



HAL
open science

New ligands for asymmetric catalysis from allenes

Avassaya Vanitcha

► **To cite this version:**

Avassaya Vanitcha. New ligands for asymmetric catalysis from allenes. Catalysis. Université Pierre et Marie Curie - Paris VI, 2015. English. NNT: 2015PA066714 . tel-01403115

HAL Id: tel-01403115

<https://theses.hal.science/tel-01403115>

Submitted on 25 Nov 2016

HAL is a multi-disciplinary open access archive for the deposit and dissemination of scientific research documents, whether they are published or not. The documents may come from teaching and research institutions in France or abroad, or from public or private research centers.

L'archive ouverte pluridisciplinaire **HAL**, est destinée au dépôt et à la diffusion de documents scientifiques de niveau recherche, publiés ou non, émanant des établissements d'enseignement et de recherche français ou étrangers, des laboratoires publics ou privés.

Université Pierre et Marie Curie

Ecole Doctorale de Chimie Moléculaire de Paris Centre

Institut Parisien de Chimie Moléculaire / Equipe Méthode et Applications en Chimie Organique

**News Ligands for Asymmetric Catalysis
from Allenes**

Par Avassaya VANITCHA

Thèse de Doctorat de Chimie Moléculaire

Dirigée par Pr. Louis FENSTERBANK et Dr. Virginie MOURIÈS-MANSUY

Présentée et soutenue publiquement le 16 octobre 2015

Devant un jury composé de :

M. Vincent GANDON	Professeur	Rapporteur
M. Florian JAROSCHIK	Chargé de Recherche	Rapporteur
M. Philippe BELMONT	Professeur	Examinateur
M. Giovanni POLI	Professeur	Examinateur
M. Louis FENSTERBANK	Professeur	Examinateur
Mme Virginie MOURIÈS-MANSUY	Maître de Conférences	Examinateur

ACKNOWLEDGEMENTS

This work was carried out from October 2012 to October 2015 under the guidance of Prof. Louis Fensterbank and Dr. Virginie Mouriès-Mansuy in the laboratory “Méthodes et Applications en Chimie Organique (MACO)” at Institut Parisien de Chimie Moléculaire (IPCM), University Pierre and Marie Curie and involved many people to whom I would like to express my deep gratitude.

First of all, I would like to thank the members of jury for accepting to be the reviews of this thesis: Prof. Vincent Gandon from University of Paris-Sud (Orsay), Dr. Florian Jaroschik from University of Reims, Prof. Philippe Belmont from University Paris Descartes, and Prof. Giovanni Poli from University Pierre and Marie Curie. Their invaluable comments and suggestions have helped me improve the quality of this thesis.

I wish to express many thanks to my supervisor, Prof. Louis Fensterbank, who welcomed me in his laboratory, for giving me a good opportunity to pursue my PhD at IPCM and for his kind attention and excellent guidance throughout the past three years and a half of my research. Because of his help for applying scholarship, I am a good opportunity to study in France. He taught me many things in chemistry, as well as languages. Especially, I would thank him for his valuable encouragement of comfort during difficult time and his patience in the correction of my thesis. He also allowed and supported me to participate in the conferences at Bordeaux and Italy for oral presentations.

I am truly grateful to Dr. Virginie Mouriès-Mansuy, my co-advisor, for her help and supports in the project “allene ligands”, that gives me a chance to work with her since my Master 2. For three years and a half, she advised me a lot, not only chemistry and also French culture. I would thank her patience to teach me and to correct my thesis, especially résumé in French. She is very kind and cheerful. She always says “bon courage” when my reaction did not work, that motivates me to achieve the goal.

I have to specially thank to Dr. Nicolas Vanthuyne from Institute des Sciences Moléculaires de Marseille (iSm2, Aix-Marseille Université) for HPLC analysis and separate my chiral gold complexes to conduct my thesis, Dr. Etienne Derat (MACO team, IPCM, UPMC) for all calculations and beautiful structures, and M. Geoffrey Gontard (IPCM, UPMC) for good X-ray crystallographic data. Also, I want to mention my intern students (M2 and L3), who help me conduct my research, are Cécilia Damelincourt (Merci beaucoup pour tes complexes de l'or),

Tanguy Jousselin, Charrotte Radal and Antoine Renaudeau. Moreover, I thank to Omar Khaled, Elsa Caytan and Aurélie Bernard for mass and NMR analysis.

My appreciation is also given to Prof. Véronique Bellosta, Dr. Alejandro Penez-luna and Dr. Frédéric Liron, who are my committees in “*comité suivi doctoral*”, for their suggestions my works and their questions to achieve my research.

I would like to say many thanks to MACO team (IPCM), like my second home. I will say “*Je vous remercie tous permanents* ”: Dr. Corinne Aubert, who is the director of IPCM, for her kindness; Dr. Marc for his guide in my first publication and security in the Lab; Dr. Marion B. for her kindness and advice; Dr. Marine for cheering up when I wrote my thesis; Dr. Cyril for all suggestions in chemistry and organize seminars; Dr. Anna-Lise for her helps and guidance in my Master; Dr. Muriel for her kindness to help and proof my writing, for sending my products to Marseille and for advice about post-doctoral position that changed my life to have a good chance in Ohio State, USA.

I also say “*Merci beaucoup*” to all my current and former colleagues in MACO team, Dr. Sara Kyne, who proof-read my thesis and help me in English; also Brendan (Brendy), Irish friend in Lab 215, for your technique “Black magic recrystallization”, for our communication in English and French and many thanks for English correction; Dr. Vincent for his guide in chemistry, advice, and his help in this thesis; Fridaaaaa!! (my best friend) for many helps and suggestions in chemistry, lab and life. I am very enjoyable when we traveled in Bordeaux together with Melanie. Also many thanks to Laura, for her help in French summary (résumé), French expressions, her kindness and her advice about alcohol drinks; Simon for his advice in French and labo, his organization for drinking and Laser game, his correction of experimental part; Jérémy (djédjé) for his kindness, French-teaching and many helps; Coralie for some substrates for gold catalysis, her technique in gold chemistry, and HPLC analysis; Thomas (our team in room 213) for his excellent calculations with his intern student Cédric B., beautiful IBOs structures, proof-reading in calculation parts and many helps for glassware team; Ludwig, for his kindness and helps; Caleb and Christophe for his helps about French grammar and lab; Fabrizio for a few Italy words and Alejandro for thesis suggestion and cheer-up when I wrote my thesis; Dr. Cédric, my little French teacher, for many helps in the lab, glassware and his suggestion about thesis and explanation about systems and steps to defend thesis with our doctoral school; Dr. Elise (last big boss of Lab 215) for her kindness, her helps in the lab and my thesis, and her cheer-up (Miss you). Moreover, I also thanks Marion Daniel (My tutor radical chemistry), Sandrine, Hugo, Antoine, Alex, Dr. David for your helps and chemical and laboratory suggesting when I was first years of Ph.D. I also thank to all

secretaries; Patricia, Sylvie P.J., Sylvie L., Dominique, Florence and Irene for your helps about my grant documents.

I would like to thank to other teams; ROCS: Dr. Julie Oble for her kindness and advice, Elise R., Valentin; GOBS and Chembio: Bo, Sha, Dmitri, Xialei, Jérémy S. Specially thanks to Mélanie, who is the first of my French friend, for many helps since my Master, her suggestions and cheer-up. We were enjoyable when we went to Italy conference together. Also, I would thank Pinglu for our French communication, which we started from zero together (Now, she can speak better than me Lol).

I would like to express thankfulness to the Franco-Thai Scholarship by French Embassy in Thailand (Campus France) and IPCM (MACO team) to give me an excellent opportunity to study and support my study.

I am very thanks my Thai friends who give me a lot of suggestion, teaching French, checking grammar, cheering up: P' Tawan, P' Namsom, P' A, Nath, P' Lek, N' Nam, Kla, P'Tum, P' Feas, Aj Dana and others. I also thank to Dr. Sumrit Wacharasindhu for your guide and suggestion.

ขอบคุณเพื่อนๆ ทุกคนในฝรั่งเศสและไทยมากค่ะ ที่ช่วยเหลือ ให้คำปรึกษา ให้กำลังใจ ในการเรียนและสำเร็จได้ค่ะ

/

Finally, I thank my family for their love and their continue efforts to understand what I study. Their supports and cheering up can make me success in my life. ขอบคุณทุกกำลังใจและ

สนับสนุนมาตลอดค่ะ

Je vous remercie infiniment!

Avassaya (Ploy) Vanitcha

“Let me tell you the secret that has led me to my goal, my strength lies solely in my tenacity”

Louis Pasteur

Contents

Acknowledgements	3
Contents	6
Abbreviations	10
Résumé	13
General introduction	35
Chapter 1. Organophosphorus Compounds and Their Applications in Gold Chemistry	39
1. Introduction	41
2. Organophosphorus chemistry	42
2.1. Phosphine ligand and analogues	43
2.1.1. Historical overview	44
2.1.2. Phosphine ligands in asymmetric catalysis	49
2.2. Phosphine oxide derivatives	51
3. Organophosphorus compounds in gold chemistry	57
3.1. Generation of gold-phosphine complexes	57
3.1.1. Mononuclear gold bisphosphine complexes	60
3.1.2. Dinuclear gold bisphosphine complexes	61
3.1.3. Gold complexes bearing phosphine and phosphine oxide moieties	63
3.2. Functionalization of gold(I) complexes bearing organophosphorus groups	64
3.2.1. Formation of Au-C bond	64
3.2.1.1. <i>Via</i> transmetalation of organometallic reagents (RLi and RMg)	64
3.2.1.2. <i>Via</i> transmetalation of boron reagents	65
3.2.1.3. <i>Via</i> intramolecular gold-catalyzed cyclization reactions	65
3.2.2. Formation of C-H and C-X bonds	67
3.3. Gold(I) complexes bearing organophosphorus groups in catalysis	68
3.3.1. Cycloisomerization of 1,6-enynes in the absence nucleophile	70
3.3.1.1. Skeletal rearrangements	71
3.3.1.2. Cyclopropanation reactions	72
3.3.2. Cycloisomerization of 1,6-enyne in the presence of nucleophiles	73
3.3.2.1. Addition of carbon nucleophile	74
3.3.2.2. Addition of oxygen and nitrogen nucleophiles	76
4. Conclusion and perspective	78

Chapter 2. Allene Syntheses and Applications	79
1. Introduction	81
2. General synthesis of allenes	82
2.1. Organometallic reagents for allene formation	82
2.1.1. Organolithium reagents	83
2.1.2. Organocopper reagents	85
2.1.3. Aluminum reagents	88
2.2. Metal-catalyzed allene formation	89
2.3. Isomerization reactions	92
2.3.1. Metallotropic rearrangement	93
2.3.2. [2,3]-Sigmatropic rearrangement	95
2.3.2.1. With phosphoryl group	95
2.3.2.2. With alkoxy group	96
3. Allenes in catalysis	97
3.1. Chiral allene catalysts	97
3.2. Allene ligands	99
4. Allenes in gold chemistry	103
4.1. Gold(I)-allene complexes	104
4.2. Gold(I)-catalyzed cyclization reactions	108
4.2.1. Heteroatom-nucleophilic cyclization	110
4.2.1.1. Hydroalkoxylation reactions	111
4.2.1.2. Hydroamination reactions	114
4.2.2. Carbonucleophilic cyclization	116
5. Conclusion and perspective	118
Chapter 3. Allenes Bearing Phosphine Oxide Groups and Their Reactivity toward Gold Complexes	121
1. Introduction	123
2. Objectives of the project	123
3. Synthesis of allenes bearing monophosphine oxide groups	124
3.1. Synthesis of allenes bearing monophosphine oxides	124
3.1.1. Synthesis of propargyl ketone (2)	124
3.1.2. Synthesis of propargylic acetate (4)	125
3.1.3. Synthesis of allenes bearing monophosphine oxides (5-13)	125
3.1.3.1. Copper(I)-mediated S_N2' reactions	125

3.1.3.2. Palladium-catalyzed coupling reactions	127
3.2. Synthesis of pyridinyl-containing allenyl phosphine oxides	129
3.2.1. Synthesis of ethynylpyridines	129
3.2.2. Synthesis of propargylic ketone (22)	130
3.2.3. Synthesis of propargylic acetate (24)	130
3.2.4. Synthesis of pyridinyl allenes bearing mono-phosphine oxides (25)	131
3.3. Synthesis of allenyl bisdiphenylphosphine oxides	132
4. Allene cyclization	134
4.1. Investigation on the reaction of allenes with cationic gold complexes	134
4.2. Chirality transfer	136
5. Cationic vinyl complex featuring a triphenylphosphine gold(I) moiety	137
5.1. Synthesis of cationic vinyl gold complex (31)	137
5.2. Post-functionalization of cationic vinylgold complex (31)	139
6. Vinyl complex bearing a chlorogold(I) group	141
6.1. Preliminary test in the presence of gold(I) complex	141
6.2. Synthesis of vinyl-gold complexes	142
6.3. Computational calculations towards the reactivity of gold complex (41)	144
6.4. Investigations on the reactivity of vinyl gold complex (41b)	148
6.4.1. Preliminary tests	148
6.4.2. Vinyl gold complex (41b) in catalysis	149
6.4.2.1. Bibliographical background: Gold carbene complexes in catalysis	149
6.4.2.2. Cycloisomerization with 1,6-enynes	153
6.4.2.3. Cyclopropanation	156
6.4.2.4. Cyclohydroalkoxylation	156
6.4.2.5. Cyclohydroamination	158
6.4.3. Electronic properties	159
6.4.4. Optical Resolution	160
6.4.5. Investigations on asymmetric catalysis	161
7. Conclusion and perspectives	162
Chapter 4. Allenyl Bisphosphine Ligands for Metal Catalysis	165
1. Introduction	167
2. Synthesis of allenyl bisphosphine	167
3. Metal-allenyl bisphosphine complexes	169
3.1. Platinum-allenyl bisphosphine complex	169

3.2. Palladium-allenyl bisphosphine complex	171
3.3. Gold-bisphosphine complexes	172
3.3.1. Mononuclear gold-phosphine complex	172
3.3.2. Dinuclear gold-bisphosphine complex	172
4. Gold(I)-catalyzed cyclization reactions	174
4.1. Preliminary catalytic tests	174
4.2. Broadening the scope of substrates	175
4.2.1. Nitrogen-tethered 1,6-enynes	175
4.2.2. Malonate group-tethered 1,6-enynes	181
4.3. Electronic properties	181
4.3.1. Evaluation by selenide complexes	181
4.3.1.1. Preparation of selenide derivatives	181
4.3.1.2. Ligand properties	182
4.3.2. Evaluation by using diagnostic allene diene	183
5. Resolution of racemic allenes	184
5.1. Using chiral cyclopalladated complexes	184
5.2. Using preparative chiral HPLC	188
6. Asymmetric palladium-catalyzed allylic alkylation	189
6.1. Preparation of chiral allenyl bisphosphine	189
6.2. Palladium-bearing bisphosphine in asymmetric allylic alkylation	190
7. Asymmetric catalysis with chiral gold complex (113)	191
7.1. Asymmetric cycloisomerization of 1,6-enynes	191
7.2. Asymmetric methoxycyclization	193
7.3. Asymmetric cycloalkoxylation	194
7.4. Asymmetric olefin cyclopropanation	195
8. Modification of chiral gold complexes	195
8.1. Selected models of chiral gold complexes	196
8.2. Preparation of new gold complexes	197
8.3. Electronic properties	198
8.3.1. Evaluation by selenide complexes	198
8.3.2. Evaluation by using diagnostic allene diene	199
8.4. Reactivity of gold complexes (116) in asymmetric catalysis	200
9. Conclusion and perspectives	201
General conclusion	203
Experimental part	209

Abbreviations

°C	degree Celsius
Ac	acetyl
Ac ₂ O	acetic anhydride
AgClO ₄	silver perchlorate
AgOTf	silver triflate
AgSbF ₆	silver hexafluoroantimonate
aq.	aqueous
Ar	aryl
Au	gold
atm	atmosphere
BINAP	2,2'-bis(diphenylphosphino)-1,1'-binaphthyl
BIPNOR	2,2',3,3'-tetraphenyl-4,4',5,5'-tetramethyl-6,6'-bis-1-phosphanorborna-2,5-dienyl
Bn	benzyl
Boc ₂ O	di- <i>tert</i> -butyl dicarbonate
BPE	1,2-bis(phospholano)ethane
BPPFA	<i>N,N</i> -dimethyl-1-[1,2-bis(diphenylphosphino)ferrocenyl]ethylamine
BPPFOH	1',2-bis(diphenylphosphino)ferrocenyl]ethyl alcohol
BPPM	(2 <i>S</i> ,4 <i>S</i>)- <i>N</i> -butoxycarbonyl-4-diphenylphosphino-2-diphenylphosphinomethylpyrrolidine
CAMP	2-methoxyphenyl(methyl)cyclohexylphosphine
cat.	catalytic
Cbz	carbobenzyloxy
CDCl ₃	chloroform- <i>d</i>
Chiralpak AD	amylose tris(3,5-dimethylphenylcarbamate) coated
Chiralpak IE	amylose tris(3,5-dichlorophenylcarbamate) coated
COD	cyclooctadiene
conv.	Conversion
CuBr	copper bromide
CuI	copper iodide
DCE	dichloroethane
DCM	dichloromethane
<i>de</i>	diastereomeric excess
DFT	density functional theory
DHP	dihydropyrane
DIBAL-H	diisobutylaluminum hydride
DIOP	2,3- <i>o</i> -isopropylidene-2,3-dihydroxy-1,4-bis(diphenylphosphino)butane
DIPAMP	1,2-bis[(2-methoxyphenyl)phenylphosphino]ethane
CHIRAPHOS	bis(diphenylphosphino)butane

DMAP	4-dimethylaminopyridine
DMF	dimethylformamide
DMP	dess-martin periodinane
DMPU	1,3-dimethyl-3,4,5,6-tetrahydro-2-pyrimidinone
DMSO	dimethyl sulfoxide
dppe	1,2-bis-diphenylphosphinoethane
<i>dr</i>	diastereomeric ratio
DuPHOS	1,2-bis(phospholano)benzene
E	electrophile
<i>ee(s)</i>	enantiomeric excess(es)
equiv	equivalent
ESI	electrospray ionization
Et	ethyl
Et ₃ N	triethylamine
EtOAc	ethyl acetate
h	hour
HCl	hydrochloric acid
HMDS	bis(trimethylsilyl)amine
HMPA	hexamethylphosphoramide
HOMO	highest occupied molecular
HPLC	high performance liquid chromatography
HRMS	high resolution mass spectrometry
IBOs	intrinsic bond orbitals
IMes	1,3-bis(2,4,6-trimethylphenyl)imidazole-2-ylidene
<i>i</i> -Pr	<i>iso</i> -propyl
IPr	<i>N,N'</i> -bis(2,6-di(2-propyl)phenyl)imidazol-2-ylidene
IR	infrared
<i>J</i>	coupling constant
KOH	potassium hydroxide
L	ligand
L*	chiral ligand
L-DOPA	L-3,4-dihydroxyphenylalanine
LiAlH ₄	lithium aluminum hydride
LiBr	lithium bromide
LiCl	lithium chloride
LiHMDS	lithium hexamethyldisilazane
LUMO	lowest occupied molecular
Lux-Cellulose-2	cellulose tris(3-chloro-4-methylphenyl-carbamate) coated
Lux-Cellulose-4	cellulose tris(4-chloro-3-methylphenyl-carbamate) coated
m	meta
M	molar (mol/L)
m.p.	melting point
<i>m</i> -CPBA	<i>m</i> -chloroperoxybenzoic acid
Me	methyl
mg	milligram (s)
MHz	megahertz

min	minute (s)
mL	milliliter (s)
mmol	millimole (s)
Ms	mesyl
MsCl	methanesulfonyl chloride
MW	molecular weight
Na ₂ S ₂ O ₃	sodium thiosulfate
NaCl	sodium chloride
NaH	sodium hydride
NaI	sodium iodide
NBS	<i>N</i> -bromosuccinimide
n.d.	not determined
<i>n</i> -BuLi	<i>n</i> -buthyllithium
nd	not determined
NHC	<i>N</i> -heterocyclic carbene
NIS	<i>N</i> -iodosuccinimide
NMR	nuclear magnetic resonance
Nu	nucleophile
<i>o</i>	ortho
<i>p</i>	para
PAMP	2-methoxyphenyl(methyl)phenylphosphine
PCC	pyridinium chlorochromate
Ph	phenyl
PPTS	pyridinium <i>p</i> -toluenesulfonate
PROPHOS	propane-1,2-diylbis(diphenylphosphine)
quant	quantitative
rt	room temperature
sat	saturated solution
SEGPPOS	5,5'-bis(diphenylphosphino)-4,4'-bi-1,3-benzodioxole
SIMes	1,3-bis(2,4,6-trimethylphenyl)-4,5-dihydroimidazol-2-ylidene
S _N 2	bimolecular nucleophilic substitution
(<i>S,S</i>)-Whelk-O1	(<i>3R,4S</i>)-4-(3,5-dinitrobenzamido)-3-[3-(dimethylsilyloxy)propyl]-1,2,3,4-tetrahydrophenanthrene
T	temperature
TBAF	tetra- <i>n</i> -butylammonium fluoride
Tf	trifluoromethanesulfonyl
<i>t</i> -BuLi	<i>tert</i> -buthyllithium
THF	tetrahydrofuran
TLC	thin layer chromatography
Ts	toluenesulfonyl
vs	versus
ZnCl ₂	zinc chloride

Résumé

La catalyse asymétrique donne directement accès à des composés énanti enrichis. Les ligands optiquement purs coordonnés à des catalyseurs métalliques sont importants pour induire l'énantiosélectivité des réactions et permettre l'obtention privilégiée d'un énantiomère. La chiralité axiale des allènes est intéressante pour être utilisée comme inducteur de chiralité dans ces réactions. Dans la littérature peu d'exemples ont été reportés. Il a été montré de façon intéressante qu'il était possible de coordiner des allènes fonctionnalisés à différents métaux tels que l'Ag^[1] et l'Au^[2-4] sans détruire le motif allénique. De façon confidentielle l'équipe de Ready a isolé et caractérisé un complexe de rhodium^[5] portant comme ligand asymétrique, une diphosphine allénique, où le rhodium est à la fois coordonné aux atomes de phosphore et à une des doubles liaisons de l'allène. Ce complexe a été utilisé de façon efficace dans l'addition asymétrique d'aryle acide boronique sur des α -cétosters. (Figure R1)

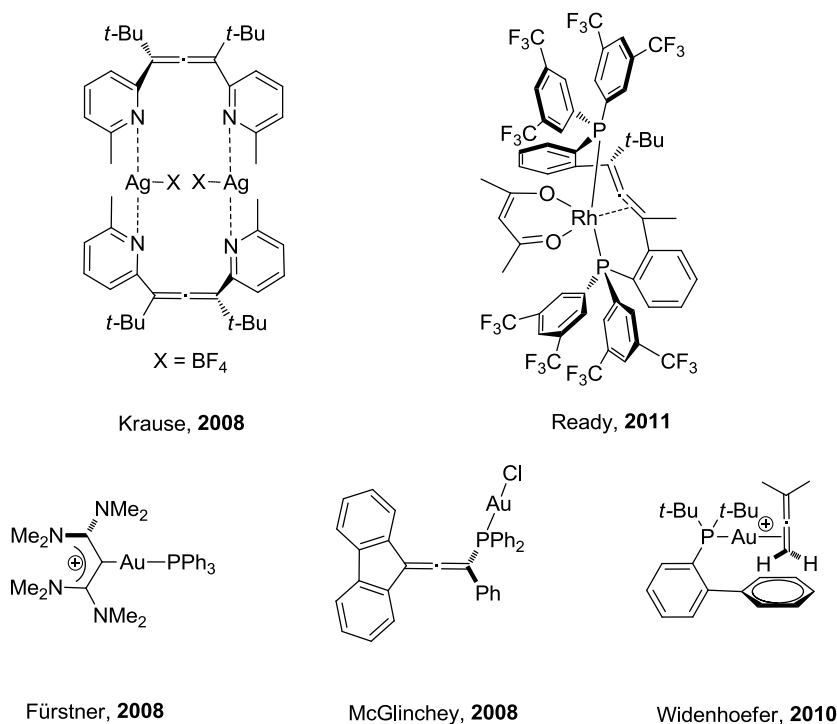


Figure R1. Les complexes d'allènes d'or.

Mon travail de thèse a été de développer de nouveaux systèmes catalytiques obtenus à partir de diverses phosphine-allènes (Figure R2) et de complexes d'or(I). En effet, au début de ce travail, aucun complexe d'or portant une mono ou diphosphine-allène comme ligand n'avait été utilisé en catalyse aussi bien en version racémique qu'en version asymétrique (Figure R2).

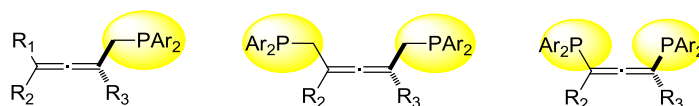


Figure R2. Allènes chiraux portant des groupements phosphiques.

Cette thèse se compose de quatre chapitres

Le premier chapitre introduit les principaux dérivés phosphiniques, couramment utilisés comme ligands de métaux de transition et leurs applications en catalyse asymétrique. Plus particulièrement les biphosphines chirales à Symétrie C_2 , comme la BINAP, le MeOBIPHEP, la SEGPHOS et ses analogues qui sont couramment utilisée comme inducteur de chiralité afin d'obtenir des produits énantiomériquement purs. La synthèse et la fonctionnalisation des phosphines seront présentées ainsi que leurs réactivités dans différentes réactions. Notre intérêt étant la catalyse asymétrique à l'or.

Le deuxième chapitre présente les différentes synthèses de dérivés alléniques et leurs utilisations. Notre attention s'est portée sur trois méthodologies de synthèse. D'abord, les réactifs organométalliques qui peuvent être employés pour la synthèse d'allènes par réaction de substitution nucléophile de type S_N2' . La seconde méthodologie est basée sur la catalyse métallique ; par exemple, l'utilisation de complexes de palladium(0) en présence d'organozinciques. Le dernier exemple met en jeu les réactions d'isomérisation de précurseurs propargyliques dilithiés ainsi que les réarrangements [2,3] de Wittig.

Le troisième chapitre concerne nos résultats. Il porte sur la synthèse d'allènes contenant des fonctions oxydes de phosphine et sur l'étude de leurs réactivités. Dans une première approche, nous avons préparé des allènes portant des groupements mono ou diphenyl oxydes de phosphine ainsi que différents substituants aryles et alkyles. Ces allènes ont été préparés à partir des trois acétates propargyliques **4**, **24a** et **24b** par le biais soit d'une réaction de substitution au cuivre de type S_N2' ou d'une réaction de couplage catalysée au palladium faisant intervenir un réactif organozincique (Schéma 1). Ces réactions ont permis l'obtention des allènes **5-13**, **17-18** et **25** avec des rendements allant de 50% à 92% (Figure R3).

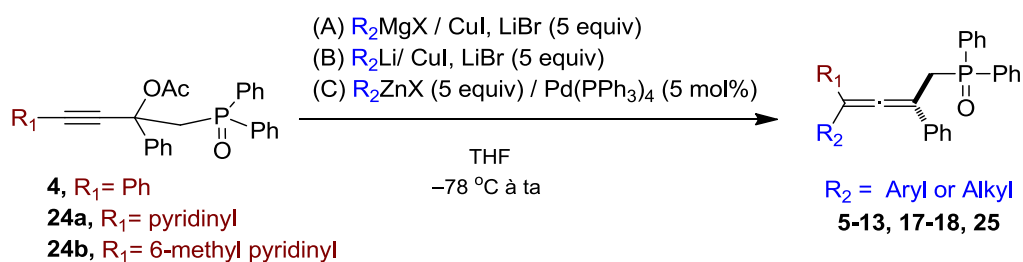


Schéma 1. Synthèse des allènes portant des groupements oxydes des phosphine à partir d'acétates propargyliques.

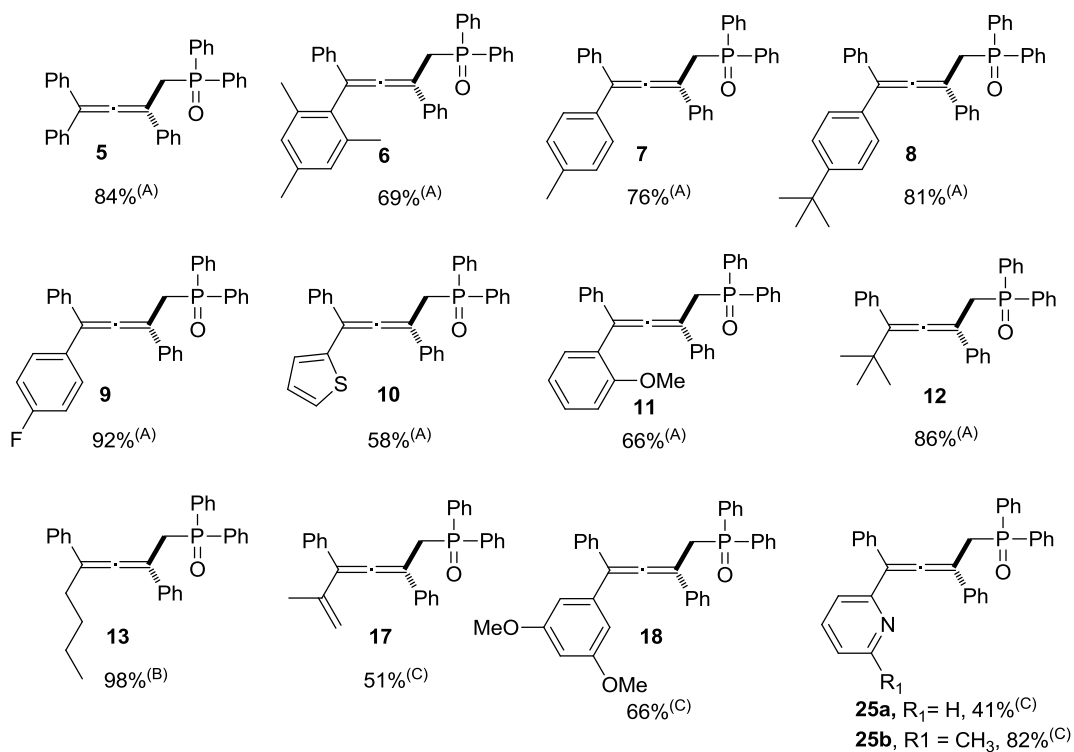
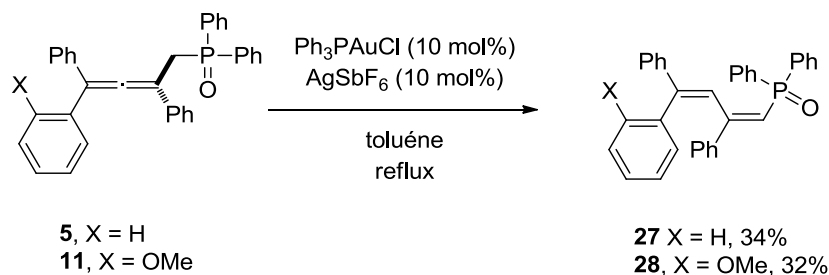


Figure R3. Monophosphine-allènes.

a) Cyclisations des allènes

Tout d'abord, nous avons étudié la réactivité des allènes portant des groupements oxyde de monophosphine en présence de catalyseur d'or(I) dans des réactions de cyclisations. Les précurseurs **5** et **11** mis en présence du système catalytique cationique PPh₃AuCl/AgSbF₆ (10 mol%), n'ont pas permis la formation des dérivés cycliques attendus, mais à celle des diènes **27** et **28** avec des rendements modérés de 34% et 32% respectivement (Schéma 2).

Schéma 2. Formation des diènes **27** et **28**.

Nous avons estimé que le groupement phényle, dans ces deux cas, n'était pas suffisamment nucléophile pour permettre la réaction de cyclisation. En revanche dans le cas des allènes **17** et **18**

les produits de cyclisations **29** et **30** ont été obtenus avec de bons rendements de 71 et 85% respectivement *via* l'intermédiaire carbénique **A**. (Schéma 3).

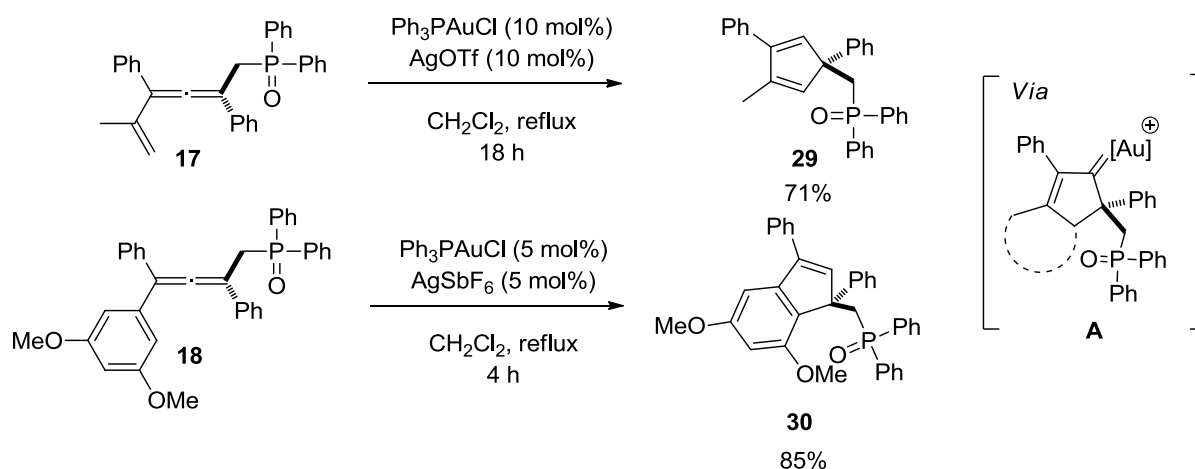


Schéma 3. Synthèses du cyclopentadiène **29** et de l'indenylphosphine **30** par cycloisomérisation.

Le défi suivant était d'étudier la possibilité de réaliser cette réaction de cyclisation à partir d'allènes optiquement purs afin de réaliser un transfert de chiralité lors de la réaction. En collaboration avec le Dr. Nicolas Vanthuynne (Laboratoire iSm2, Aix-Marseille Université) l'allène **18** a été résolu par HPLC préparative chirale. Les deux énantiomères ont été obtenus avec des *ee* > 98%. La réaction de l'isomère (–, CD 254 nm)-**18** traité avec 5 mol% d'or(I) cationique a donné le composé (–, CD 254 nm)-**30** avec un *ee* de 97 %, mettant en évidence un transfert de chiralité presque total (Schéma 4). Il est intéressant de noter ici qu'il s'agit du premier transfert de chiralité réalisé, avec succès, à partir d'un allène tétrasubstitué.

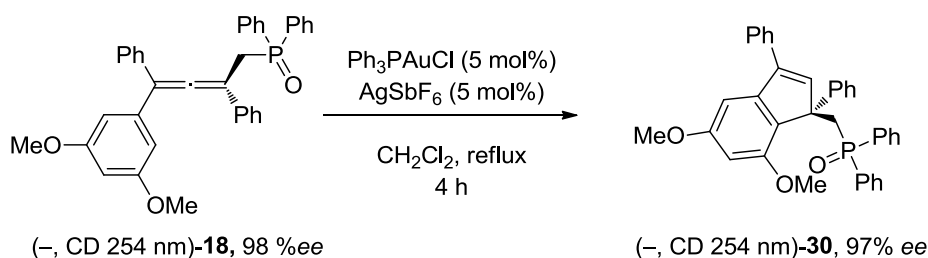


Schéma 4. Transfert de chiralité.

b) Complexe cationique vinylique comportant un fragment triphénylphosphine d'or(I)

Nous avons ensuite étudié la réaction à partir de l'allène pyridine **25a**, en utilisant les mêmes conditions de réaction que celles décrites Schéma 4. Nous n'avons pas isolé le produit de

cyclisation **32** attendu mais de façon intéressante, nous avons observé, en très faible quantité, le complexe d'or **31** (Schéma 5).

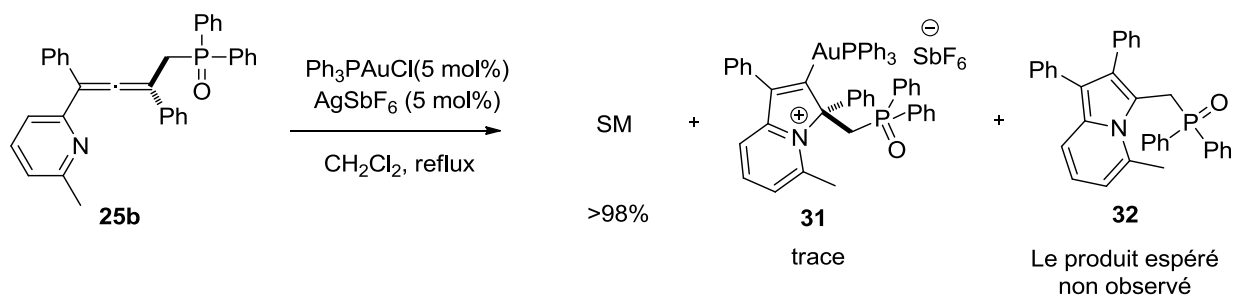


Schéma 5. Réaction de l'allène **25b** avec le cationique d'or.

Sur la base de ce résultat, nous avons tenté d'optimiser la réaction de formation du complexe d'or **31**. L'allène **25b** a été mis en réaction avec 0,7 équivalent d'un mélange 1:1 de Ph_3PAuCl et AgOTf . Le complexe **31** correspondant a été isolé avec un rendement de 81% (Schéma 6). Les données spectrales obtenues en RMN ^{31}P ont permis d'identifier ce complexe, avec des déplacements chimiques à 42,7 ppm pour le phosphore du groupement AuPPh_3 , et 23,6 ppm pour le phosphore impliqué dans la fonction phosphoryle. La RMN ^{13}C a permis d'identifier le carbone quaternaire vinylique portant AuPPh_3 avec un déplacement du chimique caractéristique à 203 ppm (doublet, $^2J_{\text{CP}} = 114$ Hz), correspondant à des complexes d'or de vinyne semblables à ceux décrit par les équipes d'Hammond^[6] et Shi.^[7]

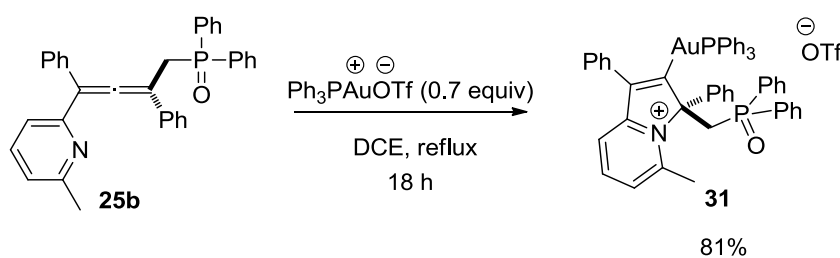
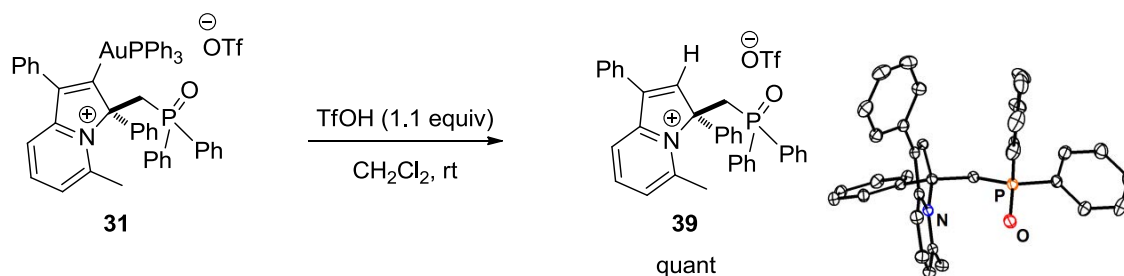
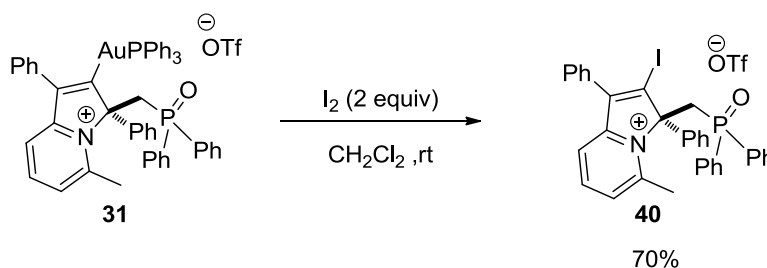


Schéma 6. Réaction de l'allène **25b** avec 0,7 équivalent d'or cationique.

En présence de 1,1 équivalents d'acide triflique, Le complexe **31** subit une protodeauration. Le composé indolizinium **39** est obtenu de façon quantitative. Sa structure a été caractérisée par analyse aux rayons X (Schéma 7).

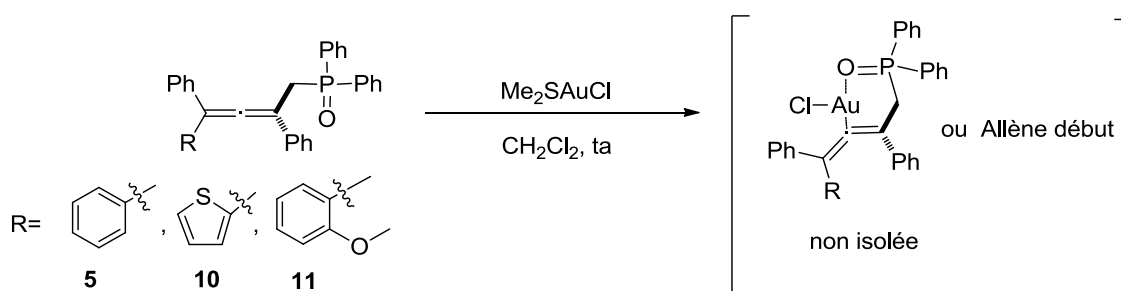
Schéma 7. Protodeauration de **31** par TfOH.

Nous avons également étudié la réaction d'iodolise de **31** par addition de 2 équivalents de diode fraîchement sublimé. Le dérivé vinyl-iodo **40** a été obtenu avec un bon rendement de 70 % (Schéma 8).

Schéma 8. Iodation de **31**.

c) Les complexes vinyliques avec le groupement de chlore d'or(I)

Devant les résultats obtenus à partir de complexes cationique d'or(I), nous avons étudié la capacité de complexation de nos différents allènes par le complexe Me_2SAuCl . Pour ce faire, les allènes **5**, **10** et **11** ont été mis en réaction en présence d'un équivalent de complexe Me_2SAuCl . Malheureusement, aucun des complexes recherchés n'a été isolé (Schéma 9).

Schéma 9. Activation des allènes **5**, **10** et **11** par Me_2SAuCl .

En revanche, dans le cas des allènes pyridiniques **25a** et **25b**, les complexes indolizinium **41a** et **41b** ont été isolés de façon quantitative. Ces composés peuvent exister sous deux formes limites

(Schéma 10). Les structures des composés **41a** et **41b** ont été caractérisées par diffraction des rayons X, la distance Au-C mesurée est de 1.993 Å et 1.984 Å respectivement (Figure R4).

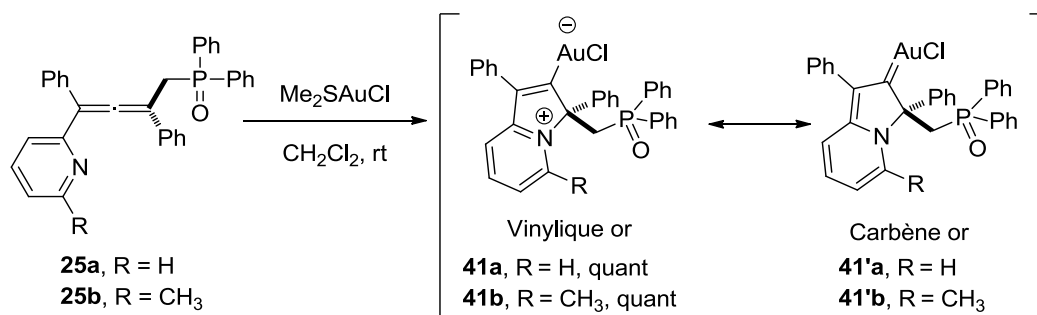


Schéma 10. Synthèse des complexes d'or pyridiniques **41** ou **41'**.

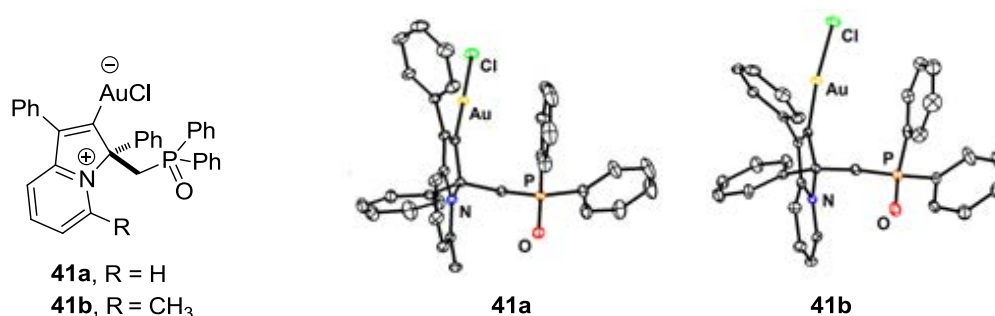


Figure R4. Cristallographies de complexes d'or vinyliques **41a** et **41b**.

Par ailleurs, une étude théorique a été faite sur ces complexes **41** pour obtenir des informations sur les propriétés électroniques et structurales. Les calculs DFT ont été effectués en utilisant le progiciel Turbomole (v6.4), la fonctionnelle B3LYP, complétée par la correction D3 et la base def2-SV(P). Nous avons effectué ce calcul pour obtenir une meilleure connaissance des structures mésomères et pour comprendre la différence entre **41** et le carbène d'or **41'**. L'analyse de l'ordre de liaison de Mayer (Figure R5A) conclut que la forme mésomère privilégiée est **41b**, puisque l'ordre de liaison entre l'or (Au) et le carbone (C1) est de 0,7559, ceci correspondant à une liaison simple. D'autre part, une visualisation des orbitales moléculaires montre qu'au moins une orbitale moléculaire implique des interactions entre le fragment AuCl et le carbène (Figure R5B). Cette étude au niveau orbitalaire révèle que la liaison π entre l'or et le chlorure est délocalisée avec le groupement pyridinium. De plus, le tracé du potentiel électrostatique (Figure R5C) montre que le fragment Au-Cl est riche en électrons et le carbène créé *in-situ* a un potentiel électrostatique positif, représentant ainsi un bon accepteur d'électrons.

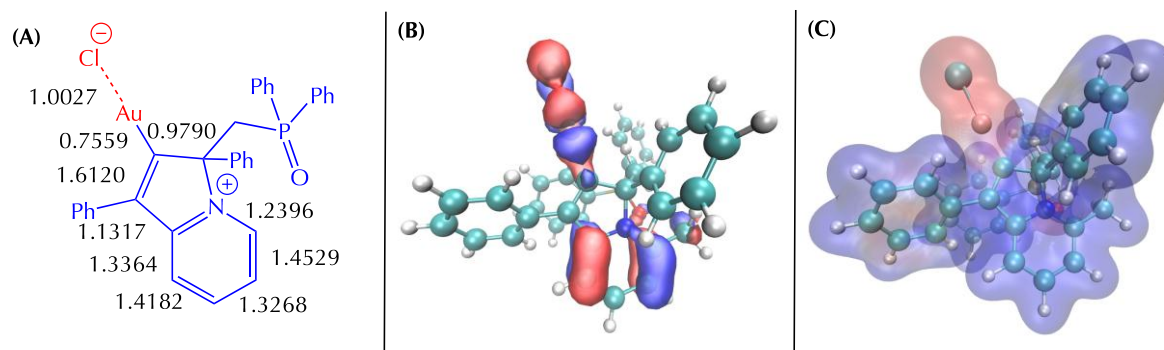


Figure R5. Calculs théoriques pour le complexe **41b** : (A) L'ordre de liaison Mayer (B) L'orbitale moléculaire montrant la délocalisation entre AuCl et carbène (C) Le potentiel électrostatique (bleu: positif; rouge: négative).

Néanmoins, ces informations ne sont insuffisantes pour décrire les propriétés du ligand pyridinium. Le calcul des énergies HOMO/LUMO du ligand **41b** sans AuCl permet de le comparer à d'autres ligands pour l'or (IPr, SPhos, and PPh₃). Le calcul indique que ce ligand est un bon π -accepteur. La comparaison d'orbitales liantes obtenus par la méthode IBOs (Intrinsic Bond Orbitals) permet de localiser sur le carbène ou l'or les électrons des orbitales σ -donneur et π -accepteur. La Figure R6 montre quatre orbitales IBOs, qui illustrent la propriété de ligand pyridinium à AuCl.

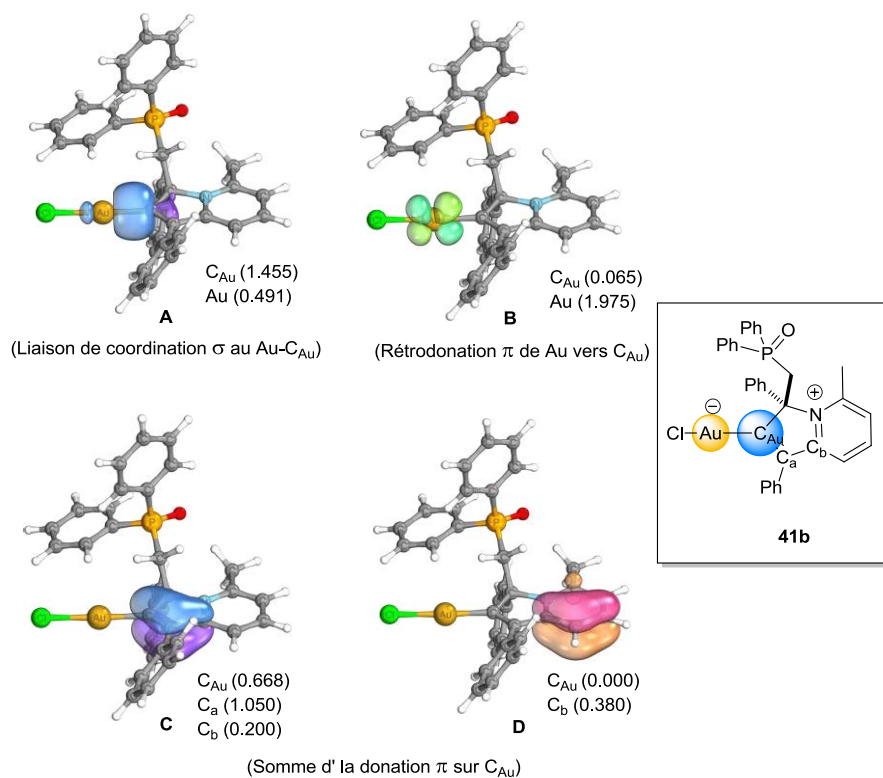
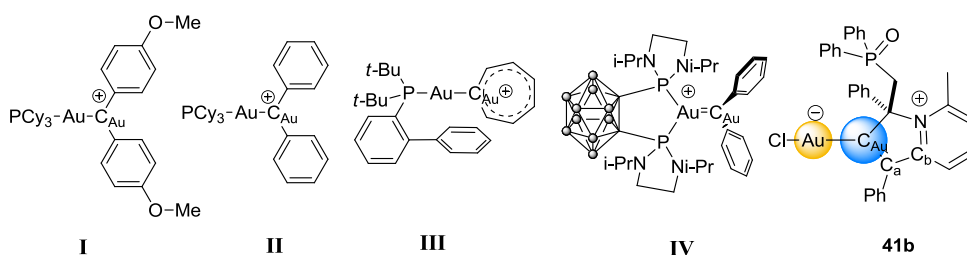


Figure R6. Orbitales IBOs partiellement localisées sur le carbène **41b**. Les nombres indiquent entre parenthèses le nombre d'électrons de l'orbitale localisés sur chaque atome.

Dans l'analyse IBOs (Figure R6) de la Table R1, le complexe **41b** se révèle moins π -accepteur que l'or complexe **IV** de l'équipe de Bourrisou, qui est très bon π -accepteur (Table R1, entry 2). Mais, c'est un bon σ -donneur comme les complexes **I**, **II** et **III** (Table R1, entries 1 et 3). Pour mieux comprendre les propriétés du complexe d'or **41b**, la réactivité a été étudiée expérimentalement.

Table R1. Nombre d'électron occupant les orbitales IBO pour des complexes d'or : I, II, III, IV et 41b



Entry	IBOs (Figure R6)	I	II	III	IV	41b
1	A (Liaison de coordination σ Au-C _{Au}) 	0.473 ^[a] (1.444) ^[b]	0.452 ^[a] (1.463) ^[b]	0.477 ^[a] (1.452) ^[b]	0.494 ^[a] (1.412) ^[b]	0.491 ^[a] (1.455) ^[b]
2	B (Rétrodonation π de Au vers C _{Au}) 	0.057	0.074	0.051	0.175	0.065
3	C + D [Somme d'la donation π sur C _{Au}] ^[c] 	0,598	0,551	0,731	0,404	0.668

^[a]Nombre d'électron localisé sur Au. ^[b] Nombre d'électron localisé sur C_{Au} ^[c] Somme de la contribution de tous les substituants aromatiques.

Suite à cette étude sur les propriétés intrinsèques du complexe d'or **41b**, celui-ci a été testé en tant que catalyseur dans des réactions de cycloisomérisation. A partir de 5 mol% du complexe racémique (\pm)-**41b** et de 5 mol% d'AgSbF₆, le complexe d'or cationique formé a permis de catalyser la réaction de cycloisomérisation de l'ényne 1,6, **63**. Les diènes **94a** et **94b** ont été obtenus dans un rapport 2:1 avec un rendement globale de 78% (Schéma 11). Devant ce résultat encourageant nous avons testé d'autres substrats

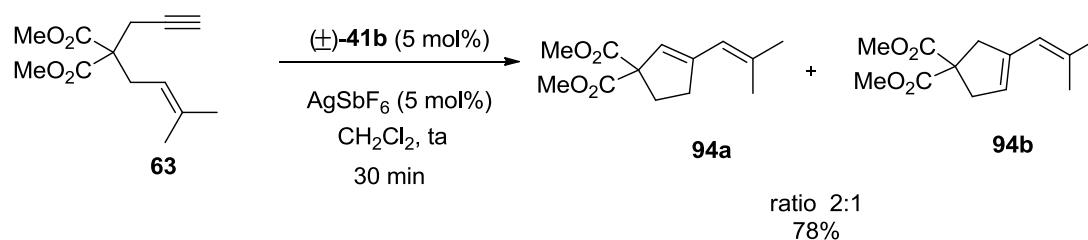


Schéma 11. Cycloisomérisation de l'ényne malonate 69 avec le réactif d'or cationique.

L'ényne *N*-Tosyl **50** a été mis en réaction dans les mêmes conditions. Cependant seul le produit de départ a été isolé (Schéma 12, eq. 1). Pour tenter d'expliquer cette absence de réactivité, on s'est basé sur les études des groupes d'Echavarren^[8] et Fensterbank.^[9] En effet, tous deux suggèrent que la préparation *in situ* d'espèces actives d'or(I) cationiques peut générer un complexe dinucléaire d'or(I) possédant un chlorure ponté. Dans ce cas, l'addition d'un excès de sel d'argent permettrait de rompre le pont chlorure et ainsi de générer des espèces actives. En effet en présence d'un léger excès de sels d'argent (3,5 mol%), les produits de cycloisomérisation **82** et **95** attendus, issus des énynes **50b** et **63**, ont été obtenus avec des rendements respectifs de 75% et 50% (Schéma 12, eq. 2 et 3).

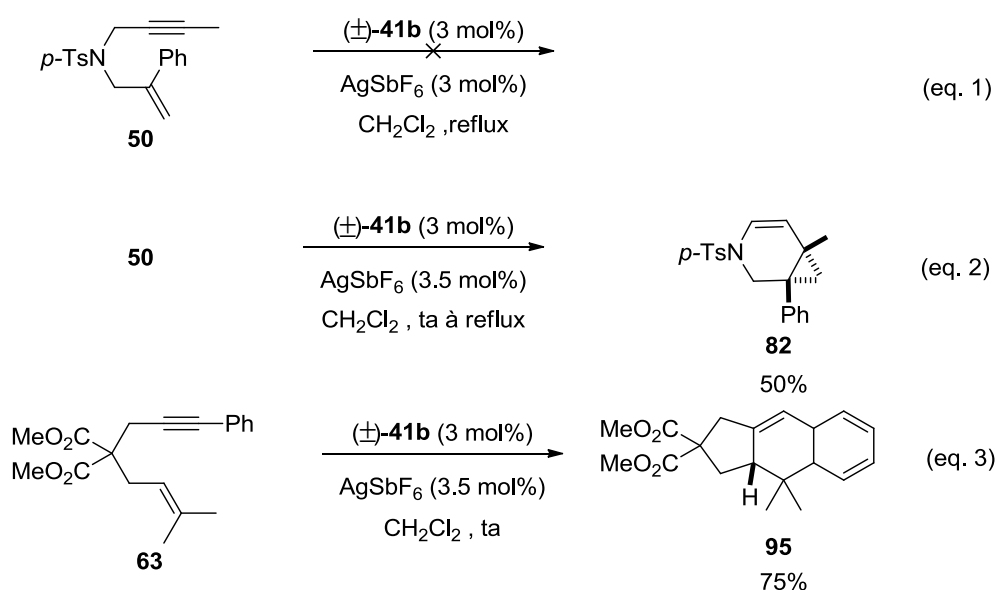


Schéma 12. Cycloisomérisation des énynes de 50 et 63 avec de l'or cationique 41b.

Nous avons effectué d'autres types de cyclisation à partir de substrats modèles différents afin d'étudier la réactivité du complexe d'or. Les réactions de cyclohydroalkoxylation et de cyclohydroamination du γ -allenol **68** et γ -allenylamine **71** ont été effectuées en présence de (±)-**41b** (3 mol%) et d'AgOTs (4,5 mol%) dans le toluène à température ambiante. La réaction n'étant

pas totale la température a été augmentée jusqu'au reflux du toluène, les produits **99** et **101** ont été obtenus avec des rendements optimisés de 76% et 70% respectivement (Schéma 13).

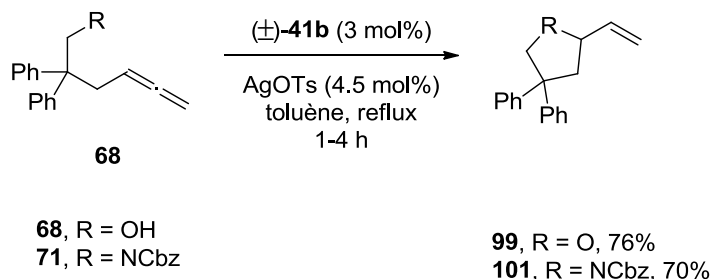


Schéma 13. Cyclohydroalkoxylation et cyclohydroamination des allènes **69** et **71**.

L'allène cyclohexyle **69**, en présence (±)-**41b** (3 mol%) et d'AgSbF₆ (4,5 mol%), à température ambiante dans le dichlorométhane, a donné le composé 2-(cyclohexylidéneméthyl) tétrahydrofurane **100** avec un rendement de 81%. Dans le cas de l'allène **72**, à température ambiante dans le toluène et en présence de (±)-**41b** (3 mol%) et d'AgOTs (4,5 mol%), le produit **102** a été obtenu avec un rendement modéré (40%) (Schéma 14).

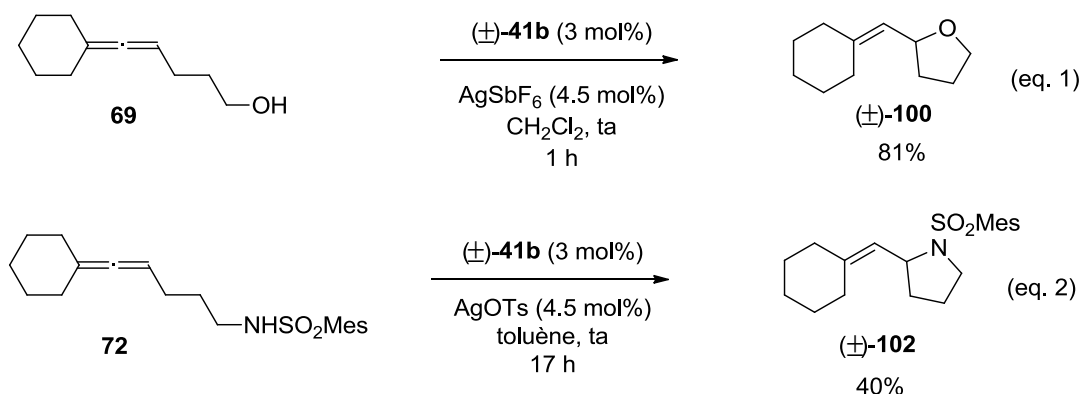
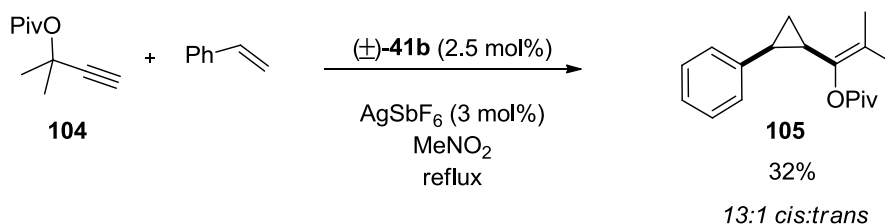
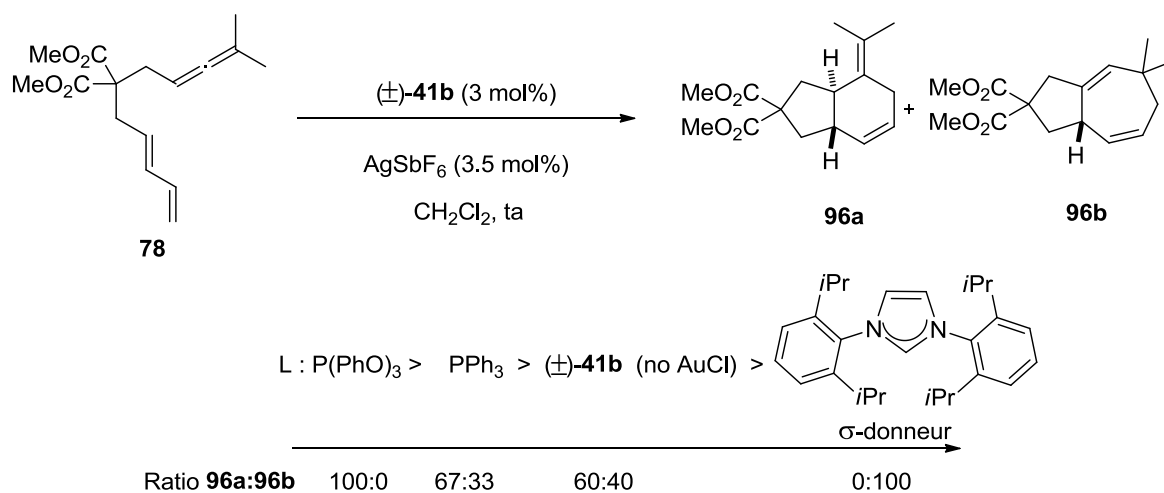


Schéma 14. Hydroalkoxylation et hydroamination des allènes **69** et **72**.

Nous avons examiné ensuite les réactions de cyclopropanation d'oléfine. Cette réaction met en jeu le pivaloate de propargyl **104** avec du styrène en présence du catalyseur d'or cationique, préparé à partir de (±)-**41b** (2,5 mol%) et d'AgSbF₆ (3 mol%). Le cyclopropane **105** a pu être synthétisé avec un rendement faible de 32% (13:1 *cis:trans*) (Schéma 15).



Afin d'évaluer les propriétés électroniques de notre ligand pyridinium, nous avons effectué la réaction de cyclisation de l'allène-diène **78**, qui est utilisée comme substrat modèle. La réactivité du complexe d'or (\pm) -**41b** a donc été comparée à celle d'autres complexes d'or portant des ligands $P(\text{PhO})_3$, PPh_3 , et carbène *N*-hétérocyclique (IPr). Lorsque que le ligand est π -accepteur le produit **96a** de type [4+2] est obtenu majoritairement tandis que dans le cas d'un ligand σ -donneur c'est le composé **96b** provenant d'une réaction de type [4+3] qui sera formé majoritairement. La réaction de l'allène-diène **78** en présence de (\pm) -**41b** (3 mol%) et AgSbF_6 (3,5 mol%), donne un mélange de **96a** et **96b** dans le ratio 67:40. Ce rapport montre que dans notre cas le ligand est moins π -accepteur que $P(\text{PhO})_3$ et PPh_3 , mais plus que IPr (Schéma 16).



Devant la bonne réactivité de notre complexe d'or nous l'avons préparé énantiomériquement pur. Une résolution de l'allène **25b** par HPLC chirale sur support Lux-Cellulose en utilisant le mélange hexanes/éthanol (50/50) comme phase mobile, a été effectué par le Dr. Nicolas Vanthuyne. L'énantiomère (*αR*)-**25b** a été obtenu avec un $ee > 99\%$ ($[\alpha]_D -55,9$, c 0,5, CHCl_3) et de façon analogue à la préparation du complexe racémique, le complexe optiquement pur (*R*)-**41b** ($[\alpha]_D -64,1$, c 0,5, CHCl_3) a été obtenu de façon quantitative (Figure R7).

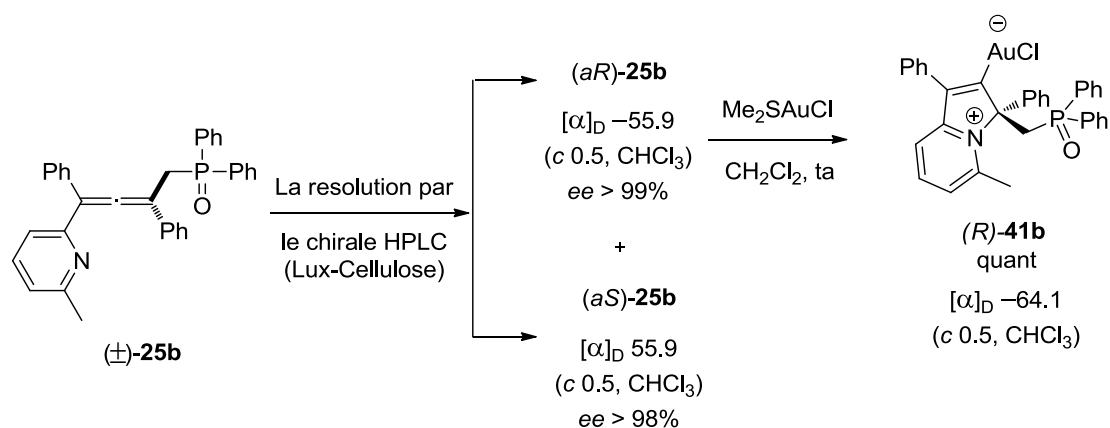


Figure R7. Résolution optique de l'allène racémique $(\pm)\text{-25b}$ par le chirale préparative HPLC et la préparation de complexe d'or $(R)\text{-41b}$.

Il était intéressant de savoir si le complexe d'or $(R)\text{-41b}$ pouvait induire de l'énantiosélectivité. Nous l'avons testé dans la réaction d'hydroalkoxylation du γ -allenol **68** en présence de 3 mol% d'or $(R)\text{-41b}$, et 4,5 mol% d'AgOTs dans du toluène à température ambiante. Cette réaction a conduit à la formation du dérivé tétrahydrofurane **99**, obtenu ici avec un rendement de 58% et un excès énantiomérique encourageant de 38% (Schéma 17). Cette réaction est en cours d'étude afin d'optimiser l'énantiosélectivité.

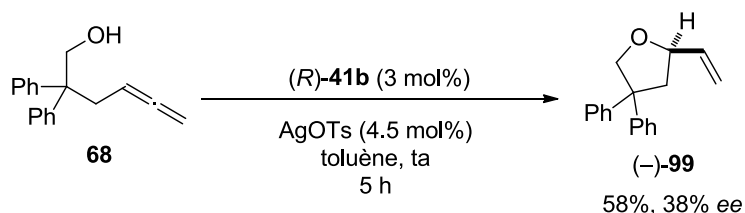
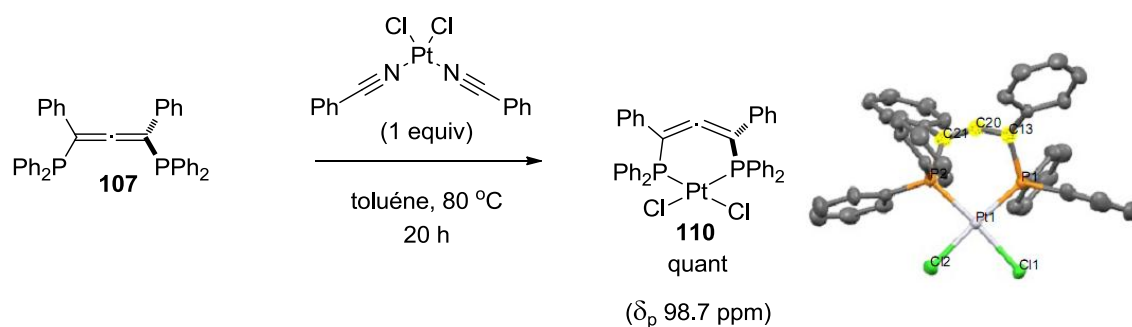


Schéma 17. Cycloisomérisation du γ -allenol **68**.

Le chapitre quatre présente d'une part la synthèse de nouveaux complexes de métaux possédant des ligands diphosphine alléniques, et d'autre part leurs applications en catalyse. La bisphosphine allène **107** a été préparée en se basant sur le travail de Schmidbaur.^[10] Nous avons d'abord examiné sa capacité à se coordiner à différentes espèces métalliques comme le platine(II). Le mélange d'un équivalent de *cis*-bis(benzonitrile)dichloroplatine(II) et d'un équivalent d'allène **107** a permis la formation du complexe mononucléaire de platine allénylique bisphosphine **110** avec un rendement quantitatif (Schéma 18).

Schéma 18. Synthèse du complexe de platine **110**.

La structure de ce complexe a été caractérisée par cristallographie aux rayons X. De façon intéressante la fonction allénique est très pliée et présente un angle de $151,8^\circ$ (liaison C=C=C). Les bent-allène acyclique **A** et cyclique **B** ont été décrits par Weber^[11] et Regitz^[12] avec un angle de courbure du motif C=C=C de $170,1^\circ$ et de $155,8^\circ$. Dans le cas de notre complexe **110** le fait que le motif allénique soit contraint dans un cycle expliquerait la valeur de $151,8^\circ$ qui est presque similaire à celui de l'allène cyclique **B** (Figure R8). Malheureusement, ce complexe **110** n'est pas très stable à l'air et à l'humidité, ce qui limite son champ d'application.

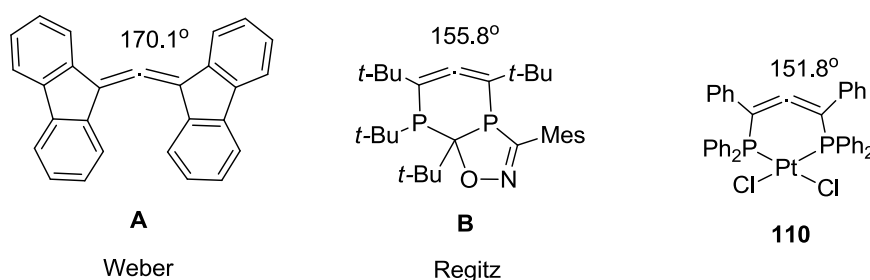
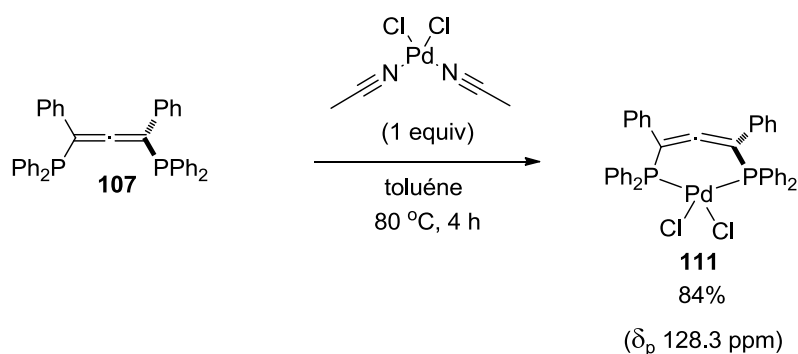
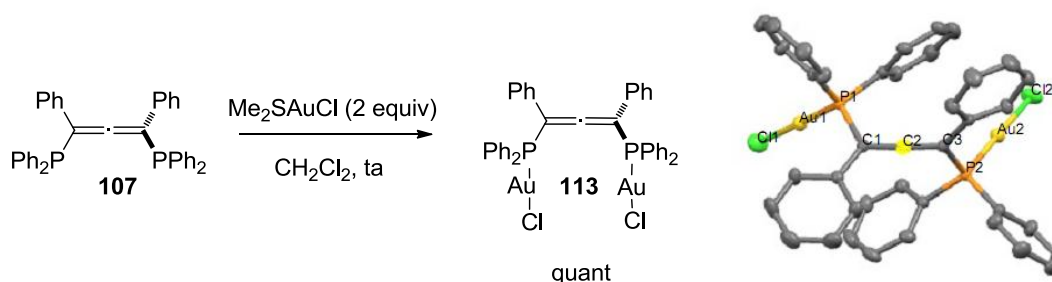


Figure R8. Exemples des bent-allènes.

Nous avons aussi tenté de préparer le complexe de palladium(II). La combinaison d'un équivalent du *cis*-bis(acétonitrile)dichloro(II) et d'un équivalent d'allène **107** a généré le complexe mononucléaire allène diphosphinique de palladium **111** avec un rendement quantitatif (Schéma 19).

Schéma 19. Synthèse du complexe du palladium **111**.

L'allène diphosphinique **107** a été utilisé comme ligand de l'or(I). Dans un premier temps, l'allène **107** a été mis en présence de deux équivalents de Me_2SAuCl . Le complexe bimétallique d'or **113** a été obtenu de manière quantitative. Ce complexe d'or a été caractérisé par cristallographie aux rayons X (Schéma 20).

Schéma 20. Synthèse du complexe d'or-allène **113**.

De façon intéressante le motif allénique reste inchangé. La distance entre les deux atomes d'or étant trop grande, aucune interaction Au-Au n'est observée. Les propriétés électroniques de ce ligand ont été étudiées par formation du dérivé sélénié **109**. La valeur de la constante de couplage $^1J_{P-Se}$, mesurée en RMN ^{31}P , permet de déduire les propriétés électroniques des ligands phosphines.^[13] La valeur de cette constante de couplage dans le composé **109** est de 750 Hz. Par rapport à la valeur mesurée pour $\text{Se}=\text{PPh}_3$, l'allène **107** est davantage π -accepteur. Cependant, sa constante est inférieure à celle de $\text{Se}=\text{P}(\text{PhO})_3$ qui est de 1027 Hz (Figure R9).

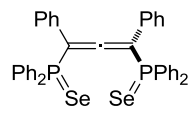
	π -accepteur	σ -donneur
	$\text{Se}=\text{P}(\text{OPh})_3$	$\text{Se}=\text{PPh}_3$
	<	<
	 109	
$J_{31\text{P},77\text{Se}}$ (HZ) dans CDCl_3	1027	736
$\delta_{31\text{P}}$ (ppm)	58.6	35.2

Figure R9. Comparaison des constantes de couplage $^1J_{\text{P-Se}}$ et des déplacements chimiques ^{31}P .

Les propriétés électroniques de **107** ont aussi été contrôlées lors de la réaction du complexe **113** avec le substrat modèle **78**. Un mélange des adduits **96a** et **96b** a été obtenu dans un ratio 80:20. Par comparaison aux résultats obtenus pour la PPh_3 , l'allène **107** est davantage attracteur d'électrons, puisque le ligand PPh_3 fournit le mélange de **96a** et **96b** avec un ratio 67:33, cependant beaucoup moins σ -donneur que IPr (Schéma 21).

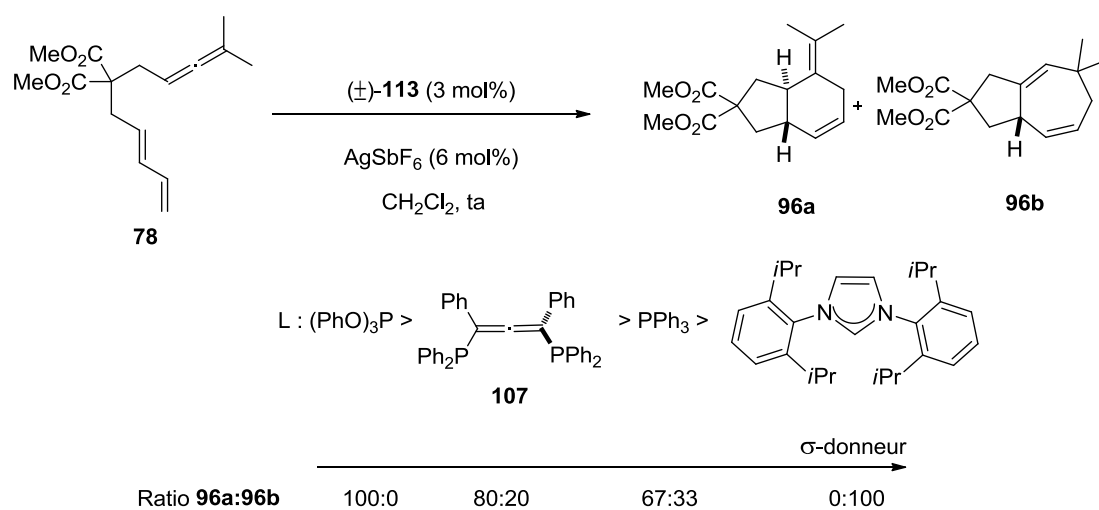


Schéma 21. Evaluation des propriétés électroniques ligands de notre allène **107**

Le complexe d'or (\pm)-**113** a été utilisé comme précatalyseur dans des réactions de cyclisation. Nous avons considéré dans un premier temps l'effet du sel d'argent sur (\pm)-**113**. L'étude a été effectuée par le mélange d'un équivalent d' AgSbF_6 et d'un équivalent de (\pm)-**113**. Le produit obtenu a été caractérisé par spectroscopie de masse qui montre la formation du complexe dinucléaire d'or(I) (\pm)-**114** possédant un chlorure ponté (m/z 989.2) (Schéma 22). Nous avons donc décidé pour notre étude sur la réactivité du complexe (\pm)-**113** de mettre 2 équivalents de sel d'argent afin de casser ce pont chlorure et d'augmenter la réactivité du complexe d'or(I) formé.

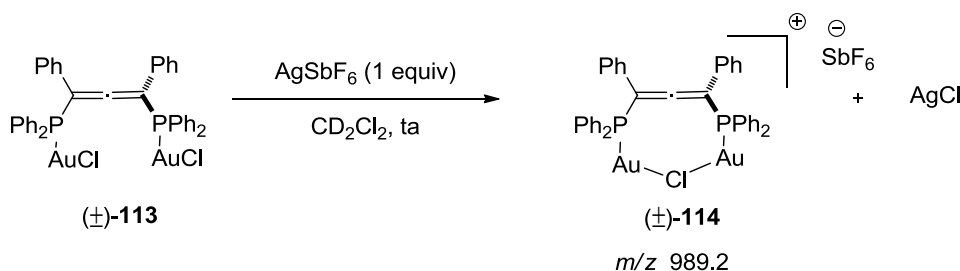


Schéma 22. Formation du complexe dinucléaire d'or(I) (±)-114 possédant un chlorure ponté.

Les réactions de diverses énynes (**49-54** et **57-58**) en présence d'un catalyseur d'or cationique, produit à partir du mélange de 3% en mole du complexe racémique (±)-113 et 6 mol% d'AgSbF₆, ont permis la formation des produits bicycliques **81-86** et **89-90** contenant un motif cyclopropane avec des rendements variant de 60 % à quantitatif (Schéma 23).

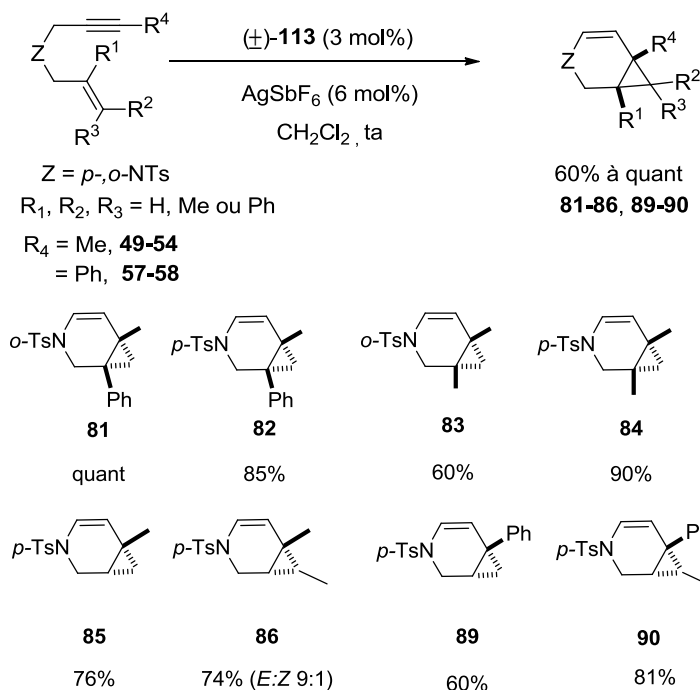


Schéma 23. Cycloisomérisations des énynes.

Dans le cas de l'ényne **59** portant un groupement fonctionnel prényl, la réaction à température ambiante n'a pas permis de générer le produit **92** contenant le motif cyclopropane de façon majoritaire. En effet, dans ces conditions la réaction a donné le produit cyclique **91** avec un rendement de 61%, et seulement des traces du produit **92** initialement attendu. En revanche, lorsque la réaction a été effectuée à une température de 0 °C, le produit **93** a été obtenu majoritairement, avec 79% de rendement contre 11% pour le produit minoritaire **91**. Le produit

92 n'a quant à lui pas été observé (Schéma 24). Nous supposons que le nouveau produit **93** est formé *via* une réaction du type Friedel-Crafts de l'intermédiaire cationique d'or(I).

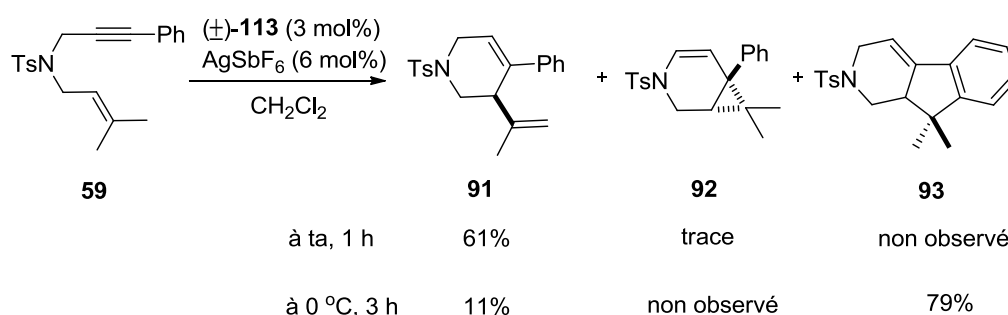


Schéma 24. Cycloisomérisation de l'ényne **59** à différentes températures.

Toujours dans la série des énynes, nous avons également réalisé la cyclisation de l'ényne **65** possédant cette fois-ci une jonction carbonée. Dans ce cas, le produit tricyclique **95** a été formé de manière quantitative, grâce au traitement de l'ényne avec le catalyseur d'or cationique généré à partir de 3 mol% (±)-**113** et 6 mol% d'AgSbF₆ (Schéma 25).

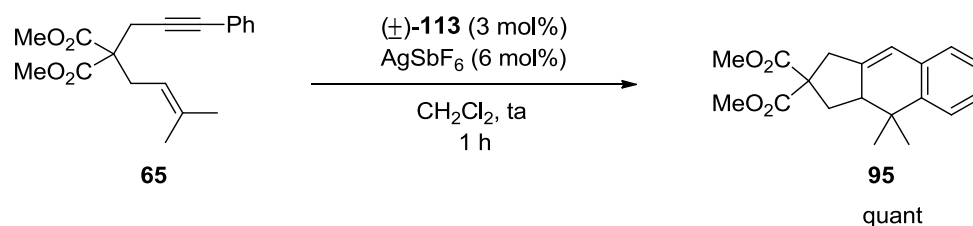


Schéma 25. Cycloisomérisation de l'ényne malonate **65**.

Devant les bon résultats obtenus avec le complexe racémique d'or (±)-**113**, nous avons effectué la résolution optique de **107** par formation d'amine bicyclique de palladium avec le complexe de palladium(II) **120**, suivie d'une recrystallisation pour obtenir les deux diastéréoisomères (*αS,S_oS_c*)-**121a** (43%) et (*αR,S_oS_c*)-**121b** (27%) (configuration déterminée par cristallographie aux rayons X). La décomplexation de chaque énantiomère **121** a été réalisée en présence de cyanure de sodium dans un mélange de dichlorométhane et de l'eau pour donner les allènes optiquement pur (*αS*)- et (*αR*)-**107** (Schéma 26).

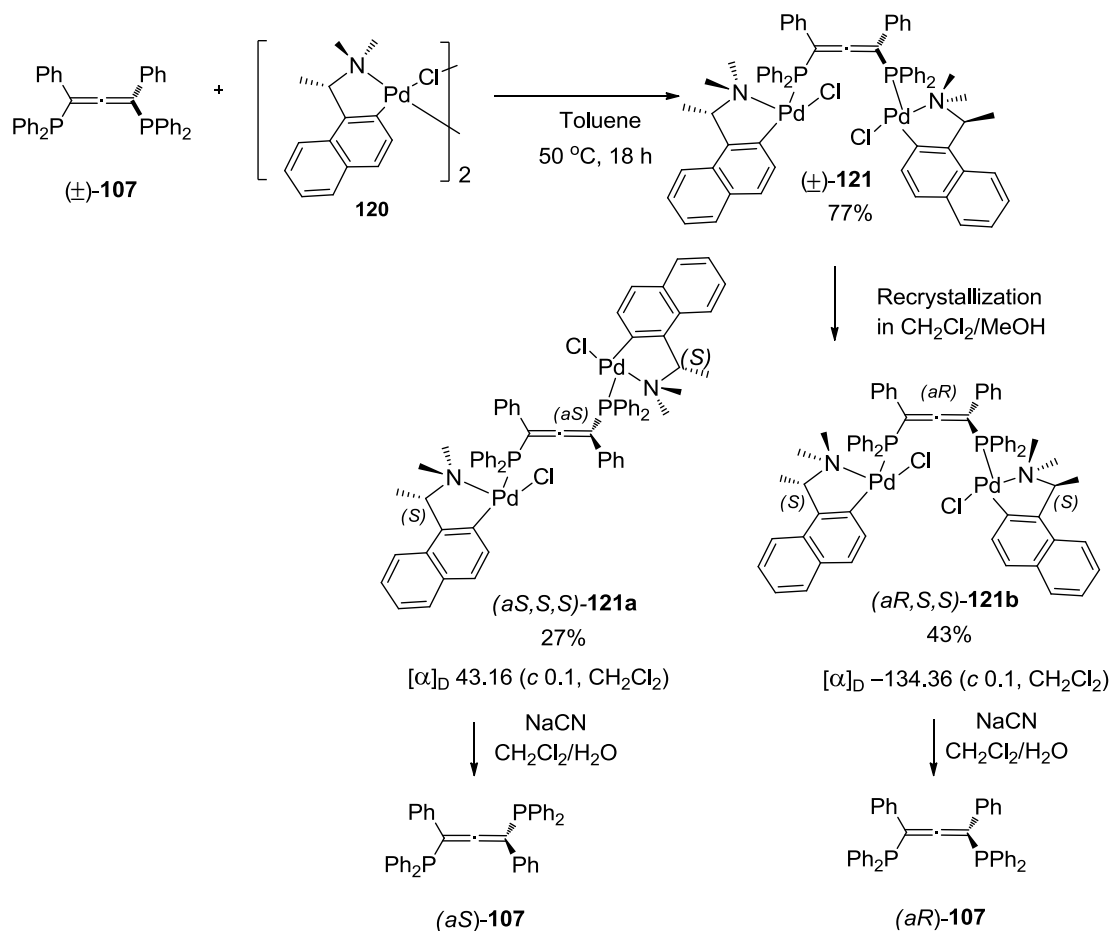


Schéma 26. Résolution optique de l'allène racémique **107** par la séparation des complexes de palladium.

L'allène chiral (*aR*)-**107** a été testé directement en tant que ligand du palladium(0) et le complexe correspondant a été engagé dans une réaction d'allylation entre l'acétate 1,3-diphényl-2-propényl **123** et l'anion diméthylmalonate. Le produit d'allylation **124** a été obtenu avec un rendement de 78% (Schéma 27). La réactivité d'un catalyseur de palladium(II) a été sondée à l'aide de chlorure allylpalladium sans les ligands chiraux, ce qui a montré que le catalyseur est non réactif. L'excès énantiomérique a été analysé en utilisant une technique HPLC chirale. Cette analyse est toujours en cours, en collaboration avec le Dr Nicolas Vanthuyne.

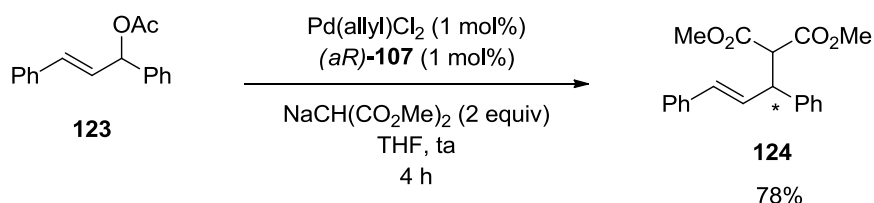


Schéma 27. Alkylation allylique asymétrique de **123** catalysée par le palladium portant le ligand (*aR*)-**107**.

Une autre résolution optique a été réalisée directement sur le complexe d'or **113**. Les énantiomères du complexe (\pm)-**113** ont été séparés avec succès par HPLC préparatif chirale, sur colonne Chiralpak IE dans le mélange d'heptane/2-PrOH/chloroforme (5/2/3) utilisé comme phase mobile. Les deux énantiomères ont été obtenus avec des *ees* > 98%, (*aR*)-**113** ($[\alpha]_D$ 28,2, *c* 0,17, CH₂Cl₂) et (*aS*)-**113** ($[\alpha]_D$ -28,2, *c* 0,17, CH₂Cl₂), la configuration absolue a été déterminée par cristallographie aux rayons X.

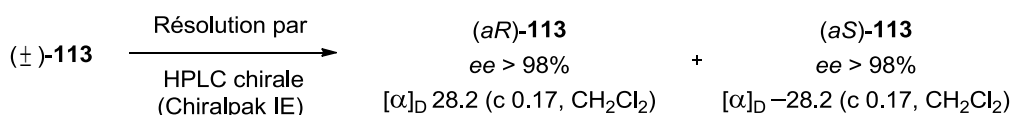


Schéma 28. Résolution optique du complexe d'or (\pm)-**113** par HPLC préparative chirale.

Le complexe (*aR* ou *aS*)-**113** a été engagé dans les mêmes réactions de cycloisomérisations décrites précédemment. Les réactions de cycloisomérisation des composés **49** et **50**, ont permis la formation des produits cycliques **81** et **82** avec des rendements respectifs de 90 et 100%, et des *ees* de 32 et 29% (Schéma 29).

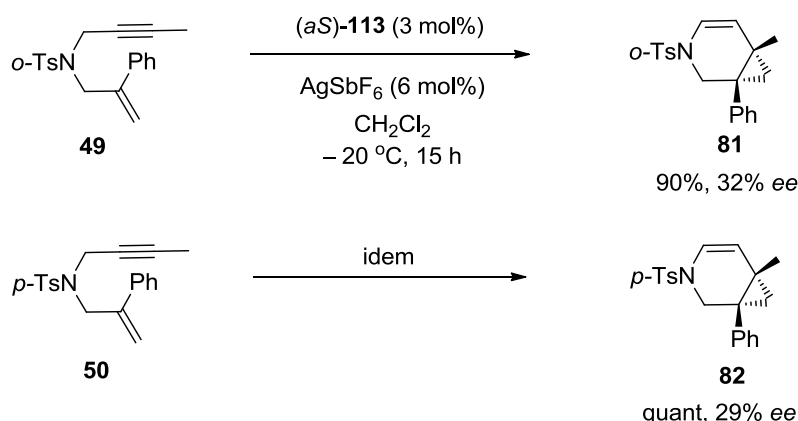
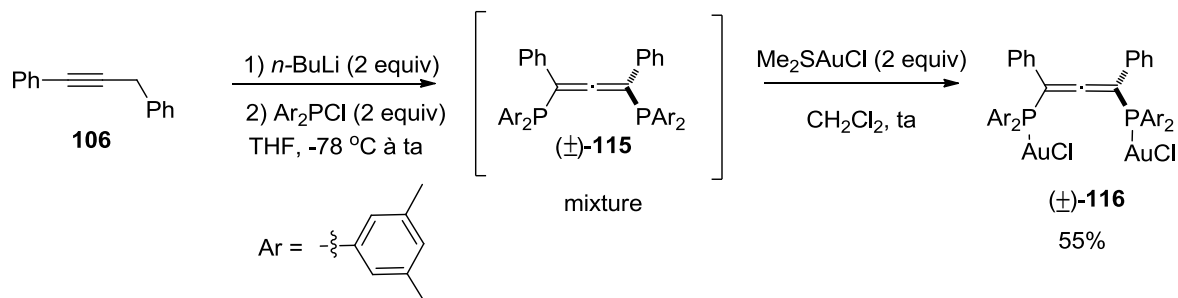


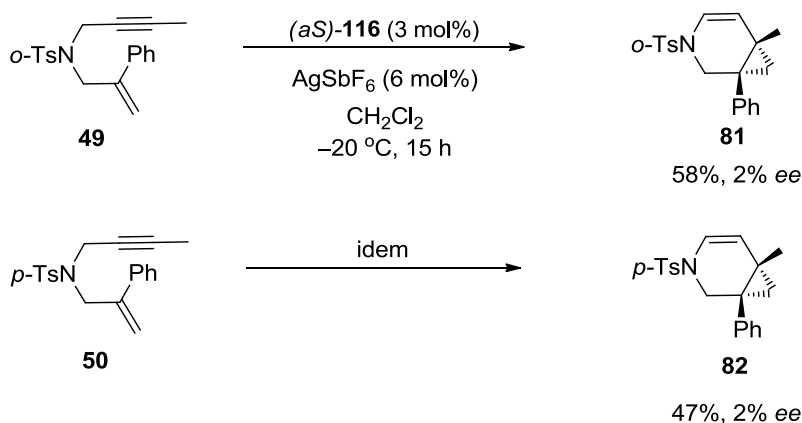
Schéma 29. Cycloisomérisation asymétrique des ényne **49** et **50**.

Afin d'augmenter les *ee* lors des réactions nous avons décidé d'introduire des groupements méthyles sur les aryles portés par le phosphore et de préparer les complexes d'or(I) correspondant. La synthèse de l'allène portant des groupes fonctionnels 3,5-Me₂C₆H₃ a été effectuée suivant le mode opératoire utilisé pour la synthèse de l'allényl bisphosphine **107**. Le traitement de l'alcyne **106** par deux équivalents de *n*-butyllithium, suivie de l'addition deux équivalents de Ar₂PCl (Ar = 3,5-Me₂C₆H₃), a permis d'obtenir un mélange d'allène (\pm)-**115**. Puis l'addition de deux équivalents de Me₂SAuCl a entraîné la formation du complexe d'or racémique

(±)-**116** avec un rendement de 55% (Schéma 30). Les deux énantiomères de ce complexe (*aR*)-**116** et (*aS*)-**116** ont été séparés par HPLC préparative chirale.



Le complexe d'or chiral (*aS*)-**116** a été engagé dans la réaction de cycloisomérisation des composés **49** et **50**. Cependant, les réactions ne donnent que les produits racémiques **81** et **82** (Schéma 31). Pour comprendre ces résultats, il faut se concentrer sur la structure de complexe d'or. On constate que les deux atomes d'or ne semblent pas pouvoir se rapprocher pour favoriser une catalyse plus énantiosélective. La structure de **116** déterminée par cristallographie aux rayons X montre que la distance entre les deux atomes d'or dans **116** ($d(\text{Au-Au})_{116} = 6,875 \text{ \AA}$) est plus long que dans **113** ($d(\text{Au-Au})_{113} = 6,498 \text{ \AA}$) (Figure R10).



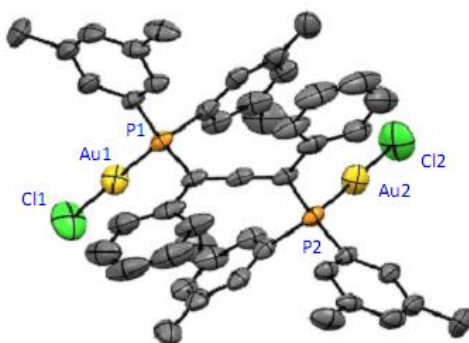


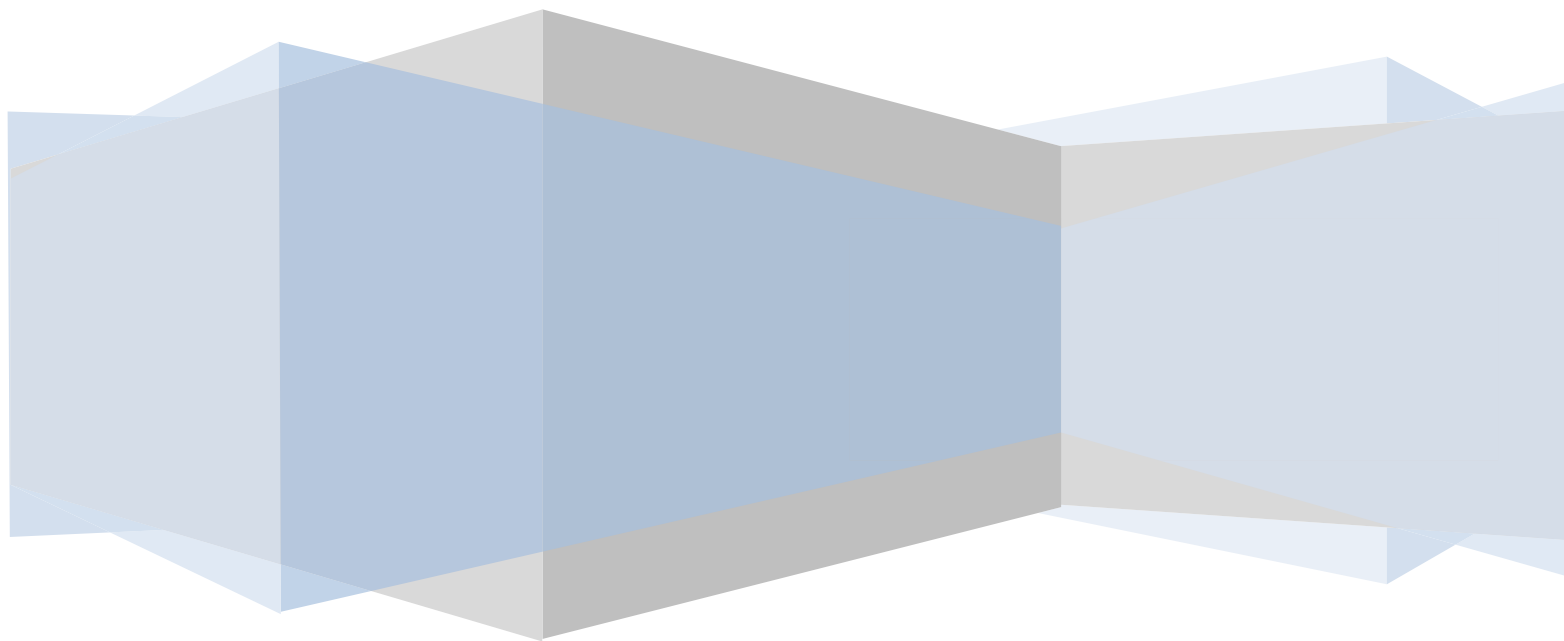
Figure R10. Structure du complexe d'or (±)-116

Pour conclure, quelle sont les perspectives à envisager ? Celles-ci devraient porter sur l'utilisation des deux types de catalyseurs d'or(I)-pyridinyle **41b** et allényle d'or **113** dans le but d'approfondir les connaissances sur leur réactivité en catalyse asymétrique, et d'améliorer l'énantiosélectivité des réactions catalysées par ces complexes.

Références (Résumé)

- [1] S. Löhr, J. Averbeck, M. Schürmann, N. Krause, *Eur. J. Inorg. Chem.* **2008**, 2008, 552–556.
- [2] A. Fürstner, M. Alcarazo, R. Goddard, C. W. Lehmann, *Angew. Chem.* **2008**, 120, 3254–3258.
- [3] E. V. Banide, J. P. Grealis, H. Müller-Bunz, Y. Ortin, M. Casey, C. Mendicute-Fierro, M. Cristina Lagunas, M. J. McGlinchey, *J. Organomet. Chem.* **2008**, 693, 1759–1770.
- [4] T. J. Brown, A. Sugie, M. G. Dickens, R. A. Widenhoefer, *Organometallics* **2010**, 29, 4207–4209.
- [5] F. Cai, X. Pu, X. Qi, V. Lynch, A. Radha, J. M. Ready, *J. Am. Chem. Soc.* **2011**, 133, 18066–18069.
- [6] L. P. Liu, G. B. Hammond, *Chem. Soc. Rev.* **2012**, 41, 3129–3139.
- [7] Y. Chen, D. Wang, J. L. Petersen, N. G. Akhmedov, X. Shi, *Chem. Commun.* **2010**, 46, 6147–6149.
- [8] A. Homs, I. Escofet, A. M. Echavarren, *Org. Lett.* **2013**, 15, 5782–5785.
- [9] F. Schröder, C. Tugny, E. Salanouve, H. Clavier, L. Giordano, D. Moraleda, Y. Gimbert, V. Mouriès-Mansuy, J.-P. Goddard, L. Fensterbank, *Organometallics* **2014**, 33, 4051–4056.
- [10] H. Schmidbaur, C. M. Frazão, G. Reber, G. Müller, *Chem. Ber.* **1989**, 122, 259–263.
- [11] E. Weber, W. Seichter, B. Hess, G. Will, H.-J. Dasting, *J. Phys. Org. Chem.* **1995**, 8, 94–96.
- [12] M. A. Hofmann, U. Bergsträßer, G. J. Reiß, L. Nyulászi, M. Regitz, *Angew. Chem. Int. Ed.* **2000**, 39, 1261–1263.
- [13] D. W. Allen, L. A. March, I. W. Nowell, *J. Chem. Soc. Dalton Trans.* **1984**, 483–485

General Introduction



General Introduction

Organophosphorus derivatives have been used as versatile ligands for various transition metals. The structure of organophosphorus ligand can control the reactivity and selectivity of reactions by their steric and electronic properties. Homogenous gold catalysis has been applied to a formation of C-C bonds. Gold complexes with donating ligands, such as organophosphorus derivatives, have been used as catalysts for building molecular complexity in catalytic reactions. Different types of organophosphorus ligands would help to different modulations of Lewis acidic character and/or electron back donation, and optimize their properties for a given selective transformation.

Since the early 1970s, chiral bisphosphine compounds have played an important role as bidentate ligands for rhodium and ruthenium in hydrogenation reactions. Most of the chiral organophosphorus types bear the chirality on stereogenic carbon or phosphorus atoms. Among latter, C_2 -Symmetric bisphosphines (axial bisphosphines) such as BINAPs and their analogues are widely used as ligands to optimize highly enantioselectivity of catalytic reactions. Recently, gold complexes with axially chiral phosphine ligands have been extended to asymmetric cycloisomerization reactions, which draw our attention to examine and design chiral phosphine ligands for enantioselective products.

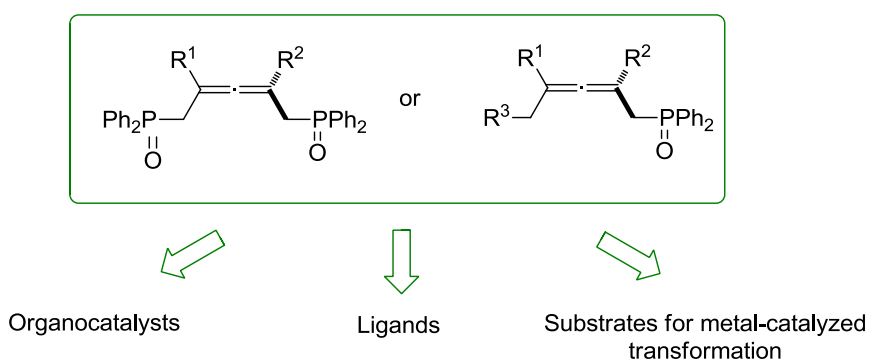
Allene motifs composed of two orthogonal double bonds, forming 1,2-diene-based axial chirality have been use as a ligand for metals. However, only the Ready group disclosed their application in asymmetric catalytic reactions. Thus, this thesis focuses on the invention of new platforms bearing axial chiral information that are new families of phosphine-containing allene ligands for metal catalysis. Our allenes are expected to enhance the stereoselectivity of products in asymmetric catalysis. Furthermore, allenyl phosphine compounds were also experimented as chiral substrates with appropriated nucleophiles for the formation of new organophosphorus-cyclic compounds.

The thesis will be divided in four chapters dealing respectively with the literature backgrounds and our attempts in the synthesis of new allene derivatives and their applications for organometallic catalysis.

The first chapter demonstrates various examples of organophosphorus derivatives as ligands for transition metals and organocatalysts. Particularly, their reactivity towards gold complexes is concerned in various catalytic reactions.

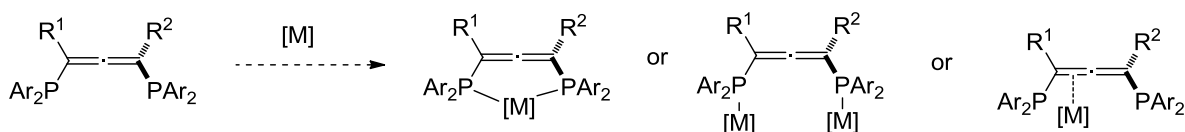
The second chapter describes synthetic methods of allene derivatives to form new allene derivatives. Moreover, their applications as organocatalysts and allenes as ligands for gold(I) complexes are presented.

The third chapter focuses on the synthesis of phosphine oxide-containing allenes and their applications. Allene bearing bisphosphine oxide group are tested to synthesize and applied them as an organocatalyst. Another allene bearing monophosphine moiety are used as ligands from a preparation of new gold(I) complexes. In addition, allenes are engaged in metal-catalyzed reactions for the extended formation of various organophosphorus derivatives (Scheme I1).



Scheme I1. The applications of new allene derivatives.

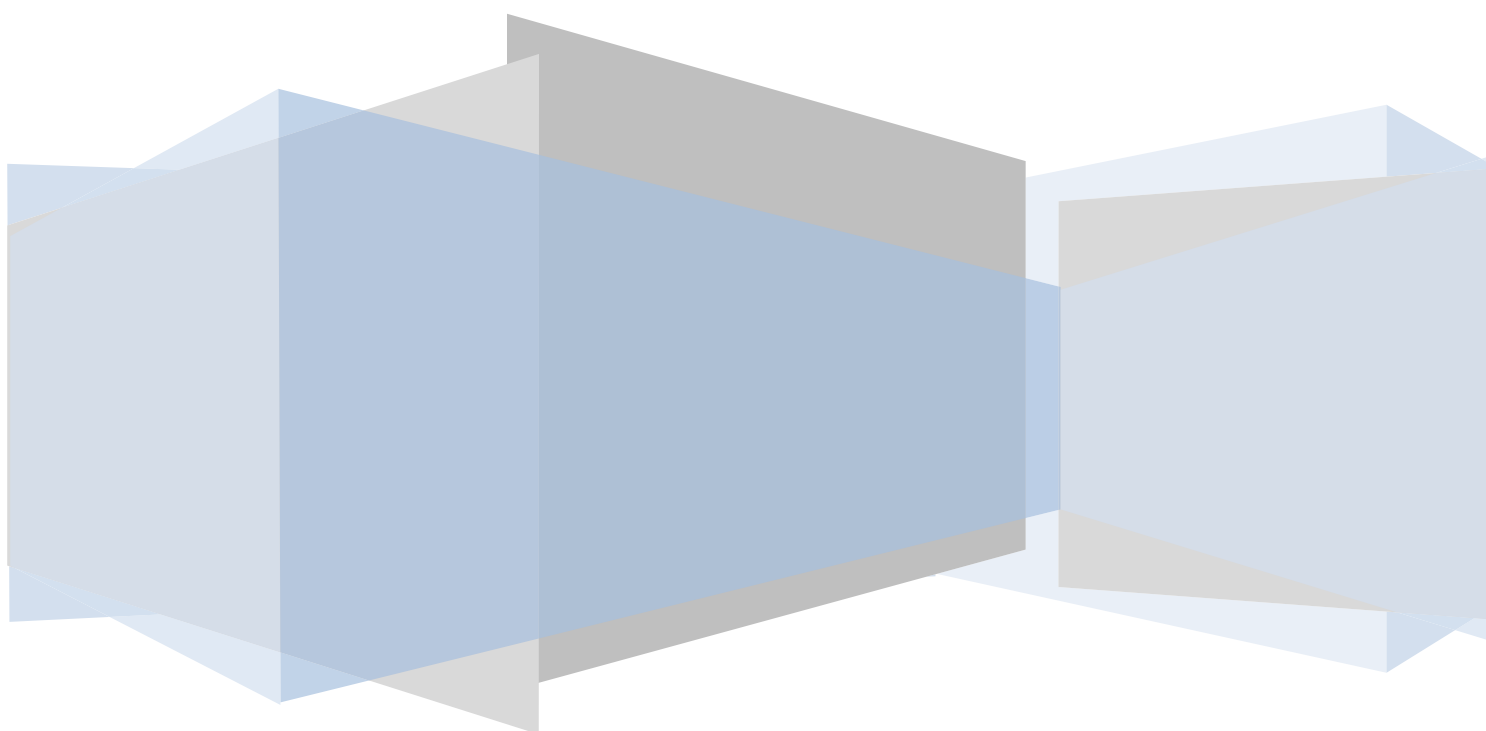
The last chapter presents the extended use of allenyl bisphosphine compounds as ligands for metals and investigated on their reactivity as metal catalysts. The preparation of metal-allenyl phosphine complexes are challenging to isolate the stable complexes. The metal might coordinate to both phosphine groups as mono- and dinuclear metal complexes, or to a π -allene bond (Scheme I2). Moreover, the chiral allene ligands would be concerned for metal to prepare various chiral cyclic products in asymmetric catalysis.



Scheme I2. Possible coordination modes of metal-allenylphosphine complexation.

Chapter 1

Organophosphorus Compounds and Their Applications in Gold Chemistry



CHAPTER 1

Organophosphorus Compounds and Their Applications in Gold Chemistry

1. Introduction

Organophosphorus compounds have been widely used as reagents in organic synthesis, such as in the Wittig and Mitsunobu reactions, and as organocatalysts, among other applications. Also, they represent a variety of interesting compounds for chemical industry and pharmaceutical companies. For example, *PALA* (*N*-Phosphonoacetyl-*L*-aspartic acid) is a potent anticancer drug and *Fosinopril* has antihypertensive activity (Figure 1).¹

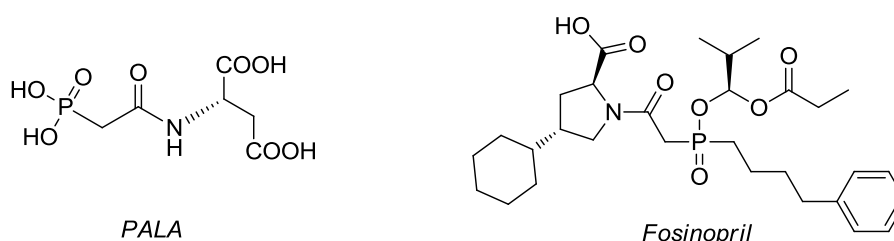


Figure 1. Examples of organophosphorus drugs: *PALA* and *Fosinopril*.

Focusing on catalytic reactions, the utilization of organophosphorus compounds as achiral or chiral ligands for transition metal-catalyzed transformations has emerged rapidly in both industrial production and academic research. (*R*)-PAMP, (*S*)-PHOX, XPhos and BINAP ligands (Figure 2) have been used as ligands of transition metals to prepare various carbo- and heterocyclic compounds for industrial scale in homogeneous catalysis.²

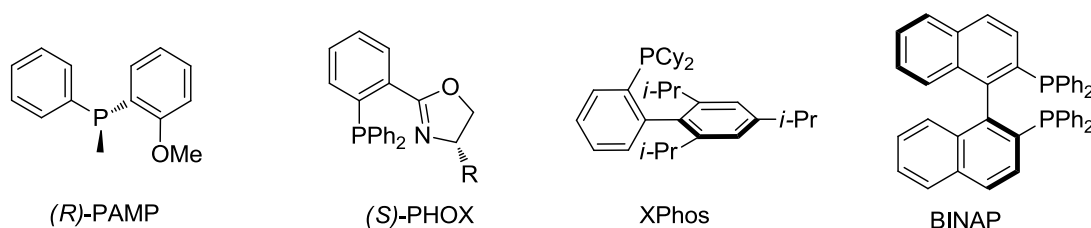
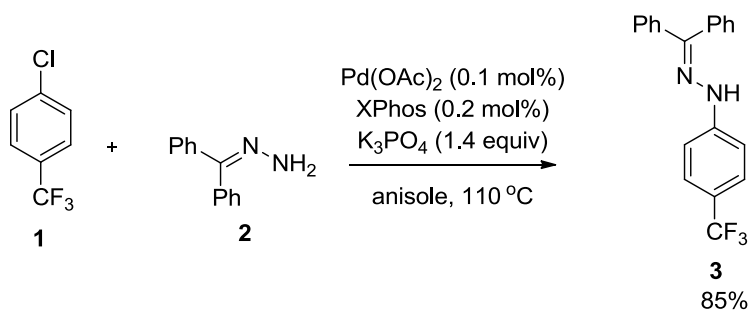


Figure 2. Examples of organophosphorus ligands for industrially relevant homogenous catalysis.

¹ L. D. Quin, *A Guide to Organophosphorus Chemistry*, Wiley, New York, N.Y., **2000** (Chapter 11).

² Y. Li, S. Das, S. Zhou, K. Junge, M. Beller, *J. Am. Chem. Soc.* **2012**, *134*, 9727–9732.

As a corresponding research, XPhos was used as a ligand by Mauger and Mignani for a palladium catalyst in a preparation of hydrazones on large scale.³ For example, the coupling reaction of *p*-chlorotrifluoromethylbenzene (**1**) and benzophenone hydrazone (**2**) in the presence of the palladium catalyst bearing this ligand afforded hydrazone **3** in a good yield (85%) (Scheme 1).



Scheme 1. Synthesis of *p*-trifluoromethyl phenylbenzophenone hydrazone (**3**).

To date, transition metal catalysis has emerged as a powerful tool for the formation of products in one-step process and atom-economic reactions. Not only palladium, but also gold catalysis draws our attention in term of mild synthetic conditions, clean reactions, and short time of reactions. The ligands of metals are significant candidates to afford regioselective or enantioselective products. In this chapter, different types of organophosphorus ligands and their catalytic applications, in particular gold catalytic reactions, will be introduced. Moreover, the formation of gold salts and organophosphine ligands will also be considered to provide stable gold complexes and further applied in catalysis.

2. Organophosphorus chemistry

Organophosphorus compounds contain carbon-phosphorus bonds (P-C) as in triphenylphosphine, for instance. The π -accepting property on the phosphorus atom can be modified *via* replacement of the P-C bonds with P-heteroatom bonds such as P-O and P-N bonds. These changes lead to various types of organophosphorus compounds as shown in Figure 3. Nevertheless, phosphines are the most encountered ligands in organometallic catalysis. In this section, we will discuss the properties of phosphines and their analogues, and the uses of organophosphorus as ligands of metals in several catalytic reactions. In addition, organophosphorus oxides will be presented as catalysts in asymmetric organocatalysis.

³ C. Mauger, G. Mignani, *Adv. Synth. Catal.* **2005**, *347*, 773–782.

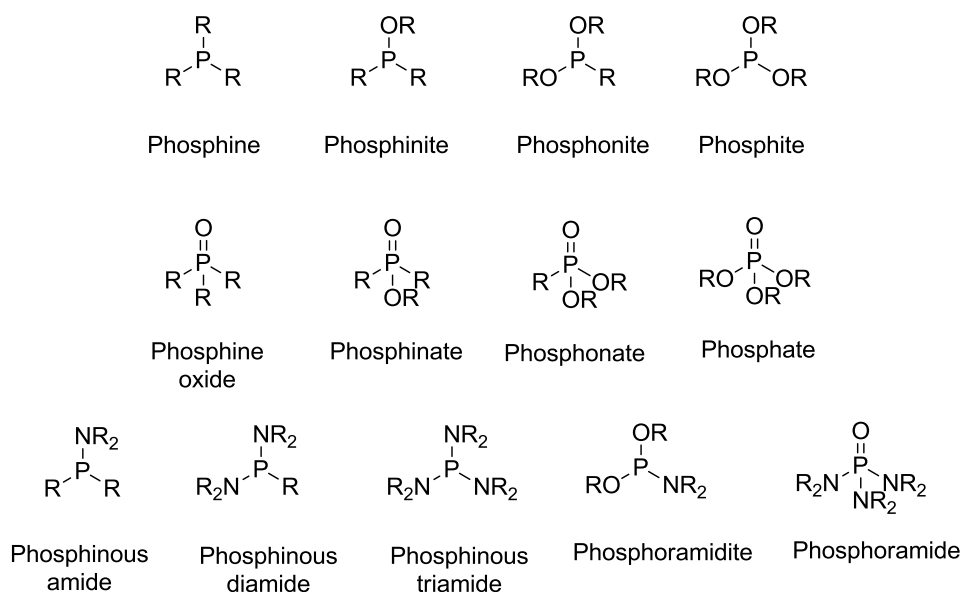


Figure 3. Examples of organophosphorus compounds.

2.1. Phosphine ligands and analogues

Phosphine compounds are excellent soft-donor ligands. A phosphorus atom selectively coordinates to the metal center forming transition metal-phosphorus coordination. The lone pair of electrons from the phosphorus atom donates to the metal atom (σ -donation), while the lone pair of electrons from the d -orbitals of the metal donates (π -back donation) to an empty d -orbital of the phosphorus to make a complex (Figure 4).⁴

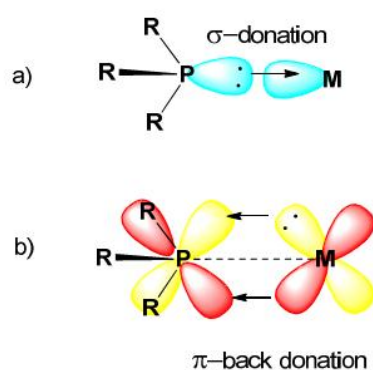


Figure 4. Metal (M)-Phosphorus (P) bonding interactions in metal-phosphine complex: (a) P to M σ -donation, (b) M to P π -back-donation by d_{π} - d_{π} overlap (Figure reproduced from reference 4)

⁴ A. G. Orpen, N. G. Connelly, *Organometallics* **1990**, 9, 1206–1210.

R group with strong electronegativity, or bulky group attached on phosphorus atom play a significant role in the reactivity of the metal complexes to promote selectivity of reactions. In addition, the phosphorus ligands are able to bind to a metal in a number of different coordination modes such as monodentate, bidentate, or polydentate (Figure 5).⁵

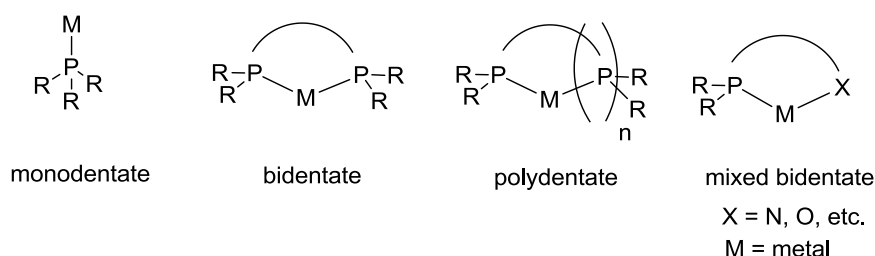


Figure 5. Organophosphorus ligands classified by coordination modes with metal (M = metal).

2.1.1. Historical overview

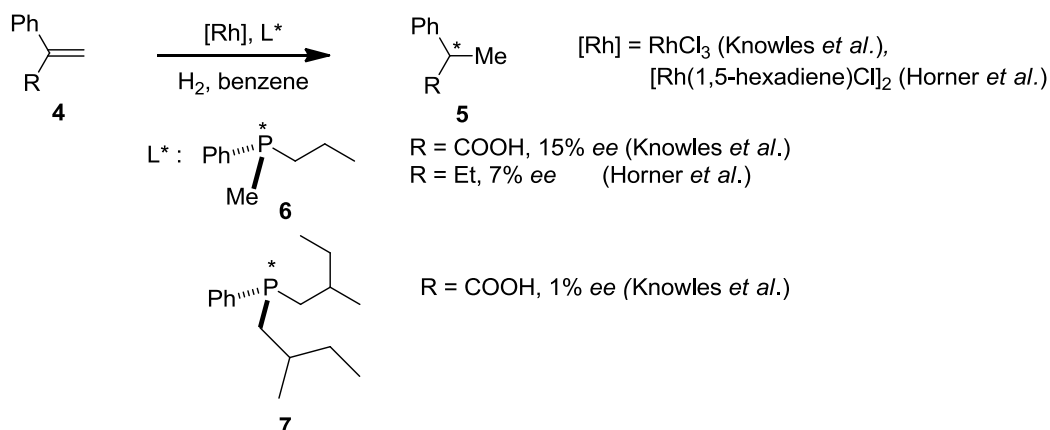
Triphenylphosphine (PPh_3) is a monodentate ligand of transition metals such as palladium, nickel, rhodium, and ruthenium that has proved for some time now to be useful in various organic transformations, due to its nucleophilicity and reductive properties. In 1966, the Wilkinson group was the first to study the hydrogenation reaction of olefins using a rhodium chloro[bis(triphenylphosphine)] complex $[\text{RhCl}(\text{PPh}_3)_3]$ as a catalyst to give achiral or racemic products.⁶ Because significant chiral compounds have been used in pharmaceutical or industrial process, the demand to synthesize enantioenriched products was increased. Optically pure phosphine derivatives combined with metal catalysts can produce enantiopure compounds from achiral precursors in asymmetric catalysis. Pioneering studies by Knowles⁷ and Horner⁸ showed that using optically *P*-stereogenic phosphines such as **6** and **7** (Scheme 2) instead of the achiral triphenylphosphine ligands could provide stereoselective compounds. The chiral rhodium catalysts were tested in the hydrogenation of alkene **4**. However, these ligands **6**, and **7** bearing alkyl moieties could not promote satisfactory enantioselectivity of the reaction, giving the product **5** with low *ees*.

⁵ H. Fernández-Pérez, P. Etayo, A. Panossian, A. Vidal-Ferran, *Chem. Rev.* **2011**, *111*, 2119–2176.

⁶ J. A. Osborn, F. H. Jardine, J. F. Young, G. J. Wilkinson, *J. Chem. Soc. (A)* **1966**, 1711–1732.

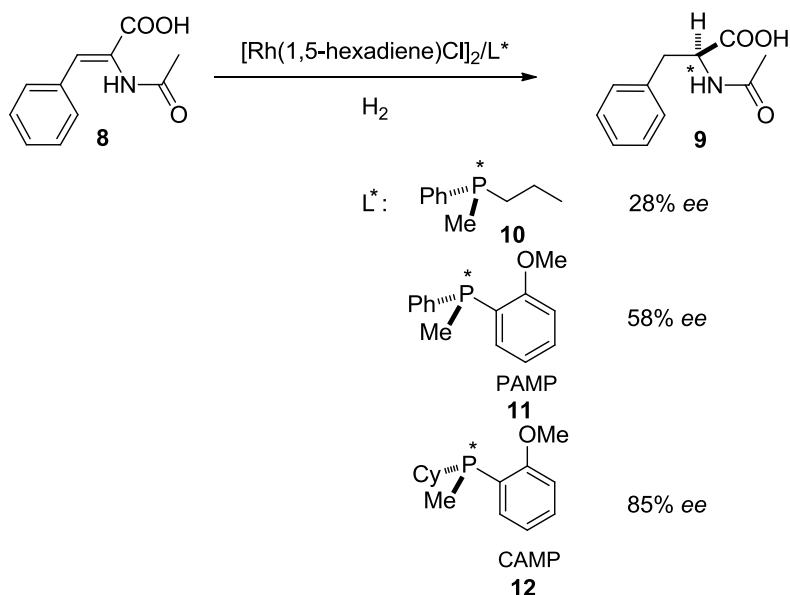
⁷ W. S. Knowles, M. J. Sabacky, *Chem. Commun. Lond.* **1968**, 1445–1446.

⁸ L. Horner, H. Siegel, H. Büthe, *Angew. Chem. Int. Ed. Engl.* **1968**, *7*, 942.



Scheme 2. Enantioselective hydrogenation reactions of alkene 4.

Continuing the study of enantioselective reactions, Knowles was interested in the synthesis (*S*)-L-DOPA, which is used to treat Parkinson's disease, by using *P*-stereogenic ligands.⁹ Initially, he tested the simple phenylalanine derivatives as 2- α -acetamidocinnamic acid (**8**) to study the reactivity of chiral ligands in hydrogenation reactions. The reactions of **8** in the presence of rhodium complexes bearing different chiral phosphines (**10-12**) were screened (Scheme 3). The reaction of **8** with the rhodium catalyst bearing CAMP (**12**) ligand with an *o*-anisyl group afforded product **9** with quite good enantioselectivity (85% ee).¹⁰ These examples show that the *P*-stereogenic ligands, in particular ligand **12** brings the chiral environment close enough to the metal, where the catalytic process takes place.



Scheme 3. Asymmetric hydrogenation of 8.

⁹ W. S. Knowles, *Angew. Chem. Int. Ed.* **2002**, 41, 1998–2007, *Adv. Synth. Catal.* **2003**, 345, 3–13.

¹⁰ W. S. Knowles, M. J. Sabacky and B. D. Vineyard, *J. Chem. Soc., Chem. Commun.* **1972**, 10–11.

Later, two major breakthroughs were made in the asymmetric hydrogenation by Kagan and Knowles who introduced bisphosphines (Figure 6) as a new type of chiral phosphine ligands in asymmetric catalysis. In 1971, Kagan presented the use of the chelating C_2 -diphosphine DIOP (**13**) bearing chirality on the carbon backbone.¹¹ In the same line, Knowles disclosed (*R,R*)-DIPAMP (**14**) as a *P*-stereogenic ligand for use in asymmetric hydrogenation reactions in 1975.¹² Under a similar test with amino acid **8** of Scheme 3, the rhodium bearing ligand **14** catalyzed the hydrogenation reaction and afforded higher enantioselectivity (96% *ee*) than using ligands **12** (85% *ee*) and **13** (83% *ee*). Consequently, the ligand **14** of rhodium complex was then applied for the preparation of (*S*)-L-DOPA (Scheme 4).¹³ The reaction of **15** as a precursor of **17** gave the L-isomer amino derivative **16** in 95% *ee*. Following acidic treatment **17** was obtained with 95% *ee*.

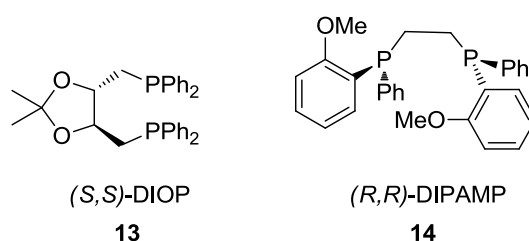
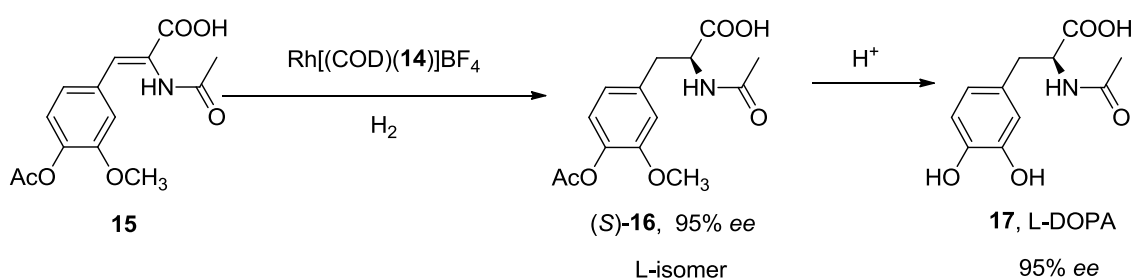


Figure 6. (*S,S*)-DIOP (**13**) and (*R,R*)-DIPAMP (**14**).



Scheme 4. Synthesis of L-DOPA (**17**) using rhodium complex bearing ligand **14**.

Subsequent to these works, other successful chiral phosphorous ligands were developed which extended the scope of reactions to afford various essential chiral products, as exemplified by ferrocene (**18**),¹⁴ BPPM (**19**),¹⁵ CHIRAPHOS (**20**)¹⁶ and PROPHOS (**21**)¹⁷ ligands (Figure 7).

¹¹ T. Dang and H. B. Kagan, *J. Chem. Soc., Chem. Commun.* **1971**, 481.; H. B. Kagan and T. Dang, *J. Am. Chem. Soc.* **1972**, *94*, 6429–6433.

¹² W. S. Knowles, M. J. Sabacky, B. D. Vineyard and D. J. Weinkauff, *J. Am. Chem. Soc.* **1975**, *97*, 2567–2568.

¹³ W. S. Knowles, *Angew. Chem. Int. Ed.* **2002**, *41*, 1998–2007, *Adv. Synth. Catal.* **2003**, *345*, 3–13.

¹⁴ T. Hayashi, T. Mise, M. Kumada, *Tetrahedron Lett.* **1979**, 425–428.

¹⁵ K. Achiwa, *J. Am. Chem. Soc.* **1976**, *98*, 8265–8266.

¹⁶ M. D. Fryzuk, B. Bosnich, *J. Am. Chem. Soc.* **1977**, *99*, 6262–6267.

¹⁷ M. D. Fryzuk, B. Bosnich, *J. Am. Chem. Soc.* **1978**, *100*, 5491–5494.

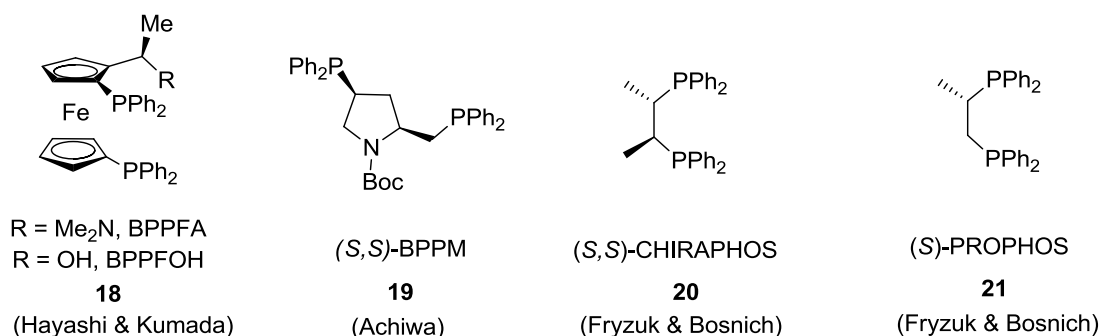
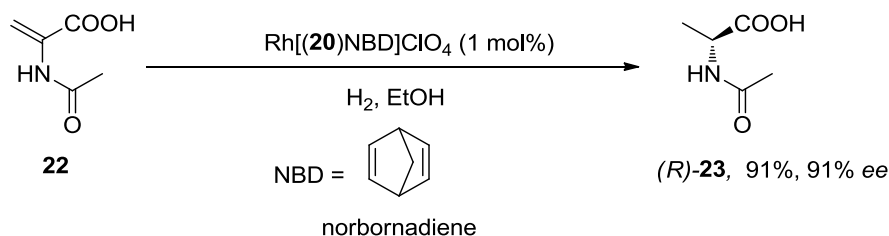


Figure 7. Example of phosphine ligands (18-21)

As an example of these ligands in hydrogenation reactions, the efficiency of using the rhodium complex bearing ligand **20** as a catalyst in the reaction of ketone **22**, gave (*R*)-alanine **23** with excellent enantioselectivity (91% *ee*) (Scheme 5).

Scheme 5. Synthesis of (*R*)-alanine (**23**) in the presence of Rh[(**20**)NBD]ClO₄ catalyst.

The 1980s carried an advance of catalytic synthesis. Particularly significant was the synthesis of the bidentate phosphine ligand, BINAP (**24**, **25**) by the Noyori group (Figure 8), which has been one of the most successful ligands in asymmetric catalysis.¹⁸ The stereogenicity of BINAP and its analogues arises from the stereogenic axis, which is due to restricted rotation along the ligand backbone. This phenomenon is called atropisomerism and refers to axial chirality. Optically pure BINAPs have been used as bidentate ligands for transition metals such as ruthenium, rhodium, and palladium.^{19, 20} For example, RuCl₂(**25**) was an excellent chiral catalyst in asymmetric hydrogenation reaction of methyl-3-oxobutanoate (**26**), giving an enantiomerically pure product **27** in 96% yield and >99% *ee* (Scheme 6).²¹

¹⁸ (a) A. Miyashita, A. Yasuda, H. Takaya, K. Toriumi, T. Ito, T. Souchi, R. Noyori, *J. Am. Chem. Soc.* **1980**, *102*, 7932–7934.; (b) A. Miyashita, H. Takaya, T. Souchi, R. Noyori, *Tetrahedron* **1984**, *40*, 1245–1253.

¹⁹ For some reviews, see: (a) M. Lin, G. Y. Kang, Y. A. Guo, Z. X. Yu, *J. Am. Chem. Soc.* **2012**, *134*, 398–405.; (b) I. J. S. Fairlamb, *Angew. Chem. Int. Ed.* **2004**, *43*, 1048–1052.

²⁰ W. Fang, H. Zhu, Q. Deng, S. Liu, X. Liu, Y. Shen, T. Tu, *Synthesis* **2014**, *46*, 1689–1708

²¹ R. Noyori, T. Ohkuma, M. Kitamura, H. Takaya, N. Sayo, H. Kumobayashi, S. Akutagawa, *J. Am. Chem. Soc.* **1987**, *109*, 5856–5858.

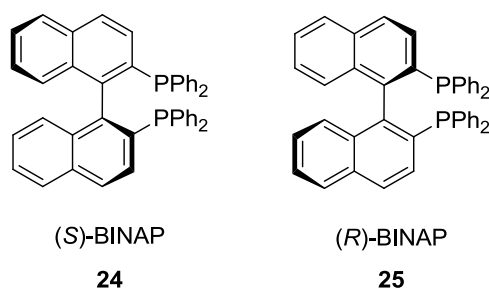
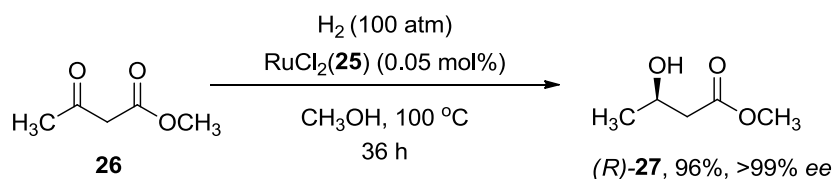


Figure 8. (S)-, (R)-BINAP (24, 25).

Scheme 6. Asymmetric hydrogenation reaction of 26 by $\text{RuCl}_2(\mathbf{25})$.

As another important breakthrough, biaryl monophosphine ligands **28** were synthesized by Buchwald and co-workers in 1988 (Figure 9).²² Bulky and electron-rich mono[dialkyl(biaryl)-phosphines] with different R and R' functional groups have been widely used in a large number of metal-catalyzed C-C, C-N, and C-O bond formation reactions. In palladium coupling reactions, the electronic and steric characteristics of the ligands **28** are favorable for accelerating the rates of the oxidative addition, transmetalation, and reductive elimination steps in the catalytic cycle.²⁰

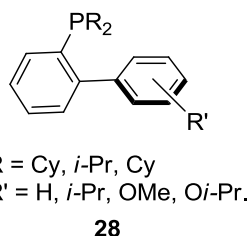


Figure 9. Mono[dialkyl(biaryl)phosphine] ligands (28).

To extend the variety of ligands in asymmetric hydrogenation reactions, chiral bisphosphine ligands have been developed for optimizing the enantioselectivity. For example, DUPHOS (**29**) and BPE (**30**) (Figure 10) were used in the enantioselective hydrogenation of α -(acylamino)acrylic acids, enamides, enol acetates, β -keto esters, unsaturated carboxylic acids, and itaconic acids.²³ In addition, the Mathey group prepared *P*-chiral bisphosphane ligand, BIPNOR

²² D. W. Old, J. P. Wolfe, S. L. Buchwald, *J. Am. Chem. Soc.* **1998**, 120, 9722–9723.

²³ (a) W.A. Nugent, T. V. RajanBabu, M.J. Burk, *Science* **1993**, 259, 479–483.; (b) M.J. Burk, *Acc. Chem. Res.* **2000**, 33, 363–372.

(**31**) which was effective in the enantioselective hydrogenation of α -(acetamido)cinnamic acids and itaconic acids.²⁴

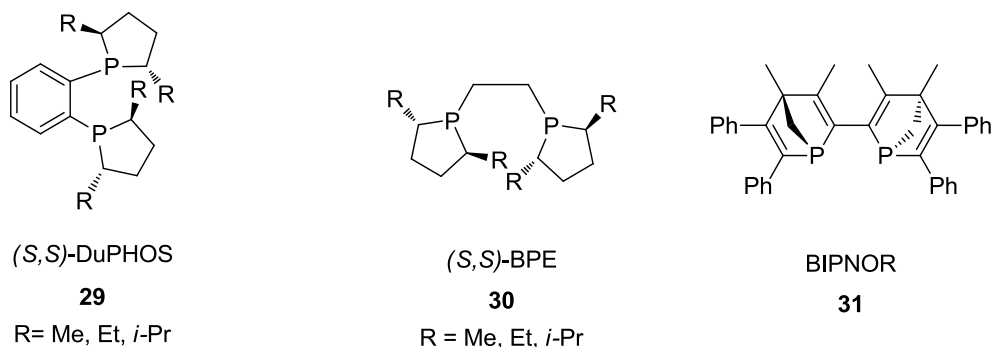


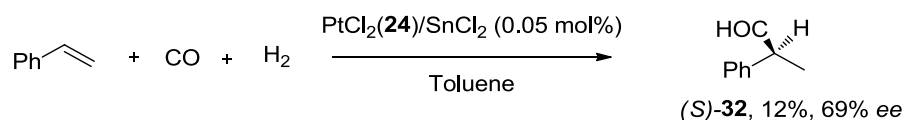
Figure 10. (*S,S*)-DUPHOS (**29**), (*S,S*)-BPE (**30**) and BINOP (**31**).

To date, axially chiral ligands are commonly selected in enantioselective metal-catalyzed asymmetric reactions, in particular axially chiral BINAPs and analogues. Our research aimed to design new axially chiral ligands in order to broaden the family of available ligands and investigate on their reactivity and selectivity in asymmetric reactions.

2.1.2. Phosphine ligands in asymmetric catalysis

Axially chiral ligands have been used in combination with transition metals to induce stereoselectivity of the desired products. In this section, we focus on some interesting examples using axially chiral ligands such as BINAPs (**24**, **25**) and their analogues in different types of asymmetric reactions.

Apart from asymmetric hydrogenation reactions, enantioselective hydroformylation reactions have been developed by the Kollár group.²⁵ They were the first to apply **24** as a ligand for PtCl₂ in the presence of SnCl₂ for hydroformylation reaction of styrene. The aldehyde **32** was obtained with high enantioselectivity (69% *ee*) (Scheme 7).

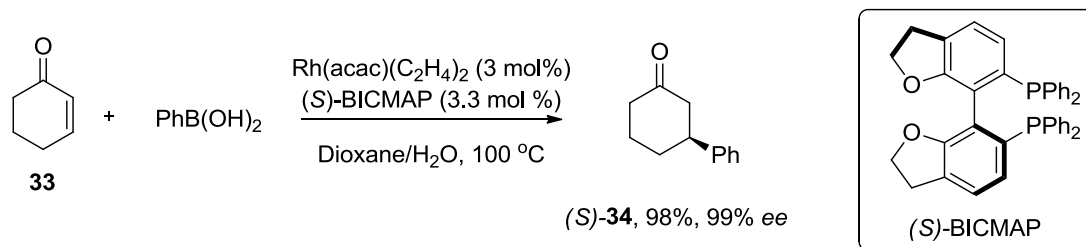


Scheme 7. Hydroformylation reaction of styrene.

²⁴ (a) F. Robin, F. Mercier, L. Ricard, F. Mathey, M. Spagnol, *Chem. Eur. J.* **1997**, *3*, 1365–1369.; (b) F. Mathey, F. Mercier, F. Robin, L. Ricard, *J. Organomet. Chem.* **1998**, *577*, 117–120.

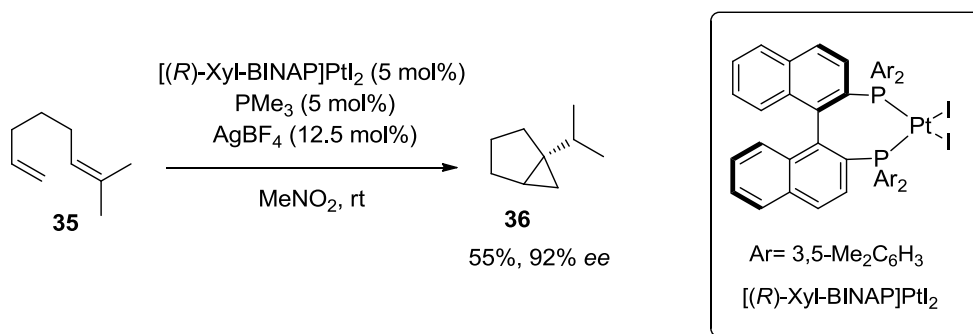
²⁵ L. Kollár, P. Sándor, G. Szalontai, *J. Mol. Catal.* **1991**, *67*, 191–198

Chiral cyclic enones can also be obtained from the rhodium(I)-catalyzed 1,4-addition of aryl- and alkenylboronic acids.²⁶ (*S*)-BICMAP was also used as a ligand for rhodium. The species formed catalyzed the formation (*S*)-3-phenylcyclohexanone (**34**) from ketone **33** in excellent yield and *ee* (Scheme 8).



Scheme 8. Asymmetric 1,4-addition reaction of ketone **33** with phenylboronic acid.

Asymmetric intramolecular cycloisomerization reactions have been devised. For example, platinum catalysts bearing axially chiral ligands have been used in this manner, as reported by Gagné.²⁷ The optically pure (*R*)-Xyl-BINAP ligand is first complexed with platinum(II) diiodide. In the presence of PMe_3 , [(*R*)-Xyl-BINAP] PtI_2 reacted with AgBF_4 to generate a cationic platinum (II) complex, [(*R*)-Xyl-BINAP] PtPMe_3^{2+} . This complex catalyzed the cycloisomerization reaction of diene **35** to provide bicyclic product **36** in 55% yield with excellent enantioselectivity (92% *ee*) (Scheme 9).



Scheme 9. Cycloisomerization of diene **35** in the presence of platinum(II) catalyst.

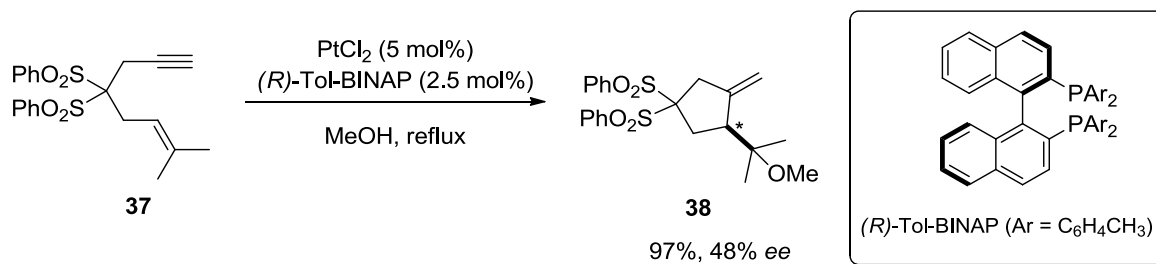
The scope of carbocyclic syntheses has also been extended. For example, platinum(II) complexed with chiral bidentate phosphine ligands^{28, 29} such as Tol-BINAP, were employed in asymmetric alkoxy cyclization reactions. The cationic platinum(II) complex, generated *in-situ* from

²⁶ T. Mino, M. Hashimoto, K. Uehara, Y. Naruse, S. Kobayashi, M. Sakamoto, T. Fujita, *Tetrahedron Lett.* **2012**, 53, 4562–4564.

²⁷ J. A. Feducia, A. N. Campbell, M. Q. Doherty, M. R. Gagné, *J. Am. Chem. Soc.* **2006**, 128, 13290–13297.

²⁸ L. Charruault, V. Michelet, R. Taras, S. Gladiali, J. P. Genêt, *Chem. Commun.* **2004**, 850–851

PtCl₂ and (*R*)-Tol-BINAP ligand, reacted with enyne **37** in MeOH to afford the cyclic product **38** in excellent yield and moderate enantioselectivity (48% *ee*) (Scheme 10).²⁹

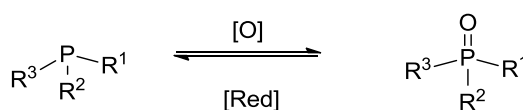


Scheme 10. Enantioselective alkoxyacyclization of enyne **37**.

As presented several examples of catalytic reactions, axially chiral organophosphorus ligands are continuing to be modified for specific selective reactions to reach enantioselective products with high *ee*. These reactions are documented to further investigate the reactivity and selectivity of our chiral phosphine ligands for metal catalysis.

2.2. Phosphine oxide derivatives

Oxidized organophosphorus compounds are also interesting compounds for asymmetric reactions. Phosphine oxides have been synthesized from the oxidation of free phosphine compounds. The most typical reagents used are peroxy reagents such as H₂O₂, *t*-BuOOH and *m*-CPBA, which can deliver the phosphine oxide quantitatively and stereoselectivity, giving retention of configuration at the phosphorus atom.³⁰ Moreover, air can be an oxidant, but often leads to impure products.³¹ In addition, reducing agents such as HSiCl₃ can reduce the phosphine oxide back to the free phosphine precursor with retention of configuration (Scheme 11).³²



Scheme 11. Interconversion between phosphines and phosphine oxides

²⁹ M. P. Muñoz, J. Adrio, J. C. Carretero, A. M. Echavarren, *Organometallics* **2005**, *24*, 1293–1300.

³⁰ (a) L. Horner, *Pure Appl. Chem.* **1964**, *9*, 225–244.; (b) D. B. Denney and J. W. Hanifin, *Tetrahedron Lett.*, **1963**, *4*, 2177–2180.; (c) Y. Hamada, F. Maturuta, M. Oku, K. Hatano and T. Shiori, *Tetrahedron Lett.* **1997**, *38*, 8961–8964.; (d) S. Matsukawa, H. Sugama and T. Imamoto, *Tetrahedron Lett.* **2000**, *41*, 6461–6465.

³¹ K. M. Pietrusiewicz and M. Zablocka, *Chem. Rev.* **1994**, *94*, 1375–1411.

³² L. Horner and W. D. Balzer, *Tetrahedron Lett.*, **1965**, *6*, 1157–1162.

The first optically pure phosphine oxide, ethylmethylphenylphosphine oxide (**39**) was synthesized originally by Meisenheimer and Lichtenstadt in 1911.³³ Fifteen years later, they also prepared and optically resolved the enantioenriched benzylmethylphenylphosphine oxide (**40**) (Figure 11).³⁴

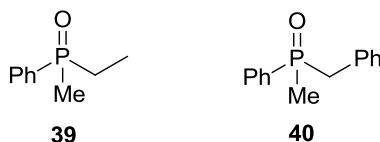


Figure 11. Ethylmethylphenylphosphine oxide (**39**) and benzylmethylphenylphosphine oxide (**40**).

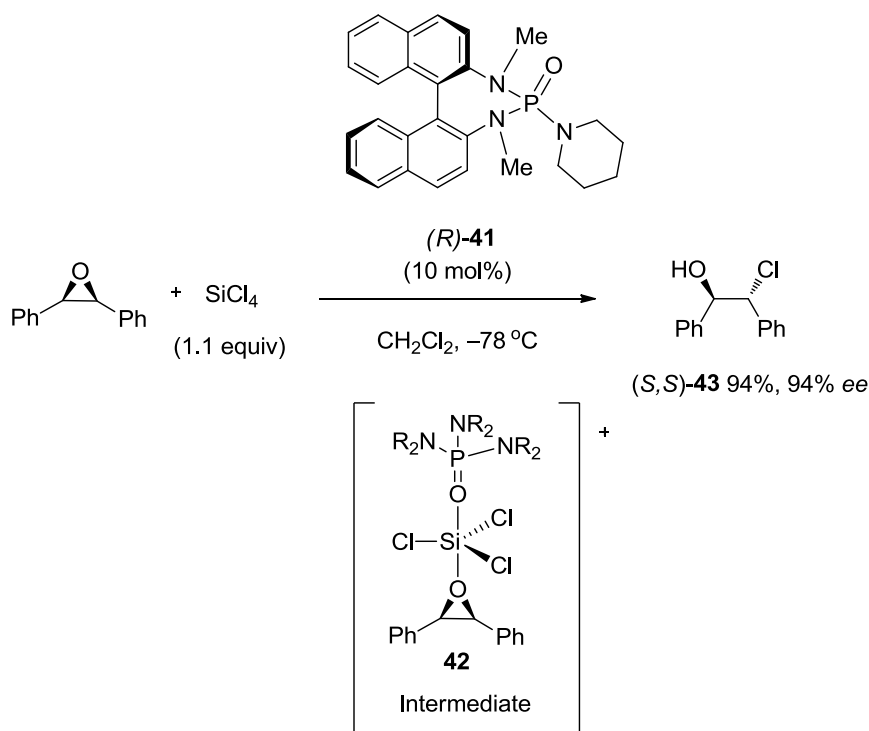
Inspired by these pioneering works, chemists have been interested in the generation of new chiral phosphine oxide families and their subsequent application in asymmetric reactions. Chiral phosphine oxides can be used as organocatalysts in asymmetric catalysis. The desymmetrization reactions of *meso*-epoxides with tetrachlorosilane was studied in the presence of chiral phosphine oxide catalysts. In preliminary studies, Lewis bases such as HMPA, DMPU or pyridine were applied in aldol additions of trichlorosilyl enolates.³⁵ In 1998, the Denmark group reported that chiral phosphoramidate (**41**) could act as Lewis bases to promote the enantioselective ring opening of *meso*-epoxides.³⁶ Activation of the epoxide is achieved through complexation of the chiral phosphorus oxide and silicon trichloride to form the corresponding cationic intermediate **42**. The chloride ion then acts as a nucleophile and attacks in an S_N2 fashion, opening the epoxide. The optically active chlorohydrin (*S,S*)-**43** is cleanly obtained in excellent yield (94%) and enantioselectivity (94% *ee*) (Scheme 12).

³³ J. Meisenheimer, L. Lichtenstadt, *Chem. Ber.*, **1911**, *44*, 356–359.

³⁴ J. Meisenheimer, J. Casper, M. Horing, W. Lauter, L. Lichtenstadt, W. Samuel, *Liebigs Ann. Chem.*, **1926**, 213–248.

³⁵ (a) S. E. Denmark, S. B. D. Winter, X. Su, K.-T. Wong, *J. Am. Chem. Soc.* **1996**, *118*, 7404–7405.; (b) S. E. Denmark, K.-T. Wong, R. A. Stavenger, *J. Am. Chem. Soc.* **1997**, *119*, 2333–2334.

³⁶ S. E. Denmark, P. A. Barsanti, K.-T. Wong, R. A. Stavenger, *J. Org. Chem.* **1998**, *63*, 2428–2429.



Scheme 12. Desymmetrization of *meso*-epoxide with tetrachlorosilane in the presence of (*R*)-41 catalyst.

Further extending the family of Lewis bases, Nakajima and co-workers reported the use of chiral bisphosphine oxide BINAPO as an organocatalyst for the reaction of Scheme 12 and also added diisopropylethylamine (1.5 equiv) to trap hydrochloric acid from silicon tetrachloride.³⁷ The reaction produced the chiral chlorohydrin efficiently in high enantioselectivity (90% *ee*). In the same line, they have also explored other chiral bisdiphenylphosphine oxide ligands to investigate on their reactivity and selectivity.³⁸ (*S*)-Tol-BINAPO, (*S*)-Xyl-BINAPO, (*S*)-H₈-BINAPO, (*S*)-SEGPHOSO and (*R,R*)-DIOPO have all been employed under the same reactions (Figure 12). In particular, (*S*)-H₈-BINAPO and (*S*)-SEGPHOSO promoted high *ees* of 86% and 88% respectively. Whereas, (*S*)-Tol-BINAPO, (*S*)-Xyl-BINAPO and (*R,R*)-DIOPO provided the product in high yields, lower *ees*. Thus, no ligand was able to provide higher *ee* than the original (*S*)-BINAPO.³⁹

³⁷ E. Tokuoka, S. Kotani, H. Matsunaga, T. Ishizuka, S. Hashimoto, M. Nakajima, *Tetrahedron Asymmetry* **2005**, *16*, 2391–2392.

³⁸ S. Kotani, H. Furusho, M. Sugiura, M. Nakajima, *Tetrahedron* **2013**, *69*, 3075–3081.

³⁹ For a recently review see: P.-A. Wang, *Beilstein J. Org. Chem.* **2013**, *9*, 1677–1695.

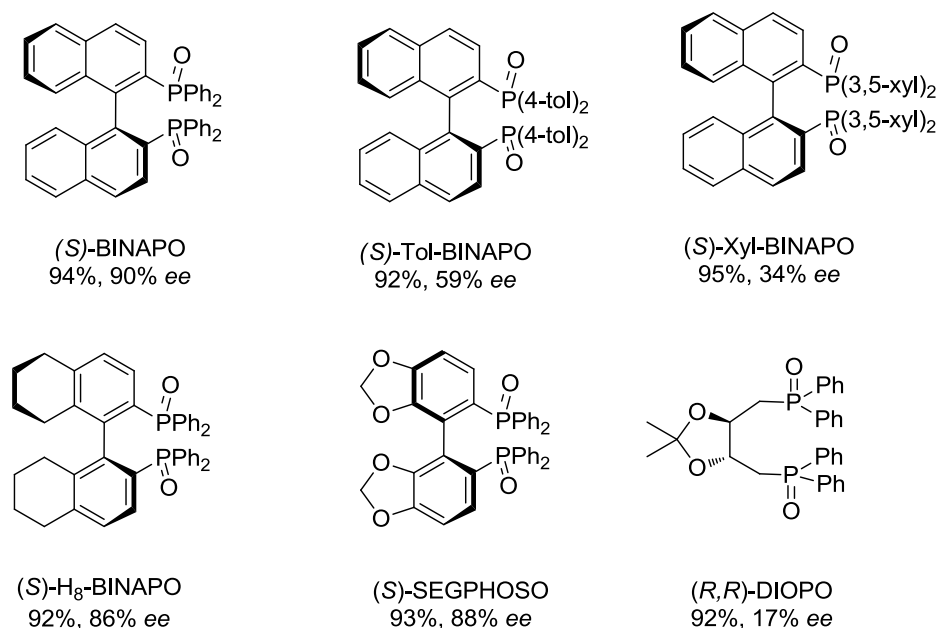


Figure 12. Screening of chiral phosphine oxides in the desymmetrization of *meso*-epoxide with tetrachlorosilane

Phosphine oxides were also reported as Lewis base promoters in allylation reactions of aldehydes.^{40, 41} For example, Zhang reported a new class of axial chiral 5,5'-bridged biphenyl diphosphine ligands such as C₁₀-BridePHOS **44** and the corresponding oxide **45** (Figure 13).⁴² In particular, the chiral C₁₀-BridePHOS Oxide **45** was applied for the allylation reaction of aldehyde **46** with allyltrichlorosilane. This organocatalyst successfully promoted the formation of chiral homoallylic alcohol **47** in excellent yield (96%) and high enantioselectivity (92% ee) (Scheme 13).⁴¹

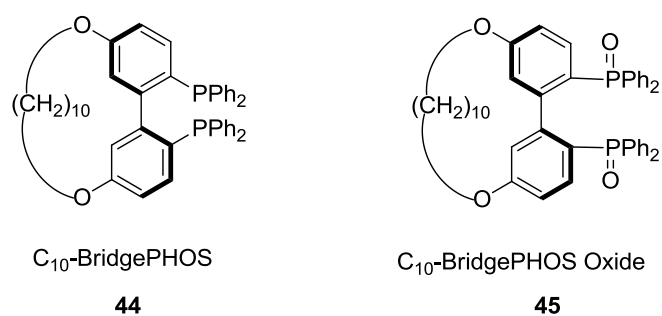


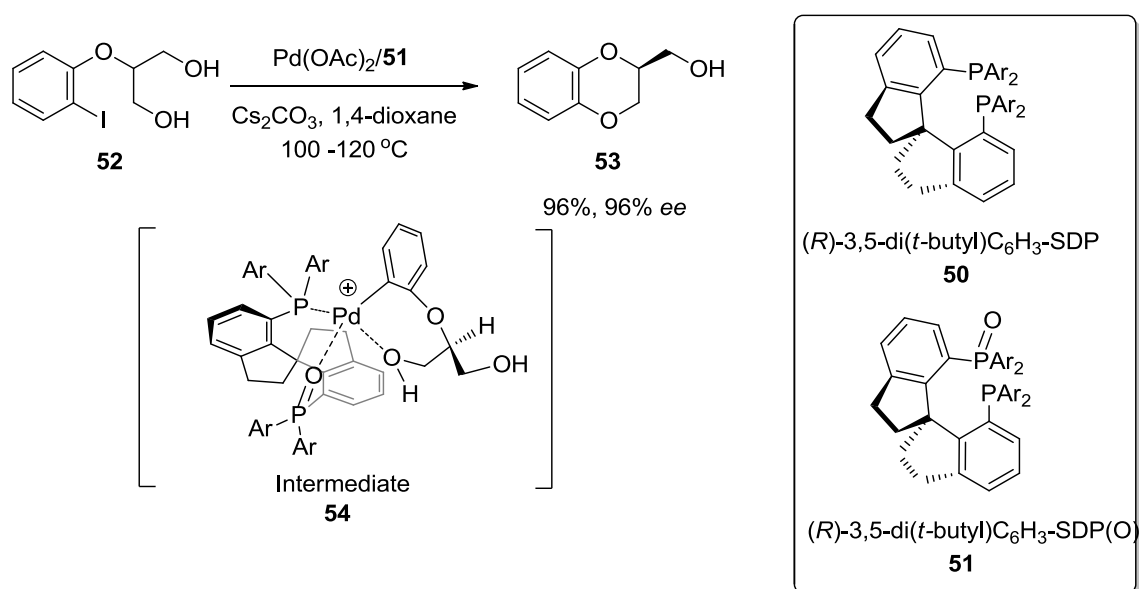
Figure 13. C₁₀-BridePHOS (**44**) and its oxide (**45**)

⁴⁰ (a) S. E. Denmark, J. Fu, D. M. Coe, X. Su, N. E. Pratt, B. D. Griedel, *J. Org. Chem.* **2006**, *71*, 1513–1522. (b) S. E. Denmark, J. Fu, M. J. Lawler, *J. Org. Chem.* **2006**, *71*, 1523–1536.

⁴¹ J. Chen, D. Liu, D. Fan, Y. Liu, W. Zhang, *Tetrahedron* **2013**, *69*, 8161–8168.

⁴² (a) H. Wei, Y. J. Zhang, Y. Dai, J. Zhang, W. Zhang, *Tetrahedron Lett.* **2008**, *49*, 4106–4109.; (b) Z.-C. Duan, X.-P. Hu, C. Zhang, D.-Y. Wang, S.-B. Yu, Z. Zheng, *J. Org. Chem.* **2009**, *74*, 9191–9194.; (c) C. Wang, G. Yang, J. Zhuang, W. Zhang, *Tetrahedron Lett.* **2010**, *51*, 2044–2047.

in this reaction; however, the reaction afforded 2-substituted 1,4-benzodioxane (**53**) in poor yields (25%) and only 60% *ee*. In addition, dehalogenated byproduct was obtained in 12%. In similar manner, the corresponding chiral monophosphine ligand **51** demonstrated better selectivity than the spirodiphosphine counterpart to afford **53** in 96% yield and 96% *ee* (Scheme 14). As a result of the palladium coordination with the oxygen atom as in corresponding intermediate **54**, the spirobiindane backbone at the phosphine oxide is forced to block the space below the palladium coordination plane, which creates an asymmetric chiral environment. Moreover, the weaker binding of phosphine oxide and metal than the phosphine, the arene substrate favors the *cis*-position of the phosphine and avoids *trans*-influence to form **53** selectively.



Scheme 14. Stereoselective palladium-catalyzed asymmetric aryl C–O bond formation of **52** in the presence of **51**.

In conclusion, a number of phosphine compounds bearing centered or axial chirality are readily used as ligands for asymmetric catalysis to access optically pure products in stereoselective reactions. Similarly in asymmetric metal-free reactions, their corresponding chiral phosphine oxides play an important role as organocatalysts, for instance, in the desymmetrization reaction of *meso*-epoxides and the allylation reactions of aldehydes. In addition, mix-phosphine and phosphine oxide ligands have been recently attempted to increase the reactivity and enantioselectivity in catalytic reactions. However, the reactivity and selectivity of the reactions depend on nature of ligands and metals. Gold salts are interesting catalysts in terms of mild condition reactions. To deepen the scope of organophosphorus ligands in organometallic reactions, we will now focus on the reactivity of organophosphorus ligands for gold(I) salts. In the

following section, the generations of gold-phosphine complexes and their applications will be presented.

3. Organophosphorus compounds in gold chemistry

Besides the phosphines and their oxides combining with rhodium, ruthenium, platinum, and palladium as presented in the previous section, recently gold catalysts bearing organophosphorus ligands have elicited interest in asymmetric catalysis. Gold(I) coordinates in a linear geometry with two ligands, which is different from other metals such as rhodium(I), platinum(II), palladium(II) and ruthenium(II) which all favor a square planar geometry due to their d^8 electronic configuration.⁴⁵ Gold(I) exhibits a d^{10} electronic configuration, which favors coordination of “soft” ligands such as phosphines and C-C π -bonds. The challenge in asymmetric catalysis is to apprehend the reactive coordination site of the gold complex. It is far removed from the chirality-inducing ligand environment, compared for instance with a rhodium complex (Figure 15). In this section, we focus on gold(I) coordination with phosphine ligands, in particular their reactivity in catalytic reactions.

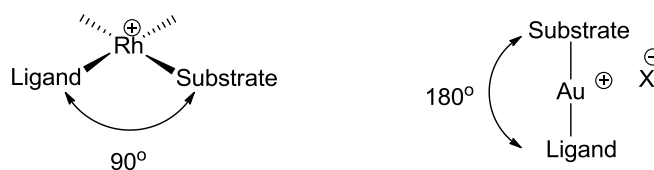


Figure 15. Unique geometry of gold(I)-complexes compared to rhodium complex.

3.1. Generation of gold-phosphine complexes

In the mid-1960s, common gold halides AuX and AuX_3 were studied to access a variety of organogold complexes. This was at the same time as the chemistry of olefin combined with many metals such as platinum catalysts emerged.⁴⁶ In 1965, Hüttel started his pioneering work on gold-olefin complexes and identified them by elemental analysis, vibrational spectroscopy, crystallography, and mass spectroscopy.⁴⁷ The formation of the gold-olefin complexes composed of gold salts such as $AuCl$, $AuBr$, $AuCl_3$ and $AuBr_3$ as the acceptors with linear or cyclic olefins such

⁴⁵ P. Pyykkö, *Chem. Rev.* **1988**, *88*, 563–594.

⁴⁶ B. Armer, H. Schmidbaur, *Angew. Chem., Int. Ed. Engl.* **1970**, *9*, 101–113.

⁴⁷ R. Hüttel, H. Dietl, *Angew. Chem., Int. Ed. Engl.* **1965**, *4*, 438–439.

as propene, butene and cyclohexene as the donors was isolated.⁴⁸ To broaden a variety of bonding modes, alkynes or phosphines have then been applied as soft ligands for gold complexes.⁴⁹ In the gold(I)-coordination mode, the ligands can be neutral (L) or anionic (X), generally coordinating to gold(I) species in the form of [L-Au-L] or [X-Au-X]/L-Au-L⁺ in a linear geometry arrangement. Moreover, tri- and tetracoordinated gold(I) complexes also exist with appropriated ligands.⁵⁰

More recently, the use of gold catalysts as carbophilic π -acids has become a good choice for building molecular complexity in an atom-economical fashion under mild conditions.⁵¹ Currently, gold(I) species bearing phosphine ligands are intensively studied in catalytic reactions such as hydration of alkynes,^{51c, 52} C-C bond forming reactions,⁵³ hydroarylation reactions,⁵⁴ and carbon-heteroatom bond forming reactions.^{55, 56} In addition, some gold(I)-phosphine species exhibit some antitumor activity. These include neutral, linear, two-coordinate gold(I) complexes such as Et₃PAuCl and tetraacetylthioglucose gold(I) phosphine complex (auranofin), and cationic tetrahedral bis-chelated gold(I) phosphine complexes such as [Au(dppe)₂]⁺Cl⁻ (Figure 16), which cause mitochondrial dysfunction that leads to cell death.⁵⁷

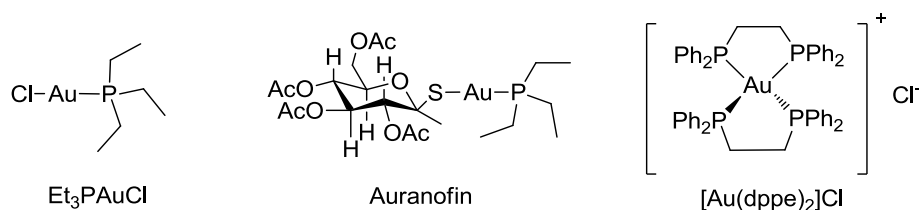


Figure 16. Examples of gold(I) phosphine antitumor complexes.

New gold complexes have attracted attention in a variety of novel catalytic reactions. These complexes bearing organophosphorus ligands can be prepared *via* coordination between

⁴⁸ R. Hüttel, H. Reinheimer, K. Nowak, *Chem. Ber.* **1968**, 101, 3761–3776.

⁴⁹ H. Schmidbaur, A. Schier, *Organometallics* **2010**, 29, 2–23.

⁵⁰ M. C. Gimeno, A. Laguna, *Chem. Rev.* **1997**, 97, 511–522.

⁵¹ For some reviews, see (a) E. Jiménez-Núñez, A. M. Echavarren, *Chem. Rev.* **2008**, 108, 3326–3350.; (b) Z. Li, C. Brouwer, C. He, *Chem. Rev.* **2008**, 108, 3239–3265.; (c) S. M. Inamdar, N. T. Patil, *Org Chem Front* **2015**, 2, 995–998.

⁵² J. H. Teles, S. Brode, M. Chabanas, *Angew. Chem., Int. Ed.* **1998**, 37, 1415–1418.

⁵³ (a) J. J. Kennedy-Smith, S. T. Staben, F. D. Toste, *J. Am. Chem. Soc.* **2004**, 126, 4526–4527.; (b) S. T. Staben, J. J. Kennedy-Smith, F. D. Toste, *Angew. Chem., Int. Ed.* **2004**, 43, 5350–5352.

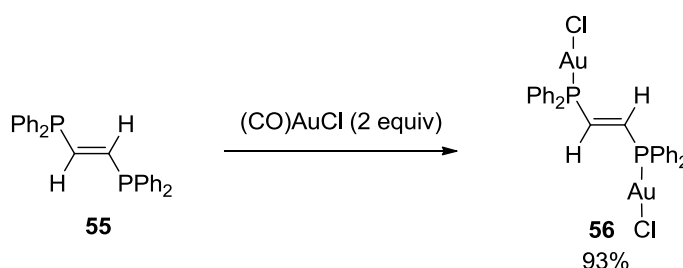
⁵⁴ (a) M. T. Reetz, K. Sommer, *Eur. J. Org. Chem* **2003**, 3485–3496.; (b) C. Nevado, A. M. Echavarren, *Chem. Eur. J.* **2005**, 11, 3155–3164.; (c) C. Ferrer, A. M. Echavarren, *Angew. Chem., Int. Ed.* **2006**, 45, 1105–1109.

⁵⁵ (a) S. Antoniotti, E. Genin, V. Michelet, J. P. Genêt, *J. Am. Chem. Soc.* **2005**, 127, 9976–9977.; (b) A. Buzas, F. Gagosz, *Org. Lett.* **2006**, 8, 515–518.; (c) E. Mizushima, T. Hayashi, M. Tanaka, *Org. Lett.* **2003**, 5, 3349–3352.

⁵⁶ For recently reviews, see R. Dorel, A. M. Echavarren, *Chem. Rev.* **2015**, DOI 10.1021/cr500691k

⁵⁷ (a) S. J. Berners-Price, R. J. Bowen, P. Galettis, P. C. Healy, M. J. McKeage, *Coord. Chem. Rev.* **1999**, 185–186, 823–836.; (b) P. J. Barnard, S. J. Berners-Price, *Coord. Chem. Rev.* **2007**, 251, 1889–1902.; (c) O. Rackham, S. J. Nichols, P. J. Leedman, S. J. Berners-Price, A. Filipovska, *Biochem. Pharmacol.* **2007**, 74, 992–1002.

gold salts and phosphorus donors to form gold-phosphorus (Au-P) bond. In an early example of synthesis of gold-phosphine complexes, Schmidbaur studied the formation of gold complexes bearing bisphosphine ligands. Ethene-*trans*-bis(diphenylphosphino)chlorogold(I) complexes (**56**) was synthesized by a mixture of 1:2 equivalents of bis(diphenylphosphino)ethane (**55**) and (CO)AuCl (Scheme 15).⁵⁸ These structures characterized by X-ray crystallography showed that gold(I) species coordinated to the phosphorus atoms in linear coordination modes. Both gold atoms are very far apart at opposite sides of the plane of the olefinic skeleton and the gold coordination on the π -bond of the olefin motif was not observed.

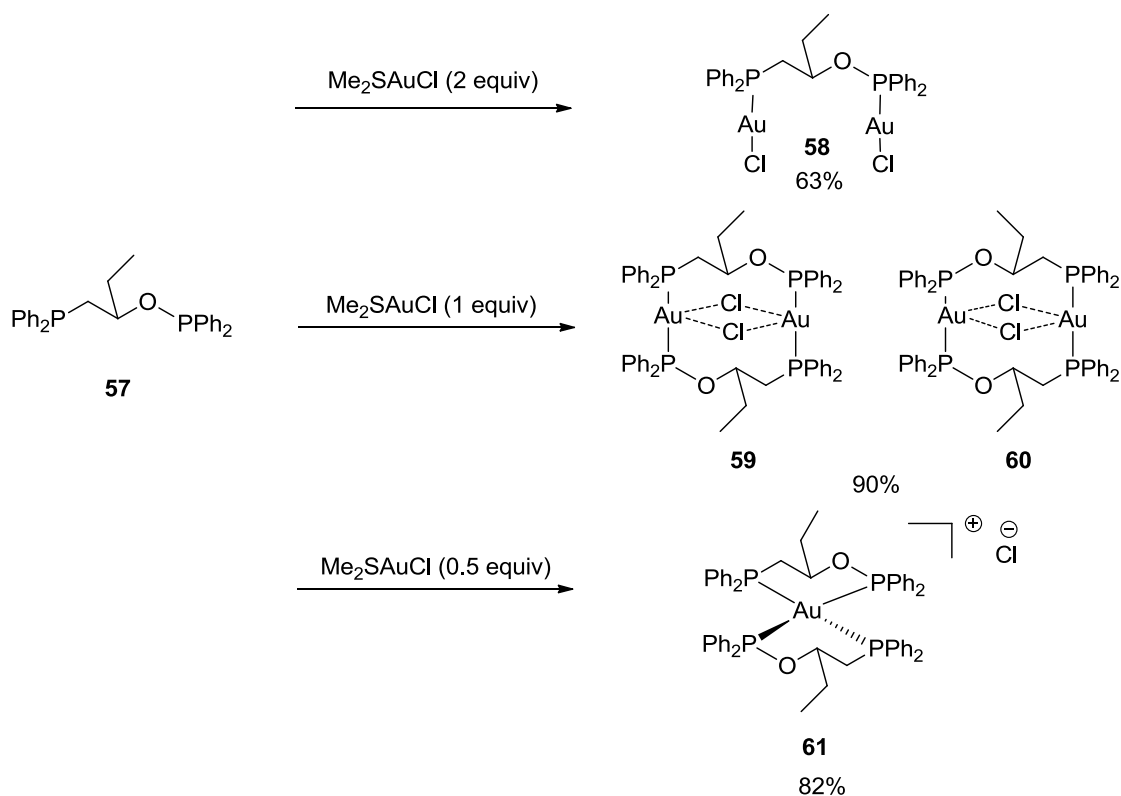


Scheme 15. Synthesis of ethene-*trans*-bis(diphenylphosphino)chlorogold(I) (**56**)

Schmidbaur also designed different types of bisphosphine ligands to study the metal-ligand coordination modes.⁵⁹ In this case, he used (1-diphenylphosphino-but-2-yl)diphenylphosphinite ligands (**57**) for gold(I) salt (Me₂SAuCl). As shown in Scheme 16, three forms of gold coordination modes were observed depending on the number of equivalents of Me₂SAuCl. Using two equivalents of Me₂SAuCl for one equivalent of ligand could provide linear coordination complex between each gold and phosphine group selectively as in complex **58**. With a 1:1 mixture of ligand and Me₂SAuCl, a mixture of annular dinuclear complexes was formed with metal linked to two phosphines from head-to-tail **59** and head-to-head **60** patterns in 90% yield. These crystals show the gold bridging by the two ligands as dimers, forming 12-membered rings. Two chloride atoms are also bridged trans-annularly with both gold atoms. Interestingly, the 2:1 complex between the ligands and Me₂SAuCl promoted cationic bisphosphine-chelated complex **61** as four coordination mode, forming the gold center with two six-membered rings.

⁵⁸ H. Schmidbaur, G. Reber, A. Schier, F. E. Wagner, G. Müller, *Inorganica Chim. Acta* **1988**, *147*, 143–150.

⁵⁹ A. Bayler, A. Schier, H. Schmidbaur, *Inorg. Chem.* **1998**, *37*, 4353–4359.

Scheme 16. Synthesis of **58-61** in difference ratio of gold and phosphine ligand.

In summary, gold(I) species interact well with phosphorus atoms selectively to form P-Au bond as linear two-coordinated complexes. When dealing with polydentate phosphine, stoichiometry of gold and the ligand becomes crucial as the formation of unusual four-coordinated complex **61**.⁵⁰ The next section will present some examples of the preparation of gold-bisphosphine complexes in mononuclear and dinuclear coordination modes. In addition, mix-phosphine and phosphine oxide ligands for gold catalysis will also be described.

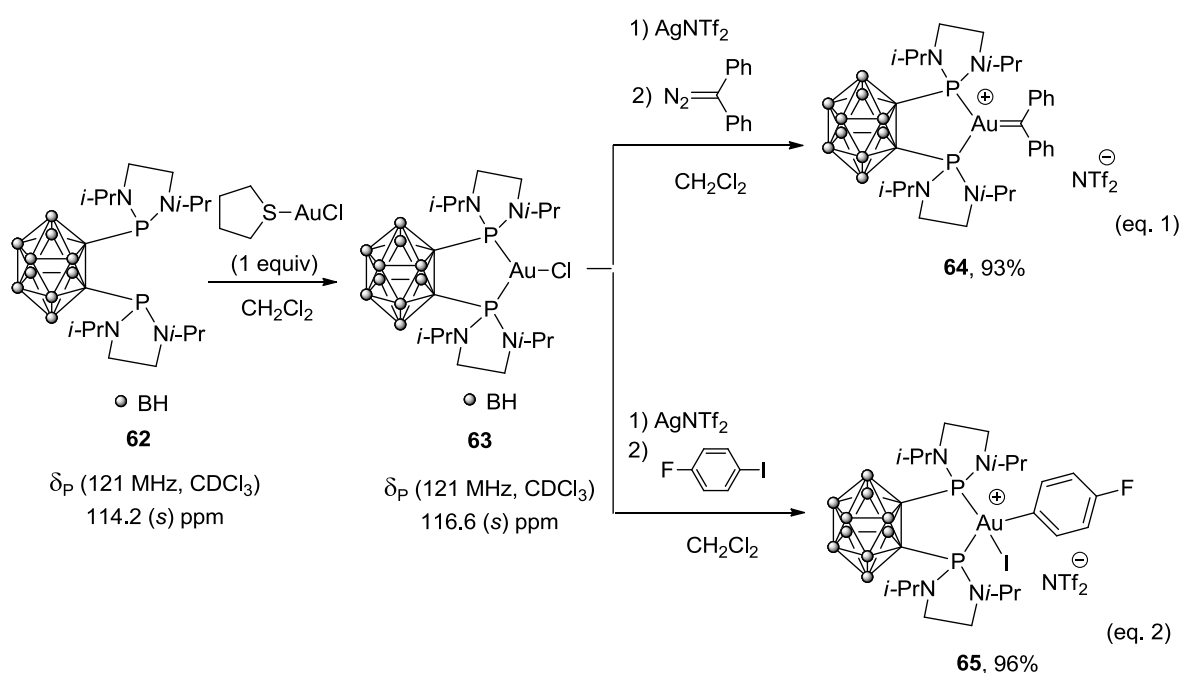
3.1.1. Mononuclear gold bisphosphine complexes

Seeing that neutral gold(I) complexes most commonly formed linear dicoordination, the use of bisphosphine ligands for mononuclear coordination is challenging for forming stable complexes. For example, carborane diphosphine **62**⁶⁰ has been recently used as a bidentate ligand of gold(I) species by the Bourissou group.⁶¹ The reaction of **62** in the presence of one equivalent of chloro(tetrahydrothiophene) gold(I) provided mononuclear gold(I) chloride complex **63**. The ³¹P NMR of **63** (δ_p 116.6 ppm) showed a downfield chemical shift from **62** (δ_p 114.2 ppm), suggesting

⁶⁰ O. Crespo, M. C. Gimeno, A. Laguna, P. G. Jones, *J. Chem. Soc. Dalton Trans.* **1992**, 1601–1605.

⁶¹ (a) M. Joost, L. Estévez, S. Mallet-Ladeira, K. Miqueu, A. Amgoune, D. Bourissou, *Angew. Chem. Int. Ed.* **2014**, *53*, 14512–14516. (b) M. Joost, L. Estévez, S. Mallet-Ladeira, K. Miqueu, A. Amgoune, D. Bourissou, *Angew. Chem. Int. Ed.* **2014**, *53*, 14512–14516.

electron depletion by metal coordination. The complex **63** was then applied to the preparation of cationic gold complexes. Upon cationization with AgNTf_2 , the resulting cationic complex reacts with diphenyldiazomethane to give carbonyl complex **64** in 93% yield (Scheme 17, eq. 1).⁶² The Au–C bond length (1.984 Å) determined from the crystal structure is significantly shorter than previously reports of gold carbenes (2.010–2.046 Å),⁶³ which suggests the strong π -backdonation for the gold(I) catalysts. Moreover, the cationic gold(I) carborane diphosphine could undergo oxidative addition of 4-fluoriodobenzene to provide the gold(III) species **65** in 96% yield (Scheme 17, eq. 2).



Scheme 17. Mononuclear gold(I) complex **63** and their functionalization.

3.1.2. Dinuclear gold bisphosphine complexes

Chiral bisphosphine compounds such as BINAP, BIPHEP, MeOBIPHEP and SEGPHOS derivatives (Figure 17) have been reported as good ligands for gold (I) salts as dinuclear gold complexes in enantioselective homogeneous catalytic reactions⁶⁴ such as cycloisomerization,⁶⁵ hydroalkoxylation,⁶⁶ hydroamination^{66, 67, 68} and olefin cyclopropanation.⁶⁹

⁶² M. Joost, A. Zeineddine, L. Estévez, S. Mallet-Ladeira, K. Miqueu, A. Amgoune, D. Bourissou, *J. Am. Chem. Soc.* **2014**, *136*, 14654–14657.

⁶³ For a very interesting discussion and comparison of Au–C length, see Y. Wang, M. E. Muratore, A. M. Echavarren, *Chem. Eur. J.* **2015**, *21*, 1–9.

⁶⁴ For some reviews, see: (a) E. Jiménez-Núñez, A. M. Echavarren, *Chem. Rev.* **2008**, *108*, 3326–3350.; (b) D. J. Gorin, B. D. Sherry, F. D. Toste, *Chem. Rev.* **2008**, *108*, 3351–3378.; (c) V. Michelet, P. Y. Toullec, J. P. Genêt, *Angew. Chem. Int.*

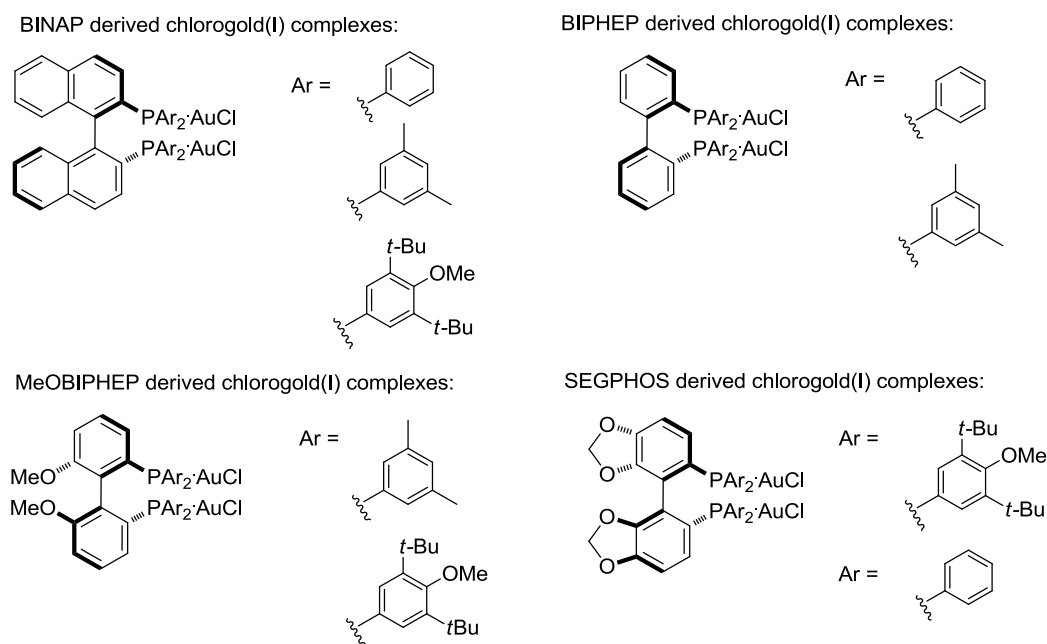


Figure 17. Examples of chiral dinuclear gold precatalysts in catalytic reactions.

The enantioselectivity of asymmetric reactions depends on the abilities of chiral ligands. The steric and electronic properties of chiral ligands are key factors to induce the asymmetry in the transition state. Dinuclear gold complexes possessing C_2 -Symmetry is usually good candidate for enantioselective compounds. Generally, the molecules of racemic gold complexes can rotate on carbon backbone to thermodynamically favorable forms. The chiral ligands would block this rotation in transition state and also induce the asymmetry of reaction to promote chiral forms. On the chiral gold-bisphosphine complexes, X-ray crystallography could be observed an intramolecular interaction such as aurophilic (Au-Au) in the range form 2.50-3.50 Å and/or π - π stacking interaction.⁷⁰ These rigidity interactions promote enantioselective products. For example, chiral Tol-BINAP²⁹ and Xylyl-BINAP⁷¹ have π - π stacking interactions between the two-aryl groups on the phosphine, which were used in gold-catalyzed asymmetric cycloisomerization of enynes and eneallenes respectively with quite good *ee* (50-72%).⁷ Chiral BIPHEP(AuCl)₂ was observed the

Ed. **2008**, *47*, 4268–4315.; (d) A. Fürstner, *Chem. Soc. Rev.* **2009**, *38*, 3208–3221.; (e) M. Rudolph, A. S. K. Hashmi, *Chem. Soc. Rev.* **2012**, *41*, 2448–2462.

⁶⁵ For some reviews, see: (a) A. Pradal, P. Toullec, V. Michelet, *Synthesis* **2011**, *2011*, 1501–1514; (b) M. Bandini, A. Eichholzer, *Angew. Chem. Int. Ed.* **2009**, *48*, 9533–9537.; (c) M. J. Johansson, D. J. Gorin, S. T. Staben, F. D. Toste, *J. Am. Chem. Soc.* **2005**, *127*, 18002–18003.

⁶⁶ G. L. Hamilton, E. J. Kang, M. Mba, F. D. Toste, *Science* **2007**, *317*, 496–499

⁶⁷ K. Aikawa, M. Kojima, K. Mikami, *Angew. Chem. Int. Ed.* **2009**, *48*, 6073–6077.

⁶⁸ A. Homs, I. Escofet, A. M. Echavarren, *Org. Lett.* **2013**, *15*, 5782–5785.

⁶⁹ M. J. Johansson, D. J. Gorin, S. T. Staben, F. D. Toste, *J. Am. Chem. Soc.* **2005**, *127*, 18002–18003.

⁷⁰ H. Schmidbaur, A. Schier, *Chem. Soc. Rev.* **2011**, *41*, 370–412.

⁷¹ M. A. Tarselli, A. R. Chianese, S. J. Lee, M. R. Gagné, *Angew. Chem. Int. Ed.* **2007**, *46*, 6670–6673., *Angew. Chem.* **2007**, *119*, 6790–6793.

Au-Au distance of 3.10 Å, which have been used in asymmetric hydroamination of aminoallene to provide high yields and *ees* (up to 91% *ee*).⁶⁷

3.1.3. Gold complexes bearing phosphine and phosphine oxide moieties

Gold complexes coordinated to mixed phosphine and phosphine oxide ligands have been synthesized and their applications studied. For example, Healy and co-workers synthesized bromo-gold phosphine **66**, featuring a phosphine oxide functional group.⁷² Hahn and co-workers reported the mononuclear gold complex **67** (Figure 18).⁷³ The P-donor atom promoted linearly two-coordinate P–Au–X (X= Br or Cl) complexes. Both complexes **66** and **67** characterized by crystallography are demonstrated by the absence of any distortion from a linear P–Au–X bond with angles of 178.53° and 179.04° respectively. The weak interaction between the gold atom and phosphine oxide group of **66** and **67** shows Au···O contact of 3.274 Å and 3.057 Å. Hahn also applied **67** on hydroarylation reaction of alkyne derivatives.^{51C, 74, 75} Treatment of ethylpropiolate and pentamethylbenzene in the presence of **67** as a precatalyst and silver tetrafluoroborate as an additive yielded 96% of product **68** (Scheme 18).

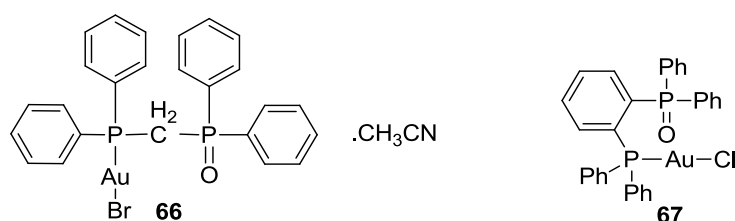
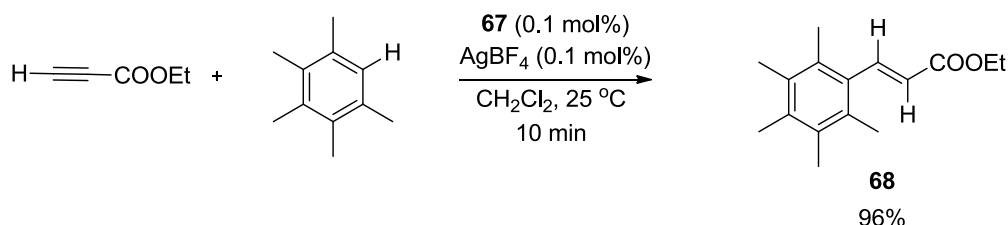


Figure 18. Organogold complexes with mixed phosphine-phosphine oxide ligands **66** and **67** by Healy and Hahn.



Scheme 18. Synthesis of **68** from ethylpropiolate and pentamethylbenzene in the presence of **67** and AgBF₄.

⁷² M. L. Williams, S. E. Boyd, S. P. C. Dunstan, D. L. Slade, P. C. Healy, *Acta Crystallogr. Sect. E Struct. Rep. Online* **2003**, 59, m768–m770.

⁷³ C. Hahn, L. Cruz, A. Villalobos, L. Garza, S. Adeosun, *Dalton Trans* **2014**, 43, 16300–16309.

⁷⁴ N. Marion, R. S. Ramón, S. P. Nolan, *J. Am. Chem. Soc.* **2009**, 131, 448–449.

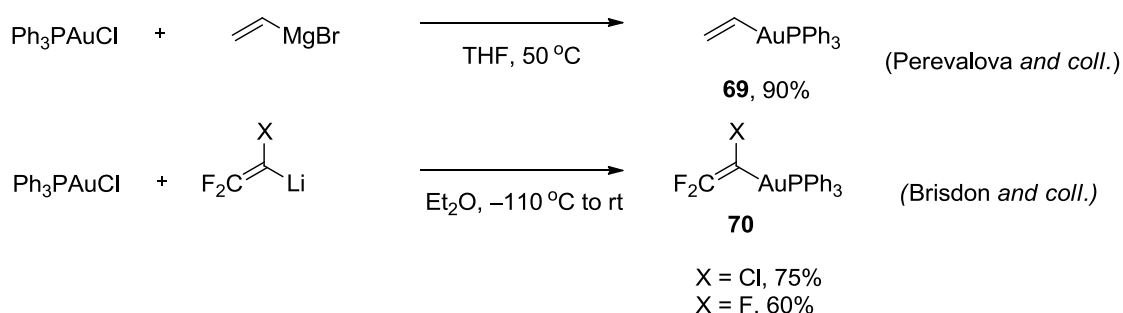
⁷⁵ C. Tubaro, M. Baron, A. Biffis, M. Basato, *Beilstein J. Org. Chem.* **2013**, 9, 246–253

3.2. Functionalization of gold(I) complexes bearing organophosphorus groups

3.2.1. Formation of Au-C bond

3.2.1.1. Via transmetalation of organometallic reagents (RLi and RMg)

Aryl, alkyl and vinylgold complexes can be formed *via* transmetalation between a gold(I) salt bearing a phosphine ligand and organometallic reagents such as lithium reagent⁷⁶ or a Grignard reagent.^{46, 77} Pioneering work in 1972 by the Perevalova group described the synthesis of vinylgold(I) compounds **69**, Ph₃PAu(CH=CH₂) using vinyl magnesium bromide as transmetalating agent.⁷⁸ In 2000, Brisdon also synthesized and structurally characterized two halogenated hydrocarbon gold complexes **70**, Ph₃PAu(CX=CF₂) (X=Cl, F) from Ph₃PAuCl and the corresponding organolithium reagent CF₂=CXLi (Scheme 19).⁷⁹



Scheme 19. Preparation of vinyl gold complexes **69** and **70** from the groups of Perevalova and Brisdon.

To extend the scope of gold complexes, the Thibonnet group synthesized arylgold(I) complexes **71** bearing vinyl and methoxy substituents, as well as a fluorine atom on the aryl group prepared by either Grignard or lithium reagents and Ph₃PAuCl in high yields (Scheme 20).⁸⁰

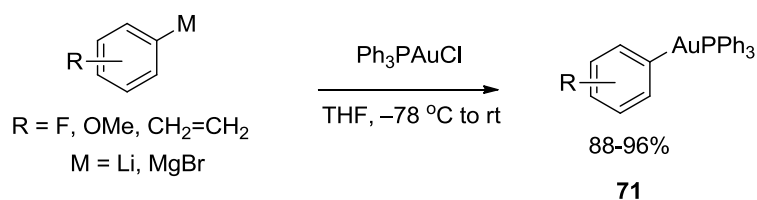
⁷⁶ (a) K. A. Porter, A. Schier, H. Schmidbaur, *In Perspectives in Organometallic Chemistry*, Screttas, C. G., Steele, B. R., Eds.; The Royal Society of Chemistry: **2003**, 74.; (b) M. A. Bennett, S. K. Bhargava, K.D. Griffiths, G. B. Robertson, *Angew. Chem., Int. Ed. Engl.* **1987**, *26*, 260–261.

⁷⁷ W. Y. Heng, J. Hu, J.H. K. Yip, *Organometallics* **2007**, *26*, 6760–6768.

⁷⁸ A. N. Nsmeyanov, E. G. Perevalova, V. V. Krivykh, A. N. Kosina, K. I. Grandberg, E. I. Smyslova, *Izv. Akad. Nauk. SSSR, Ser. Khim.* **1972**, 653–654.

⁷⁹ N. A. Barnes, A. K. Brisdon, W. I. Cross, J. G. Fay, J. A. Greenall, R. G. Pritchard, J. Sherrington, *J. Organomet. Chem.* **2000**, *616*, 96–105.

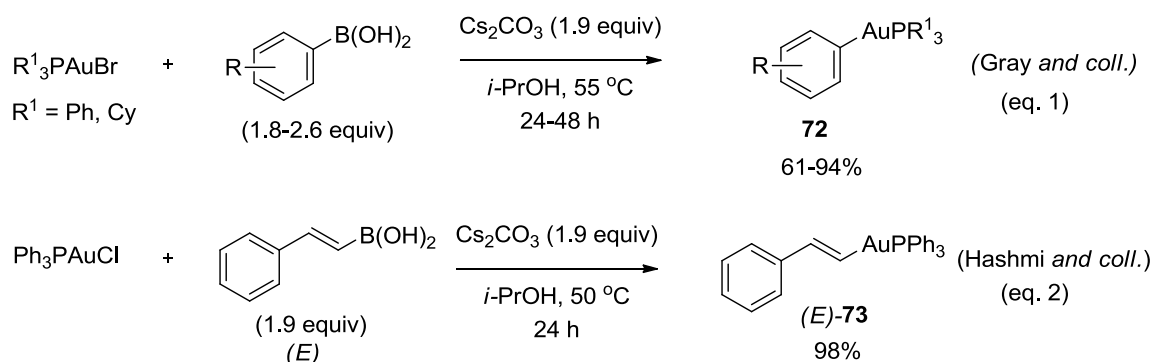
⁸⁰ C. Croix, A. Balland-Longeau, H. Allouchi, M. Giorgi, A. Duchêne, J. Thibonnet, *J. Organomet. Chem.* **2005**, *690*, 4835–4843.



Scheme 20. Preparation of arylgold complexes **71** by lithium or Grignard reagents.

3.2.1.2. Via transmetalation of boron reagents

Organogold compounds can be prepared from boron reagents. A base-assisted auration methodology using arylboronic acids was first reported by Gray and co-workers in 2005.⁸¹ A combination of gold(I) salts and arylboronic acids in the presence of a mild base (cesium carbonate) and isopropyl alcohol provided aryl gold complexes **72** in 61-94% yields, depending on the nature of substrates (Scheme 21, eq. 1). In 2009, Hashmi and co-workers also applied this method for the preparation of styrylgold complex (*E*)-**73** compounds (Scheme 21, eq. 2). The reactivity of **73** was further assessed to use in reactions with Michael acceptors and sources of electrophilic halogens and protons.⁸²



Scheme 21. Preparation of **72** and **73** by transmetalation of arylboronic acids.

3.2.1.3. Via intramolecular gold-catalyzed cyclization reactions

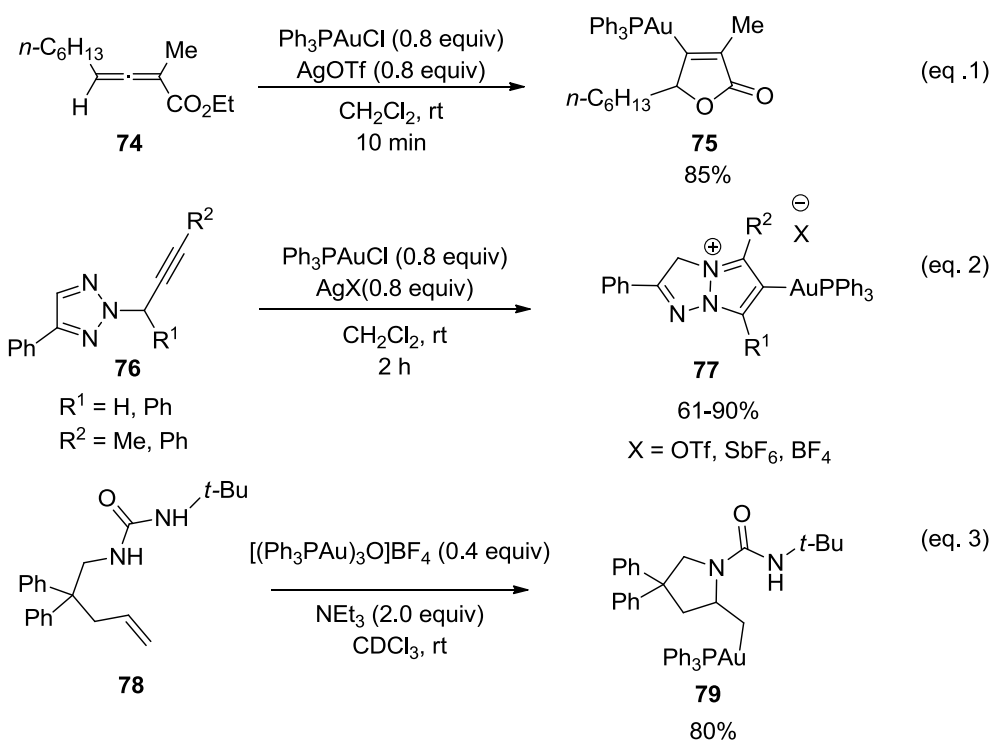
The last examples devoted to the preparation of organogold complexes by gold(I)-catalyzed cyclization reactions from allene, alkyne and alkene substrates (Scheme 22).⁸³ In 2008, Hammond and co-workers demonstrated that stable lactone-containing gold complex **75**

⁸¹ D. V. Partyka, M. Zeller, A. D. Hunter, T. G. Gray, *Angew. Chem. Int. Ed.* **2006**, *45*, 8188–8191.

⁸² A. S. K. Hashmi, T. D. Ramamurthi, F. Rominger, *J. Organomet. Chem.* **2009**, *694*, 592–597.

⁸³ (a) A. S. K. Hashmi, A. M. Schuster, F. Rominger, *Angew. Chem. Int. Ed.* **2009**, *48*, 8247–8249.; (b) A. S. K. Hashmi, T. D. Ramamurthi, F. Rominger, *Adv. Synth. Catal.* **2010**, *352*, 971–975.

accessed to cyclization of allenolate **74**.⁸⁴ Treatment of **74** in the presence of a 1:1 mixture of Ph_3PAuCl and AgOTf afforded **75** in 85% yield *via* cyclization process (Scheme 22, eq. 1). In the same line, the Shi group also prepared in 2010 a new class of cationic vinylgold complexes from propargylic triazoles **76** *via* 5-*endo-dig* cyclization.⁸⁵ Under catalytic conditions identical to Hammond's work, the reaction of **76** afforded the corresponding product **77** in 61-90% yields (Scheme 22, eq. 2). The organogolds **77** are remarkably stable compounds to air and moisture. The high stability of the C-Au bond may be attributable to the extreme electron-deficiency of the cationic heterocycles. In contrast to alkynes and allenes, the activation of alkenes with gold(I) is less documented. Alkylgold complexes have been pointed out as key intermediates in the intramolecular hydroamination of alkenes. Toste disclosed the aminoauration reaction of terminal pentenyl amides and carbomates with gold-oxo trimer, $[(\text{Ph}_3\text{PAu})_3\text{O}]\text{BF}_4$ in the presence of base (Et_3N).⁸⁶ Following addition of the nitrogen moiety onto the activated π -bond, alkene **78** underwent ring-closing process delivering alkylgold **79** in 80% yield (Scheme 22, eq. 3).



Scheme 22. Preparation of organogold complexes **75**, **77** and **79** *via* gold(I)-catalyzed cyclization reaction.

⁸⁴ L.-P. Liu, B. Xu, M. S. Mashuta, G. B. Hammond, *J. Am. Chem. Soc.* **2008**, *130*, 17642–17643.

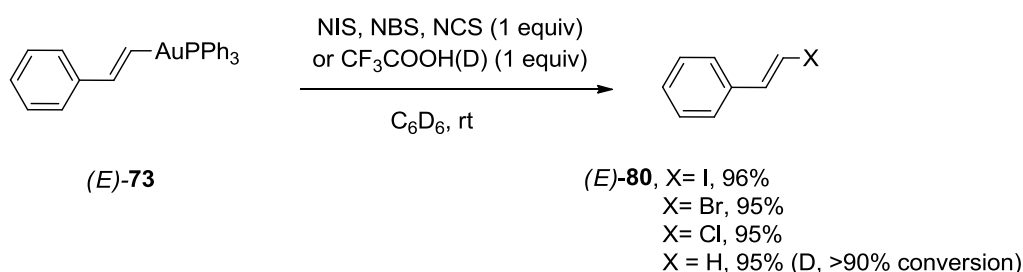
⁸⁵ Y. Chen, D. Wang, J. L. Petersen, N. G. Akhmedov, X. Shi, *Chem. Commun.* **2010**, *46*, 6147–6149

⁸⁶ R. L. LaLonde, W. E. Brenzovich, Jr., D. Benitez, E. Tkatchouk, K. Kelley, W. A. Goddard, III, F. D. Toste, *Chem. Sci.* **2010**, *1*, 226–233.

Apart from the transmetalation of organolithium, Grignard, organoboron reagents and catalytic cyclization reactions, other methods have also been devised to prepare different types of gold(I) species such as C-H activation reactions,⁸⁷ cycloaddition reactions,⁸⁸ and transmetalation with other late transition metals such as palladium, nickel, iron and zirconium.⁸⁹ Some gold complexes have been applied for functionalization by trapping gold phosphine moieties with electrophilic reagents or cross-coupling reactions.⁹⁰

3.2.2. Formation of C-H and C-X Bonds

Post-functionalization of vinylgold complexes has been studied through the addition of electrophilic halide sources and protodeauration in order to trap gold(I) species. According to a report by Hashmi and co-workers, electrophilic addition was carried out on styrylgold derivatives.⁸² The synthesis of (*E*)-styrylgold(I) compound **73** has already reported in Scheme 21 (eq. 2). Here, we focused on trapping the gold functional group (AuPPh₃) of (*E*)-**73** by using various electrophilic halogen sources such as NIS, NBS, NCS or by protodeauration with trifluoroacetic acid (Scheme 23). In each case, reactions were successful to yield 95-96% of vinylproducts **80** and no side product was observed. Moreover, a complete diastereoselectivity transfer could be noted during the protodeauration step when preformed with CF₃CO₂D. When using the (*E*)-**73**, the reaction only gave (*E*)-deuterostyrene with 90% conversion.



Scheme 23. Electrophilic additions of (*E*)-**73**.

Another type of vinyl gold complexes displaying this time, a lactone pattern has been disclosed by the Hammond group.⁸⁴ The gold complex **75** could be isolated as a stable intermediate stemming from the cyclization process (Scheme 24, eq. 1). It was treated with TsOH

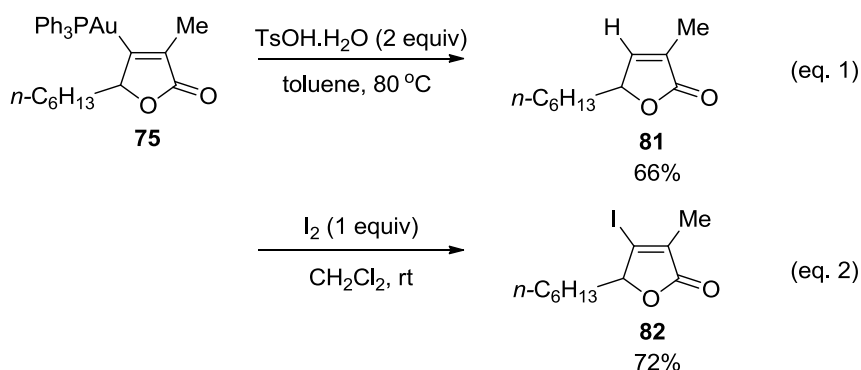
⁸⁷ P. Lu, T. C. Boorman, A. M. Z. Slawin, I. Larrosa, *J. Am. Chem. Soc.* **2010**, *132*, 5580–5581

⁸⁸ (a) L. Gao, D. V. Partyka, J. B. Updegraff, N. Deligonul, T. G. Gray, *Eur. J. Inorg. Chem.* **2009**, *2009*, 2711–2719.; (b) D. V. Partyka, L. Gao, T. S. Teets, J. B. Updegraff, N. Deligonul, T. G. Gray, *Organometallics* **2009**, *28*, 6171–6182.

⁸⁹ (a) S. A. Blum, J. J. Hirner, Y. Shi, *Acc. Chem. Res.* **2011**, *44*, 603–613.; (b) Y. Shi, S. D. Ramgren, S. A. Blum, *Organometallics* **2009**, *28*, 1275–1277.; (c) Y. Shi, S. A. Blum, *Organometallics* **2011**, *30*, 1776–1779.

⁹⁰ (a) A. S. K. Hashmi, R. Döpp, C. Lothschütz, M. Rudolph, D. Riedel, F. Rominger, *Adv. Synth. Catal.* **2010**, *352*, 1307–1314.; (b) L.-P. Liu, G. B. Hammond, *Chem. Soc. Rev.* **2012**, *41*, 3129.

to afford the corresponding protodeauration product **81** in 66% yield. In addition, the lactone could be reacted with iodine and produce *via* iodination γ -iodolactone **82** in 72% yield effectively (Scheme 24, eq. 2).



Scheme 24. Protodeauration (eq. 1) and iodination (eq. 2) reaction of **75**.

Overall, these reports represent early and recent examples of the preparation and isolation of gold complexes. The post-functionalization of goldphosphine complex could be achieved based on various processes. The next challenge is to apply these processes for catalytic reactions by generation of gold complexes as intermediate and then *in-situ* post-functionalization and recovery of the catalytic entity. The isolation of gold intermediates is thus quite useful for the understanding of reaction mechanisms. Moreover, the use of isolated gold complexes as catalysts is an intriguing opportunity.

3.3. Gold(I) complexes bearing organophosphorus groups in catalysis

Nowadays, metal-catalyzed reactions play an important role in the synthesis of functionalized carbo- and heterocyclic structures.⁹¹ Noble metals, such as palladium and platinum, have proved to be outstanding catalysts in several processes. Herein, we focus on gold catalyzed reactions. Gold(I) complexes bearing phosphine ligands are usually used as precatalysts. Silver salts have been used for the activation of neutral gold chloride complexes through anion metathesis to form cationic gold complexes as active catalysts for the reactions. The phosphine is an electron donor ligand which enhances catalytic reactivity. In the absence of such stabilizing

⁹¹ For some reviews, see (a) L. Zhang, J. Sun, S. A. Kozmin, *Adv. Synth. Catal.* **2006**, *348*, 2271–2296.; (b) B. M. Trost, F. D. Toste, A. B. Pin-kerton, *Chem. Rev.* **2001**, *101*, 2067–2096.; (c) G. C. Lloyd-Jones, *Org. Biomol. Chem.* **2003**, *1*, 215–236.; (d) C. Aubert, O. Buisine, M. Malacria, *Chem. Rev.* **2002**, *102*, 813–834.; (e) I. Ojima, M. Tzamarioudaki, Z. Y. Li, R. J. Donovan, *Chem. Rev.* **1996**, *96*, 635–636.

ligands, gold(I) generally prefers to disproportionate to gold(III) and gold(0).⁹² Few reports mention the use of AuCl as a catalyst. However, the reactions are often sluggish and provide products in poor yield⁹³ or undesired products.⁹⁴ In 2006, Toste disclosed the efficient cationic gold triphenylphosphine (AuPPh₃⁺X⁻) catalyst and successfully applied it in the total syntheses of natural products such as (+)-lycopoladine A,⁹⁵ (+)-fawcettimine,⁹⁶ and ventricosene⁹⁷ (Figure 19).

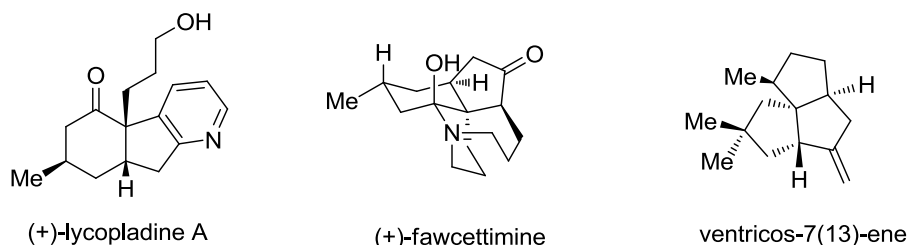


Figure 19. Natural products prepared by cationic gold(I) complexes.

The use of gold catalysts for the electrophilic gold-activation of the π -system of substrates such as alkenes, alkynes, and allenes has been intensely studied.^{64e, 92, 98, 99} The formation of cationic gold intermediate would allow the attack of nucleophiles such as carbon, nitrogen, and oxygen functional groups to form the desired products *via* intra- or intermolecular reactions.

Organophosphorus ligands can have a significant impact for increasing the regio- or stereoselectivity of reactions. Various chiral organophosphorus ligands have been investigated to provide enantiopure products. Moreover, chirality transfers from optically pure substrates in the presence of achiral catalysts have also been studied. This following section will present some illustrative transformations, especially the cycloisomerization reactions of 1,6-enynes, classified according to the nature of the nucleophile, and also the successful utilization of chiral phosphine ligands in these reactions to reach high enantioselectivity.

⁹² (a) A. S. K. Hashmi, *Chem. Rev.* **2007**, *107*, 3180–3211.; (b) G. Lemièrre, V. Gandon, N. Agenet, J.-P. Goddard, A. de Kozak, C. Aubert, L. Fensterbank, M. Malacria, *Angew. Chem. Int. Ed.* **2006**, *45*, 7596–7599.

⁹³ C. Nieto-Oberhuber, M. P. Muñoz, S. López, E. Jiménez-Núñez, C. Nevado, E. Herrero-Gómez, M. Raducan, A. M. Echavarren, *Chem. Eur. J.* **2006**, *12*, 1677–1693.

⁹⁴ C. Nieto-Oberhuber, M. P. Muñoz, E. Buñuel, C. Nevado, D. J. Cárdenas, A. M. Echavarren, *Angew. Chem. Int. Ed.* **2004**, *43*, 2402–2406.

⁹⁵ S.T. Staben, J. J. Kennedy-Smith, D. Huang, B. K. Corkey, R. A. LaLonde, F. D. Toste, *Angew. Chem. Int. Ed.* **2006**, *45*, 5991–5994.

⁹⁶ X. Linghu, J. J. Kennedy-Smith, F.D. Toste, *Angew. Chem. Int. Ed.* **2007**, *46*, 7671–7673.

⁹⁷ S. T. Staben, J. J. Kennedy-Smith, D. Huang, B. K. Corkey, R. A. LaLonde, F. D. Toste, *Angew. Chem. Int. Ed.* **2006**, *45*, 5991–5994.

⁹⁸ (a) L. Fensterbank, M. Malacria, *Acc. Chem. Res.* **2014**, *47*, 953–965.; (b) C. Aubert, L. Fensterbank, P. Garcia, M. Malacria, A. Simonneau, *Chem. Rev.* **2011**, *111*, 1954–1993.

⁹⁹ V. Gandon, G. Lemièrre, A. Hours, L. Fensterbank, M. Malacria, *Angew. Chem. Int. Ed.* **2008**, *47*, 7534–7538.

3.3.1. Cycloisomerization of 1,6-enynes in the absence nucleophile

The synthesis of five- or six-membered rings continues to draw attention due to a variety of relevant carbo- or heterocycles, which contain these structural units.^{100, 101} Pioneering catalytic reactions were studied by Trost and co-workers using $[\text{Ph}_3\text{PPd}(\text{OAc})_2]$ as a catalyst for a skeletal rearrangement of 1,6-enynes to prepare five-cyclic products.¹⁰² After these works, other transition metals such as ruthenium, rhodium, iridium, platinum, and gold were investigated, focusing on their reactivity and selectivity.¹⁰³ However, the mechanistic pathway depends on metals. In particular gold(I) catalysis exhibits unique features. The activation of 1,6-enynes by gold(I) proceeds by forming cyclopropyl metal carbenes *via* 5-*exo-dig* or 6-*endo-dig* processes. Echavarren and co-workers have studied more deeply the mechanism of this process on the basis of DFT calculations and labeling experiments (Scheme 25).^{51a} The catalytic reaction starts with gold coordinating to π -bond of alkyne (**A**). The π -alkene moiety then attacks the resulting electrophilic gold complex, generating cyclopropyl gold carbenes **B** *via* a 5-*exo-dig*¹⁰⁴ or **C** *via* a 6-*endo-dig*¹⁰⁵ cyclization processes, which depends on the nature of substrates.

¹⁰⁰ (a) B. M. Trost, *Chem. Soc. Rev.* **1982**, *11*, 141–170.; (b) T. L. B. Boivin, *Tetrahedron* **1987**, *43*, 3309–3362.

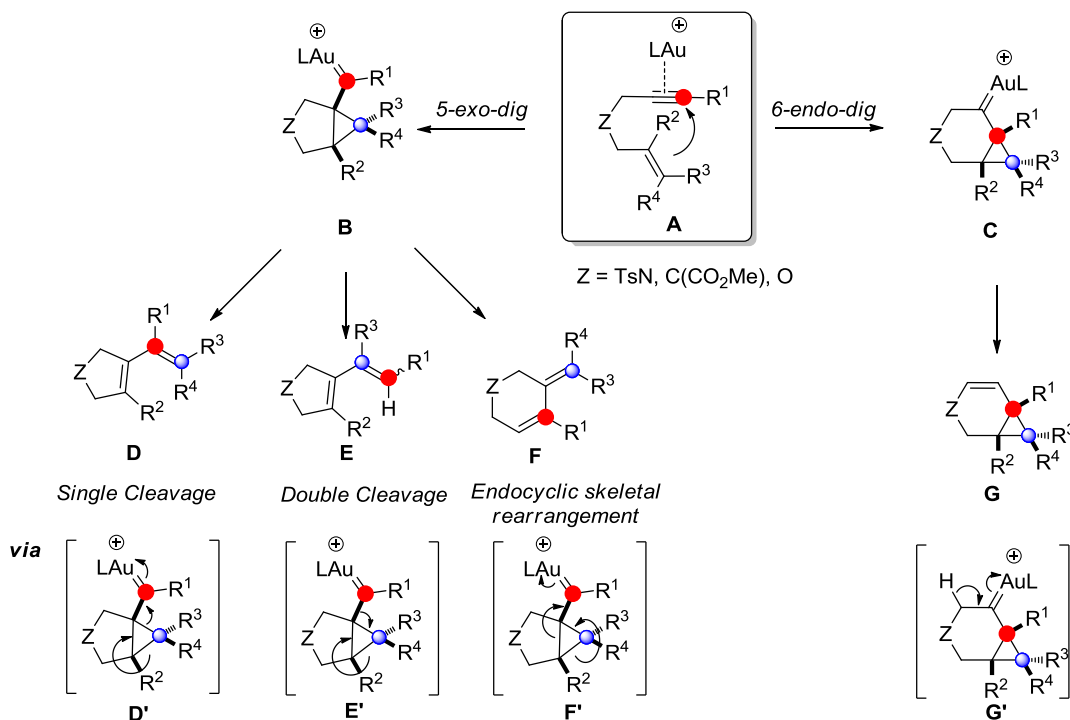
¹⁰¹ S. G. Sethofer, T. Mayer, F. D. Toste, *J. Am. Chem. Soc.* **2010**, *132*, 8276–8277.

¹⁰² B. M. Trost, M. Lautens, *J. Am. Chem. Soc.* **1985**, *107*, 1781–1783.

¹⁰³ For some reviews of Ru, see: (a) N. Chatani, T. Morimoto, T. Muto, S. Murai, *J. Am. Chem. Soc.* **1994**, *116*, 6049–6050. For Rh, see: (b) N. Chatani, K. Kataoka, S. Murai; N. Furukawa, Y. Seki. *J. Am. Chem. Soc.* **1998**, *120*, 9104–9105.; (c) K. Ota, N. Chatani, *Chem. Commun.* **2008**, 2906–2907.; (d) K. Ota, S. I. Lee, J.-M. Tang, M. Takachi, H. Nakai, T. Morimoto, H. Sakurai, K. Kataoka, N. Chatani, *J. Am. Chem. Soc.* **2009**, *131*, 15203–15211.; (e) S. Y. Kim, Y. K. Chung, *J. Org. Chem.* **2010**, *75*, 1281–1284. For Ir, see: (f) M. Barbazanges, M. Augé, J. Moussa, H. Amouri, C. Aubert, C. Desmarets, L. Fensterbank, V. Gandon, M. Malacria, C. Ollivier, *Chem. Eur. J.* **2011**, *17*, 13789–13794.; (g) E. Benedetti, A. Simonneau, A. Hours, H. Amouri, A. Penoni, G. Palmisano, M. Malacria, J.-P. Goddard, L. Fensterbank, *Adv. Synth. Catal.* **2011**, *353*, 1908–1912. For Pt, see: (h) N. Chatani, N. Furukawa, H. Sakurai, S. Murai, *Organometallics* **1996**, *15*, 901–903.; (i) A. Fürstner, F. Stelzer, H. Szillat, *J. Am. Chem. Soc.* **2001**, *123*, 11863–11869. For Au, see (j) M. Méndez, M. P. Muñoz, C. Nevado, D. J. Cárdenas, A. M. Echavarren, *J. Am. Chem. Soc.* **2001**, *123*, 10511–10520.

¹⁰⁴ C. Nieto-Oberhuber, S. López, M. P. Muñoz, D. J. Cárdenas, E. Buñuel, C. Nevado, A. M. Echavarren, *Angew. Chem. Int. Ed.* **2005**, *44*, 6146–6148.

¹⁰⁵ N. Cabello, E. Jiménez-Núñez, E. Buñuel, D. J. Cárdenas, A. M. Echavarren, *Eur. J. Org. Chem.* **2007**, *2007*, 4217–4223.



Scheme 25. The mechanistic process of gold(I)-catalyzed cycloisomerization of 1,6-enynes.

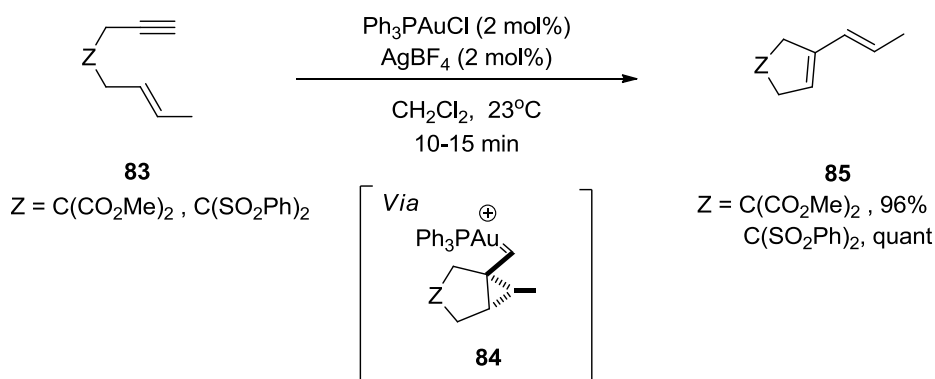
In the absence of nucleophiles, the intermediate **B** can evolve into the three possible products (**D**–**G**) *via* a skeletal rearrangement process. In the first case, the cyclopropylcarbene **B** undergoes cleavage of one C–C bond of the cyclopropane (**D'**), and then loses the cationic gold moieties [AuL⁺] *via* 1,2-H shift and demetalation to furnish the single cleavage product **D**. For a 1,6-enyne bearing methyl substituent (R¹ = Me, R^{2–4} = H), double cleavage was reported and consisted of a concerted dyotropic rearrangement of carbene **B**.¹⁰⁶ This process involves a 1,2-H shift of carbene **B**, concomitant with the cleavage of the C–C bond of the cyclopropane as in **E'** to eventually produce **E**. The last possibility consists of endocyclic skeletal rearrangement **F** through pathway **F'**. Unsubstituted enynes bearing weak electron-withdrawing substituents at the tether (R^{1–4} = H) favor this pathway. In the case of the 6-*endo-dig* rearrangement process,⁹⁴ cyclopropane **C** is able to undergo directly 1,2-H shift and demetalation to afford product **G**.

3.3.2.1. Skeletal rearrangements

In 2004, Echavarren and co-workers reported the gold(I)-catalyzed reactions of 1,6-enynes by using a cationic gold complex.⁹⁴ The enynes **83** activated by cationic gold complex underwent rearrangement through gold carbene intermediate **84** *via* a 5-*exo-dig* cyclization. The intermediate **84** was then rearranges in a single cleavage pathway, leading in good yields to 1,3-

¹⁰⁶ M. T. Reetz, *Angew. Chem. Int. Ed. Engl.* **1972**, *11*, 129–131.

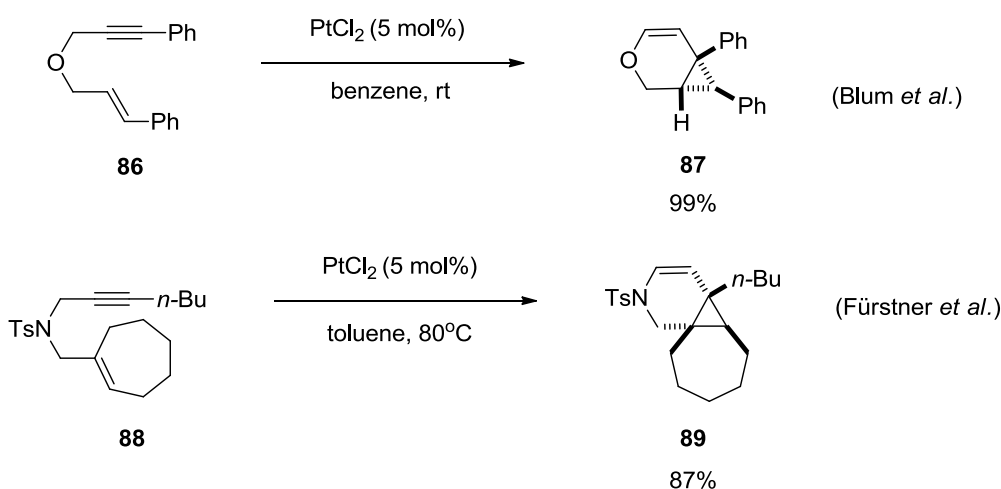
dienes **85** bearing malonate and sulfonyl groups (96% yield and quantitative respectively) (Scheme 26).



Scheme 26. Exo-skeletal rearrangement of 1,6-enynes **83**.

3.3.2.2. Cyclopropanation reactions

A pioneering study of rearrangement of an enyne-ether **86** was disclosed by the Blum group in 1995.¹⁰⁷ The reaction was run in the presence of platinum catalyst to afford bicycle[4.1.0]heptene derivative **87** in excellent yield. A few years later, Fürstner expanded the scope of substrates such as *N*-Tosyl-enyne **88** and came upon similar catalytic reactions *via* a 6-*endo-dig* cycloisomerization process to diastereoselectively afford tricyclic product **89** in 87% yield (Scheme 27).¹⁰⁸

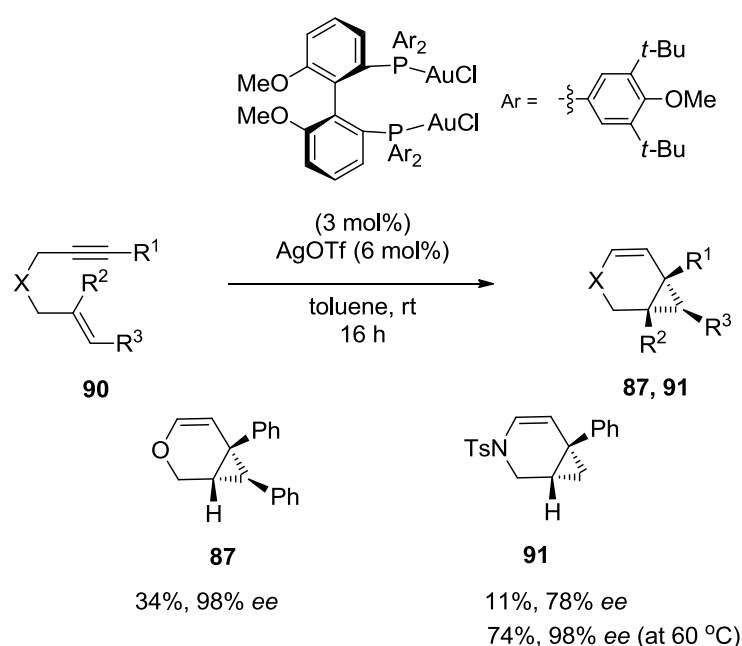


Scheme 27. Cyclopropanation of enynes **86** and **88** in the presence of platinum(II) catalyst.

¹⁰⁷ J. Blum, H. Beer-Kraft, Y. Badrieh, *J. Org. Chem.* **1995**, *60*, 5567–5569.

¹⁰⁸ A. Fürstner, H. Szillat, F. Stelzer, *J. Am. Chem. Soc.* **2000**, *122*, 6785–6786.

Gold(I) catalyst can also be engaged for these reactions. Concerning cyclopapane derivatives bearing stereogenic centers, Michelet and co-workers reported the use of chiral phosphine gold complexes as precatalysts for the preparation of enantiopure bicyclo[4.1.0]heptene derivative.¹⁰⁹ (*R*)-4-MeO-3,5-(*t*-Bu)₂-MeOBIPHEP(AuCl)₂ precatalyst associated with AgOTf provided an active cationic catalyst for the cyclization reactions of oxygen atom and *N*-Tosyl-1,6-enynes **90**. Although, the reactions afforded the product **87** and **91** in moderated yields (34% and 11%), this chiral ligand can induce excellent enantioselectivities of the reactions with 93% and 78% *ees* respectively. Moreover, in the case of *N*-Tosyl group tether (substrate **90**), the optimized reaction condition involved high temperature (60 °C). In that case, the reaction yielded 74% of product **91** with 98% *ee* (Scheme 28).



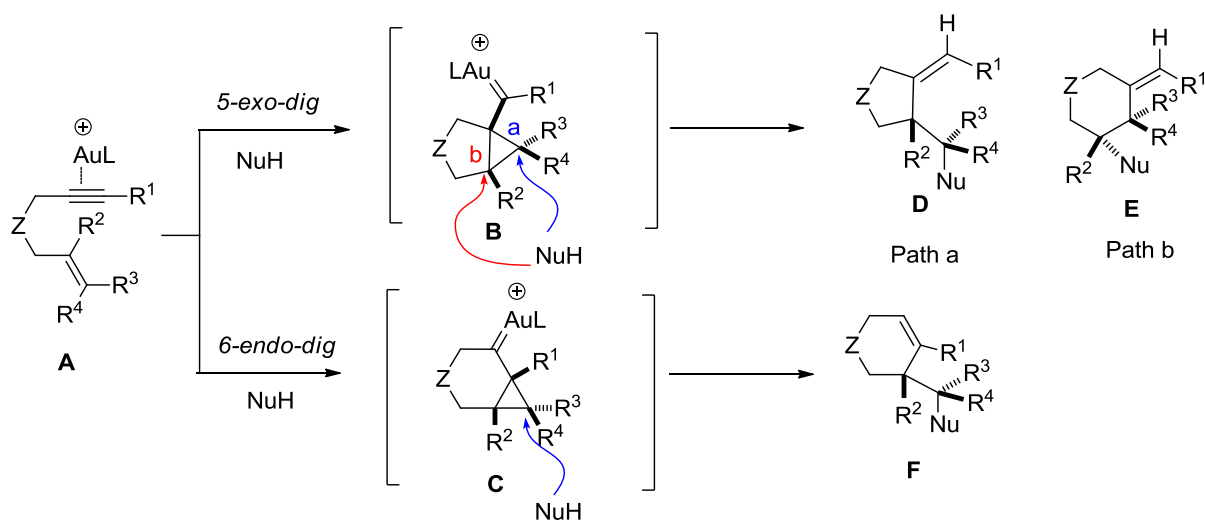
Scheme 28. Synthesis of bicyclo[4.1.0]heptene derivative **87** and **91**.

3.3.2. Cycloisomerization of 1,6-enyne in the presence of nucleophiles

Electron rich functions such as alkenes and congeners are valuable sources of nucleophiles, as found in enynes, diene-yne and allenenes. In the same manner, heteroatom nucleophiles, such as oxygen and nitrogen reagents, have been involved to attack the electrophilic gold intermediate to produce various heterocycles. The proposed reaction mechanism with 1,6-enynes in the presence of nucleophiles was also involved gold-carbene intermediates originating

¹⁰⁹ (a) C.-M. Chao, D. Beltrami, P. Y. Toullec, V. Michelet, *Chem. Commun.* **2009**, 6988.; (b) C.-M. Chao, M. R. Vitale, P. Y. Toullec, J.-P. Genêt, V. Michelet, *Chem. Eur. J.* **2009**, *15*, 1319–1323.

from *5-exo-dig* (**B**) or *6-endo-dig* (**C**) cyclization reactions. Nucleophiles can then attack cyclopropyl carbenes **B** or **C** to form cyclic products **D-F** (Scheme 29).⁹³ In the case of intermediate **B**, the nucleophilic attack on the cyclopropane carbene follows two pathways, whether in position a (path a) or in position b (path b). Subsequent protodeauration step liberates products **D** or **E**. In the case of cyclopropane intermediate **C**, it is generally attacked by a nucleophile in a single pathway to provide **F** after protodeauration.

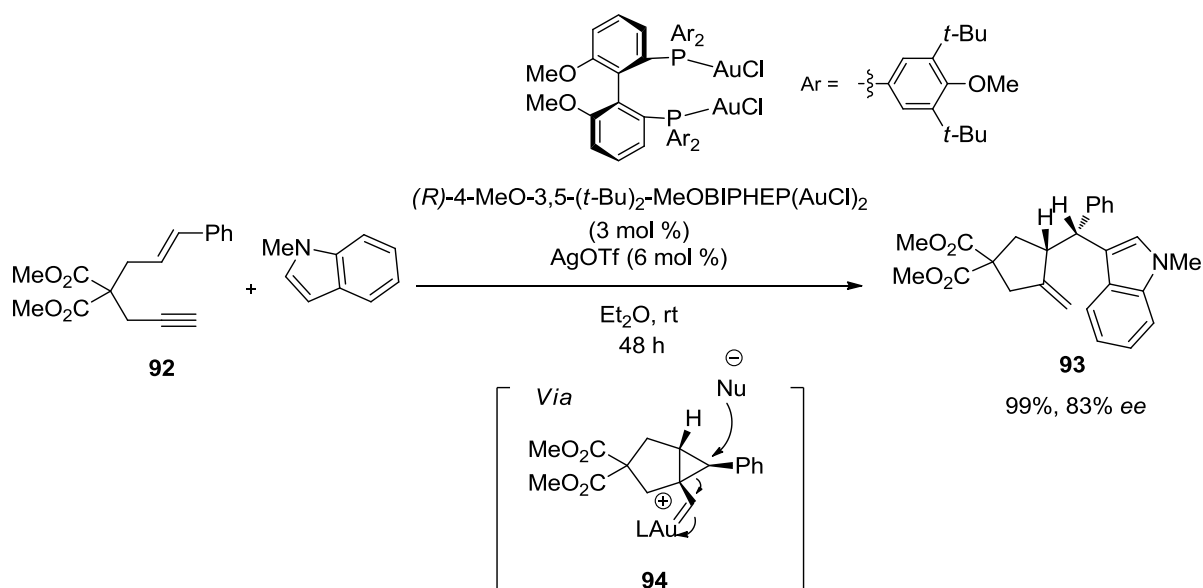


Scheme 29. Proposed mechanism of gold(I)-catalyzed reaction of 1,6-enynes in the presence of nucleophiles.

The following section will briefly deal with examples related to the use of carbon nucleophiles and heteroatom nucleophiles (O, N) in the catalytic reaction of 1,6-enynes. Moreover, different types of organophosphorus ligands have been involved to control regio- and enantioselectivities.

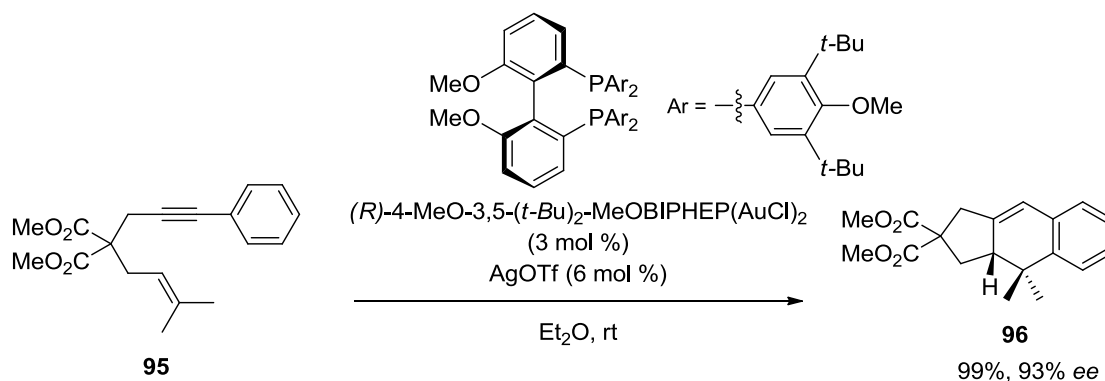
3.3.2.1. Addition of carbon nucleophile

Michelet and Echavarren groups have reported the successful addition of indoles such as 1-methylindole as an external carbon nucleophile to 1,6-enynes. In asymmetric reaction, Michelet used a gold complex bearing a chiral bisphosphine ligand, (*R*)-4-MeO-3,5-(*t*-Bu)₂-MeOBIPHEP(AuCl)₂, as a precatalyst.^{109b} As an example, the reaction of enyne **92** with methylindole provided cyclic product **93** in high yield (99%) and *ee* (93%), presumably *via* intermediate **94** (Scheme 30).



Scheme 30. Enantioselective gold(I)-catalyzed cyclization of 1,6-enyne **92**.

Intramolecular reactions of 1,6-enynes bearing aryl or alkenyl substituents produce formal [4+2] adducts. Using similar gold catalyst as before, the enantioselective cyclization of malonate enyne **95** afforded the tricyclic product **96** in excellent yield (99%) and enantioselectivity (93% ee) (Scheme 31).^{109b}

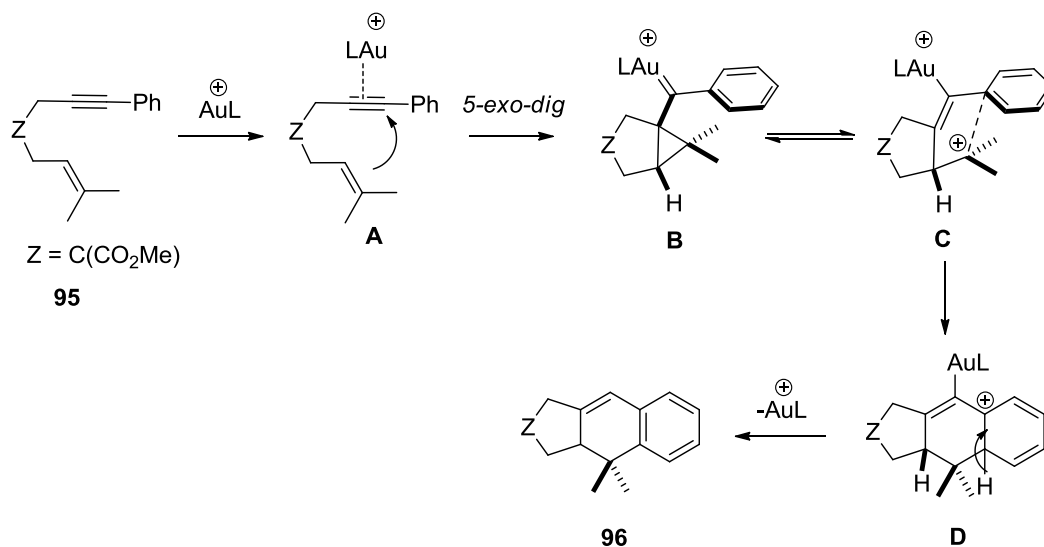


Scheme 31. Cycloisomerization of **95** with cationic gold complexes from (R) -4-MeO-3,5-(*t*-Bu)₂-MeOBIPHEP(AuCl)₂.

The mechanism was proposed on the basis of DFT calculations by Echavarren.^{51a, 110} After activation of cationic gold on alkyne bond (**A**), the malonate enyne **95** evolves into cyclopropylcarbene **B**. Its opening (**C**) leads to aryl-stabilized π -cation, where the stereochemical information of the double bond is retained. The intermediate **C** then underwent a Friedel-Crafts type reaction to form intermediate **D**. After rearomatization and protodeauration, the tricyclic

¹¹⁰E. Jiménez-Núñez, A. M. Echavarren, *Chem. Rev.* **2008**, *108*, 3326–3350.

product **96** bearing a stereogenic carbon was obtained (Scheme 32). This methodology has been applied to the polycyclization reaction of polyene-yne.¹⁰¹



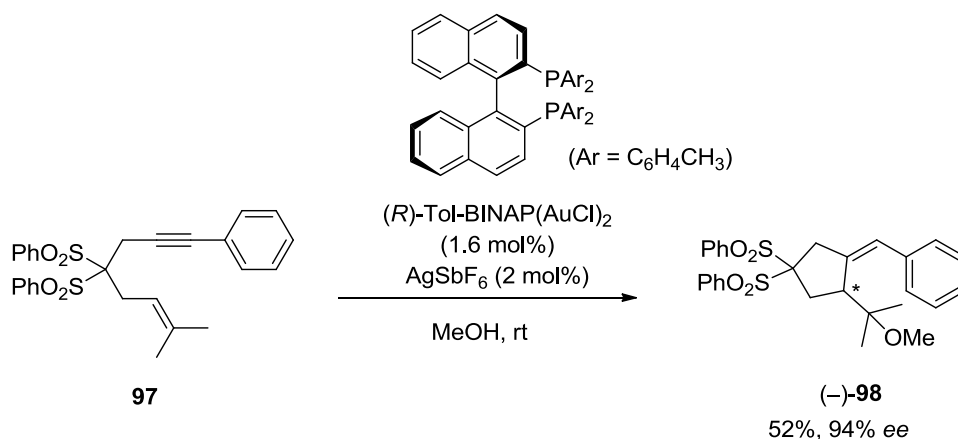
Scheme 32. Proposed mechanism of gold(I)-catalyzed cycloisomerization of enyne **95**.

3.3.2.2. Addition of oxygen and nitrogen nucleophiles

Alkoxy- and hydroxycyclization of 1,6-enynes have been readily reported by Echavarren in the presence of platinum dichloride in refluxing methanol.^{111, 112} The cationic gold complexes are the most competitive catalysts, which can produce similar products, giving clean reactions at room temperature.^{29, 93} Naturally, asymmetric versions have been developed. As an example by the Echavarren group relied on the use of chiral (*R*)-Tol-BINAP(AuCl), which was activated by silver salt (AgSbF₆) and used to catalyze the enyne **97** in the presence of methanol at room temperature (Scheme 33). An asymmetric gold-catalyzed alkoxycyclization reaction *via* a 5-*exo-dig* cyclization took place, giving cyclic product **98** in good yield and *ee* (94%).²⁹

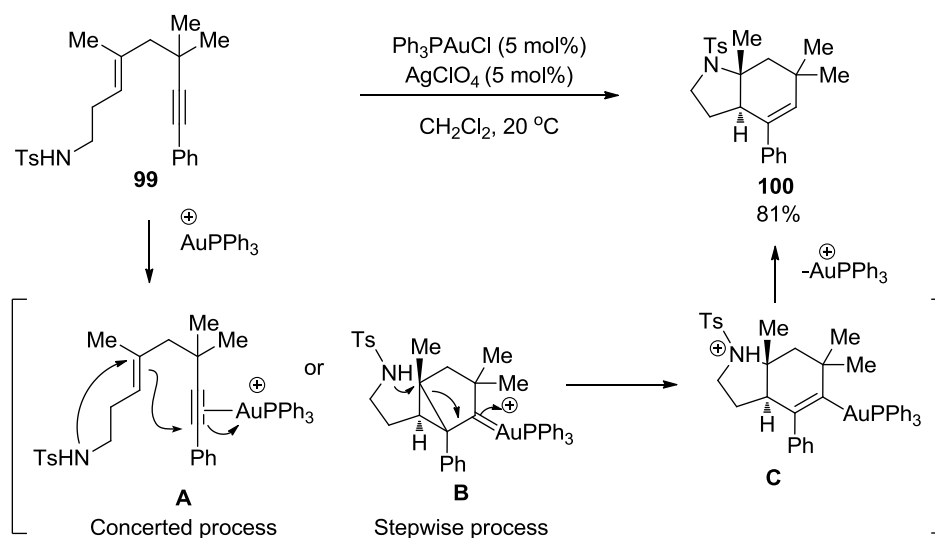
¹¹¹ M. Méndez, M. P. Muñoz, C. Nevado, D. J. Cárdenas, A. M. Echavarren, *J. Am. Chem. Soc.* **2001**, *123*, 10511–10520.

¹¹² M. Méndez, M. P. Muñoz, A. M. Echavarren, *J. Am. Chem. Soc.* **2000**, *122*, 11549–11550.



Scheme 33. Enantioselective alkoxyacyclization of enyne **97** with (R) -Tol-BINAP(AuCl)₂.

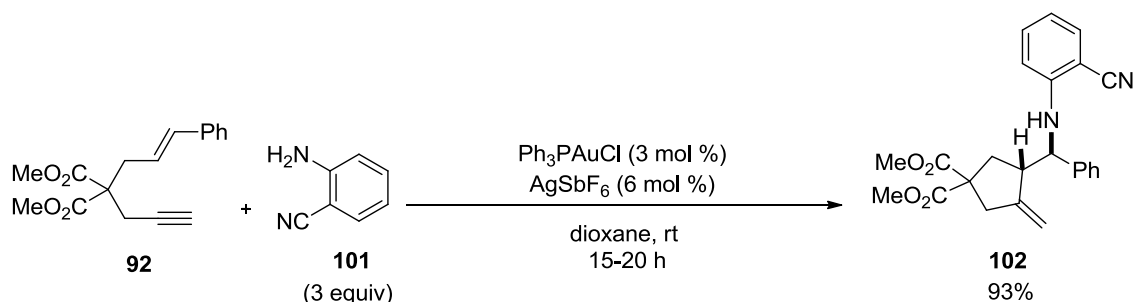
Pioneering work in gold catalysis featured the intramolecular gold(I)-catalyzed aminocyclization reactions of 1,5-enynes to form hetero-bicyclic products by Zhang and Kozmin in 2005.¹¹³ When treated by a 1:1 mixture of Ph₃PAuCl and AgClO₄, enyne-sulfonamide **99** furnished *trans*-oxabicyclo[4.3.0]nonenes **100** with excellent diastereoselectivity (Scheme 34). To get more insight into the mechanism, they proposed two possible pathways for double cyclization process. These could be either a concerted pathway (**A**) or a stepwise route (**B**). The pathway **A** would consist in an *anti*-addition to the activated alkyne from the nucleophilic alkene and concerted addition of the amine on the alkene. In contrast, the stepwise route (**B**) involves the nucleophilic opening of cyclopropyl gold carbene **B**. Both lead to bicyclic gold intermediate **C**. Consecutive proton loss and protodeauration of **C** yields to the bicyclic product, obtained as a single diastereomer **100** without side-product.



Scheme 34. Gold(I)-catalyzed reactions of 1,5-enynes sulfonamide **99**.

¹¹³ L. Zhang, S. A. Kozmin, *J. Am. Chem. Soc.* **2005**, *127*, 6962–6963.

The Michelet group reported a hydroamination/cyclization reaction closely related to alkoxy cyclization using external amino nucleophiles.¹¹⁴ For example, the same enyne **92** was used as a model substrate in this line. Similar mechanistic pathway to alkoxy cyclization reaction in the presence of cationic gold(I) with the external amine **101** afforded product **102** in excellent yield (93%) (Scheme 35).



Scheme 35. Gold(I)-catalyzed hydroamination/cycloisomerization reaction of enyne **92**.

4. Conclusion and perspective

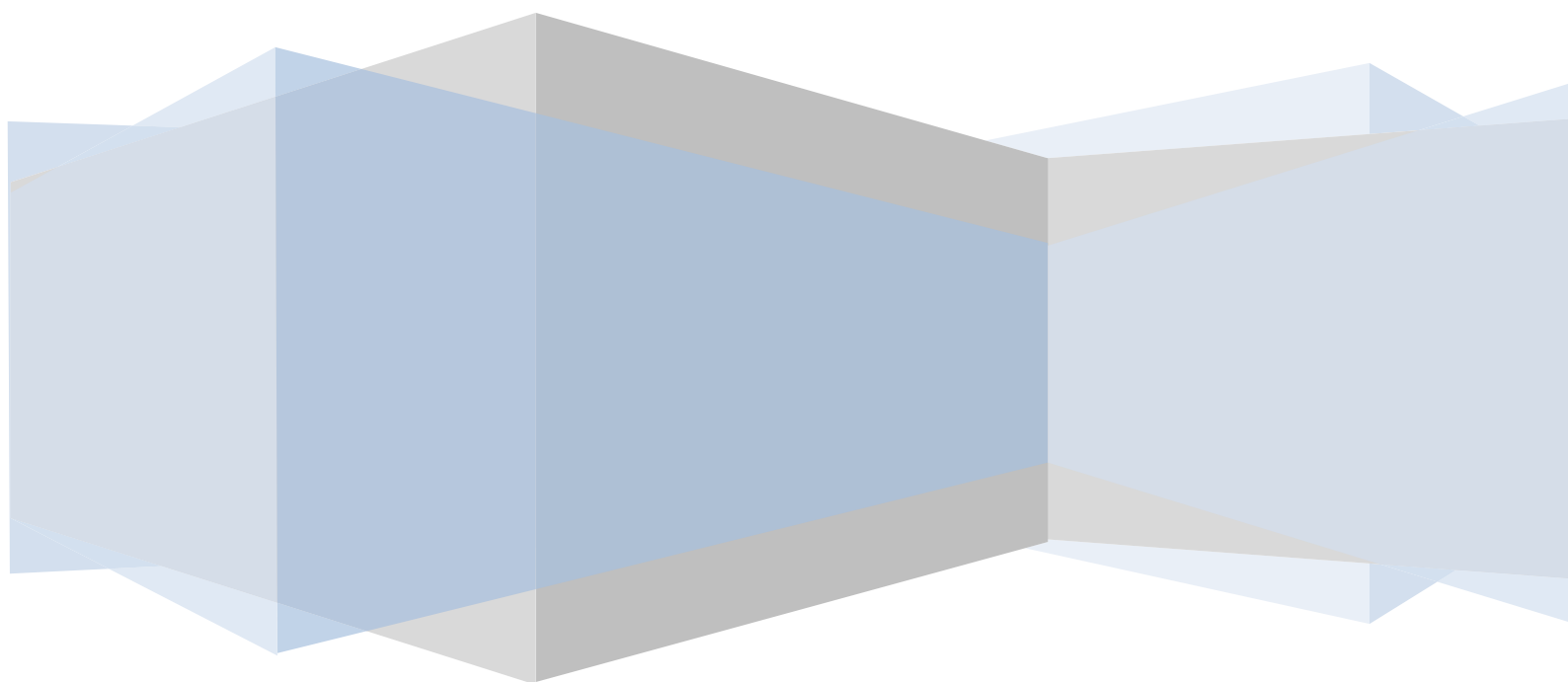
Organophosphorus compounds have raised considerable interest as ligands in metal-coordination and have been utilized in a variety of catalytic reactions. The regio- and enantioselectivity of catalytic reactions can be induced by these chiral ligands. Their oxides are also active as organocatalysts in asymmetric reactions. In the field of gold chemistry, the organophosphorus compounds are usually used as monodentate or bidentate ligands of gold(I) species *via* an interaction of the P-donor atom with the gold atom. Organogold complex bearing phosphorus moieties were isolated and determined by X-ray crystallography in order to understand the coordination mode and investigate them in catalytic reactions.

We have seen in this section through several examples that the nature of the organophosphorus ligands plays a significant role to improve the selectivity of the reactions and notably their enantioselectivity. For instance, C_2 -Symmetrical bisphosphine ligands such as chiral BINAP and their analogues have successfully provided products with high *ees* in gold catalytic reactions. To extent the scope of chiral phosphine ligands, we aimed to design new axially chiral ligands, which possess C_2 -Symmetry. These will be developed in Chapter 3 and 4.

¹¹⁴ L. Leseurre, P. Y. Toullec, J.-P. Genêt, V. Michelet, *Org. Lett.* **2007**, *9*, 4049–4052.

Chapter 2

Allene Syntheses and Applications



CHAPTER 2

Allene Syntheses and Applications

1. Introduction

Allenes are known as valuable building blocks towards the total synthesis of complex molecular targets. Their intrinsic and original properties allow the access to novel applications in the synthesis of a variety of industrial and biologically active products. The allene motif has also been found in over 150 biologically active natural compounds, such as an insect pheromone and *anti*-fungal activity, as well as marketed drugs such as Enprostil[®], Fenprostalene[®], and Prostalene[®] (Figure 20).^{115, 116} The allene is unique unsaturated hydrocarbon in comparison with an alkene and alkyne, due to the 1,2-diene-based axial chirality. The structure is composed of a central *sp*-hybridized carbon, which forms two orthogonal double bonds bearing terminal *sp*²-hybridized carbons. The orthogonal π -systems prevent the conjugation between these cumulated double bonds.¹¹⁷ Because of the non-free rotation of the double bonds, allenes are molecules that can present an axial chirality (*C*₂-Symmetry). Notably the axial chirality property sets them apart from all other functional groups and results in their incorporation in new methodologies both as racemic and valuable chiral building blocks. The ongoing interest in allene chemistry is demonstrated by the development of numerous catalytic methodologies in either racemic or enantioenriched forms. In this chapter, we will present a general overview of the recent methodologies for the synthesis of allenes, as well as their applications in catalysis.

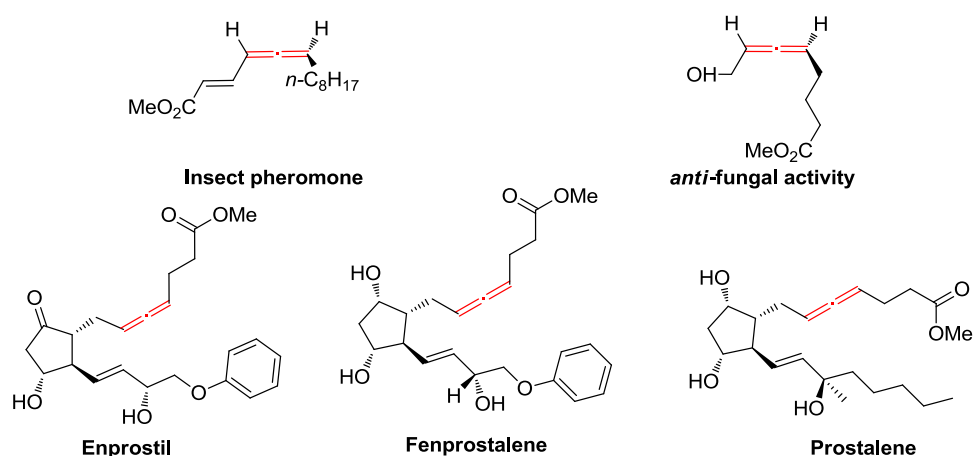


Figure 20. Allene derivatives in biologically active natural compounds and marketed drugs.

¹¹⁵ N. Krause, A. S. Hashmi, *Modern Allene Chemistry*, Wiley-VCH, Weinheim, **2004**, 997–1039.

¹¹⁶ R. K. Neff, D. E. Frantz, *ACS Catal.* **2014**, *4*, 519–528.

¹¹⁷ J. Clayden, *Organic Chemistry*, Oxford University Press, Oxford ; New York, **2012**.

2. General synthesis of allenes

Allene was firstly disclosed the correct structure and its axial chirality in 1875 by Van't Hoff.¹¹⁸ This allowed chemists to propose new synthetic methodologies. Until 1887, Burton and Pechmann reported the first synthesis of an allene, called Glutinic acid (Figure 21).¹¹⁹ However, the paucity of analytical technique makes it difficult to distinguish from the corresponding alkynes. In 1954, Jones and co-workers confirmed and identified this allene's structure.¹²⁰ In addition, the discovery of naturally occurring allene is Pyrethrolone (Figure 21), which was isolated from Pyrethrum flowers by Staudinger and Ruzicka in 1924.¹²¹



Figure 21. Glutinic acid and Pyrethrolone.

Recently, a variety of preparative methodologies have been developed to access substituted allenes. They can be obtained using several classical reactions (addition, elimination, substitution, rearrangement), including transition metal mediated processes. In this manuscript, some interesting synthetic methodologies for the preparation of allenes have been reviewed according to three principal types of reactions.

2.1. Organometallic reagents for allene formation

The use of organometallic reagents is a very common approach for the synthesis of a large variety of allenes. This part deals with the use of stoichiometric amounts of organometallic reagents for the generation of allenic target molecules. The fundamental reactions suitable for metal-mediated syntheses of allenes are generally S_N2' nucleophilic substitution reactions of propargylic electrophile **1**, as well as 1,4-additions to enyne substrate **2**, and 1,6-addition reaction to acceptor-substituted enyne **3** (Scheme 36).¹²²

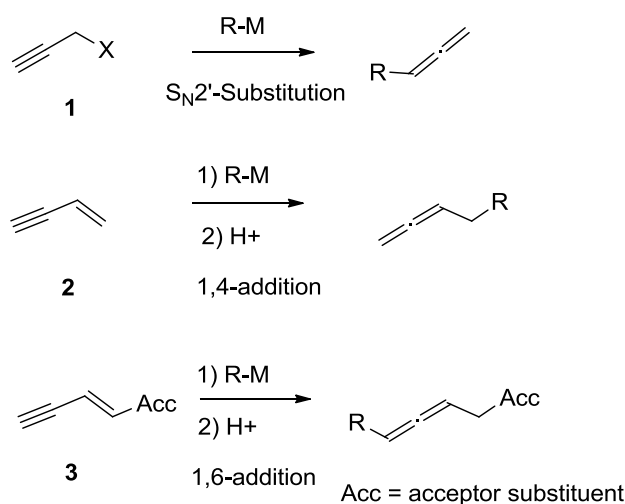
¹¹⁸ J. H van't Hoff, *La Chimie dans l'Espace*; Bazendijk: Rotterdam, **1875**, 29.

¹¹⁹ B. S. Burton, H. von Pechmann, *Ber. Dtsch. Chem. Ges.* **1887**, *20*, 145–149.

¹²⁰ E.R.H. Jones, G.H. Mansfield, M.L.H. Whiting *J. Chem. Soc.* **1954**, 3208–3212.

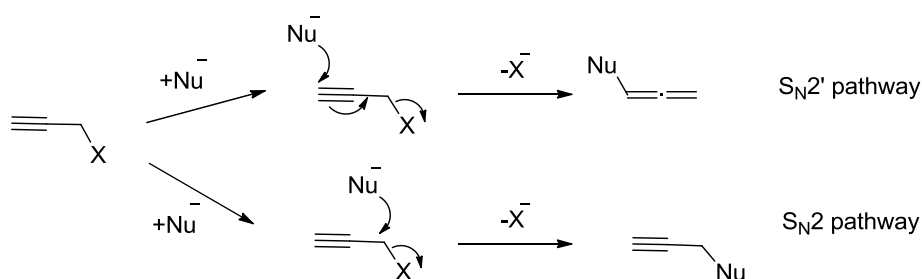
¹²¹ H. Staudinger, L. Ruzicka, *Helv. Chim. Acta.* **1924**, *7*, 177–201

¹²² N. Krause, A. Hoffmann-Röder, *Tetrahedron* **2004**, *60*, 11671–11694.



Scheme 36. Metal-mediated reactions for allene synthesis.¹²²

Herein, we focus on the use of basic organometallic reagents based on organolithium, organocopper, and aluminum (DIBAL-H and LiAlH_4). The reagents effectively in either addition or substitution reactions. In the case of substitution reactions, two possible nucleophilic substitutions can be involved, according to $\text{S}_{\text{N}}2$ or $\text{S}_{\text{N}}2'$ pathways. However only $\text{S}_{\text{N}}2'$ pathway can afford the formation of allenes *via* nucleophilic addition (Nu^-) and subsequent elimination of the leaving group. The organometallic reagent plays the role of the nucleophile which adds to the alkyne bond (Scheme 37).



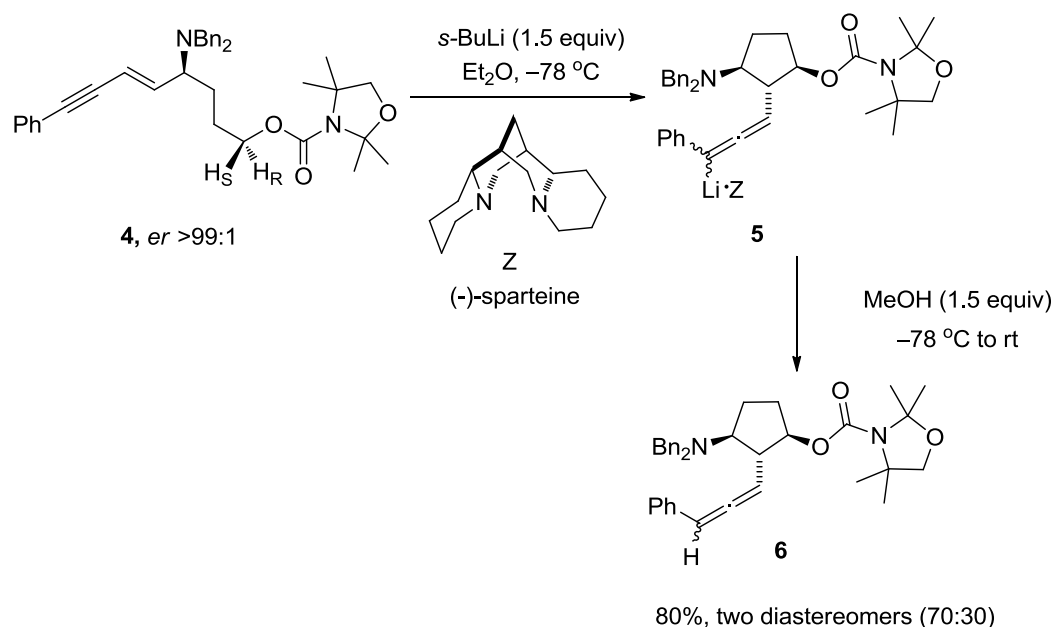
Scheme 37. Formation of allenes by substitution reactions.

2.1.1. Organolithium reagents

There are a few examples of $\text{S}_{\text{N}}2'$ substitution reactions of propargylic electrophiles with organolithium reagents. One example reported by Oestreich and Hoppe describes the 1,4-addition of organolithium derivatives to conjugated enynes.¹²³ They reported the enantioselective deprotonation of the enyne carbamate **4** with *sec*-butyllithium in the presence of (–)-sparteine.

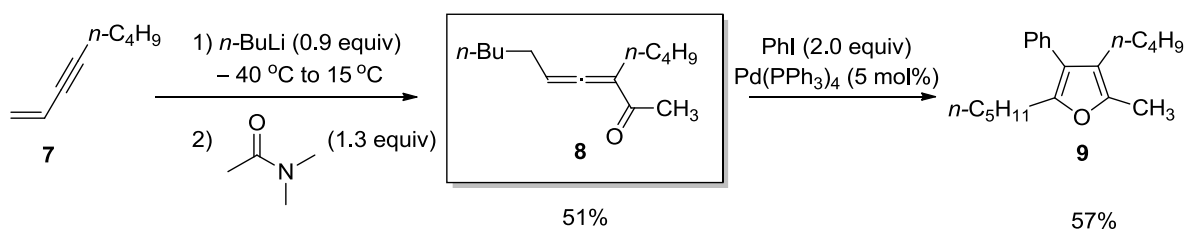
¹²³ M. Oestreich, D. Hoppe, *Tetrahedron Lett.* **1999**, *40*, 1881–1884.

The chiral (–)-sparteine can promote the stereoselective intramolecular cyclization process. As a result, stereoselective abstraction of the H_S atom allows the corresponding organolithium intermediate to undergo an enantioselective intramolecular 1,4-addition onto the enyne pattern. The diastereomeric allenyl lithium species **5** was formed. Subsequent protonation with MeOH furnishes the two diastereomeric allenes **6**. (Scheme 38)



Scheme 38. Enantioselective intramolecular 1,4-addition of enyne carbamate ester **4**.

In 2003, the 1,4-addition of organolithium reagents was also reported by the Zhang group.¹²⁴ α,γ -Disubstituted-1,2-allenylketone (**7**) was prepared by one-pot stepwise reactions of an enyne derivatives with an alkyl lithium reagents such as *n*-butyllithium followed by the addition of an *N,N*-dimethyl formamide. The corresponding product **8** is valuable substrate that can be used to generate the 2,3,4,5-tetrasubstituted furan derivative **9** via Pd(PPh₃)₄-catalyzed cyclization with iodobenzene as shown in Scheme 39.

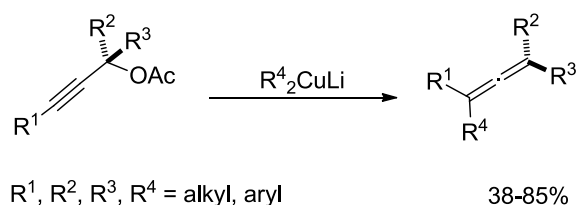


Scheme 39. Synthesis of 1,2-allenyl ketone **8**.

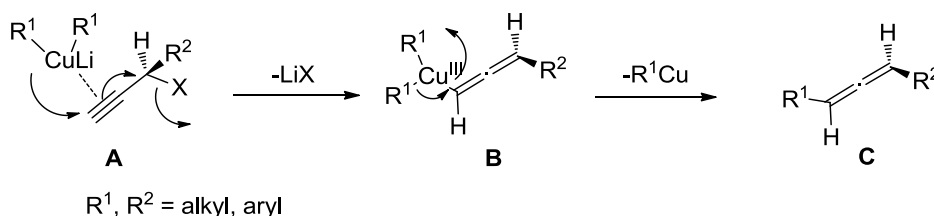
¹²⁴ S. Ma, J. Zhang, L. Lu, *Chem. Eur. J.* **2003**, *9*, 2447–2456.

2.1.2. Organocopper reagents

Organocopper reagents are usually prepared *via* stoichiometric transmetalation of the corresponding organolithium or organomagnesium derivatives. Pioneering work in 1968 by Rona and Crabbé¹²⁵ demonstrated the efficiency of copper-mediated S_N2' substitution processes. The reaction of propargylic acetates with lithium dialkylcuprates led to the formation of allenes with moderate to good yields (Scheme 40). The proposed mechanism involves an organocopper(III) intermediate. The *in-situ* generated organocuprate would first coordinate to the acetylenic moiety of the propargylic derivatives to form a copper (III) π -complex **A**, which would evolve to the formation of the σ -organocopper(III) intermediate **B** after antiperiplanar elimination of the leaving group ($X = \text{OAc}, \text{OMe}, \text{etc.}$)¹²⁶. Finally, the intermediate **B** undergoes a reductive elimination of an alkyl group to furnish the *anti*-substituted allene **C** (Scheme 41).



Scheme 40. Synthesis of allenes *via* organocuprate S_N2' substitution.



Scheme 41. Mechanistic model for *anti*-stereoselective S_N2' substitution.

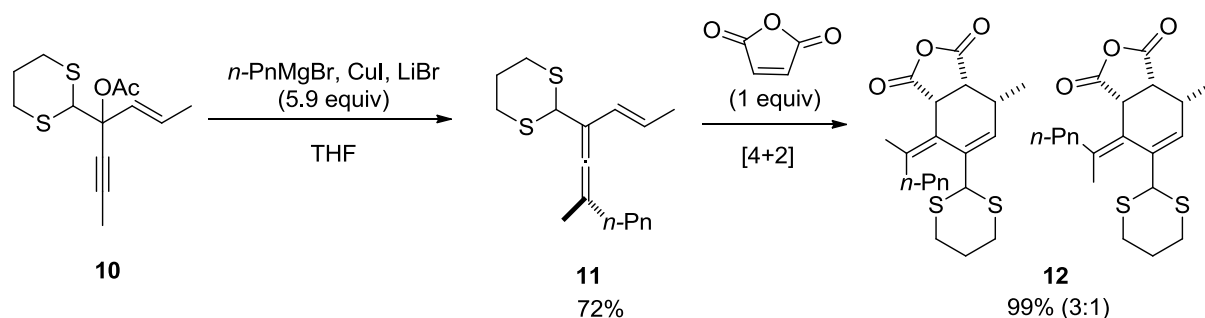
The organocopper-mediated substitution reactions have been constantly applied in synthetic methodology, notably for the development of stereoselective synthesis. One application of the copper-promoted S_N2' stereoselective reaction was developed by the Spino group in 1998.¹²⁷ The reaction of propargylic acetate **10** bearing an alkene moiety in the presence of organocuprate, prepared from a mixture of *n*-pentylmagnesium bromide and CuI/LiBr, afforded the desired vinylallene **11** in high yield (72%) (Scheme 42). The latter can be used as substrates for

¹²⁵ P. Rona, P. Crabbé, *J. Am. Chem. Soc.* **1968**, *90*, 4733–4734.

¹²⁶ For some examples of methoxyl (OMe) leaving group, see: (a) I. Marek, P. Mangeney, A. Alexakis, J. F. Normant, *Tetrahedron Lett.* **1986**, *27*, 5499–5502.; (b) A. Alexakis, I. Marek, P. Mangeney, J. F. Normant, *J. Am. Chem. Soc.* **1990**, *112*, 8042–8047. For various leaving groups, see: (c) L. I. Olsson, A. Claesson, L. E. Thornell, *Acta Chem. Scand.* **1979**, *33b*, 679–684.

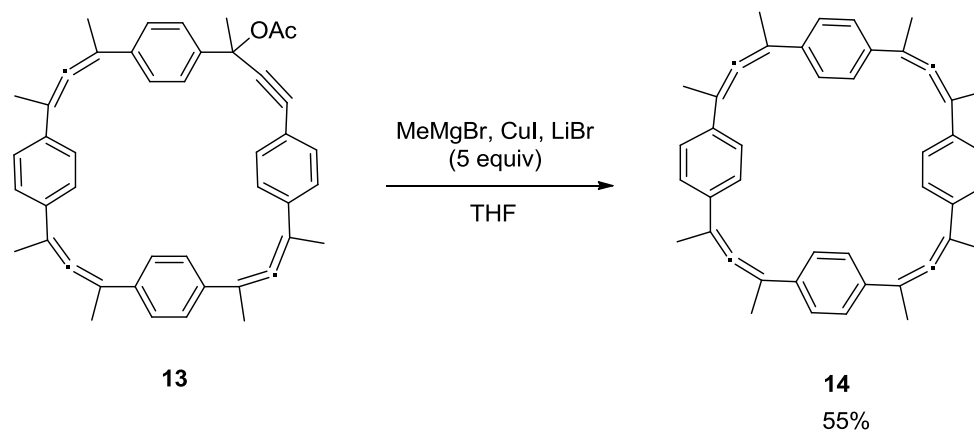
¹²⁷ C. Spino, C. Thibault, S. Gingras, *J. Org. Chem.* **1998**, *63*, 5283–5287.

[4+2]-cycloaddition reactions to generate the corresponding stereoselective tetrasubstituted exocyclic alkenes **12**.



Scheme 42. Synthesis of vinylallene **11** for [4+2]-cycloaddition.

Interestingly, the synthesis of allenic macrocycles is also reported *via* the use of organocopper reagents. Krause and co-workers presented the synthesis of [3₄] Allenophan (**14**) with four allenic bridges.¹²⁸ They were successively formed through the S_N2' substitution reaction of propargylic acetate **13** with methylmagnesium cuprate (Scheme 43).

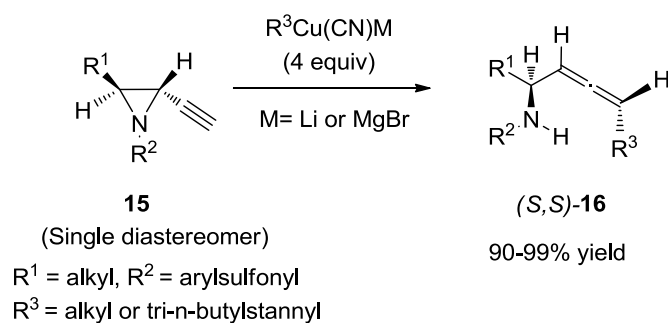


Scheme 43. Synthesis of [3₄] Allenophan (**14**)

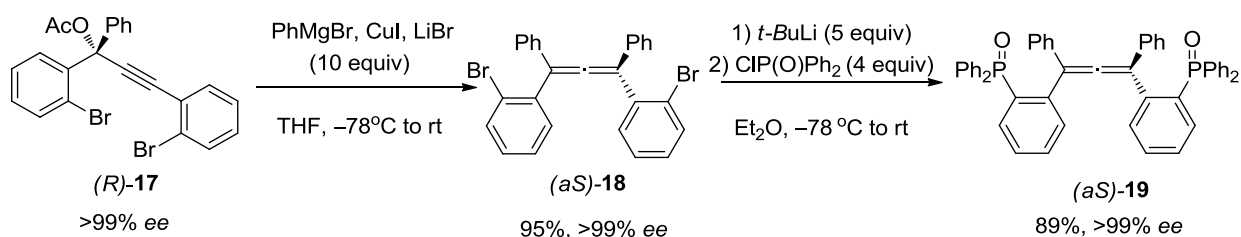
The organocopper-mediated substitution reactions have been constantly applied in synthetic methodology, notably for the development of stereoselective synthesis. For example, some chiral amino allenes were synthesized by the Ohno group in 2000.¹²⁹ These chiral amino allenes were prepared from single diastereomeric 3-alkyl-2-ethynylaziridines. The reaction of (2*R*,3*S*)-2,3-*trans*-3-alkyl-2-ethynylaziridines **15** with organocyanocuprates (RCu(CN)M, M=Li or MgX) afforded the chiral (*S,S*)-amino-allenes **16** in excellent yields (90-99%) and a stereoselective manner *via anti*-S_N2' nucleophilic addition (Scheme 44).

¹²⁸S. Thorand, F. Vögtle, N. Krause, *Angew. Chem.* **1999**, *111*, 3929–3931.

¹²⁹H. Ohno, A. Toda, N. Fujii, Y. Takemoto, T. Tanaka, T. Ibuka, *Tetrahedron* **2000**, *56*, 2811–2820.

Scheme 44. Synthesis of (*S,S*)-amino allenes **16** from (*2R,3S*)-**15**.

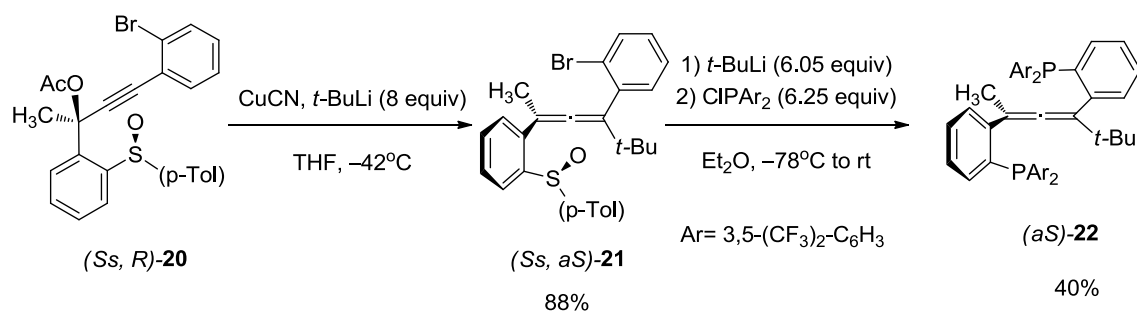
Phosphines bearing an allene moiety have been recently discovered as new ligands. In 2009, Ready presented the synthesis of allenes with bisphosphine oxide substituents.¹³⁰ The involved organocopper, which was generated from the mixture of phenylmagnesium bromide, CuI and LiBr, underwent the S_N2' substitution on the propargylic acetate (*R*)-**17** to afford a bis(2-bromobenzene) allene (*aS*)-**18**. Subsequent treatment with *tert*-butyllithium and chlorodiphenyl phosphine oxide furnished allene (*aS*)-**19** bearing diphenylphosphine oxides in 95% yield (Scheme 45). The allene was then applied as organocatalyst in the ring-opening reaction of *meso*-epoxides to generate chiral alcohol derivatives.

Scheme 45. Synthesis of allene (*aS*)-**19**.

In a similar fashion, the same group has also developed the synthesis of allenes with bisphosphine groups in 2011.¹³¹ The reaction involves an organocyanocuprate reagent, prepared from CuCN and *tert*-butyllithium, and an enantiomerically pure propargylic acetate **20** to form allenyl sulfoxide **21**. In the second step, chlorodiphenylphosphine is used as electrophile reagent after treatment with *tert*-butyllithium to yield 40% of chiral allene **22** bearing diphenylphosphines (Scheme 46). This allene could be employed as a chiral ligand of rhodium(I) species in order to generate new chiral organometallic catalyst that has shown reactivity in enantioselective rhodium(I)-catalyzed addition of arylboronic acids to α -keto esters.

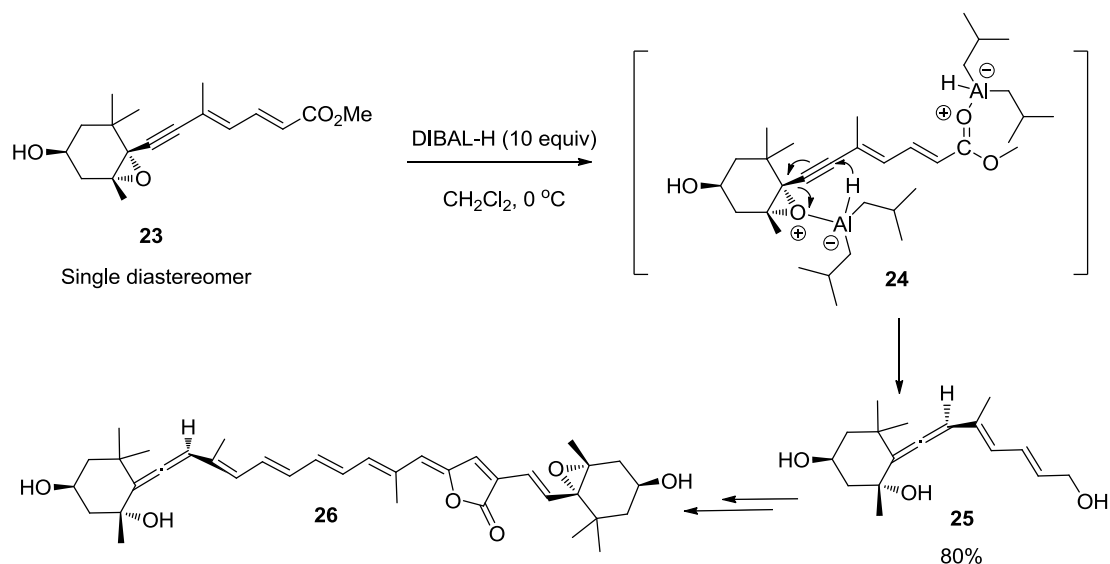
¹³⁰ X. Pu, X. Qi, J. M. Ready, *J. Am. Chem. Soc.* **2009**, *131*, 10364–10365.

¹³¹ F. Cai, X. Pu, X. Qi, V. Lynch, A. Radha, J. M. Ready, *J. Am. Chem. Soc.* **2011**, *133*, 18066–18069.

Scheme 46. Synthesis of allenes bearing bisphosphine moieties (*aS*)-**22**.

2.1.3. Aluminum reagents

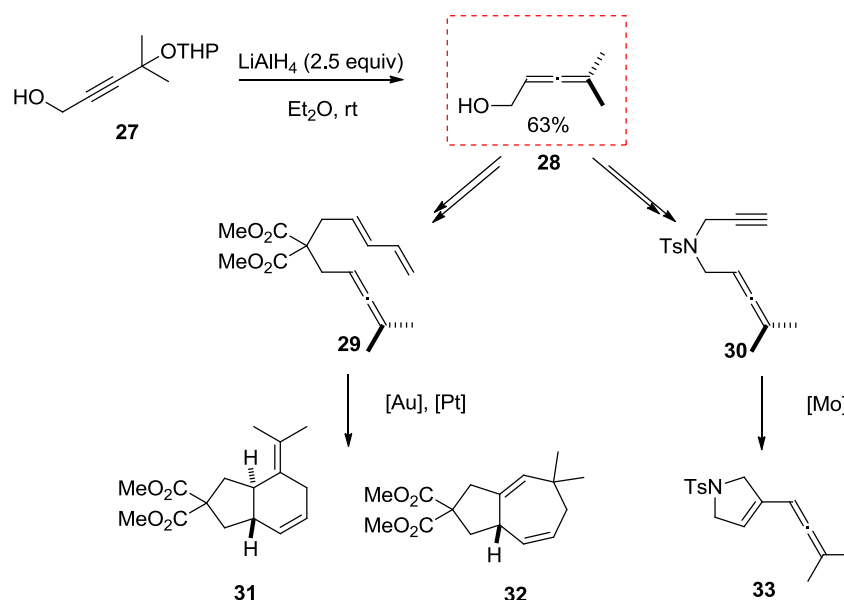
Aluminum reagents are applied as aluminum-based Lewis acids for carbon-hydrogen bond formation of the propargylic substrates. These reagents, such as LiAlH₄ and DIBAL-H, can produce various allenes from propargylic electrophiles such as alcohols, ethers, halides, etc. For example, Katsumura and co-workers reported the preparation of allylic hydroxyallene substrates for the total synthesis of the polyfunctional carotenoid peridinin (**26**).¹³² DIBAL-H was used in stereospecific S_N2' reduction of optically pure conjugated ethynylepoxyde derivative **23** via proposed formation of aluminum intermediate **24**. The reaction could produce allenyl-triol derivative **25** with 80% yield (Scheme 47).

Scheme 47. Synthesis of allenyl-triol derivative **25** for carotenoid peridinin **26**.

Another example is the synthesis of allene-diene derivatives such as malonate- and *N*-Tosyl-bridged allenyne has been recognized as versatile substrates in metal-catalyzed cyclization

¹³² N. Furuichi, H. Hara, T. Osaki, H. Mori, S. Katsumura, *Angew. Chem. Int. Ed.* **2002**, *41*, 1023–1026.

reactions, such as gold,¹³³ platinum,¹³⁴ and molybdenum¹³⁵ catalysts. According to Murakami's report,¹³⁵ dimethyl substituted- α -allenol **28** was successfully prepared from a propargylic alcohol **27** by LiAlH_4 reagent (Scheme 48). Subsequent modifications of this allene substrate **28** allowed the access to substrates **29** and **30** that could undergo cycloisomerization reactions to afford the corresponding cyclic products **31-33**.



Scheme 48. Synthesis of allene **29** and **30** from **28** using LiAlH_4 reagent.

2.2. Metal-catalyzed allene formation

As presented above, the synthetic methodology based on the use of organometallic reagents has been considered for the preparation of the allenes. However, in some cases direct substitution of the propargylic substrates by way of a $\text{S}_{\text{N}}2$ pathway may compete with the $\text{S}_{\text{N}}2'$ displacement. The transition metal-catalyzed coupling reaction has been developed to obtain high levels of regioselectivity.

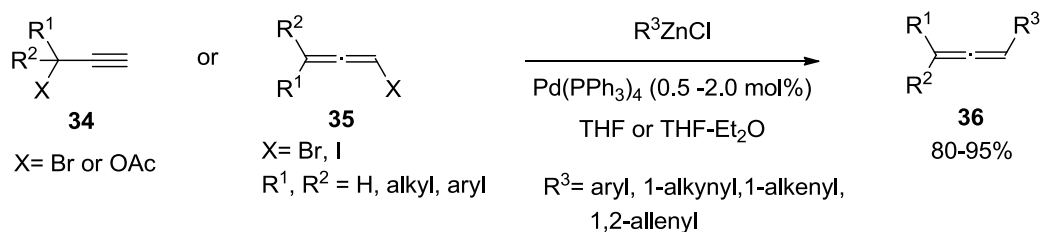
Palladium complexes are often used to prepare allenes. Pioneering report of palladium-catalyzed reaction was presented by Vermeer in 1981.¹³⁶ The reaction of propargylic halides/acetates **34** or allenic halides **35** with organozinc reagents could afford allenes **36** in excellent yields (80-95%). This coupling reaction led to understand the mechanism and to further extend the methodology to substituted allenes (Scheme 49).

¹³³ P. Mauleón, R. M. Zeldin, A. Z. González, F. D. Toste, *J. Am. Chem. Soc.* **2009**, *131*, 6348–6349.

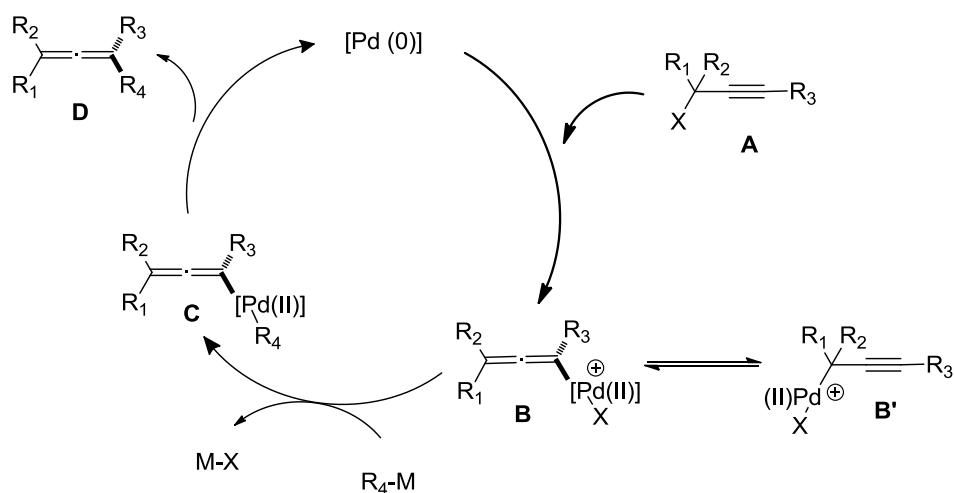
¹³⁴ B. Trillo, F. López, M. Gullías, L. Castedo, J. L. Mascareñas, *Angew. Chem. Int. Ed.* **2008**, *47*, 951–954.

¹³⁵ M. Murakami, S. Kadowaki, T. Matsuda, *Org. Lett.* **2005**, *7*, 3953–3956.

¹³⁶ K. Ruitenbergh, H. Kleijn, C. J. Elsevier, J. Meijer, P. Vermeer, *Tetrahedron Lett.* **1981**, *22*, 1451–1452.

Scheme 49. Palladium(0)-catalyzed reaction of the synthesis of **36**.

For the proposed mechanism as shown in Scheme 50, catalytic amounts of tetrakis(triphenylphosphine)palladium [Pd(PPh₃)₄] activate on propargylic derivatives **A** via an oxidative addition process to form palladium complex **B'**, following isomerized to form (σ-allenyl)-palladium(II) intermediate **B** in equilibrium. The intermediate **B** then reacts with a carbon nucleophile, such as organozinc or organoboron reagents to form **C** via a transmetalation step. The intermediate **C** is followed by a reductive elimination to give a substituted allene **D** and a regeneration of the palladium(0) catalyst.¹³⁷

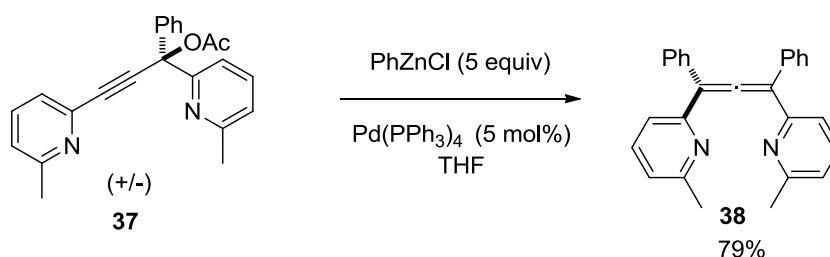


Scheme 50. Plausible mechanism of palladium(0)-catalyzed allene formation.

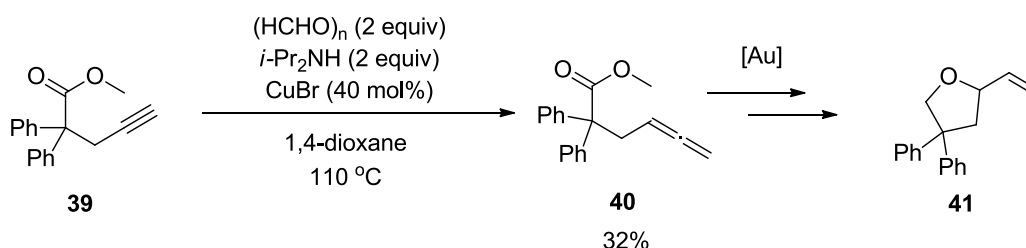
A noteworthy interesting example has been described for the synthesis of allenic bipyridines by the Krause group in 2008.¹³⁸ PhZnCl was used as a nucleophile for the transmetalation step in palladium catalytic process. Allene **38** was then obtained in high yields from propargylic acetate **37** (Scheme 51). It was applied as ligand for coordination with transition metals such as copper(I) and silver (I).

¹³⁷ M. Ogasawara, T. Hayashi, in *Mod. Allene Chem.* (Eds.: N. Krause, A.S.K. Hashmi), Wiley-VCH Verlag GmbH, Weinheim, Germany, **2004**, pp. 93–140.

¹³⁸ S. Löhrl, J. Averbek, M. Schürmann, N. Krause, *Eur. J. Inorg. Chem.* **2008**, *2008*, 552–556.

Scheme 51. Synthesis of allenic bipyridine **38**.

Copper salts have also been investigated as catalysts in this reaction. Pioneering works presented by Crabbé in 1979 dealt with the efficient copper-catalyzed synthesis of functionalized terminal allenes.¹³⁹ Since, numerous reactions have been developed towards the same goal, one interesting application of this copper-catalyzed reaction was provided by the Widenhoefer group.¹⁴⁰ They aimed to synthesize allenyl acetate derivatives as substrates for the formation of vinyltetrahydrofurans (**41**) via gold-catalyzed cyclization. As shown in Scheme 52, γ -acetylenic ester **39** was engaged in the presence of paraformaldehyde, diisopropylamine and copper bromide catalyst in refluxing 1,4-dioxane to afford **40** in a moderate yield (32%).

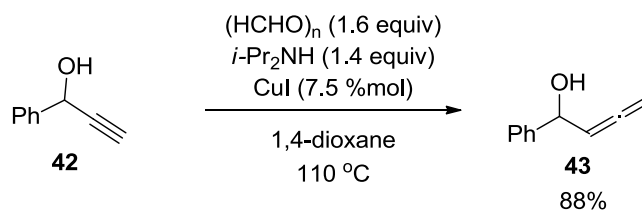
Scheme 52. Synthesis of **40** in the presence of copper(I) catalyst.

In similar fashion, Luo and Ma¹⁴¹ developed the synthesis of β -allenol derivatives from propargylic alcohols by using copper iodide as a catalyst. The effective copper(I)-catalyzed reaction, based on the same procedure, provided the allenols. As shown in Scheme 53, the copper catalytic reaction with 1-phenyl-2-propyn-1-ol (**42**) as starting material yielded 88% of the desired α -allenol product **43**.

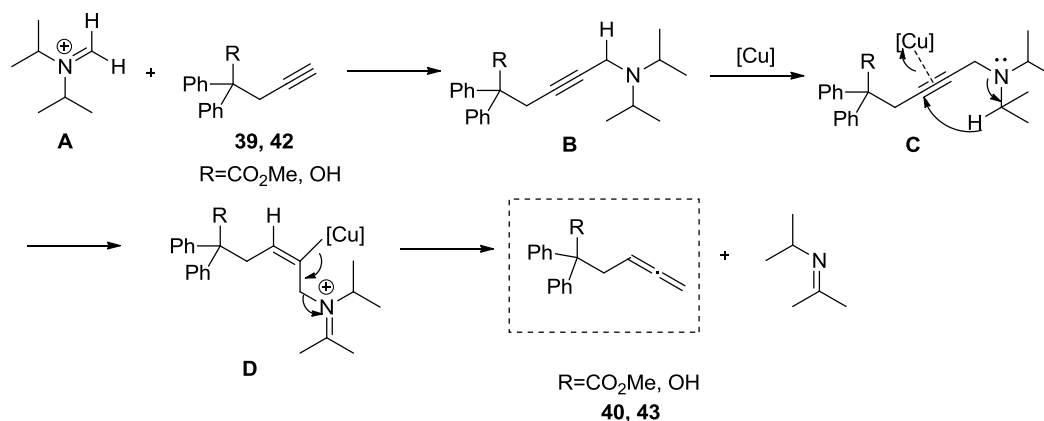
¹³⁹ P. Crabbé, H. Fillion, D. André, J.-L. Luche, *J. Chem. Soc. Chem. Commun.* **1979**, 859–860.

¹⁴⁰ Z. Zhang, C. Liu, R. E. Kinder, X. Han, H. Qian, R. A. Widenhoefer, *J. Am. Chem. Soc.* **2006**, *128*, 9066–9073.

¹⁴¹ H. Luo, S. Ma, *Eur. J. Org. Chem.* **2013**, *2013*, 3041–3048.

Scheme 53. Synthesis of γ -allenol **43**.

The proposed mechanism of copper(I)-catalyzed allenylation involved the formation of iminium ion **A** from $i\text{-Pr}_2\text{NH}$ and formaldehyde *via* Mannich reaction. It was reacted by the deprotonated of γ -acetylenic ester or alcohol **39**, **42** in basic condition, formed intermediate **B**. In the presence of CuBr catalyst, **B** was activated by a copper catalyst, leading to 1,5-sigmatropic rearrangement of hydride (**C**) to provide organocopper **D**. After abstraction of copper and eliminate the latter amine group, allenyl ester **40** or allenol **43** were obtained (Scheme 54).¹⁴²



Scheme 54. Proposed mechanism of copper(I)-catalyzed allenylation.

2.3. Isomerization reactions

Isomerization reaction represents an alternative approach to synthesize allenes from propargylic derivatives. The reaction is the process by which one molecule is transformed into another molecule without the change of the empirical formula.¹⁴³ The migration of a substituent (such as H, alkyl, alkoxy and stannyl) at β -position on alkyne occurs *via* an intramolecular isomerization, which is a special case of a molecular rearrangement. Nevertheless, isomerization does not necessarily imply molecular rearrangement, such as in the case of the interconversion of conformational isomers. In following section, the isomerization from propargylic substrates to

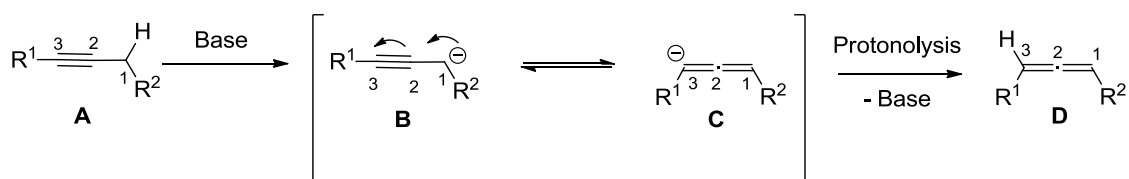
¹⁴² H. Nakamura, T. Sugiishi, Y. Tanaka, *Tetrahedron Lett.* **2008**, 49, 7230–7233.

¹⁴³ N. Krause, A. S. Hashmi, *Modern Allene Chemistry*, Wiley-VCH, Weinheim, **2004**, 3–36.

allenes will be focused on two types, which are metallotropic rearrangement and [2,3]-sigmatropic rearrangement.

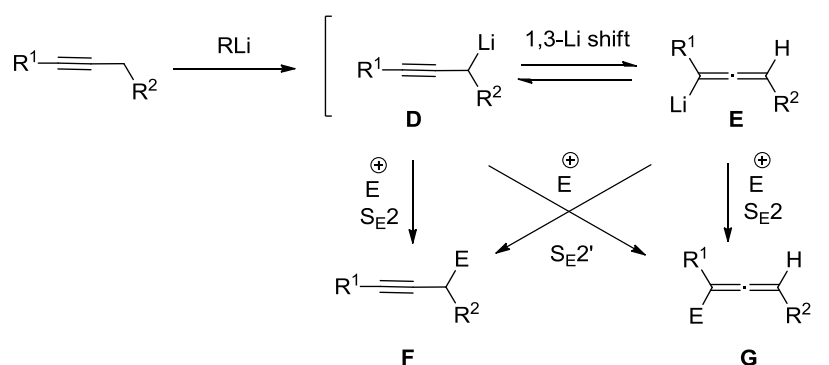
2.3.1. Metallotropic rearrangement

Under basic conditions, the isomerization step of an alkyne (**A**) takes place by deprotonation at C₁ and generation of an alkynyl anion as a free carbene intermediate (**B**). It proceeds localizing to C₃ to form an allenyl anion (**C**) in equilibrium (Scheme 55). The anion form **C** then undergoes protonolysis to afford a proton-substituent allene (**D**).¹⁴⁴



Scheme 55. Isomerization reaction of an alkyne in the base condition.

In the case of using organometallic reagents, a isomerization proceeds through a particular case of a metallotropic rearrangement.¹⁴⁵ We focused on the use of organolithium reagents such as LDA and *n*-buthyllithium to provide an allene. As illustrated in Scheme 56, alkynyllithium intermediate (**D**) is generated by deprotonation of an alkyne, leading to form allenyl and/or propargyllithium (**E**) species in an equilibrium mixture. The process can provide electrophilic-substituted products **F** and **G** by either S_E2 or S_E2' pathways, depending on an electrophile and a reaction condition.¹¹⁵

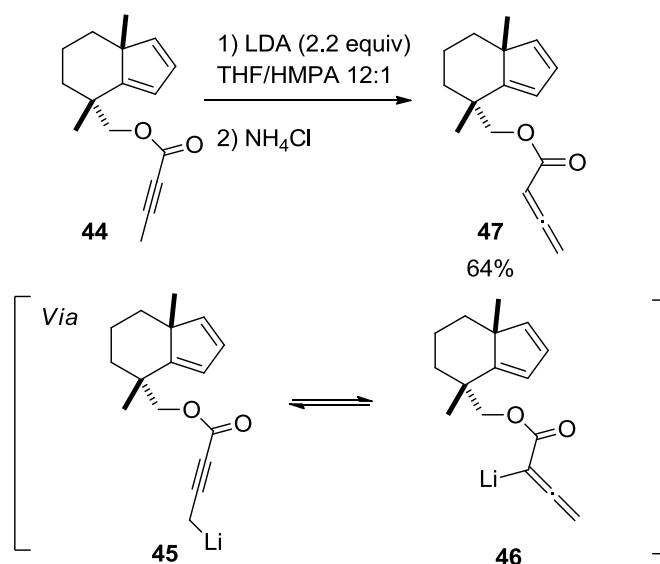


Scheme 56. Metallotropic rearrangement of an alkyne and electrophilic substitution reactions of **D** and **E**.

¹⁴⁴ M. D. Carr, L. H. Gan, I. Reid, *J. Chem. Soc. Perkin Trans. 2* **1973**, 668–672.

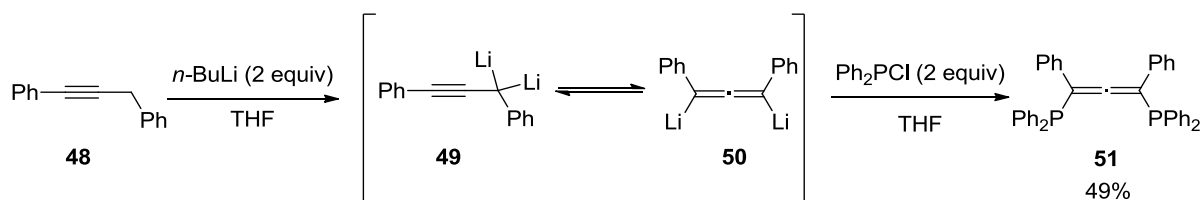
¹⁴⁵ J. J. Eisch, *Prod. RD* **1975**, *14*, 11–21.

An corresponding example was given by the Winterfeldt group at the occasion of the synthesis of (–)-myltaylenol.¹⁴⁶ In this synthetic strategy, allenyl esters were examined as synthetic intermediates. A selective isomerization by the protonation of α -alkynyl ester **44** in the presence of LDA provided alkynyllithium **45**, which underwent an isomerization process to form allenyllithium **46**. After hydrolysis, allenyl ester **47** was obtained in 64% yield (Scheme 57).



Scheme 57. Synthesis of allenyl ester **47**.

Another interesting example devoted to the synthesis of allenes bearing phosphine moieties was presented by the Schmidbaur group in 1989.¹⁴⁷ So far, this is the only study for the synthesis of allene bisphosphines *via* an isomerization of the alkyne and electrophilic trapping. The reaction begins from 1,3-diphenyl-1-propyne (**48**) in the presence of two equivalents of *n*-butyllithium as a reagent to deprotonate the two acidic protons at the propargylic position. In the same line, two possible intermediates were also generated in equilibrium mixture, which are alkynyllithium **49** and allenyllithium **50**. The allenyllithium **50** would react to chlorodiphenyl phosphine. The allenyl bisphosphine **51** was obtained in 49% yield (Scheme 58).



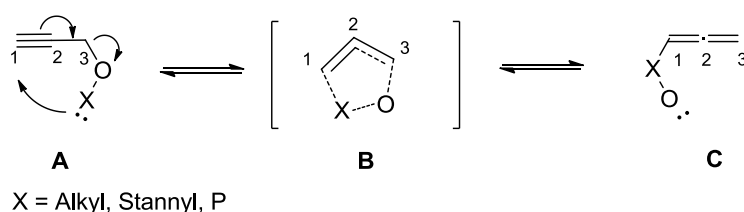
Scheme 58. Synthesis of bisdiphenylphosphine allene **51**.

¹⁴⁶ S. Doye, T. Hotopp, R. Wartchow, E. Winterfeldt, *Chem. Eur. J.* **1998**, *4*, 1480–1488.

¹⁴⁷ H. Schmidbaur, C. M. Frazão, G. Reber, G. Müller, *Chem. Ber.* **1989**, *122*, 259–263.

2.3.2. [2,3]-Sigmatropic rearrangement

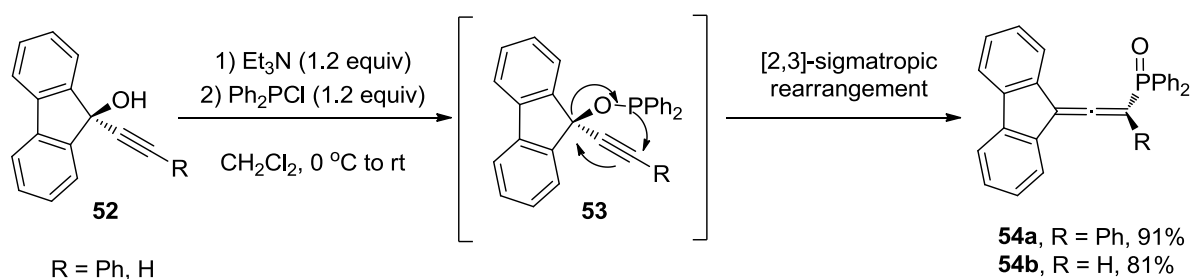
Among various isomerization reactions useful for the synthesis of allenes, the [2,3]-sigmatropic rearrangement constitutes an interesting pathway. This isomerization reaction proceeds through a six-electron, five-membered cyclic transition state. It occurs when an alkyne precursor bearing a functional group such as alkoxide, stannyl or phosphenyl groups at C-3 position as depicted in Scheme 59. The group (X-O) tethered-carbon at position 3 of **A** can migrate to another carbon at position 1, leading to form allene **C** via an isomerization of intermediate **B**.¹⁴⁸ There are various types of [2,3]-sigmatropic rearrangement reported in difference of migrated groups. We focused on two types of alkyne substrates bearing a phosphorus and an alkoxide groups to provide corresponding allenes.



Scheme 59. [2,3]-Sigmatropic Rearrangement of propargyl precursor **A** to form allene **C**.

2.3.2.1. With phosphoryl group

An interesting report was disclosed by the McGlinchey group in 2008.¹⁴⁹ They synthesized an allenylphosphine oxides from propargylic alcohols and chlorodiphenylphosphine reagent via [2,3]-sigmatropic rearrangement. For example, the reaction of **52** with chlorodiphenylphosphine in the presence of Et₃N provides an alkynyl intermediate **53**, which undergoes spontaneous migration of the phosphinoyl moiety to give directly the allenyl phosphine oxides **54a, b** in excellent yields (Scheme 60).



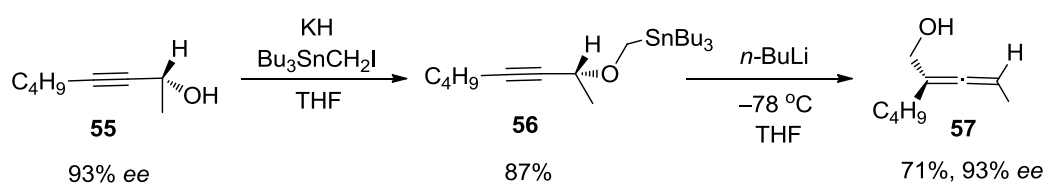
Scheme 60. Synthesis of **54** via [2,3]-sigmatropic rearrangement.

¹⁴⁸ T. Nakai, K. Mikami, *Chem. Rev.* **1986**, 86, 885–902.

¹⁴⁹ E. V. Banide, J. P. Grealis, H. Müller-Bunz, Y. Ortin, M. Casey, C. Mendicute-Fierro, M. Cristina Lagunas, M. J. McGlinchey, *J. Organomet. Chem.* **2008**, 693, 1759–1770.

2.3.2.2. With alkoxy group

In 1989, Marshall reported the synthesis of allenyl alcohols by [2,3]-Wittig rearrangement of stannyl group. This rearrangement was induced by a tin-lithium exchange.¹⁵⁰ The reaction is based on the use of propargylic tin-containing ether **56**, prepared from optically pure (*R*)-propargylic alcohol **55** via deprotonation of hydroxyl group and organotin substitution. The chiral allene **57** was obtained upon treatment with *n*-butyllithium at low temperature. The product showed the completely transfer of chirality from the substrate with 93% *ee* (Scheme 61).



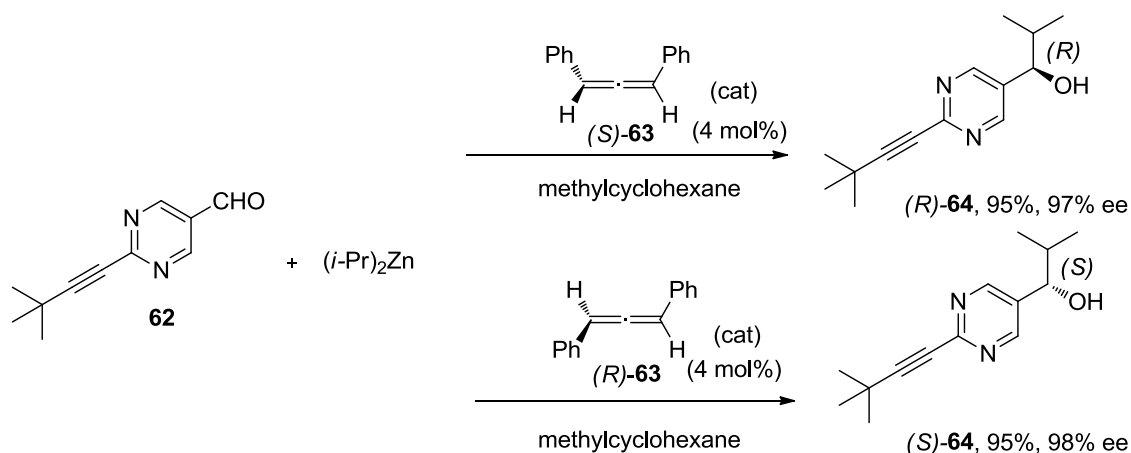
Scheme 61. [2,3]-Wittig rearrangement of propargylic tin-containing ether **57**.

Inspired by this good result for the synthesis of chiral allenes, they also developed a more valuable method without the use of toxic tin derivatives.¹⁵¹ The chiral propargylic ether **59** bearing acetic acid group was prepared from a deprotonation of hydroxyl group and an alkylation reaction with chloroacetic acid of the optically pure propargylic alcohol **58**. Upon treatment with LDA, **59** underwent high stereoselective [2,3]-rearrangement in THF at -78°C . Subsequent esterification with diazomethane afforded α -(*S*)-hydroxy- β -(*R*)-allenic methyl ester **60** with a complete transfer of chirality and a diastereoselectivity (*de* >90%). This product was then engaged in a cyclization process to prepare the optically pure 1,5-dihydrofurans **61** upon treatment with $\text{AgNO}_3\text{-CaCO}_3$, PhSeCl or NBS (Scheme 62).

¹⁵⁰ J. A. Marshall, E. D. Robinson, A. Zapata, *J. Org. Chem.* **1989**, *54*, 5854–5855.

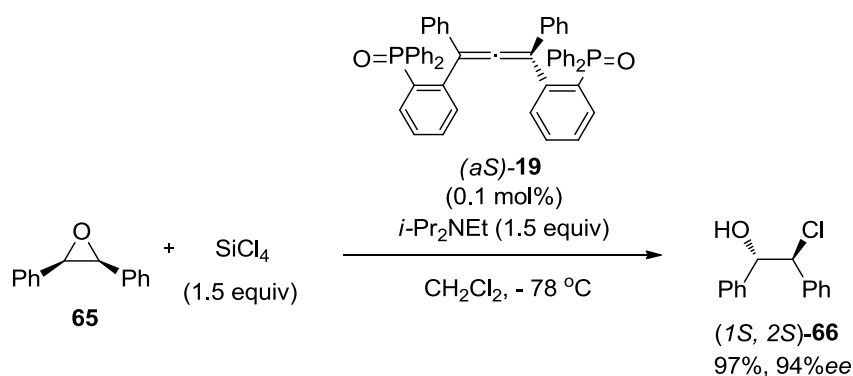
¹⁵¹ J. A. Marshall, W. Xiao-J., *J. Org. Chem.* **1990**, *55*, 2995–2996.

substrates afforded (*R*)- and (*S*)-pyrimidin-5-yl alkanol (**64**) in excellent yields and *ees*, showing the inverse configurations of the chiral allene catalysts **63** (Scheme 63).



Scheme 63. Enantioselective addition of $(i\text{-Pr})_2\text{Zn}$ to aldehyde **62** in the presence of catalyst **63**.

According to the preparation of optically pure allenyl phosphine oxides (**19**) by Ready in Scheme 45,¹³⁰ the chiral allenes can induce some high efficiencies and enantioselectivities in catalytic reactions as well. The successful use of **19** as a chiral catalyst, similar to chiral phosphoramides from Denmark's reports (Scheme 12),^{36, 154} for the ring-opening reaction of *meso*-epoxides. For example, the reaction of **65** with SiCl_4 in the presence of (*aS*)-**19** catalyst provided a diastereoselective chlorohydrin (*1S*, *2S*)-**66** in 97% yield and 94% *ee* (Scheme 64).



Scheme 64. Asymmetric ring opening of *meso*-epoxide **65**.

Although allenes have been found in the limited contributions to asymmetric catalysis, these two reports show the attractive properties of allene catalysts for inducing the asymmetry to prepare enantiomerically pure compounds. These works would be noted for our attempts in the use of new allenes as catalysts for asymmetric catalysis.

¹⁵⁴ S. E. Denmark, P. A. Barsanti, G. L. Beutner, T. W. Wilson, *Adv. Synth. Catal.* **2007**, *349*, 567–582.

3.2. Allene ligands

Allenes have been reported as ligands for transition metals in plenty of literature. A η^2 -coordination mode between an allene-double bond and a metal has often been observed. For example in Figure 22, allene complexes of tungsten,¹⁵⁵ cobalt,¹⁵⁶ platinum,¹⁵⁷ manganese,¹⁵⁸ and osmium¹⁵⁹ are successfully isolated and characterized by X-ray crystallography and NMR analysis.

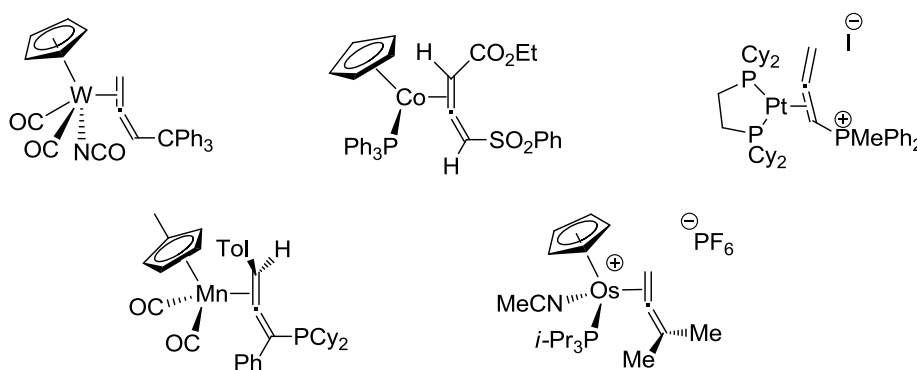


Figure 22. Examples of η^2 -(metal-allene) coordinations.

Substituted functional groups on allenes groups could also coordinate to transition metals. In Krause's work, allenic bipyridine ligands have been synthesized (See Scheme 51).¹³⁸ Their complexation to silver and copper salts was studied to form the corresponding complexes through nitrogen coordination of the pyridine groups, characterized by mass spectrometry (ESI), NMR spectroscopy, and X-ray crystallography. These analyses show that the complexation of allenes **67** with silver salts gives a 2:2 (Ligand/Ag) cluster **68** via the coordination of two silver atoms to both nitrogen atoms of each ligand (Scheme 65). On the other hand, the complexation with copper salts forms two types of complexes **69** and **70**, 2:1 and 1:1 complexes (Ligand/Cu) depending on the temperature. At 296 K, the complex formed is the 2:1 association of ligands and metal (**69**). In contrast, at low temperature (236 K), the copper complexation led to the 1:1 complex (**70**) (Scheme 66).

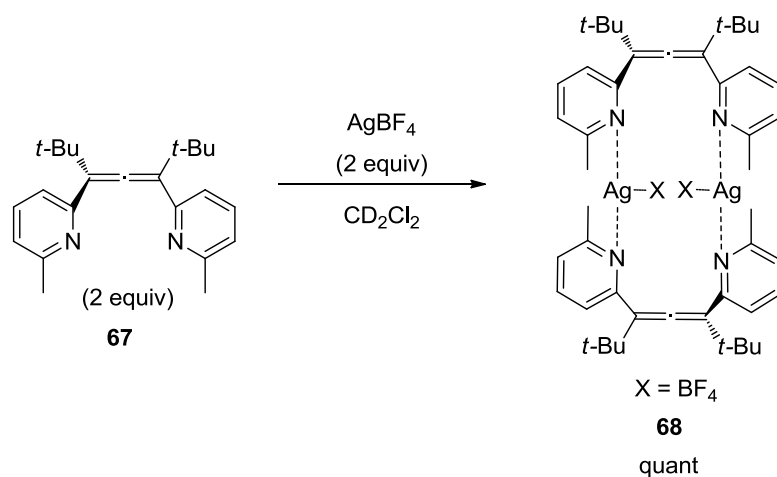
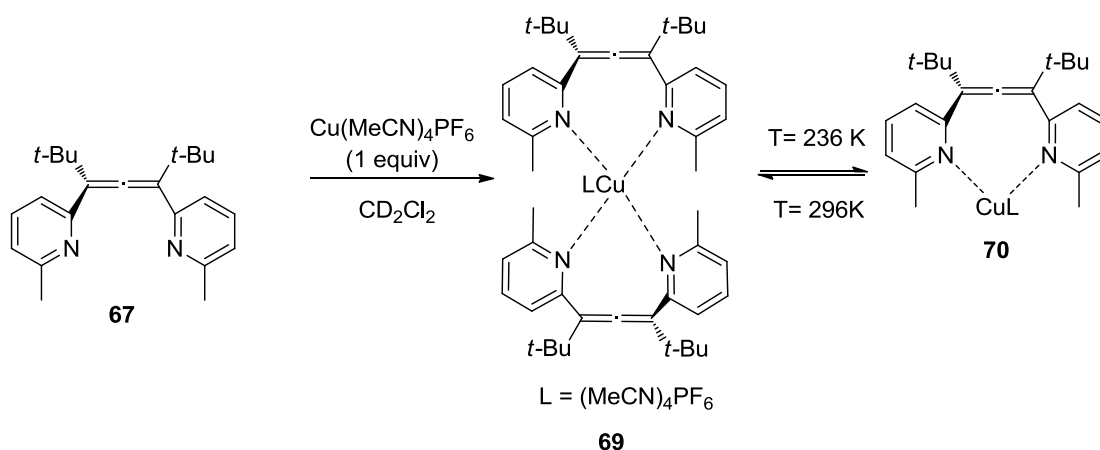
¹⁵⁵ L. Lee, I.-Y. Wu, Y.-C. Lin, G.-H. Lee, Y. Wang, *Organometallics* **1994**, *13*, 2521–2526.

¹⁵⁶ J. M. O'Connor, M.-C. Chen, B. S. Fong, A. Wenzel, P. Gantzel, A. L. Rheingold, I. A. Guzei, *J. Am. Chem. Soc.* **1998**, *120*, 1100–1101.

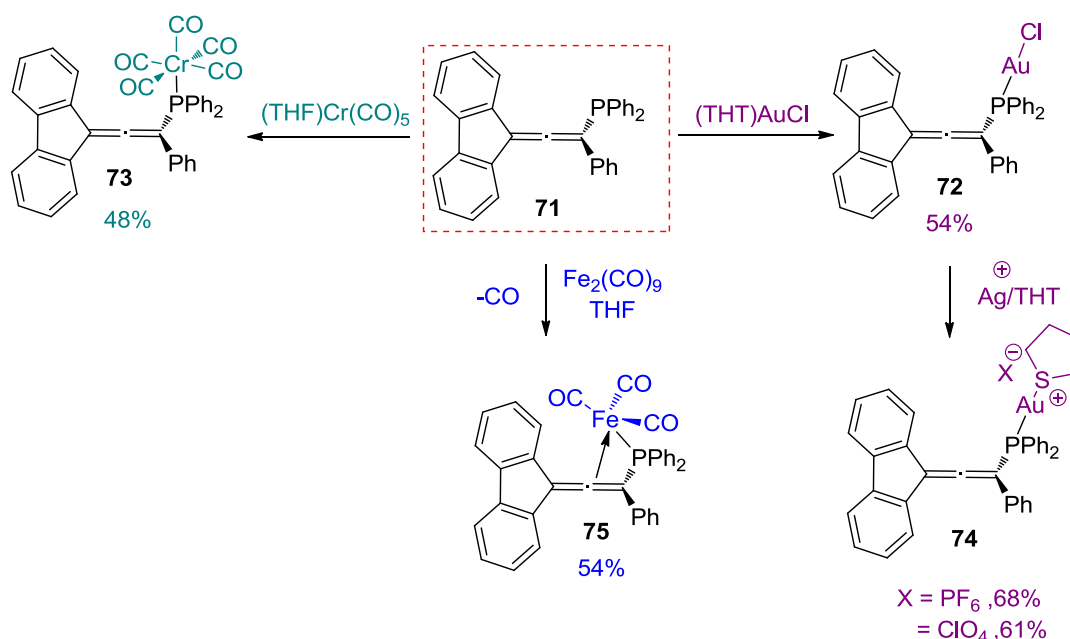
¹⁵⁷ M. A. Bennett, L. Kwan; A. D.Rae; E. Wenger; A. C. Willis, *Dalton Trans.* **2002**, 226–233.

¹⁵⁸ S. Sentets, R. Serres, Y. Ortin, N. Lugan, G. Lavigne, *Organometallics* **2008**, *27*, 2078–2091.

¹⁵⁹ R. Castro-Rodrigo, M. A. Esteruelas, A. M. López, S. Mozo, E. Oñate, *Organometallics* **2010**, *29*, 4071–4079.

Scheme 65. Allene complexation mode (**68**) of silver salt 2:2 (Ligand/Ag).Scheme 66. Allene complexation modes (**69** and **70**) of copper salt 2:1 and 1:1 (Ligand/Cu).

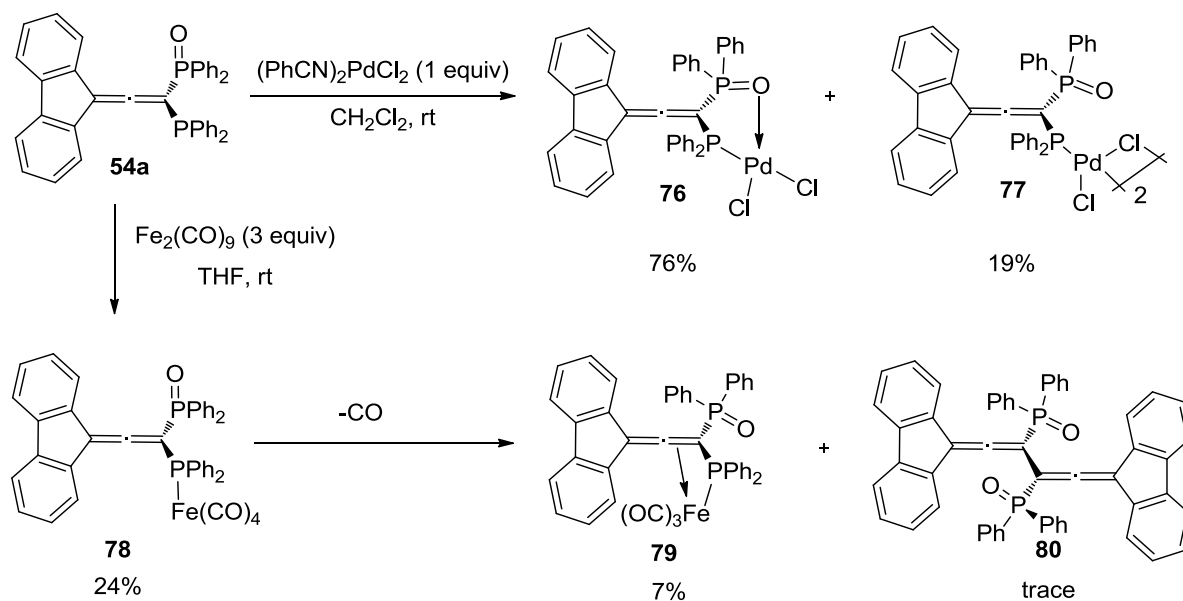
In their studies regarding the synthesis of novel alkylidenecyclobutanes and tetracene derivatives as electroluminescent compounds through dimerization of fluorenylidene-derived allenes, McGlinchey and co-workers reported the synthesis of various allenyl phosphine **71** (See Scheme 60) and their reactions with metals.¹⁴⁹ Several metals such as gold, chromium, and iron were examined in order to evaluate the coordination properties of these ligands. As shown in Scheme 67, with gold and chromium, the favored coordination occurs with the mono-phosphine group rather than with the allene to form complexes **72** and **73**, because of the better electron-donor properties of the phosphorous ligand to stabilize metals. In addition, the gold complex **74** could be generated as the stable cationic gold(I) species by the activation of **72** with silver salt. In contrast, iron is able to coordinate on both the π -allene bond and phosphine group. After loss of a carbonyl ligand, vacant site on iron moiety was occupied by the adjacent π -bond of the allene to form complex **75**. All metal-complexes structures were elucidated by NMR spectroscopy and X-ray crystallography characterizations.



Scheme 67. Preparation of metal-allene complexes from **71**.

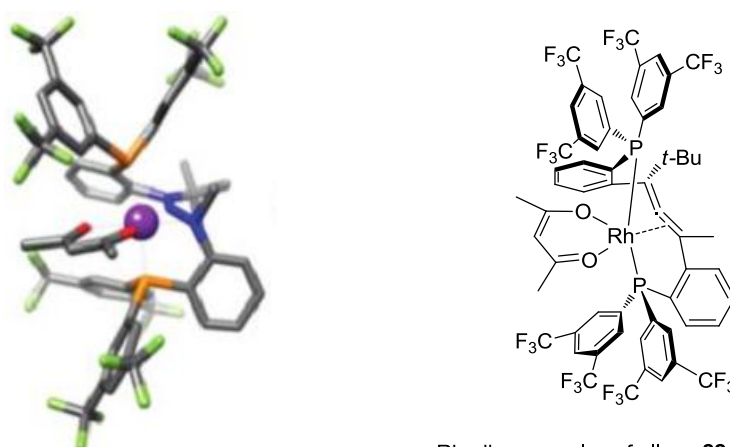
Later, McGlinchey pursued his studies on allenylphosphine reactivity.¹⁶⁰ A bifunctional ligand **54a** (See Scheme 60) could complex to $(\text{PhCN})_2\text{PdCl}_2$ between oxygen and phosphorus to give the palladium complex **76** as a major product (76%), in which the metal is coordinated to both phosphorus and oxygen of phosphine oxide, and minor chlorine-bridged **77** (19%) (Scheme 68). Moreover, di-iron nonacarbonyl with ligand **54a** also formed a phosphorus-bonded- $\text{Fe}(\text{CO})_4$ species **78**. After loss of a carbonyl ligand, the adjacent allene double bond was able to coordinate to iron as **79**, leaving the phosphine oxide uncoordinated, characterized by NMR analyses and X-ray crystallography. The reaction also gave trace amount of side-product **80**.

¹⁶⁰ S. Milosevic, E. V. Banide, H. Müller-Bunz, D. G. Gilheany, M. J. McGlinchey, *Organometallics* **2011**, *30*, 3804–3817.



Scheme 68. The coordination modes of **54a** to $\text{Fe}_2(\text{CO})_9$ and $(\text{PhCN})_2\text{PdCl}_2$.

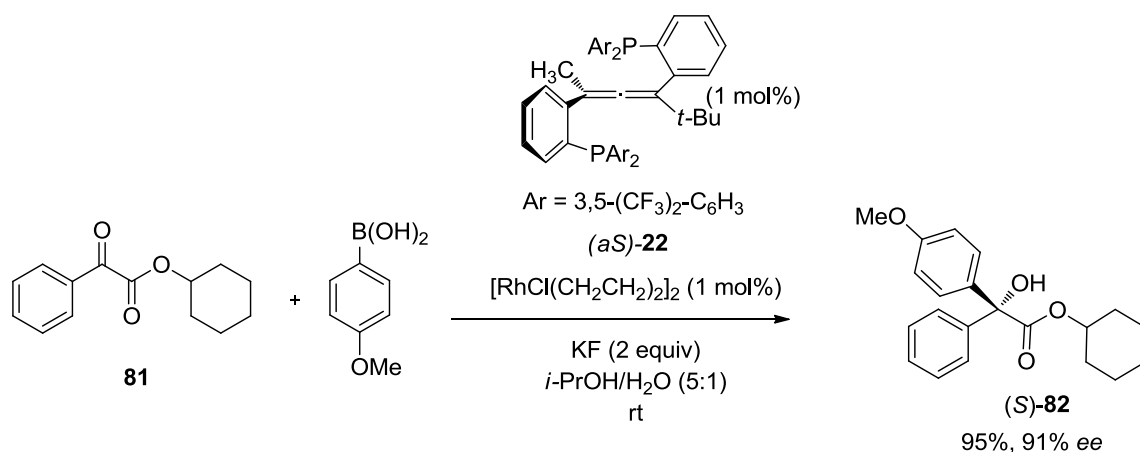
However, the isolated metal-allene complexes have less evidence in applications. Only an example that described the applications of the metal-allene complexes have been presented by the Ready group in 2011.¹³¹ For example, allenyl bisphosphines **22** have been synthesized (See Scheme 46) and applied them as axially chiral ligands for rhodium(I) in asymmetric catalysis. Interestingly, the coordination complex could be isolated and characterized by X-ray analysis. It demonstrated the coordination of rhodium center with both two phosphine groups and one allene bond (Figure 23). This was efficiently applied in the enantioselective rhodium(I)-catalyzed addition of arylboronic acids to α -keto ester **81** to generate the corresponding enantioenriched alcohol ester **82** in high yield (95%) and excellent *ee* (91%) (Scheme 69).



Rhodium complex of allene **22** and ester **81**

Figure 23. X-ray crystal structure of rhodium(I) complex intermediate in the arylation of **81**.

(Figure reproduced from reference 131)



Scheme 69. Enantioselective rhodium(I)-catalyzed addition of arylboronic acid to **81**.

A large range of allene-metal complexes have been reported in literature using various transition metals. Depending on metal species and their intrinsic properties, the complexes could be formed according to different coordination modes. The isolation of these complexes and their full characterization could allow to better understand their properties for further applications. However, the opportunities offered by allene ligands have not been widely studied in asymmetric catalysis reactions. Thus, it is challenging to study the metal properties and prepare the suitable allene ligands in order to try to develop new asymmetric process.

4. Allenes in gold chemistry

Gold catalysts have been employed to activate alkenes,⁸⁶ alkynes,¹⁶¹ and allenes^{49, 51b, 64, 162} as well heteroatoms from carbonyls and imines, thanks to their soft and carbophilic character (Figure 24).^{65a, 163} Mostly, the gold catalyst can promote the allene cyclization to generate cyclic products. Isolated gold intermediates and computational analyses can help to explain their coordination modes and reactivity.

¹⁶¹ (a) A. Corma, V. R. Ruiz, A. Leyva-Pérez, M. J. Sabater, *Adv. Synth. Catal.* **2010**, *352*, 1701–1710.; (b) C.-F. Xu, M. Xu, L.-Q. Yang, C.-Y. Li, *J. Org. Chem.* **2012**, *77*, 3010–3016.

¹⁶² (a) H. C. Shen, *Tetrahedron* **2008**, *64*, 3885–3903.; (b) E. Álvarez, P. García-García, M. A. Fernández-Rodríguez, R. Sanz, *J. Org. Chem.* **2013**, *78*, 9758–9771.

¹⁶³ (a) A. S. K. Hashmi, T. M. Frost, J. W. Bats, *J. Am. Chem. Soc.* **2000**, *122*, 11553–11554.; (b) A. Pradal, P. Toullec, V. Michelet, *Synthesis* **2011**, *2011*, 1501–1514.

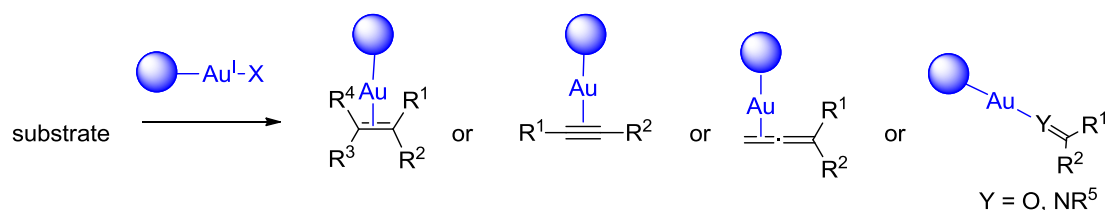
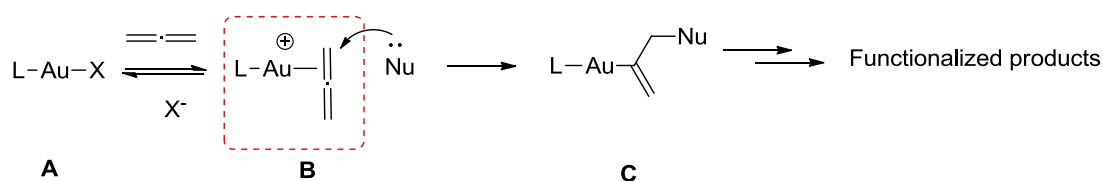


Figure 24. Possible gold coordination modes with different types of substrates
(Figure reproduced from reference 163b).

The gold activation allows the generation of an electrophilic unsaturated bond which can be attacked by a nucleophile. In the case of allene substrates (**A**), gold(I)-allene complexes are the attractive species as they can show a particular reactivity due to their potential for multiple coordination modes. The η^2 -mode (**B**) has often been presented as reactive intermediates in gold(I)-catalyzed activation processes, facilitating their functionalization by addition of nucleophiles (**C**).¹⁶⁴ The intermediates are supported by computational analyses as well by complete characterization after isolation. (Scheme 70).



Scheme 70. Formation of a cationic η^2 -gold allene complex from the activation of gold(I) on allene.

4.1. Gold(I)-allene complexes

The activation of gold catalyst on allene scaffold can form three possible coordination modes between allene and cationic gold(I) species: η^2 -allene, η^1 -allene and η^1 -allylic cation (Figure 25). These modes have also been studied theoretically in order to rationalize the different reaction pathways.^{165, 166} In 2008, Gandon, Fensterbank and co-workers explained the coordination of gold(I) species in various types of allenic structures by means of computational studies.⁹⁹ In this manner, the interaction of an allene in the presence of AuX_3 ($\text{X} = \text{Cl}$ or Br) shows that η^2 -allene complexes, generated through the coordination of one of the two orthogonal C=C bonds, are the most stable forms.

¹⁶⁴ A. J. L. Pombeiro, *Advances in Organometallic Chemistry and Catalysis: The Silver / Gold Jubilee International Conference on Organometallic Chemistry Celebratory Book*, John Wiley & Sons, **2013**, 209.

¹⁶⁵ M. Malacria, L. Fensterbank, V. Gandon, *Top. Curr. Chem.* **2011**, 302, 157–182.

¹⁶⁶ E. Soriano, I. Fernandez, I. *Chem. Soc. Rev.* **2014**, 43, 3041–3105.

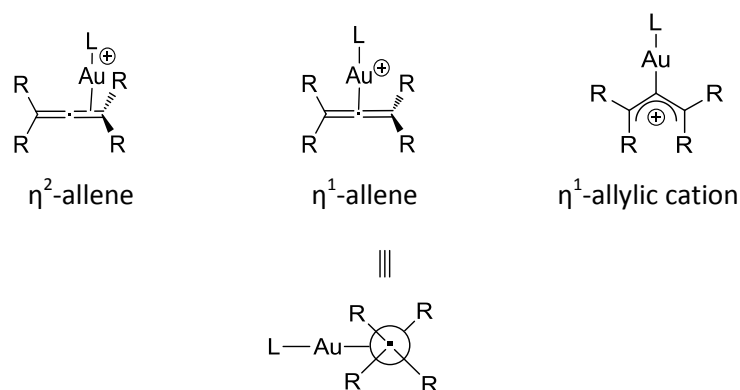


Figure 25. Potential coordination modes accessible for gold(I) allene complexes (R= Me).

Generally, cationic gold complexes are described following three resonance structures based on carbene (Au=C bond order of 2), carbenium (Au-C bond order of 1) and carbenoid (AuC bond order of 0) characters (Figure 26).¹⁶⁷ These resonance forms are expected to react differently in further organometallic applications.

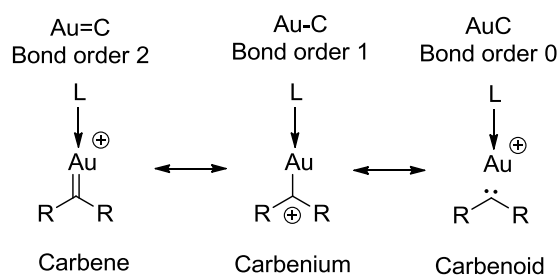
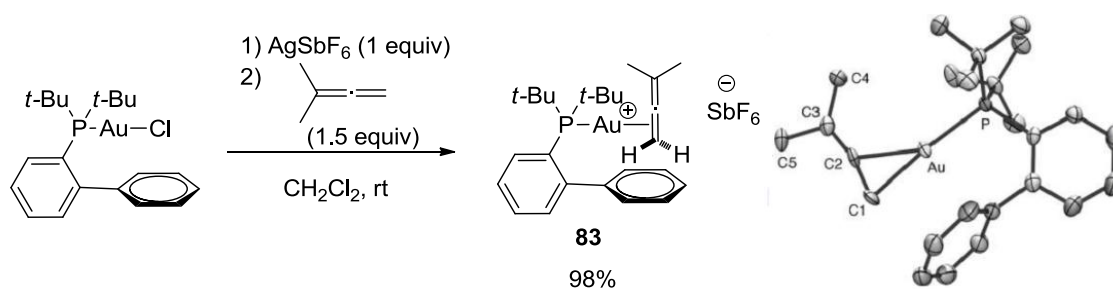


Figure 26. Au-C bond orders of cationic gold(I) resonance structures.

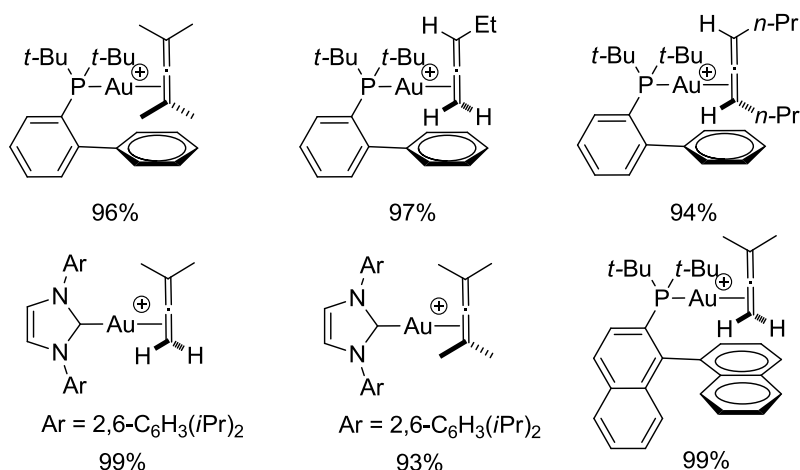
The isolation and characterization of allene-gold(I) complexes is crucial in order to better understand the allene coordination mode into metal. In 2010, the Widenhoefer group isolated the first cationic gold η^2 -allene complex, which was obtained after complexation with a gem-disubstituted allene.¹⁶⁸ This complex is observed in the η^2 -allylic cationic form as a stable form in the solid state. The treatment of $[P(t\text{-Bu})_2\text{o-biphenyl}]AuCl$ with $AgSbF_6$ (1:1) and dimethylallene at room temperature resulted in an excellent yield of the isolated dimethylallene- $Au^+SbF_6^-$ complex **83** (98%) (Scheme 71). The crystal structure demonstrated that the gold atom coordinated to the less substituted of two orthogonal C=C π bonds.

¹⁶⁷ M. W. Hussong, F. Rominger, P. Krämer, B. F. Straub, *Angew. Chem. Int. Ed.* **2014**, *53*, 9372–9375.

¹⁶⁸ T. J. Brown, A. Sugie, M. G. Dickens, R. A. Widenhoefer, *Organometallics* **2010**, *29*, 4207–4209.

Scheme 71. Synthesis of complex **83**. (Figure reproduced from reference 168)

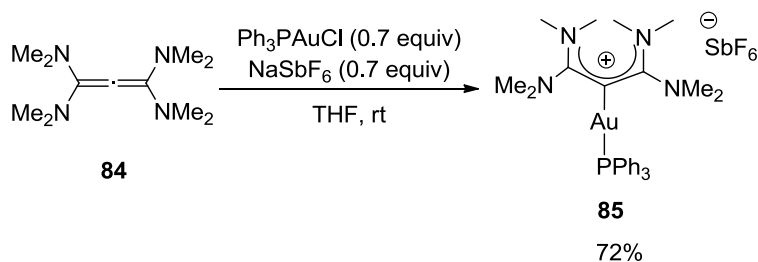
Later in 2012, the Widenhoefer group isolated in excellent yields of various cationic gold-allene complexes with electron-rich supporting ligands such as phosphine derivatives and *N*-heterocyclic carbenes (NHCs) (Figure 27).¹⁶⁹ These gold complexes would be used as catalysts for organic transformations.

Figure 27. η^2 -gold allene complexes.

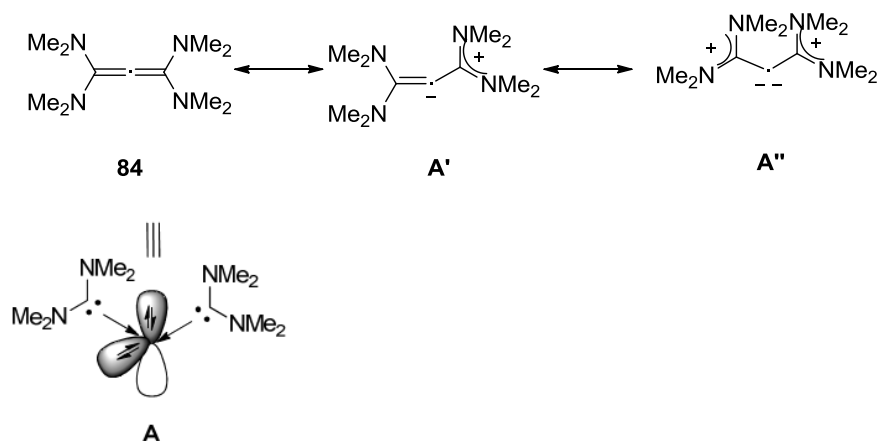
Gold complexes containing heteroatom-substituted ligands are also noteworthy. In 2008, Fürstner reported the synthesis and isolation of gold-enamine complexes. The reaction of tetradimethylaminoallene **84** and Ph₃PAuSbF₆, prepared from Ph₃PAuCl and NaSbF₆, provided the gold complex **85** as the trigonal planar coordination in 72% yield (Scheme 72).¹⁷⁰ The X-ray analysis of these complexes revealed a η^1 -coordination involving an allylic cation.

¹⁶⁹ T. J. Brown, A. Sugie, M. G. D. Leed, R. A. Widenhoefer, *Chem. Eur. J.* **2012**, *18*, 6959–6971.

¹⁷⁰ A. Fürstner, M. Alcarazo, R. Goddard, C. W. Lehmann, *Angew. Chem. Int. Ed.* **2008**, *47*, 3210–3214., *Angew. Chem.* **2008**, *120*, 3254–3258.

Scheme 72. Synthesis of gold complex **85**.

The ligand **84** was described as C(0) system (L→C←L), involving two lone pairs of electrons of strongly donating diamino-stabilized carbene (L) entities (carbodicarbene **A**) (Scheme 73). The central carbon atom (C(0)) of allene ligand was indicated as being zerovalent character, containing two lone pairs of electrons on occupying σ and π type orbitals. Theoretical analysis of the bonding situation demonstrated that the mesomeric bent allene form **A''** makes a substantial contribution to the ground-state structure. This form contains four-electron donors at the carbon center. In this case, only one lone pair of electrons would reside on the central carbon atom of **84**, bonding to gold center to form **85**.

Scheme 73. Bonding situation in **84** and their mesomeric forms.

In the same line of bent acyclic allenes (Figure 28), Tonnor and Frenking also presented carbodicarbene ligand **86** from two NHCs-substituted allene. The conjugation of a lone pair of electron from NHCs with the adjacent C=C π bond leads to the extremely distorted allene π -system as C=C=C angle of 131.8° . Similarly to Bertrand's work, carbodicarbene **87** from bis(N-methylbenzimidazol-2-yl)methane was developed by increasing the conjugation on the benzene ring, resulting in a less bent allene as C=C=C angle of 134.8° .¹⁷¹ In contrast, less electron-donating group on an allene π -bond can induced lower bending in the allenes. For example, Weber and co-

¹⁷¹ C. A. Dyker, V. Lavallo, B. Donnadieu, G. Bertrand, *Angew. Chem. Int. Ed.* **2008**, *47*, 3206–3209.

workers identified a remarkably bent bis(biphenyl-2,2'-diyl)allene **88**, involving a C=C=C bond angle of 170.1° .¹⁷² In the case of bent cyclic allene, Regitz presented the diphosphorus containing six-membered ring **89** as a cyclic allene, a bent allene with C=C=C angle of 155.8° ,¹⁷³ which is larger than carbodicarbene ligands **86** and **87**. The results show that the substituent on allene skeleton plays a significant role in distorting the linear π -bond which can increase the reactivity of ligands to complex with metals *via* a η^1 -coordination mode on a carbon center.

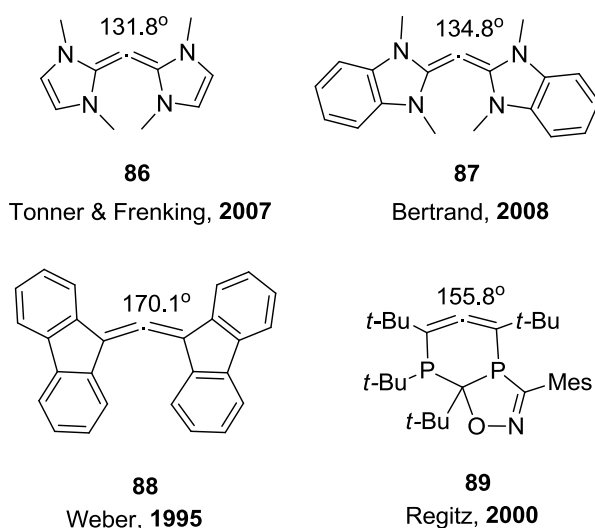


Figure 28. Examples of bent acyclic and cyclic allenes

To conclude, in order to promote different coordinated stable forms for allene-gold complexes, the design of the allene ligand substitution is significant. Particularly, phosphines and NHCs in the gold coordination sphere with the allene favor the η^2 -allene coordination mode. The functional groups on an allene are also significant in increasing electron-donating properties in order to stabilize metals *via* the formation of bent acyclic or cyclic forms. Thus, η^1 -allylic coordination mode is also stable when using bent acyclic allenes such as carbodicarbene ligands.

4.2. Gold(I)-catalyzed cyclization reactions

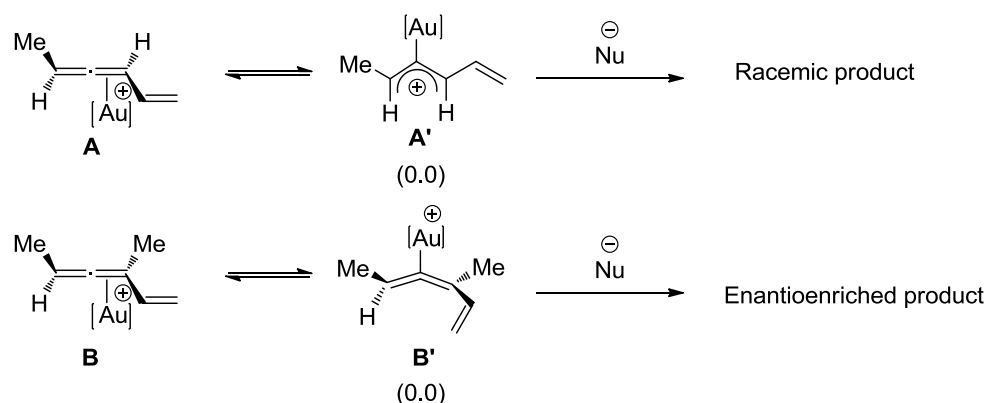
Allenes are valuable synthetic precursors to generate carbocyclic or heterocyclic products *via* gold(I)-catalyzed cyclization.^{98, 99, 168, 174} The activation of allenes is promoted by the gold coordination on the double bonds of an allene in order to generate the active intermediate in transition state based on η^1 or η^2 -coordination modes. The transition state of gold-catalyzed

¹⁷² E. Weber, W. Seichter, B. Hess, G. Will, H.-J. Dasting, *J. Phys. Org. Chem.* **1995**, *8*, 94–96.

¹⁷³ M. A. Hofmann, U. Bergsträßer, G. J. Reiß, L. Nyulászi, M. Regitz, *Angew. Chem. Int. Ed.* **2000**, *39*, 1261–1263.

¹⁷⁴ For reviews, see: N. Krause, C. Winter, *Chem. Rev.* **2011**, *111*, 1994–2009.

reactions has been studied by using optically pure allene substrates to promote the enantioenriched products. As the study by the group of Gandon and Fensterbank,¹⁶⁵ the catalytic gold reactions of optically pure vinylallenes could evaluate the chirality transfer in cycloisomerization step (Scheme 74). They found that the gold intermediate bearing substituent allene **A** would generate the allylic cation **A'** as a planar form in ground state ($\Delta H^\ddagger_{298} = 0.0$ kcal/mol). The chiral allene would be racemized in this step and produce the racemic corresponding compound after nucleophilic attack. In the case of trisubstituted **B**, the ground state still is a C_2 -coordinated allene **B'**. The trisubstituted allene could prevent the formation of planar structure and transfer the chirality to the corresponding products.



Scheme 74 Two examples of gold complexes of hexa-1,3,4-triene. [Au] = {Au(PMe₃)}. Relative enthalpies in kcal/mol barrier heights indicated in parentheses.

Gold catalysts bearing chiral mono- or dinuclear ligands have been examined in asymmetric reactions to promote enantioselective products.¹⁷⁵ In the case of dinuclear gold complex, only one gold moiety activates on π -allene (Figure 29). Another gold atom might block the molecule rotation by intramolecular interactions, such as Au-Au or Au- π bond interactions, to promote highly enantioselectivity.^{67, 176, 177} However, the enantioselectivity depends on the nature of substrates and chiral ligands, and reaction conditions.

¹⁷⁵ W. Yang, A. S. K. Hashmi, *Chem. Soc. Rev.* **2014**, *43*, 2941–2955.

¹⁷⁶ E. Herrero-Gómez, C. Nieto-Oberhuber, S. López, J. Benet-Buchholz, A. M. Echavarren, *Angew. Chem. Int. Ed.* **2006**, *45*, 5455–5459.

¹⁷⁷ (a) C. Michon, F. Medina, M.-A. Abadie, F. Agbossou-Niedercorn, *Organometallics* **2013**, *32*, 5589–5600.; (b) M.-A. Abadie, X. Trivelli, F. Medina, F. Capet, P. Roussel, F. Agbossou-Niedercorn, C. Michon, *ChemCatChem* **2014**, *6*, 2235–2239.

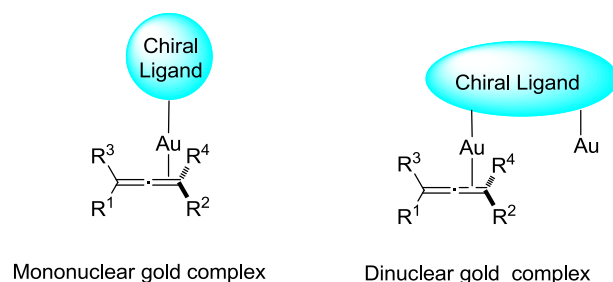
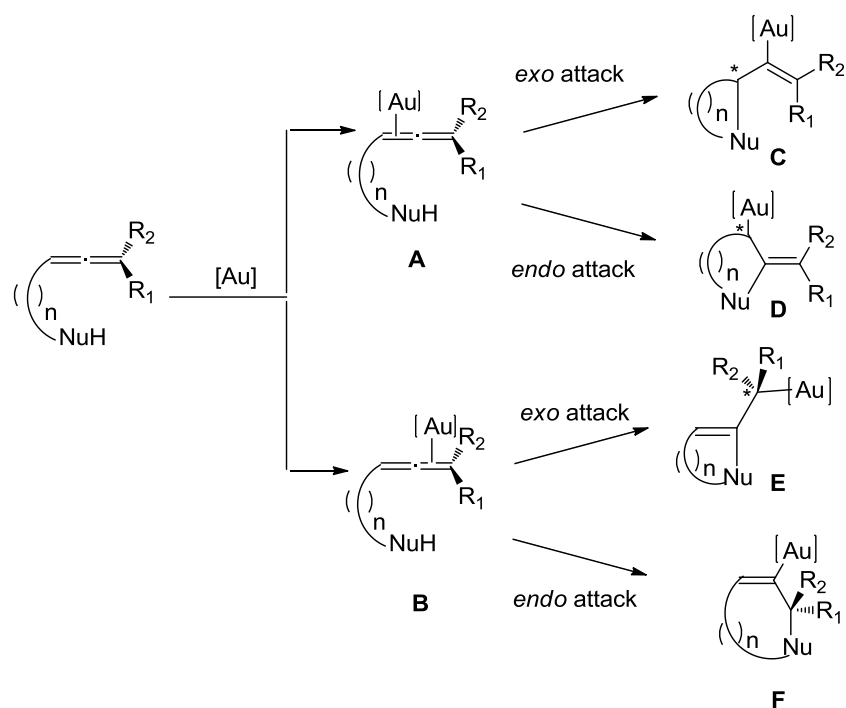


Figure 29. Activation of allenes by mono- and dinuclear gold complexes.

In this section, allenes could be model substrates to investigate their reactivities as with gold catalysts towards heteroatom- and carbonucleophilic substitutions. We focus on allene cyclization reactions by study chirality transfer from optically pure allenes and chiral gold(I) catalysts in asymmetric version.

4.2.1. Heteroatom-nucleophilic cyclization

Allenes bearing heteroatom functional groups are considered in the preparation of heterocyclic products. Nitrogen- and oxygen-containing heterocyclic compounds are significant biological components. The development of new and efficient synthetic methods is more attractive. Allenes bearing hydroxyl or amino groups are focused on the formation of heterocyclic derivatives. The oxygen and nitrogen atoms play an important role as internal nucleophiles for cyclization processes. In the first step, the metal coordinates to one or the other double bonds of the allene as a η^2 -coordination mode (**A** or **B**) (Scheme 75), promoting the *exo*- or *endo*-attacks to terminal or internal carbons. Depending on the length of the tether-connecting allene and a nucleophile, four types of intramolecular cyclization products can be obtained to form different sized heterocycles. Five- and six-membered rings are often favored *via* σ -gold species **C** or **F**, formed by the nucleophilic attack at the terminal allenic carbon atom. In contrast, products arising from the nucleophilic attack at the central allenic carbon atom *via* intermediate **D** and **E** are rare. These cyclization processes also generated chiral products to be accessed in a stereoselective manner.¹⁷⁵



Scheme 75. Possible mechanism for gold(I)-catalyzed cyclization of allenols and amino allenes.

We focus on two-reaction types: gold(I)-catalyzed hydroalkylation and hydroamination reactions to prepare enantioenriched heterocyclic derivatives by using optically pure allenes and chiral gold catalysts.

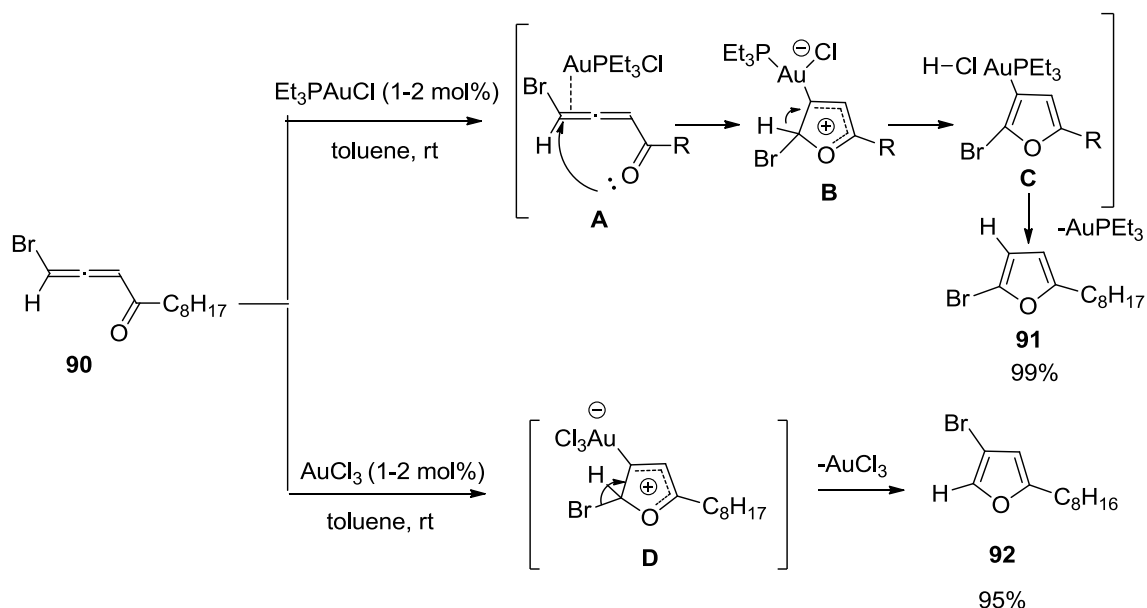
4.2.1.1. Hydroalkoxylation reactions

Gold (III) species was first studied for the formation of alkyl and aryl substituted furans from allenic ketones by Hashmi and co-workers in 2000.¹⁷⁸ The Gevorgyan group demonstrated the synthesis of halogenated furans from bromo-allenones by gold(I) in comparison to gold (III) catalysts in 2005.¹⁷⁹ Interestingly, different bromo-substituted furans were obtained. In the presence of triethylphosphine gold(I) chloride, the cycloisomerization of bromoallenic ketone **90** led to 2-bromofurans **91**, whereas the reaction with gold(III) chloride afforded 3-bromofurans **92** (Scheme 76). These remarkable results and computational studies by Soriano and Fernández¹⁶⁶ allowed them to propose a mechanism in two pathways for the selective formation of bromofurans **91** and **92**. When using triethylphosphine gold(I) chloride catalyst, π -philic gold(I) species coordinated to the distal double bond of allene (**A**), and followed the intermolecular attack of oxygen to form gold carbenoid **B**. The reaction then underwent a 1,2-hydride shift

¹⁷⁸ A. S. K. Hashmi, L. Schwarz, J.-H. Choi, T. M. Frost, *Angew. Chem. Int. Ed.* **2000**, *39*, 2285–2288.

¹⁷⁹ A. W. Sromek, M. Rubina, V. Gevorgyan, *J. Am. Chem. Soc.* **2005**, *127*, 10500–10501.

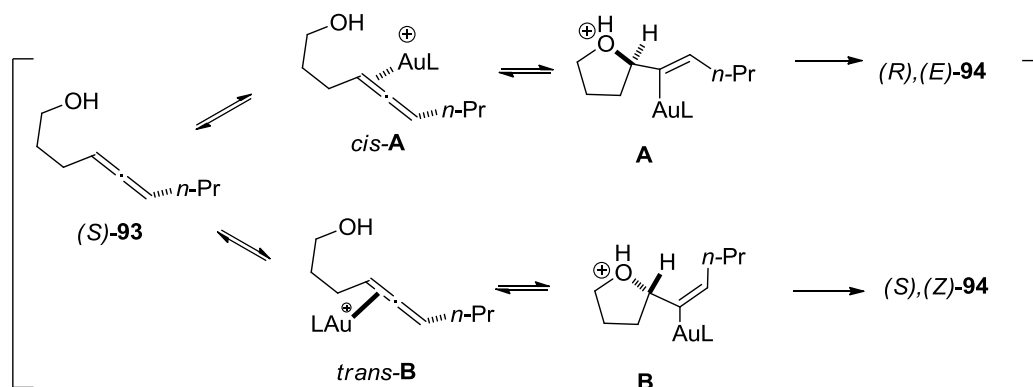
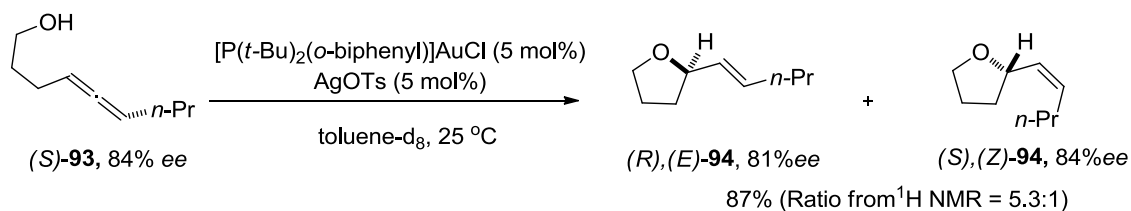
process **(B)** and protodeauration **(C)** to furnish **91**. In the case of gold(III) chloride, oxophilic gold(III) species **D** was formed as cyclic zwitterionic intermediates. The latter underwent a kinetically favored 1,2-bromo-migration to give **92**.



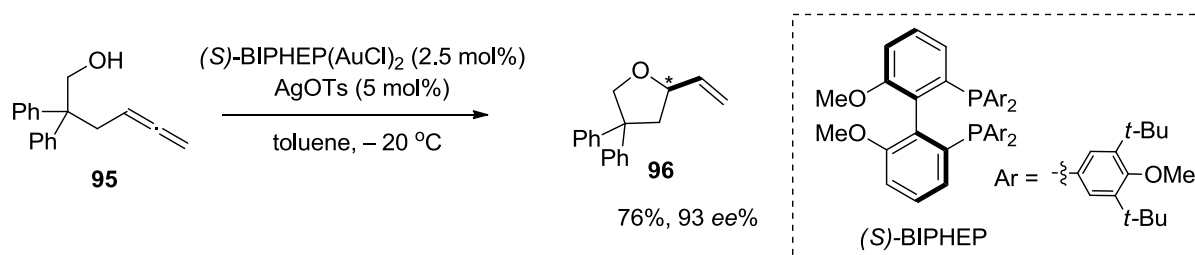
Scheme 76. Gold-catalyzed cycloisomerization of **90**.

Since the publication of these studies, gold(I) and gold(III) (pre)catalysts have been widely used in the cycloisomerization of allenones, as well as allenols, for the formation of aromatic heterocycles.¹⁷⁴ However, the use of gold(III) chloride catalysts in some reactions could promote undesired products.¹⁸⁰ Alternatively, the use of gold(I) complex as a precatalyst has also been suggested. In 2007, Widenhoefer and co-workers were the first to study the gold(I)-catalyzed *exo*-hydroalkoxylation reaction of optically pure γ -allenol derivatives.¹⁴⁰ For example, chiral allenol (*S*)-**93** was treated with 5 mol% of cationic gold complex bearing biarylphosphine ligand. Gold intermediates **A** and **B** in transition state resulted from the competitive outer-sphere attack of the hydroxyl group on the diastereomeric η^2 -gold-allene complexes (*cis*-**A** and *trans*-**B**). After protodeauration, a 5.3:1 mixture of (*R*),(*E*)-**94** and (*S*),(*Z*)-**94** was obtained in 87% yield, with almost complete transfer of chirality (Scheme 77).

¹⁸⁰ A. S. K. Hashmi, M. C. Blanco, D. Fischer, J. W. Bats, *Eur. J. Org. Chem.* **2006**, 2006, 1387–1389.

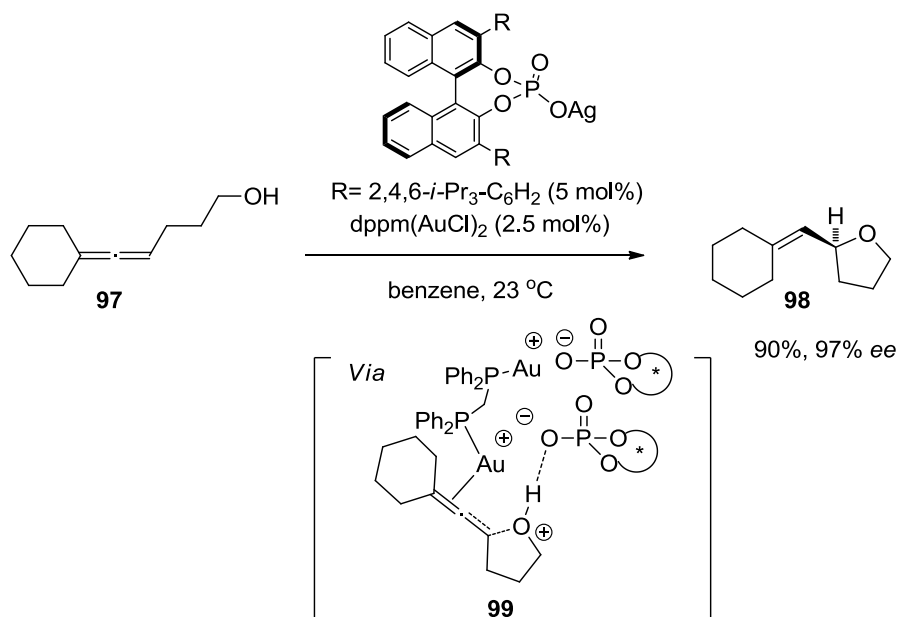
Scheme 77. Synthesis of **94** from (*S*)-**93**.

Moreover, the Widenhoefer group also used chiral digold complex to afford other enantiomerically pure 2-vinyltetrahydrofuran derivatives.^{140, 181} The β -gem-disubstituted- γ -allenol **95** carried out in the presence of (*S*)-BIPHEP(AuCl)₂ (2.5 mol%) and AgOTs (5 mol%) in toluene at –20 °C. Chiral 2-vinyltetrahydrofuran **96** was obtained in 76% yield and 93% ee (Scheme 78).

Scheme 78. Asymmetric hydroalkoxylation of allenols **95**.

The last interesting example from the Toste group extended the series of substrates and chiral gold catalyst for Hydroalkoxylation reactions. Cyclohexyl substituted- γ -allenol **97** and chiral dinuclear gold complexes bearing (*R*)-BINAP and (*R*)-SEPHOS as precatalysts were used. However, the corresponding product **98** was obtained in poor enantioselectivity.⁶⁶ To improve the enantioselectivity, Toste used a chiral silver anion and dppm(AuCl)₂ in the presence of **97**. We proposed that the gold catalyst and chiral silver anion could be formed as reactive intermediate **99**. The enantiomerically pure product **98** was obtained successfully in 90% yield and 97% ee.

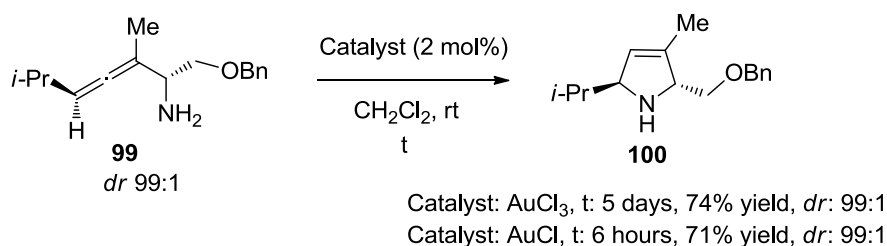
¹⁸¹ Z. Zhang, R. A. Widenhoefer, *Angew. Chem.* **2007**, *119*, 287–289.



Scheme 79. Asymmetric hydroalkylation of **97** with a chiral silver anion and dppm(AuCl)_2 .

4.2.1.2. Hydroamination reactions

In 2004, Morita and Krause pioneered the intramolecular hydroamination of allenes.¹⁸² They trialed the treatment of optically pure α -aminoallene **99** with gold(III) chloride to afford the corresponding 3-pyrroline **100** with completely transfer of diastereomeric ratio. However, they found that this reaction with gold(III) catalyst took long reaction times for full conversion of the desired product.¹⁸³ Interestingly, the reaction employed the gold(I) chloride catalyst took only six hours and gave the product **100** in 71% yield (Scheme 80). Thus, the gold(I) salts are usually applied in hydroamination reactions.

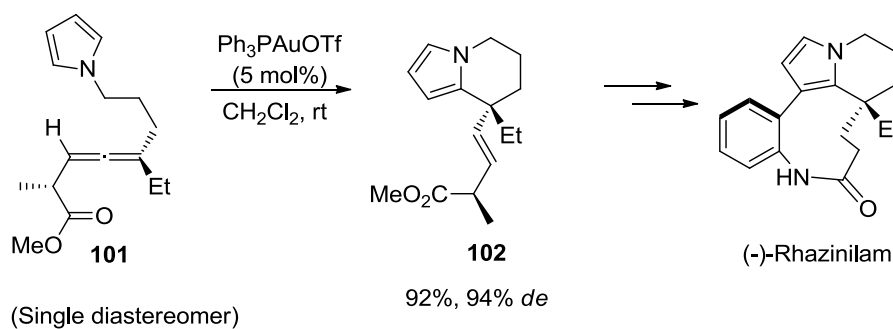


Scheme 80. Gold-catalyzed cycloisomerization of α -aminoallene **99**.

¹⁸² N. Morita, N. Krause, *Org. Lett.* **2004**, *6*, 4121–4123.

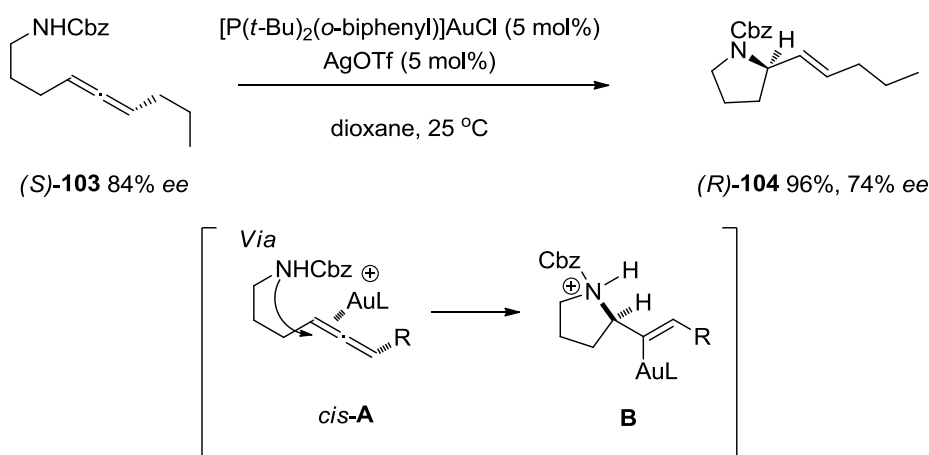
¹⁸³ N. Morita, N. Krause, *Eur. J. Org. Chem.* **2006**, *2006*, 4634–4641.

The Nelson group also reported the use of the cationic gold-catalyzed allene cyclization as a key step for the synthesis of (–)-Rhazinilam.¹⁸⁴ Ph_3PAuOTf was employed as a catalyst in order to activate allene **101** bearing a pyrrole substituent. The pyrrole ring, which acts as a nucleophile, attacks the activated allene bond to deliver with high yield and excellent chirality transfer (92%, 94% *de*) of the tetrahydroinolizine **102**, which is a precursor of the alkaloid (–)-Rhazinilam (Scheme 81).



Scheme 81. Synthesis of **102** from allene **101**.

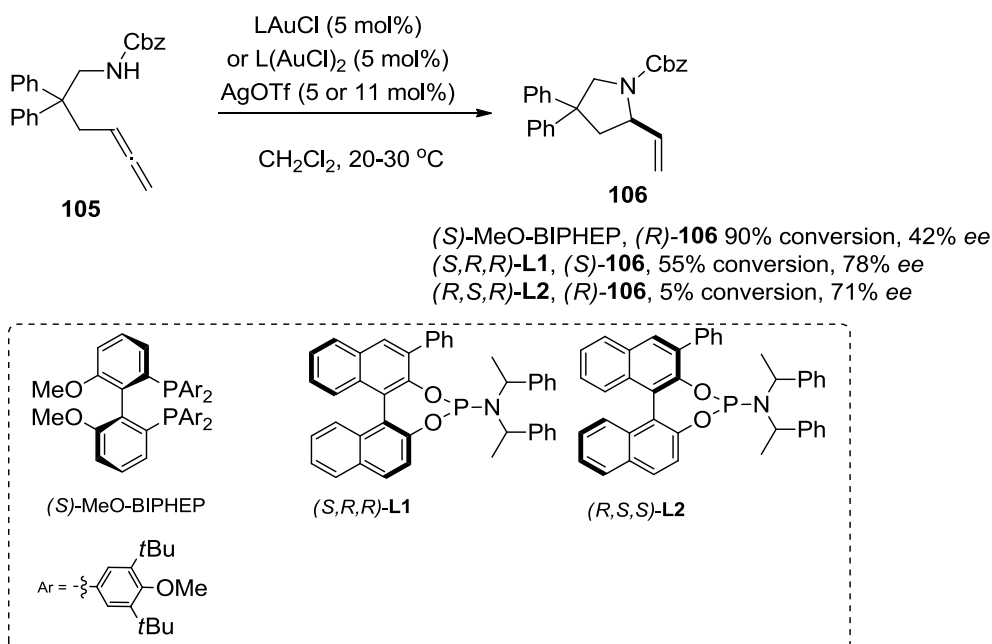
Widenhoefer also studied gold-catalyzed intramolecular *exo*-selective hydroaminations to enantioenriched pyrrolidine derivatives.¹⁴⁰ The reaction of enantioenriched (*S*)-*N*-allenyl carbamate **103** with 84% *ee* in the presence of 5 mol% of cationic gold, prepared by $\text{P}(t\text{-Bu})_2(o\text{-biphenyl})\text{AuCl}$ and AgOTf , afforded (*R*)-pyrrolidine **104** in 96% yield and 74% *ee*. The lost 10% *ee* from the substrate (84% *ee*) is thought to have resulted from the incompletely chirality transfer in transition state in the transformation of gold intermediate **B** from *cis*-**A**. (Scheme 82).



Scheme 82. Intramolecular hydroamination of (*S*)-**103**.

¹⁸⁴ Z. Liu, A. S. Wasmuth, S. G. Nelson, *J. Am. Chem. Soc.* **2006**, *128*, 10352–10353.

To continue the preparation of enantioenriched pyrrolidine derivatives, Michon and co-workers developed the synthesis of 2-vinylpyrrolidine **123**¹⁴⁰ from monosubstituted γ -aminoallene **122** by gold catalysts with different chiral ligands.^{177a} A digold complex bearing (*S*)-MeO-BIPHEP were the first to investigate. The treatment of allene carbamate **105** with (*S*)-MeO-BIPHEP(AuCl)₂ and AgOTf catalyst afford **106** in moderate *ee* (42%). Moreover, mononuclear gold complexes bearing bulky functional group were investigated to improve the enantioselectivity. Among various ligands examples, the phosphoramidite complexes are used to improve enantioselectivity. The more bulky phosphoramidites such as phosphoramidites bearing phenyl substituents (*S,R,R*)-**L1** and (*R,S,S*)-**L2** could improve the enantioselectivity of the reaction by up to 78% *ee* (Scheme 83).



Scheme 83. Asymmetric gold(I)-catalyzed cyclization of **105**.

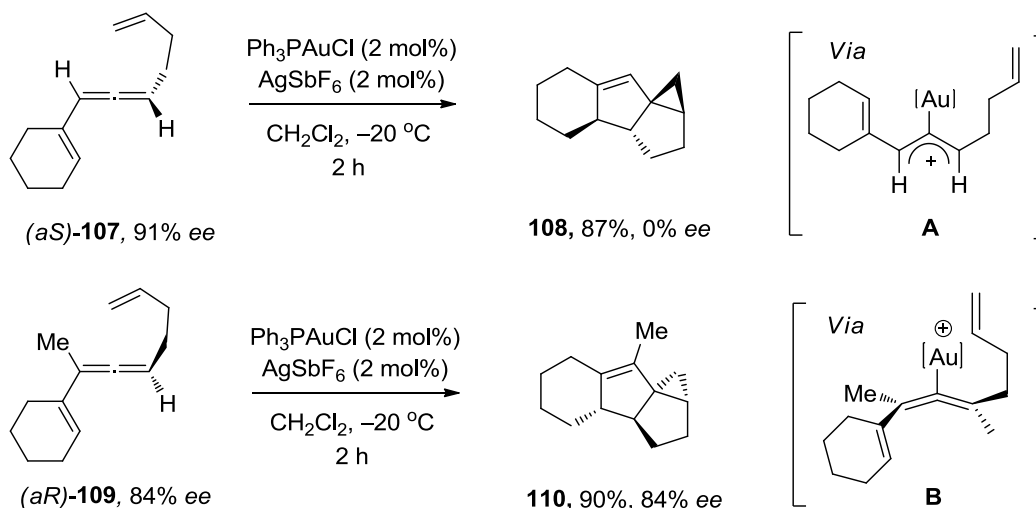
4.2.2. Carbonucleophilic cyclization

Electron-rich moieties such as vinyl group-containing allenes are more attractive as *in-situ* nucleophiles to enhance carbonucleophilic cyclization process.^{185, 186} Our group is interested in the synthesis of cyclopentadiene derivatives towards the preparation of polycyclic compounds *via*

¹⁸⁵ J. H. Lee, F. D. Toste, *Angew. Chem. Int. Ed.* **2007**, *46*, 912–914.

¹⁸⁶ C. Santelli-Rouvier, M. Santelli, *Synthesis* **1983**, 429–442. See also: (a) A. J. Frontier, C. Collison, *Tetrahedron* **2005**, *61*, 7577–7606.; (b) M. A. Tius, *Eur. J. Org. Chem.* **2005**, 2193–2206.; (c) M. Rueping, W. Ieawsuwan, A. P. Antonchick, B. J. Nachtsheim, *Angew. Chem.* **2007**, *119*, 2143–2146.; (d) I. Walz, A. Togni, *Chem. Commun.* **2008**, 4315–4317.

gold catalytic reactions.¹⁸⁷ The reaction of disubstituted ene-vinylallene (*aS*)-**107** with 91% *ee* led to racemic tetracyclic compound **108**, due to the formation of achiral planar allylic cation (**A**). In contrast, the cyclization of trisubstituted ene-vinylallene (*aR*)-**109** with 84% *ee* gave the enantio-pure polycyclic product **110**, rising to a perfect transfer of chirality. Consequently, more substituted functional group on the allene can keep the stereometric information of optically pure allenes to afford totally transfer of chirality. (Scheme 84)

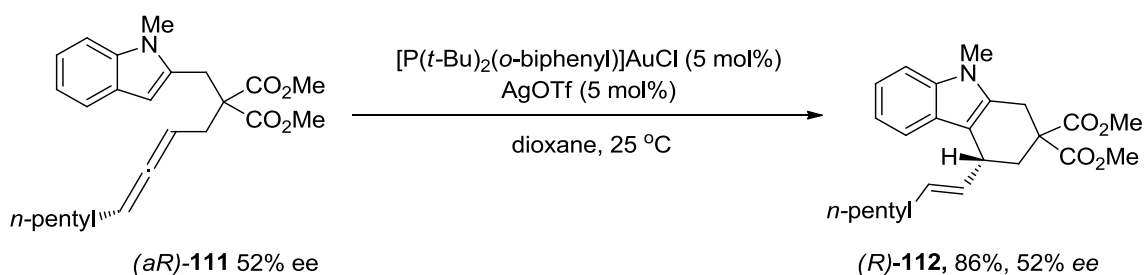


Scheme 84. Gold(I)-catalyzed cycloisomerization of (*aS*)-**107** and (*aR*)-**109**.

The last series of carbonucleophilic cyclization is devoted to hydroarylation reaction of a combination of allene and arene. This reaction is described as the Friedel-Crafts type cyclization when the addition of an arene takes place across an unsaturated π -system of alkene, alkyne, allene, or benzyne.¹⁸⁸ In 2006, Windenhoefer reported successfully hydroarylation reactions of allene derivatives.¹⁴⁰ For example, the reaction of optically pure allnylindole (*aR*)-**111** in the presence of gold catalyst bearing Buchwald biaryl phosphine yielded 86% of (*R*)-**112**. It was proven the totally transfer of chirality, thanks to the steric indole moiety induced the asymmetry (Scheme 85).

¹⁸⁷ G. Lemière, V. Gandon, K. Cariou, A. Hours, T. Fukuyama, A.-L. Dhimane, L. Fensterbank, M. Malacria, *J. Am. Chem. Soc.* **2009**, *131*, 2993–3006

¹⁸⁸ (a) M. T. Reetz, K. Sommer, *Eur. J. Org. Chem.* **2003**, 3485–3496.; (b) Z. Shi, C. He, *J. Org. Chem.* **2004**, *69*, 3669–3671.; (c) A. S. K. Hashmi, M. C. Blanco, *Eur. J. Org. Chem.* **2006**, 4340–4342.

Scheme 85. Hydroarylation reactions of *(aR)*-111.

To summary, a large number of hetero- and carbopolycyclic derivatives can be synthesized from well-designed allene substrates and active carbo- or heteroatom-nucleophiles in gold(I)-catalyzed cyclization reactions. The generation of stereoselective compounds with high enantiomeric excess is more challenging by using chiral catalysts or optically pure allenes as in several examples to enhance the selectivity of products.

5. Conclusion and perspective

Allene derivatives are valuable compounds as versatile substrates, catalysts, and ligands of metals. The allenes are often prepared from propargylic acetates by the substitution of nucleophiles *via* S_N2' reactions or by the catalytic reactions using metal catalysts such as palladium(0), copper(I) salts. Alternatively, the isomerization reactions of alkyne substrates to form allenes is also mentioned in studies. The main focus of studies on allenes centred on attempts to use them as chiral organocatalysts and ligands for enhancing in the stereoselective products in asymmetric catalysis. The isolation of metal-allene complexes could allow us to understand their coordination modes and to predict the metal-allene intermediates in transition state. In addition, metal complexes have been recognized as very useful catalysts for the straightforward cyclization of allenes as substrates, leading to a wide range of monocyclic and polycyclic compounds. In particular, gold(I) complexes have already been reported as catalysts for this process in the presence of nucleophiles.

Owing to the great examples of allene applications in gold chemistry, our perspective is to consider the design of new allene derivatives bearing phosphine moieties as depicted in Figure 30. We aimed to apply them as chiral organocatalysts, as ligands for various metals, particularly gold(I) salts, and chiral substrates in gold(I)-catalyzed allene cyclization, which is more attractive to enhance their synthetic utility with the synthesis of more complexes and designed molecules in mild reactions.

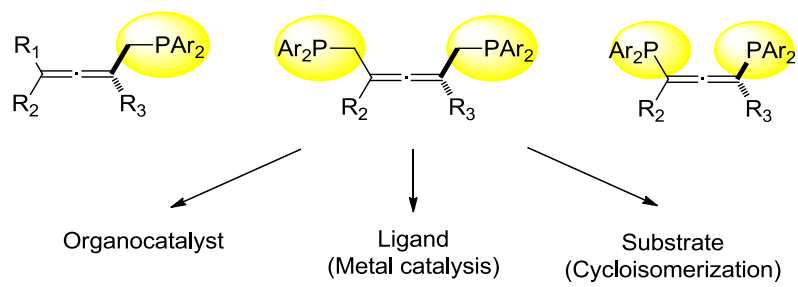
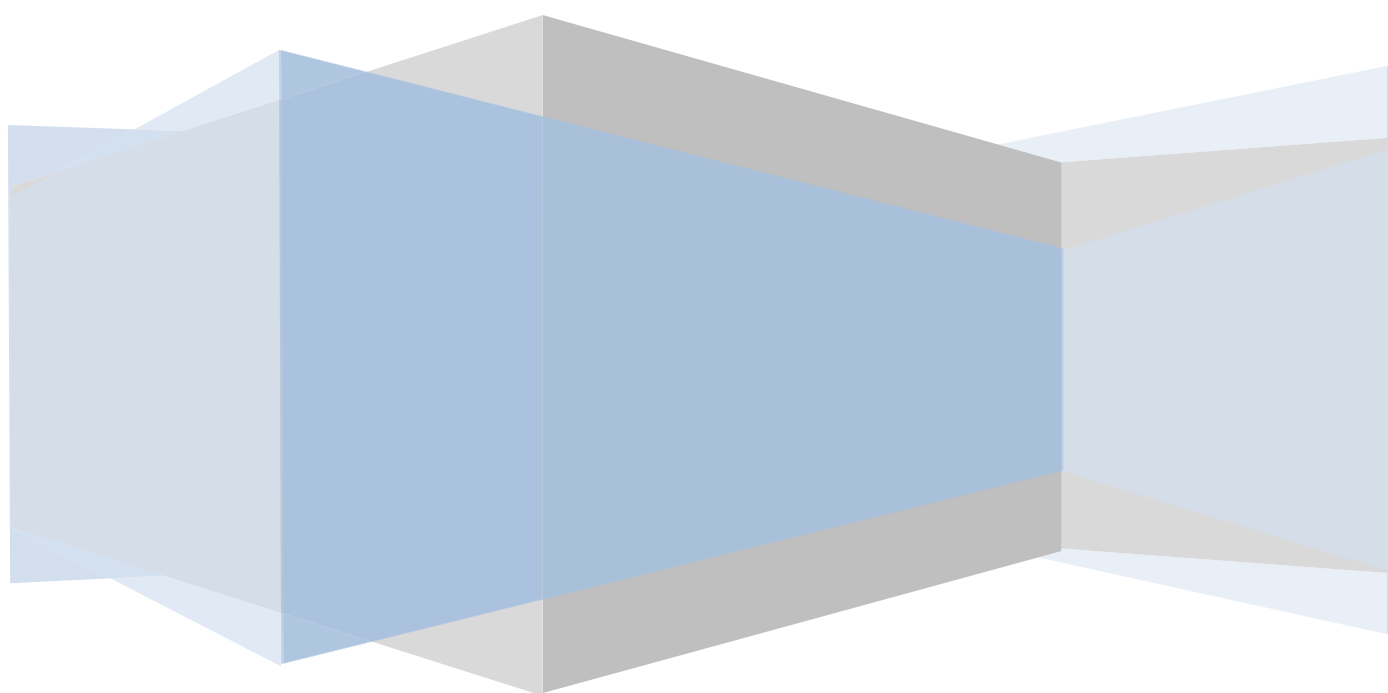


Figure 30. Allenes with phosphine moieties

Chapter 3

Allenes Bearing Phosphine Oxide Groups and
Their Reactivity towards Gold Complexes



CHAPTER 3

Allenes Bearing Phosphine Oxide Groups and Their Reactivity towards Gold Complexes

1. Introduction

Chiral phosphine ligands have proven their significant role in metal-mediated asymmetric catalytic (See Chapter 1). Axially chiral allenes are highly valuable precursors for preparative organic chemistry but also promising ligands for transition metals (See Chapter 2). However, research devoted to the study of the reactivity of mixed allene-phosphine ligands remains quite limited in the field of asymmetric catalysis. Of special interest, gold complexes bearing allene ligands have been disclosed in a few reports (Figure 31). For example, McGlinchey reported gold complexes containing allene moieties *via* a coordination of gold and phosphorus atoms.¹⁴⁹ Fürstner isolated a gold complex bearing diamino group, which was formed as η^1 -coordination mode.^{170b} In contrast, Widenhoefer has reported the isolation of an η^2 -coordinated-cationic allene gold complexes.^{168, 169} These motivate us to design new gold complexes bearing mixed allene-phosphine ligands and to investigate their reactivity towards gold salts.

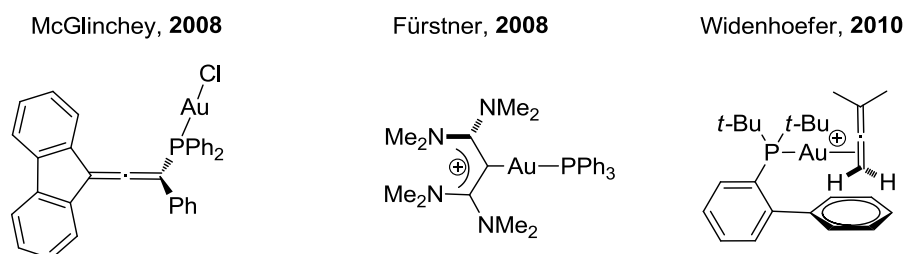
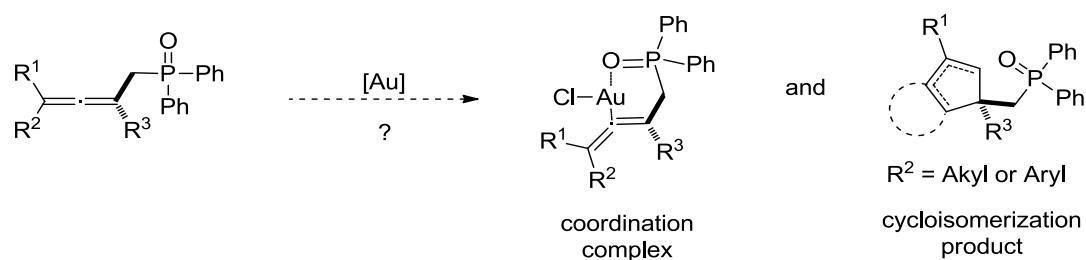


Figure 31. Allene-gold complexes.

2. Objectives of the project

We aimed at synthesizing allenes bearing phosphine oxide groups as new chiral ligands for gold(I) species. They will be used as probes for two types of applications (Scheme 86). The first type is based on previous studies discussed. We expected to generate original organogold complexes featuring polycoordination mode.^{50, 73} Indeed, both the allene and the oxygen atom of the phosphine oxide group could coordinate to gold(I) species. The second objective was to involve these substrates in cycloisomerization reactions when using appropriate R^2 substituent on allene in order to deliver new chiral organophosphorus substrates.



Scheme 86. Objectives of allene compounds.

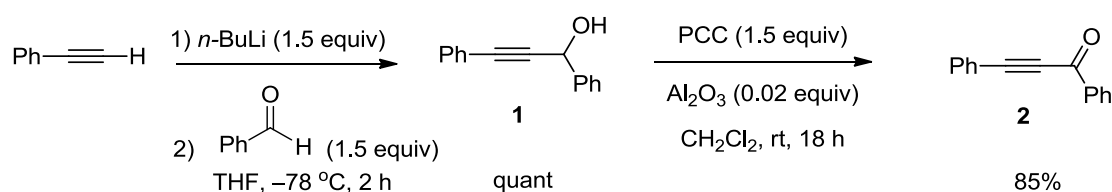
3. Synthesis of allenes bearing monophosphine oxide groups

We envisaged the preparation of various allenes bearing one or two phosphine oxide groups, following a general strategy reported by the groups of Krause¹³⁸ and Ready¹³⁰ involving common intermediates such as propargylic acetate precursors. The latter can then undergo a S_N2' substitution *via* copper catalysis or a cross-coupling reaction *via* palladium catalysis with appropriate organometallic derivatives, leading to the formation of the desired allene function. The following section will describe these synthetic methodologies and their results.

3.1. Synthesis of allenes bearing monophosphine oxides

3.1.1. Synthesis of propargyl ketone (2)

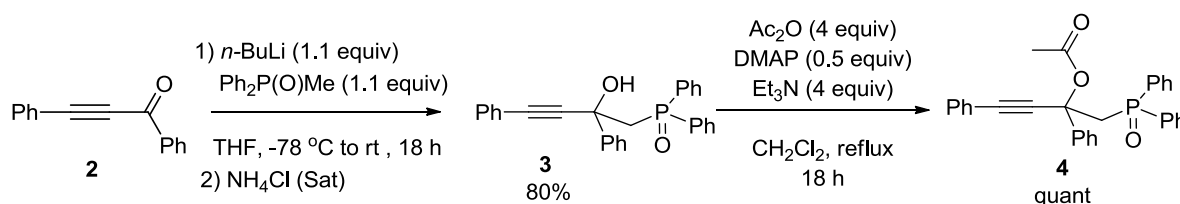
Allenes bearing monophosphine oxides requires the corresponding propargylic acetates as precursors, which were prepared from the alkylation reaction of propargyl ketones. First step was devoted to the synthesis of propargyl ketone **2**. Deprotonation of phenylacetylene with *n*-butyllithium followed by condensed onto benzaldehyde gave alcohol **1** in quantitative yield.¹⁸⁹ Oxidation of **1** in the presence of PCC gave propargyl ketone **2** in 85% yield. (Scheme 87)

Scheme 87. Synthesis of propargyl ketone **2**.

¹⁸⁹ P. G., Cozzi, S., Alesi, *Chem. Comm.* **2004**, 2448–2449.

3.1.2. Synthesis of propargylic acetate (**4**)

The ketone **2** was then substituted through an alkylation reaction using lithium methyl-diphenylphosphine oxide, prepared by deprotonation of methyl-diphenylphosphine oxide with *n*-butyllithium. After hydrolysis, the reaction gave alcohol **3** in 80% yield. The corresponding propargylic acetate precursor **4** was obtained in quantitative yield through an efficient protection of the hydroxyl group with acetic anhydride under classical conditions (Scheme 88).



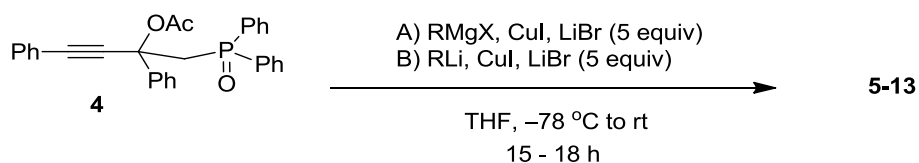
Scheme 88. Synthesis of propargylic acetate **4**.

3.1.3. Synthesis of allenes bearing monophosphine oxides (5-13)

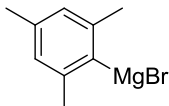
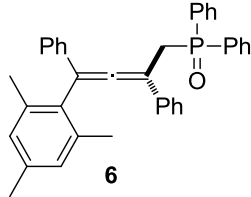
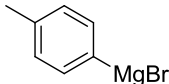
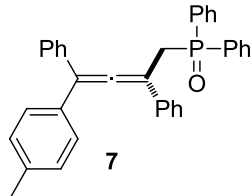
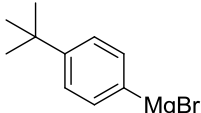
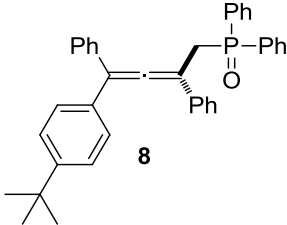
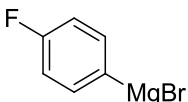
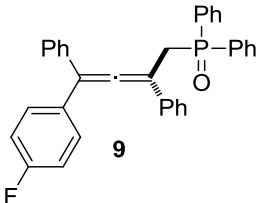
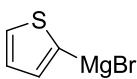
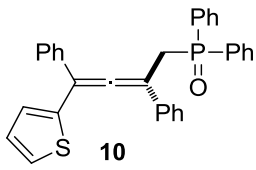
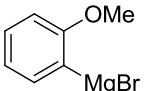
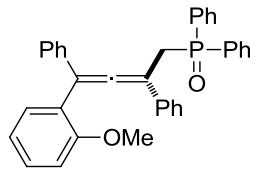
3.1.3.1. Copper(I)-mediated S_N2' reactions

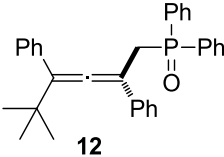
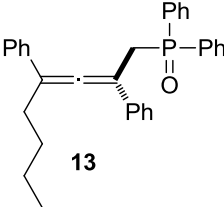
A first series of allenes bearing monophosphine oxides was prepared by modifying the nature of the organometallic reagents (RLi, RMgX), presenting an alkyl or an aryl function. Depending on the nature of the organometallic species, the displacement of the acetate group from propargylic acetate **4** could occur under classical copper iodide-mediated S_N2' substitution under Ready's conditions¹³⁰ with satisfactory yields (Table 1, entries 1-9).

Table 1. Preparation of allenes *via* copper-mediated S_N2' reactions.



Entry	Condition	Reagent	Product	Yield (%)
1	A	PhMgBr		84

2	A			69
3	A			76
4	A			81
5	A			92
6	A			58
7	A			66

8	A	<i>t</i> -BuMgCl	 12	78
9	B	<i>n</i> -BuLi	 13	98

3.1.3.2. Palladium-catalyzed coupling reactions

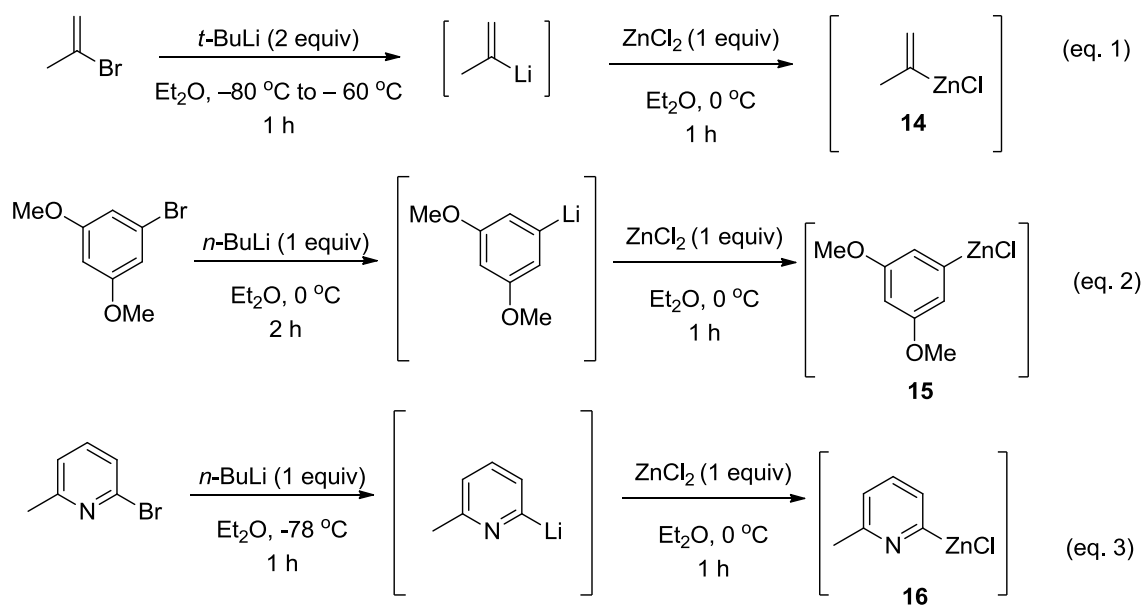
In some cases, the non-productive transmetalation process between copper and the organometallic reagent (RLi, RMgX) prevents the S_N2' substitution pathway. Alternatively, organocopper reagents are unreactive. A palladium-catalyzed coupling reaction was attempted to use for the preparation of some allenes that contain vinyl **17**, 3,5-dimethoxyphenyl **18**, and pyridyl **19** functional groups, using the corresponding organozinc derivatives.

a) Preparation of organozinc reagents

The organozinc reagents were prepared from the corresponding organolithium reagents by transmetalation using $ZnCl_2$ salts. Isopropenyllithium (Scheme 89, eq. 1) was prepared from a 2:1 mixture of *tert*-buthyllithium and isopropenyl bromide *via* lithium-bromo exchange, according to the procedure by Lautens.¹⁹⁰ In a similar manner, the preparation of 3,5-dimethoxybenzyl- and 2-pyridinyl lithium reagents (Scheme 89, eq. 2 and 3) was achieved following the procedure of Alexakis¹⁹¹ by using *n*-buthyllithium (1 equiv) with the corresponding bromide reagents. The latter organolithium reagents were directly added to a $ZnCl_2$ solution, leading to the precipitation of LiCl salt *via* lithium-zinc transmetalation. The freshly prepared organozinc chloride reagents were directly used for the palladium-catalyzed reactions with propargylic acetate substrates to afford the corresponding allenes.

¹⁹⁰ D. A. Candito, M. Lautens, *Angew. Chem. Int. Ed.* **2009**, *48*, 6713–6716.

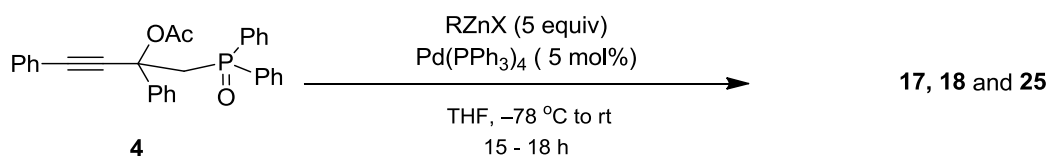
¹⁹¹ D. Müller, L. Guénée, A. Alexakis, *Eur. J. Org. Chem.* **2013**, *2013*, 6335–6343.

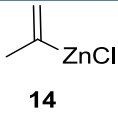
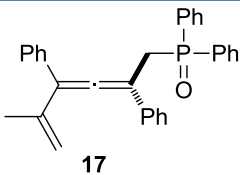
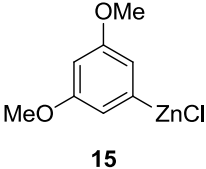
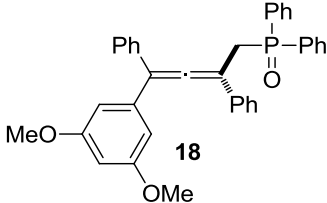
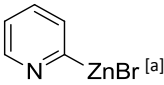
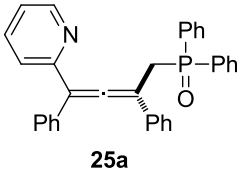
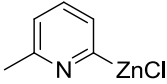
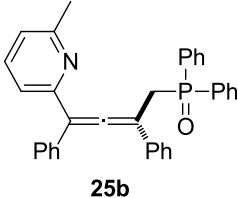


Scheme 89. Preparation of organozinc reagents.

b) The use of organozinc reagents in palladium-catalyzed coupling reactions.

In the next step, the propargylic acetate **4** was added in the presence of $\text{Pd}(\text{PPh}_3)_4$ to the solution of freshly prepared organozinc reagents. The activation of palladium(0) catalyst on acetate **4** allows the generation of a palladium-allene complex which undergoes transmetalation with the organozinc reagent (See the proposed mechanism in Scheme 50). After the reductive elimination of palladium, the reaction affords the desired allenes. The preparations of allenes **17**, **18**, and **25** were envisaged in this manner and summarized in Table 2 (entries 10-13). Following Krause's condition¹³⁸, allenes **17**, **18** and **25a** were obtained in moderate to fair yields. However, the product **25b** was not obtained. This reaction (Table 2, entry 13) gave a mixture of propargylic alcohol **3** and starting propargylic acetate **4**. We surmised that the problem came from the incomplete formation of the organozinc compound that also led to deacylation of the acetoxy group of **4** by the pyridinyl-lithium reagent to form **3**.

Table 2. Preparation of allenes *via* palladium-catalyzed coupling reactions.

Entry	Condition	Reagent	Yield (%)
10	 14	 17	51
11	 15	 18	75
12	 12	 25a	41
13	 13	 25b	^[b]

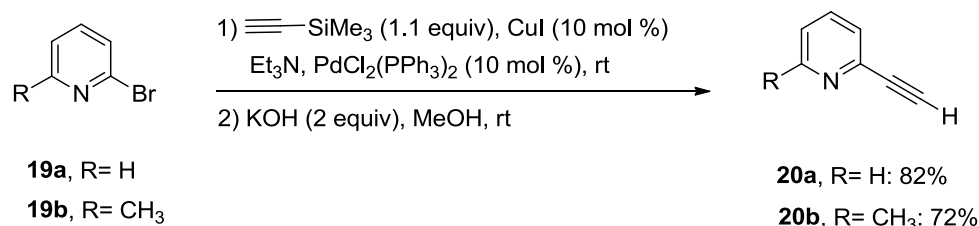
^[a] 2-pyridinyl zinc bromide is a commercial reagent from Sigma-Aldrich®. ^[b] The reaction with 6-methyl-2-pyridinyl zinc chloride did not afford **25b**.

3.2. Synthesis of pyridinyl-containing allenyl phosphine oxides

Following unsatisfying results of pyridinyl allenes from propargylic acetate **4**, the preparation of pyridinyl propargylic acetates was attempted in order to use them as substrates for palladium-catalyzed allene formations.

3.2.1. Synthesis of ethynylpyridines.

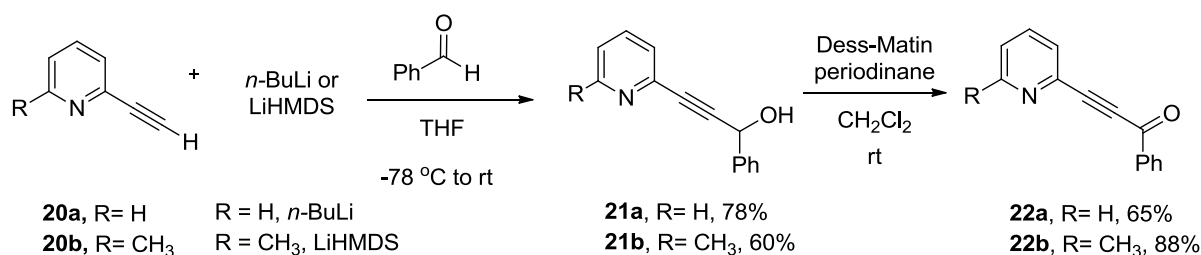
Ethynylpyridines were synthesized to access the corresponding ketone substrates as well. Treatment of 2-bromopyridines **19** and trimethylsilyl acetylene in the presence of palladium catalysts gave cross coupling reactions, followed by the elimination of trimethylsilyl group by KOH to afford **20a** and **20b** (Scheme 90).



Scheme 90. Synthesis of ethynylpyridines.

3.2.2. Synthesis of propargylic ketone (22)

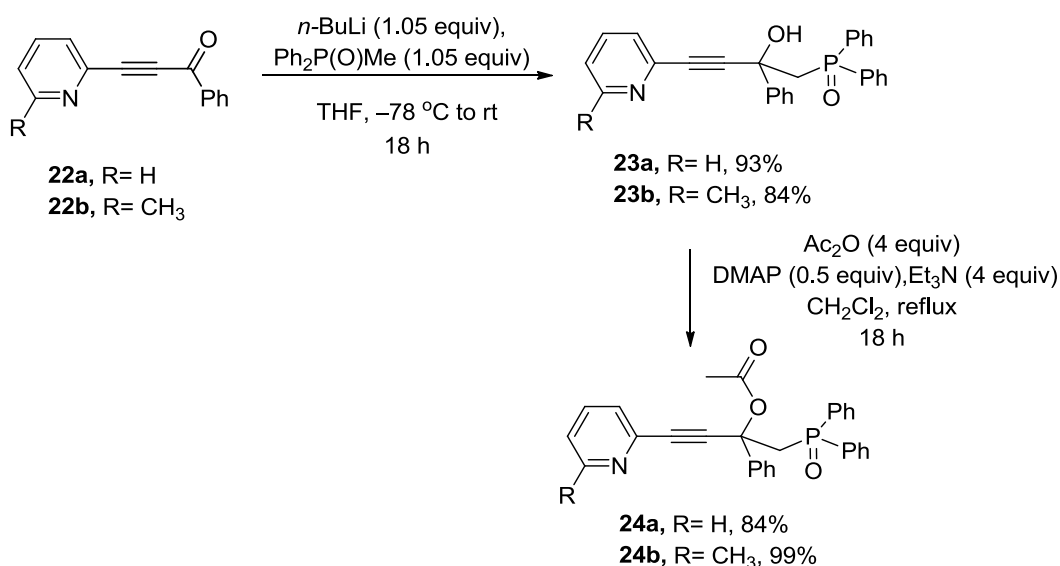
The ethynylpyridines **20a** and **20b** were deprotonated with *n*-butyllithium for **20a** and a milder base, LiHMDS, for **20b** respectively. Condensation with benzaldehyde afforded propargyl alcohols **21a** and **21b** in 60 % and 78% yields respectively. The alcohols **21a** and **21b** were then oxidized by Dess-Martin periodinane to afford propargyl ketones **22a** and **22b** in 65% and 88% yields (Scheme 91). Notably, PCC was not used to prepare these ketones. It was not a selective oxidizing agent and it led to only poor conversion to ketones. Dess-Martin periodinane, which is a less toxic agent, worked effectively under milder conditions with short reaction times.



Scheme 91. Synthesis of pyridyl ketones 5a and 5b.

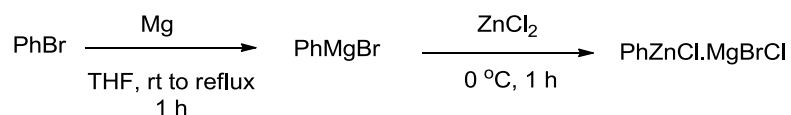
3.2.3. Synthesis of propargylic acetate (24)

In a similar manner to the preparation of propargylic acetate **4**, the ketones **22a** and **22b** were also alkylated by lithium methyl-diphenylphosphine oxide *via* alkylation reaction. After the protection of the hydroxyl group with acetic anhydride, the propargylic acetate precursors **24a** and **24b** were obtained in excellent yields (84% and 99%) (Scheme 92).

Scheme 92. Synthesis of propargylic acetate **24a** and **24b**.

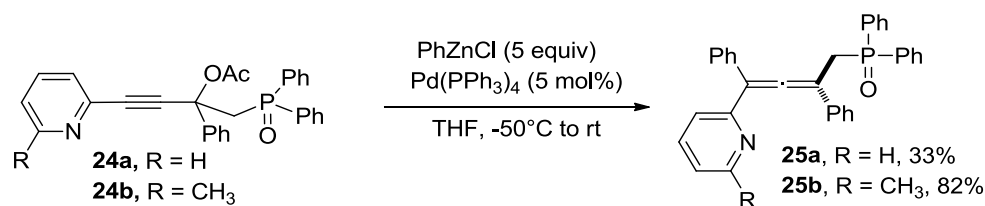
3.2.4. Synthesis of pyridinyl allenes bearing mono-phosphine oxides (25)

Phenylzinc chloride reagent was prepared from freshly obtained phenylmagnesium bromide, prepared from bromobenzene and magnesium turnings, and the ZnCl₂ solution in Et₂O at 0 °C *via* a magnesium-zinc transmetalation (Scheme 93), following Krause's method.¹³⁸ Phenylzinc chloride was applied for the *in-situ* palladium-catalyzed reactions with propargylic acetate substrates to afford the corresponding allenes.



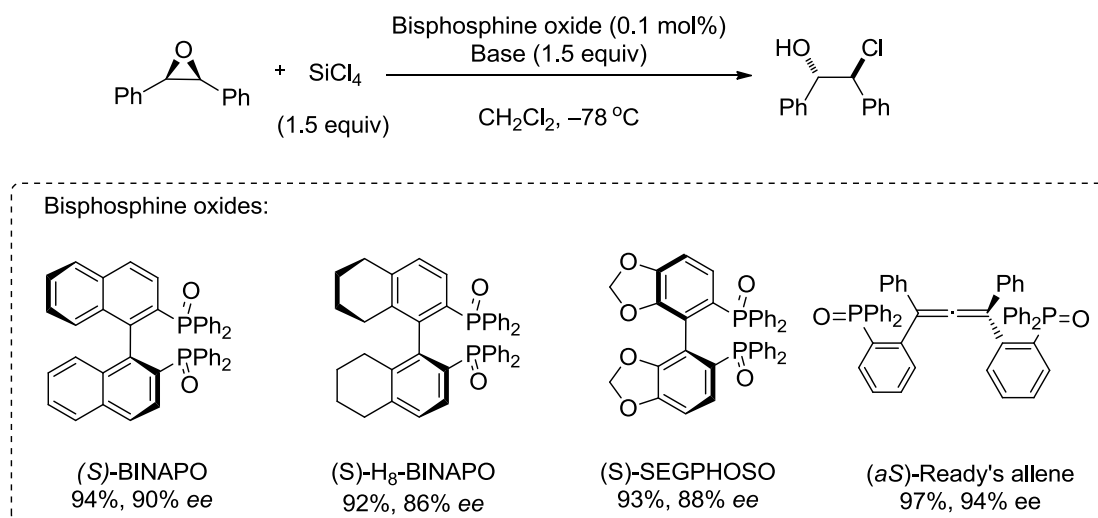
Scheme 93. Preparation of phenylzinc chloride reagent.

Based on the fact that the synthesis of allene **25a** and **25b** bearing a pyridine substituent could not be realized with high yields starting from propargylic acetate **4**, we envisaged to use pyridinyl propargylic acetates **24** as precursors in a palladium coupling reaction with freshly prepared phenylzinc chloride reagent (Scheme 94). Under palladium catalysis, as in the previous synthesis of allene **25a** and **25b**, the phenylzinc chloride directly was directly engaged. The coupling reaction produced the desired pyridinyl-allenes **25a** in moderate yield (33%) and **25b** in excellent yield (82%).

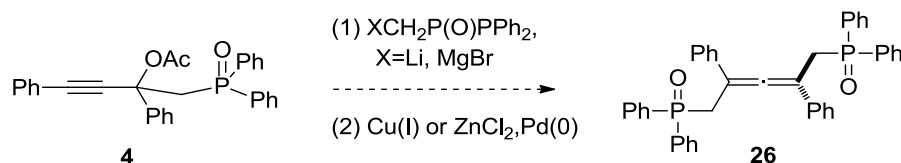
Scheme 94. Synthesis of pyridyl allenes **25a** and **25b**.

3.3. Synthesis of allenyl bisphosphine oxides

Bisphosphine oxide derivatives have been successfully used as organocatalysts in asymmetric reactions. As presented in chapter I, axially chiral bisphosphine oxides such as (*S*)-BINAPO, (*S*)-H₈-BINAPO, and (*S*)-SEGPHOSO were reported as chiral catalysts in asymmetric desymmetrization of *meso*-epoxides to afford chiral alcohol derivatives (Scheme 95).³⁸ Bisphosphine oxide groups act as Lewis bases for chelating to silicon tetrachloride reagent and induce highly enantioselectivity of products. Ready also introduced the first chiral allenes bearing bisphosphine oxide moieties, which succeeded as catalysts in this type of reaction to afford 94% *ee* of the desired chiral alcohol.¹³⁰

Scheme 95. Asymmetric desymmetrization of *meso*-epoxides.

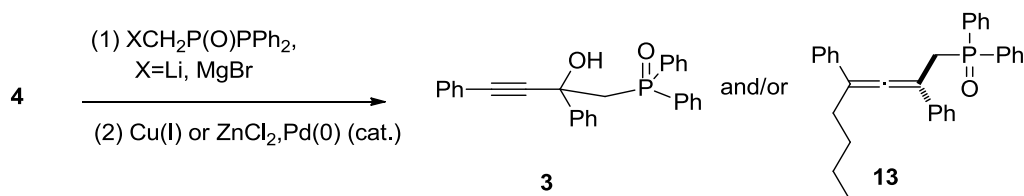
As a result, we envisaged the preparation of allene **26** bearing two phosphine oxide groups for this application. Reactions were attempted to test different phosphino-organocopper reagents *via* copper-mediated S_N2' substitution, and as well *via* a palladium coupling with phosphine-organozinc reagents using the organometallic methyldiphenylphosphine oxide (XCH₂P(O)Ph₂, X = Li or MgBr) as a precursor (Scheme 96).



Scheme 96. Preparation of allene **26 bearing bisphosphine oxide group.**

Unfortunately, two non-desired products (**3**, **13**) were obtained besides the formation of the expected allene **26** depending on the reaction conditions. The different conditions employed and the corresponding results are compiled in Table 3. For the experimental results, side reactions appeared as deacylation of the acetoxy group (**3**) and/or substitution by the butyl anion (**13**) from *n*-butyllithium reagent.

Table 3. Results regarding the synthesis of allenyl bis-diphenylphosphine oxides under different conditions.



Entry	Reagent (1)	Reagent (2)	Product (% yield)
1	MeP(O)Ph ₂ , <i>n</i> BuLi	CuI, LiI	3 (8%) ^[b] , 13 (quant) ^[a] ,
2	MeP(O)Ph ₂ , <i>n</i> BuLi	CuI, LiBr	6 (quant) ^[a]
3	1)MePPh ₂ , <i>n</i> BuLi 2)MgBr ₂	CuI, LiBr	3 (31%) ^[b] , 13 (quant) ^[a]
4	1)MePPh ₂ , <i>n</i> BuLi 2) MgBr ₂	ZnCl ₂ , Pd(PPh ₃) ₄ (5% mol)	No reaction ^[a]

^[a] Determination of the major product by ¹H NMR without isolation. ^[b] Isolated yield.

Reactions (Table 3, entries 1-2) of **4** with copper methyl-diphenylphosphine oxide reagent, prepared from lithium methyl-diphenylphosphine oxide in the presence of CuI and different types of lithium salts (LiI and LiBr), were not effective. Unfortunately, the alcohol **3** was produced as a major product. The latter could arise through the addition of cuprous species on the carbonyl group of the acetate moiety to give corresponding alcohol **3**. When the organometallic reagent was changed to the Grignard reagent of methyl-diphenylphosphine in association with CuI and LiBr (Table 3, entry 3), the reaction also conducted to the alcohol **3** as the major product and a small amount of allene **13**. Consequently, the reactions were envisaged *via* the coupling of an organozinc in the presence of the palladium catalyst (Table 3, entry 4). However, organozinc

reagent, prepared from the transmetalation of lithium methyl diphenylphosphine and ZnCl_2 , did not react with the substrate **4** under palladium catalytic conditions.

To summary, the classical reaction conditions (copper-mediated $\text{S}_{\text{N}}2'$ substitution and palladium-catalyzed coupling) were not applicable to the synthesis of the desired allene **26** bearing two phosphine oxide groups. In these conditions, we found that the alcohol **3** was often obtained as a major product. A possible explanation would be that coordination of the cuprous reagent at the phosphine oxide would bring both favors the attack on the acetoxy group. In the same line, the allene **13** came from the unsuccessful synthesis of the preparation of organometallic reagents (RCu and RZnCl) *via* transmetalation of the organolithium reagent, leading to the attack of butyl anion at π -bond of **4** *via* $\text{S}_{\text{N}}2'$ substitution. Thus, we had to envisage other alternatives to develop a synthetic methodology to attempt the synthesis of allene **26**.

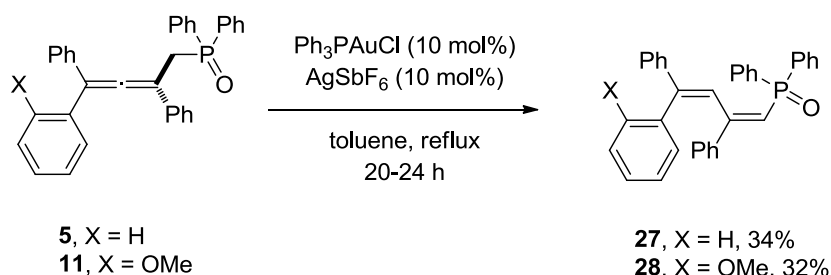
4. Allene cyclization

4.1. Investigation on the reaction of allenes with cationic gold complexes

Gold salts have already shown the ability to activate on an allene bond, which was determined by X-ray crystallography of isolated an gold-allene intermediate^{168-170, 192} and computational calculations⁹⁹ which exhibit different coordination modes. The intermediate can undergo rearrangement or cyclization in the presence of internal or external nucleophiles. Our allenes with difference substituents were engaged in gold catalytic reactions. We predicted that the substituents on allene or phosphine oxide moieties could behave as nucleophiles to afford intramolecular cyclic products.

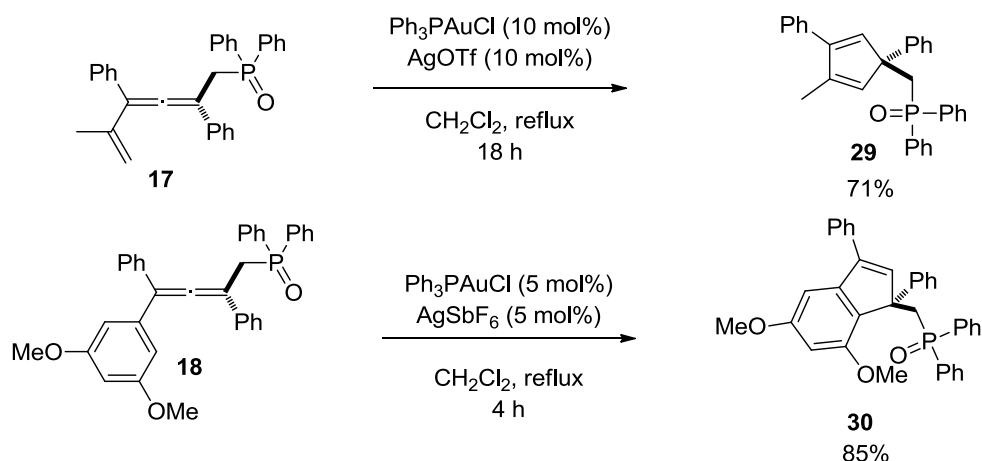
Firstly, we examined the reactivity of allenes **5** and **11** in the presence of catalytic quantities of Ph_3PAuCl and AgSbF_6 (10 mol%) in dichloromethane. However, the reaction did not afford any new products in either room temperature or refluxing in this solvent. To observe conversion, it was necessary to run these reactions in toluene at reflux. These reactions were sluggish to give dienic products **27** and **28** as the major compounds with 34% and 32% yields respectively (Scheme 97).

¹⁹² R. E. M. Brooner, R. A. Widenhoefer, *Angew. Chem. Int. Ed.* **2013**, 52, 11714–11724.



Scheme 97. Formation of dienes **27** and **28** via cationic gold(I) catalysis.

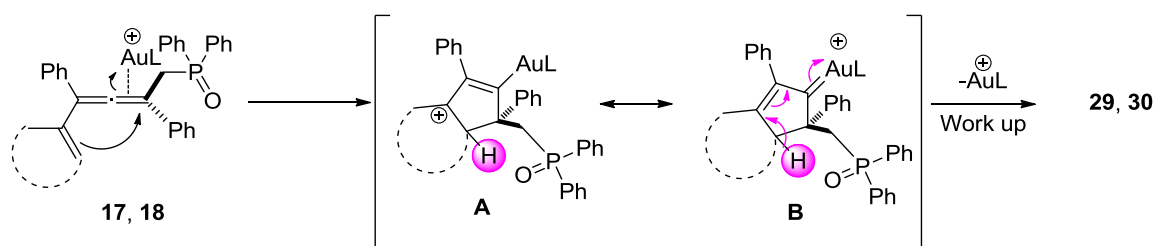
We were interested to know if we could observe an improved reactivity by using a more electron rich aryl group. Accordingly, vinylallene **17**¹⁹³ and allene **18** bearing a 3,5-dimethoxyphenyl substituent were engaged. To our delight, allenes **17** and **18** underwent gold(I)-catalyzed rearrangement and hydroarylation reactions providing the corresponding cyclopentadiene **29** and indenyl phosphine oxide **30** in 71% and 85% yields respectively (Scheme 98).



Scheme 98. Synthesis of cyclopentadiene-phosphine oxide **29** and indenylphosphine oxide **30**.

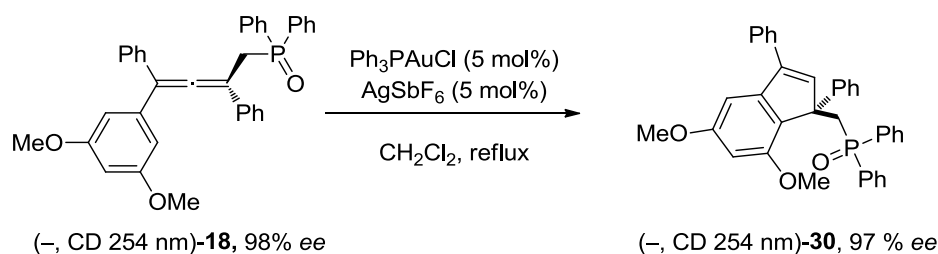
In these cases, we propose a first intramolecular addition of the nucleophile onto the activated allenes **17** and **18**, furnishing the cationic vinylgold intermediates **A** and **B** that can also be seen as carbenic resonance forms. Then, proton loss in the α -position on carbocation would be favored, leading to the desired product **29** and **30** after protodeauration (Scheme 99).

¹⁹³ (a) H. Funami, H. Kusama, N. Iwasawa, *Angew. Chem. Int. Ed.* **2007**, *46*, 909-911.; (b) J. H. Lee, F. D. Toste, *Angew. Chem. Int. Ed.* **2007**, *46*, 912-914.; (c) G. Lemièrre, V. Gandon, K. Cariou, T. Fukuyama, A.-L. Dhimane, L. Fensterbank, M. Malacria, *Org. Lett.* **2007**, *9*, 2207-2209.; (d) G. Lemièrre, V. Gandon, K. Cariou, A. Hours, T. Fukuyama, A.-L. Dhimane, L. Fensterbank, M. Malacria, *J. Am. Chem. Soc.* **2009**, *131*, 2993-3006.

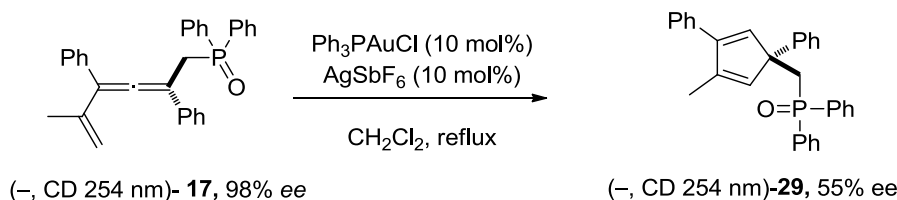
Scheme 99. Proposed mechanism of the formation of indenyl phosphine oxide **29** and cyclopentadiene **30**.

4.2. Chirality transfer

The next challenge was to study the possible chirality transfer to products **29**, **30** from optically pure allenes **17**, **18** in this efficient cycloisomerization step. We surmised that if a chirality transfer takes place in the cycloisomerization step, then an access to novel enantiopure phosphineoxides in which chirality relies on a quaternary center in the β -position to the phosphorus atom should be possible. This investigation was performed in collaboration with Dr. Nicolas Vanthuyne from Institut des Sciences Moléculaires de Marseille (iSm2, Aix-Marseille Université). A preparative chiral HPLC on racemic **17** and **18** could separate both corresponding to enantiomers with *ees* > 98%. We first engaged the (–, CD 254 nm)-**18**, under the same reaction conditions. Gratifyingly, the reaction gave the isolated (–, CD 254 nm)-**30** with a 97% *ee* evidencing an almost complete transfer of chirality (Scheme 100).

Scheme 100. Synthesis of (–, CD 254 nm)-**30**.

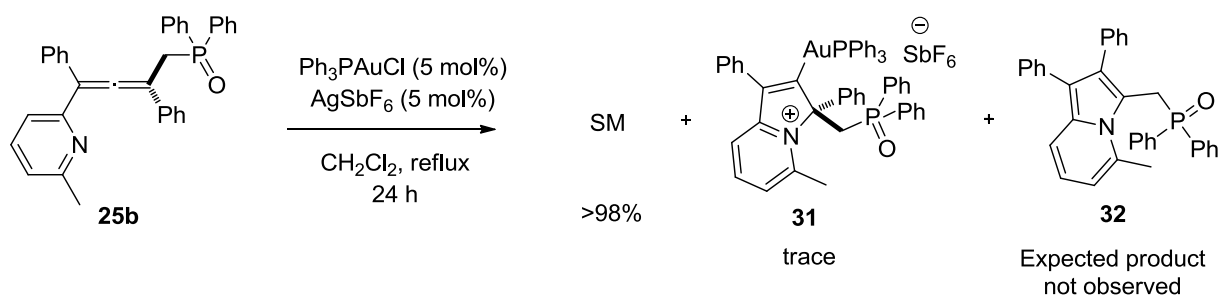
The chirality transfer from vinylallene **17** was also studied by the treatment of the optically pure vinylallene (–, CD 254 nm)-**29** in the presence of 10 mol% of cationic gold catalyst. However, the (–, CD 254 nm)-**29** was isolated with a moderate 55% *ee*, suggesting a less efficient chirality transfer (Scheme 101).

Scheme 101. Synthesis of (–, CD 254 nm)-**29**.

5. Cationic vinyl complex featuring a triphenylphosphine gold(I) moiety

5.1. Synthesis of cationic vinyl gold complex (**31**)

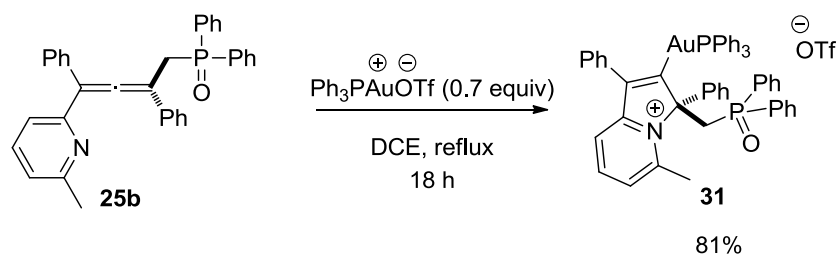
Following the satisfying results obtained with allene **17** and **18** bearing electron-rich functional groups in the preparation of cyclic products, we aimed to test the generality of the formation of heterocyclic products using a cationic gold complex in the presence of allene **25b** bearing a pyridinyl group. Unfortunately, pyridinyl allene **25b** could not generate the expected cyclic products **32** that would form through 1,2-phenyl migration¹⁹⁴ *via* trapping of the gold carbene intermediate (Scheme 102). Then, the starting allene **25b** was fully recovered with only a trace amount of the new gold complex **31**, corresponding mainly to the quantity of generated cationic gold.

Scheme 102. Reactivity of pyridyl allene **25b** under cationic gold catalysis.

The generation of trace amount of gold complex **31** by cationic gold-catalyzed reaction was considered. We decided to foster this reaction by using 0.7 equivalent of a 1:1 mixture of Ph_3PAuCl and AgOTf in the presence of pyridinyl-allene **25b**. The corresponding complex **31** was obtained this time in 81% yield with a complete conversion of the starting material (Scheme 103).

¹⁹⁴ For some reports of 1,2-phenyl migration, see: (a) K.-H. Chen, Y. J. Feng, H.-W. Ma, Y.-C. Lin, Y.-H. Liu, T.-S. Kuo, *Organometallics* **2010**, *29*, 6829–6836.; (b) D. J. Gorin, N. R. Davis, F. D. Toste, *J. Am. Chem. Soc.* **2005**, *127*, 11260–11261.; (c) A. V. Gulevich, A. S. Dudnik, N. Chernyak, V. Gevorgyan, *Chem. Rev.* **2013**, *113*, 3084–3213.; (d) Y. Chen, L. Wang, N. Sun, X. Xie, X. Zhou, H. Chen, Y. Li, Y. Liu, *Chem. Eur. J.* **2014**, *20*, 12015–12019.

Although no X-ray crystallography data could be obtained, characteristic spectral data, based on ^{31}P NMR (Figure 32a) corresponding to the PPh_3 and $\text{P}=\text{O}$ groups at 42.7 and 23.6 ppm respectively and ^{13}C NMR displacement (Figure 32b) of vinylic quaternary carbon at 203.9 ppm (doublet, $^2J_{\text{CP}} = 114$ Hz), allowed us to diagnostic the formation of a vinyl gold species (Figure 32).



Scheme 103. Preparation of gold complex 31 from pyridyl allene 25b with 0.7 equivalent of cationic gold.

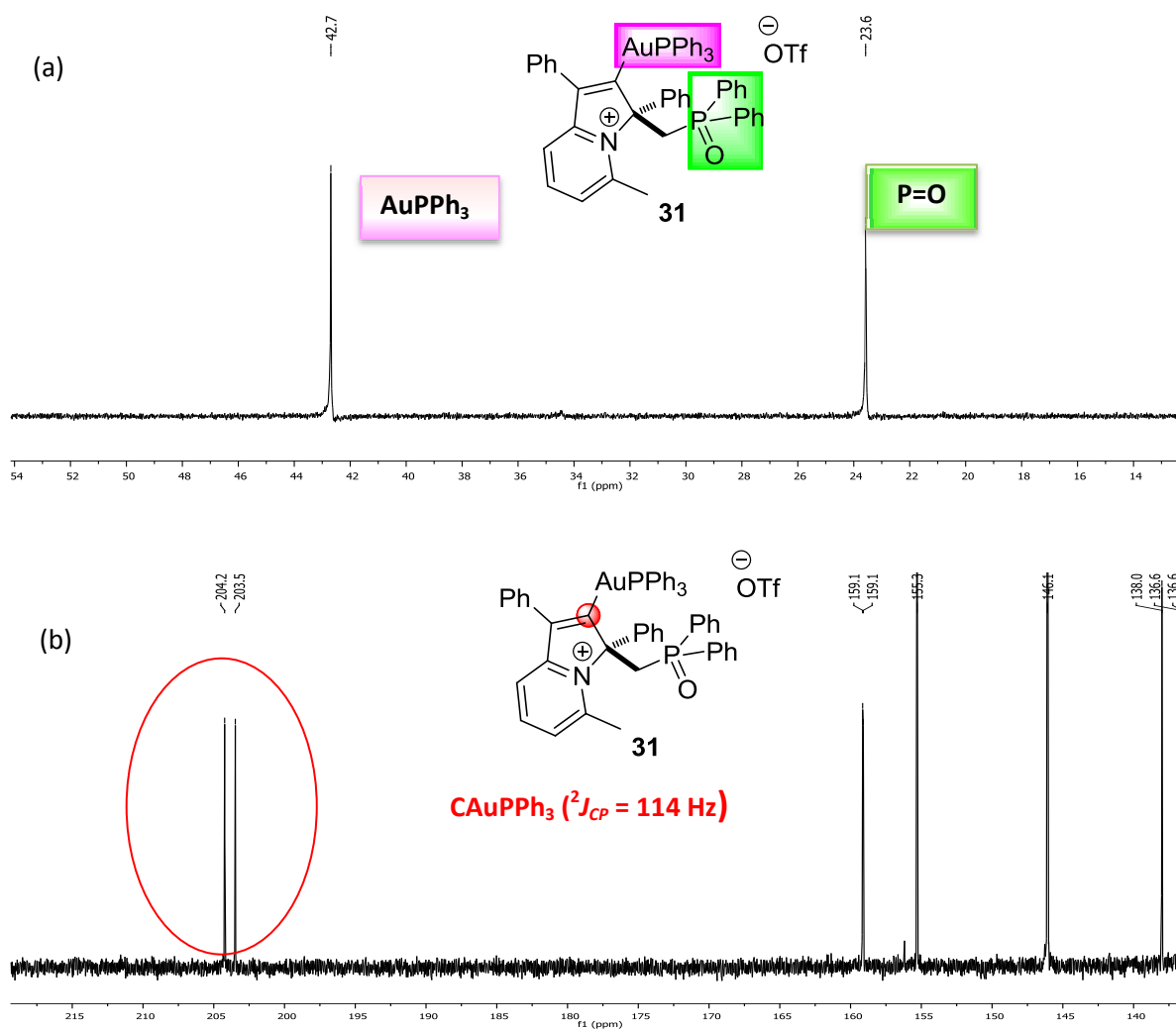
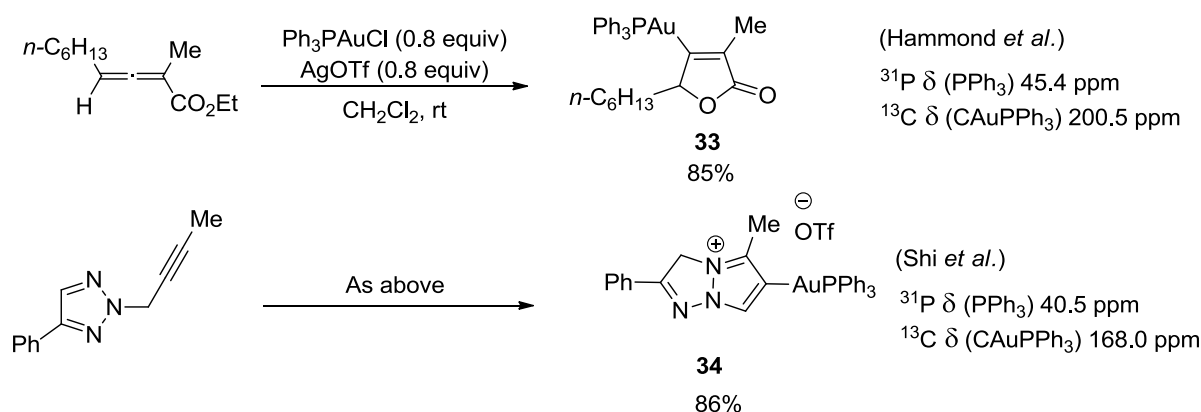


Figure 32 The NMR spectra of 31: (a) ^{31}P NMR (122 MHz, CD_2Cl_2) and (b) ^{13}C NMR (151 MHz, CD_2Cl_2).

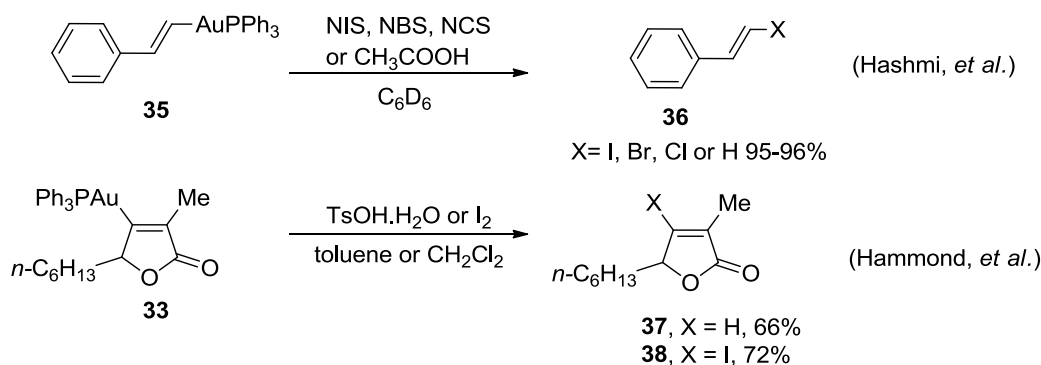
According to previous studies, a few vinyl-gold complexes could be synthesized by mixing alkynes and cationic gold catalysts. Two examples described by Shi⁸⁵ and Hammond⁸⁴ focus on the characterizations of vinyl gold complexes **33** and **34** respectively (Scheme 104). In these complexes, the ³¹P NMR of the AuPPh₃ group is observed at 40.5 (**33**) and 45.4 ppm (**34**) confirming the presence of this type of AuPPh₃ group in our complex **31** ($\delta = 42.7$ ppm). As well, ¹³C NMR of complex **33** shows a peak at 200.5 ppm (doublet, ²J_{CP} = 112.4 Hz), characteristic for a vinylic quaternary carbon. This type of signal can be also observed in a similar range for our complex **31** (Figure 32b), probing the formation of a stable vinyl gold complex.



Scheme 104. Previous organogold complexes from Shi (**33**) and Hammond (**34**).

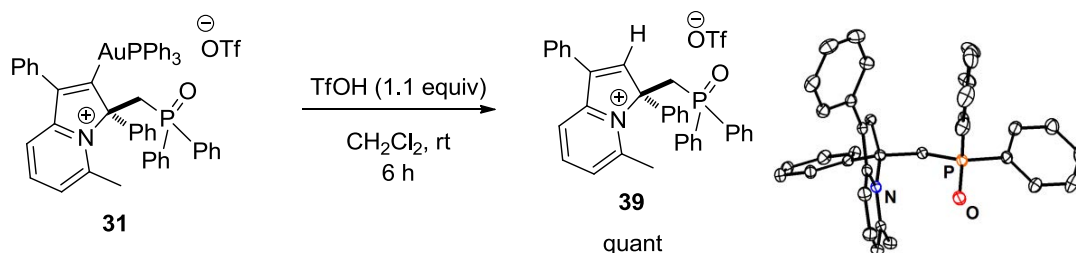
5.2. Post-functionalization of cationic vinylgold complex (**31**)

Post-functionalization of vinylgold complexes through addition of electrophilic halide sources and protodeauration to trap the AuPPh₃ are reviewed in Chapter 2. Here, we focus on the methods developed by the group of Hashmi⁸² and Hammond⁸⁴. Hashmi and co-workers used electrophiles such as NIS, NBS, NCS and proton from CH₃COOH trapping AuPPh₃ group of styrenyl-gold complex **35** to form **36** in high yields. In the same vein, the Hammond group used TsOH and iodine (I₂) reagents to treat the lactone-containing gold complexes **33** *via* protodeauration and iodination. These reactions afforded functionalized products **37** and **38** respectively (Scheme 105).



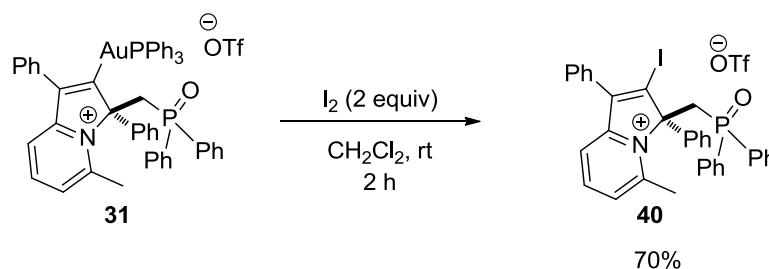
Scheme 105. Post-functionalization of **35** and **33** by the groups of Hashmi⁸² and Hammond⁸⁴.

Inspired by these works, we envisaged examining the protodeauration and iodination reaction onto the vinyl gold complex **31** in order to generate new pyridinium derivatives bearing a stereogenic center. We first engaged the complex **31** in a protodeauration reaction by trapping of the gold phosphine group with triflic acid (TfOH). The reaction successfully gave a quantitative yield of indolizinium salt **39**, whose structure was confirmed by X-ray crystallography (Scheme 106).



Scheme 106. Protodeauration reaction of **31** with TfOH reagent.

In addition, we also studied the functionalization of complex **31** by adding sublimated iodine as an electrophile in order to trap the gold phosphine group. The iodination reaction worked well to yield 70% of vinyliodide derivative **40** (Scheme 107).



Scheme 107. Iodination reaction of the vinyl gold complex **31**.

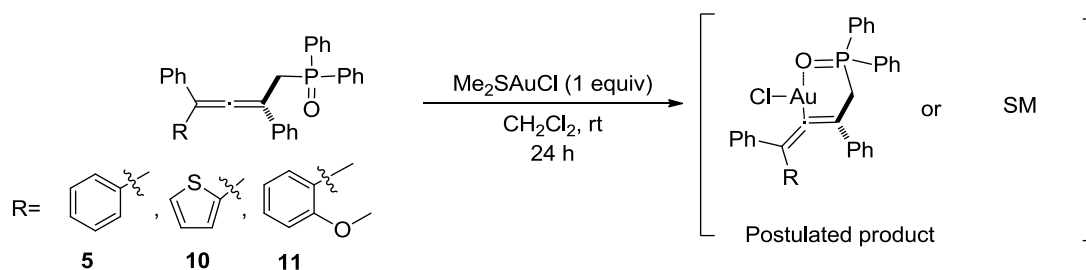
In conclusion, the vinyl gold complex **31** was successfully functionalized by protodeauration and iodination reactions. In homogeneous gold catalysis study, these results demonstrate the reactivity of this organogold complex **31**, implying that the proto- and iodoauration step could be involved in gold-catalyzed reactions through the formation of intermediate gold complex **31**. Interestingly, these reactions afforded new chiral products **39**, **40** containing a pyridinium pattern. Some of our perspectives are now to pursue on the post-functionalization reactions of the complex **31** with various electrophilic reagents in order to obtain an interesting library of heterocyclic products. Moreover, the asymmetric synthesis of heterocyclic products is also of interest and could be reached by studying the chirality transfer process.

6. Vinyl complex bearing a chlorogold(I) group

With a variety of allenes in hand, we envisaged their ability to complex with gold(I) chloride in order to prepare new gold(I) complexes and to examine their post-functionalization with either nucleophiles or electrophiles.

6.1. Preliminary test in the presence of gold(I) complex

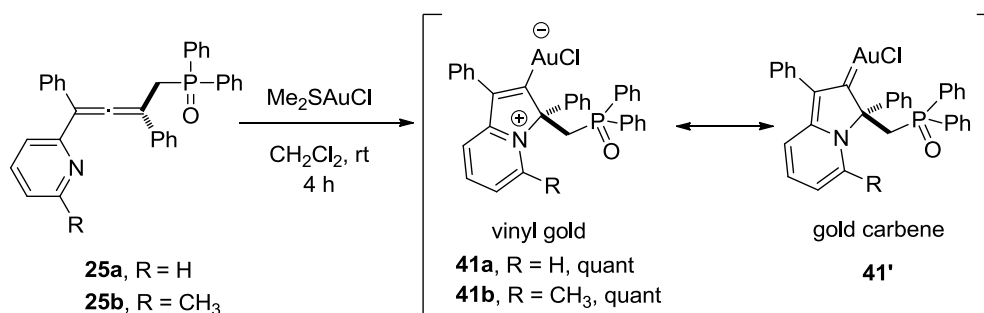
We attempted to prepare a variety of gold complexes bearing allene ligands. Initially, one equivalent of allene was reacted with one equivalent of Me_2SAuCl in dichloromethane at room temperature. Determined by NMR spectroscopy, the crude products showed the similar chemical shifts to the allene substrates in ^1H NMR and broad singlet peak in ^{31}P NMR. Unfortunately, no complexes were isolated in the case of allene with phenyl **5**, thionyl **10**, and 2-methoxyphenyl **11** substituents (Scheme 108).



Scheme 108. The reaction tests of allene **5**, **10**, and **11** bearing monophosphine with Me_2SAuCl .

6.2. Synthesis of vinyl-gold complexes

In the next attempt, we hypothesized that allenes bearing an additional Lewis-base functional group such as a pyridinyl group might contribute to the coordination with gold species. Indeed, we were pleased to observe that allenes bearing a pyridine substituent **25a** and **25b** could react with gold(I) chloride generating new gold complexes **41a** and **41b** in quantitative yields (Scheme 109).



Scheme 109. Preparation of pyridinyl-gold complexes **41** or **41'**.

Their structures were confirmed by X-ray crystallography analysis (Figure 33). There is only limited number of literature reports regarding the formation and characterization of this new type of gold complexes. The latter exist in two mesomeric forms, the vinyl gold complex **41**, and the gold carbene complex **41'**.

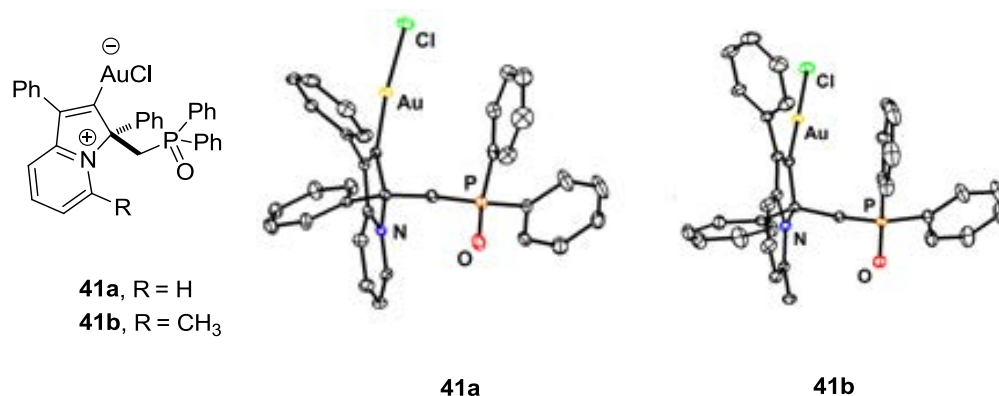
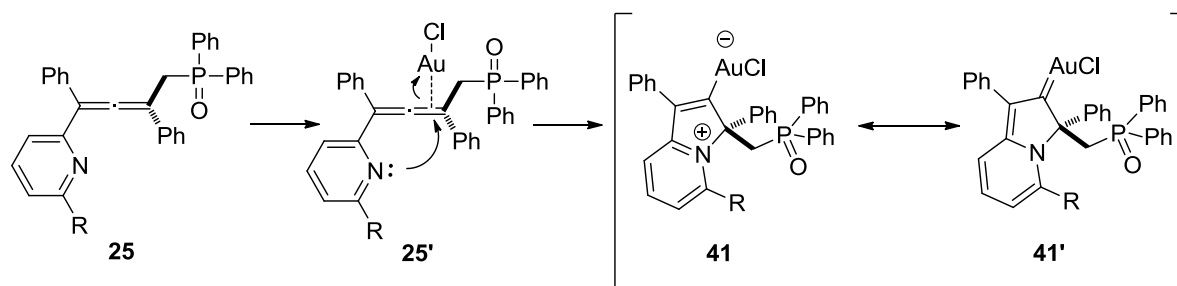


Figure 33. Structures of pyridinyl-gold complexes **41a** and **41b**.

A proposed mechanism for the formation of these gold complexes is depicted as shown in Scheme 110 and recalls the previous reported synthesis of pyrroles from alkynyl imines using

metal-catalyzed cycloisomerization by Gevorgyan and co-workers.¹⁹⁵ The π -philic gold(I) species would coordinate to the double bond of allene (**25'**). Intramolecular *5-endo-dig* attack of the nitrogen atom of the pyridine group would conduct to the formation of the gold complex **41** or as well to the gold carbene species **41'**.



Scheme 110. Proposed mechanism for the synthesis of gold(I) complexes **41** or **41'**.

To get more insight their characterizations from their crystal structures of **41a** and **41b**, Au-C bond distances of 1.993 Å for **41a** and 1.984 Å for **41b**. These are in the low range of previously isolated gold carbenes,^{63, 196} such as the gold complexes from the groups of Aumann¹⁹⁷ and Fürstner¹⁹⁸. They are in the same range as *o*-carborane diphenylphosphine gold(I) diphenylcarbene complex prepared by the Bourissou group, observing the shortest Au-C bond distances of 1.984 Å.⁶¹ Moreover, this group demonstrated that *o*-carborane diphenylphosphine ligand contains the excellent π -electron accepting property and promote the electron back-donating property of gold(I). We predicted that the gold complex **41a** and **41b** might bear similar property (Figure 34).

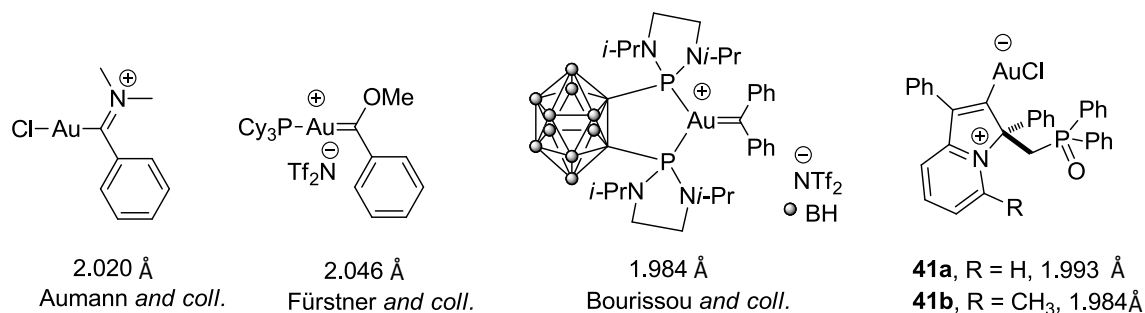


Figure 34. Examples of previous gold carbenes showing the comparison of Au-C bond distances comparing to **41**.

¹⁹⁵ (a) D. Chernyak, S. B. Gadamsetty, V. Gevorgyan, *Org. Lett.* **2008**, *10*, 2307–2310.; (b) T. Schwier, A. W. Sromek, D. M. L. Yap, D. Chernyak, V. Gevorgyan, *J. Am. Chem. Soc.* **2007**, *129*, 9868–9878.; (c) A. V. Gulevich, A. S. Dudnik, N. Chernyak, V. Gevorgyan, *Chem Rev* **2013**, *113*, 3084–3213.

¹⁹⁶ (a) D. Benitez, N. D. Shapiro, E. Tkatchouk, Y. Wang, W. A. Goddard, F. D. Toste, *Nat. Chem.* **2009**, *1*, 482–486.; (b) L. Nunes dos Santos Comprido, J. E. M. N. Klein, G. Knizia, J. Kästner, A. S. K. Hashmi, *Angew. Chem. Int. Ed.* **2015**, *54*, 1–6.

¹⁹⁷ U. Schubert, K. Ackermann, R. Aumann, *Cryst. Struct. Commun.* **1982**, *11*, 591–594.

¹⁹⁸ (a) G. Seidel, B. Gabor, R. Goddard, B. Heggen, W. Thiel, A. Fürstner, *Angew. Chem. Int. Ed.* **2014**, *53*, 879–882.; (b) G. Seidel, A. Fürstner, *Angew. Chem. Int. Ed.* **2014**, *53*, 4807–4811.

6.3. Computational calculations towards the reactivity of gold complex (41)

DFT calculation and optimization was also realized for these gold structures **41a** and **41b**, and performed in collaboration with Dr. Etienne Derat (MACO Team, IPCM), using the Turbomole program package (V6.4). B3LYP, supplemented by the D3 correction, which was used as functional and the def2-SV(P) as basis set. The structure **41b** was optimized starting from X-ray crystallographic data, which allowed us to better understand the electronic structure of this unusual gold-carbene complex. Firstly, the Mayer bond order analysis was used to understand the difference between the vinylgold **41** and gold carbene **41'** (Figure 35A). The bond order between gold (Au) and carbon (C₁) is 0.7559 referred as a single bond. In comparison, the bond order between carbon (C₁) and carbon (C₂) is 1.6120 referred as double bond that concluded that the main mesomeric form for complex is **41b**. According to the electronic interaction between a metal and a ligand *via* σ -donation, and π -back-donation to access metal-ligand coordination,¹⁹⁹ our study of the molecular orbitals shows a specific reactivity of this complex in relation with interactions between the AuCl fragment and the carbene (Figure 35B). We suggest that the π -bonding interaction between gold and chloride is delocalized in the pyridinium moiety of the carbene, thus enhancing what is traditionally described as the back-donation. As shown in the plotting of the electrostatic potential (Figure 35C), the AuCl fragment is found to be electron-rich and the *in-situ* created carbene moiety has a positive electrostatic potential as a good electron-acceptor.

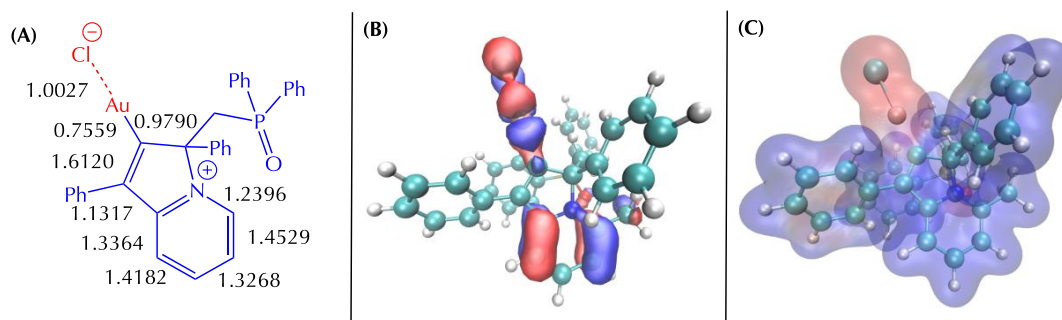


Figure 35. Summary of calculations for complex **41b** (A) Mayer bond order (B) molecular orbital showing the delocalization between AuCl and carbene (C) electrostatic potential (blue: positive; red: negative).

To further substantiate these findings, comparisons were made with other classical gold ligands. HOMO/LUMO energies of a typical phosphine (PPh₃), a standard carbene (IPr), a π -

¹⁹⁹ D. Marchione, L. Belpassi, G. Bistoni, A. Macchioni, F. Tarantelli, D. Zuccaccia, *Organometallics* **2014**, *33*, 4200–4208.

acceptor phosphine (SPhos, Buchwald ligand)²⁰⁰ and carbene **41b** was calculated and analyzed.²⁰¹ The HOMO-LUMO energy diagrams are presented in Figure 36. The σ -donating molecular orbital generally corresponds to HOMO, whereas the π -accepting one corresponds to LUMO.²⁰² The energy gap between HOMO and LUMO are significant for the properties of carbene. The narrow energy gap infers an excellent π -acceptor carbene. The carbene derived from **41b** without AuCl appears more electrophilic than a usual σ -donating carbene (IPr) with a high HOMO and in the same range with both phosphines, especially the SPhos or Buchwald phosphine and triphenylphosphine (PPh₃). The lowest energy of LUMO refers to strong π -acceptor ligand, whereas the highest energy of HOMO refers to strong σ -donor ligand. This carbene **41b** has the lowest energy at LUMO and the highest energy at HOMO level energy of other ligands. We hypothesize that this special new carbene ligand **41b** for gold species can certainly promote catalytic reactions in different reactivity and selectivity than the others.

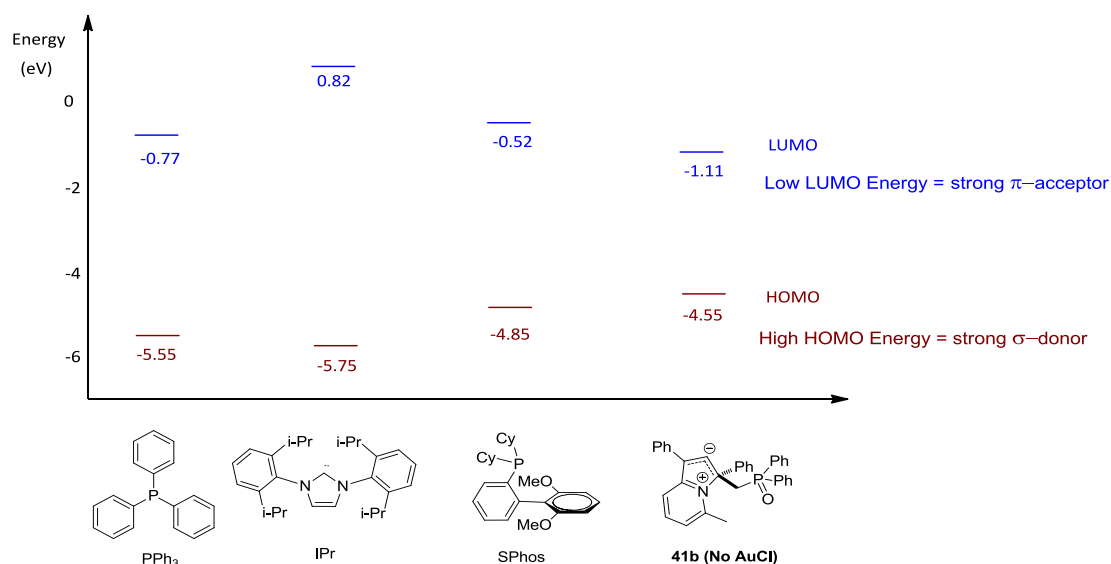


Figure 36. Comparisons of HOMO-LUMO energy diagram of PPh₃, IPr, SPhos and **41b** (No AuCl).

However, the HOMO-LUMO energy diagram is calculated from complex **41b** without gold chloride. We can ask the question, what is the effect of the gold chloride moiety on the carbene? To clarify and strengthen the observations of **41b**, we also investigated the bonding and the stabilizing effect using IBOs method (Intrinsic Bond Orbitals).²⁰³ The IBO values indicate the number of electrons of occupied orbitals assigned to the individual contribution. This method can

²⁰⁰ D. S. Surry, S. L. Buchwald, *Angew. Chem. Int. Ed.* 2008, 47, 6338–6361.

²⁰¹ The calculation was performed by Mr. Cédric Barcha, who is an intern student (L3, IPCM) under supervision of Dr. Etienne Derat (MACO Team, IPCM)

²⁰² D. S. Laitar, P. Müller, T. G. Gray, J. P. Sadighi, *Organometallics* 2005, 24, 4503–4505.

²⁰³ G. Knizia, *J. Chem. Theory Comput.* 2013, 9, 4834–4843.

depict occupied orbitals and allow a direct interpretation of chemical bonding. Recently, Hashmi, Kästner and co-workers reported computational calculations using IBO method to analyze several gold carbene complexes^{196b} such as complexes **I**,^{198b, 204} **II**,^{198a} **III**,²⁰⁵ and **IV**⁶¹ in Table 4. The comparison of the numbers of electrons of IBO orbitals can identify the interaction between gold and a carbene ligand related to accepting or donating properties. We calculated the bonding and stabilizing effects of complex **41b** using this method, based on DFT computations.²⁰⁶ C_{Au} -stabilizing IBOs of gold complex **41b** are illustrated in Figure 37, involving the number of electrons in orbitals, which are summarized in Table 4.

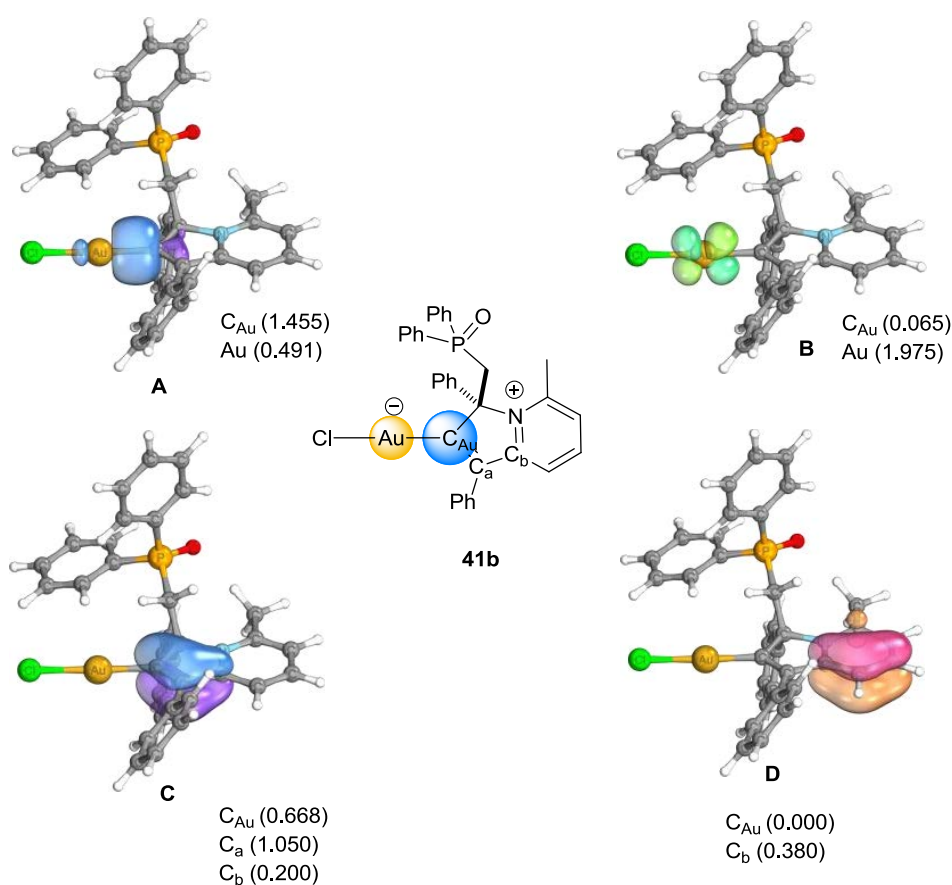


Figure 37. C_{Au} -stabilizing IBOs of gold complex **41b**. Numbers in parentheses indicate the number of electrons of the doubly occupied orbital. (C_{Au} is carbon atom (carbene) bonding to gold atom)

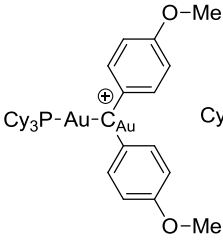
²⁰⁴ (a) A. Fürstner, L. Morency, *Angew. Chem. Int. Ed.* **2008**, *47*, 5030–5033; *Angew. Chem.* **2008**, *120*, 5108–5111.; (b) A. S. K. Hashmi, *Angew. Chem. Int. Ed.* **2008**, *47*, 6754–6756; *Angew. Chem.* **2008**, *120*, 6856–6858.; (c) G. Seidel, R. Mynott, A. Fürstner, *Angew. Chem. Int. Ed.* **2009**, *48*, 2510–2513; *Angew. Chem.* **2009**, *121*, 2548–2551.

²⁰⁵ R. J. Harris, R. A. Widenhoefer, *Angew. Chem. Int. Ed.* **2014**, *53*, 9369–9371.

²⁰⁶ The calculation was performed by Mr. Thomas Driant, who is a PhD student under supervision of Dr. Etienne Derat (MACO Team, IPCM).

Four occupied orbitals of **41b** described the π -stabilized pyridinium ligand to AuCl fraction. The first IBO orbital (Figure 37, orbital **A**) represents the number of electrons in σ -coordination between Au and carbene (C_{Au}). This lone pair is largely located at carbon atom (C_{Au}), consistent with coordinative bonding (σ -donation). Our carbene **41b** can donate electron to gold in the same range as other carbenes **I-IV**, in particular **IV** (Table 4, entry 1). The second IBO (Figure 37, orbital **B**) indicates the electrons, which delocalized at the gold atom and adjusted to potential π -backbonding. The number of electrons of **41b** is 0.065 that is weaker π -acceptor than carbene **IV** (0.175) and similar range to the other donor carbenes **I**, **II** and **III** (Table 4, entry 2). This result contradicts that the pyridinium ligand is not good π -acceptor ligand, even if the bond distance between AuCl and C_{Au} is similar range with carbene **IV**.^{61, 63} Finally, the last two IBO orbitals (Figure 37, orbitals **C** and **D**) show that the delocalized electron from the π -system of aromatic rings stabilize C_{Au} coordinated to gold. The sum of electron π -donation of both aromatic rings of **41b** (orbital **C** and **D**) in entry 3 (Table 4) is 0.668. It shows the π -donation character is better than **I**, **II** and **IV**, but less than **III**. This explains that the electrons from π -aromatic rings are delocalized to C_{Au} and stabilize the bonding between carbene and AuCl.

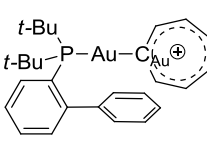
Table 4. Number of electrons in occupied orbital IBOs for gold complexes **I**, **II**, **III**, **IV** and **41b**^[a]



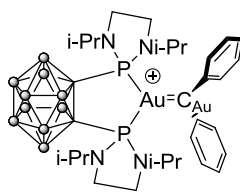
I



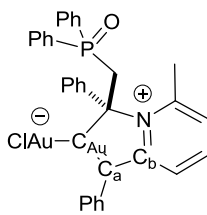
II



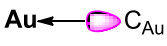
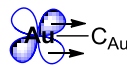
III

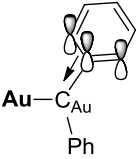


IV



41b

Entry	IBOs (Figure 37)	I	II	III	IV	41b
1	A [σ -Coordination of Au and C_{Au}] 	0.473 ^[b] (1.444) ^[c]	0.452 ^[b] (1.463) ^[c]	0.477 ^[b] (1.452) ^[c]	0.494 ^[b] (1.412) ^[c]	0.491 ^[b] (1.455) ^[c]
2	B [π -Backbonding of Au and C_{Au}] 	0.057	0.074	0.051	0.175	0.065

3	C + D	0,598	0,551	0,731	0,404	0.668
[Sum of π -donation] ^[d]						
						
^[a] Number of electrons on Au. ^[b] Number of electrons on C _{Au} . ^[c] Sum of the contribution from all aromatic substituents						

In summary, calculations of gold complexes **41b** have been performed to gain insight the electronic structure, chemical bonding, and reactivity, and to apply this complex in other reactions. DFT calculations were used to give informations to extend the family of the molecule **41b**. The structure was first optimized and performed Mayer bond order analysis. Also, the delocalization of electron density between AuCl and carbene was demonstrated by the molecular orbital and electrostatic potential. Nevertheless, this information is not enough to conclude on the reactivity of this ligand. The calculation of the HOMO/LUMO energies of ligand **41b** without AuCl compared to other ligands for gold (IPr, SPhos, and PPh₃) indicated that the pyridinium carbene is a good π -acceptor. However, gold chloride moiety has an effect on the ligand property. As seen in IBO analysis, **41b** is special donating ligand. Other calculations are currently performed to reconcile the various points of view.

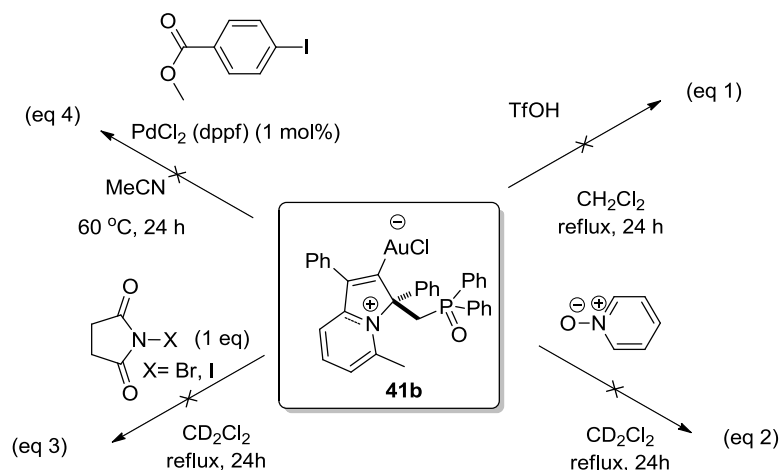
6.4. Investigations on the reactivity of vinyl gold complex (41b)

6.4.1. Preliminary tests

Several reactions have been tested to achieve the post-functionalization of this gold complex **41b** *via* nucleophilic or electrophilic substitutions in order to gain insight into the mesomeric form of these gold complexes. However, complex **41b** proved to be relatively unreactive through the treatment with TfOH for the protodeauration (Scheme 111, eq 1) and pyridine *N*-oxide (Scheme 111, eq 2) for formal oxidation reaction. The addition of electrophilic halide sources (NBS, NIS) (Scheme 111, eq 3) and the attempts of palladium coupling with methyl 4-iodobenzoate (Scheme 111, eq 4) proved also to be unsuccessful with this complex **41b**.^{207, 208}

²⁰⁷ For reviews of functionalized gold complexes by pyridine *N*-oxide; G. Henrion, T. E. J. Chavas, X. Le Goff, F. Gagosz, *Angew. Chem. Int. Ed.* **2013**, *52*, 6277–6282.

²⁰⁸ For reviews of functionalized gold complexes by halide sources, see: (a) A. S. K. Hashmi, R. Döpp, C. Lothschütz, M. Rudolph, D. Riedel, F. Rominger, *Adv. Synth. Catal.* **2010**, *352*, 1307–1314.; For a review of functionalized gold complexes by palladium-coupling reaction, see: (b) X. Zeng, R. Kinjo, B. Donnadieu, G. Bertrand, *Angew. Chem. Int. Ed.* **2010**, *49*, 942–945.



Scheme 111. Attempts of the post-functionalization of gold complex **41b**.

In this work, several reactions with the gold complex **41**, such as protodeauration and electrophilic substitutions have been explored thoroughly. Unfortunately, the complexes are stable and unreactive. However, by understanding thanks to DFT calculations the electronic properties of our gold carbene complexes, we are now interested in applying these gold complexes as catalysts in cycloisomerization. We hypothesize that the gold carbenes would activate alkynes or allenes undergoing the cyclization reactions, similar to other gold carbene complexes such as *N*-heterocyclic carbene gold(I) complexes [(NHC)AuCl].

6.4.2. Vinyl gold complex (**41b**) in catalysis

6.4.2.1. Bibliographical backgrounds: Gold carbene complexes in catalysis

N-heterocyclic compounds, which consist of the family of nitrogen-tethered carbene compounds, have been frequently used as ligands for metals such as rhodium, ruthenium, and gold in homogeneous catalytic reactions since 1995.^{209, 210} Their behaviors, compared to the phosphine analogues, show stronger σ -donating properties, including tighter binding to metals and greater thermal stability.

²⁰⁹ For some reviews of Rh and Au complexes, see: (a) C. Köcher, W. A. Herrmann, *J. Organomet. Chem.* **1997**, 532, 261–265.; (b) A. Arnanz, C. González-Arellano, A. Juan, G. Villaverde, A. Corma, M. Iglesias, F. Sánchez, *Chem. Commun.* **2010**, 46, 3001–3003.; For Ru, see: (c) D. Patel, S.T. Liddle, S.A. Mungur, M. Rodden, A.J. Blake, P.L. Arnold, *Chem. Commun.* **2006**, 1124.

²¹⁰ For some reviews of Au, see: (a) N. Marion, S. P. Nolan, *Chem. Soc. Rev.* **2008**, 37, 1776–1782.; (b) D. Gatineau, J.-P. Goddard, V. Mouriès-Mansuy, L. Fensterbank, *Isr. J. Chem.* **2013**, 53, 892–900.; (c) F. López, J. L. Mascareñas, *Beilstein J. Org. Chem.* **2013**, 9, 2250–2264.; (d) D. J. Gorin, B. D. Sherry, F. D. Toste, *Chem. Rev.* **2008**, 108, 3351–3378.; (e) C. Nieto-Oberhuber, S. López, A. M. Echavarren, *J. Am. Chem. Soc.* **2005**, 127, 6178–6179.; (f) A. S. K. Hashmi, T. M. Frost, J.W. Bats, *J. Am. Chem. Soc.* **2000**, 122, 11553–11554.

In 2003, Herrmann disclosed the first example of using NHC-gold complex for the hydration of alkyne.²¹¹ Two year later, Nolan and co-workers prepared gold complexes with different types of NHC ligands such as IMes, SIMes and IPr (Figure 38).²¹²

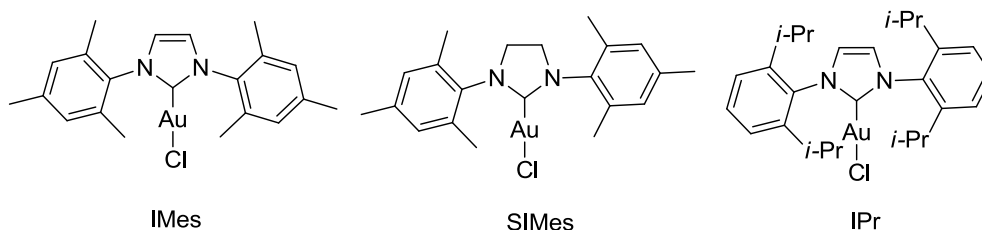
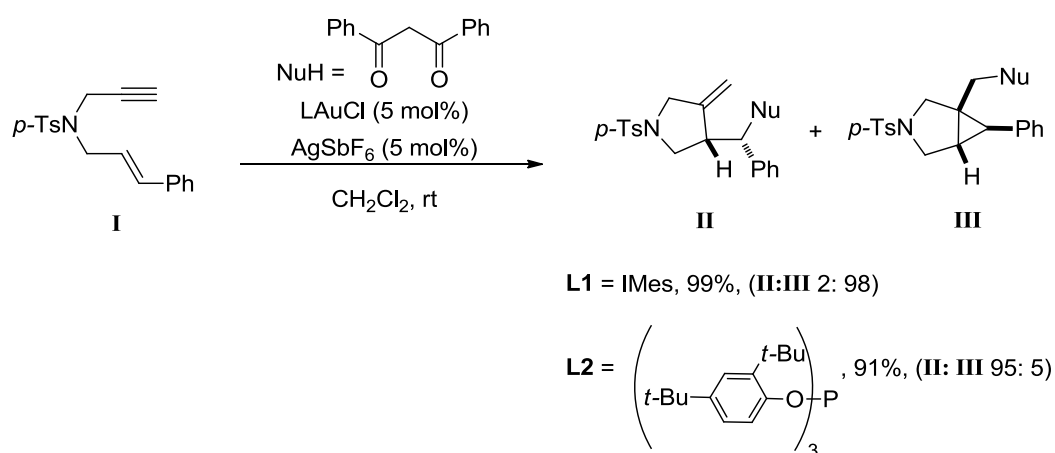


Figure 38. Examples of NHC-gold(I) species.

Our group have readily reviewed and compared the reactivity of NHC ligands to organophosphorus ligands in gold catalysis.^{210b} As seen an example by Echavarren and co-workers in 2008,²¹³ the catalytic use of IMesAuCl in addition of dibenzolymethane to enyne **I** was reported (Scheme 112). The reaction with this donating ligand (**L1**) could afford a major cyclopropyl product **III**, resulting from the addition of the nucleophile on the carbene carbon of the intermediate. In contrast, the use of phosphite-gold (**L2**) complex promoted selectively exo-methylene cyclopropyl derivative **II** as the major product.



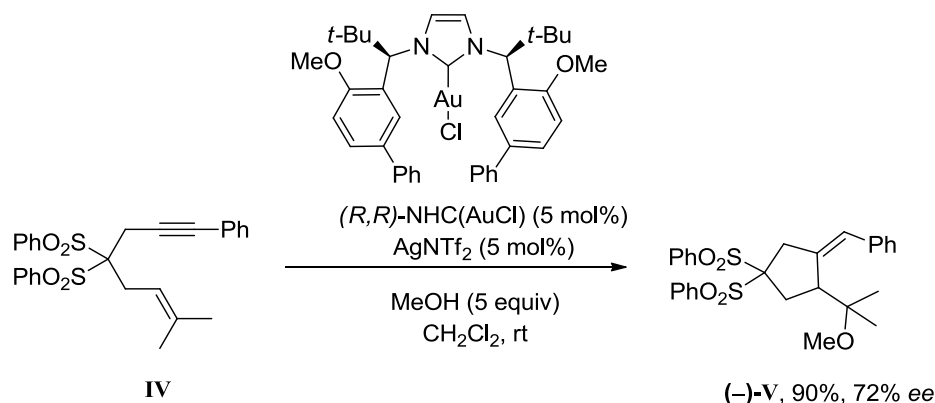
Scheme 112. Au(I)-catalyzed cyclization of enyne **I** in the presence of dibenzoylmethane.

²¹¹ S. K. Schneider, W. A. Herrmann, E. Herdtweck, *Z. Anorg. Allg. Chem.* **2003**, 629, 2363–2370.

²¹² P. de Frémont, N. M. Scott, E. D. Stevens, S. P. Nolan, *Organometallics* **2005**, 24, 2411–2418.

²¹³ H. M. Amijs, V. López-Carrillo, M. Raducan, P. Pérez-Galán, C. Ferrer, A. M. Echavarren, *J. Org. Chem.* **2008**, 73, 7721–7730.

In enantioselective manner, versatile chiral NHC-gold complexes were designed to apply in asymmetric gold(I)-catalyzed reactions.²¹⁴ For example, Kündig and co-workers developed bulky chiral NHC-gold complexes for asymmetric intramolecular methoxycyclization reactions of 1,6-enynes.^{214d} The best result presented the reaction of enyne **IV** in the presence of (*R,R*)-NHC(AuCl) (5 mol%), AgNTf₂ (5 mol%) and methanol (5 equiv) in dichloromethane at room temperature. The enantioselective cyclopentane (–)-**V** was obtained in high yield (90%) and excellent *ee* (72%) (Scheme 113).

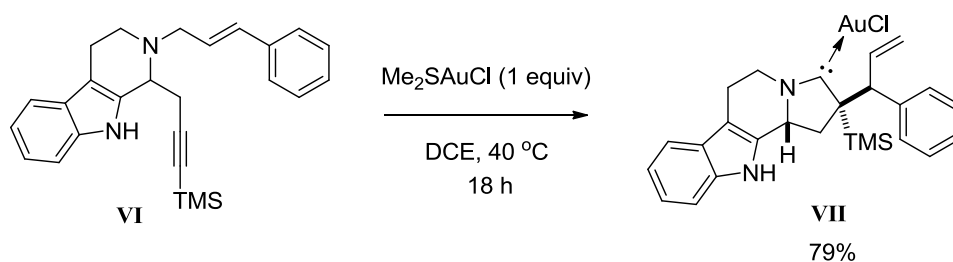


Scheme 113. Asymmetric intramolecular methoxycyclization reaction of enyne **IV**.

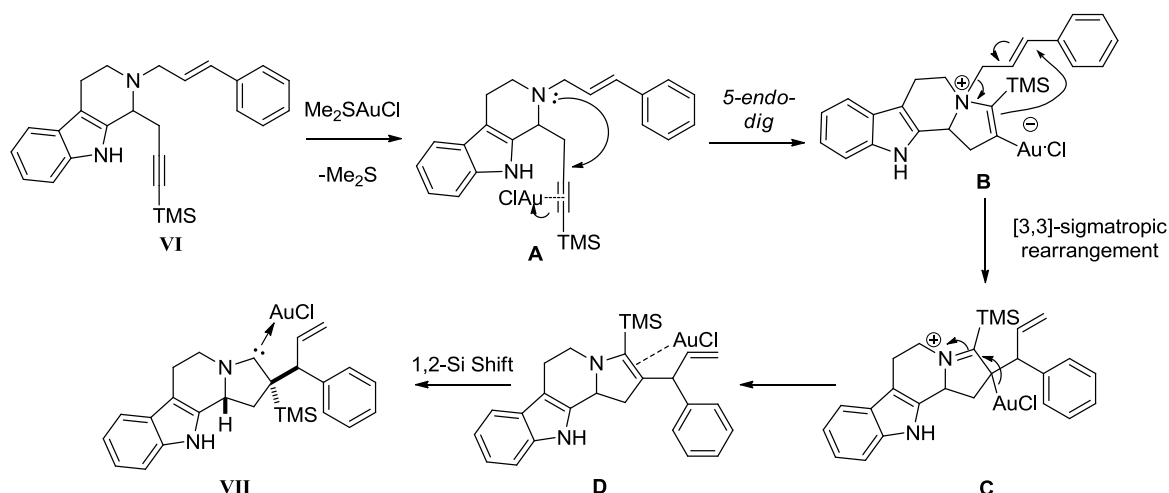
Quite recently, the group of Kumar and Waldmann disclosed the synthesis of chiral cyclic alkyl aminocarbene gold complexes by gold(I)-catalyzed cyclization and rearrangement reactions. In this case, the gold(I) source promoted the cyclization and rearrangement of alkyneamines for the preparation of new gold complexes. For example, aminocarbene gold complex **VII** was prepared successfully in 69% yield from a 1:1 mixture of 1,7-enyne **VI** and Me₂SAuCl in dichloroethane at 40 °C (Scheme 114).²¹⁵ The structure determined by X-ray crystallography showed an Au-C bond distance of 1.985 Å, which is in the same range of our gold carbene **41b** (1.984 Å).

²¹⁴ Some examples of NHC in asymmetric gold catalysis, see: (a) Y. Matsumoto, K. B. Selim, H. Nakanishi, K. Yamada, Y. Yamamoto, K. Tomioka, *Tetrahedron Lett.* **2010**, *51*, 404–406.; (b) A. Aranz, C. González-Arellano, A. Juan, G. Villaverde, A. Corma, M. Iglesias, F. Sánchez, *Chem. Commun.* **2010**, *46*, 3001–3003.; (c) J. Francos, F. Grande-Carmona, H. Faustino, J. Iglesias-Sigüenza, E. Díez, I. Alonso, R. Fernández, J. M. Lassaletta, F. López, J. L. Mascareñas, *J. Am. Chem. Soc.* **2012**, *134*, 14322–14325.; (d) D. Banerjee, A. K. Buzas, C. Besnard, E. P. Kündig, *Organometallics* **2012**, *31*, 8348–8354.

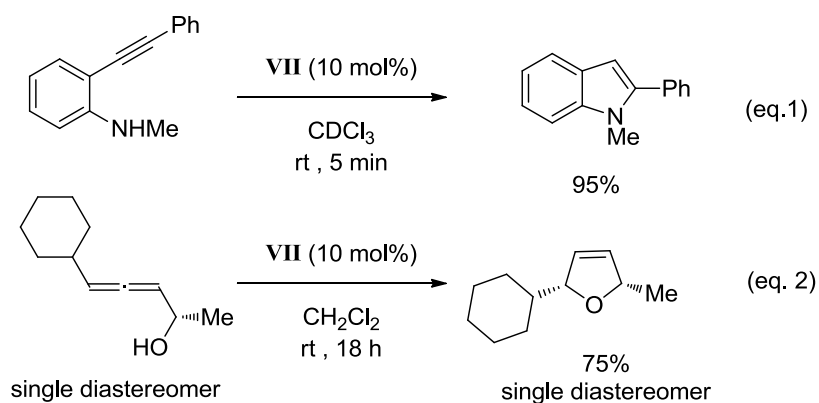
²¹⁵ F. Kolundžić, A. Murali, P. Pérez-Galán, J. O. Bauer, C. Strohmann, K. Kumar, H. Waldmann, *Angew. Chem. Int. Ed.* **2014**, *53*, 8122–8126.

Scheme 114. Preparation of cyclic alkyl aminocarbene gold complex **VII**.

The proposed mechanism in Scheme 115 showed that a *5-endo-dig* cyclization of alkynylamine **VI** led to the formation of zwitterionic vinyl-gold complex **B** after the activation on π -bond (**A**) by gold(I) species. An aza-Cope type sigmatropic rearrangement of **B** yielded iminium intermediate **C**, which eventually formed the gold(I)-olefin complex **D**. After 1,2-silicon migration, the final product **VII** was obtained in good yield (79%). The complex **VII** and its derivatives are biologically active products, including activity against cancer cells. For instance, they could inhibit the growth of human ovarian cancer cell line (A2780), involving excellent IC_{50} range (0.55 μM to 2.52 μM).

Scheme 115. Proposed mechanism of gold(I)-catalyzed reaction and rearrangement process of alkynylamine **VI**.

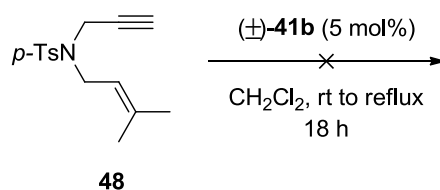
This polycyclic gold carbene **VII** was used as a catalyst (10 mol%) without silver salt in two intramolecular cyclization reactions. The first reaction carried out *N*-methyl-2-(2-phenylethynyl)aniline in the presence of 10 mol% of gold complex **VII** in CDCl_3 at room temperature (Scheme 116, eq. 1). The cyclohydroamination reaction yielded 95% of corresponding indole. The other success used allenol substrate with the same catalyst in dichloromethane (Scheme 116, eq. 2). The substituted dihydrofuran as a single diastereomer was obtained in 75% yield.²¹⁵



Scheme 116. Gold complex VII-catalyzed cyclization reactions.

6.4.2.2. Cycloisomerization with 1,6-enynes

Based on previously described results in gold catalysis (See Chapter 1), we were interested to investigate the cycloisomerization of 1,6-enynes using our gold(I) complexes. Generally, when reacting with cationic gold complexes bearing phosphine moieties, 1,6-enyne substrates can furnish cyclic products effectively. However, except the work of Kumar and Waldmann, there is no literature report using such type of gold carbenes as catalysts. Thus, *N*-Tosyl-enyne **48** was selected as a model substrate.^{51, 216} Our initial experiment was realized using enyne **48** and racemic gold complex (\pm)-**41b** as a catalyst (5 mol%) at room temperature. Unfortunately, no satisfactory result was observed. Although the temperature was increased at reflux for 18 hours, the gold complex (\pm)-**41b** cannot promote the formation of any cyclic product (Scheme 117).

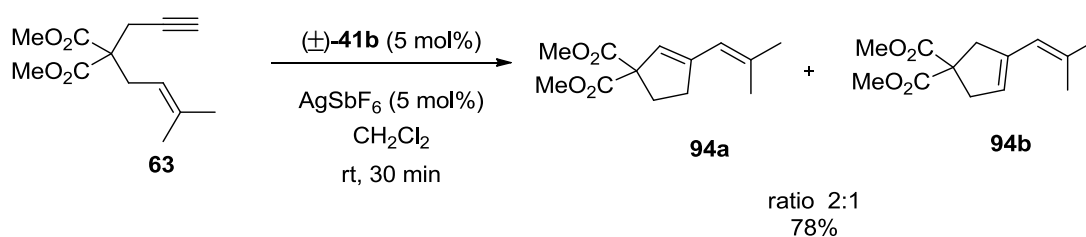
Scheme 117. Reaction of enyne **48** in the presence of gold complex (\pm)-**41b** only.

We found that **41b** is unreactive toward enyne **48** to initiate the reaction. According to most previous works in the preparation of cationic gold catalysts,⁵¹ silver salt were used as co-catalyst. However, *N*-Tosyl-enyne **48** has been recognized as a suitable substrate in silver-

²¹⁶ F. Schröder, C. Tugny, E. Salanouve, H. Clavier, L. Giordano, D. Moraleda, Y. Gimbert, V. Mouriès-Mansuy, J.-P. Goddard, L. Fensterbank, *Organometallics* **2014**, *33*, 4051–4056.

catalyzed cyclization to produce the desired product.^{216, 217, 218} Therefore, we decided to change the substrate to malonate-tethered enyne **63**. Before starting, we tested the blank reaction with only AgSbF₆ as plausible catalyst with this enyne. In that case, only starting enyne **63** was recovered.

The use of 5 mol% of both gold complex (±)-**41b** and AgSbF₆ was examined at room temperature. In this case, the cationic gold catalyst promoted the cyclization of enyne **63** successfully with a high yield (78%), giving a mixture of cyclopentenes **94a** and **94b** in a 2:1 ratio as shown in Scheme 118.

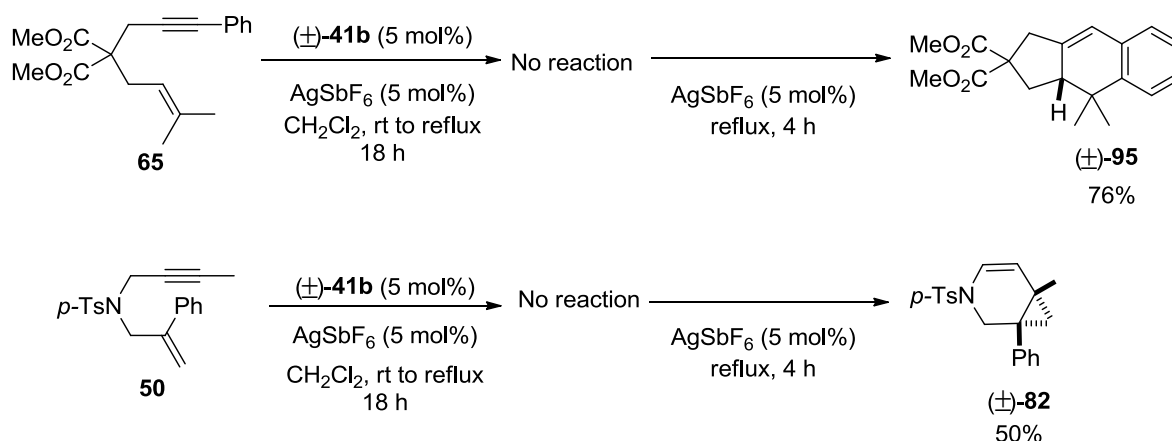


Scheme 118. Cycloisomerization of malonate-tethered enyne **63**.

Due to this excellent result, the reactivity of this cationic gold complex, prepared from (±)-**41b** and silver salt was further investigated in other enyne cycloisomerization reactions. Other enynes such as a malonate-tethered enyne with a phenyl substituent on the alkyne bond **65** and *p*-*N*-Tosyl-enyne **50** were tested with the same reaction condition. However, both reactions did not afford any new products in either room temperature or refluxing conditions. Satisfyingly, when adding the silver salt in excess (10 mol%), the reaction of **65** can afford the tricyclic product (±)-**95** in high yield (76%) (Scheme 119). Similarly, the reaction of **50** provides the corresponding cyclic product (±)-**82** in moderate yield (50%). As our test reactions with only silver catalyst cannot promote the cycloisomerization process for these two 1,6-enynes, our results demonstrated an alternative role of silver in adjunction to gold complexes.

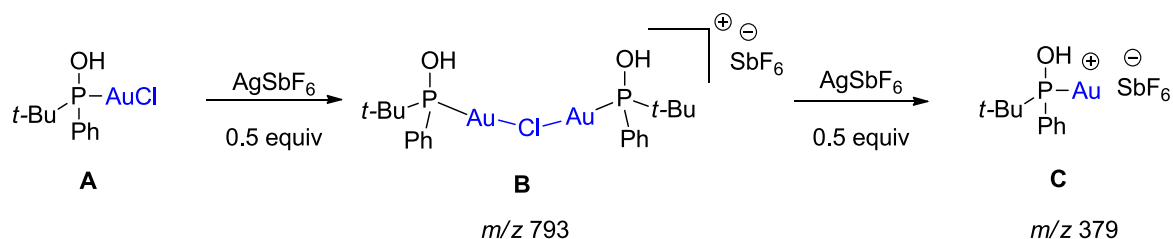
²¹⁷ V. Michelet, P. Y. Toullec, J.P. Genêt, *Angew. Chem. Int. Ed.* **2008**, *47*, 4268–4315.

²¹⁸ J. Koo, H.S. Park, S. Shin, *Tetrahedron Lett.* **2013**, *54*, 834–839.



Scheme 119. Cycloisomerization of enynes **65** and **50** with cationic gold complex (\pm) -**41b**.

The use of silver salts to activate gold complexes has been thoroughly studied by the groups of Schmidbaur²¹⁹, Echavarren,²²⁰ Widenhoefer,²²¹ and Jones²²² among others, which isolated and characterized chloride-bridged gold complexes. Our group has also reported the formation of a cationic secondary phosphine oxide-Au(I) complex **A** by using an excess of silver salts.²¹⁶ The chloride-bridged dinuclear gold complex **B** was observed by mass spectrometry (m/z 793). The addition of another equivalent of silver salt could break the chloride-bridged species to afford the more active cationic gold species **C** (Scheme 120). In our case, we presumed that the enyne substrate was not able to break the intermediate gold chloride-bridged, so it was necessary to add an excess of silver in the medium to observe the generation of an active cationic gold complex.



Scheme 120. Effects of silver salt on a neutral gold complex **A**.

To confirm the hypothesis of the formation of a gold chloride-bridged species, we conducted the previous reactions using this time a 1:1.2 ratio of gold complex (\pm) -**41** and silver salt. The reactions of enyne **65** and **50** were performed by using 3 mol% of **41b** and 3.5 mol% of

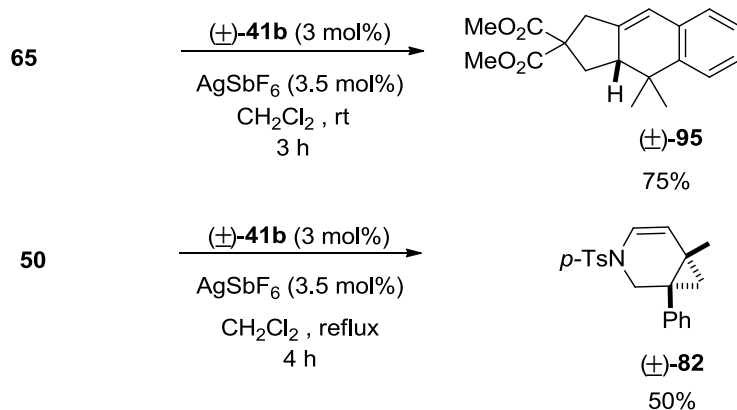
²¹⁹ A. Bayler, A. Bauer, H. Schmidbaur, *Chem. Ber./Recueil*. **1997**, *130*, 115–118.

²²⁰ A. Homs, I. Escofet, A. M. Echavarren, *Org. Lett.* **2013**, *15*, 5782–5785.

²²¹ R. E. M. Brooner, T. J. Brown, R. A. Widenhoefer, *Chem. Eur. J.* **2013**, *19*, 8276–8284.

²²² Y. Zhu, C. S. Day, L. Zhang, K. J. Hauser, A. C. Jones, *Chem. Eur. J.* **2013**, *19*, 12264–12271.

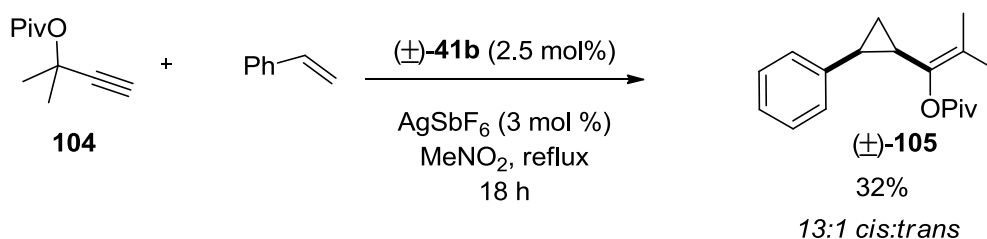
AgSbF₆. The reactions went with complete conversion suggesting efficient formation of the cationic gold complex and afforded the desired products **95** and **82** as well, with similar yields as the previous two-step procedure (Scheme 121).



Scheme 121. Cycloisomerization of enynes **64** and **50**.

6.4.2.3. Cyclopropanation

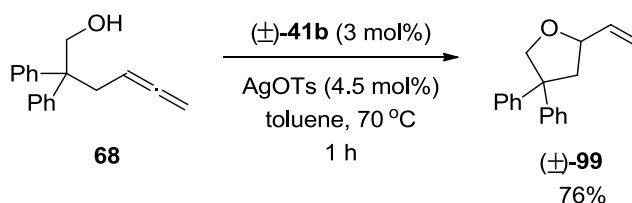
Different types of cyclization reactions with other model substrates were carried out in order to screen the reactivity of the gold complex (\pm) -**41b**. Inspired by Toste's research,⁶⁹ the gold-catalyzed cyclopropanation reaction of propargylic esters and olefins was attempted. The reaction of propargylic pivaloate **104** with styrene was run in the presence of the cationic gold complex (Scheme 122). However, the reaction was sluggish to give cyclopropane (\pm) -**105** in moderate yield (32%) as a 13:1 mixture of *cis*: *trans* diastereomers.



Scheme 122. Olefin cyclopropanation reaction.

6.4.2.4. Cyclohydroalkoxylation

Cyclohydroalkoxylation reaction have been disclosed with the use of gold(I) catalysts, for instance, by the groups of Widenhoefer,^{140, 181} Toste²²³ and Mikami²²⁴ in the preparation of oxygen-tethered cyclic products. Pioneering works by Widenhoefer and co-workers have focused on the successful synthesis of 2-vinyltetrahydrofuran derivatives from β -gem-disubstitued- γ -allenols **68** by means of gold-catalyzed hydroalkoxylation in excellent yield and high enantioselectivity with chiral gold complex, (*S*)-BIPHEP(AuCl)₂.^{140, 181} In this case, they used AgOTs as co-catalyst for activating gold complex instead of AgSbF₆ or AgOTf and the reaction was run in toluene. This silver salt improved the selectivity of the reaction to afford 2-vinyltetrahydrofuran **99** via only a 5-*exo-trig* cyclization. In the same line, we envisaged to apply our gold complex (\pm)-**41b** on this catalytic reaction. Initially, the reaction of **68** in the presence of cationic gold, prepared from the combination of (\pm)-**41b** (3 mol%) and AgOTs (4.5 mol%) in toluene at room temperature. However, the full conversion of product could not be obtained. Thus, the reaction was run in reflux toluene only one hour and afforded the product (\pm)-**99** selectively in 76% yield (Scheme 123).

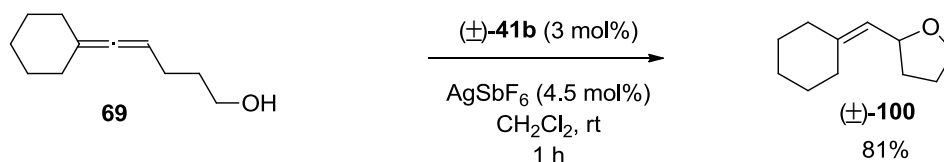


Scheme 123. Hydroalkoxylation reaction of γ -allenol **68**.

The next attempts focused on the preparation of 2-(cyclohexidenemethyl)tetrahydrofuran **100** from cyclohexyl substituted- γ -allenol **69**. Toste and co-workers have been reported this reaction by using the combination of dppm(AuCl)₂ and a chiral silver anion provided product **100** in high yields (90%) and *ee* (97%).²²³ Inspired from Toste' work, we attempted to use our gold (\pm)-**41b** with AgSbF₆ for the similar allene substrate **69**. The reaction was run in dichloromethane at room temperature to afford **100** in 81% yield (Scheme 124).

²²³ G. L. Hamilton, E. J. Kang, M. Mba, F. D. Toste, *Science* **2007**, 317, 496–499.

²²⁴ K. Aikawa, M. Kojima, K. Mikami, *Adv. Synth. Catal.* **2010**, 352, 3131–3135.

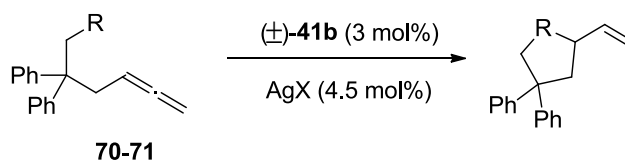


Scheme 124. Hydroalkoxylation reaction of allenol 69.

6.4.2.5. Cyclohydroamination

We also envisaged cyclohydroamination reactions of allenyl substrates **70-71** bearing amino groups to afford a variety of heterocyclic products by analogy with Widenhoefer's works on model γ -allenyl carbamate derivatives.¹⁴⁰ To investigate the reactivity of our gold complex (\pm)-**41b**, the first reaction engaged γ -allenyl amine **70** (Table 5, entry 1) in previous conditions. Unfortunately, the starting allene **70** was recovered and we also observed a slow decomposition of starting allene. Secondly, allenyl carbamate **71** was employed in the presence of (\pm)-**41b** (3 mol%) and AgOTs (4.5 mol%) in toluene. Notably, AgOTs cannot dissolve well in dichloromethane. The reaction was carried out at room temperature. However, no conversion was observed (Table 5, entry 2). To our delight, when the reaction of **71** was run in reflux toluene, a full conversion of product **101** was obtained in 70% yield (Table 5, entry 3).

Table 5. Hydroamination reaction of allenyl amine 70-71



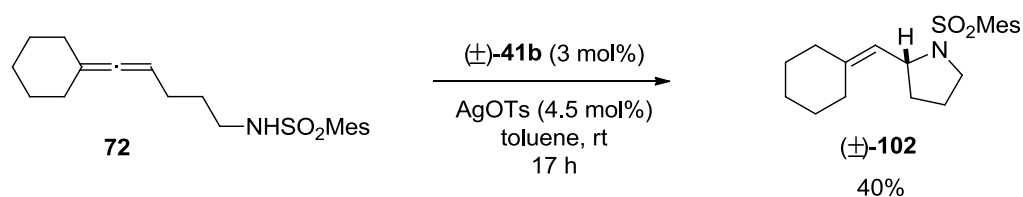
Entry	R	AgX	Solvent	T (°C)	t (h)	Yield
1	NH ₂ (70)	AgSbF ₆	CH ₂ Cl ₂	rt	2	No reaction ^(a)
2	NHCbz (71)	AgOTs	toluene	rt	20	No reaction
3	NHCbz (71)	AgOTs	toluene	reflux	4	70% (101)

^(a) SM slowly decomposed

To broaden the scope of products, we are interested in using *N*-protected γ -allenyl-mesylamide **72** as a model substrate following the reference experiment by the groups of Toste²²⁵

²²⁵ R. L. LaLonde, B. D. Sherry, E. J. Kang, F. D. Toste, *J. Am. Chem. Soc.* **2007**, *129*, 2452–2453.

and Gade.²²⁶ The reaction of **72** was run under the same catalytic condition in Table 5 (entry 2). However, a product **102** was obtained in moderate yield (40%) (Scheme 125).



Scheme 125. Cyclohydroamination of *N*-protected γ -allenyl-mesylamide **72**.

6.4.3. Electronic properties

The gold complex (\pm)-**41b** is an effective and valuable catalyst for gold(I)-catalyzed cyclization to produce several cyclic derivatives as presented in previous sections. A better understanding of the electronic properties of the pyridinyl carbene ligand would be then necessary in order to control the selectivity and the reactivity of each reaction investigated to access the desired products. As described by Toste and Mascareñas groups,²²⁷ allene diene **78** was used as a diagnostic precursor in order to investigate and study the electronic properties of various gold ligands. The cationic-gold catalyzed cyclization of **78** as a model reaction can afford two possible products **96a** and **96b** *via* formal [4+2] and [4+3] cycloadditions respectively, depending on the nature of the employed ligand.

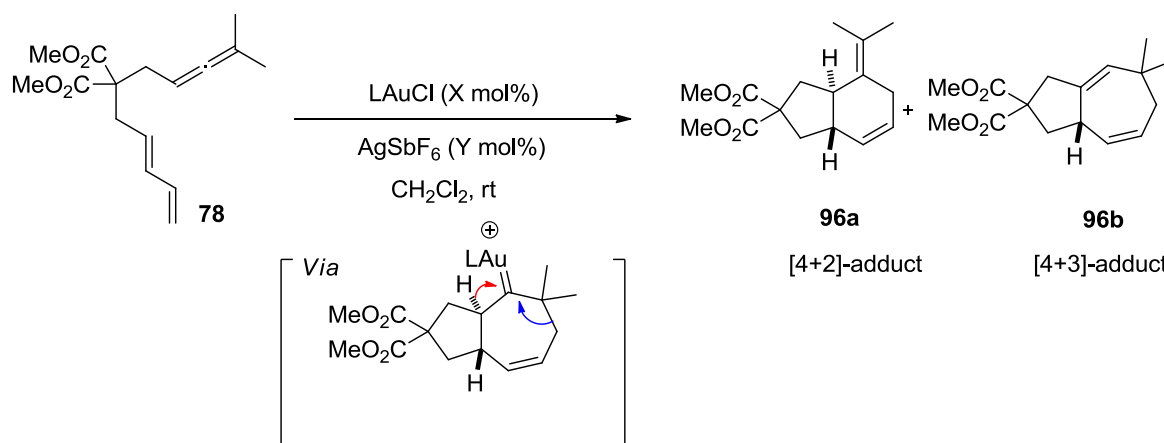
We wished to compare the properties of our gold complex (\pm)-**41b** with selected gold complexes bearing different ligands in catalytic reaction of allene diene **78** and the results were summarized in Table 6. From previous studies, triphenylphosphite ($\text{P}(\text{PhO})_3$) is known as a good electron π -acceptor. In contrast, NHC ligands are usually strong electron σ -donors. Indeed, the cationic gold complex bearing $\text{P}(\text{PhO})_3$ ligand affords only product **96a** selectively (Table 6, entry 1).^{227a} This π -acceptor ligand would induce the ring contraction to stabilize the cationic gold intermediate and form [4+2]-product **96a** after protodeauration. In contrast, IPr, the electron-donating ligand would be able to favor the relative stability of the seven-membered ring carbene intermediate, evolving through a 1,2-H shift in order to afford the formal [4+3] **96b** (Table 6, entry 4).^{227c} In the case of PPh_3 (Table 6, entry 2), which is a common ligand for gold(I), a 67:33 (**96a**:**96b**) was observed.^{227a} It shows that this ligand is closely to be an electron-withdrawing ligand but less than $\text{P}(\text{PhO})_3$.

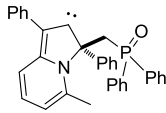
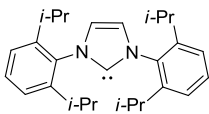
²²⁶ L.-I. Rodríguez, T. Roth, J. Lloret Fillol, H. Wadepohl, L. H. Gade, *Chem. Eur. J.* **2012**, *18*, 3721–3728.

²²⁷ (a) P. Mauleón, R. M. Zeldin, A. Z. González, F. D. Toste, *J. Am. Chem. Soc.* **2009**, *131*, 6348–6349.; (b) A. Z. González, F. D. Toste, *Org. Lett.* **2010**, *12*, 200–203.; (c) B. Trillo, F. López, S. Montserrat, G. Ujaque, L. Castedo, A. Lledós, J. L. Mascareñas, *Chem. Eur. J.* **2009**, *15*, 3336–3339.

In our attempt, the gold complex (\pm)-**41b** can also give the mixture of **96a** and **96b** (ratio 60:40) (Table 6, entry 3). Interestingly, the proportion of these products is lower than the obtained one with the use of PPh₃. It suggests that the pyridinyl ligand of (\pm)-**41b** is a more electron-donating ligand than PPh₃. Taking in account this property, further studies need to be realized.

Table 6. Allene diene cycloisomerizations using different gold(I) complexes.

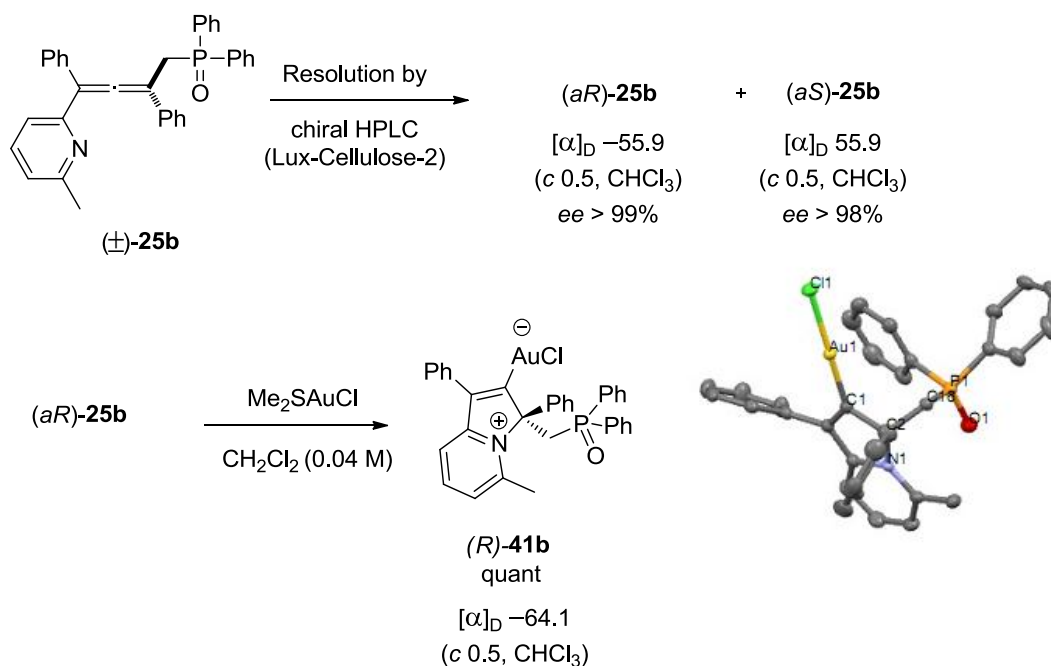


Entry	Ligand (L)	LAuCl (mol %)	AgSbF ₆ (mol %)	Yield (%)	96a:96b
1	P(PhO) ₃	5	5	89	100:0 ^{227a}
2	PPh ₃	5	5	80	67:33 ^{227a}
3	 (\pm)- 41b (no AuCl)	3	3.5	67	60:40
4		10	10	79	0:100 ^{227c}

6.4.4. Optical resolution

Thanks to successful results with gold precatalyst (\pm)-**41b**, we focused on the use of **41b** in asymmetric gold catalysis since it bears a stereogenic center. In collaboration with Dr. Nicolas Vanthuyne (iSm2, Aix-Marseille Université), we decided to separate both enantiomers of pyridinyl allene (\pm)-**25b** by preparative chiral HPLC. Dr. Nicolas Vanthuyne carried out the optical resolution of racemic allene (\pm)-**25b** by chiral HPLC on Lux Cellulose in the mixture hexanes/ ethanol (50/50) as mobile phase. Both enantiomers were obtained with *ees* > 98%. The first enantiomer (*aR*)-**25b**

with $ee > 99\%$ ($[\alpha]_D -55.9$, c 0.5, CHCl_3) was then used to prepare optically pure gold complex **41b** in the presence of Me_2SAuCl . The chiral gold complex (*R*)-**41b** was formed in quantitative yield and its absolute configuration of (*R*)-**41b** ($[\alpha]_D -64.1$, c 0.5, CHCl_3) determined by X-ray crystallography (Scheme 126). It was ready to apply as chiral precatalyst in the previous presented reactions.



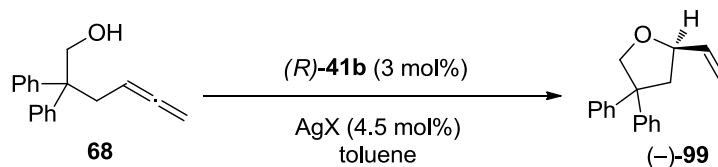
Scheme 126. Resolution of (\pm)-**25b** to prepare chiral gold complex **41b**.

6.4.5. Investigations on asymmetric catalysis

With chiral gold complexes **41b** in hand, we aimed to apply them on asymmetric reactions. According to previous successful results in the preparation of various cyclic products bearing stereogenic centers, we envisaged those reactions (cycloisomerization of 1,6-enynes, cyclopropanation, cyclohydroalkoxylation and cyclohydroamination reactions) with chiral gold (*R*)-**41b**. To our delight, the chiral gold complex (*R*)-**41b** could induce an asymmetry of cycloalkoxylation of γ -allenol **68** as shown in Table 7, whereas the reactions with other model substrates afforded the corresponding products in racemic mixtures. In this case, **68** was treated with the combination of (*R*)-**41b** and AgOTs in toluene at room temperature (Table 7, entry 1). The 2-vinyltetrahydrofuran ($-$)-**99** was obtained in 58% yield and 38% ee . To test the effect of silver salt catalyst, the blank reaction was carried out in the presence of AgOTs under the same conditions. The starting γ -allenol **68** was all recovered without the formation of any products. We

also tested to carry out the reactions at low temperature. Unfortunately, the reaction, when run at 0 °C, cannot afford any products (Table 7, entry 2).

Table 7. Asymmetric cycloalkoxylation of γ -allene **68**

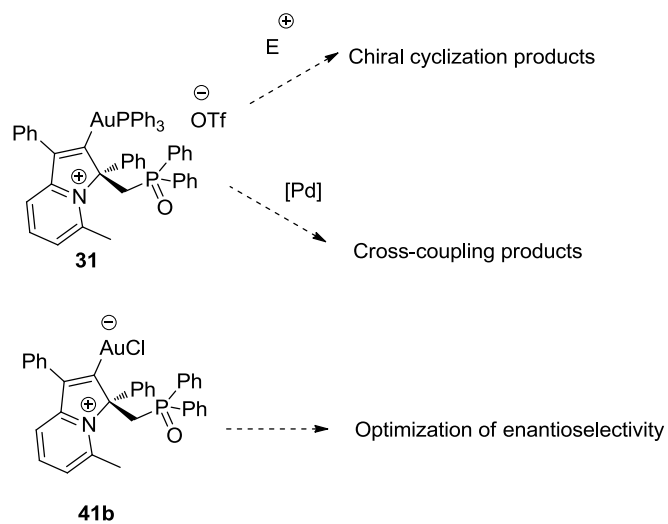


Entry	AgX	Solvent	T (°C)	t (h)	Yield (ee)
1	AgOTs	toluene	Rt	5	58% (38%)
2	AgOTs	toluene	0	41	No reaction

7. Conclusion and perspectives

This study reports the successful synthesis of functionalized allenes bearing mono-diphenyl phosphine oxide groups *via* either organocopper-mediated S_N2' reaction or palladium-catalyzed coupling reaction. However, allenes with bisphosphine oxide functional groups could not be synthesized under similar methods. We have applied these allenes in several settings, focusing on gold coordination chemistry. Firstly, with a nucleophilic component bearing a labile proton such as allenes **17** and **18**, gold(I)-catalyzed cycloisomerization takes place and delivers highly valuable cyclopentadienyl-**29** and indenylphosphine oxide **30** products. To our delight, a complete axial-to-centered chirality transfer was observed in the formation of enantiomerically pure indenylphosphine **30** from optically pure allene **18**. With a pendant pyridine moiety, allene **25b** could be transformed into cationic phosphinylvinylgold complex **31** by using a cationic gold complex in stoichiometric amount. This gold complex **31** was post-functionalized by trapping the goldphosphine functional group to give indolizium salt **39** after deprotonation and vinyl iodide **40** after iodolysis. Moreover, pyridinyl allenes **25** successfully allows access to generate new vinylgold complexes **41a** and **41b** with no adjacent heteroatoms. These pyridinyl gold complexes have been isolated and fully characterized, both analytically and theoretically. Gold complexes **41a,b** perfectly work as precatalysts in gold(I)-catalyzed reactions.

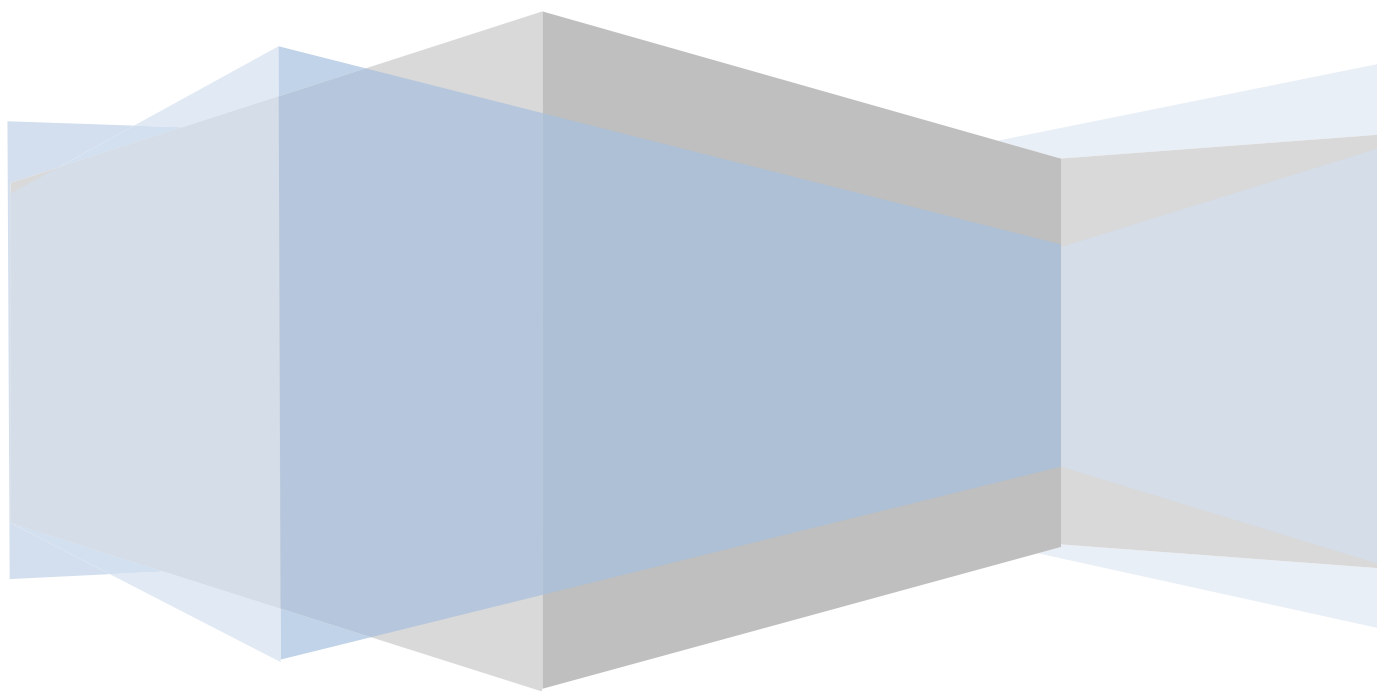
As perspectives (Scheme 127), we are continuing to investigate the ability of optically pure vinylgold complex **31** to produce the various chiral products. Moreover, palladium-gold cross-coupling reactions could be attempted. Our gold precatalyst **41b** would be engaged in several other asymmetric reactions to delineate its potential.



Scheme 127. Perspectives in the application of gold complexes 41b and 31.

CHAPTER 4

Allenyl Bisphosphine Ligands for Metal Catalysis



CHAPTER 4

Allenyl Bisphosphine Ligands for Metal Catalysis

1. Introduction

Chiral allene ligands bear interesting properties for metals complexation. With regard to Ready's work (Figure 39), allene ligands bearing free-bisphosphine functional groups were described for the successful formation of rhodium(I) and platinum(II) complexes.^{130, 131} Interestingly, rhodium complexes bearing chiral allene moieties can be isolated and used as catalysts in asymmetric arylation reactions of ketones. Schmidbaur also presented allenyl bisphosphine (Figure 39), however, applications on these compounds as valuable ligands have not been reported.¹⁴⁷ Encouraged by these works, we made an attempt to prepare allene ligands bearing a free phosphine functional group for transition metals such as palladium, platinum and gold. Moreover, optical resolution of racemic allenes has been experimented for the preparation of chiral metal complexes for asymmetric reactions.

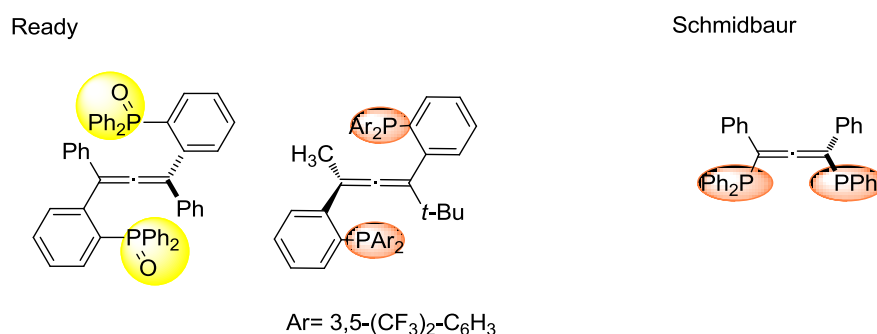


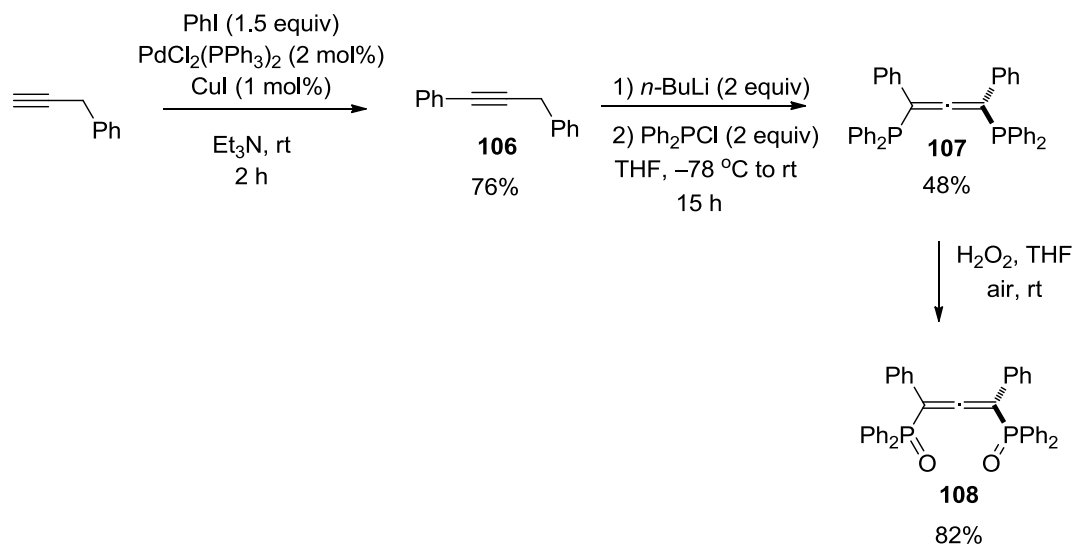
Figure 39. Allene ligands from Ready^{130, 131} and Schmidbaur.¹⁴⁷

2. Synthesis of allenyl bisphosphine

The synthesis of allenyl bisphosphine derivatives was first reported in the work of Schmidbaur.¹⁴⁷ 1,3-diphenyl-1-propyne **106** was used as a precursor for allenyl bisphosphine **107**, which was prepared *via* a palladium coupling reaction of 2-propynylbenzene and iodobenzene.²²⁸ The precursor **106** was deprotonated with two equivalents of *n*-butyllithium to generate an alkynyllithium intermediate, by undergoing the isomerization to form an allenyllithium intermediate in equilibrium. After adding two equivalents of chlorodiphenylphosphine, the

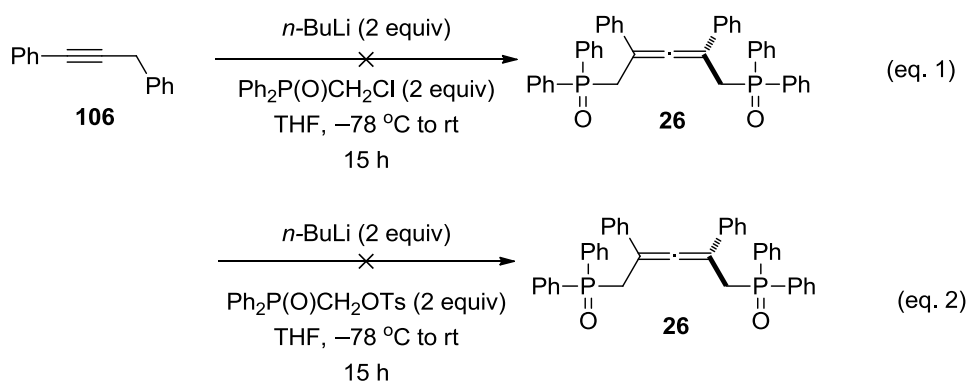
²²⁸ X. Zhang, S. Sarkar, R. C. Larock, *J. Org. Chem.* **2006**, *71*, 236–243.

reaction afforded allenyl bisphosphine **107** in 48% yield (Scheme 128). The evaluation of its electrophilic properties was attempted in view to the complexation with transition metals. Moreover, a corresponding allenyl bisphosphine oxide **108** was prepared by adding hydrogen peroxide into **107** yielding 82%.¹⁴⁷



Scheme 128. Synthesis of allenyl bisphosphines **107** and the corresponding oxide **108**.

To extend the scope of allenyl bisphosphine oxides, the synthesis of allene **26** was aimed. We prepared organolithium intermediate from **106** with *n*-butyllithium under the same conditions of allenyl bisphosphines **107**. During the first attempt, we used (chloromethyl)diphenylphosphine oxide as an electrophile, but this reagent was unreactive to form the product **26** (Scheme 129, eq. 1). ³¹P NMR of this reaction was recorded and gave a major peak of P=O bond at 33 ppm, which corresponds to (chloromethyl)diphenylphosphine oxide reagent. There were several small peaks occurring in the range of 29-33 ppm, which were unable to be isolated. During the second attempt, we changed the electrophilic reagent to (diphenylphosphoryl)methyl-4-methylbenzenesulfonate bearing tosyl group (OTs), which is a better leaving group. However, the reaction did not afford the allene **26** (Scheme 129, eq. 2). ³¹P NMR showed the major peak of reagent at 26 ppm.



Scheme 129. Screening electrophilic reagents to prepare allene 26.

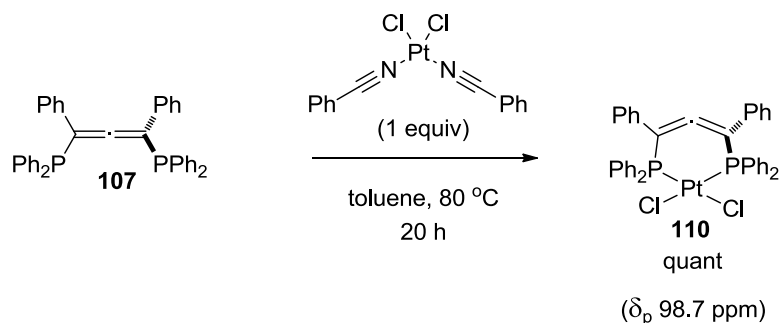
3. Metal-allenyl bisphosphine complexes

Allene motifs and organophosphorus compounds have been reported to have the ability to coordinate with noble metals. However, the study of allenes bearing phosphine moieties with metal has found in only a limited number of reports. It was challenging to observe whether the allenyl bisphosphine **107** could act as a ligand for transition metals. In this case, we focused on using one equivalent or two equivalents of metals, such as platinum(II), palladium(II) and gold(I).

3.1. Platinum-allenyl bisphosphine complex

Platinum complexes bearing phosphine moieties have also been reported in the literature.²²⁹ We envisaged the preparation of a new platinum complex with allene **107**. In this case, a 1:1 mixture of *cis*-bis(benzonitrile)dichloroplatinum(II) and **107** afforded the mononuclear platinum-allene bisphosphine complex **110** in quantitative yield (Scheme 130). It was recrystallized by diffusion of toluene into the solution of crude product in CHCl_3 . ^{31}P NMR shows the central peak of P-Pt at 98.7 ppm with two small satellite peaks of ^{195}Pt with a $^1J_{\text{P-Pt}}$ of 4371 Hz. Moreover, the peak of central carbon of allene ($\text{C}=\text{C}=\text{C}$) in ^{13}C NMR is at 198.9 ppm, which is more shielded than allene **107** (209.9 ppm, doublet). This triplet carbon peak is observed, because of the coupling of two non-equivalent phosphorus atoms caused by the coordination with metal.

²²⁹ See some reviews: (a) V. Michelet, L. Charruault, S. Gladiali, J.-P. Genêt, *Pure Appl. Chem.* **2006**, *78*, 397–407.; (b) X. Han, R. A. Widenhoefer, *Org. Lett.* **2006**, *8*, 3801–3804.; (c) D. Brissy, M. Skander, H. Jullien, P. Retailleau, A. Marinetti, *Org. Lett.* **2009**, *11*, 2137–2139.; (d) K. Ishida, H. Kusama, N. Iwasawa, *J. Am. Chem. Soc.* **2010**, *132*, 8842–8843.; (e) C. Liu, X. Han, X. Wang, R. A. Widenhoefer, *J. Am. Chem. Soc.* **2004**, *126*, 3700–3701.



Scheme 130. Synthesis of platinum complex **110**.

The characterization of complex **110** by X-ray crystallography shows the mononuclear platinum complex bearing bidentate allenyl ligand (Figure 40). The observed structure is a bent cyclic allene, showing an allene (C=C=C) angle of 151.8°.

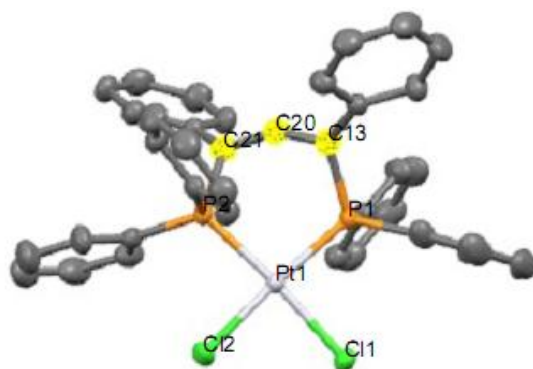


Figure 40. Crystal structure of platinum-allenyl bisphosphine complex **110** at solid state. Selected bond lengths (Å): P1-Pt1 2.258, P2-Pt1 2.246, P1-C13 1.854, P2-C21 1.854. Allene angle (C21=C20=C13) 151.8°.

The bent acyclic allene and cyclic allenes have been discussed in previous sections (See Chapter II). For example, bent acyclic allene **A** by Weber¹⁷² shows an allene angle of 170° (Figure 41A). In contrast, Regitz presented bent cyclic allene **B** with an allene angle of 155.8° (Figure 41B).¹⁷³ However, the severe bending in an allene, which necessary constrains the C=C=C π system into a ring, eventually leads to very unstable compounds.²³⁰ Consequently, the cyclic allene complex **110** is not stable in the air and humidity.

²³⁰ For some discussions, see (a) R. Warmuth, M. A. Marvel, *Angew. Chem.* **2000**, *112*, 1168–1171.; (b) K. J. Daoust, S. M. Hernandez, K. M. Konrad, I. D. Mackie, J. Winstanley, R. P. Johnson, *J. Org. Chem.* **2006**, *71*, 5708–5714.; (c) M. M. Hänninen, A. Peuronen, H. M. Tuononen, *Chem. Eur. J.* **2009**, *15*, 7287–7291.

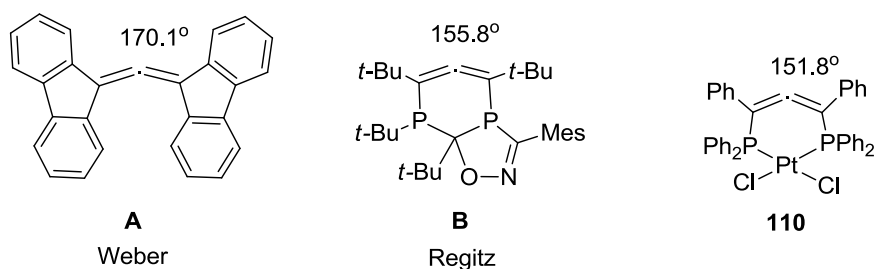
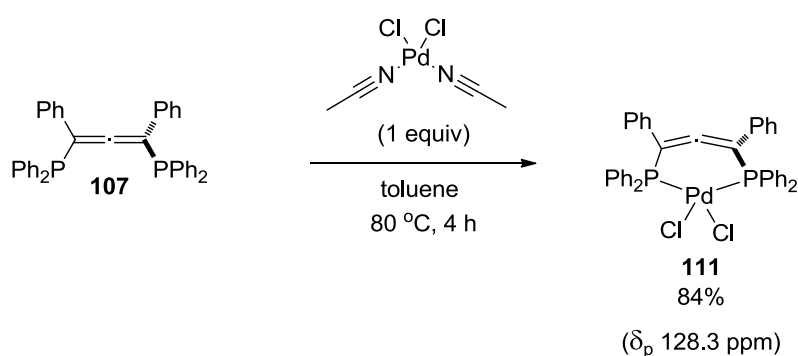


Figure 41. Bent acyclic and cyclic allenyls by Weber (A), Regitz (B), and platinum complex **110**.

3.2. Palladium-allenyl bisphosphine complex

Palladium salts have been used for the complexation with organophosphine ligands. The corresponding complexes applied in catalytic reactions in order to stabilize the metal and promote the selectivity of reactions.^{20, 231} In this case, we also attempted to prepare palladium complex allene **111** from a 1:1 mixture of *cis*-bis(acetonitrile)dichloropalladium(II) and **107** in reflux toluene. The reaction yielded 84% of the palladium complex (Scheme 131).³¹ P NMR of **111** shows a singlet peak at 128.3 ppm and central carbon of allene (C=C=C) peak in ¹³C NMR is also observed as triplet peak at 193.3 ppm in the same range as platinum complex **110**. Because of the similarity with **110**, the product **111** was assumed to be cyclic mononuclear palladium(II) complex bearing the allene ligand. The complex **111** was recrystallized under the same conditions of **110**. The characterization by X-ray crystallography is in process.



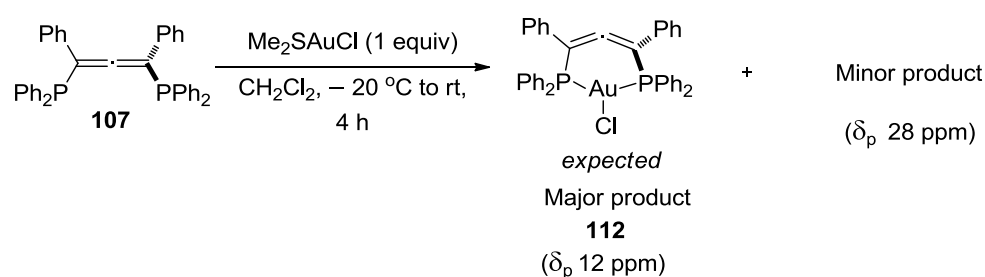
Scheme 131. Synthesis of mononuclear palladium-allenyl bisphosphine complex **111**.

²³¹ For some reviews, see: (a) D. S. Surry, S. L. Buchwald, *Angew. Chem. Int. Ed.* **2008**, *47*, 6338–6361.; (b) C. Li, J. Chen, G. Fu, D. Liu, Y. Liu, W. Zhang, *Tetrahedron* **2013**, *69*, 6839–6844.; (c) T. T. Dang, B. Ramalingam, S. P. Shan, A. M. Seayad, *ACS Catal.* **2013**, *3*, 2536–2540.; (d) W. Fang, H. Zhu, Q. Deng, S. Liu, X. Liu, Y. Shen, T. Tu, *Synthesis* **2014**, *46*, 1689–1708.

3.3. Gold-bisphosphine complexes

3.3.1. Mononuclear gold-phosphine complex

The allene **107** was also attempted to prepare mononuclear gold complex. The solution of **107** in dichloromethane was slowly adding the solution of Me_2SAuCl at $-20\text{ }^\circ\text{C}$. The reaction was warmed to room temperature for 4 hours to afford a mixture of products in quantitative yield (Scheme 132). ^{31}P NMR (162 MHz, CD_2Cl_2) of the mixture shows two peaks at 12 (broad singlet) as major and 28 ppm (singlet) as minor products. The major product was assumed to be a mononuclear gold(I) complex **112**. The mixture was recrystallized by diffusion of pentane into the solution of product in dichloromethane. The characterization by X-ray crystallography is still in process.



Scheme 132. Synthesis of gold complex **112**.

3.3.2. Dinuclear gold-bisphosphine complex

Dinuclear gold complexes bearing axial chiral ligands (C_2 -Symmetry) have been successfully prepared by gold(I) salts and applied in asymmetric catalytic reactions.^{109, 232} To attempt this, our approach was to use two equivalents of Me_2SAuCl for allene **107**. Gratifyingly, the gold(I) coordinated to the phosphorus atoms of **107** selectively to afford the dinuclear gold-bisphosphine complex **113** in quantitative yield without other side-products coordinated to allene bond (Scheme 133). ^{31}P NMR analysis showed a singlet peak at 30.2 ppm. The gold complex **113** was characterized by X-ray crystallography (Figure 42).

²³² (a) A. Pradal, C.-M. Chao, M. R. Vitale, P. Y. Toullec, V. Michelet, *Tetrahedron* **2011**, *67*, 4371–4377.; (b) M.-A. Abadie, X. Trivelli, F. Medina, F. Capet, P. Roussel, F. Agbossou-Niedercorn, C. Michon, *ChemCatChem* **2014**, *6*, 2235–2239.; (c) Y.-M. Wang, A. D. Lackner, F. D. Toste, *Acc. Chem. Res.* **2014**, *47*, 889–901.

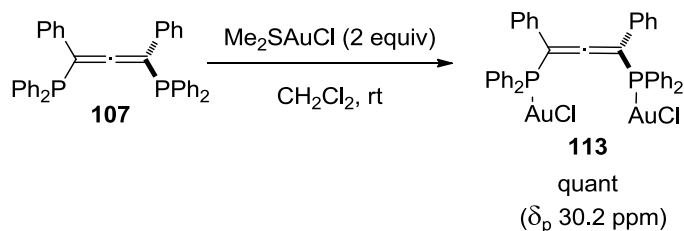
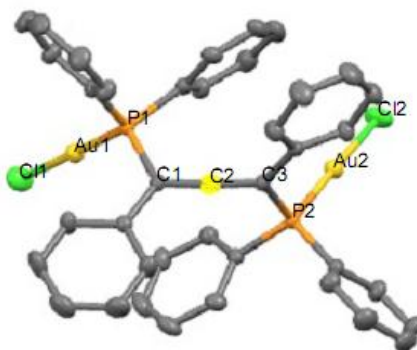
Scheme 133. Synthesis of gold-allene bisphosphine complex **113**.

Figure 42. Crystal structure of gold-allene bisphosphine complex **113** at solid state of racemic product. Selected bond lengths (Å): Au1-Au2 6.498, P1-Au1 2.228, P2-Au2 2.232, P1-C1 1.838, P2-C3 1.833. Allene angle (C1=C2=C3) 175.11°

No coordination between η^2 -allene and gold, and the gold-gold interaction (Au-Au) were observed. The gold complex **113** shows that the bond length of Au \cdots Au is 6.498 Å, which is too far for the gold atoms to interact. The distances of intramolecular Au-Au interactions are often less than 3.6 Å.^{49, 233} Moreover, the weak interaction between gold and phenyl group *via* η^2 -interaction of the *ortho* phenyl group with the gold center as well as bulky biphenylphosphanes ligands (Figure 43), and the π - π interaction of both phenyl groups were not observed as disclosed by Echavarren and co-workers.¹⁷⁶ Thus, the gold complex **113** were attempted to test the reactivity in catalytic reactions.

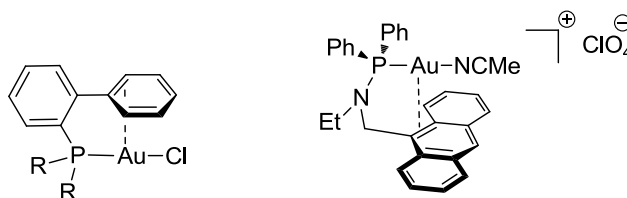


Figure 43. Examples of η^2 -interaction of the *ortho* phenyl group with the gold center.¹⁷⁶

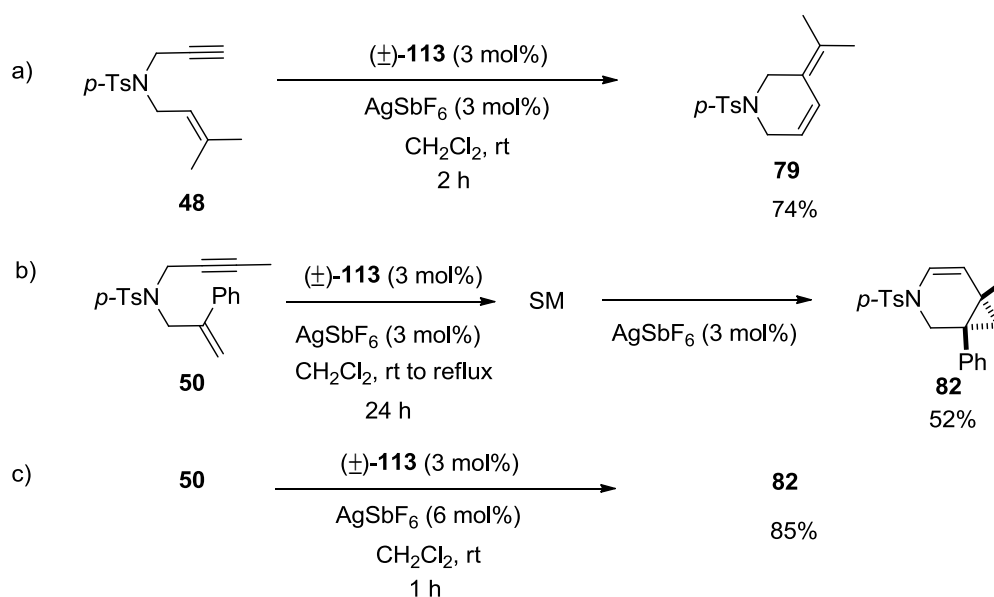
²³³ H. Schmidbaur, A. Schier. *Chem. Soc. Rev.* **2012**, *41*, 370–412.

4. Gold(I)-catalyzed cyclization reactions

We decided to test the racemic digold-bisphosphine complex (\pm)-**113** as a precatalyst in cycloisomerization reactions of 1,6-enyne substrates to examine the reactivity and selectivity.

4.1. Preliminary catalytic tests

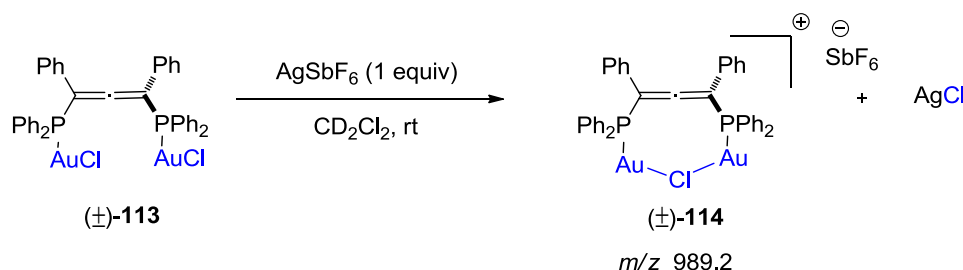
Firstly, the reaction was run using enyne **48** and 3 mol% of our cationic gold catalyst. This cyclization reaction gave six-membered cyclic product **79** in high yield (Scheme 134a). In contrast, when we experimented with enyne **50** under the same conditions, no product was observed. The reaction required to add a second equivalent of AgSbF_6 for (\pm)-**113**. The cyclic product **82** containing two stereogenic carbons-containing cyclopropane was obtained in 52% yield (Scheme 134b). We thus decided to use two equivalents of AgSbF_6 to react one equivalent of gold complex (\pm)-**113** (Scheme 134c). This reaction of **50** could provide **82** in high yield (85%).



Scheme 134. Preliminary catalytic tests in cycloisomerization of enyne **48** and **50** with (\pm)-**113**.

We considered the effect of the silver salt on the gold complexes and tested the reaction that employed one equivalent of AgSbF_6 and one equivalent of (\pm)-**113**. The obtained product was characterized by Mass Spectroscopy and showed the detrimental formation of chloride-bridged dinuclear gold(I) complex (\pm)-**114** (m/z 989.2) (Scheme 135). The results correlated well with previous research from Schmidbaur,²¹⁹ Echavaren,²²⁰ Widenhoefer,²²¹ Jones,²²² and our group.²¹⁶ An excess silver salt was required in order to break the *in-situ* generated gold-chloride bridged species and generate the active cationic gold complex. In the case of condition in Scheme 134a,

the enyne **48** could be a good nucleophile to cleavage the gold-chloride bridged species ((±)-**114**) to afford **79**, whereas another substrate **50** could not react. Thus, ((±)-**114**) must be cleaved by substrates like **48** or by the addition of an excess of silver salts. Following the reaction condition in Scheme 134c, we decided to use two equivalents of silver salts for the gold complex ((±)-**113**) in order to evaluate the reactivity of ((±)-**113**) in racemic catalytic reactions.



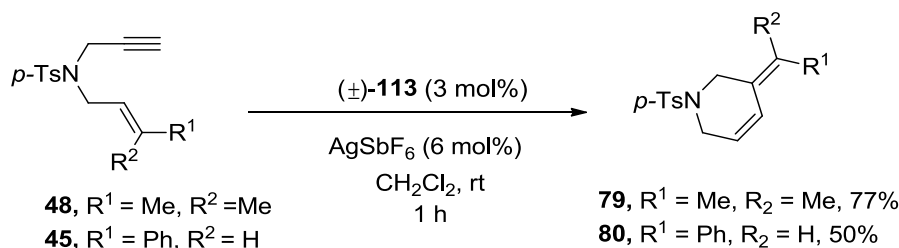
Scheme 135. Formation of chloride-bridged dinuclear gold(I) complex ((±)-**114**.

4.2. Broadening the scope of substrates

We next attempted to evaluate the reactivity and selectivity of our gold complex ((±)-**113**) with different substrates, such as *N*-Tosyl and malonate group-tethered 1,6 enyne, in skeletal rearrangement reactions under the condition reaction in Scheme 134c.

4.2.1. Nitrogen-tethered 1,6-enynes

Nitrogen tethered-1,6 enynes such as *N*-Tosyl (*p*-TsN)-substituted-enynes are considered as model precursors^{234, 235} for catalytic testing by employing gold complex ((±)-**113**). As Initial testing, two enyne precursors **48**, which were tested in condition Scheme 134a, and **45** were examined by treatment with our cationic gold complex under the reaction conditions in Scheme 134c. Reactions gave birth to six-membered cyclic products **79** and **80** in 77% and 50% yields respectively (Scheme 136).



Scheme 136. Synthesis of cyclic products **79** and **80**.

²³⁴ E. Jiménez-Núñez, A. M. Echavarren, *Chem. Rev.* **2008**, *108*, 3326–3350.

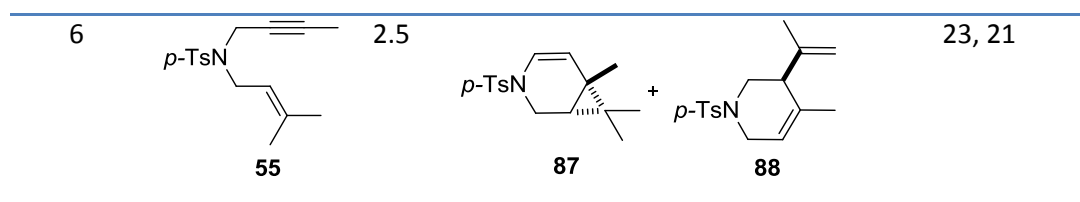
²³⁵ C. Nieto-Oberhuber, M. P. Muñoz, S. López, E. Jiménez-Núñez, C. Nevado, E. Herrero-Gómez, M. Raducan, A. M. Echavarren, *Chem. Eur. J.* **2006**, *12*, 1677–1693.

A second series of enyne substrates with a methyl substituent on the alkyne was investigated.^{216, 236} Several enynes **49-55** were evaluated in a similar catalytic system (Table 8). In the case of enynes **49**, **51-54** (Table 8, entries 1-5), reactions afforded the cyclic products **81**, **83-86** in 60% to quantitative yields. However, the reaction with enyne **55** (Table 8, entry 6), formed two products **87** and **88**, owing to the prenyl substituted-alkene. The reaction was sluggish to give these products **87** and **88** in 23% and 21% yields respectively.

Table 8. Gold-catalyzed cyclization of enynes **49-55**.

Entry	Substrate	t (h)	Product	Yield (%)
1		1		Quant
2		1		60
3		2		90
4		1		76
5		1		74

²³⁶ (a) H. Teller, M. Corbet, L. Mantilli, G. Gopakumar, R. Goddard, W. Thiel, A. Fürstner, *J. Am. Chem. Soc.* **2012**, *134*, 15331–15342.; (b) S. I. Lee, S. M. Kim, S. Y. Kim, Y. K. Chung, *Synlett.* **2006**, *14*, 2256–2260.; (c) S. I. Lee, S. M. Kim, M. R. Choi, S. Y. Kim, Y. K. Chung, W.-S. Han, S. O. Kang, *J. Org. Chem.* **2006**, *71*, 9366–9372.



N-tethered enynes with phenyl substituent on the alkyne were also attempted. We selected the three enynes **57**, **58** and **59** under our standard conditions. As shown in Table 9 (entries 1 and 2), the reactions of enynes **57** and **58** gave products **89** and **90** in 60% and 81% yields respectively. In contrast, the reaction of the enyne **59** bearing a prenyl functional group (Table 9, entry 3) could not afford similar cycloisomerization pattern as product **92**. The reaction gave a major cyclic product **91** instead. When the reaction was carried out at room temperature, the major product **91** yielded 61% and a trace amount of **92**. Interestingly, when the reaction was carried out at 0 °C, it gave new major product **93** in 79% yield, which was determined the structure by NMR spectrometry (1D and 2D), and minor product **91** in 11% yield. However, the product **92** was not observed in this condition. The new product **93** is in process to determine the structure by X-ray crystallography.

Table 9. Gold-catalyzed cyclization of enynes 57-59.

57-59 (\pm) -**113** (3 mol%)
 AgSbF₆ (6 mol%)
 CH₂Cl₂, rt
 t

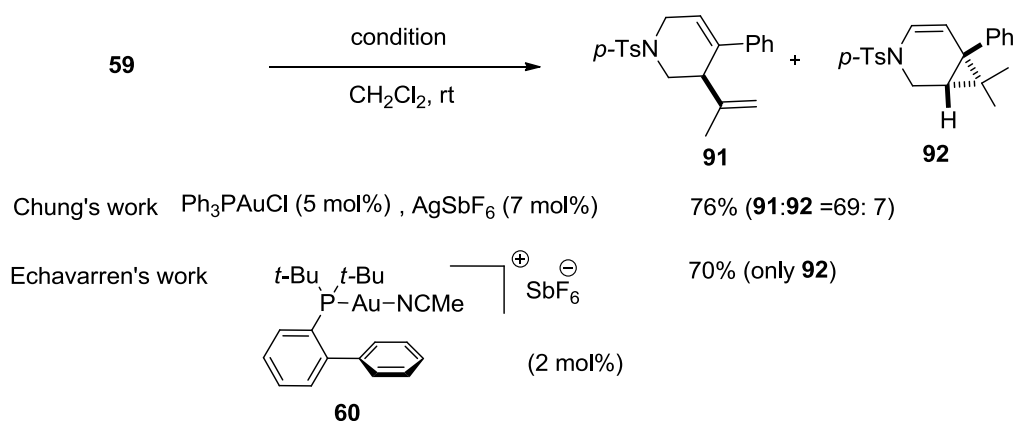
89-90, 92 **91**

Entry	Substrate	t (h)	Product	Yield (%)
1		2.5		60
	57		89	
2		2.5		81
	58 (<i>E</i> : <i>Z</i> = 9:1)		90 (<i>E</i> : <i>Z</i> = 9:1)	

3		1		61, trace
4	59	3		11 ^(a) , 79 ^(a)

^(a)The condition was performed at 0 °C

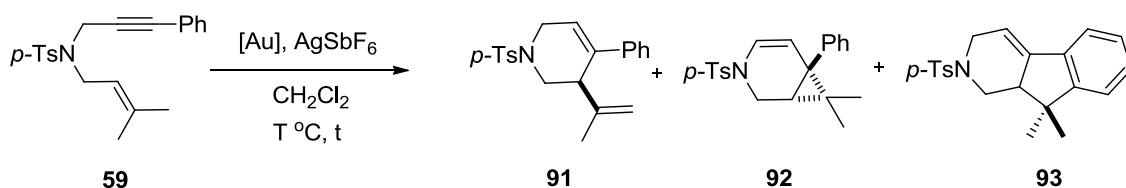
According to the similar tests in gold catalytic reactions reported by the groups of Chung^{236b} and Echavarren,²³⁷ the reaction of **59** was examined with different gold(I) catalysts (Scheme 137). The treatment of **59** in the presence of Ph₃PAuCl (5 mol%) and AgSbF₆ (7 mol%) afforded a cyclic product **91**, with a minor product **92** (a 69:7 ratio). In the other case, the reaction with bulky gold complex (**60**, 2 mol%) gave the cyclic product **92** selectively.



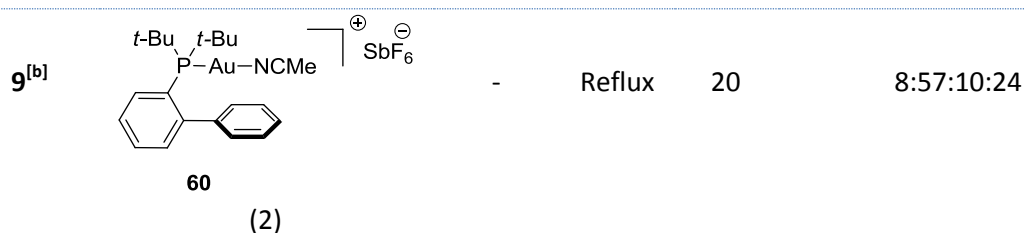
Scheme 137. Gold(I)-catalyzed cycloisomerization of enynes **59** in different catalysts.

To probe the selectivity of (±)-**113**, the results from entries 3 and 4 suggested that the reagent ratios and temperatures were significant factors that control the reaction for the generation of **91**, **92** or new product **93**. Thus, we proceeded to explore the reaction of enyne **59** in various temperature and catalysts. The results were summarized in Table 10.

²³⁷ C. Nieto-Oberhuber, P. Pérez-Galán, E. Herrero-Gómez, T. Lauterbach, C. Rodríguez, S. López, C. Bour, A. Rosellón, D. J. Cárdenas, A. M. Echavarren, *J. Am. Chem. Soc.* **2008**, *130*, 269–279.

Table 10. Screening of conditions using the enyne **59**.

Entry	Au (mol%)	AgSbF ₆ (mol%)	T °C	t (h)	Ratio from ¹ H NMR (91:92:93:59)
1	-	6	rt	18	0:0:0:100
2	(±)- 113 (3)	6	rt	1	93:7:0:0
3	(±)- 113 (3)	6	0	3	12:0:88:0
4	(±)- 113 (3)	3	rt	22	28:11:57:4
5 ^[a]	Ph ₃ PAuCl (5)	7	rt	0.5	60:20:20:0
6	Ph ₃ PAuCl (5)	7	0	3	42:24:42:34
7	Ph ₃ PAuCl (2)	2	rt	0.5	37:15:15:33
8	Ph ₃ PAuCl (2)	2	0	3	12:1:51:36



^[a] The reaction was optimized by using Chung's condition.^{236b} ^[b] The reaction was optimized by using Echavarren's condition.²³⁷

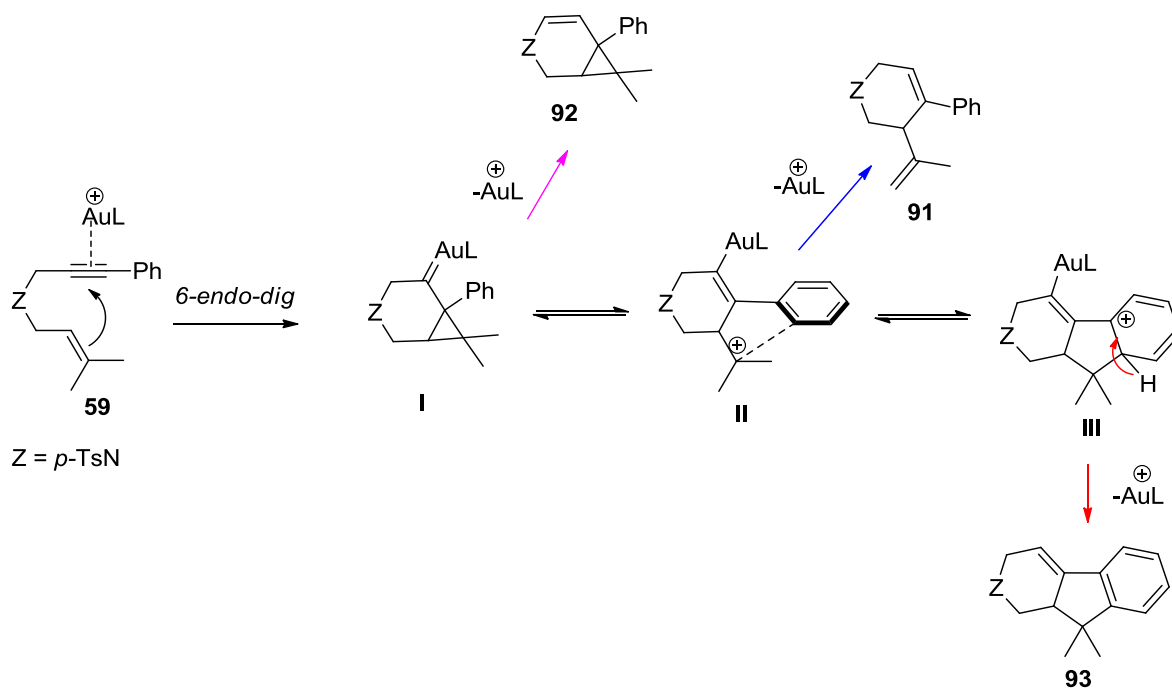
First of all, enyne **59** was tested with only 6 mol% AgSbF₆ (Table 10, entry 1). The result showed only starting material was recovered. When used 6 mol% of AgSbF₆ and 3 mol% of (±)-**113** at room temperature (Table 10, entry 2), the reaction gave **91** as a major product and a small amount of product **92**, whereas running the reaction at 0 °C (Table 10, entry 3) gave **93** as the major product. When the silver salt was decreased to only 3 mol% (Table 10, entry 4), the reaction gave **93** as a major product and increased the ratio of products **91** and **92**. Thus, the temperature and the quantity of silver salt were significant in determining the reaction outcome.

Another series by using a cationic gold, prepared from 5 mol% of Ph₃PAuCl and 7 mol% of AgSbF₆ was tested (Table 10, entries 5 and 6). The reaction (Table 10, entry 5) involving these catalytic conditions at room temperature formed **91** as the major product, along with a mixture of **92** and **93** as minor products. At low temperature, the reaction found the sluggish production of

91 and **93** in similar quantity (Table 10, entry 6). However, the reaction with 2 mol% of cationic gold (Table 10, entries 7-8) under the same conditions was slow to give products. These reactions were not complete to afford the products with full conversion.

Finally, we tested Echavarren's conditions (Table 10, entry 9). The catalyst **60** promoted the reaction of enyne **59** to obtain **92** as the major product in a better ratio (57% yield from ^1H NMR) than the other two gold complexes. However, we also observed the formation of a minor amount of **91** and **93**.

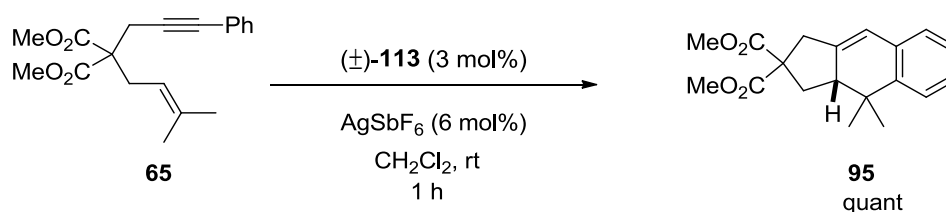
The proposed mechanisms for the formations of **91** and **92** have been reported by the groups of Chung^{236b} and Echavarren.²³⁷ Our group realized and proposed the formation of **93** via the Friedel-Crafts type cyclization reaction. The activation of enyne **59** by cationic gold catalyst to afforded cyclopropane-gold intermediate **I**, which is followed by 6-endo-dig cyclization. The first possibility of **I** underwent β -hydride elimination to trap the gold(I) species and then gave product **92**. The second possibility continued to cleave a cyclopropane ring to stabilize gold carbene. The carbocation intermediate **II** was then generated. After β -hydride elimination and protodeauration, the intermediate **II** transformed as product **91** selectively. However, the phenyl-stabilized π -cation might be occurred when the reaction was run at low temperature. We surmised the third possibility that the intermediate **II** could undergo the Friedel-Crafts type cyclization to form intermediate **III**. After rearomatization and protodeauration, the tricyclic compound **93** was obtained (Scheme 138).



Scheme 138. Proposed mechanism of cycloisomerization using enyne **59**.

4.2.2. Malonate group-tethered 1,6-enynes

A series of malonate group-tethered 1,6-enynes substrates were tested in gold(I)-catalyzed cyclization. We selected enyne **65**⁶⁴ to engage in similar catalytic reaction. The reaction afforded tricyclic product **95** in quantitative yield (Scheme 139).



Scheme 139. Gold-catalyzed cyclization of enyne **65**.

4.3. Electronic properties

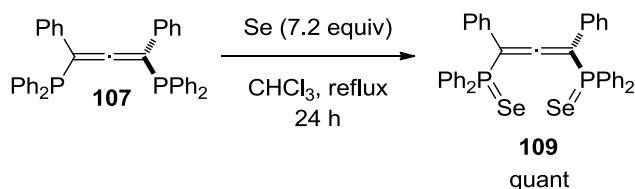
4.3.1. Evaluation by selenide complexes

Electronic properties of ligands can be observed by the formation of the selenide compounds. Nowell and co-workers have disclosed the electronic properties of arylphosphines towards selenium acceptor in 1984.²³⁸ The selenium can coordinate to phosphine group selectively and indicate the properties of phosphine ligands by the characterization of ³¹P NMR analysis. Generally, chemical element selenium has five naturally stable isotopes, which are ⁷⁴Se, ⁷⁶Se, ⁷⁷Se, ⁷⁸Se, and ⁸⁰Se. Only ⁷⁷Se has an effect on magnetic resonance of ³¹P to give two small peaks occurring in ³¹P NMR. The increasing coupling constant (*J*) of phosphorus (³¹P) with selenium (⁷⁷Se) indicates that the attached groups to the phosphine become a good π -acceptor ligand. The electron-withdrawing groups would increase *s*-character of a phosphorus lone-pair orbital in the bonding to selenium and provide shorter bonding between phosphorus and selenium than electron-rich ligands.

4.3.1.1. Preparation of selenide derivatives

The synthesis of allenyl selenide **109** has been reported by Schmidbaur and co-workers.¹⁴⁷ It was prepared from the combination of ligand **107** (1.0 equiv) and selenium (7.2 equiv) in chloroform at reflux. The lone pair of electrons of both phosphorus atoms was donated to two selenium atoms to form the product **109** in quantitative yield (Scheme 140).

²³⁸ D. W. Allen, L. A. March, I. W. Nowell, *J. Chem. Soc. Dalton Trans.* **1984**, 483–485.



Scheme 140. Synthesis of allenyl selenide **109**.

4.3.1.2. Ligand properties

The properties of allenyl selenide **109** were compared with some selected phosphine selenide compounds, which are $\text{P}(\text{OPh})_3$ and PPh_3 . As shown in Figure 44, ^{31}P NMR spectrum in CDCl_3 demonstrates the peak ($^{31}\text{P}=\text{Se}$) at 33.2 ppm and small doublets ($^{31}\text{P}=\text{Se}$) at 30.9 and 35.5 ppm. The $^1J_{^{31}\text{P}-^{77}\text{Se}}$ coupling constant is 750 Hz and $^4J_{^{31}\text{P}-^{31}\text{P}}$ are 16 Hz.

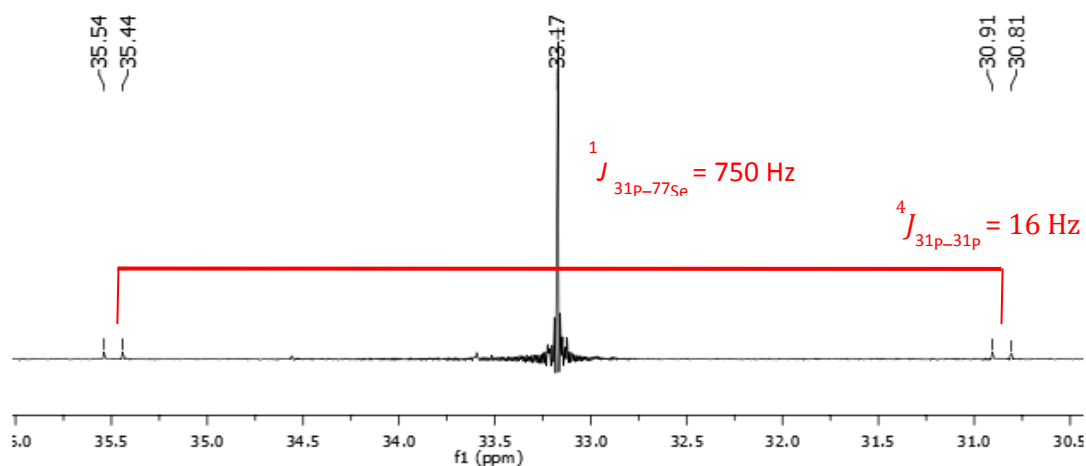


Figure 44. ^{31}P NMR in CHCl_3 of allenyl selenide **109**.

The comparison of coupling constants of **109**, $\text{Se}=\text{P}(\text{OPh})_3$ and $\text{Se}=\text{PPh}_3$ is summarized in Figure 45. Compared with the coupling constant of the $\text{Se}=\text{PPh}_3$ (736 Hz),²³⁹ the allenyl ligand **107** is a weaker σ -donating ligand than PPh_3 . However, this ligand **107** is a stronger σ -donating ligand than $\text{P}(\text{PhO})_3$ (1027 Hz).²³⁹ Consequently, **107** might promote different reactivity in catalytic reactions.

²³⁹ C. Glidewell, E.J. Leslie. *J. Chem. Soc. Dalton Trans.*, **1977**, 527–531.

	$\xrightarrow{\sigma\text{-donor}}$		
	P(OPh) ₃	> 107 >	PPh ₃
<i>J</i> _{³¹P-⁷⁷Se} (HZ) value in CDCl ₃	1027	750	736
$\delta_{31\text{P}}$ (ppm)	58.6	33.2	35.2

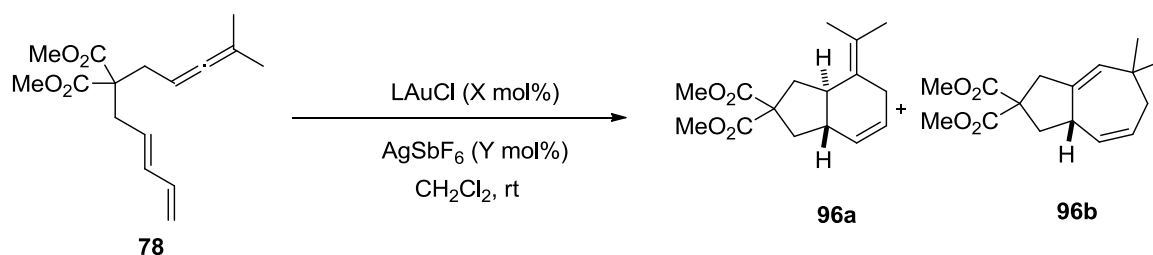
Figure 45. Comparison of *J* coupling constant of ³¹P-⁷⁷Se and ³¹P chemical shift in CHCl₃.²³⁹

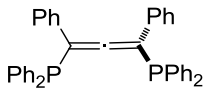
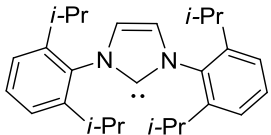
4.3.2. Evaluation by using diagnostic allene diene

To examine the ability of ligand **107** for providing selective products, we also studied the electronic properties of various ligands by the preparation of gold complexes to examine the catalytic reaction of a diagnostic allene diene substrate **78**.²²⁷ The gold complex (\pm)-**113** is also investigated its property under the same conditions in order to control the selectivity and the reactivity of each reaction investigated to access the desired products. We compared the properties of (\pm)-**113** and selected ligands: P(PhO)₃, PPh₃ and IPr, are summarized in Table 11.²²⁷ P(PhO)₃ as a strong π -acceptor produced only **96a** from [4+2] cyclization (Table 11, entry 1), whereas IPr as strong σ -donor gave **96b** from [4+3] cyclization (Table 11, entry 4).

In the case of allene ligand **107**, the gold(I)-catalyzed reaction of allene diene **78** afforded a mixture of the [4+3] and [4+2] cycloadducts (**96a** and **96b**) in the ratio 80:20 (Table 11, Entry 2). Compared to the results obtained with the PPh₃ ligand, based on Ph₃PAuCl catalyst, this ratio shows that the allene **107** is better π -accepting property than PPh₃^{227a} (Table 11, entry 3). This property can enhance the carbocation-like character of the intermediates by decreasing the electron density around gold to promote **96a** as a major selective product.

Table 11. Gold-catalyzed cycloisomerization reaction of allene diene **78** in different ligands for gold



Entry	Ligand (L)	LAuCl (mol %)	AgSbF ₆ (mol %)	Yield (%)	96a:96b
1	(PhO) ₃ P	5	5	89	100:0
2	 107	3	6	67	80:20
3	PPh ₃	5	5	80	67:33
4	 IPr	10	10	79	0:100

In relative terms, the allene ligand **107** has strong π -acceptor and weak σ -donating properties than PPh₃, which is common phosphine ligand for a gold complex. We expected that this ligand **107** might generate different selectivity of reaction from using PPh₃ in metal catalysis, in particular gold catalytic reactions. Moreover, the asymmetric reaction would be focused on the induction of enantioselectivity of products by the chiral allene ligand **107**. In order to test this; we required the optical resolution of racemic allene **107** to study the catalyst's behavior asymmetric catalysis version.

5. Resolutions of racemic allenes

5.1. Using chiral cyclopalladated complexes

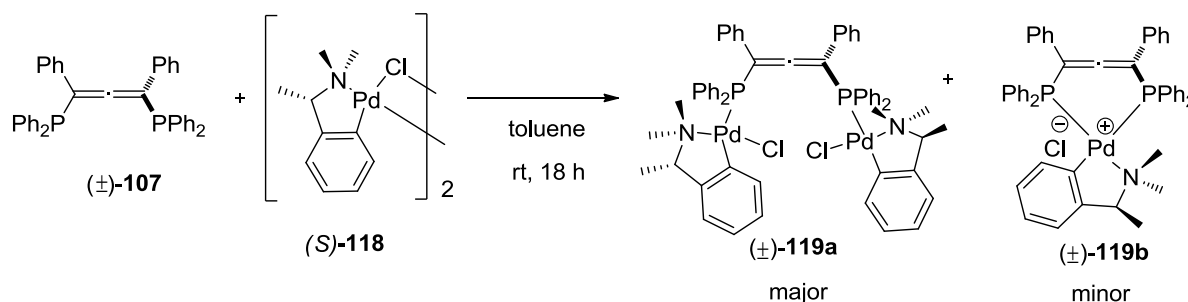
Optically pure phosphine ligands are significant to prepare chiral catalysts for inducing the asymmetry in catalytic process. Pietrusiewicz and Zabloc have conducted a thorough review on a variety of examples of resolutions of racemic phosphine compounds in order to obtain optically pure phosphines.²⁴⁰ One method involves the use of palladium metallacycles. Moreover, direct resolution is also accomplished by the use of preparative HPLC system, which is another choice to obtain optically pure phosphine derivatives in large quantities.²⁴¹

Chiral palladium(II) complexes **118** have been used to separate phosphine ligands *via* the formation of two diastereomerically dinuclear palladium-phosphine complexes, which can be

²⁴⁰ K. M. Pietrusiewicz, M. Zablocka, *Chem. Rev.* **1994**, *94*, 1375–1411.

²⁴¹ T. Imamoto, H. Tsuruta, Y. Wada, H. Masuda, K. Yamaguchi, *Tetrahedron Lett.* **1995**, *36*, 8271–8274.

separated by recrystallization.²⁴² After removing chiral palladium moieties by NaCN or KCN, two chiral phosphine ligands would be obtained. In our study, the reaction of palladium complex **118** and racemic allene (\pm)-**107** gave two types of palladium complexes, which are a major dinuclear palladium complex **119a** and a minor mononuclear one **119b** (Scheme 141). ³¹P NMR of **119a** shows two main peaks around 42.5 ppm, referring to the two diastereomers of complexes. Another four small doublet peaks at 41.5, 40.9, 26.2 and 25.9 ppm, approximately, refers to a mixture of mononuclear palladium complexes **119b**. The four doublet peaks related to the coupling between phosphorus and palladium atoms (Figure 46). The palladium complex **119a** was isolated by recrystallization. Its structure was characterized by X-ray crystallography (Figure 47).



Scheme 141. Formation of diastereomers of palladium complexes (\pm)-**119a** and (\pm)-**119b**.

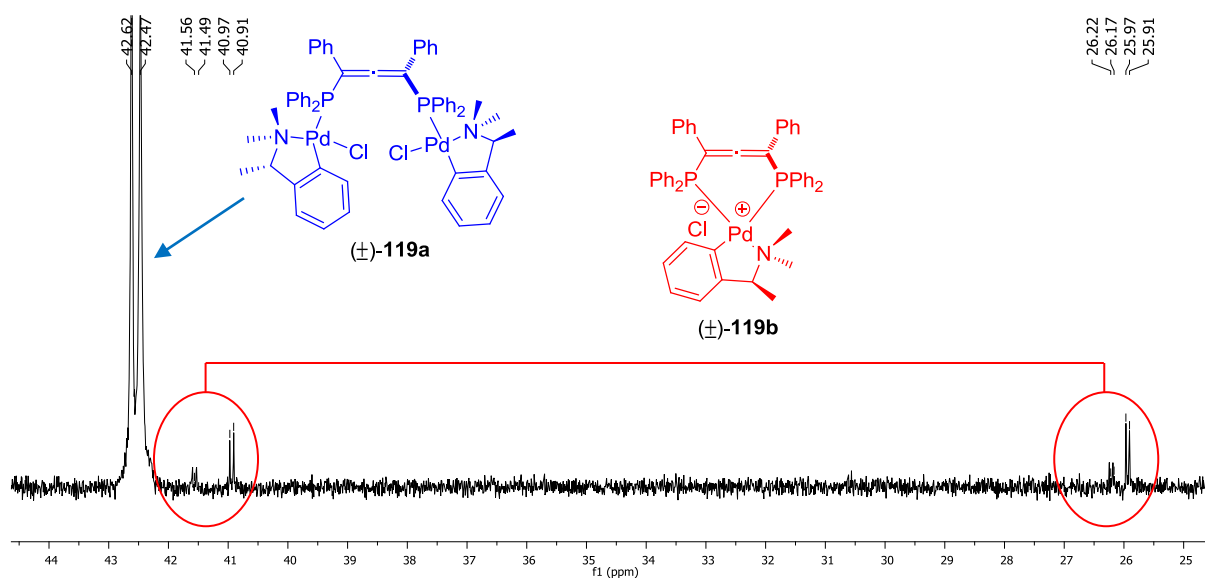


Figure 46. ³¹P NMR of the complexes (\pm)-**119a** and (\pm)-**119b**

²⁴² (a) A. Otsuka, A. Nakamura, T. Kano, K. Tani, *J. Am. Chem. Soc.* **1971**, *93*, 4301–4303.; (b) A. Miyashita, A. Yasuda, H. Takaya, K. Toriumi, T. Ito, T. Souchi, R. Noyori, *J. Am. Chem. Soc.* **1980**, *102*, 7932–7934.

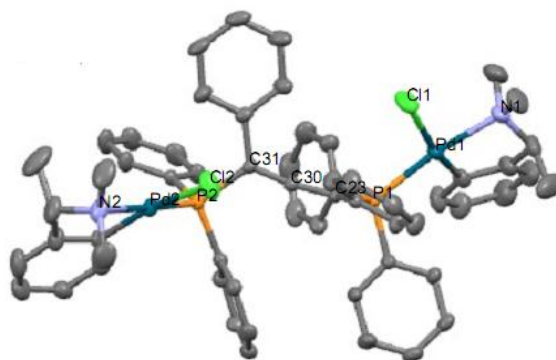
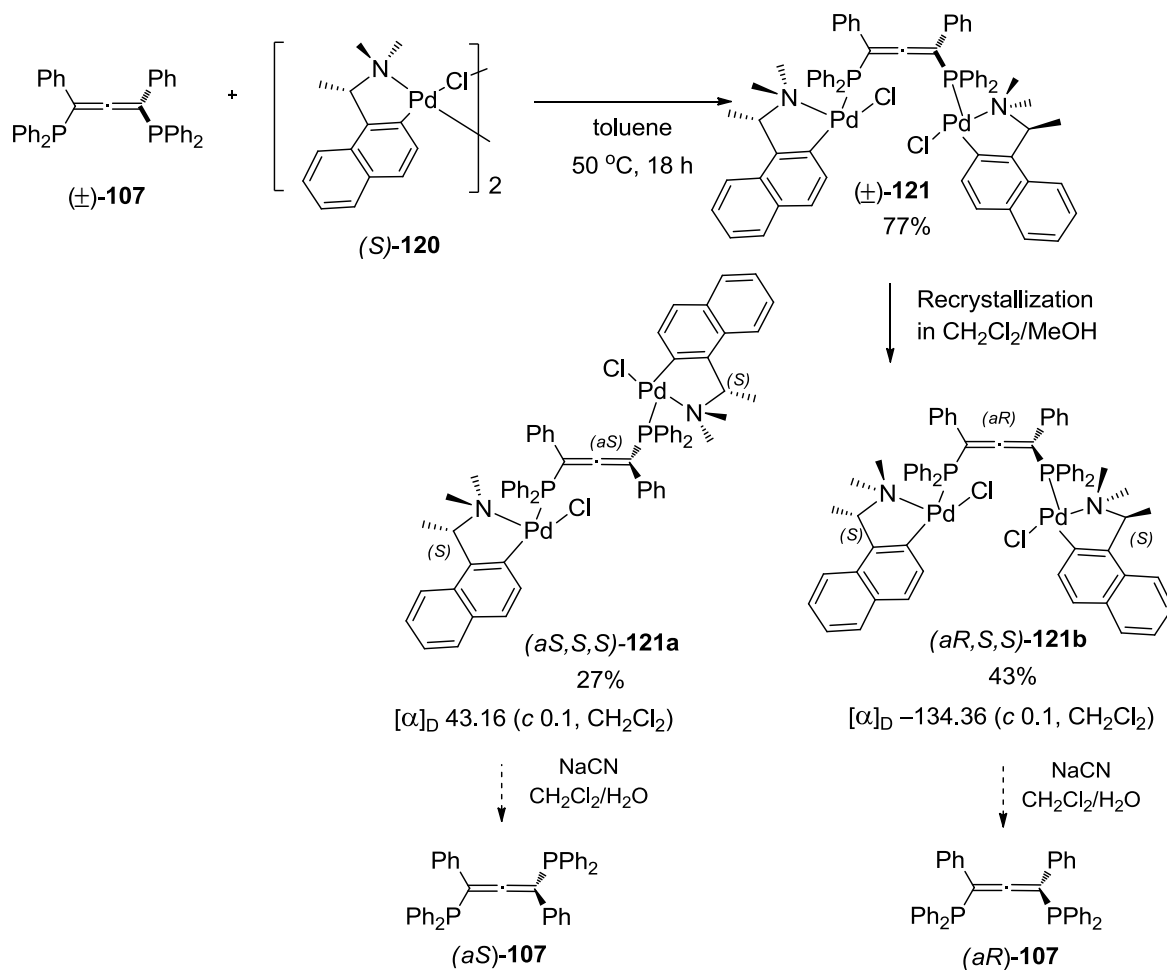
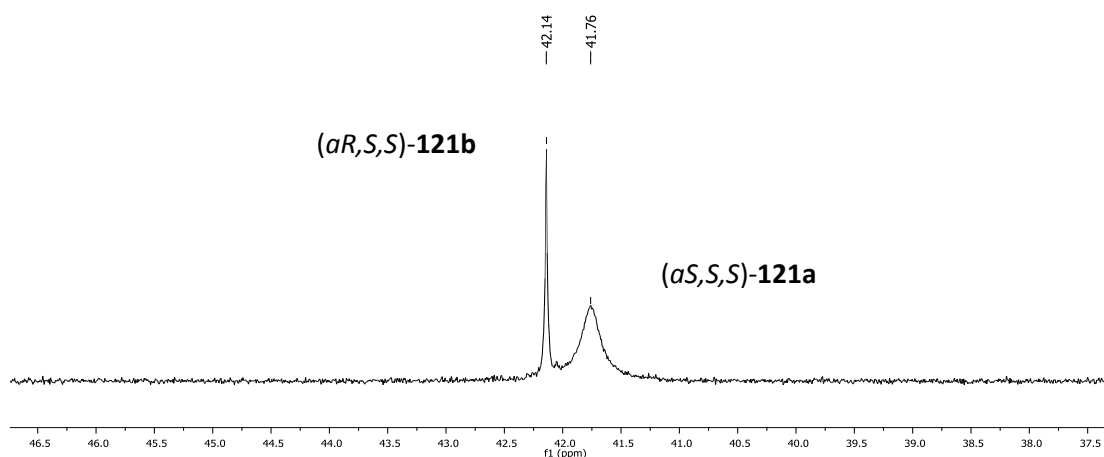


Figure 47. Crystal structure of (±)-**119a** at solid state. Selected bond lengths (Å): P1-Pd1 2.265, P2-Pd2 2.255, P1-C23 1.846, P2-C31 1.841. Allene angle (C23=C30=C31) 167.1°.

The two diastereomeric palladium complexes with phenyl group **119a** cannot be separated. The chiral palladium containing a naphthyl functional group **120** (Di- μ -chlorobis[(*S,S*)-(1-(dimethylamino-ethyl))-2-naphthylamine-C,N]-dipalladium(II))²⁴³ was tested under similar conditions. The results found that the reaction gave only two diastereomerically dinuclear complexes (±)-**121**, due to the steric hindrance of naphthyl group prevented the formation of a mononuclear complex (Scheme 142). The complexes (±)-**121** were recrystallized by diffusion of methanol slowly into a product in a small amount of dichloromethane to give two diastereomers **121a** and **121b**. ³¹P NMR shows two main peaks at 41.8 and 42.1 ppm respectively (Figure 48). The solid crystal was characterized by X-ray crystallography, and was shown to be diastereomer (*Sc,Sc,Ra*)-**121b** as a major product ($[\alpha]_D -134.36$ (c 0.1, CH₂Cl₂) (Figure 49). Another diastereomer is (*Sc,Sc,Sa*)-**121a** in mother liquor ($[\alpha]_D 43.16$ (c 0.1, CH₂Cl₂). These optically pure diastereomers were tested to remove the palladium groups on both phosphine groups by NaCN and prepare enantioenriched allenes **107**.

²⁴³ (a) S. Sabater, J. A. Mata, E. Peris, *Organometallics* **2013**, *32*, 1112–1120.; (b) D. H. Kim, J. K. Im, D. W. Kim, H. Lee, H. Kim, H. S. Kim, M. Cheong, D. K. Mukherjee, *Transit. Met. Chem.* **2010**, *35*, 949–957.

Scheme 142. The optical resolution of racemic (\pm) -107.Figure 48. ^{31}P NMR (121.5 Hz, CHCl_3) of the chiral naphthyl palladium complexes 121a and 121b

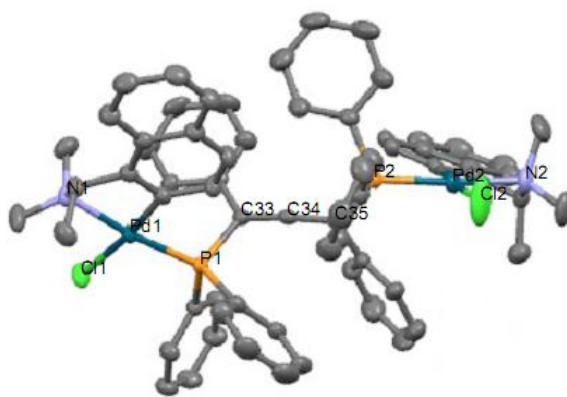


Figure 49. Crystal structure of complex (*aR,S,S*)-**121b** at solid state. Selected bond lengths (Å): P1-Pd1 2.261, P2-Pd2 2.253, P1-C33 1.856, P2-C35 1.855. Allene angle (C33=C34=C35) 172.5°.

5.2. Using preparative chiral HPLC

We are interested in the separation of two enantiomers of racemic allene (\pm)-**107** in large scale by using preparative chiral HPLC. This analysis was performed in collaboration with Dr. Nicolas Vanthuyne (iSm2, Aix-Marseille Université). Unfortunately, only small amount of two enantiomers (*aR*)- and (*aS*)-**107** were obtained (<25% yields). The oxidized phosphine functional groups on allene **107**, such as mono- and bisphosphine oxide-containing allenes were occurred. Therefore, we then changed to racemic digold complex (\pm)-**113**, which is more stable than allene (\pm)-**107**, to separate both enantiomers of gold complexes directly. The separation was conducted by Chiralpak IE column and detecting by UV-detection at 254 nm (Figure 50a) and circular dichroism (Figure 50b) by Dr. Nicolas Vanthuyne. Two enantiomers of (*aR*)-**113** with $[\alpha]_D = 28.2$ (*c* 0.17, CH₂Cl₂) and (*aS*)-**113** with $[\alpha]_D = -28.2$ (*c* 0.17, CH₂Cl₂) were obtained in excellent enantiomeric excess (*ees*>98%). Their absolute configurations were determined by X-ray crystallography.

Method description : Chiralpak IE, Heptane/Isopropanol/Chloroforme 50/20/30, 1 ml/min, DAD and CD254nm

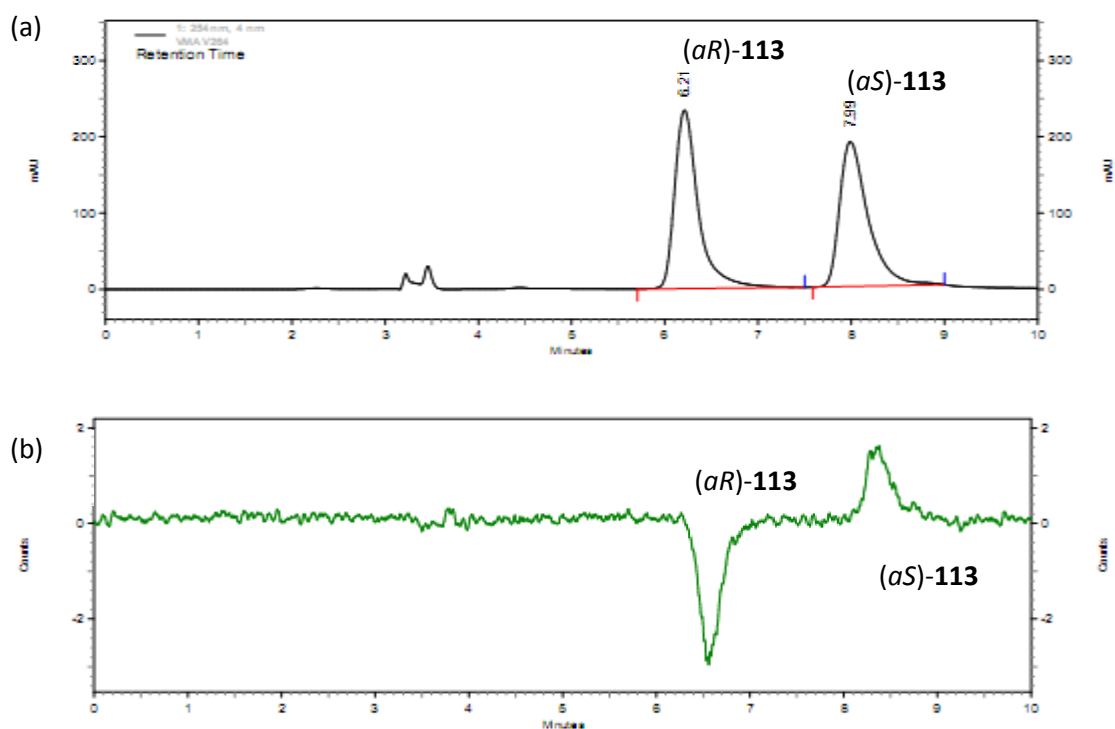


Figure 50. Preparative chiral HPLC of (±)-113. The chromatographic conditions: Chiralpak IE (250x10 mm), hexanes/ 2-*i*PrOH/ Chloroform (5/2/35) as mobile phase, flow-rate = 5 mL/min, (a) UV detection at 254 nm and (b) circular dichroism detection

6. Asymmetric palladium-catalyzed allylic alkylation

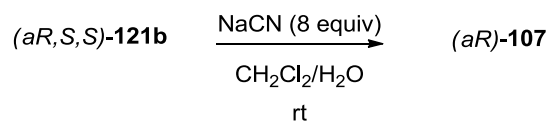
The preliminary test of chiral allene ligand was to investigate the ability of chiral allene (±)-**107** as a chiral ligand for the palladium-catalyzed asymmetric allylic alkylation²⁴⁴ using 1,3-diphenyl-2-propenyl acetate with dimethyl malonate. According to the optical resolution of palladium complex (±)-**121**, the diastereomeric palladium complex (*aR,S,S*)-**121b** was selected to engage in the asymmetric catalytic system.

6.1. Preparation of chiral allenyl bisphosphine

The asymmetric reaction was designed to use this allenyl bisphosphine ligand directly to make a chiral metal catalyst in order to prevent the oxidation of both phosphorus groups on

²⁴⁴ For some reviews, see: (a) P. R. Auburn, P. B. Mackenzie, B. Bosnich, *J. Am. Chem. Soc.* **1985**, *107*, 2033–2046.; (b) G. Helmchen, *J. Organomet. Chem.* **1999**, *576*, 203–214.; (c) T. Mino, Y. Naruse, S. Kobayashi, S. Oishi, M. Sakamoto, T. Fujita, *Tetrahedron Lett.* **2009**, *50*, 2239–2241.; (d) T. Mino, M. Ishikawa, K. Nishikawa, K. Wakui, M. Sakamoto, *Tetrahedron Asymmetry* **2013**, *24*, 499–504.

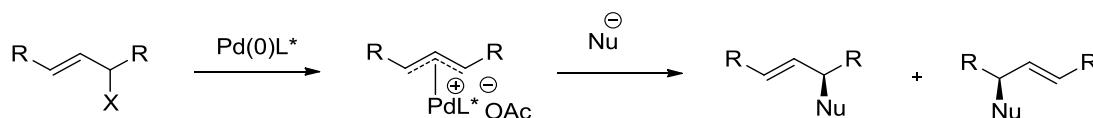
allene **107**. Initially, the complex (*aR,S,S*)-**121b** was treated by NaCN in the mixture of degassed dichloromethane and water under argon atmosphere.^{244a} After depalladation, the chiral allene (*aR*)-**107** was obtained (Scheme 143).



Scheme 143. Preparation of enantioenriched allene ligand (*aR*)-**107**.

6.2. Palladium-bearing bisphosphine in asymmetric allylic alkylation

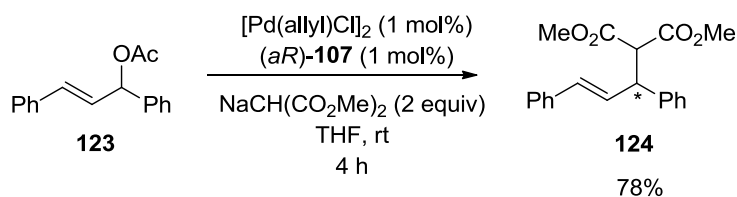
Phosphines have been reported their ability or accelerate the palladium catalytic alkylation reaction. The first attempt was studied by Trost and co-workers using a stoichiometric palladium-catalyzed allylic substitution.²⁴⁵ To achieve enantioselectivity, the chiral ligands were engaged to furnish chiral products *via* cationic palladium allylic intermediate (Scheme 144).



Scheme 144. Palladium(0)-catalyzed allylic alkylation reaction.

The chiral allene ligand (*aR*)-**107** was generated in this line by complexation with a palladium catalyst. Allylpalladium(II) chloride was used as a catalyst source to prepare *in-situ* chiral palladium(0) catalyst by adding chiral ligand (*aR*)-**107** directly. Following the Mathey's procedure of using chiral BIPNOR ligand,²⁴ the 1,3-diphenyl-2-propenyl acetate substrate (**123**) was catalyzed by palladium(0) catalyst bearing (*aR*)-**107** ligand. After underwent the nucleophilic substitution by dimethylmalonate anion, the allyl product **124** was obtained in 78% yield (Scheme 145). The reactivity of palladium(II) catalyst was probed by using allylpalladium(II) chloride without chiral ligands that showed unreactive catalyst for giving similar product. The product was analyzed the enantiomeric excess by using chiral HPLC technique. This analysis is performed by the collaboration with Dr. Nicolas Vanthuyne, which is still in process.

²⁴⁵ B. M. Trost, T. J. Fullerton, *J. Am. Chem. Soc.* **1973**, *95*, 292–294.



Scheme 145. Palladium bearing (*aR*)-**107** ligand-catalyzed asymmetric allylic alkylation of **123**.

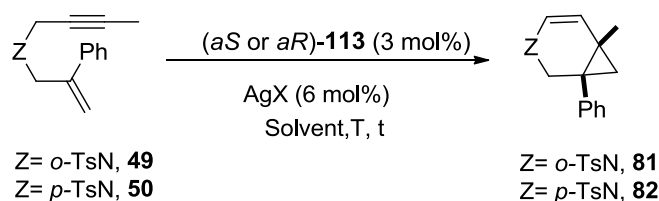
7. Asymmetric catalysis with chiral gold complex (**113**)

The successful optical resolution of racemic gold complex (\pm)-**113** was separated the chiral forms by preparative chiral HPLC. The (*aS*)- and (*aR*)-**113** were next used in asymmetric catalytic reactions. We selected some interesting asymmetric reactions, which presented to use chiral C_2 -Symmetric ligands, in order to test the ability of chiral ligand **107** for gold(I) catalyst to access enantioselective products.

7.1. Asymmetric cycloisomerization of 1,6-enynes

According to the successful cycloisomerization of 1,6-enynes by using racemic gold complex (\pm)-**113**, we explored the reactivity of chiral gold complex (*R*)- or (*S*)-**113** in this manner and optimized the conditions to afford highly enantiomeric excess. *N*-Tosyl-enynes (**49-55** and **57-59**), and malonate-tethered enyne **65** were treated in the presence of our cationic gold catalyst, generated from 3 mol% of (*aS*)-**113** and 6 mol% of AgSbF₆ in dichloromethane at -20°C . Under this catalytic condition, only the reactions of enynes **49** and **50** were successfully in giving enantioselective products **81** and **82** with 32% and 29% *ees* respectively (Table 12, entries 1 and 4).

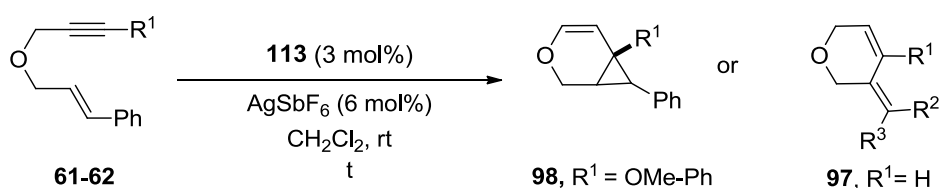
The anion that was generated from the combination of a gold complex and a silver salt might play an important role in transition state in term of promote the enantioselectivity.^{65, 224} To improve the enantioselectivity, we attempted to optimize these conditions of reactions by vary the nature of silver salts. Unfortunately, the reactions of **49** and **50** using cationic gold, prepared from (*aR*)-**113** and AgBF₄ in chloromethane at -20°C , gave even less enantioselectivity of the cyclic products **81** and **82** with 5% and 8% *ees* respectively (Table 12, entries 2 and 5). When using (*aR*)-**113** and AgOTf in toluene at 60°C , the reactions also afforded the products **81** and **82** with 18% and 13% *ees* (Table 12, entries 3 and 6), which has lower enantioselectivity than entries 1 and 4. Notably, these reactions were necessary to increase the temperature to afford fully conversion of desired products.

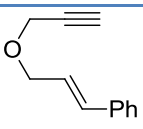
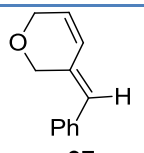
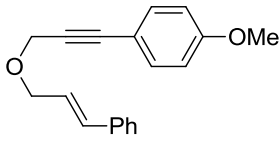
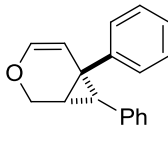
Table 12. Screening conditions of using chiral gold catalyst **113** in asymmetric cycloisomerization of enyne **49** and **50**.

Entry	Z	113	AgX	Solvent	T (°C)	t (h)	%Yield (%ee)
1	<i>o</i> -TsN	(<i>aS</i>)- 113	AgSbF ₆	CH ₂ Cl ₂	-20	15	91 (32)
2	<i>o</i> -TsN	(<i>aR</i>)- 113	AgBF ₄	CH ₂ Cl ₂	-20	18	74 (5)
3	<i>o</i> -TsN	(<i>aR</i>)- 113	AgOTf	toluene ^[a]	60	4	42 (18)
4	<i>p</i> -TsN	(<i>aS</i>)- 113	AgSbF ₆	CH ₂ Cl ₂	-20	15	quant (29)
5	<i>p</i> -TsN	(<i>aR</i>)- 113	AgBF ₄	CH ₂ Cl ₂	-20	18	46 (8)
6	<i>p</i> -TsN	(<i>aR</i>)- 113	AgOTf	toluene ^[a]	60	4	75 (13)

^[a] The reactions were necessarily prepared in toluene because AgOTf is able to be soluble completely in dichloromethane

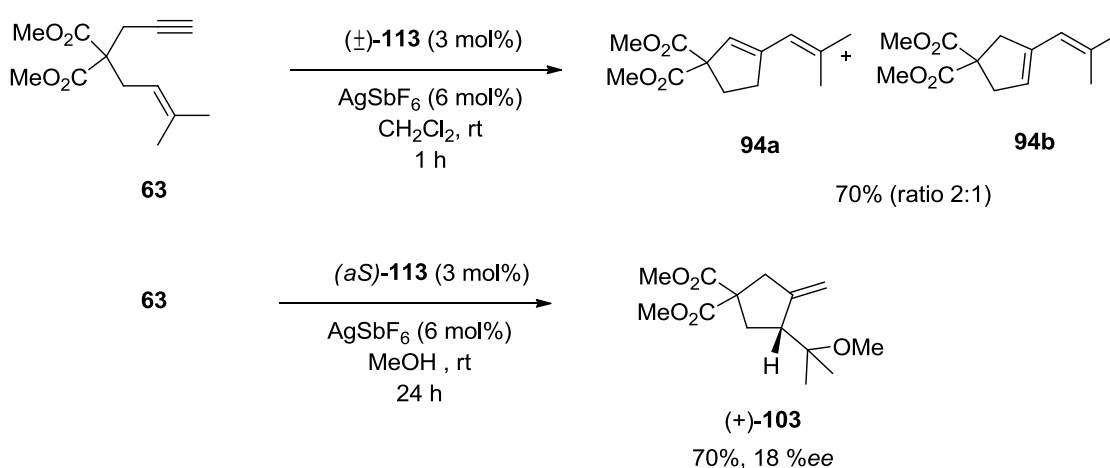
According to Michelet's report, the bicyclo[4.1.0] heptene derivatives have been successfully synthesized using a chiral bimetallic gold(I) complex bearing C₂-Symmetric ligand, (*R*)-4-MeO-3,5-(*t*-Bu)₂-MeOBIPEP, with excellent enantioselectivity.¹⁰⁹ Inspired by this work, we tested the reactivity of our gold complex (\pm)-**113** with enyne **61** (Table 13, entry 1). Unfortunately, the catalytic reaction underwent an endocyclic skeletal rearrangement process to form product **97**. At the second stage, we ran the reaction with enyne **62** bearing a 4-MeO-phenyl functional group on the terminal alkyne in the presence of (*aR*)-**113** and AgSbF₆ in dichloromethane (Table 13, entry 2). Nevertheless, the reaction yielded only 40% of cyclic product **98** without any enantioselectivity. Consequently, the chiral gold complex (*aR*)-**113** cannot successfully induce the asymmetry for this type of enynes in cycloisomerization reactions under these conditions.

Table 13. Cycloisomerization of oxygen-tethered 1,6 enynes **61-62**.

Entry	Substrate	113	Time (h)	Product	%Yield (% <i>ee</i>)
1	 61	(±)- 113	3	 97	20 (-)
2	 62	(<i>aR</i>)- 113	1	 98	40 (0)

7.2. Asymmetric methoxycyclization

The chiral gold complex **113** was next tested in methoxycyclization reactions, as well as chiral bisphosphine ligands by the groups of Michelet^{109, 232a} and Echavarren^{111, 112}. Firstly, the reaction was tested for the reactivity of racemic cationic gold complex, prepared from (±)-**113** and AgSbF₆ with enyne **63** without a nucleophile. The reaction underwent *exo*-skeletal rearrangement and yielded 70% of the mixture of **94a** and **94b**. In the presence of methanol as a nucleophile, the reaction of **63** under chiral cationic condition gave (+)-**103** in 70% yield and 18% *ee* (Scheme 146). It is shown that the chiral gold complex (*aS*)-**113** can induce slightly enantioselectivity in the cycloisomerization process; however, *ee* is lower than the previous work from the Michelet group^{232a} using (*R*)-4-MeO-3,5-(*t*-Bu)₂MeOBIPHEP(AuCl)₂ (44% *ee*) and AgOTf.



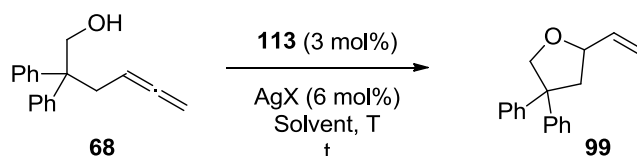
Scheme 146. Gold(I)-catalyzed skeletal rearrangement and methoxycyclization of enyne **63**.

7.3. Asymmetric cycloalkoxylation

Allenol substrates have been reported to produce tetrahydrofuran derivatives *via* gold-catalyzed cycloalkoxylation.^{140, 181} We aimed to study whether the use of our chiral gold complex **113** would be beneficial to furnish the enantioselective products. Initially, we tested the reactivity of racemic gold complex (\pm)-**113** with γ -allenol **68** and summarized in Table 14. Firstly, the allenol **68** was treated with the cationic gold catalyst under the same cationic condition (Table 14, entry 1). The reaction gave 2-vinyltetrahydrofuran **99** in poor yield (26%). Therefore, we decided to use AgOTs for activating gold complex (\pm)-**113** (Table 14, entries 2-4). However, the reaction in dichloromethane at reflux cannot furnish any product (Table 14, entry 2). As the optimization in different solvent and temperature, the reaction in the presence of (\pm)-**113** and AgOTs in toluene at room temperature (Table 14, entry 3) yielded 43% of **99**. To our delight, good condition by running the reaction in toluene at 70 °C (Table 14, entry 4) could provide **99** in 75% yield.

We next attempted to use chiral gold (*aR*)-**113** under this condition. The product **99** was obtained in 70% yield. Unfortunately, the enantiomeric excess by chiral HPLC analysis showed only 4% *ee* (Table 14, entry 5). We surmised that the high temperature might promote the formation of racemic product rapidly before the induction of chiral ligand in the cyclization step. The control temperature will be attempted to improve the enantioselectivity.

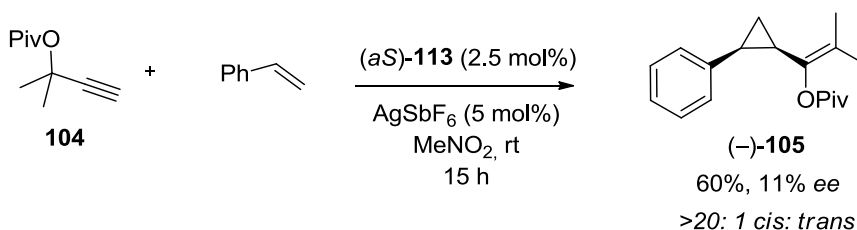
Table 14. Gold-catalyzed cycloalkoxylation of γ -allenol **99**.



Entry	113	AgX	Solvent	T (°C)	t (h)	%Yield (% <i>ee</i>)
1	(\pm)- 113	AgSbF ₆	CH ₂ Cl ₂	rt	1.5	26 (-)
2	(\pm)- 113	AgOTs	CH ₂ Cl ₂	reflux	24	No reaction
3	(\pm)- 113	AgOTs	toluene	rt	3	43 (-)
4	(\pm)- 113	AgOTs	toluene	70	1	75 (-)
5	(<i>aR</i>)- 113	AgOTs	toluene	70	1	70 (4)

7.4. Asymmetric olefin cyclopropanation

Lastly, we investigated the asymmetric olefin cyclopropanation of propargyl ester derivatives and styrene. The catalytic conditions was followed pioneering report by the Toste group in asymmetric gold(I)-catalyzed stereoselective olefin cyclopropanation reactions.⁶⁹ The propargyl esters **104** was treated with 2.5 mol% of (*aS*)-**113** activated by 5 mol% of AgSbF₆. The cyclopropane (–)-**105** was obtained in 60% yield with a >20:1 mixture of *cis*: *trans* diastereomers, but afforded only 11% *ee* (Scheme 147).

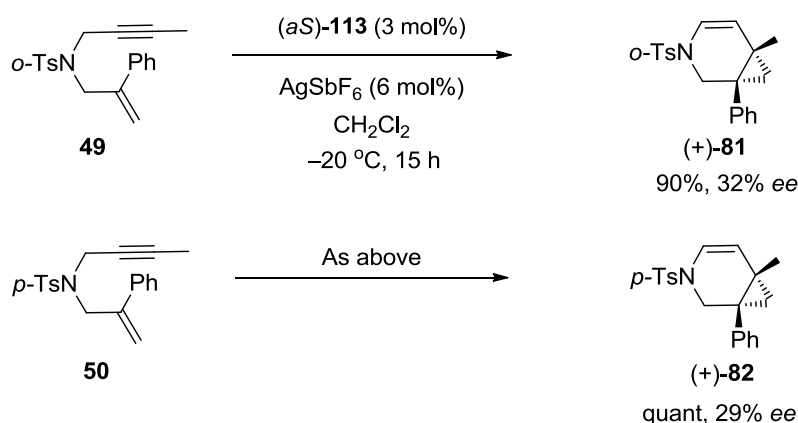


Scheme 147 Gold(I)-catalyzed cyclopropanation of propargyl ester **104**.

To conclude, our gold complex **113** bearing allenyl phosphine moiety are a good precatalyst in various reactions: cycloisomerization, methoxycyclization, cycloalkoxylation and olefin cyclopropanation reactions to afford the racemic cyclic products in moderate to good yields. The reactivities of chiral gold (*aR*)- and (*aS*)-**113** in asymmetric reactions can provide the enantioenriched products in moderate *ees* (29–32% *ees*). Some optimized conditions were tested to improve better the enantioselectivity by changing the type of silver salts, playing on the size of anions, or controlling the reaction's temperature. Unfortunately, these chiral gold complexes could not provide the products with good *ees*. We surmised that the structure of gold complex **113** could not induce the asymmetry of reaction effectively. The next attempt is devoted to modify the structure of allenyl-bisphosphine ligand **107**.

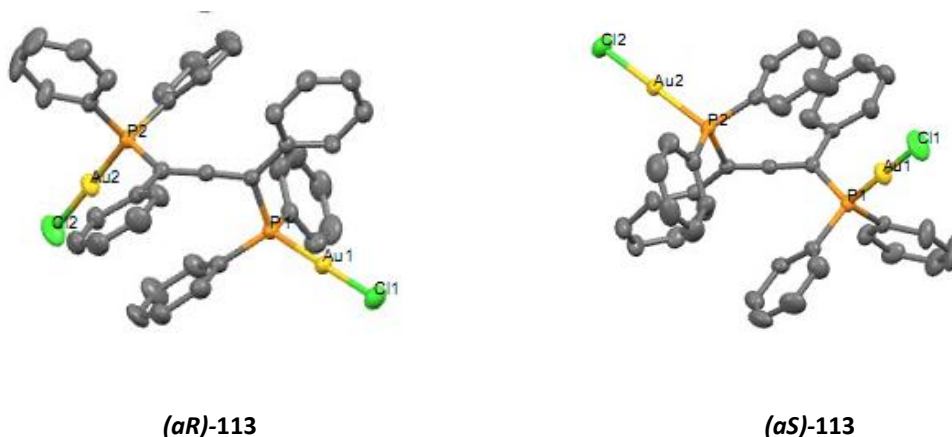
8. Modification of chiral gold complexes

The asymmetric reactions by using chiral gold complex **113** were attempted to improve the enantioselectivity by the modification of its ligand. The asymmetric cycloisomerization reactions of *N*-Tosyl-ene-yne substrates **49** and **50** represented the best reactivity of chiral gold complex **113** to afford the products (+)-**81** and (+)-**82** in 32% and 29% *ees* respectively (Scheme 148). Thus, we planned to design new chiral gold complexes in order to investigate their reactivity in these reactions.


 Scheme 148 Asymmetric cycloisomerization of enyne **49** and **50**.

8.1. Selected models of chiral gold complexes

According to the crystal structure of chiral gold complexes (aR) - and (aS) -**113** (Figure 51), the interaction between Au_1 and Au_2 ($d(\text{Au}_1 \cdots \text{Au}_2) = 6.498$) or Au and π -aryl were not observed. We surmised that these interactions are significant to block the rotation of intermediates, which were catalyzed by gold atom on one side of allene.


 Figure 51. Structures of (aR) - and (aS) -**113**. (The hydrogen atoms are omitted for clarity)

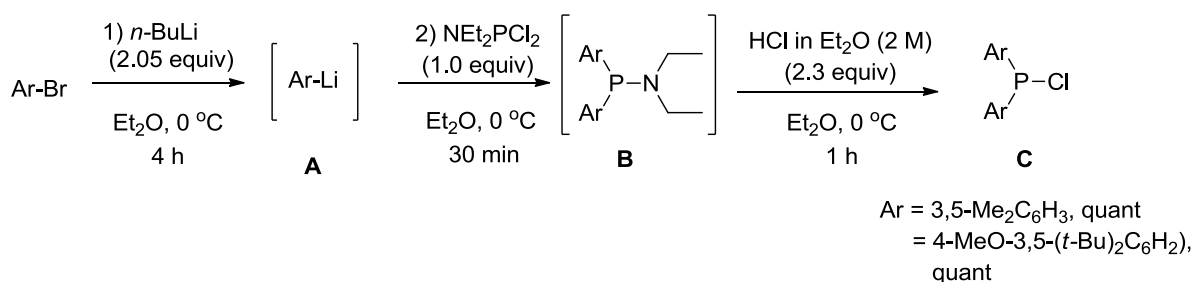
Recently, Hii and co-workers reported the correlations between the $\text{Au} \cdots \text{Au}$ distances for the biaryl series of phosphine ligands such as BINAP (aryl = 3,5- $\text{Me}_2\text{C}_6\text{H}_3$)²²⁵ and MeOBIPHEP (aryl = 4-MeO-3,5- $(t\text{-Bu})_2\text{C}_6\text{H}_3$)^{109a, 246}. They indicated that auropophilic interactions are significant to promote highly enantioselectivity in asymmetric cycloisomerization of 1,6-enynes. Thus, we attempted to design two chiral allene ligands bearing bulky bis(arylphosphine) groups (aryl = 3,5-

²⁴⁶ E. M. Barreiro, E. V. Boltukhina, A. J. P. White, K. K. M. Hii, *Chem. Eur. J.* **2015**, *21*, 2686–2690.

$\text{Me}_2\text{C}_6\text{H}_3$ and 4-MeO-3,5-(*t*-Bu) $_2\text{C}_6\text{H}_2$) by a modification of allenyl bisphosphine ligand **107**. The bulky groups on allenes were expected to increase the Au⁺-Au interaction in digold complexes to promote high enantioselectivity.

8.2. Preparation of new gold complexes

The preparation of new gold complexes was performed in collaboration with Cécilia Damelin-court, master student (Master 2, 2015) under supervisions of Dr. Virginie Mouriés-Mansuy.²⁴⁷ Firstly, we prepared corresponding chlorodiarylphosphine reagents for the formation of desired allenes, following the procedure from the Alexakis group.¹⁹¹ The reaction starts from the Li-Br exchange to generate aryllithium **A** intermediate. Dichloro-diethylphosphinamine (NEt_2PCl_2) was added as an electrophile to be trapped by two equivalents of aryl anion from intermediate **A**, led to form diaryl diethylphosphinamine (**B**). The amine group was removed by the solution of hydrochloric acid 2 M in Et_2O to furnish chlorodiarylphosphines (**C**) in quantitative yield (Scheme 149).

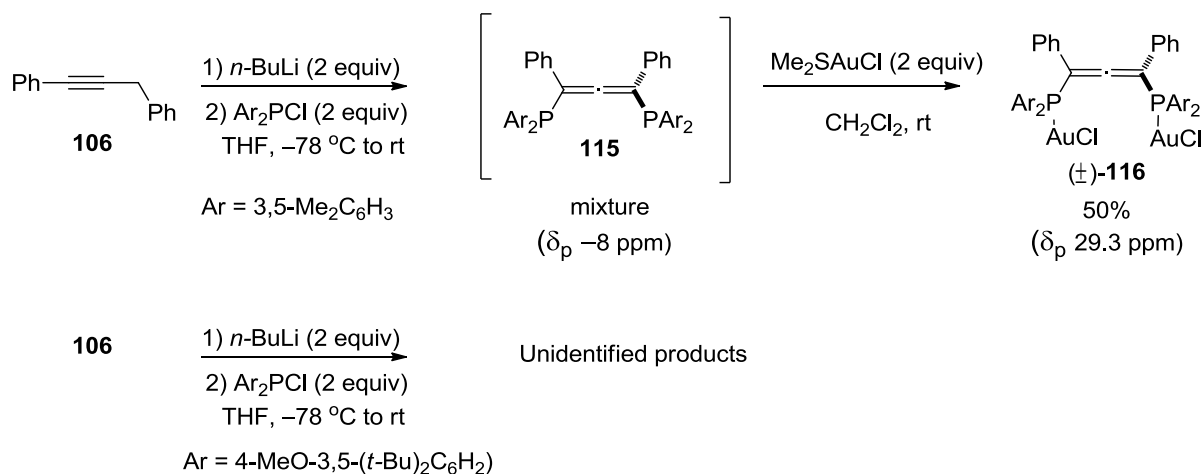


Scheme 149. Synthesis of chlorodiarylphosphine reagents (**C**).

The next step was concentrated on the synthesis of allenyl bisarylphosphine ligands. Following the Schmidbauer's procedure of preparation allene **107**,¹⁴⁷ the alkyne **106** was deprotonated with two equivalents of *n*-butyllithium and followed by the addition of two equivalents of Ar_2PCl ($\text{Ar} = 3,5\text{-Me}_2\text{C}_6\text{H}_3$) to furnish allene **115**. However, the allene **115** could not be purified by recrystallization. Accordingly, the crude mixture was added with two equivalents of Me_2SAuCl . The racemic allenyl gold complex (\pm)-**116** was obtained in 50% yield after a precipitation in a mixture of dichloromethane and hexanes (1/7) (Scheme 150). The total yield of these reactions is in the same range as the gold complex (\pm)-**113** (49% yield). In another case with Ar_2PCl ($\text{Ar} = 4\text{-MeO-3,5-(}t\text{-Bu)}_2\text{C}_6\text{H}_2$) reagent, the reaction did not give the desired allene product.

²⁴⁷ C. Damelin-court, *Rapport de Stage 5C101: Les allènes en catalyse organométallique: réactifs, ligands, catalyseurs*, UPMC, 2015.

^{31}P NMR shows several peaks, corresponding to phosphine oxide complexes arising from Ar_2PCL and unidentified products.

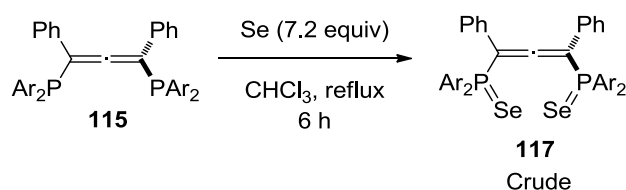


Scheme 150. Synthesis of allenyl gold complexes (\pm)-**116**.

8.3. Electronic properties

8.3.1. Evaluation by selenide complexes

Electronic properties of allene ligand **115** were also determined by preparation of selenide complex. The selenide complex **117** was prepared by adding excess selenium, following Schmidbaur's method.¹⁴⁷ The reaction was run in reflux chloroform to afford crude product **117** (Scheme 151).



Scheme 151. Preparation of selenide complex **117**.

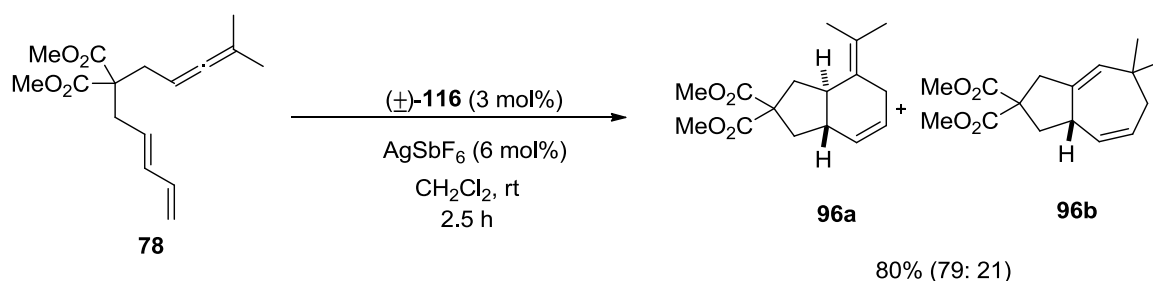
The crude product **117** characterized by ^{31}P NMR was evaluated the electronic properties comparing to allene ligand **107**, PPh_3 and $\text{P}(\text{OPh})_3$, which are summarized in Figure 52.²³⁹ The coupling constant ($^1J_{31\text{p},77\text{se}}$) of **117** shows 744 Hz referring to a stronger σ -donating ligand than ligand **107** (750 Hz) and $\text{P}(\text{OPh})_3$ (1027 Hz), but weaker than PPh_3 (736 Hz). The methyl substituents on aryl groups have an effect on the inductive donating electron to metal better than diphenylphosphine of **107**.

	σ-donor ←						
	PPh ₃	<	115	<	107	<	P(OPh) ₃
$J_{31\text{P},77\text{Se}}$ (HZ)	736		744		750		1027
value in CDCl ₃							
$\delta_{31\text{P}}$ (ppm)	35.2		33.7		33.3		58.6

Figure 52. Comparison of J coupling constant of ^{31}P - ^{77}Se and ^{31}P chemical shift in CHCl_3

8.3.2. Evaluation by using diagnostic allene diene

We also investigated on the reactivity of allene ligand **115** in the preparation of selective products *via* gold-catalyzed reaction using allene diene **78** as a precursor. According to the previous study using gold complex (\pm)-**113**, the allenylphosphine ligand can induce the selective product **96a** *via* [4+2]-cyclization better than **96b** *via* [4+3]-cyclization in the ratio 80:20. In the case, the gold complex (\pm)-**116** was treated under the same reaction. The reaction gave the mixture of products **96a** and **96b** in the ratio 79:21 (Scheme 152). The result show the π -electron acceptor property of ligand **115** is in the same range as ligand **107**, which is better π -accepter than PPh₃, but worse than P(PhO)₃.²²⁷

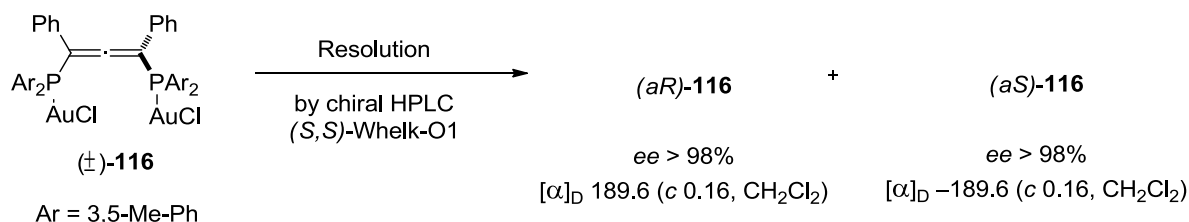


Scheme 152. Evaluation of (\pm)-**116** in cycloisomerization reaction of **78**.

Thus, the effect of methyl groups on arylphosphine of ligand **115** show a little σ -donating property than the ligand **107** as seen in the evaluation of selenide complex **117**. However, the study in gold catalytic reaction of allene diene **78** by gold complex (\pm)-**116** showed the ratio of product closely to gold complex (\pm)-**113**. To achieve the optimization of enantioselectivity, the gold complex (\pm)-**116** bearing allenyl arylphosphine was next attempted to test the reactivity in gold catalysis.

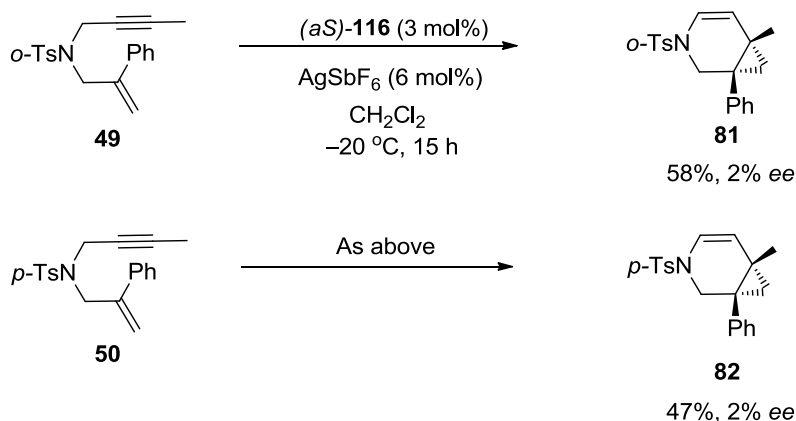
8.4. Reactivity of gold complexes (**116**) in asymmetric catalysis

The gold complex (\pm)-**116** was applied in the cycloisomerization of 1,6-enyne as the same catalytic condition of (\pm)-**113**. The racemic gold complex (\pm)-**116** was separated by preparative chiral HPLC with (*S,S*)-Whelk-O1 column (Scheme 153). Both enantiomers (*aR*)-**116** and (*aS*)-**116** were obtained with *ees* >98%.



Scheme 153. Optical resolution of racemic gold complex (\pm)-**116**.

We tested this chiral gold complex (*aS*)-**116** as a precatalyst in the cycloisomerization reaction of **49** and **50** under the same condition at $-20\text{ }^{\circ}\text{C}$ for 15 h as in Scheme 148 to optimize the enantioselectivity. The reactions afford both racemic products **81** and **82** in 58% and 47% yields respectively (Scheme 154). However, the (*aS*)-**116** could not induce the asymmetry of this reaction. We surmised that the structure of chiral gold complex bears the aryl groups, which are too far to induce the asymmetry of intermediate in cyclization process.



Scheme 154. The optimization reaction of **49** and **50** with chiral digold complex (*aS*)-**116**.

The gold complex (\pm)-**116** was recrystallized by diffusion of hexanes in the solution of product in dichloromethane in order to be characterized the structure by X-ray crystallography (Figure 53). The structure shows that the arylphosphine bearing methyl groups is not better at allowing the interaction between both gold atoms than the diphenyl group of allene **107**. The Au \cdots Au distance of gold complex **116** shows 6.875 Å, which is larger than **113** (6.498 Å).

Accordingly, this ligand cannot induce the enantioselectivity of products **81** and **82** in the cycloisomerization reactions of enynes **49** and **50**. It is challenging to investigate the bulky groups on arylphosphines that can promote the interaction of both gold atoms or the interaction between the gold atom and π -aryl group in order to improve the enantioselectivity. Thus, these works are continuing to prepare new allenyl arylphosphine ligands to achieve the enantioselective products with high *ees*.

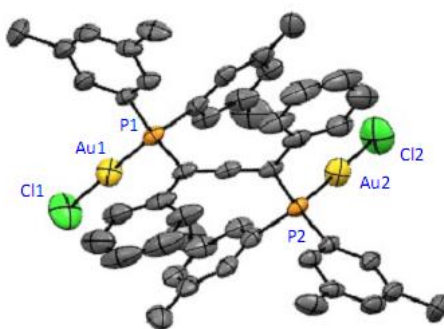


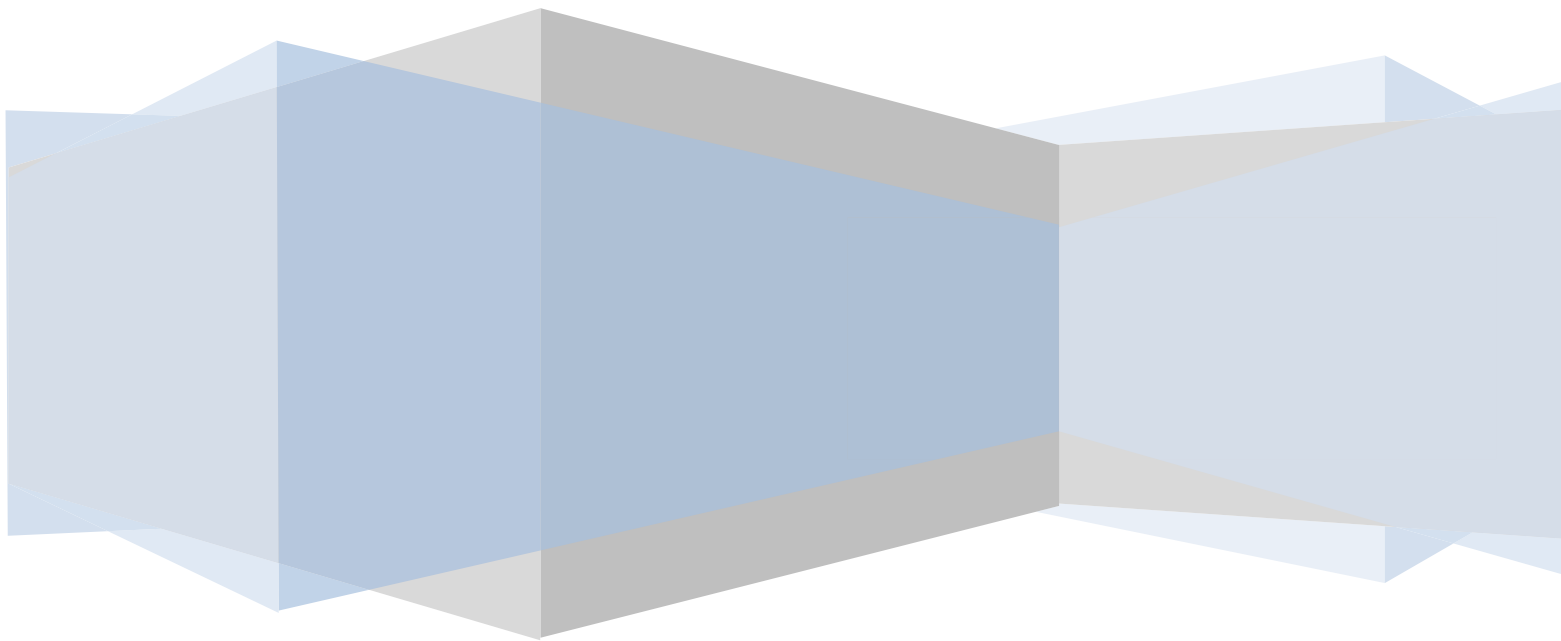
Figure 53. Crystal structure of gold-allene bisarylphosphine complex **116** at solid state of racemic product. Selected bond lengths (Å): Au1-Au2 6.875, P1-Au1 2.224, P2-Au2 2.224, P1-Cl1 1.830, P2-Cl2 1.830. Allene angle (C1=C2=C3) 179.94°

9. Conclusion and perspective

The allenyl bisphosphine ligand **107** was successfully prepared and well-coordinated to various metals such as platinum, palladium and gold furnishing metal complexes. The gold(I) complex (\pm)-**113** bearing allenyl bisphosphine complex was able to be used as a precatalyst in gold catalysis. It was initially used as a catalyst in cycloisomerization reactions with 1,6-enynes. The reaction successfully furnished the desired products in fair to excellent yields. The optical resolutions of ligand (\pm)-**107** were analyzed to prepare chiral ligands for asymmetric versions. The chiral gold complexes (*aR*)- and (*aS*)-**113** were separated by preparative chiral HPLC. These enantiomers were investigated in asymmetric reactions in order to prepare enantiomerically pure products. However, only the reactions of enynes **49** and **50** could generate products with excellent yields and fair enantiomeric excesses. To improve the enantioselectivity, new gold allene (\pm)-**116** bearing bulky aryl-containing phosphoryl groups was prepared. Unfortunately, the chiral gold allene (\pm)-**116** could not induce the higher enantiomeric excess than previous chiral gold complex (\pm)-**113** under the same catalytic condition. To achieve the potentially improvement of

the enantioselectivity, we planned to develop the phosphine functional groups of our allene ligand with other bulky aryl groups such as 3,5-(CF₃)₂C₆H₃ and naphthyl groups.

General Conclusion



General Conclusion

This Ph.D. work has been aimed to prepare new chiral ligands for asymmetric catalysis. We focused on the preparation of two families of phosphine-containing allene ligands, which possess axial chirality. All successful applications of new allenes bearing phosphine moieties are summarized in Scheme C1. Our study started first with the synthesis of allenes bearing monophosphine oxide groups (1). These ligands readily originated from phosphine oxide propargyl acetate precursors *via* copper-mediated S_N2' substitution or palladium-catalyzed coupling reaction with organozinc reagent. These reactions produced the various allenes with 50% to 92% yields successfully.

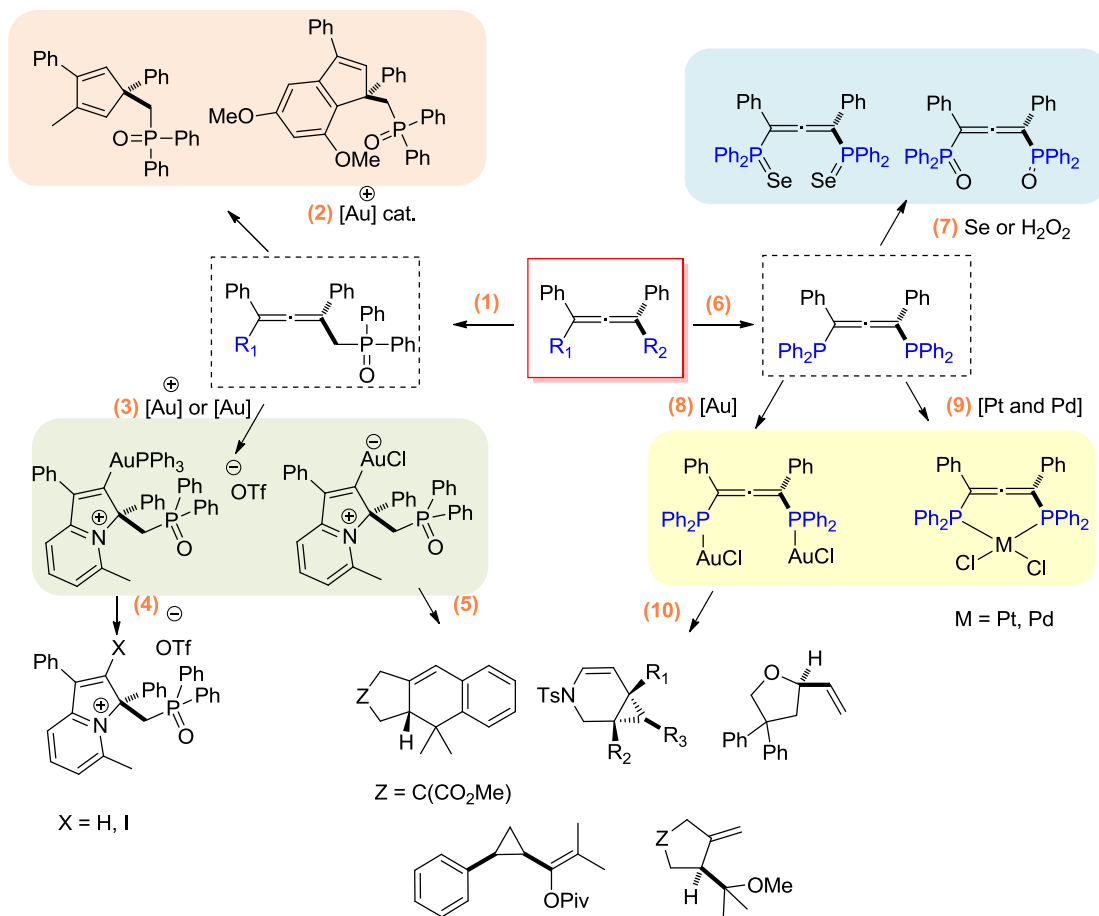
The first application uses allenes in gold(I)-catalyzed cyclization reactions (2). The allenes bearing electron rich functional groups such as vinyl or 3,5-methoxy phenyl groups were successfully cyclized by cationic gold(I) catalyst in order to obtain cyclopentadiene and indenyl phosphine oxide derivatives. Optically pure allene bearing 3,5-methoxy phenyl groups underwent transfer of chirality to the chiral cyclic product completely.

The allenes were also tested as ligands for transition metals to access organometallic complexes. It was found that pyridinyl allenes can coordinate to gold(I) species and generate new organogold complexes in quantitative yields (3). These structures were characterized by NMR analysis, X-ray crystallography, and computational calculations. One vinyl gold cationic complex was functionalized by trapping goldphosphine moiety with acids or electrophiles to obtain new indolizinium salt ($X = H$) and vinyl iodide ($X=I$) derivatives (4). In our perspectives, indolizinium derivatives will be extended by using various electrophiles. Alternatively, chiral indolizinium compounds can be prepared from optically pure pyridinyl allenes.

The other chlorovinylgold complex was used as a precatalyst in gold(I)-catalyzed cyclization reactions (5). To broaden the use in asymmetric reactions, the racemic pyridinyl allene was separated by preparative chiral HPLC to provide the enantioenriched allenes, leading to the preparation of chiral chloro vinylgold complexes. An asymmetric hydroalkoxylation of γ -allenol in the presence of this chiral gold and AgOTs produced tetrahydrofuran derivative with 50% yield and 38% *ee*. Thus, we are continuing to optimize the reactions with this catalytic system in order to improve enantiomeric excesses.

As another type of phosphine ligands, we focused on the synthesis of bisphosphine-containing allenes (6) and their derivatives were readily prepared (7). The allenyl bisphosphine was then applied as ligand for platinum(II), palladium(II) and gold(I) (8,9). Dinuclear gold complex

bearing allenyl bisphosphine ligand was also used as a digold precatalyst in cycloisomerization reactions to afford the cyclic products in satisfying yields (10).

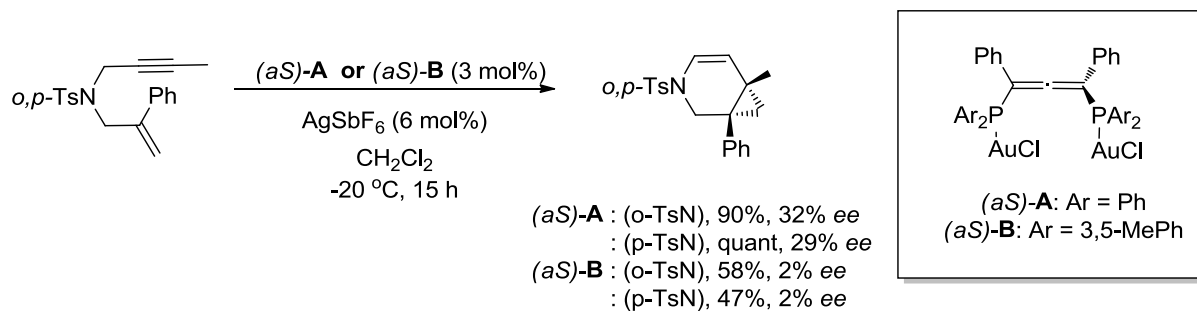


Scheme C1. Summary of new allenyl bisphosphine ligands and their applications.

The successful results from this racemic gold complex inspired us to study the optical resolutions of racemic allenyl bisphosphine ligand. The first method was carried out by formation of dinuclear palladium complexes. After recrystallization, two diastereomers were obtained. One of them was engaged in asymmetric palladium-catalyzed allylic alkylation reaction. Alternatively, preparative chiral HPLC of chiral gold complexes was done. Asymmetric reactions of *N*-Tosyl-1,6-enyne in the presence of chiral cationic gold catalyst, generated from this chiral gold complex and a silver salt, provided the cyclopropane-containing bicyclic products in high yields, but with moderate enantioselectivity (29-32% *ee*).

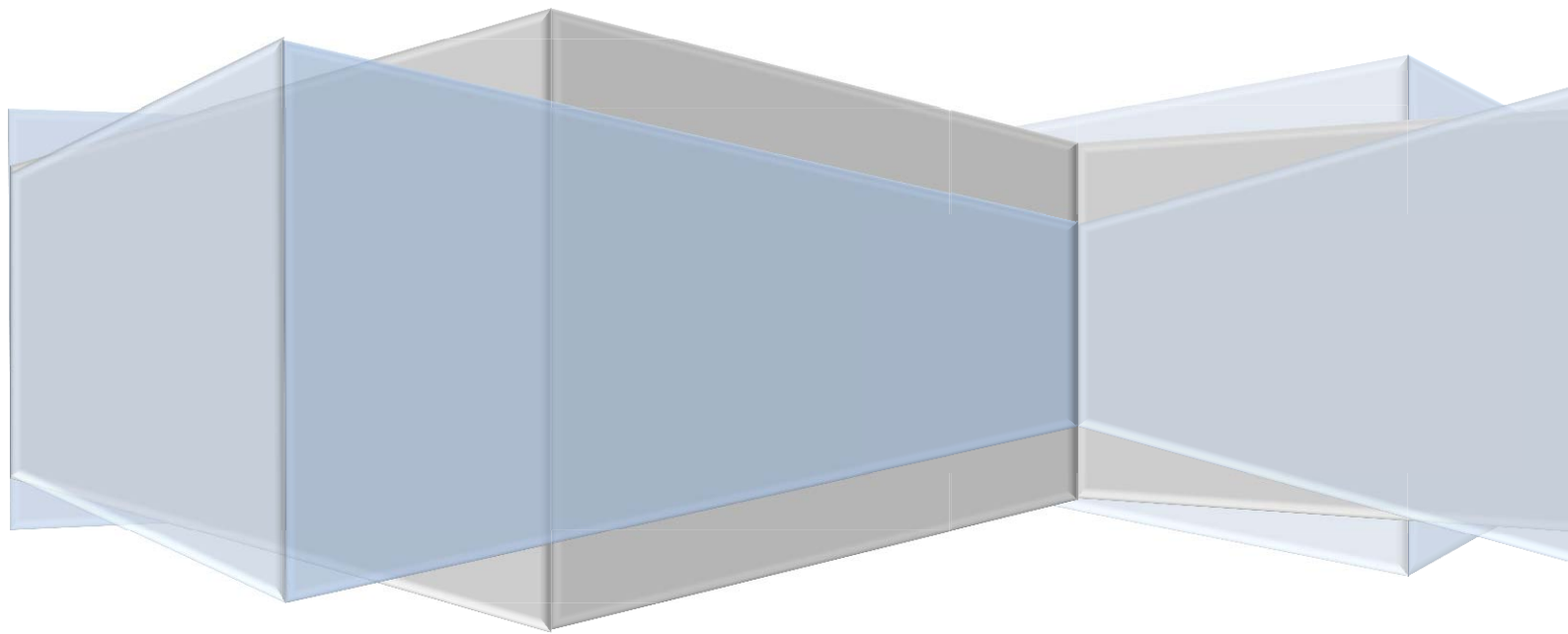
We decided to develop a chiral catalyst structure to improve the enantioselectivity. A new gold complex bearing bis(3,5-Me₂C₆H₃phosphoryl) allene ligand was prepared and expected to better induce the asymmetry of chiral product in cyclization process. The racemic gold complexes were separated by preparative chiral HPLC to obtain both enantiomerically pure gold catalysts for asymmetric catalysis. The chiral gold complex was tested in similar catalytic reactions.

Unfortunately, it did not enhance the enantioselectivity to give chiral products (Scheme C2). To improve the enantioselectivity, we attempted to prepare new chiral gold catalysts featuring bulky allene ligands and to test them in these asymmetric reactions.



Scheme C2. Asymmetric cycloisomerization of enyne in the presence of $(aS)\text{-A}$ and $(aS)\text{-B}$ precatalysts.

Experimental part



Experimental part

1. General information

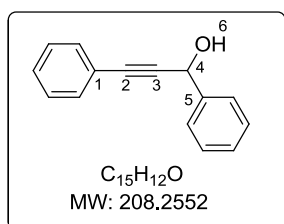
All reactions were performed in oven-dried glassware under argon atmosphere. All solvents were freshly distilled prior to use: Et₂O and THF over sodium and benzophenone; CH₂Cl₂ over CaH₂. DMF was dried and degassed before using. Technical grade solvents for extraction and chromatography were used without distillation. *n*-Butyllithium was purchased as a 2.5 M solution in hexanes and titrated before using. NaH was purchased as a 60% suspension in mineral oil and washed with pentane under argon atmosphere before using. Column chromatography was performed on Merck Geduran SI 60 A silica gel (35-70 mm). Analytical Thin-layer chromatography (TLC) was performed on Merck 60 F₂₅₄ silica gel and visualized either with a UV lamp (254 nm), or using solutions of *para*-anisaldehyde-sulfuric acid-acetic acid in EtOH or KMnO₄-K₂CO₃ in water followed by heating. ¹H NMR spectra were recorded at 400 MHz, 300 MHz or 600 MHz and data are reported as follows: chemical shift in ppm with the solvent as an internal indicator (CDCl₃ δ 7.26, CD₂Cl₂ δ 5.32, C₆D₆ δ 7.16), multiplicity (s = singlet, d = doublet, t = triplet, q = quartet or m = multiple and b = broad) and integration. ¹³C NMR spectra were recorded at 100 MHz, 75 MHz or 151 MHz and data are reported as follows: chemical shift in ppm with the solvent as an internal indicator (CDCl₃ δ 77.16, CD₂Cl₂ δ 54.00, C₆D₆ δ 128.06). ³¹P NMR spectra were recorded at 122 MHz or 162 MHz and data are reported as follows: chemical shift in ppm with an internal probe of H₃PO₄ (85% in H₂O, δ 0.0). Coupling constants (*J*) are given in Hertz (Hz). High resolution mass spectra (HRMS) were obtained using a mass spectrometer MicroTOF from Bruker with an electron spray ion source (ESI) and a TOF detector at Institut Parisien de Chimie Moléculaire. Melting points (m.p.) were recorded with a SMP3 Stuart Scientific melting point apparatus. Infrared (IR) spectra were measured using Tensor 27 (ATR Diamond) Bruker spectrometer. IR data are reported as characteristic band (cm⁻¹) in their maximal intensity. Optical rotations were determined using a JASCO P2000. Chiral HPLC analyses were achieved on an Agilent 1260 infinity unit with pump, autosampler, oven, DAD and Jasco CD-2095 circular dichroism detector, controlled by a SRA Instrument software (Marcy l'Etoile, France) at Institut des Sciences Moléculaires de Marseille (iSm2).

2. Experimental Details and Analytical Data (Related to Chapters 3 and 4)

2.1. Preparation of allene derivatives

2.1.1. Synthesis of phenyl propargylic acetate (4)

1,3-Diphenylprop-2-yn-1-ol (1)



To a solution of phenylacetylene (5.5 mL, 50 mmol, 1 equiv) in THF (50 mL) was added *n*-BuLi (24 mL of 2.2 M in hexanes, 75 mmol, 1.5 equiv) at $-78\text{ }^{\circ}\text{C}$. After stirring for 10 min, a solution of benzaldehyde (7.6 mL, 75 mmol, 1.5 equiv) was added and the reaction mixture was stirred for 2 h at rt and completion of reaction (TLC monitoring). The reaction

mixture was diluted with EtOAc (50 mL) and quenched with a saturated aqueous NH_4Cl solution (50 mL). The aqueous phase was extracted with EtOAc (2x30 mL). The combined organic layers were washed with brine (20 mL), dried over anhydrous MgSO_4 , filtered and concentrated under reduced pressure. Purification by column chromatography on silica gel using EtOAc/pentane (1/4) as eluent afforded alcohol **1** (11.2 g, quant) as a colourless oil.

The characterization data were identical to those previously reported.^[1]

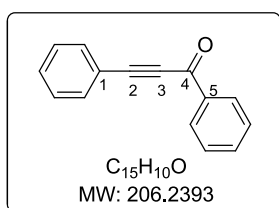
$R_f = 0.48$ (EtOAc/ pentane: 1/4).

IR (neat): $\tilde{\nu}$ (cm^{-1}) = 3062, 3034, 2959, 2197, 1964, 1907, 1638, 1282, 1031.

$^1\text{H NMR}$ (300 MHz, CDCl_3) δ 7.75-6.92 (m, 10H, H_{ar}), 5.62 (d, $J = 6.0$ Hz, 1H, H_6), 3.03 (d, $J = 6.1$ Hz, 1H, H_4).

$^{13}\text{C NMR}$ (75 MHz, CDCl_3) δ 140.7 (C, C_5), 131.8 (2CH), 128.6 (2CH), 128.6 (CH), 128.4 (2CH), 128.3 (CH), 126.8 (2CH), 122.5 (CH), 88.9 (C, C_3), 86.6 (C, C_2), 65.0 (CH, C_4).

1,3-Diphenylprop-2-yn-1-one (2)



A solution of **1** (5.0 g, 24 mmol, 1 equiv) in CH_2Cl_2 (10 mL) was added to a mixture of PCC (7.8 g, 36 mmol, 1.5 equiv) and Al_2O_3 (50 g, 0.50 mmol, 0.02 equiv) in CH_2Cl_2 (30 mL) and stirred at rt. After 18 h, the mixture was filtered through a short pad of silica, washed with CH_2Cl_2 and

concentrated the solvent under reduced pressure. Purification by column chromatography on silica gel using EtOAc/pentane (1/4) as eluent afforded ketone **2** (4.2 g, 85% yield) as a yellow solid.

The characterization data were identical to those previously reported.^[2]

R_f = 0.57 (EtOAc/ pentane: 1/4).

m.p. = 49–53 °C.

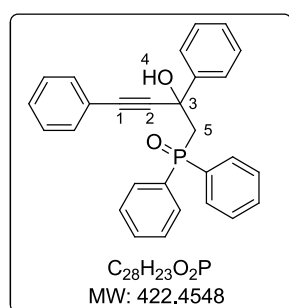
IR (neat): $\tilde{\nu}$ (cm⁻¹) = 3061, 2958, 2197, 1721, 1638, 1448.

¹H NMR (300 MHz, CDCl₃) δ 8.21 (d, J = 7.9 Hz, 1H), 7.65 (d, J = 7.2 Hz, 2H, H_{ar}), 7.60-7.56 (m, 1H, H_{ar}), 7.53-7.34 (m, 6H, H_{ar}).

¹³C NMR (100 MHz, CDCl₃) δ 177.8 (C, C₄), 136.8 (C, C₅), 134.0 (CH), 133.0 (2CH), 130.8 (CH), 129.5 (2CH), 128.6 (4CH), 120.0 (C, C₁), 93.0 (C, C₃), 86.9 (C, C₂).

HRMS (ESI) calcd for C₁₅H₁₀NaO ([M + Na]⁺) 229.0624 found 229.0626.

(2-Hydroxy-2,4-diphenylbut-3-yn-1-yl)diphenylphosphineoxide (**3**)



To a solution of methyl diphenylphosphine oxide (5.47 g, 25.3 mmol, 1.1 equiv) in THF (70 mL) was added *n*-BuLi (13.0 mL of 1.95 M solution in hexanes, 25.3 mmol, 1.1 equiv) at -78 °C and slowly warmed to 0 °C. After stirring for 1 h, the mixture was cooled down to -78 °C and the solution of **2** (4.75 g, 23.0 mmol, 1 equiv) in THF (10 mL) was slowly added. After stirring for 18 h at rt, the reaction mixture was quenched with a saturated aqueous NH₄Cl solution (50 mL) and diluted with EtOAc (30 mL). The aqueous layer was extracted with EtOAc (3x30 mL). The combined organic layers were washed with brine (30 mL), dried over anhydrous MgSO₄, filtered and concentrated under reduced pressure. Purification by column chromatography on silica gel using EtOAc/pentane (3/7) as eluent afforded **3** (7.76 g, 80% yield) as a white solid.

R_f = 0.25 (EtOAc/pentane: 3/7).

m.p. = 163–165 °C.

IR (neat): $\tilde{\nu}$ (cm⁻¹) = 3290, 3058, 2958, 1489, 1313, 1272, 1120, 1098.

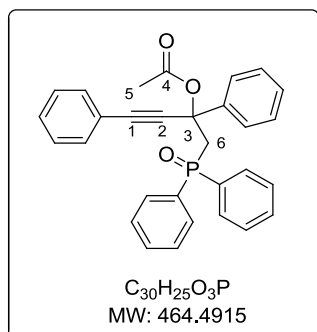
¹H NMR (300 MHz, CDCl₃) δ 7.97-7.90 (m, 2H, H_{ar}), 7.80-7.77 (m, 2H, H_{ar}), 7.68-7.61 (m, 2H, H_{ar}), 7.52-7.15 (m, 11H, H_{ar}), 6.98-6.95 (m, 2H, H_{ar}), 6.89 (s, 1H, H_{ar}), 3.14 (dd, J = 15.0, 5.7 Hz, 1H, H₅), 3.00 (dd, J = 15.0, 10.8 Hz, 1H, H₅).

¹³C NMR (100 MHz, CDCl₃) δ 145.1 (d, J = 10.1 Hz, C), 134.7 (C), 133.7 (C), 132.1 (C), 132.0 (d, J = 3.0 Hz, C), 131.9 (d, J = 2.9 Hz, C), 131.8 (2C), 131.1 (d, J = 10.1 Hz, CH), 130.3 (d, J = 9.1 Hz, CH), 128.9 (d, J = 2.0 Hz, 2CH), 128.8 (d, J = 2.0 Hz, 2CH), 128.5 (2CH), 128.4 (d, J = 10.1 Hz, 2CH), 127.9 (d, J = 7.1 Hz, CH), 127.9 (2CH), 125.3 (2CH), 122.3 (CH), 91.0 (d, J = 5.1 Hz, C, C₂), 87.2 (C, C₁), 70.9 (d, J = 5.1 Hz, C, C₃), 44.1 (d, J = 67.7 Hz, CH₂, C₅).

³¹P NMR (162 MHz, CDCl₃) δ 33.0.

HRMS (ESI) calcd for $C_{28}H_{23}NaO_2P$ ($[M + Na]^+$) 445.1328 found 445.1331.

1-(Diphenylphosphoryl)-2,4-diphenylbut-3-yn-2-yl acetate (**4**)



To a solution of **3** (1.48 g, 3.51 mmol, 1 equiv) in CH_2Cl_2 (30 mL) were added DMAP (0.21 g, 1.76 mmol, 0.5 equiv) and Et_3N (1.95 mL, 14.0 mmol, 4 equiv). After stirring for 20 min, Ac_2O (1.33 mL, 14.0 mmol, 4 equiv) was added and the mixture was refluxed for 18 h. The reaction mixture was quenched with a saturated aqueous NH_4Cl solution (20 mL) and diluted with CH_2Cl_2 (20 mL). The aqueous layer was extracted with CH_2Cl_2 (3x20 mL) and the combined organic

layers were washed with brine (20 mL), dried over anhydrous $MgSO_4$, filtered and concentrated under reduced pressure. Purification by precipitation with petroleum ether afforded acetate **4** (1.63 g, quant yield) as a pale yellow solid.

$R_f = 0.25$ (EtOAc/pentane: 1/1).

m.p. = 115–119 °C.

IR (neat): $\tilde{\nu}$ (cm^{-1}) = 3429, 3057, 2921, 2851, 2228, 1752, 1491, 1301, 1217, 1196, 1117, 1071.

1H NMR (400 MHz, $CDCl_3$) δ 7.62-7.59 (m, 4H, H_{ar}), 7.47-7.45 (m, 2H, H_{ar}), 7.29-7.24 (m, 8H, H_{ar}), 7.16-7.08 (m, 6H, H_{ar}), 3.27 (d, $J = 10.4$ Hz, 2H, H_6), 1.73 (s, 3H, H_5).

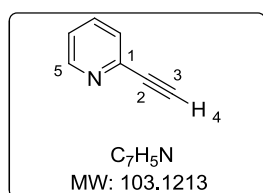
^{13}C NMR (100 MHz, $CDCl_3$) δ 168.5 (C, C_4), 141.6 (d, $J = 6.1$ Hz, C), 134.3 (d, $J = 52.5$ Hz, C), 133.3 (d, $J = 52.5$ Hz, C), 132.2 (2CH), 131.6 (d, $J = 3.0$ Hz, 2CH), 131.5 (d, $J = 3.0$ Hz, 2CH), 131.2 (d, $J = 9.1$ Hz, 2CH), 131.0 (d, $J = 10.1$ Hz, 2CH), 128.7 (d, $J = 22.2$ Hz, CH), 128.5 (2CH), 128.3 (d, $J = 10.1$ Hz, 2CH), 128.2 (2CH), 125.4 (2CH), 122.2 (CH), 89.8 (C, C_1), 87.0 (d, $J = 6.1$ Hz, C, C_2), 75.8 (d, $J = 4.0$ Hz, C, C_3), 44.0 (d, $J = 67.7$ Hz, CH_2 , C_6), 21.6 (CH_3 , C_5).

^{31}P NMR (162 MHz, $CDCl_3$) δ 24.9.

HRMS (ESI) calcd for $C_{30}H_{25}NaO_3P$ ($[M + Na]^+$) 487.1434 found 487.1434.

2.1.2. Synthesis of pyridinyl propargylic acetate (**24**)

2-Ethynylpyridine (**20a**)



To a solution of 2-bromopyridine (4 mL, 42.0 mmol, 1 equiv) in Et_3N (60 mL) was added trimethylsilylacetylene (6.4 mL, 46.2 mmol, 1.1 equiv), CuI (0.4 g, 4.20 mmol, 0.1 equiv) and $PdCl_2(PPh_3)_2$ (2.9 g, 4.20 mmol, 0.1 equiv) and stirred at rt. After stirring for 15 h, the black solid was removed by filtered on a short pad of Celite® and washed with Et_2O . The solution was hydrolyzed

with water (30 mL) and diluted with Et₂O (30 mL). The aqueous layer was extracted with Et₂O (3x30 mL). The combined organic layers were washed with brine (20 mL), dried over anhydrous MgSO₄, filtered and concentrated under reduced pressure. Purification by silica gel chromatography with Et₂O/pentane (1/9) afforded 2-((trimethylsilyl)ethynyl)pyridine (6.63 g, 90% yield) as a yellow oil. $R_f = 0.24$ (Et₂O/pentane: 1/9).

To a solution of KOH (5.0 g, 75.6 mmol, 2 equiv) in MeOH (70 mL) was added the solution of 2-((trimethylsilyl)ethynyl) pyridine (6.63 g, 37.8 mmol, 1 equiv) and stirred for 70 min at rt. The reaction was hydrolyzed with water (70 mL) and diluted with EtOAc (40 mL). The aqueous layer was extracted with EtOAc (3x30 mL) and the combined organic layers were washed with brine (40 mL), dried over anhydrous MgSO₄, filtered and concentrated under reduced pressure to afford **20a** (3.21 g, 82% yield) as a colorless oil. (*Note*: the product is volatile).

The spectral data obtained for this compound matched those reported in the literature.^[3]

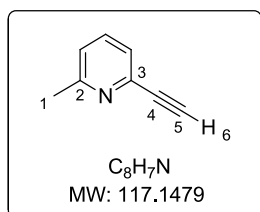
$R_f = 0.11$ (Et₂O/pentane: 1/9).

IR (neat): $\tilde{\nu}$ (cm⁻¹) = 3296, 3052, 3005, 2304, 2109, 1726, 1583, 1561, 1461, 1428, 1243, 1150, 1091, 1045, 991, 779.

¹H NMR (400 MHz, CDCl₃) δ 8.56 (d, $J = 4.3$ Hz, 1H, H₅), 7.74-7.58 (m, 1H, H_{ar}), 7.45 (d, $J = 7.8$ Hz, 1H, H_{ar}), 7.31-7.16 (m, 1H, H_{ar}), 3.13 (s, 1H, H₄).

¹³C NMR (100 MHz, CDCl₃) δ 149.2 (CH, C₅), 141.5 (C, C₁), 135.5 (CH), 126.8 (CH), 122.8 (CH), 82.2 (C, C₂), 76.9 (CH, C₃).

2-Ethynyl-6-methylpyridine (20b)



To a solution of 2-bromo-6-methylpyridine (5.0 mL, 43.9 mmol, 1 equiv) in Et₃N (75 mL) was added trimethylsilylacetylene (6.8 mL, 48.3 mmol, 1.1 equiv), CuI (0.80 g, 4.39 mmol, 0.1 equiv) and PdCl₂(PPh₃)₂ (3.1 g, 4.39 mmol, 0.1 equiv) and stirred at rt. After stirring for 15 h, the black solid was removed by filtration on a short pad of Celite® and washed with Et₂O. The solution was hydrolyzed with water (60 mL) and diluted with Et₂O (60 mL). The aqueous layer was extracted with Et₂O (3x30 mL). The combined organic layers were washed with brine (20 mL), dried over anhydrous MgSO₄, filtered and concentrated under reduced pressure. Purification by silica gel chromatography with Et₂O/pentane (1/9) afforded 2-methyl-6-((trimethylsilyl)ethynyl)pyridine (7.75 g, 93% yield) as a yellow oil. $R_f = 0.24$ (Et₂O/pentane: 1/9).

To a solution of KOH (5.80 g, 103.5 mmol, 2 equiv) in MeOH (100 mL) was added the solution of 2-methyl-6-((trimethylsilyl) ethynyl)pyridine (9.80 g, 51.7 mmol, 1 equiv) and stirred

for 30 min. The reaction was quenched with water (100 mL) and diluted with EtOAc (50 mL). The aqueous layer was extracted with EtOAc (3x30 mL) and the combined organic layers were washed with brine (40 mL), dried over anhydrous MgSO₄, filtered and concentrated under reduced pressure to afford **20b** (5.6 g, 92% yield) as a colorless oil.

The spectral data obtained for this compound matched those reported in the literature.^[3]

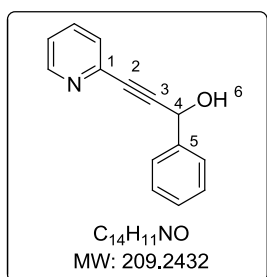
R_f = 0.11 (Et₂O/pentane: 1/9).

IR (neat) = 2921, 2851, 2362, 1621, 1488, 1377, 1037, 794, 696.

¹H NMR (400 MHz, CDCl₃) δ 7.28 (m, 1H, H_{ar}), 7.11–6.92 (m, 1H, H_{ar}), 6.95–6.75 (m, 1H, H_{ar}), 2.97 (s, 1H, H₆), 2.29 (s, 3H, H₁).

¹³C NMR (100 MHz, CDCl₃) δ 158.5(C, C₂), 141.0(C, C₃), 136.0 (CH), 124.1 (CH), 122.9 (CH), 82.6 (C, C₄), 76.6 (C, C₅), 24.0 (CH₃, C₁).

1-Phenyl-3-(pyridin-2-yl)prop-2-yn-1-ol (**21a**)



To a solution of **20a** (3.21 g, 31.1 mmol, 1 equiv) in THF (100 mL) was added *n*-BuLi (14.9 mL of 2.2 M in hexanes, 32.7 mmol, 1.05 equiv) at –78 °C. After stirring for 1.5 h, benzaldehyde (3.5 mL, 34.2 mmol, 1.1 equiv) was added at –60 °C and slowly warmed to rt. After stirring for 18 h and completion of reaction (TLC monitoring), the reaction mixture was quenched with a saturated aqueous NH₄Cl solution (30 mL) and diluted

with EtOAc (20 mL). The aqueous phase was extracted with EtOAc (2x20 mL). The combined organic layers were washed with brine (20 mL), dried over anhydrous MgSO₄, filtered and concentrated under reduced pressure. Purification by column chromatography on silica gel using EtOAc/pentane (1/1) as eluent afforded **21a** (5.2 g, 80% yield) as a brown solid.

R_f = 0.29 (EtOAc/pentane: 1/1).

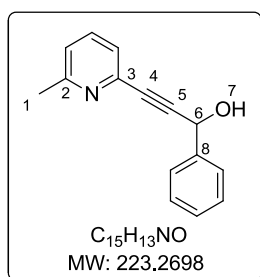
m.p. = 70–73 °C.

IR (neat): $\tilde{\nu}$ (cm⁻¹) = 3201, 3062, 2924, 2855, 2227, 1585, 1563, 1466, 1429, 1275, 1039, 1001, 971, 778, 728, 698.

¹H NMR (300 MHz, CDCl₃) δ 8.38 (d, *J* = 4.7 Hz, 1H, H_{ar}), 7.62–7.44 (m, 3H, H_{ar}), 7.35–7.14 (m, 4H, H_{ar}), 7.11–7.04 (m, 1H, H_{ar}), 5.66 (s, 1H, H₄), 5.09 (s, 1H, H₆).

¹³C NMR (75 MHz, CDCl₃) δ 149.6 (CH), 142.7 (C, C₁), 140.6 (C, C₅), 136.5 (CH), 128.6 (2CH), 128.2 (CH), 127.4 (CH), 126.9 (CH), 123.1 (CH), 90.4 (C, C₂), 84.9 (C, C₃), 64.4 (CH, C₄).

HRMS (ESI) calcd for C₁₄H₁₁NNaO ([M + Na]⁺) 232.0733 found 232.0738.

3-(6-Methylpyridin-2-yl)-1-phenylprop-2-yn-1-ol (21b)

To a solution of HMDS (0.62 mL, 2.90 mmol, 1.5 equiv) in THF 10 mL was added *n*-BuLi (1.2 mL of a 2.5 M solution in hexanes, 2.90 mmol, 1.5 equiv) at 0 °C. After 1 h, the mixture was cooled at – 78 °C and **20b** was added (0.23 g, 1.96 mmol, 1 equiv) in THF 10 mL. The mixture was warmed again to 0 °C and stirred for 1.5 h. Benzaldehyde (0.30 mL, 2.95 mmol, 1.5 equiv) was then added at – 40 °C and the mixture was slowly warmed to rt. After stirring for 18 h, a saturated aqueous NH₄Cl solution (20 mL) was added, followed by Et₂O (20 mL). The aqueous layer was extracted with Et₂O (2x10 mL) and the combined organic layers were washed with brine (20 mL), dried over anhydrous MgSO₄, filtered and concentrated under reduced pressure. Purification by silica gel chromatography with EtOAc/pentane (1/2) afforded **21b** (262 mg, 60% yield) as a brown solid.

R_f = 0.45 (EtOAc/pentane: 1/1).

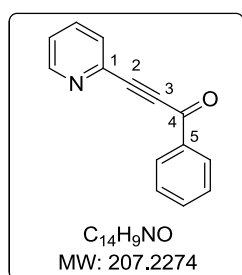
m.p. = 102–108 °C.

IR (neat): $\tilde{\nu}$ (cm⁻¹) = 3183, 3086, 3062, 2923, 2687, 2319, 1586, 1568, 1493, 1452, 1052, 1031, 1015, 818, 763, 745, 699.

¹H NMR (400 MHz, CDCl₃) δ 7.62-7.60 (m, 2H, H_{ar}), 7.49 (d, *J* = 1.5 Hz, H_{ar}), 7.35-7.22 (m, 4H, H_{ar}), 7.05 (d, *J* = 7.8 Hz, 1H, H_{ar}), 5.77 (s, 1H, H₆), 2.50 (s, 3H, H₁).

¹³C NMR (100 MHz, CDCl₃) δ 158.8 (C, C₂), 140.7 (C, C₃), 136.7 (C, C₈), 128.6 (3CH), 128.2(CH), 126.9, 126.9 (CH), 126.8 (2CH), 123.1 (CH), 85.2 (C, C₄), 76.8 (CH, C₆), 64.4 (C, C₅), 24.2 (CH₃, C₁).

HRMS (ESI) calcd for C₁₅H₁₃NNaO ([M + Na]⁺) 246.0889, found 246.0896.

1-Phenyl-3-(pyridine-2-yl)prop-2-yn-1-one (22a)

A solution of Dess-Martin Periodinane (240 mg, 0.58 mmol, 1.2 equiv) in CH₂Cl₂ (2.5 mL) was added to a solution of **21a** (100 mg, 0.48 mmol, 1 equiv) in CH₂Cl₂ (2 mL). After stirring for 18 h at rt and monitoring the completion of reaction by TLC, the mixture was quenched with a saturated aqueous NH₄Cl solution (10 mL) and diluted with CH₂Cl₂ (10 mL). The aqueous phase was extracted with CH₂Cl₂ (2x20 mL). The combined organic layers were washed with brine (20 mL), dried over anhydrous MgSO₄, filtered and concentrated under reduced pressure. Purification by column chromatography on silica gel using EtOAc/pentane (1/1) as eluent afforded the ketone **22a** (65 mg, 65% yield) as a pale brown solid.

R_f: 0.41 (EtOAc/pentane: 1/1).

m.p. = 65–69 °C.

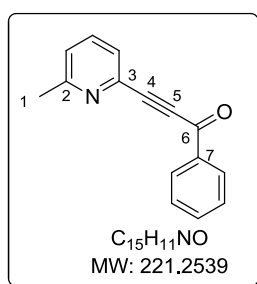
IR (neat): $\tilde{\nu}$ (cm⁻¹) = 3059, 2918, 2850, 2207, 1639, 1597, 1578, 1460, 1450, 1314, 1279, 1214, 1174, 1047, 1031, 778.

¹H NMR (300 MHz, CDCl₃) δ 8.69 (s, 1H, H_{ar}), 8.34–8.12 (m, 2H, H_{ar}), 7.87–7.34 (m, 6H, H_{ar}).

¹³C NMR (75 MHz, CDCl₃) δ 177.8 (C, C₄), 150.7 (CH), 141.0 (C, C₁), 136.6 (CH), 134.5 (C, C₅), 129.8 (2CH), 129.0, (CH), 128.7 (2CH), 124.8 (CH), 115.1 (CH), 90.5 (C, C₃), 84.9 (C, C₂).

HRMS (ESI) calcd for C₁₄H₉NNaO ([M + Na]⁺) 230.0576 found 230.0585.

3-(6-Methylpyridin-2-yl)-1-phenylprop-2-yn-1-one (22b)



A solution of Dess-Martin periodinane (16 g, 37.7 mmol, 1.2 equiv) in CH₂Cl₂ (100 mL) was added to a solution of **21b** (7.0 g, 31.4 mmol, 1 equiv) in CH₂Cl₂ (50 mL). After stirring for 18 h at rt, the reaction was quenched with the aqueous solution of Na₂S₂O₃ (0.1 M, 60 mL) and diluted with CH₂Cl₂ (30 mL). The aqueous layer was extracted with CH₂Cl₂ (2x30 mL) and the combined organic layers were washed with brine (20 mL), dried over anhydrous MgSO₄, filtered and concentrated under reduced pressure. Purification by silica gel chromatography with Et₂O/pentane (1/1) as eluent afforded the ketone **22b** (6.80 g, 98% yield) as a dark green solid.

R_f = 0.65 (Et₂O/pentane: 1/1).

m.p. = 85–90 °C.

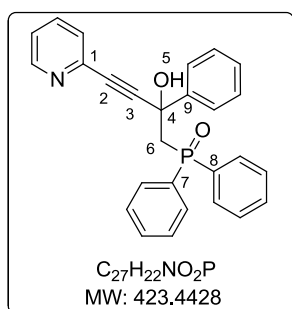
IR (neat): $\tilde{\nu}$ (cm⁻¹) = 3046, 2918, 2201, 1905, 1723, 1630, 1580, 1564, 1449, 1315, 1296, 1047, 902, 791, 687, 631.

¹H NMR (400 MHz, CDCl₃) δ 8.21 (d, *J* = 1.2 Hz, 1H, H_{ar}), 8.19 (d, *J* = 1.5 Hz, 1H, H_{ar}), 7.62–7.56 (m, 2H, H_{ar}), 7.47–7.43 (m, 3H, H_{ar}), 7.21–7.18 (m, 1H, H_{ar}), 2.57 (s, 3H, H₁).

¹³C NMR (100 MHz, CDCl₃) δ 177.7 (C, C₆), 159.7 (C, C₂), 140.1 (CH), 136.7 (CH), 136.5 (CH), 134.4 (CH), 129.8 (2CH), 128.7 (2CH), 126.1 (CH), 124.7 (CH), 90.8 (C, C₄), 84.6 (C, C₅), 24.5 (CH₃, C₁).

HRMS (ESI) calcd for C₁₅H₁₁NNaO ([M + Na]⁺) 244.0733, found 244.0742.

(2-Hydroxy-2-phenyl-4-(pyridin-2-yl)but-3-yn-1-yl)diphenylphosphine oxide (23a)



To a solution of methyl diphenylphosphine oxide (1.64 g, 7.59 mmol, 1.05 equiv) in Et₂O (120 mL) was added *n*-BuLi (3.88 mL of 1.95 M solution in hexanes, 7.59 mmol, 1.05 equiv) at – 78 °C and slowly warmed to 0 °C. After stirring for 2 h, the mixture was cooled down to

– 78 °C and the solution of **22a** (1.50 g, 7.22 mmol, 1 equiv) was slowly added. After stirring for 18 h at rt, the reaction mixture was quenched with a saturated aqueous NH₄Cl solution (100 mL) and diluted with Et₂O (30 mL). The aqueous phase was extracted with Et₂O (3x50 mL) and the combined organic layers were washed with brine (30 mL), dried over anhydrous MgSO₄, filtered and concentrated under reduced pressure. Purification by column chromatography on silica gel using EtOAc/pentane (9/1) as eluent afforded **23a** (2.85 g, 93% yield) as a brown solid.

R_f = 0.25 (EtOAc/pentane: 7/3).

m.p. = 65–67 °C.

IR (neat): $\tilde{\nu}$ (cm⁻¹) = 3267, 3057, 2230, 2141, 1583, 1463, 1437, 1428, 1156, 1119, 779, 737, 722.

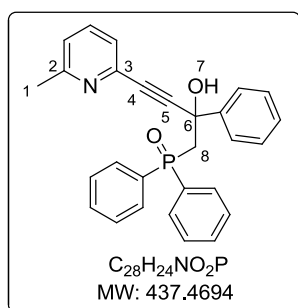
¹H NMR (400 MHz, CDCl₃) δ 8.44 (ddd, *J* = 4.8, 1.6, 0.8 Hz, 1H, H_{ar}), 7.88-7.83 (m, 2H, H_{ar}), 7.74-7.72 (m, 2H, H_{ar}), 7.60-7.54 (m, 2H, H_{ar}), 7.48-7.21 (m, 10H, H_{ar}), 7.13 (ddd, *J* = 7.6, 4.8, 1.2 Hz, 1H, H_{ar}), 6.98 (dt, *J* = 7.6, 1.2 Hz, 1H, H_{ar}), 6.88 (bs, 1H, H_{ar}), 3.15 (dd, ¹*J*_{HP} = 15.2, 6.4 Hz, 1H, H₆), 2.99 (dd, *J* = 15.2, 10.8 Hz, 1H, H₆).

¹³C NMR (100 MHz, CDCl₃) δ 149.6 (2CH), 144.1 (d, *J* = 9.1 Hz, C), 142.5 (CH), 135.7 (2CH), 132.8 (d, *J* = 45.0 Hz, C), 132.1 (d, *J* = 3.0 Hz, C), 131.6 (d, *J* = 3.0 Hz, C), 131.0 (d, *J* = 9.1 Hz, 2CH), 130.2 (d, *J* = 9.1 Hz, 2CH), 128.8 (d, *J* = 10.1, 2CH), 128.7 (d, *J* = 10.1 Hz, 2CH), 128.4 (2CH), 127.3 (CH), 125.5 (2CH), 122.9 (CH), 91.0 (d, *J* = 6.1 Hz, C, C₃), 86.3 (C, C₂), 70.9 (d, *J* = 6.1 Hz, C, C₄), 43.8 (d, *J* = 67.7 Hz, CH₂, C₆).

³¹P NMR (162 MHz, CDCl₃) δ 33.5.

HRMS (ESI) calcd for C₂₇H₂₂NNaO₂P ([M + Na]⁺) 446.1280 found 446.1285.

2-Hydroxy-4-(6-methylpyridin-2-yl)-2-phenylbut-3-yn-1-yl diphenylphosphine oxide (**23b**)



To a solution of methyl diphenylphosphine oxide (1.51 g, 7.00 mmol, 1 equiv) in Et₂O (60 mL) was added *n*-BuLi (3.1 mL of a 2.5 M solution in hexanes, 7.68 mmol, 1.1 equiv) at – 78 °C. Then, the reaction mixture was warmed to 0 °C and stirred for 2 h. The solution of pyridine ketone **22b** (1.55 g, 7.00 mmol, 1 equiv) in Et₂O (20 mL) was added dropwise at – 40 °C and then the reaction mixture slowly warmed to

– 10 °C. After 18 h at rt, a saturated aqueous NH₄Cl solution (50 mL) was added and diluted with EtOAc (50 mL). The aqueous layer was extracted with EtOAc (3x20 mL). The combined organic layers were washed with brine (20 mL), dried over anhydrous MgSO₄, filtered and concentrated under reduced pressure. Purification by silica gel chromatography with EtOAc/cyclohexane (8/2) as eluent afforded **23b** (2.57 g, 84% yield) as a yellow solid.

R_f = 0.13 (EtOAc/cyclohexane: 1/1).

m.p. = 57–58°C.

IR (neat): $\tilde{\nu}$ (cm⁻¹) = 3269, 3957, 2916, 2178, 2165, 2132, 1584, 1452, 1438, 1158, 1119, 737, 697, 539.

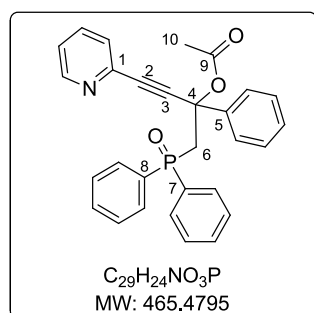
¹H NMR (400 MHz, CDCl₃) δ 7.89-7.84 (m, 2H, H_{ar}), 7.73 (d, *J* = 8.0 Hz, 2H, H_{ar}), 7.60-7.55 (m, 2H, H_{ar}), 7.47-7.21 (m, 10H, H_{ar}), 7.01 (d, *J* = 8.0 Hz, 1H, H_{ar}), 6.85 (s, 1H, H_{ar}), 6.82 (d, *J* = 7.6 Hz, 1H, H_{ar}), 3.17 (dd, *J* = 14.8, 6.4 Hz, 1H, H₈), 3.01 (dd, *J* = 14.8, 10.4 Hz, 1H, H₈), 2.49 (s, 3H, H₁).

¹³C NMR (100 MHz, CDCl₃) δ 158.4 (C), 144.2 (d, *J* = 9.1, C), 141.8 (C), 135.9 (CH), 131.9 (d, *J* = 3.0 Hz, 2CH), 131.6 (d, *J* = 3.0 Hz, 2CH), 131.1 (d, *J* = 9.1 Hz, C), 130.2 (d, *J* = 10.1 Hz, 2C), 128.8 (d, *J* = 8.1 Hz, 2CH), 128.7 (d, *J* = 9.1 Hz, 2CH), 128.6 (CH), 128.3 (2CH), 127.9 (CH), 125.4 (2CH), 124.6 (CH), 122.7 (CH), 90.6 (d, *J* = 8.0 Hz, C, C₅), 86.4 (C, C₄), 71.0 (d, *J* = 5.0 Hz, C, C₆), 43.8 (d, *J* = 67.7 Hz, CH₂, C₈), 24.5 (CH₃, C₁).

³¹P NMR (162 MHz, CDCl₃) δ 33.4.

HRMS (ESI) calcd for C₂₈H₂₄NNaO₂P ([M + Na]⁺) 460.1437, found 460.1443.

1-(Diphenylphosphoryl)-2-phenyl-4-(pyridin-2-yl)but-3-yn-2-yl acetate (**24a**)



To a solution of **23a** (2.94 g, 6.95 mmol, 1 equiv) in CH₂Cl₂ (150 mL) were added DMAP (0.42 g, 3.50 mmol, 0.5 equiv) and Et₃N (3.86 mL, 27.8 mmol, 4 equiv) at rt. After stirring for 20 min, Ac₂O (2.63 mL, 27.8 mmol, 4 equiv) was added. The mixture was refluxed for 24 h. The reaction mixture was quenched with a saturated aqueous NH₄Cl solution (100 mL) and diluted with CH₂Cl₂ (30 mL). The aqueous phase was extracted with CH₂Cl₂ (3x30 mL). The combined organic

layers were washed with brine (30 mL), dried over anhydrous MgSO₄, filtered and concentrated under reduced pressure. Purification by column chromatography on silica gel using EtOAc/pentane (8/2) as eluent afforded the acetate **24a** (2.72 g, 84% yield) as a pale yellow solid.

R_f = 0.09 (EtOAc/ pentane: 7/3).

m.p. = 68–69 °C.

IR (neat): $\tilde{\nu}$ (cm⁻¹) = 3267, 3057, 2230, 2141, 1583, 1463, 1437, 1428, 1156, 1119, 779, 737, 722, 694.

¹H NMR (400 MHz, CDCl₃) δ 8.56 (bd, *J* = 4.8 Hz, 1H, H_{ar}), 7.74-7.67 (m, 4H, H_{ar}), 7.60-7.56 (m, 3H, H_{ar}), 7.45-7.32 (m, 7H, H_{ar}), 7.25-7.17 (m, 4H, H_{ar}), 3.54 (dd, *J* = 15.2, 11.6 Hz, 1H, H₆), 3.38 (dd, *J* = 15.2, 9.6 Hz, 1H, H₆), 1.89 (s, 3H, H₁₀).

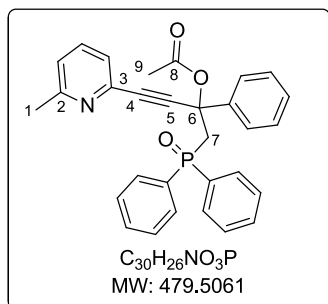
¹³C NMR (100 MHz, CDCl₃) δ 169.2 (C, C₉), 149.7(2CH), 142.4 (C), 140.5 (d, *J* = 5.1 Hz, C), 135.9 (2CH), 134.0 (d, *J* = 55.6, C), 133.0 (d, *J* = 55.6 Hz, C), 131.4 (d, *J* = 2.0 Hz, 2CH), 131.3 (d, *J* = 3.0 Hz,

CH), 130.8 (CH), 130.7 (CH), 130.7 (CH), 128.4 (d, $J = 10.1$ Hz, CH), 128.3 (2CH), 128.2 (d, $J = 11.1$ Hz, CH), 128.2 (CH), 127.8 (CH), 125.2 (2CH), 123.2 (CH), 88.3 (C, C₂), 87.0 (d, $J = 7.1$ Hz, C, C₃), 75.3 (d, $J = 4.0$ Hz, C, C₄), 43.4 (d, $J = 66.7$ Hz, CH₂, C₆), 21.4 (CH₃, C₁₀).

³¹P NMR (162 MHz, CDCl₃) δ 24.5.

HRMS (ESI) calcd for C₂₉H₂₄NNaO₃P ([M + Na]⁺) 488.1386 found 488.1373.

1-(Diphenylphosphoryl)-4-(6-methylpyridin-2-yl)-2-phenylbut-3-yn-2-yl acetate (24b)



A solution of **23b** (0.63 g, 1.45 mmol, 1 equiv) and DMAP (0.090 g, 0.72 mmol, 0.5 equiv) in CH₂Cl₂ (4.1 mL) was added Et₃N (0.80 mL, 5.80 mmol, 4 equiv) and stirred 10 min. Ac₂O (0.50 mL, 5.80 mmol, 4 equiv) was added and refluxed for 18 h. A saturated aqueous NH₄Cl solution (20 mL) and diluted with CH₂Cl₂ (50 mL). The aqueous phase was extracted with CH₂Cl₂ (3x20 mL). The combined

organic layers were washed with brine (10 mL), dried over anhydrous MgSO₄, filtered and concentrated under reduced pressure. Purification by silica gel chromatography with EtOAc/petroleum ether (8/2) as eluent afforded the acetate **24b** (0.69 g, 99% yield) as a pale yellow solid. $R_f = 0.14$ (EtOAc/ petroleum ether: 8/2).

m.p. = 62–66°C.

IR (neat): $\tilde{\nu}$ (cm⁻¹) = 3058, 2923, 2219, 2122, 1978, 1751, 1584, 1568, 1450, 1438, 1218, 734, 697, 534.

¹H NMR (300 MHz, CDCl₃) δ 7.71-7.59(m, 6H, H_{ar}), 7.49 (t, $J = 10.4$ Hz, 1H, H_{ar}), 7.41-7.17 (m, 10H, H_{ar}), 7.08 (d, $J = 7.8$ Hz, 1H, H_{ar}), 3.60 (dd, $J = 15.3, 11.4$ Hz, 1H, H₇), 3.38 (dd, $J = 15.3, 9.9$ Hz, 1H, H₇), 2.55 (s, 3H, H₁), 1.91 (s, 3H, H₉).

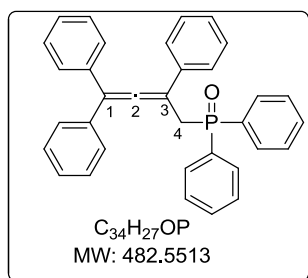
¹³C NMR (75 MHz, CDCl₃) δ 168.2 (C, C₉), 158.5 (C), 141.6 (C), 140.3 (C), 136.1 (CH), 134.2 (d, $J = 49.5$ Hz, CH), 132.8 (d, $J = 49.5$ Hz, CH), 131.3 (d, $J = 2.3$ Hz, C), 131.1 (d, $J = 3.0$ Hz, C), 130.7 (d, $J = 9.0$ Hz, 2CH), 130.6 (d, $J = 9.0$ Hz, 2CH), 128.3 (d, $J = 12.0$ Hz, 2CH), 128.2 (d, $J = 11.3$ Hz, 2CH), 128.1 (3CH), 125.3 (2CH), 125.1 (CH), 122.9 (CH), 88.2 (C, C₄), 88.7 (d, $J = 7.5$ Hz, C, C₅), 75.3 (d, $J = 4.5$ Hz, C, C₆), 43.2 (d, $J = 66.8$ Hz, CH₂, C₇), 24.4 (CH₃, C₁), 21.4 (CH₃, C₉).

³¹P NMR (162 MHz, CDCl₃) δ 24.4.

HRMS (ESI) calcd. for C₃₀H₂₆NO₃PH ([M + H]⁺) 480.17231 found 480.17281.

2.1.3. Synthesis of allenes with mono-diphenylphosphine oxides

Diphenyl (2,4,4-triphenylbuta-2,3-dien-1-yl) phosphine oxide (5)



To a solution of CuI (1.02 g, 5.37 mmol, 5 equiv) and LiBr (470 mg, 5.37 mmol, 5 equiv) in THF (16 mL) was added slowly freshly prepared PhMgBr (10.1 mL of 0.53 M in THF, 5.37 mmol, 5 equiv) at $-78\text{ }^{\circ}\text{C}$. The mixture was warmed at $0\text{ }^{\circ}\text{C}$ for 20 min, then the temperature was cooled down to $-78\text{ }^{\circ}\text{C}$ and a solution of **4** (500 mg, 1.07 mmol, 1 equiv) in THF (4 mL) was added dropwise. At the end of the addition, the mixture was warmed to rt. After stirring for 18 h, a saturated aqueous NH_4Cl solution (20 mL) was added. The aqueous phase was extracted with Et_2O (2x30 mL). The combined organic layers were washed with brine (20 mL), dried over anhydrous MgSO_4 , filtered and concentrated under reduced pressure. Purification by column chromatography on silica gel using EtOAc/pentane (1/1) as eluent afforded allene **5** (440 mg, 84% yield) as a white solid.

$R_f = 0.29$ (EtOAc/pentane: 1/1).

m.p. = $180\text{--}186\text{ }^{\circ}\text{C}$.

IR (neat): $\tilde{\nu}$ (cm^{-1}) = 3640, 3341, 3057, 3026, 2921, 1961, 1492, 1311, 1261, 1120, 839.

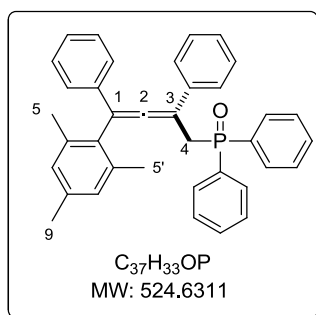
$^1\text{H NMR}$ (400 MHz, CDCl_3) δ 7.75-7.0 (m, 5H, H_{ar}), 7.52-7.49 (m, 3H, H_{ar}), 7.32-7.26 (m, 4H, H_{ar}), 7.26-7.22 (m, 13H, H_{ar}), 3.72 (d, $J = 12.8\text{ Hz}$, 2H, H_4).

$^{13}\text{C NMR}$ (75 MHz, CDCl_3) δ 209.3 (d, $J = 7.5\text{ Hz}$, C, C_2), 136.1 (d, $J = 3.0\text{ Hz}$, C), 135.9 (d, $J = 5.3\text{ Hz}$, C), 133.3 (C), 132.1 (d, $J = 2.7\text{ Hz}$, C), 131.5 (d, $J = 3.0\text{ Hz}$, C), 130.9 (d, $J = 9.0\text{ Hz}$, 4CH), 128.8 (4CH), 128.6 (4CH), 128.5 (4CH), 128.4 (2CH), 128.3 (2CH), 127.5 (2CH), 127.4 (CH), 126.3 (2CH), 114.1 (d, $J = 2.3\text{ Hz}$, C, C_3), 100.6 (d, $J = 7.5\text{ Hz}$, C, C_1), 32.9 (d, $J = 69.8\text{ Hz}$, CH_2 , C_4).

$^{31}\text{P NMR}$ (162 MHz, CDCl_3) δ 29.3.

HRMS (ESI) calcd for $C_{34}H_{27}NaOP$ ($[M + Na]^+$) 505.1692, found 505.1679.

(4-Mesityl-2,4-diphenylbuta-2,3-dien-1-yl)diphenylphosphine oxide (6)



To a solution of CuI (0.61 g, 3.22 mmol, 5 equiv) and LiBr (0.28 g, 3.22 mmol, 5 equiv) in THF (15 mL) was added 2-mesitylmagnesiumbromide (3.2 mL of 1 M in THF, 3.22 mmol, 5 equiv) slowly at $-78\text{ }^{\circ}\text{C}$. The reaction mixture was warmed to $0\text{ }^{\circ}\text{C}$ for 30 min, then the temperature was cooled down to $-60\text{ }^{\circ}\text{C}$ and a solution of **4** (0.27 g, 0.58 mmol, 1 equiv) in THF (15 mL) was added dropwise. At the end of the addition, the mixture was slowly warmed to rt. After stirring for 4 h

and completion of reaction (TLC monitoring), the reaction mixture was diluted with EtOAc (10 mL) and quenched a saturated aqueous NH_4Cl solution (10 mL) was added. The aqueous phase was extracted with EtOAc (3x20 mL). The combined organic layers were washed with brine (10 mL), dried over anhydrous MgSO_4 , filtered and concentrated under reduced pressure. Purification by column chromatography on silica gel using EtOAc/pentane (1/1) as eluent afforded allene **6** (210 mg, 69% yield) as a light yellow solid.

$R_f = 0.51$ (EtOAc/pentane: 8/2).

m.p. = 162–163.

IR (neat): $\tilde{\nu}$ (cm^{-1}) = 3056, 3026, 2918, 2855, 1928, 1734, 1609, 1595, 1491, 1437, 1120, 1119, 837.

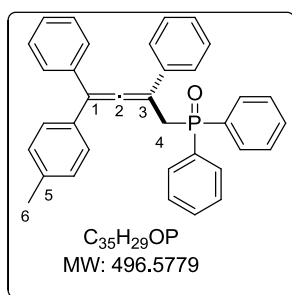
$^1\text{H NMR}$ (300 MHz, CDCl_3) δ 7.79-7.63 (m, 5H, H_{ar}), 7.43-7.28 (m, 7H, H_{ar}), 7.25-7.09 (m, 6H, H_{ar}), 6.99 (dd, $J = 6.4, 3.3$ Hz, 2H, H_{ar}), 6.91 (s, 2H, H_{ar}), 3.68 (d, $J = 13.2$ Hz, 2H, H_4), 2.33 (s, 3H, H_6), 2.11 (s, 6H, $\text{H}_{5,5'}$).

$^{13}\text{C NMR}$ (75 MHz, CDCl_3) δ 207.0 (d, $J = 9.0$ Hz, C, C_2), 137.0 (C), 136.8 (C), 135.9 (d, $J = 2.3$ Hz, C), 135.2 (d, $J = 4.5$ Hz, C), 133.9 (C), 132.6 (d, $J = 9.8$ Hz, C), 131.9 (d, $J = 3.8$ Hz, C), 131.7 (CH), 131.4 (CH), 131.2 (CH), 130.9 (CH), 130.8 (CH), 128.5 (3CH), 128.4 (4CH), 128.3 (3CH), 127.2 (2CH), 127.0 (2CH), 126.4 (3CH), 108.8 (d, $J = 3.0$ Hz, C, C_3), 100.8 (d, $J = 9.0$ Hz, C, C_1), 33.6 (d, $J = 66.8$ Hz, CH_2 , C_4), 21.1 (d, $J = 3.8$ Hz, CH_3 , C_5 or $5'$), 20.7 (d, $J = 3.8$ Hz, CH_3 , C_5 or $5'$), 14.2 (CH_3 , C_6).

$^{31}\text{P NMR}$ (162 MHz, CDCl_3) δ 29.4.

HRMS (ESI) calcd for $\text{C}_{37}\text{H}_{33}\text{NaOP}$ ($[\text{M} + \text{Na}]^+$) 547.2161 found 547.2181.

(2,4-Diphenyl-4-(*p*-tolyl)buta-2,3-dien-1-yl)diphenylphosphine oxide (**7**)



To a solution of CuI (410 mg, 2.15 mmol, 5 equiv) and LiBr (190 mg, 2.15 mmol, 5 equiv) in THF (15 mL) was added *p*-tolylmagnesium bromide (5.3 mL of a 0.4 M in THF, 2.15 mmol, 5 equiv) slowly at -78 $^{\circ}\text{C}$. The reaction mixture was warmed to 0 $^{\circ}\text{C}$ for 20 min, the temperature was cooled down to -60 $^{\circ}\text{C}$ and a solution of **4** (0.20 g, 0.42 mmol, 1 equiv) in THF (15 mL) was added dropwise. At the end of

the addition, the mixture was slowly warmed to rt. After stirring for 20 h, the reaction mixture was diluted with EtOAc (10 mL) and quenched a saturated aqueous NH_4Cl solution (10 mL) was added. The aqueous phase was extracted with EtOAc (3x20 mL). The combined organic layers were washed with brine (10 mL), dried over anhydrous MgSO_4 , filtered and concentrated under reduced pressure. Purification by column chromatography on silica gel using EtOAc/pentane (6/4) as eluent afforded allene **7** (162 mg, 76% yield) as a yellow solid.

$R_f = 0.63$ (EtOAc/pentane: 8/2).

m.p. = 175–180 °C.

IR (neat): $\tilde{\nu}$ (cm⁻¹) = 3056, 3024, 2919, 2851, 1903, 1735, 1596, 1512, 1492, 1438, 1182, 1119, 820.

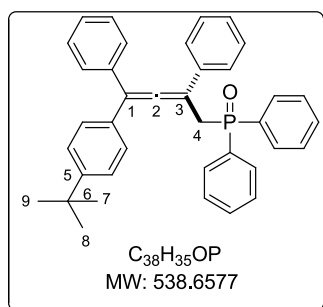
¹H NMR (300 MHz, CDCl₃) δ 7.79-7.67 (m, 4H, H_{ar}), 7.52 (dd, $J = 7.6, 1.8$ Hz, 2H, H_{ar}), 7.35-7.13 (m, 16H, H_{ar}), 7.09 (d, $J = 7.9$ Hz, 2H, H_{ar}), 3.72 (d, $J = 12.9$ Hz, 2H, H₄), 2.37 (s, 3H, H₆).

¹³C NMR (75 MHz, CDCl₃) δ 209.1 (d, $J = 8.3$ Hz, C, C₂), 137.2 (C, C₅), 136.1 (d, $J = 3.0$ Hz, C), 135.9 (d, $J = 5.3$ Hz, C), 133.0 (d, $J = 3.8$ Hz, C), 131.9 (d, $J = 3.8$ Hz, C), 131.4 (CH), 130.8 (d, $J = 9.0$ Hz, 2CH), 129.0 (3CH), 128.7 (3CH), 128.6 (3CH), 128.5 (3CH), 128.4 (3CH), 128.3 (3C), 127.3 (d, $J = 8.3$ Hz, 2CH), 126.2 (2CH), 113.9 (d, $J = 2.3$ Hz, C, C₃), 100.3 (d, $J = 7.5$ Hz, C, C₁), 32.8 (d, $J = 69.8$ Hz, CH₂, C₄), 21.2 (d, $J = 3.8$ Hz, CH₃, C₆).

³¹P NMR (162 MHz, CDCl₃) δ 29.3.

HRMS (ESI) calcd for C₃₅H₂₉NaOP ([M + Na]⁺) 519.1848 found 519.1840.

(4-(4-(*Tert*-butyl)phenyl)-2,4-diphenylbuta-2,3-dien-1-yl)diphenyl phosphine oxide (**8**)



To a solution of CuI (410 mg, 2.15 mmol) and LiBr (190 mg, 2.15 mmol, 5 equiv) in THF (20 mL) was added dropwise *tert*-butylphenyl magnesiumbromide (4.3 mL of a 0.5 M in THF, 2.15 mmol, 5 equiv) at -78 °C. The reaction mixture was warmed to 0 °C for 30 min, then the temperature was cooled down to -60 °C and a solution of **4** (0.20 g, 0.42 mmol, 1 equiv) in THF (10 mL) was added dropwise. At the end of the addition, the mixture was slowly warmed to rt. After stirring for 18 h, the reaction mixture was diluted with EtOAc (20 mL) and quenched a saturated aqueous NH₄Cl solution (20 mL). The aqueous phase was extracted with EtOAc (3x20 mL). The combined organic layers were washed with brine (10 mL), dried over anhydrous MgSO₄, filtered and concentrated under reduced pressure. Purification by column chromatography on silica gel using EtOAc/pentane (7/3) as eluent afforded allene **8** (184 mg, 81% yield) as a yellow solid.

$R_f = 0.57$ (EtOAc/pentane: 8/2).

m.p. = 73–80 °C.

IR (neat): $\tilde{\nu}$ (cm⁻¹) = 3054, 2961, 2866, 2318, 2223, 1959, 1510, 1437, 1197, 1117, 907, 828.

¹H NMR (400 MHz, CDCl₃) δ 7.69 (s, 4H, H_{ar}), 7.47 (s, 2H, H_{ar}), 7.31-7.06 (m, 18H, H_{ar}), 3.69 (d, $J = 12.9$ Hz, 2H, H₄), 1.33 (s, 9H, H₇₋₉).

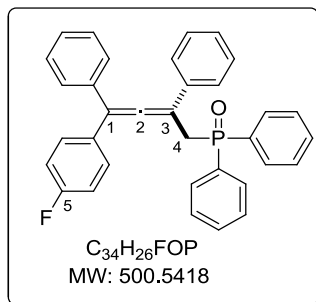
¹³C NMR (100 MHz, CDCl₃) δ 209.3 (d, $J = 8.1$ Hz, C, C₂), 150.4 (C, C₅), 136.2 (d, $J = 2.0$ Hz, C), 135.9 (d, $J = 5.1$ Hz, C), 132.9 (d, $J = 3.0$ Hz, C), 131.5 (d, $J = 2.0$ Hz, C), 130.9 (d, $J = 9.1$ Hz, 3CH), 128.8

(3CH), 128.6 (4CH), 128.5 (d, $J = 3.0$ Hz, CH), 128.4 (2CH), 128.3 (2CH), 127.8 (4CH), 127.3 (d, $J = 11.1$ Hz, 2CH), 126.3 (2CH), 125.3 (2CH), 113.9 (d, $J = 2.0$ Hz, C, C₃), 100.3 (d, $J = 7.1$ Hz, C, C₁), 34.6 (C, C₆), 32.9 (d, $J = 72.7$ Hz, CH₂, C₄), 31.5 (3CH₃, C₇₋₉).

³¹P NMR (162 MHz, CDCl₃) δ 29.4.

HRMS (ESI) calcd for C₃₈H₃₅Na OP ([M + Na]⁺) 561.2318 found 561.2296.

(4-(4-Fluorophenyl)-2,4-diphenylbuta-2,3-dien-1-yl)diphenylphosphineoxide (9)



To a solution of CuI (400 mg, 2.15 mmol, 5 equiv) and LiBr (190 mg, 2.15 mmol, 5 equiv) in THF (15 mL) was added 4-fluorophenyl magnesium bromide (6.94 mL of a 0.31 M in Et₂O, 2.15 mmol, 5 equiv) slowly at -78 °C. The mixture was warmed to 0 °C for 20 min, then the temperature was cooled down to -78 °C and a solution of **4** (0.20 g, 0.42 mmol, 1 equiv) in THF (15 mL) was added dropwise.

At the end of the addition, the mixture was warmed rt. After stirring for 4 h and completion of reaction (TLC monitoring), the reaction mixture was diluted with EtOAc (20 mL) and quenched a saturated aqueous NH₄Cl solution (10 mL) and NH₃ solution (5 mL) was added. The aqueous phase was extracted with EtOAc (3x20 mL) and the combined organic layers were washed with brine (10 mL), dried over anhydrous MgSO₄, filtered and concentrated under reduced pressure. Purification by column chromatography on silica gel using EtOAc/pentane (1/1) as eluent afforded **9** (199 mg, 92% yield) as a yellow solid.

R_f = 0.34 (EtOAc/petroleum ether: 1/1).

m.p. = 183–185 °C.

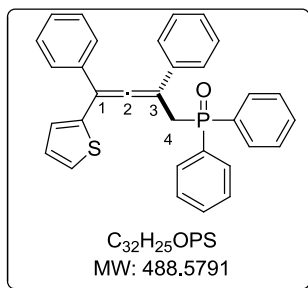
IR (neat): $\tilde{\nu}$ (cm⁻¹) = 3057, 2922, 2216, 2191, 2160, 2113, 2054, 1994, 1598, 1505, 1492, 1437, 1197, 1158, 833.

¹H NMR (300 MHz, CDCl₃) δ 7.70 (dd, $J = 11.4, 7.3$ Hz, 4H, H_{ar}), 7.46 (d, $J = 7.6$ Hz, 3H, H_{ar}), 7.24 (s, 15H, H_{ar}), 6.94 (d, $J = 8.4$ Hz, 2H, H_{ar}), 3.68 (d, $J = 12.7$ Hz, 2H, H₄).

¹³C NMR (100 MHz, CDCl₃) δ 209.1 (d, $J = 7.1$ Hz, C, C₂), 162.4 (d, ¹J_{CF} = 247.5 Hz, C, C₅), 136.0 (d, $J = 2.0$ Hz, C), 135.9 (d, $J = 6.1$ Hz, C), 133.0 (C), 132.4 (C), 132.0 (d, $J = 3.0$ Hz, CH), 131.6 (CH), 131.5 (CH), 130.9 (CH), 130.8 (CH), 130.7 (CH), 130.4 (CH), 128.7 (3CH), 128.6 (4H), 128.5 (2CH), 128.4 (2CH), 127.5 (d, $J = 11.1$ Hz, CH), 126.2 (4CH), 115.3 (CH), 115.1 (CH), 113.4 (d, $J = 2.0$ Hz, C, C₃), 100.5 (d, $J = 7.0$ Hz, C, C₁), 32.7 (d, $J = 71.7$ Hz, CH₂, C₄).

³¹P NMR (122 MHz, CDCl₃) δ 29.2.

HRMS (ESI) calcd for C₃₄H₂₆FOPNa ([M + Na]⁺) 523.15975 found 523.15926.

(2,4-Diphenyl-4-(thiophen-2-yl)buta-2,3-dien-1-yl)diphenylphosphine oxide (10)

To a solution of CuI (180 mg, 0.96 mmol, 3 equiv) and LiBr (80 mg, 0.96 mmol, 3 equiv) in THF (4 mL) was slowly added 2-thienylmagnesium bromide (0.96 mL of a 1 M in THF, 0.96 mmol, 3 equiv) at $-78\text{ }^{\circ}\text{C}$. The mixture was warmed to $0\text{ }^{\circ}\text{C}$ for 20 min, then the temperature was cooled down to $-60\text{ }^{\circ}\text{C}$ and a solution of **4** (150 mg, 0.32 mmol, 1 equiv) in THF (4 mL) was added dropwise. At the end of the addition, the mixture was slowly warmed to rt. After stirring for 20 h, the reaction mixture was quenched with a saturated aqueous NH_4Cl solution (10 mL) and diluted with EtOAc (10 mL). The aqueous phase was extracted with EtOAc (3x20 mL). The combined organic layers were washed with brine (10 mL), dried over anhydrous MgSO_4 , filtered and concentrated under reduced pressure. Purification by column chromatography on silica gel using EtOAc/pentane (1/1) as eluent afforded **10** (90 mg, 58% yield) as a yellow solid.

$R_f = 0.39$ (EtOAc/pentane: 6/4).

m.p. = $153\text{--}154\text{ }^{\circ}\text{C}$.

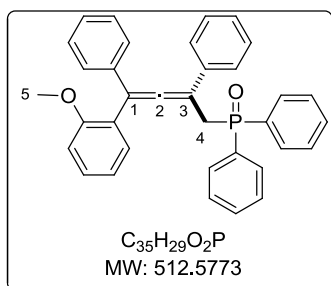
IR (neat): $\tilde{\nu}$ (cm^{-1}) = 3057, 2185, 2152, 2028, 1959, 1593, 1494, 1439, 1201, 1121, 828.

$^1\text{H NMR}$ (400 MHz, CDCl_3) δ 7.77-7.67 (m, 4H, H_{ar}), 7.51-7.48 (m, 2H, H_{ar}), 7.40-7.34 (m, 3H, H_{ar}), 7.31-7.25 (m, 8H, H_{ar}), 7.22-7.18 (m, 4H, H_{ar}), 6.95-6.93 (m, 2H, H_{ar}), 3.71 (d, $J = 13.6\text{ Hz}$, 2H, H_4).

$^{13}\text{C NMR}$ (100 MHz, CDCl_3) δ 209.0 (d, $J = 8.1\text{ Hz}$, C, C_2), 139.1 (d, $J = 3.0\text{ Hz}$, C), 135.7 (d, $J = 2.0\text{ Hz}$, C), 135.6 (d, $J = 5.1\text{ Hz}$, C), 133.5 (d, $J = 23.2\text{ Hz}$, C), 132.5 (d, $J = 22.0\text{ Hz}$, C), 131.6 (d, $J = 3.0\text{ Hz}$, CH), 131.5 (d, $J = 3.0\text{ Hz}$, CH), 131.0 (CH), 130.9 (d, $J = 7.1\text{ Hz}$, 2CH), 130.8 (d, $J = 8.1\text{ Hz}$, CH), 128.6 (2CH), 128.5 (2CH), 128.4 (3CH), 128.3 (2CH), 128.2 (CH), 127.9 (CH), 127.5 (CH), 127.3 (CH), 126.7 (CH), 126.5 (2CH), 125.5 (CH), 108.8 (d, $J = 3.0\text{ Hz}$, C, C_3), 101.1 (d, $J = 7.1\text{ Hz}$, C, C_1), 32.9 (d, $J = 69.7\text{ Hz}$, CH_2 , C_4).

$^{31}\text{P NMR}$ (162 MHz, CDCl_3) δ 29.4.

HRMS (ESI) calcd for $\text{C}_{32}\text{H}_{25}\text{OPSNa}$ ($[\text{M} + \text{Na}]^+$) 511.12559 found 511.12517.

(4-(2-Methoxyphenyl)-2,4-diphenylbuta-2,3-dien-1-yl)diphenylphosphine oxide (11)

To a solution of CuI (410 mg, 2.15 mmol, 5 equiv) and LiBr (190 mg, 2.15 mmol, 5 equiv) in THF (20 mL) was added slowly, 2-methoxyphenylmagnesium bromide (2.15 mL of a 1 M in THF, 2.15 mmol, 5 equiv) at $-60\text{ }^{\circ}\text{C}$. The reaction mixture was warmed to $0\text{ }^{\circ}\text{C}$ for 1h, then the temperature was cooled down to $-60\text{ }^{\circ}\text{C}$ and a

solution of **4** (200 mg, 0.43 mmol) in THF (20 mL) was added dropwise. At the end of the addition, the mixture was slowly warmed to rt. After stirring for 17 h, the reaction mixture was quenched with a solution of saturated aqueous a 2:1 $\text{NH}_4\text{Cl}:\text{NH}_3$ solution and diluted with EtOAc (10 mL). The aqueous phase was extracted with EtOAc (3x20 mL). The combined organic layers were washed with brine (10 mL), dried over anhydrous MgSO_4 , filtered and concentrated under reduced pressure. Purification by column chromatography on silica gel using EtOAc/pentane (1/1) as eluent afforded **11** (146 mg, 66% yield) as a light yellow solid.

$R_f = 0.33$ (EtOAc/pentane: 1/1).

m.p 173–175 °C.

IR (neat): $\tilde{\nu}$ (cm^{-1}) = 3080, 3057, 2931, 2917, 2361, 2340, 1897, 1818, 1569, 1492, 1436, 1199, 1182, 1182, 1119, 1049, 987, 837.

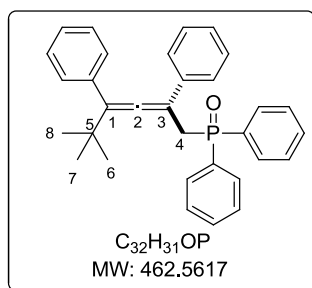
^1H NMR (400 MHz, CDCl_3) δ 7.78-7.67 (m, 4H, H_{ar}), 7.56 (bd, $J = 8.4$ Hz, 2H, H_{ar}), 7.31-7.12 (m, 14H, H_{ar}), 7.03-7.00 (m, 2H, H_{ar}), 6.95-6.88 (m, 2H, H_{ar}), 3.75 (dd, $J = 15.2, 13.2$ Hz, 2H, H_4), 3.65 (s, 3H, H_5).

^{13}C NMR (100 MHz, CDCl_3) δ 208.9 (d, $J = 9.1$ Hz, C, C_2), 157.4 (C), 136.3 (d, $J = 3.0$ Hz, C), 135.8 (d, $J = 4.0$ Hz, C), 133.3 (d, $J = 37.4$ Hz, C), 132.3 (d, $J = 37.4$ Hz, C), 131.6 (d, $J = 2.0$ Hz, CH), 131.5 (d, $J = 4.1$ Hz, 2CH), 131.5 (CH), 131.2 (d, $J = 9.1$ Hz, CH), 131.0 (d, $J = 10.1$ Hz, CH), 129.1 (CH), 128.4 (d, $J = 2.0$ Hz, CH), 128.4 (2CH), 128.3 (d, $J = 2.0$ Hz, 2CH), 128.2 (2CH), 127.2 (2CH), 127.1 (CH), 126.9 (CH), 126.8 (2CH), 125.0 (d, $J = 3.0$ Hz, C), 120.8 (2CH), 111.3 (2CH), 109.2 (d, $J = 3.0$ Hz, C, C_3), 100.2 (d, $J = 9.1$ Hz, C, C_1), 55.6 (CH_3 , C_5), 32.9 (d, $J = 69.7$ Hz, CH_2 , C_4).

^{31}P NMR (162 MHz, CDCl_3) δ 30.1.

HRMS (ESI) calcd. for $\text{C}_{35}\text{H}_{29}\text{O}_2\text{PNa}$ ($[\text{M} + \text{Na}]^+$) 535.17974 found 535.17859.

5,5-Dimethyl-2,4-diphenylhexa-2,3-dien-1-yl)diphenylphosphine oxide (**12**)



To a solution of CuI (400 mg, 2.10 mmol, 5 equiv) and LiBr (180 mg, 2.10 mmol, 5 equiv) in THF (10 mL) was added *t*-butylmagnesiumchloride (1.1 mL of a 2 M in Et_2O , 2.10 mmol, equiv) slowly at -78°C . The reaction mixture was warmed to 0°C for 20 min, then the temperature was cooled down to -60°C and a solution of **4** (0.20 g, 0.42 mmol) in THF (10 mL) was added. At the

end of the addition, the mixture was warmed to rt. After stirring for 4 h and completion of reaction (TLC monitoring), the reaction mixture was diluted with EtOAc (10 mL) and quenched a saturated aqueous NH_4Cl solution (20 mL) was added. The aqueous phase was extracted with EtOAc (3x10 mL). The combined organic layers were washed with brine (10 mL), dried over

anhydrous MgSO_4 , filtered and concentrated under reduced pressure. Purification by column chromatography on silica gel using EtOAc/pentane (7/3) as eluent afforded **12** (152 mg, 78% yield) as a yellow solid.

$R_f = 0.53$ (EtOAc/pentane: 8/2).

m.p. = 124–127°C.

IR (neat): $\tilde{\nu}$ (cm^{-1}) = 3659, 3388, 3056, 2962, 2866, 1950, 1492, 1437, 1392, 1199, 1118, 814.

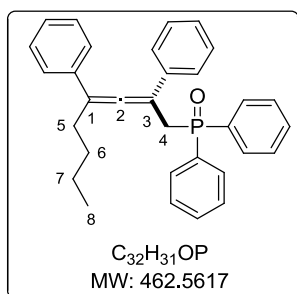
$^1\text{H NMR}$ (400 MHz, CDCl_3) δ 7.70 (dd, $J = 11.5, 7.9$ Hz, 2H, H_{ar}), 7.60 (dd, $J = 11.4, 7.9$ Hz, 2H, H_{ar}), 7.44–7.33 (m, 7H, H_{ar}), 7.22–7.13 (m, 8H, H_{ar}), 7.05–7.00 (m, 2H, H_{ar}), 3.53 (dd, $J = 13.4, 2.6$ Hz, 2H, H_4), 1.11 (d, $J = 0.9$ Hz, 9H, H_{6-8}).

$^{13}\text{C NMR}$ (100 MHz, CDCl_3) δ 204.0 (d, $J = 8.1$ Hz, C, C_2), 137.2 (d, $J = 4.0$ Hz, C), 136.7 ($J = 3.0$ Hz, C), 134.2 ($J = 6.1$ Hz, C), 133.4 ($J = 9.1$ Hz, C), 131.7 (d, $J = 3.0$ Hz, C), 131.6 (d, $J = 3.0$ Hz, CH), 131.2 ($J = 5.1$ Hz, 2CH), 131.1 ($J = 5.1$ Hz, 2CH), 129.3 (3CH), 128.7 (CH), 128.6 (CH), 128.4 (4CH), 128.3 (CH), 127.8 (3CH), 126.7 ($J = 6.1$ Hz, CH), 125.9 (2CH), 119.8 (d, $J = 2.0$ Hz, C, C_3), 97.7 (d, $J = 8.1$ Hz, C, C_1), 35.9 (d, $J = 3.0$ Hz, C, C_5), 32.9 (d, $J = 69.7$ Hz, CH_2 , C_4), 29.7 (CH_3 , C_{6-8}).

$^{31}\text{P NMR}$ (162 MHz, CDCl_3) δ 29.4.

HRMS (ESI) calcd for $\text{C}_{32}\text{H}_{31}\text{NaOP}$ ($[\text{M} + \text{Na}]^+$) 485.2005 found 485.2016.

2,4-Diphenylocta-2,3-dien-1-yl)diphenylphosphine oxide (**13**)



To a solution of CuI (47 mg, 0.26 mmol, 1.2 equiv) and LiBr (19 mg, 0.26 mmol, 1.2 equiv) in THF (5 mL) was added *n*-BuLi (0.10 mL of a 2.5 M in THF, 0.26 mmol, 1.2 equiv) slowly at -78 °C. The mixture was warmed at 0 °C for 30 min, then the temperature was cooled down -40 °C and a solution of **4** (100 mg, 0.22 mmol, 1 equiv) in THF (10 mL) was added dropwise. At the end of the addition, the mixture was

warmed to 0 °C. After stirring for 1 h and completion of reaction (TLC monitoring), a saturated aqueous NH_4Cl solution (20 mL) was added. The aqueous phase was extracted with EtOAc (3x10 mL). The combined organic layers were washed with brine (10 mL), dried over anhydrous MgSO_4 , filtered and concentrated under reduced pressure. Purification by column chromatography on silica gel using EtOAc/pentane (1/1) as eluent afforded **13** (100 mg, 98% yield) as a light yellow solid.

$R_f = 0.33$ (EtOAc/pentane: 1/1).

m.p. = 120–121 °C.

IR (neat): $\tilde{\nu}$ (cm^{-1}) = 3056, 2929, 2206, 2191, 2160, 2030, 1968, 1483, 1435, 1187, 1120, 887, 740.

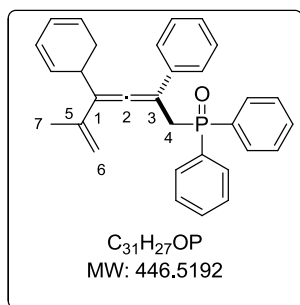
¹H NMR (300 MHz, CDCl₃) δ 7.77-7.66 (m, 4H, H_{ar}), 7.47 (d, *J* = 7.3 Hz, 1H, H_{ar}), 7.39-7.13 (m, 15H, H_{ar}), 3.66 (d, *J* = 12.8 Hz, 2H, H₄), 2.28 (dd, *J* = 9.0, 5.9 Hz, 1H, H₅), 2.21-2.07 (m, 1H, H₅), 1.29 (dd, *J* = 9.8, 6.2 Hz, 4H, H_{6,7}), 0.83 (t, *J* = 7.0 Hz, 3H, H₈).

¹³C NMR (100 MHz, CDCl₃) δ 207.6 (d, *J* = 8.1 Hz, C, C₂), 136.5 (d, *J* = 5.1 Hz, C), 135.9 (d, *J* = 2.0 Hz, C), 133.5 (d, *J* = 23.2 Hz, C), 132.5 (d, *J* = 22.2 Hz, C), 131.6 (d, *J* = 3.0 Hz, C), 131.5 (d, *J* = 3.0 Hz, CH), 131.0 (d, *J* = 3.0 Hz, CH), 130.9 (d, *J* = 3.0 Hz, 2CH), 128.5 (d, *J* = 2.0 Hz, CH), 128.4 (3CH), 128.4 (d, *J* = 1.0 Hz, CH), 128.3 (3CH), 126.9 (d, *J* = 8.1 Hz, CH), 126.3 (3CH), 126.1 (3CH), 110.5 (d, *J* = 2.0 Hz, C, C₃), 100.1 (d, *J* = 8.1 Hz, C, C₁), 32.4 (d, *J* = 70.7 Hz, CH₂, C₄), 30.2 (d, *J* = 3.0 Hz, CH₂, C₅), 30.0 (CH₂, C₆), 22.8 (CH₂, C₇), 13.9 (CH₃, C₈).

³¹P NMR (162 MHz, CDCl₃) δ 29.4.

HRMS (ESI) calcd for C₃₂H₃₁OP ([M + Na]⁺) 485.20047 found 485.19921.

(5-Methyl-2,4-diphenylhexa-2,3,5-trien-1-yl)diphenylphosphine oxide (17)



To a solution of 2-bromopropene (0.95 mL, 10.75 mmol, 5.0 equiv) in Et₂O (15 mL) was added dropwise *t*-BuLi (15.4 mL of a 1.4 M in pentane, 21.5 mmol, 10.0 equiv) at – 80 °C. The reaction was warmed to – 60 °C. After stirring for 1 h, a solution of ZnCl₂ (11.3 mL of 1 M in Et₂O, 11.3 mmol, 5.25 equiv) was added. The mixture was warmed to 0 °C for 1 h, then the temperature was cooled down to – 40 °C and the mixture of **4** (1.0 g, 2.15 mmol, 1 equiv) and Pd(PPh₃)₄ (120 mg, 0.11 mmol, 0.05 equiv) in THF (34 mL) was added dropwise. At the end of the addition, the mixture was slowly warmed to rt. After stirring for 17 h, the reaction was quenched with a saturated aqueous NH₄Cl solution (40 mL) and diluted with EtOAc (40 mL). The aqueous phase was extracted with EtOAc (2x30 mL). The combined organic layers were washed with brine (20 mL), dried over anhydrous MgSO₄, filtered and concentrated under reduced pressure. Purification by silica gel chromatography with EtOAc/Pentane (1/1) as eluent afforded **17** (490 mg, 51% yield) as yellow solid.

R_f: 0.45 (EtOAc/Pentane: 1/1).

m.p. = 120–123 °C.

IR (neat): $\tilde{\nu}$ (cm⁻¹) = 3056, 3024, 2972, 2918, 1963, 1891, 1617, 1492, 1437, 1199, 1119, 804, 765.

¹H NMR (300 MHz, CDCl₃) δ 7.81-7.69 (m, 4H, H_{ar}), 7.49-7.18 (m, 16H, H_{ar}), 5.08 (s, 1H, H₆), 4.91 (s, 1H, H₆), 3.67 (d, *J* = 13.5 Hz, 2H, H₄), 1.81 (s, 3H, H₇).

¹³C NMR (75 MHz, CDCl₃) δ 208.4 (d, *J* = 8.3 Hz, C, C₂), 140.0 (d, *J* = 3.0 Hz, C, C₅), 136.2 (d, *J* = 5.2 Hz, C), 135.9 (d, *J* = 3.0 Hz, C), 133.3 (d, *J* = 28.5 Hz, C), 132.0 (d, *J* = 28.5 Hz, C), 131.7 (d, *J* = 3.0 Hz, CH), 131.6 (d, *J* = 3.0 Hz, CH), 131.0 (d, *J* = 6.8 Hz, 2CH), 130.9 (d, *J* = 6.8 Hz, 2CH), 129.1 (2CH),

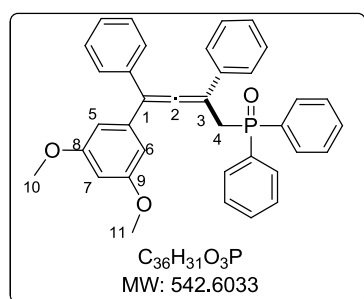
128.6 (d, $J = 12.0$ Hz, CH), 128.5 (d, $J = 12.0$ Hz, 4CH), 128.3 (CH), 128.2 (3CH), 127.2 (d, $J = 6.0$ Hz, CH), 126.2 (2CH), 116.0 (CH₂, C₆), 115.3 (d, $J = 2.2$ Hz, C, C₃), 99.7 (d, $J = 8.2$ Hz, C, C₁), 32.8 (d, $J = 69.0$ Hz, CH₂, C₄), 21.9 (CH₃, C₇).

³¹P NMR (162 MHz, CDCl₃) δ 29.3.

HRMS (ESI) calcd. for C₃₁H₂₇OPNa ([M + Na]⁺) 469.16917 found 469.16835.

Chiral HPLC separation Chromatographic conditions: Chiralpak AD-H (250 x 10 mm), hexanes/ethanol (80/20) as mobile phase, flow-rate = 5 mL/min, UV detection at 254 nm. Retention time for first enantiomer ((–, CD 254nm)-**17**) = 5.55 min (*ee* > 99%), for second enantiomer ((+, CD 254 nm)-**17**, [α_D] 65.0 (*c* 1.05, CHCl₃) = 7.44 min (*ee* > 98%).

(4-(3,5-Dimethoxyphenyl)-2,4-diphenylbuta-2,3-dien-1-yl)diphenylphosphine oxide (**18**)



To a solution of 1-bromo-3,5-dimethoxybenzene (1.65 g, 7.60 mmol, 5 equiv) in Et₂O (35 mL) was added dropwise *n*-BuLi (3.80 mL of a 2 M in hexanes, 7.60 mmol, 5 equiv) at 0 °C. After stirring for 2 h at this temperature, a solution of ZnCl₂ (7.60 mL of 1 M in Et₂O, 7.60 mmol, 5 equiv) was added and the mixture was stirred for 1 h. The temperature was cooled down to – 40 °C and a

mixture of **4** (700 mg, 1.51 mmol, 1 equiv) and Pd(PPh₃)₄ (87 mg, 0.076 mmol, 0.05 equiv) in THF (50 mL) was added dropwise. At the end of the addition, the mixture was warmed to rt. After stirring for 14 h, the reaction was quenched with saturated aqueous NH₄Cl solution (40 mL) and diluted with EtOAc (20 mL). The aqueous layer was extracted with EtOAc (2x20 mL). The combined organic layers were washed with brine (20 mL), dried over anhydrous MgSO₄, filtered and concentrated under reduced pressure. Purification by silica gel chromatography with EtOAc/Pentane (1/1) as eluent afforded **18** (613 mg, 75% yield) as a white solid.

R_f = 0.13 (EtOAc/pentane: 1/1).

m.p. = 62–63 °C.

IR (neat): $\tilde{\nu}$ (cm⁻¹) = 3080, 2935, 2837, 2222, 1714, 1591, 1438, 1203, 1155, 1103, 1066, 731.

¹H NMR (300 MHz, CDCl₃) δ 7.73-7.65 (m, 4H, H_{ar}), 7.45 (d, $J = 7.5$ Hz, 2H, H_{ar}), 7.31-7.20 (m, 14H, H_{ar}), 6.45 (d, $J = 3.0$ Hz, 2H, H_{5,6}), 6.38 (bt, $J = 2.1$ Hz, 1H, H₇), 3.73 (s, 6H, H_{10,11}), 3.69 (d, $J = 13.2$ Hz, 2H, H₄).

¹³C NMR (75 MHz, CDCl₃) δ 209.1 (d, $J = 8.3$ Hz, C, C₂), 160.7 (2C, C_{8,9}), 138.3 (d, $J = 3.0$ Hz, C), 135.9 (d, $J = 5.3$ Hz, C), 135.8 (d, $J = 3.8$ Hz, C), 133.3 (C), 132.0 (C), 131.6 (CH), 131.5 (CH), 131.0 (d, $J = 3.0$ Hz, 2CH), 130.9 (d, $J = 3.0$ Hz, 2CH), 128.8 (3CH), 128.6 (3CH), 128.5 (d, $J = 3.0$ Hz, CH), 128.4 (d, $J = 3.0$ Hz, CH), 128.3 (4CH), 127.5 (d, $J = 6.0$ Hz, CH), 126.3 (2CH), 114.1 (d, $J = 2.2$ Hz, C,

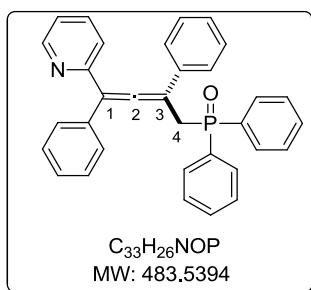
C₃), 107.1 (2CH, C₅, 6), 100.6 (d, *J* = 7.5 Hz, C₁), 99.8 (CH, C₇), 55.5 (2CH₃, C_{10,11}), 32.9 (d, *J* = 69.6 Hz, CH₂, C₄).

³¹P NMR (122 MHz, CDCl₃) δ 29.4.

HRMS (ESI) calcd. for C₃₆H₃₁O₃PNa ([M + Na]⁺) 565.1903 found 565.1921.

Chiral HPLC separation Chromatographic conditions: Lux Cellulose-4 (250 x 10 mm), hexanes/ethanol (80/20) as mobile phase, flow-rate = 5 mL/min, UV detection at 280 nm. Retention time for first enantiomer ((-, CD 254nm)-**18**, [α_D] 16.9 (c 0.5, CHCl₃)) = 8.01 min (*ee* > 98.5%), for second enantiomer ((+, CD 254 nm)-**18**) = 8.78 min (*ee* >97%).

(2,4-Diphenyl-4-(pyridin-2-yl)buta-2,3-dien-1-yl)diphenylphosphine oxide (**25a**)



Procedure 1

To a solution of acetate **4** (200 mg, 0.4 mmol, 1 equiv) in THF (3 mL) was added 2-pyridylzinc bromide (4.30 mL of a 0.5 M in THF, 2.15 mmol, 5 equiv) at – 60 °C. The mixture was slowly warmed to rt. After stirring for 23 h, the reaction mixture was quenched with a saturated aqueous NH₄Cl solution (10 mL) and diluted with EtOAc (10

mL). The aqueous phase was extracted with EtOAc (3x20 mL). The combined organic layers were washed with brine (10 mL), dried over anhydrous MgSO₄, filtered and concentrated under reduced pressure. Purification by column chromatography on silica gel using EtOAc/cyclohexane (1:1 to 3:1) as eluent afforded **25a** (88 mg, 41% yield) as a brown solid.

Procedure 2

To a solution of freshly prepared PhMgBr (10.7 mL of a 1 M in Et₂O, 10.7 mmol, 5 equiv) in THF (15 mL) was added ZnCl₂ (10.7 mL of 1 M in Et₂O, 10.7 mmol, 5 equiv) at 0 °C. After stirring for 30 min, the reaction was cooled down to – 40 °C and the mixture of pyridyl acetate **24a** (1.0 g, 2.20 mmol, 1 equiv) and Pd(PPh₃)₄ (120 mg, 0.10 mmol, 0.05 equiv) in THF (10 mL) was added dropwise. At the end of the addition, the mixture was slowly warmed to rt. After stirring for 18 h, the reaction was quenched with a saturated aqueous NH₄Cl solution (30 mL) and diluted with Et₂O (30 mL). The aqueous phase was extracted with EtOAc (2x30 mL). The combined organic layers were washed with brine (20 mL), dried over anhydrous MgSO₄, filtered and concentrated under reduced pressure. Purification by silica gel chromatography with EtOAc/toluene (6/4) as eluent afforded **25a** (350 mg, 33% yield) as a brown solid.

R_f = 0.14 (EtOAc/cyclohexane: 3/1).

m.p. = 143–145 °C.

IR (neat): $\tilde{\nu}$ (cm^{-1}) = 3055, 2918, 2224, 2018, 1987, 1585, 1564, 1493, 1468, 1437, 1195, 1119, 842.

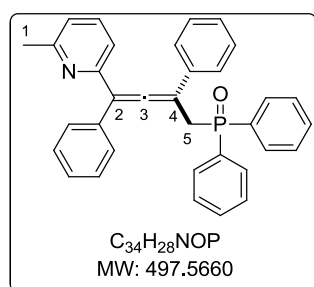
^1H NMR (300 MHz, CDCl_3) δ 8.58 (d, J = 4.5 Hz, 1H, H_{ar}), 7.78-7.66 (m, 5H, H_{ar}), 7.59-7.49 (m, 6H, H_{ar}), 7.37-7.15 (m, 13H, H_{ar}), 3.76 (d, J = 13.2 Hz, 2H, H_4).

^{13}C NMR (100 MHz, CDCl_3) δ 211.2 (d, J = 9.1 Hz, C, C_2), 155.3 (d, J = 3.0 Hz, C), 149.1 (CH), 136.6 (CH), 135.3 (d, J = 5.1 Hz, C), 134.9 (d, J = 2.0 Hz, C), 133.3 (d, J = 28.3 Hz, C), 132.3 (d, J = 32.3 Hz, C), 132.1 (d, J = 6.8 Hz, CH), 131.9 (d, J = 2.2 Hz, CH), 131.6 (d, J = 2.2 Hz, CH), 131.5 (d, J = 2.2 Hz, CH), 130.9 (d, J = 5.1 Hz, CH), 130.8 (d, J = 5.1 Hz, CH), 128.8 (2CH), 128.6 (2CH), 128.5 (d, J = 12.1 Hz, 2CH), 128.4 (d, J = 12.1 Hz, 2CH), 128.3 (d, J = 12.1 Hz, 2CH), 128.2 (2CH), 127.6 (d, J = 9.1 Hz, CH), 126.4 (CH), 124.7 (CH), 121.9 (CH), 114.5 (d, J = 3.0 Hz, C, C_1), 101.5 (d, J = 7.1 Hz, C, C_3), 31.7 (d, J = 70.7 Hz, CH_2 , C_4).

^{31}P NMR (162 MHz, CDCl_3) δ 29.3.

HRMS (ESI) calcd for $\text{C}_{33}\text{H}_{27}\text{NOP}$ ($[\text{M} + \text{Na}]^+$) 484.18248 found 484.18260.

4-(6-Methylpyridin-2-yl)-2,4-diphenylbuta-2,3-dien-1-yl)diphenylphosphine oxide (**25b**)



To a solution of freshly prepared PhMgBr (12.6 mL of a 1 M in THF, 12.6 mmol, 5 equiv) in THF (15 mL) was added ZnCl_2 (12.6 mL of a 1 M in Et_2O , 12.6 mmol, 5 equiv) at 0 °C. After stirring for 30 min, the reaction was cooled down to -40 °C and the mixture of acetate **24b** (1.21 g, 2.5 mmol, 1 equiv) and $\text{Pd}(\text{PPh}_3)_4$ (150 mg, 0.13 mmol, 0.05 equiv) in THF (10 mL) was added dropwise. At the end of the

addition, the mixture was warmed to rt. After stirring for 18 h, a saturated aqueous NH_4Cl solution (50 mL) was added and diluted with Et_2O (50 mL). The aqueous phase was extracted with EtOAc (2x30 mL). The combined organic layers were washed with brine (20 mL), dried over anhydrous MgSO_4 , filtered and concentrated under reduced pressure. Purification by silica gel chromatography with EtOAc /toluene (6/4) as eluent afforded **25b** (1.02 g, 82% yield) as yellow solid.

R_f = 0.32 (EtOAc /toluene: 6/4).

m.p. = 143–145 °C.

IR (neat): $\tilde{\nu}$ (cm^{-1}) = 3055, 2960, 2927, 2873, 2189, 2094, 1998, 1587, 1571, 1492, 1438, 1193, 1118, 1091, 948, 904.

^1H NMR (400 MHz, CDCl_3) δ 7.76-7.71 (m, 4H, H_{ar}), 7.55 (d, J = 8.0 Hz, 2H, H_{ar}), 7.46 (t, J = 7.6 Hz, 1H, H_{ar}), 7.33-7.17 (m, 15H, H_{ar}), 7.00 (d, J = 7.6 Hz, 1H, H_{ar}), 3.73 (dd, J = 12.8, 3.6 Hz, 2H, H_5), 2.51 (s, 3H, H_1).

¹³C NMR (100 MHz, CDCl₃) δ 211.2 (d, *J* = 9.1 Hz, C, C₃), 157.8 (2C), 154.7 (d, *J* = 3.0 Hz, C), 136.8 (CH), 135.4 (d, *J* = 5.1 Hz, C), 134.9 (d, *J* = 3.0 Hz, C), 133.5 (C), 132.6 (d, *J* = 15.2 Hz, CH), 131.6 (CH), 131.5 (d, *J* = 3.0 Hz, CH), 131.4 (d, *J* = 3.0 Hz, CH), 131.0 (d, *J* = 9.1 Hz, CH), 130.9 (d, *J* = 9.1 Hz, CH), 128.7 (3CH), 128.4 (3CH), 128.3 (CH), 128.1 (2CH), 127.4 (d, *J* = 13.1 Hz, 3CH), 126.5 (2CH), 121.7 (d, *J* = 13.1 Hz, 2CH), 114.3 (d, *J* = 9.0 Hz, C₄), 101.6 (d, *J* = 7.1 Hz, C, C₂), 32.9 (d, *J* = 69.7 Hz, CH₂, C₅), 24.7 (CH₃, C₁).

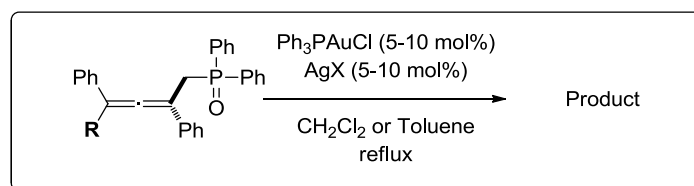
³¹P NMR (162 MHz, CDCl₃) δ 29.6.

HRMS (ESI) calcd. for C₃₄H₂₈NOPH ([M + H]⁺) 498.19813 found 498.19824.

Chiral HPLC separation Chromatographic conditions: Lux Cellulose-2 (250 x 10 mm), hexanes/ethanol (50/50) as mobile phase, flow-rate = 5 mL/min, UV detection at 254 nm. Retention time for (*aR*)-**25b** = 5.24 min (*ee* > 99%, [*α*_D] –55.9 (c 0.5, CHCl₃)); for (*aS*)-**25b** = 6.27 min (*ee* > 98%, [*α*_D] 55.9 (c 0.5, CHCl₃)).

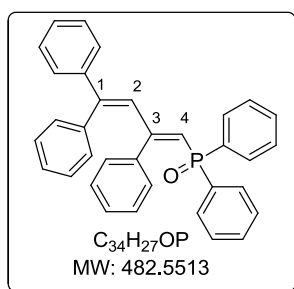
2.2. Gold(I)-catalyzed reactions

GP1: General procedure for gold(I)-catalyzed reactions



To a solution of Ph₃PAuCl (0.05-0.10 equiv) in dry and degassed solvent was added AgSbF₆ or AgOTf (0.05 - 0.10 equiv). After 5 min stirring at rt, the formation of AgCl was observed as a white solid. Then, a solution of allene (1 equiv) in dry and degassed solvent (final concentration 0.05 M) was added. The reaction was stirred at reflux temperature and monitored by TLC. When the reaction was complete, the mixture was filtered through a short pad of Celite® and washed with Et₂O and CH₂Cl₂. The solution was concentrated under reduced pressure. Subsequent purification by flash-chromatography on silica gel afforded the desired products.

(Z)-Diphenyl(2,4,4-triphenylbuta-1,3-dien-1-yl)phosphineoxide (27)



The compound was prepared according to the general procedure **GP1** using Ph₃PAuCl (10 mg, 0.02 mmol), AgSbF₆ (7 mg, 0.020 mmol) and allene **5** (95 mg, 0.20 mmol) in toluene (4 mL). The reaction was refluxed for 24 h. The residue was purified by silica gel chromatography with EtOAc/pentane (1/1) as eluent to afford diene **27** (33 mg, 34% yield) as a white solid.

R_f = 0.25 (EtOAc/pentane: 1/1).

m.p. = 138–140 °C.

IR (neat): $\tilde{\nu}$ (cm⁻¹) = 3055, 2925, 2853, 1572, 1538, 1492, 1438, 1193, 1182, 1118, 753, 718.

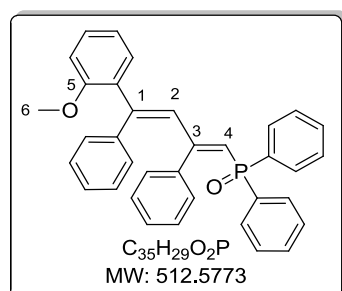
¹H NMR (300 MHz, C₆D₆) δ 8.07 (s, 1H, H₂), 7.91-7.83 (m, 4H, H_{ar}), 7.36-7.33 (m, 2H, H_{ar}), 7.11-7.04 (m, 11H, H_{ar}), 6.86-6.76 (m, 8H, H_{ar}), 6.42 (d, *J* = 22.5 Hz, 1H, H₄).

¹³C NMR (100 MHz, CDCl₃) δ 159.2 (C, C₃), 148.9 (C), 142.1 (C), 142.6 (d, *J* = 16.1 Hz, C), 139.5 (C, C₁), 135.0 (d, *J* = 105.0 Hz, C), 133.9 (C), 131.6 (d, *J* = 3.0 Hz, 2CH), 131.3 (d, *J* = 9.1 Hz, 2CH), 130.4 (3CH), 128.7 (2CH), 128.6 (2CH), 128.4 (3CH), 128.2 (d, *J* = 3.0 Hz, CH), 128.1 (3CH), 127.8 (4CH), 127.4 (2CH), 127.3 (d, *J* = 5.1 Hz, CH), 125.7 (d, *J* = 8.1 Hz, CH, C₂), 121.7 (d, *J* = 102.0 Hz, CH, C₄).

³¹P NMR (122 MHz, C₆D₆) δ 17.4.

HRMS (ESI) calcd for C₃₄H₂₇OPNa ([M + Na]⁺) 505.1692, found 505.1675.

((1Z,3E)-4-(2-Methoxyphenyl)-2,4-diphenylbuta-1,3-dien-1-yl) diphenylphosphineoxide (28)



The compound was prepared according to the general procedure **GP1** using Ph₃PAuCl (9.0 mg, 0.018 mmol), AgSbF₆ (5.0 mg, 0.018 mmol) and allene **11** (100 mg, 0.18 mmol) in CH₂Cl₂ (4 mL). The reaction was refluxed for 20 h. The residue was purified by silica gel chromatography with EtOAc/pentane (1/1) as eluent to afford diene **28** (30 mg, 32% yield) as a white solid.

R_f = 0.29 (EtOAc/pentane: 1/1).

m.p. = 159–160 °C.

IR (neat): $\tilde{\nu}$ (cm⁻¹) = 3055, 2959, 2853, 2833, 1598, 1539, 1489, 1436, 1243, 1183, 1117, 1027, 752.

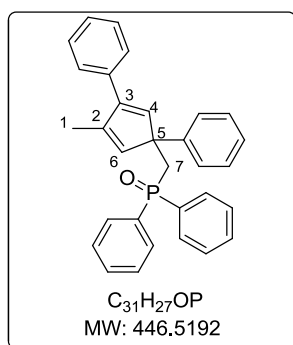
¹H NMR (300 MHz, C₆D₆) δ 8.44 (s, 1H, H₂), 7.93-7.88 (m, 4H, H_{ar}), 7.45-7.43 (m, 2H, H_{ar}), 7.13-7.11 (m, 2H, H_{ar}), 7.07-6.98 (m, 10H, H_{ar}), 6.84-6.80 (m, 4H, H_{ar}), 6.59 (t, *J* = 7.6 Hz, 1H, H_{ar}), 6.31 (dd, *J* = 22.8, 1.2 Hz, 1H, H₄), 6.06 (d, *J* = 7.6 Hz, 1H, H_{ar}), 2.94 (s, 3H, H₆).

^{13}C NMR (100 MHz, C_6D_6) δ 159.8 (C, C_3), 156.8 (C, C_5), 146.5 (C), 142.6 (d, $J = 16.2$ Hz, C), 141.8 (C, C_1), 136.2 (d, $J = 103.9$ Hz, C), 132.3 (CH), 131.6. (d, $J = 9.1$ Hz, 2CH), 131.3 (d, $J = 2.0$ Hz, CH), 129.3 (2CH), 129.1 (2CH), 128.7 (2CH), 128.6 (2CH), 128.4 (3CH), 128.2 (3CH), 127.9 (3CH), 127.7 (3CH), 127.4 (d, $J = 2.8$ Hz, CH), 126.9 (d, $J = 8.1$ Hz, CH, C_2), 122.7 (d, $J = 100.6$ Hz, CH, C_4), 120.0 (CH), 110.2 (CH), 54.4 (CH_3 , C_6).

^{31}P NMR (162 MHz, C_6D_6) δ 17.3.

HRMS (ESI) calcd for $\text{C}_{35}\text{H}_{29}\text{O}_2\text{PNa}$ ($[\text{M} + \text{Na}]^+$) 535.1797, found 535.1818.

((3-Methyl-1,4-diphenylcyclopenta-2,4-dien-1-yl)methyl)diphenylphosphineoxide (29)



The compound was prepared according to the general procedure **GP1** using Ph_3PAuCl (16 mg, 0.008 mmol), AgOTf (4 mg, 0.016 mmol) and the allene **17** (70 mg, 0.16 mmol) in CH_2Cl_2 (3 mL). The reaction was refluxed for 18 h. The residue was purified by silica gel chromatography with EtOAc/Pentane (3/7) as eluent afforded cyclic product **29** (50 mg, 71% yield) as a white solid.

$R_f = 0.25$ (EtOAc/Pentane:3/7).

IR (neat): $\tilde{\nu}$ (cm^{-1}) = 3080, 2970, 2923, 1892, 1674, 1597, 1437, 1395, 1379, 1273, 1118, 1101, 742.

^1H NMR (400 MHz, CDCl_3) δ 7.62-7.54 (m, 4H, H_{ar}), 7.35-7.21 (m, 13H, H_{ar}), 7.07-7.00 (m, 3H, H_{ar}), 6.78 (d, $J = 2.4$ Hz, 1H, H_4), 6.46 (bs, 1H, H_6), 3.02 (d, $J = 10.4$ Hz, 2H, H_7), 1.79 (s, 3H, H_1).

^{13}C NMR (100 MHz, CDCl_3) δ 145.4 (C, C_3), 141.2 (d, $J = 8.1$ Hz, C), 139.9 (d, $J = 6.1$ Hz, CH), 139.7 (C, C_2), 139.0 (d, $J = 5.1$ Hz, CH), 136.3 (C), 134.7 (d, $J = 55.6$ Hz, C), 133.7 (d, $J = 56.6$ Hz, C), 131.2 (d, $J = 2.0$ Hz, CH), 131.1 (d, $J = 2.0$ Hz, CH), 130.8 (d, $J = 10.1$ Hz, CH), 130.6 (d, $J = 9.1$ Hz, CH), 128.4 (d, $J = 11.1$ Hz, 2CH), 128.3 (3CH), 128.2 (3CH), 128.1 (2CH), 127.9 (2CH), 127.2 (3CH, $\text{C}_{4,ar}$), 126.7 (C, C_6), 57.4 (d, $J = 3.4$ Hz, C, C_5), 38.3 (d, $J = 69.7$ Hz, CH_2 , C_7), 15.2 (CH_3 , C_1).

^{31}P NMR (162 MHz, CDCl_3) δ 27.3.

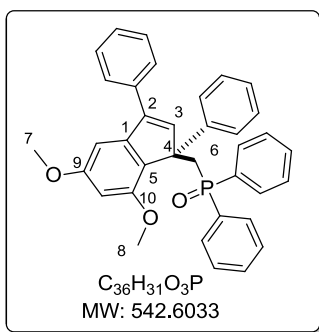
HRMS (ESI) calcd. for $\text{C}_{31}\text{H}_{27}\text{OPNa}$ ($[\text{M} + \text{Na}]^+$) 469.1692 found 469.1695.

Chirality transfer study: The isolated (–, CD 254 nm-**29**) by chiral HPLC analysis, 55 %*ee*.

((5,7-Dimethoxy-1,3-diphenyl-1H-inden-1-yl)methyl)diphenylphosphineoxide (30)

The compound was prepared according to the general procedure **GP1** using Ph_3PAuCl (4.0 mg, 0.009 mmol), AgSbF_6 (1.7 mL of 0.005 M in CH_2Cl_2 , 0.009 mmol) and the allene **18** (98 mg, 0.18

mmol) in CH₂Cl₂ (8.5 mL). The reaction was refluxed for 4 h. The residue was purified by silica gel chromatography with EtOAc/Pentane (gradient: from 3/7 until 1/1) as eluent afforded cyclic product **30** (83 mg, 85% yield) as a pale yellow solid.



R_f = 0.2 (EtOAc/pentane: 3/7).

m.p = 69–70 °C.

IR (neat): $\tilde{\nu}$ (cm⁻¹) = 3078, 2963, 1600, 1583, 1493, 1437, 1352, 1216, 1195, 1141, 1077, 696.

¹H NMR (400 MHz, CDCl₃) δ 7.78-7.73 (m, 2H, H_{ar}), 7.57-7.32 (m, 13H, H_{ar}), 7.23-7.07 (m, 5H, H_{ar}), 6.84 (bs, 1H, H₃), 6.42 (d, *J* = 1.6 Hz, 1H, H_{ar}), 5.99 (d, *J* = 2.0 Hz, 1H, H_{ar}), 3.91 (dd, *J* = 14.8, 6.0 Hz, 1H, H₆), 3.74 (s, 3H, H_{7 or 8}), 3.65 (s, 3H, H_{7 or 8}), 3.51 (d, *J* = 15.6 Hz, 1H, H₆).

¹³C NMR (100 MHz, CDCl₃) δ 161.5 (C, C_{9 or 10}), 155.8 (C, C_{9 or 10}), 145.7 (C, C₂), 143.3 (d, *J* = 3.0 Hz, CH, C₃), 142.1 (d, *J* = 13.1 Hz, C, C₅), 141.0 (C, C₁), 135.7 (d, *J* = 99.0, C), 135.5 (C), 132.2 (d, *J* = 98.0 Hz, C), 131.4 (d, *J* = 3.0 Hz, C), 130.7 (d, *J* = 10.1 Hz, CH), 130.5 (CH), 130.4 (d, *J* = 9.1 Hz, CH), 128.6 (d, *J* = 11.1 Hz, CH), 128.5 (2CH), 128.3 (2CH), 128.1 (4CH), 127.7 (2CH), 127.6 (CH), 127.5 (CH), 126.5 (4CH), 98.9 (CH), 96.5 (CH), 56.1 (d, *J* = 3.0 Hz, C, C₄), 55.6 (CH₃, C_{7 or 8}), 55.1 (CH₃, C_{7 or 8}), 35.5 (d, *J* = 71.7, CH₂, C₆).

³¹P NMR (122 MHz, CDCl₃) δ 27.5.

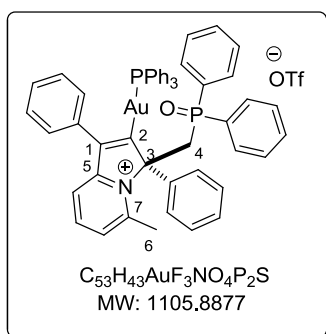
HRMS (ESI) calcd for C₃₆H₃₁NaO₃P ([M + Na]⁺) 565.1903, found 565.1917.

Chirality transfer study: The isolated (–, CD 254 nm-**30**), 97.3% *ee*, [α _D] 131.43 (c 0.5, CHCl₃)

2.3. Pyridinyl vinylphosphine oxides

2.3.1. Preparation of cationic vinylgold complex

3-((Diphenylphosphoryl)methyl)-5-methyl-1,3-diphenyl-3*H*-indolizin-4-ium-2-yl) (triphenylphosphine)aurate(I) trifluoromethanesulfonate (**31**)



A mixture of PPh₃AuCl (140 mg, 0.28 mmol, 1 equiv) and AgOTf (72 mg, 0.28 mmol, 1 equiv) in DCE (4 mL) was stirred for 3.5h at rt. The mixture was filtered to remove the AgCl and added to a solution of **25b** (200 mg, 0.39 mmol, 1.4 equiv) in DCE (10 mL) and heated at 50 °C. After 16 h, the mixture was monitored by ³¹P NMR, the peak at 45 ppm [Ph₃PAu⁺TfO⁻] disappeared. The mixture was concentrated under reduced pressure to afford **31** (250 mg, 81%

yield) as a brown solid.

m.p. = 140–144 °C.

IR (neat): $\tilde{\nu}$ (cm⁻¹) = 3056, 2925, 2302, 1618, 1480, 1436, 1257, 1148, 1110, 1029.

¹H NMR (600 MHz, CD₂Cl₂) δ 8.30 (t, *J* = 8.1 Hz, 1H, H_{ar}), 7.83-7.75 (m, 5H, H_{ar}), 7.60-7.52 (m, 7H, H_{ar}), 7.49-7.46 (m, 10H, H_{ar}), 7.42-7.39 (m, 3H, H_{ar}), 7.37 (s, 1H), 7.34-7.28 (m, 9H, H_{ar}), 7.07-7.04 (m, 2H, H_{ar}), 4.53 (dd, *J* = 15.6, 11.4 Hz, 1H, H₄), 4.03 (dd, *J* = 15.6, 12.0 Hz, 1H, H₄), 2.61 (s, 3H, H₆).

¹³C NMR (151 MHz, CD₂Cl₂) δ 203.9 (d, *J* = 113.2 Hz, C, C₂), 159.1 (d, *J* = 7.6 Hz, C, C₇), 155.3 (C, C₅), 146.1 (CH), 138.0 (C, C₁), 136.6 (d, *J* = 10.6 Hz, C), 134.7 (C), 134.6 (d, *J* = 1.5 Hz, C), 134.6 (d, *J* = 102.7 Hz, C), 134.5 (4CH), 134.4 (3CH), 134.2 (CH), 133.0 (CH), 132.7 (d, *J* = 1.5 Hz, CH), 132.3 (d, *J* = 1.5 Hz, 2CH), 132.2 (d, *J* = 1.5 Hz, 2CH), 131.8 (d, *J* = 9.1 Hz, CH), 130.5 (d, *J* = 9.1 Hz, 2CH), 130.4 (3CH), 130.0 (2CH), 129.8 (3CH), 129.7 (3CH), 129.5 (CH), 129.2 (CH), 129.1 (CH), 128.9 (CH), 128.7 (CH), 128.4 (CH), 128.3 (CH), 128.1 (C), 124.3 (CH), 122.7 (C), 120.6 (C), 117.8 (CH), 91.1 (C, C₃), 33.3 (d, *J* = 67.9 Hz, CH₂, C₄), 21.3 (CH₃, C₆).

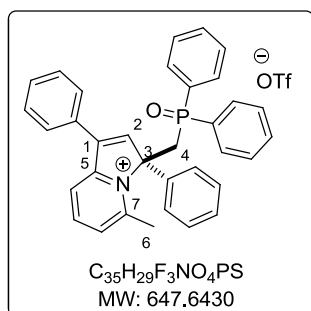
³¹P NMR (122 MHz, CD₂Cl₂) δ 42.7 (PPh₃), 23.6 (P=O).

¹⁹F NMR (282 MHz, CD₂Cl₂) δ -78.6.

HRMS (ESI) calcd. for C₅₂H₄₃AuNOP₂⁺ [M⁺] 956.2480 found 956.2514.

2.3.2. Synthesis of Cationic indolizinyll derivatives

3-((Diphenylphosphoryl)methyl)-5-methyl-1,3-diphenyl-3H-indolizin-4-ium trifluoromethanesulfonate (**39**)



To a solution of gold complex **31** (140 mg, 0.13 mmol, 1 equiv) in CH₂Cl₂ (2 mL) was added dropwise TfOH (12 μ L, 0.14 mmol, 1.08 equiv) and stirred at rt. After 6 h at rt, a black solid precipitated. The reaction was monitored by ³¹P NMR until disappearance of the peaks of the starting gold complex **31**. The black solid was removed by filtration on Celite®. Water was added to the residue (10 mL) and the

resultant mixture was diluted with CH₂Cl₂ (5 mL). The aqueous phase was extracted with CH₂Cl₂ (3x10 mL). The combined organic layers were washed with brine (10 mL), dried over anhydrous MgSO₄, filtered and concentrated under reduced pressure. The residue was purified by precipitation in CH₂Cl₂ and Et₂O to afford **39** (84 mg, quant) as a pale brown solid.

m.p. = 207–209 °C.

IR (neat): $\tilde{\nu}$ (cm⁻¹) 3057, 2924, 1632, 1573, 1496, 1437, 1279, 1152, 1102, 1031.

¹H NMR (300 MHz, CD₂Cl₂) δ 8.39 (t, *J* = 8.1 Hz, 1H, H_{ar}), 7.92-7.82 (m, 4H, H_{ar}), 7.61-7.39 (m, 15H, H_{ar}), 7.26-7.24 (m, 1H, H₂), 7.04-7.00 (m, 3H, H_{ar}), 4.53 (dd, *J* = 15.9, 11.1 Hz, 1H, H₄), 3.95 (dd, *J* = 15.9, 12.0 Hz, 1H, H₄), 2.66 (s, 3H, H₆).

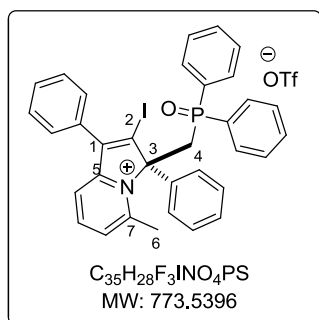
¹³C NMR (100 MHz, CD₂Cl₂) δ 156.9 (d, *J* = 5.9 Hz, C, C₇), 146.6 (CH), 146.0 (CH, C₂), 135.0 (C, C₅), 134.7 (d, *J* = 10.8 Hz, CH), 134.2 (CH), 133.7 (d, *J* = 102.9 Hz, C), 132.9 (d, *J* = 8.8 Hz, C), 132.8 (d, *J* = 9.4 Hz, C), 132.7 (C), 132.5 (d, *J* = 101.3 Hz, CH), 131.3 (d, *J* = 9.7 Hz, CH), 130.8 (d, *J* = 7.1 Hz, CH), 130.7 (d, *J* = 2.3 Hz, 2CH), 130.6 (d, *J* = 2.8 Hz, 2CH), 130.0 (2CH), 129.9 (CH), 129.8 (CH), 129.7 (CH), 129.6 (2CH), 129.5 (2CH), 129.2 (2CH), 128.3 (CH), 127.5 (2CH), 125.8 (CH), 119.7 (CH), 84.0 (d, *J* = 4.8 Hz, C, C₃), 32.2 (d, *J* = 66.3 Hz, CH₂, C₄), 21.6 (CH₃, C₆).

³¹P NMR (162 MHz, CD₂Cl₂) δ 24.1.

¹⁹F NMR (376 MHz, CD₂Cl₂) δ -78.7.

HRMS (ESI) calcd. for C₃₄H₂₉NOP⁺ [M⁺] 498.1981 found 498.1983.

3-((Diphenylphosphoryl)methyl)-2-iodo-5-methyl-1,3-diphenyl-3*H*-indolizin-4-ium (40)



To a solution of gold complex **31** (70 mg, 0.060 mmol, 1 equiv) in CH₂Cl₂ (2 mL) was added I₂ (30 mg, 0.13 mmol, 2.1 equiv). The resulting mixture was stirred at rt. After 2 h, the water was added (5 mL) and the mixture was diluted with CH₂Cl₂ (5 mL). The aqueous phase was extracted with CH₂Cl₂ (3x5 mL). The combined organic layers were dried over anhydrous MgSO₄, filtered and concentrated under reduced pressure. The residue was purified by precipitation in CH₂Cl₂ and Et₂O to afford **40** (33 mg, 70% yield) as a pale brown solid.

m.p. = 138–140 °C.

IR (neat): $\tilde{\nu}$ (cm⁻¹) 3055, 2964, 2917, 2362, 1622, 1566, 1493, 1437, 1259, 1193, 1119, 1030.

¹H NMR (400 MHz, CD₂Cl₂) δ 8.35 (t, *J* = 8.0 Hz, 1H), 7.85 (d, *J* = 12.1 Hz, 2H), 7.78-7.66 (m, 3H), 7.65-7.46 (m, 14H), 7.39 (dd, *J* = 7.8, 0.7 Hz, 1H), 7.25 (dd, *J* = 7.3, 2.2 Hz, 2H), 4.15 (dd, *J* = 15.7, 11.6 Hz, 1H), 4.00 (dd, *J* = 15.7, 10.1 Hz, 1H), 2.49 (s, 3H).

¹³C NMR (100 MHz, CD₂Cl₂) δ 157.1 (C, C₇), 156.7 (C, C₂), 147.3 (CH), 141.8 (C, C₅), 133.4 (d, *J* = 2.0 Hz, CH), 133.3 (d, *J* = 3.0 Hz, CH), 133.2 (C), 132.7 (d, *J* = 109.1 Hz, C), 132.6 (d, *J* = 112.1 Hz, C), 132.6 (d, *J* = 4.0 Hz, C), 132.5 (C), 132.2 (C), 131.6 (d, *J* = 10.1 Hz, CH), 131.4 (CH), 131.0 (CH), 130.8 (d, *J* = 9.1 Hz, CH), 129.8 (d, *J* = 4.0 Hz, CH), 129.8 (CH), 129.7 (3CH), 129.6 (d, *J* = 5.1 Hz, 2CH), 129.4 (2CH), 129.1 (d, *J* = 12.1 Hz, 2CH), 127.0 (2CH), 123.3 (CH), 119.5 (CH), 87.4 (d, *J* = 5.1 Hz, C, C₃), 31.9 (d, *J* = 64.6 Hz, CH₂, C₄), 22.1 (CH₃, C₆).

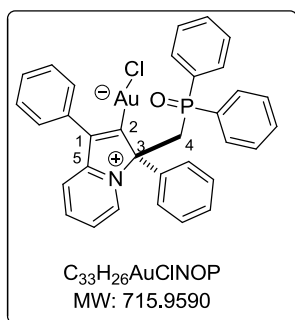
³¹P NMR (162 MHz, CD₂Cl₂) δ 22.4.

^{19}F NMR (376 MHz, CD_2Cl_2) δ -78.7.

HRMS (ESI) calcd for $\text{C}_{34}\text{H}_{28}\text{INOP}$ [M^+] 624.0948, found 624.0930.

2.4. Pyridinyl-vinylgold(I) chloride complexes

Chloro(3-((diphenylphosphoryl)methyl)-1,3-diphenyl-3H-indolizin-4-ium-2-yl)aurate(I) (**41a**)



A mixture of **25a** (50 mg, 0.11 mmol, 1 equiv) and $\text{AuCl}(\text{Me}_2\text{S})$ (40 mg, 0.14 mmol, 1 equiv) in CH_2Cl_2 (3.5 mL, 0.04 M) was stirred for 4 h. The mixture was concentrated under reduced pressure to afford gold complex **41a** (95 mg, quant) as a yellow solid. The product was recrystallized by diffusion of cyclohexane into the solution of crude product in CH_2Cl_2 to give colorless crystals quantitatively.

R_f = 0.09 (100% EtOAc).

m.p. = 229–231 °C.

IR (neat): $\tilde{\nu}$ (cm^{-1}) = 3057, 3027, 2980, 2854, 1959, 1895, 1819, 1618, 1569, 1539, 1477, 1438, 1337, 1298, 1199, 1072.

^1H NMR (600 MHz, CD_2Cl_2) δ 8.40 (d, J = 6.6 Hz, 1H, H_{ar}), 8.21 (t, J = 7.8 Hz, 1H, H_{ar}), 7.78-7.75 (m, 3H, H_{ar}), 7.73-7.69 (m, 2H, H_{ar}), 7.56-7.52 (m, 1H, H_{ar}), 7.49-7.46 (m, 3H, H_{ar}), 7.40-7.37 (m, 11H, H_{ar}), 7.22-7.20 (m, 2H, H_{ar}), 4.44 (dd, J = 15.0, 8.4 Hz, 1H, H_4), 3.57 (dd, J = 15.0, 13.8 Hz, 1H, H_4).

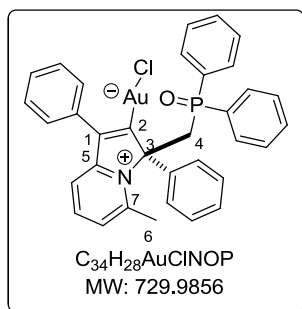
^{13}C NMR (151 MHz, CD_2Cl_2) δ 191.0 (C, C_2), 159.1 (C, C_5), 145.1 (CH), 140.8 (CH), 138.7 (d, J = 9.1 Hz, C), 136.4 (C), 135.6 (C), 135.2 (d, J = 101.2 Hz, C), 134.8 (C, C_1), 132.6 (dd, J = 4.5, 3.0 Hz, CH), 132.2 (d, J = 9.1 Hz, CH), 131.5 (d, J = 101.2 Hz, C), 130.4 (d, J = 9.1 Hz, CH), 129.3 (4CH), 129.8 (CH), 129.4 (d, J = 12.1 Hz, 3CH), 128.8 (d, J = 12.1 Hz, 4CH), 128.6 (CH), 126.2 (3CH), 120.1 (CH), 119.4 (CH), 88.9 (d, J = 4.5 Hz, C, C_3), 36.5 (d, J = 67.9 Hz, CH_2 , C_4).

^{31}P NMR (162 MHz, CDCl_3) δ 25.2.

HRMS (ESI) calcd. for $\text{C}_{33}\text{H}_{26}\text{AuClINOPNa}$ ($[\text{M} + \text{Na}]^+$) 738.0998 found 738.0095.

Chloro(3-((diphenylphosphoryl)methyl)-5-methyl-1,3-diphenyl-3H-indolizin-4-ium-2-yl)aurate(I) (**41b**)

A mixture of allene **25b** (100 mg, 0.20 mmol) and $\text{AuCl}(\text{Me}_2\text{S})$ (60 mg, 0.20 mmol) in CH_2Cl_2 (3.5 mL, 0.04 M) was stirred for 4 h. The mixture was concentrated under reduced pressure to afford the gold complex **41b** (180 mg, quant) as yellow solid. The product was recrystallized by diffusion



of cyclohexane into the solution of crude product in CH_2Cl_2 to give colorless crystals quantitatively.

$R_f = 0.09$ (100% EtOAc).

m.p. = 229–230 °C.

IR (neat): $\tilde{\nu}$ (cm^{-1}) = 3056, 3024, 2980, 2854, 1898, 1821, 1617, 1573, 1544, 1484, 1437, 1401, 1312, 1173, 1117, 1110, 999.

1H NMR (600 MHz, CD_2Cl_2) δ 8.07 (t, $J = 7.8$ Hz, 1H, H_{ar}), 7.85–7.77 (m, 4H, H_{ar}), 7.57–7.29 (m, 15H, H_{ar}), 7.22 (d, $J = 7.8$ Hz, 1H, H_{ar}), 7.12–7.10 (m, 2H, H_{ar}), 4.73 (dd, $J = 15.0, 10.2$ Hz, 1H, H_4), 3.75 (d, $J = 14.4$, 1H, H_4), 2.55 (s, 3H, H_6).

^{13}C NMR (151 MHz, CD_2Cl_2) δ 191.6 (C, C_2), 160.4 (C, C_7), 155.6 (C, C_5), 145.1 (CH), 137.5 (d, $J = 9.1$ Hz, C), 135.7 (C), 135.4 (d, $J = 101.2$ Hz, C), 135.1 (C), 134.9 (C), 132.7 (d, $J = 3.0$ Hz, CH), 132.6 (d, $J = 3.0$ Hz, CH), 132.4 (d, $J = 9.1$ Hz, CH), 131.1 (d, $J = 101.2$ Hz, CH), 130.4 (d, $J = 9.1$ Hz, CH), 130.1 (3CH), 129.5 (d, $J = 12.1$ Hz, CH), 129.4 (2CH), 129.3 (2CH), 128.9 (4CH), 128.6 (4CH), 128.4 (CH), 90.3 (C, C_3), 33.8 (d, $J = 67.9$ Hz, CH_2 , C_4), 21.6 (CH_3 , C_6).

^{31}P NMR (162 MHz, CD_2Cl_2) δ 23.9.

HRMS (ESI) calcd. for $C_{34}H_{28}AuClINOPNa$ ($[M + Na]^+$) 752.11548 found 752.11538 .

Specific optical rotation of (R)-41b (Prepared from (*aR*)-25b) $[\alpha]_D -64.1$ (*c* 0.5, $CHCl_3$)

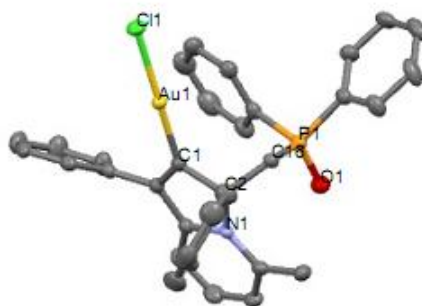


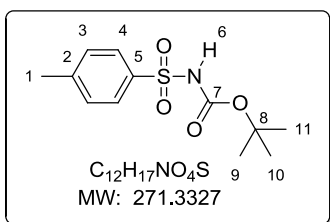
Figure S1. Structure of (R)-41b by X-ray crystallography based on (*aR*)-25b as the allene substrate. (The hydrogen atoms are omitted for clarity)

2.5. Preparation of 1,6-enyne substrates

2.5.1. Heteroatom-tethered 1,6-enynes

***N*-Boc-*p*-toluenesulfonamide (42)**

To a solution of *p*-toluenesulfonamide (7.0 g, 40.9 mmol, 1 equiv) in CH_2Cl_2 (40 mL) were added Et_3N (6.25 mL, 45.0 mmol, 1.1 equiv) and DMAP (0.5 g, 4.09 mmol, 0.1 equiv) at rt .The reaction



was cooled to 0°C and the solution of Boc₂O (10.3 g, 47.0 mmol, 1.15 equiv) in CH₂Cl₂ (80 mL) was added to the solution and then warmed to rt. After stirring for 15 h, the mixture was concentrated under reduced pressure and then dissolved in Et₂O (50 mL). A solution of 1 M HCl (20 mL) was added. The aqueous phase was extracted with Et₂O (3 x 50 mL). The combined organic layers were washed with brine (20 mL), dried over anhydrous MgSO₄, filtered and concentrated under reduced pressure. Purification by recrystallization in refluxing hexanes/Et₂O (9/1) for overnight afforded **42** (11.3 g, quant) as a white solid.

The characterization data were identical to those previously reported.^[4,5]

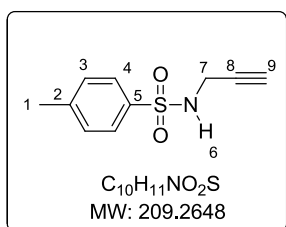
R_f = 0.13 (EtOAc/ pentane: 1/9).

IR (neat): $\tilde{\nu}$ (cm⁻¹) = 3263, 2981, 1746, 1706, 1433, 1307, 1089, 1057, 910, 704.

¹H NMR (300 MHz, CDCl₃) δ 7.90 (d, *J* = 8.4 Hz, 2H, H₄), 7.34 (d, *J* = 8.5 Hz, 2H, H₃), 2.45 (s, 3H, H₁), 1.38 (s, *J* = 0.7 Hz, 9H, H₉₋₁₁).

¹³C NMR (75 MHz, CDCl₃) δ 149.2 (C, C₇), 144.9 (C, C₅), 136.1 (C, C₂), 129.6 (2CH, C₄), 128.4 (2CH, C₃), 84.2 (C, C₈), 28.0 (3CH₃, C₉₋₁₁), 21.8 (CH₃, C₁).

4-Methyl-N-(prop-2-yn-1-yl)benzenesulfonamide (**43**)



To a solution of **42** (2.0 g, 7.4 mmol, 1 equiv) in DMF (8 mL) was added K₂CO₃ (1.5 g, 11.1 mmol, 1.5 equiv). After stirring at rt for 1 h, 3-bromoprop-1-yne (0.66 mL, 7.4 mmol, 1 equiv) was added and the resulting yellow solution was stirred for 18 h. The reaction mixture was diluted with Et₂O (20 mL) and quenched with a saturated aqueous NH₄Cl solution (30 mL). The aqueous phase was extracted with Et₂O (2x30 mL). The combined organic layers were washed with brine (20 mL), dried over anhydrous MgSO₄, filtered and concentrated under reduced pressure. The resulting crude product was dissolved in CH₂Cl₂ (6 mL) and trifluoroacetic acid (2.2 mL, 24.5 mmol, 3.3 equiv) was added. The resulting mixture was stirred for 20 h. A solution of NaHCO₃ (20 mL) was slowly added, then the mixture was diluted with CH₂Cl₂ (20 mL). The aqueous phase was extracted with CH₂Cl₂ (3x 20 mL). The combined organic layers were washed with brine (20 mL), dried over anhydrous MgSO₄, filtered and concentrated under reduced pressure. Purification by column chromatography on silica gel using EtOAc/pentane (1/9) as eluent afforded **43** (1.20 g, 77% yield) as a pale brown solid pure product **43**.

The characterization data were identical to those previously reported.^[4,5]

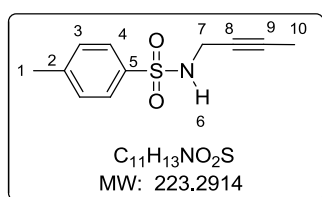
$R_f = 0.13$ (EtOAc/ pentane: 1/9).

IR (neat): $\tilde{\nu}$ (cm^{-1}) = 3267, 2125, 1597, 1474, 1430, 1323, 1156.

$^1\text{H NMR}$ (400 MHz, CDCl_3) δ 7.77 (d, $J = 8.3$ Hz, 2H, H_4), 7.32 (d, $J = 8.0$ Hz, 2H, H_3), 3.83 (d, $J = 2.5$ Hz, 2H, H_7), 2.43 (s, 3H, H_1), 2.11 (t, $J = 2.5$ Hz, 1H, H_9).

$^{13}\text{C NMR}$ (75 MHz, CDCl_3) δ 144.0 (C, C_5), 136.7 (C, C_2), 129.9 (2CH, C_4), 127.5 (2CH, C_3), 73.2 (C, C_8), 73.1 (CH, C_9), 33.0 (CH_2 , C_7), 21.7 (CH_3 , C_1).

***N*-(but-2-ynyl)-4-methyl(benzenesulfonamide (44)**



To a solution of **42** (2.0 g, 7.4 mmol, 1 equiv) in DMF (8 mL) was added K_2CO_3 (1.5 g, 11.1 mmol, 1.5 equiv). After stirring at rt for 1h, 1-bromobut-2-yne (0.66 mL, 7.4 mmol, 1 equiv) was added and the resulting yellow solution was stirred for 18 h. The reaction mixture

was diluted with Et_2O (20 mL) and quenched with a saturated aqueous NH_4Cl solution (30 mL). The aqueous phase was extracted with Et_2O (2x30 mL) and the combined organic layers were washed with brine (20 mL), dried over anhydrous MgSO_4 , filtered and concentrated under reduced pressure. The resulting crude product was dissolved in CH_2Cl_2 (6 mL) and trifluoroacetic acid (2.20 mL, 24.5 mmol, 3.3 equiv) was added. The resulting mixture was stirred overnight (24 h). The solution of NaHCO_3 (20 mL) was slowly added, then the mixture was diluted with CH_2Cl_2 (20 mL). The aqueous phase was extracted with CH_2Cl_2 (3x20 mL). The combined organic layers were washed with brine (20 mL), dried over anhydrous MgSO_4 , filtered and concentrated under reduced pressure. Purification by column chromatography on silica gel using EtOAc/pentane (1/9) as eluent afforded **44** (1.10 g, 67% yield) as a pale brown solid without purification.

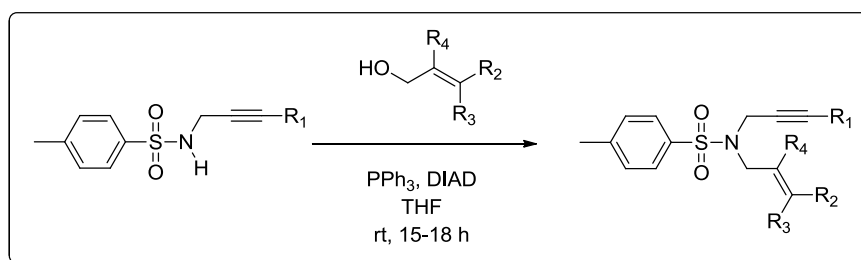
The characterization data were identical to those previously reported.^[4,5]

$R_f = 0.13$ (EtOAc/ pentane: 1/9).

IR (neat): $\tilde{\nu}$ (cm^{-1}) = 3257, 2919, 2299, 2228, 1597, 1435, 1380, 1153.

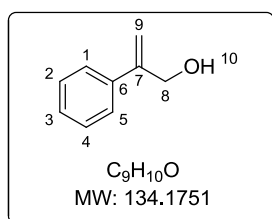
$^1\text{H NMR}$ (400 MHz, CDCl_3) δ 7.77 (d, $J = 8.3$ Hz, 2H, H_4), 7.31 (d, $J = 8.0$ Hz, 2H, H_3), 4.40 (bs, 1H, H_6), 3.77 (dq, $J = 4.9, 2.4$ Hz, 2H, H_7), 2.43 (s, 3H, H_1), 1.61 (t, $J = 2.4$ Hz, 3H, H_{10}).

$^{13}\text{C NMR}$ (100 MHz, CDCl_3) δ 143.4 (C, C_5), 136.8 (C, C_2), 129.4 (2CH, C_4), 127.4 (2CH, C_3), 80.9 (C, C_8), 73.3 (C, C_9), 33.2 (CH_2 , C_7), 21.4 (CH_3 , C_1), 3.1 (CH_3 , C_{10}).

GP2: General procedure for the synthesis of Nitrogen-tethered 1,6-enyne derivatives

To a solution of **43** (1.0 equiv) or **44** (1.0 equiv) in freshly distilled THF at rt were added triphenyl phosphine (1.5 equiv) and the desired allylic alcohol (1.5 equiv). Diisopropylazodicarboxylate (1.5 equiv) was added dropwise to the mixture. The resulting yellow-orange mixture was stirred at rt for 15-18 h. The mixture was diluted with EtOAc (50 mL) and quenched with a saturated aqueous NH_4Cl solution (50 mL). The aqueous phase was extracted with EtOAc (2x30 mL). The combined organic layers were washed with brine (20 mL), dried over anhydrous MgSO_4 , filtered and concentrated under reduced pressure. Purification by column chromatography on silica gel afforded the desired products.

The procedure and characterization of compounds **45**,^[6] **46**,^[7] **47**,^[8] **48**,^[8] **49**,^[8] **51**,^[8] **54**,^[9] **59**,^[10] **60**^[5], **61**,^[6] **62**^[5] have been described in the literature.

N*-(but-2-yn-1-yl)-4-methyl-*N*-(2-phenylallyl)benzenesulfonamide (**50**)a) Preparation of 2-Phenyl-2-propenol*

To a solution of PhMgBr (215.0 mL of 0.5 M in Et_2O , 89.30 mmol, 3 equiv) in Et_2O was added CuI (0.97g, 5.36 mmol, 0.19 equiv) at rt. The mixture was stirred for 30 min. The prop-2-yn-1-ol (1.56 mL, 28.83 mmol, 1 equiv) in Et_2O (36 mL) was then added dropwise. The reaction was stirred at reflux for 24 h. After cooling to rt, an aqueous solution of sat NH_4Cl (50 mL) was added slowly. The aqueous phase was extracted with Et_2O . The combined organic layers were washed with brine (20 mL), dried over anhydrous Na_2SO_4 , filtered and concentrated under reduced pressure. Purification by column chromatography on silica gel using EtOAc/pentane (1/10) as eluent afforded 2-Phenyl-2-propenol (1.55 g, 40% yield) as colourless oil. The characterization data were identical to those previously reported.^[11]

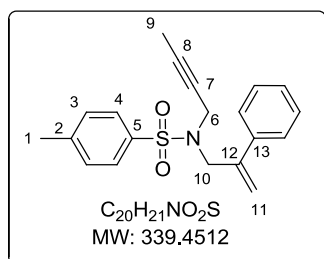
$R_f = 0.26$ (EtOAc/ pentane: 1/10).

IR (neat): $\tilde{\nu}$ (cm^{-1}) = 3264, 3056, 2922, 2860, 1948, 1898, 1875, 1631, 1573, 1495, 1407, 1234, 1111, 1024.

¹H NMR (400 MHz, CDCl₃) δ 7.55-7.23 (m, 5H, H₁₋₅), 5.49 (s, 1H, H₉), 5.37 (s, 1H, H₉), 4.53 (s, 2H, H₈), 2.32 (s, 1H, H₁₀).

¹³C NMR (75 MHz, CDCl₃) δ 146.9 (C, C₇), 138.4 (C, C₆), 128.2 (2CH, C_{1,4}), 127.6 (CH, C₃), 125.8 (2CH, C_{2,5}), 112.1 (CH₂, C₉), 64.3 (CH₂, C₈).

b) Preparation of **50**



The compound was prepared according to the general procedure **GP2** using **44** (0.64 g, 2.87 mmol, 1 equiv), 2-Phenyl-2-propenol (0.58 g, 4.31 mmol, 1.5 equiv), PPh₃ (1.13 g, 4.31 mmol, 1.5 equiv) and diisopropylazodicarboxylate (0.85 mL, 4.31 mmol, 1.5 equiv). Purification by chromatography on silica gel using EtOAc/pentane (1/20) as eluent afforded **50** (0.52 g, 53% yield) as a white solid.

The characterization data were identical to those previously reported.^[8]

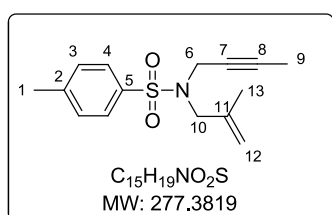
R_f = 0.33 (EtOAc/ pentane: 1/10).

IR (neat): $\tilde{\nu}$ (cm⁻¹) = 3087, 2920, 2853, 2221, 1630, 1598, 1445, 1400, 1347, 1186, 1063, 897.

¹H NMR (300 MHz, CDCl₃) δ 7.76 (d, *J* = 8.4 Hz, 2H, H₄), 7.53 (d, *J* = 1.8 Hz, 1H, H₃), 7.51 (d, *J* = 1.5 Hz, 1H, H₃), 7.37-7.29 (m, 5H, H_{ar}), 5.56 (s, 1H, H₁₁), 5.33 (d, *J* = 1.2 Hz, 1H, H₁₁), 4.23 (s, 2H, H₆), 3.93 (d, *J* = 2.4 Hz, 2H, H₁₀), 2.44 (s, 3H, H₁), 1.51 (t, *J* = 2.4 Hz, 3H, H₉).

¹³C NMR (100 MHz, CDCl₃) δ 143.3 (C, C₅), 141.5 (C, C₁₂), 137.9 (C, C₂), 135.7 (C, C₁₃), 129.2 (2CH, C₃), 128.4 (2CH, C₄), 128.0 (4CH) 126.3 (CH), 116.9 (CH₂, C₁₁), 82.0 (C, C₇), 71.3 (C, C₈), 50.0 (CH₂, C₁₀), 36.1 (CH₂, C₆), 21.5 (CH₃, C₁), 3.2 (CH₃, C₉).

N-(but-2-yn-1-yl)-4-methyl-N-(2-methylallyl)benzenesulfonamide (52)



The compound was prepared according to the general procedure **GP2** using **44** (0.5 g, 2.24 mmol, 1 equiv), 2-Phenyl-2-propenol (0.28 mL, 3.36 mmol, 1.5 equiv), PPh₃ (0.88 g, 3.36 mmol, 1.5 equiv) and diisopropylazodicarboxylate (0.66 mL, 3.36 mmol, 1.5 equiv). Purification by chromatography on silica gel using EtOAc/pentane

(1/10) as eluent afforded **52** (0.35 g, 56% yield) as a white solid.

The characterization data were identical to those previously reported.^[8]

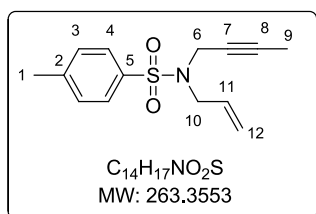
R_f = 0.32 (EtOAc/ pentane: 1/10).

IR (neat): $\tilde{\nu}$ (cm⁻¹) = 3079, 2919, 2851, 2221, 1673, 1598, 1442, 1348, 1160, 1096, 1016, 903.

¹H NMR (300 MHz, CDCl₃) δ 7.69 (d, *J* = 8.1 Hz, 2H, H₄), 7.25 (d, *J* = 8.0 Hz, 2H, H₃), 4.90 (s, 2H, H₁₂), 3.92 (d, *J* = 2.0 Hz, 2H, H₁₀), 3.65 (s, 2H, H₆), 2.37 (s, 3H, H₁), 1.71 (s, 3H, H₁₃), 1.45 (s, 3H, H₉).

^{13}C NMR (75 MHz, CDCl_3) δ 143.2 (C, C₅), 139.4 (C, C₂), 136.2 (C, C₁₁), 129.2 (2CH, C₄), 127.9 (2CH, C₃), 115.1 (CH₂, C₁₂), 81.6 (C, C₇), 71.4 (C, C₈), 52.4 (CH₂, C₁₀), 36.0 (CH₂, C₆), 21.4 (CH₃, C₁), 19.7 (CH₃, C₁₃), 3.1 (CH₃, C₉).

***N*-allyl-*N*-(but-2-yn-1-yl)-4-methylbenzenesulfonamide (53)**



The compound was prepared according to the general procedure **GP2**, using **44** (0.50 g, 2.24 mmol, 1 equiv), prop-2-en-1-ol (0.23 mL, 3.36 mmol, 1.5 equiv), PPh₃ (0.90 g, 3.36 mmol, 1.5 equiv) and diisopropylazodicarboxylate (0.70 mL, 3.36 mmol, 1.5 equiv). Purification by chromatography on silica gel using EtOAc/pentane

(1/10) as eluent to afford **53** (0.52 g, 88% yield) as a white solid.

The characterization data were identical to those previously reported.^[8]

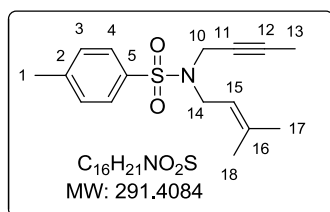
R_f = 0.29 (EtOAc/ pentane: 1/10).

IR (neat): $\tilde{\nu}$ (cm⁻¹) = 2982, 2920, 2851, 1743, 1711, 1671, 1643, 1597, 1403, 1160, 1091, 948, 898.

^1H NMR (300 MHz, CDCl_3) δ 7.65 (d, J = 8.0 Hz, 2H, H₄), 7.22 (d, J = 7.9 Hz, 2H, H₃), 5.70-5.55 (m, 1H, H₁₁), 5.22 (s, 1H, H₁₂), 5.13 (d, J = 10.3 Hz, 1H), 3.93 (s, 2H, H₆), 3.72 (d, J = 5.8 Hz, 2H, H₁₀), 2.33 (s, 3H, H₁), 1.45 (s, 3H, H₉).

^{13}C NMR (75 MHz, CDCl_3) δ 143.2 (C, C₅), 136.0 (CH, C₁₁), 132.1 (C, C₂), 129.1 (2CH, C₄), 127.8 (2CH, C₃), 119.3 (CH₂, C₁₂), 81.5 (C, C₇), 71.4 (C, C₈), 48.8 (CH₂, C₁₀), 36.2 (CH₂, C₆), 21.3 (CH₃, C₁), 3.0 (CH₃, C₉).

***N*-(but-2-yn-1-yl)-4-methyl-*N*-(3-methylbut-2-en-1-yl)benzenesulfonamide (55)**



The compound was prepared according to the general procedure **GP2**, using **44** (0.50 g, 2.24 mmol, 1 equiv), 3-methylbut-2-en-1-ol (0.34 mL, 3.36 mmol, 1.5 equiv) PPh₃ (0.6 g, 3.36 mmol, 1.5 equiv) and diisopropylazodicarboxylate (0.7 mL, 3.36 mmol, 1.5 equiv). Purification by chromatography on silica gel using EtOAc/pentane

(1/10) as eluent afforded **55** (0.65 g, quant) as yellow oil.

The characterization data were identical to those previously reported.^[5]

R_f = 0.23 (EtOAc/ pentane: 1/10).

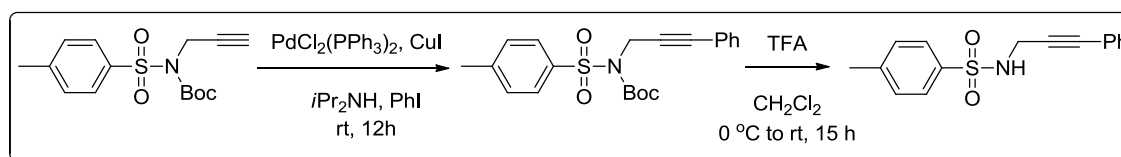
IR (neat): $\tilde{\nu}$ (cm⁻¹) = 2970, 2919, 2855, 1736, 1672, 1494, 1433, 1345, 1185, 1091, 900, 736.

¹H NMR (400 MHz, CDCl₃) δ 7.74 (d, *J* = 8.2 Hz, 2H, H₄), 7.29 (d, *J* = 7.9 Hz, 2H, H₃), 5.12-5.08 (m, 1H, H₁₅), 3.99 (q, *J* = 2.4 Hz, 2H, H₁₄), 3.78 (d, *J* = 6.9 Hz, 2H, H₁₀), 2.42 (s, 3H, H₁), 1.72 (s, 3H, H_{17 or 18}), 1.67 (s, 3H, H_{17 or 18}), 1.54 (t, *J* = 2.4 Hz, 3H, H₁₃).

¹³C NMR (75 MHz, CDCl₃) δ 143.0 (C, C₅), 138.4 (CH, C₁₅), 136.1 (C, C₂), 129.1 (2CH, C₄), 127.8 (2CH, C₃), 118.1 (C, C₁₆), 81.2 (C, C₁₁), 71.9 (C, C₁₂), 43.8 (CH₂, C₁₄), 35.9 (CH₂, C₁₀), 25.7 (CH₃, C_{17 or 18}), 21.3 (CH₃, C₁), 17.7 (CH₃, C_{17 or 18}), 3.1 (CH₃, C₁₃).

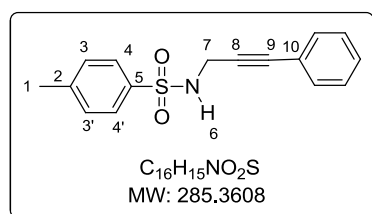
HRMS (ESI) calcd for C₁₆H₂₁NO₂SNa ([M + Na]⁺) 314.1185, found 314.1198.

GP3: General Procedure for the Sonogashira Coupling.^[4]



CuI (0.1 equiv) and [PdCl₂(PPh₃)₂] (0.05 equiv) were suspended in *i*-Pr₂NH, and the resulting mixture was stirred for 5 min. The corresponding aryl iodide (1.3 equiv) and the alkyne 1,6-enyne (1 equiv) in *i*-Pr₂NH (final concentration = 1.1 M) were added sequentially. The reaction was stirred at rt until TLC showed total conversion. The crude mixture was diluted with Et₂O, filtered over a short pad of Celite[®], and purified by chromatography (EtOAc/hexanes: 1/9).

N-(phenyl-2-ynyl)-4-methyl(benzenesulfonamide (56)



The compound was prepared according to the general procedure **GP3**, using ***N*-Boc-43** (2.0 g, 6.47 mmol, 1 equiv), iodobenzene (0.94 mL, 8.41 mmol, 1.3 equiv), CuI (0.12 g, 0.65 mmol, 0.1 equiv) and PdCl₂(PPh₃)₂ (0.23 g, 0.32 mmol, 0.05 equiv) in *i*-Pr₂NH (6 mL). Purification by chromatography on silica gel using EtOAc/pentane (1/9) as eluent afforded yellow solid (2.13 g, 92% yield). The product was dissolved in CH₂Cl₂ (9 mL) and trifluoroacetic acid (3.0 mL, 38.95 mmol, 6 equiv) was added. The resulting mixture was stirred for 20 h. The mixture was slowly added NaHCO₃ (20 mL) and CH₂Cl₂ (20 mL). The aqueous phase was extracted with CH₂Cl₂ (3x 20 mL). The combined organic layers were washed with brine (20 mL), dried over anhydrous MgSO₄, filtered and concentrated under reduced pressure to give **56** (1.50 g, 81% yield) as a pale yellow solid without purification.

The characterization data were identical to those previously reported.^[4,5]

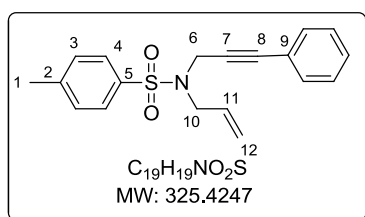
R_f = 0.25 (EtOAc/ pentane: 1/10).

IR (neat): $\tilde{\nu}$ (cm⁻¹) = 3261, 2981, 2921, 2241, 1597, 1438, 1290, 1156, 1108, 1090, 1017.

¹H NMR (400 MHz, CDCl₃) δ 7.82 (d, *J* = 8.4 Hz, 2H, H_{4,4'}), 7.29-7.26 (m, 3H, H_{ar}), 7.25-7.24 (m, 1H, H_{ar}), 7.23-7.22 (m, 1H, H_{ar}), 7.14 (d, *J* = 1.6 Hz, 1H, H₃), 7.12 (d, *J* = 2.0 Hz, 1H, H_{3'}), 4.72 (t, *J* = 6.2 Hz, 1H, H₆), 4.08 (d, *J* = 6.4 Hz, 2H, H₇), 2.35 (s, 3H, H₁).

¹³C NMR (100 MHz, CDCl₃) δ 144.0 (C, C₅), 137.1 (C, C₂), 131.8 (2CH, C_{12,14}), 129.9 (2CH, C₄), 128.7 (CH, C₁₃), 128.4 (2CH, C_{11,15}), 127.7 (2CH, C₃), 122.3 (C, C₁₀), 84.9 (C, C₉), 83.4 (C, C₈), 34.0 (CH₂, C₇), 21.7 (CH₃, C₁).

***N*-allyl-4-methyl-*N*-(3-phenylprop-2-yn-1-yl)benzenesulfonamide (57)**



The compound was prepared according to the general procedure **GP3**, using **46** (50 mg, 2.0 mmol, 1 equiv), iodobenzene (0.3 mL, 2.69 mmol, 1.3 equiv), CuI (40 mg, 0.19 mmol, 0.1 equiv) and PdCl₂(PPh₃)₂ (0.07 g, 0.10 mmol) in *i*-Pr₂NH (25 mL). Purification by chromatography on silica gel using EtOAc/pentane (1/10) as

eluent afforded **57** (0.46 g, 71% yield) as a yellow solid.

The characterization data were identical to those previously reported.^[12]

R_f = 0.32 (EtOAc/ pentane: 1/10).

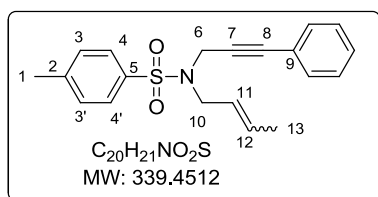
IR (neat): $\tilde{\nu}$ (cm⁻¹) = 3084, 2982, 2920, 2242, 1643, 1491, 1443, 1348, 1161, 1092.

¹H NMR (300 MHz, CDCl₃) δ 7.78 (d, *J* = 8.2 Hz, 2H, H₄), 7.28-7.20 (m, 5H, H_{ar}), 7.07 (d, *J* = 6.3 Hz, 2H, H₃), 5.86-5.74 (m, 1H, H₁₁), 5.34 (d, *J* = 17.0, 1H, H₁₂), 5.27 (d, *J* = 10.0, 1H, H₁₂), 4.31 (s, 2H, H₆), 3.90 (d, *J* = 6.4 Hz, 2H, H₁₀), 2.32 (s, 3H, H₁).

¹³C NMR (75 MHz, CDCl₃) δ 143.6 (C, C₅), 136.0 (C, C₂), 132.1 (C, C₉), 131.5 (2CH), 129.6 (2CH, C₄), 128.4 (CH), 128.1 (2CH), 127.8 (2CH, C₃), 122.2 (CH, C₁₁), 119.9 (CH₂, C₁₂), 85.8 (C, C₈), 81.7 (C, C₇), 49.3 (CH₂, C₁₀), 36.8 (CH₂, C₆), 21.4 (CH₃, C₁).

HRMS (ESI) calcd for C₁₉H₁₉NO₂SNa ([M + Na]⁺) 348.1029, found 348.1042.

***N*-(but-2-en-1-yl)-4-methyl-*N*-(3-phenylprop-2-yn-1-yl)benzenesulfonamide (58)**



The compound was prepared according to the general procedure **GP2** using **56** (0.50 g, 1.75 mmol, 1 equiv), but-2-en-1-ol (0.23 mL, 2.76 mmol, 1.5 equiv), PPh₃ (0.70 g, 2.76 mmol, 1.5 equiv) and diisopropylazodicarboxylate (0.6 mL, 2.76 mmol,

1.5 equiv). Purification by chromatography on silica gel using EtOAc/pentane (1/10) as eluent afforded **58** (*E:Z* = 9:1, 0.49 g, 82% yield) as a white solid.

The characterization data were identical to those previously reported.^[13]

$R_f = 0.27$ (EtOAc/ pentane: 1/10).

m.p. = 73–75 °C.

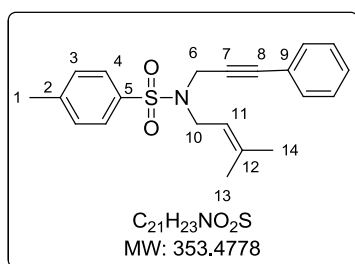
IR (neat): $\tilde{\nu}$ (cm⁻¹) = 3065, 2918, 2854, 2241, 1672, 1598, 1442, 1379, 1159, 1091, 965.

¹H NMR (400 MHz, CDCl₃) δ 7.77 (d, $J = 8.3$ Hz, 2H, H_{4,4'}), 7.28-7.21 (m, 5H, H_{ar}), 7.08 (d, $J = 1.4$ Hz, 1H, H₃), 7.06 (d, $J = 1.7$ Hz, 1H, H_{3'}), 5.77-5.72 (m, 1H, H₁₁), 5.47-5.40 (m, 1H, H₁₂), 4.29 (s, 2H, H₆), 3.82 (d, $J = 6.8$ Hz, 2H, H₁₀), 2.33 (s, 3H, H₁), 1.71 (dd, $J = 6.5, 1.6$ Hz, 3H, H₁₃).

¹³C NMR (75 MHz, CDCl₃) δ 143.5 (C, C₅), 136.3 (C, C₂), 131.7 (C, C₉), 131.6 (2CH), 129.6 (2CH, C₄), 128.5 (CH), 128.2 (2CH), 128.0 (2CH, C₃), 124.8 (CH, C₁₁), 122.5 (CH, C₁₂), 85.7 (C, C₈), 82.1 (C, C₇), 48.7 (CH₂, C₁₀), 36.6 (CH₂, C₆), 21.5 (CH₃, C₁), 17.9 (CH₃, C₁₃).

HRMS (ESI) calcd for C₂₀H₂₁NO₂SNa ([M + Na]⁺) 362.1185, found 362.1190.

4-Methyl-N-(3-methylbut-2-en-1-yl)-N-(3-phenylprop-2-yn-1-yl)benzenesulfonamide (**59**)



The compound was prepared according to the general procedure **GP2** using **56** (1.0 g, 3.49 mmol, 1 equiv), 3-methylbut-2-en-1-ol (0.35 mL, 3.49 mmol, 1 equiv), PPh₃ (0.9 g, 3.49 mmol, 1 equiv) and diisopropylazodicarboxylate (0.7 mL, 3.49 mmol, 1 equiv). Purification by chromatography on silica gel using EtOAc/pentane (1/10) as eluent to afford **59** (0.57 g, 46% yield) as a white solid.

The characterization data were identical to those previously reported.^[4]

$R_f = 0.27$ (EtOAc/pentane: 1/10).

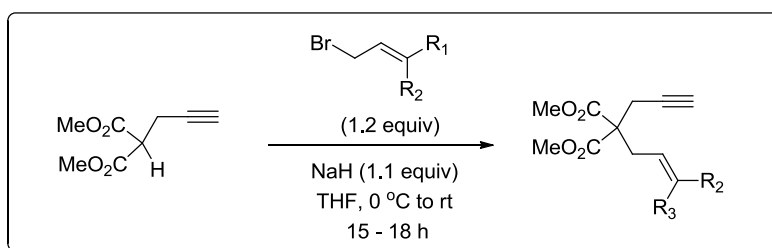
IR (neat): $\tilde{\nu}$ (cm⁻¹) = 2917, 2855, 2243, 1598, 1426, 1121, 692.

¹H NMR (300 MHz, CDCl₃) δ 7.78 (d, $J = 8.2$, 2H, H₄), 7.27-7.21 (m, 5H, H_{ar}), 7.06 (d, $J = 6.4$, 2H), 5.25- 5.10 (t, $J = 7.2$, 1H, H₁₁), 4.28 (s, 2H, H₆), 3.88 (d, $J = 7.4$ Hz, 2H, H₁₀), 2.33 (s, 3H, H₁), 1.75 (s, 3H, H₁₃ or 14), 1.70 (s, 3H, H₁₃ or 14).

¹³C NMR (100 MHz, CDCl₃) δ 143.4 (C, C₅), 139.2 (C, C₂), 136.3 (C, C₉), 131.6 (2CH), 129.6 (2CH, C₄), 128.4 (CH), 128.3 (2CH), 128.0 (2CH, C₃), 122.6 (C, C₁₂), 118.2 (CH, C₁₁), 85.6 (C, C₈), 82.4 (C, C₇), 44.3 (CH₂, C₁₀), 36.5 (CH₂, C₆), 26.0 (CH₃, C₁₃ or 14), 21.5 (CH₃, C₁), 18.0 (CH₃, C₁₃ or 14).

2.5.2. Carbon-tethered 1,6-enynes

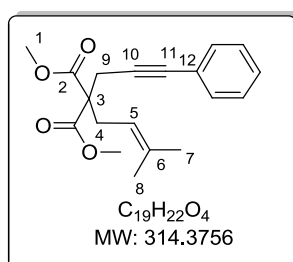
GP4: General procedure for the synthesis of Oxygen-tethered 1,6-enynes



To a solution of NaH (60 % dispersion in mineral oil, 1.1 equiv) in THF (concentration = 0.12 M) was added dimethyl-2-(prop-2-yn-1-yl)malonate (1.0 equiv) at 0 °C. The resulting mixture was stirred for 30 min. Alkene bromide (1.2 equiv) was slowly added. The reaction mixture was allowed to warm up to rt and stirred for 15–18 h. Upon completion, the reaction mixture was quenched with water (50 mL) and the aqueous phase was extracted with Et₂O (3x30 mL). The combined organic layers were washed with brine (20 mL), dried over anhydrous MgSO₄, filtered and concentrated under reduced pressure. Purification by column chromatography afforded the desired products.

The procedure and characterization of compounds **63**,^[8] **64**^[4] have been described in the literature.

Dimethyl 2-(3-methylbut-2-en-1-yl)-2-(3-phenylprop-2-yn-1-yl)malonate (**65**)



The compound was prepared according to the general procedure **GP4** using **64** (1.80 g, 7.35 mmol, 1 equiv), 1-bromo-3-methylbut-2-ene (1.0 mL, 8.82 mmol, 1.2 equiv), NaH (60 % dispersion in mineral oil, 0.3 g, 7.86 mmol, 1.1 equiv). Purification by chromatography on silica gel using EtOAc/pentane (1/15) as eluent afforded **65** (1.70 g, 74% yield) as colourless oil.

The characterization data were identical to those previously reported.^[4]

R_f = 0.3 (EtOAc/ pentane: 1/9).

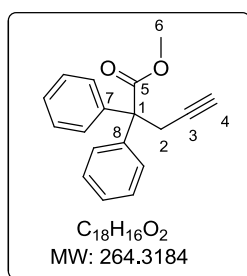
IR (neat): $\tilde{\nu}$ (cm⁻¹) = 2953, 1735, 1598, 1435, 1261, 1172, 1055.

¹H NMR (400 MHz, CDCl₃) δ 7.36-7.34 (m, 2H, H_{ar}), 7.26-7.24 (m, 3H, H_{ar}), 4.94 (m, 1H, H₅), 3.73 (s, J = 2.0 Hz, 6H, H₁), 2.98 (s, 2H, H₉), 2.84 (d, J = 7.7 Hz, 2H, H₄), 1.70 (d, J = 1.0 Hz, 3H, H_{7 or 8}), 1.67 (d, J = 0.9 Hz, 3H, H_{7 or 8}).

^{13}C NMR (100 MHz, CDCl_3) δ 170.8 (2C, C_2), 136.9 (C, C_6), 131.7 (2CH, $\text{C}_{13, 17}$), 128.3 (2CH, $\text{C}_{14, 16}$), 128.0 (CH, C_{15}), 123.4 (C, C_{12}), 117.3 (CH, C_5), 84.9 (C, C_{10}), 83.5 (C, C_{11}), 57.7 (C, C_3), 52.8 (2 CH_3 , C_1), 31.1 (CH_2 , C_4), 26.2 (CH_3 , $\text{C}_{7 \text{ or } 8}$), 23.6 (CH_2 , C_9), 18.1 (CH_3 , $\text{C}_{7 \text{ or } 8}$).

2.6. Preparation of allenol derivative

Methyl 2,2-diphenylpent-4-ynoate (**66**)



To a solution of *i*-Pr₂NH (3.25 mL, 23.1 mmol, 1.05 equiv) at 0 °C was added dropwise a solution of *n*-BuLi (13.3 mL of 2 M in hexanes, 1.2 equiv) and the reaction mixture was stirred at the same temperature for 1 h. A solution of methyl diphenylacetate (5 g, 22 mmol, 1 equiv) in THF (30 mL) was then added at –78 °C. After 15 min, the resulting solution was treated with propargyl bromide (2.60 mL of 80 wt% in toluene, 24.3 mmol, 1.05 equiv), stirred and warmed slowly to rt for 15 h. The resulting solution was quenched with saturated NH₄Cl solution (20 mL) and diluted with Et₂O (20 mL). The aqueous phase was extracted with Et₂O (3x 20 mL). The combined organic layers were washed with brine (20 mL), dried over anhydrous MgSO₄, filtered and concentrated under reduced pressure. Purification by column chromatography on silica gel using EtOAc/petroleum ether (1/10) afforded **66** (4.51 g, 78% yield) as yellow oil.

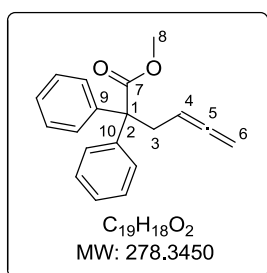
The characterization data were identical to those previously reported.^[14]

R_f = 0.28 (EtOAc/pentane: 1/10).

IR (neat): $\tilde{\nu}$ (cm⁻¹) = 3287, 2951, 1728, 1496, 1432, 1229, 954.

^1H NMR (400 MHz, CDCl_3) δ 7.33-7.31 (m, 10H, 10H_{ar}), 3.75 (s, 3H, H₆), 3.30 (dd, J = 2.6, 1.0 Hz, 2H, H₂), 1.93 (s, 1H, H₄).

^{13}C NMR (100 MHz, CDCl_3) δ 173.9 (C, C_5), 141.6 (2C, $\text{C}_{7, 8}$), 129.0 (4CH), 128.0 (4CH), 127.4 (2CH), 81.1 (C, C_3), 72.0 (CH, C_4), 60.0 (C, C_1), 52.8 (CH_3 , C_6), 29.5 (CH_2 , C_2).

Methyl-2,2-diphenylhexa-4,5-dienoate (67)

To a solution of **66** (4.5 g, 26.7 mmol, 1 equiv) in 1,4-dioxane (135 mL) were added *p*-formaldehyde (1.6 g, 53.5 mmol, 2 equiv), *i*-Pr₂NH (3.9 mL, 53.5 mmol, 2 equiv), and CuBr (1.53 g, 10.7 mmol, 0.4 equiv). The resulting mixture were refluxed for 18 h, then cooled down to rt, and concentrated under vacuum. The resulting residue was dissolved with Et₂O, filtered over a short pad of silica gel. The mixture solution was concentrated under reduced pressure. Purification by flash chromatography on silica gel using Petroleum ether/EtOAc (20/ 1) afforded **67** (2.45 g, 33% yield) as a yellow oil.

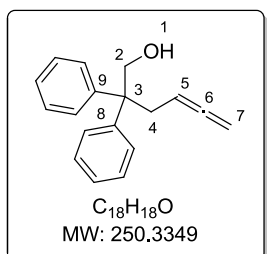
The characterization data were identical to those previously reported.^[14]

R_f = 0.38 (EtOAc/pentane: 1/10).

IR (neat): $\tilde{\nu}$ (cm⁻¹) = 3058, 3023, 2950, 1954, 1728, 1494, 1432, 1221, 1005.

¹H NMR (300 MHz, CDCl₃) δ 7.34-7.30 (m, 10H, H_{ar}), 4.97-4.92 (m, 1H, H₄), 4.53-4.48 (m, 2H, H₆), 3.73 (s, 3H, H₈), 3.28-3.17 (m, 2H, H₃).

¹³C NMR (75 MHz, CDCl₃) δ 210.1 (C, C₅), 174.4 (C, C₇), 142.3 (2C, C_{9,10}), 129.1 (4CH), 127.9 (4CH), 127.0 (2CH, C₁₂), 85.9 (CH, C₄), 73.9 (CH₂, C₆), 60.7 (C, C₁), 52.3 (CH₃, C₈), 38.2 (CH₂, C₃).

2,2-Diphenylhexa-4,5-dien-1-ol (68)

To a solution of LiAlH₄ (0.67 g, 17.60 mmol, 2 equiv) in Et₂O (120 mL) was added dropwise a solution of **67** (2.45 g, 8.80 mmol, 1 equiv) in Et₂O (42 mL). The resulting suspension was stirred for 2.5 h. The mixture was treated with 10% NaOH solution, and then filtered over a short pad of silica gel. The mixture solution was concentrated under reduced pressure to afford **68** (1.67 g, 76% yield) as colorless oil.

The characterization data were identical to those previously reported.^[14]

R_f = 0.13 (EtOAc/pentane: 1/10).

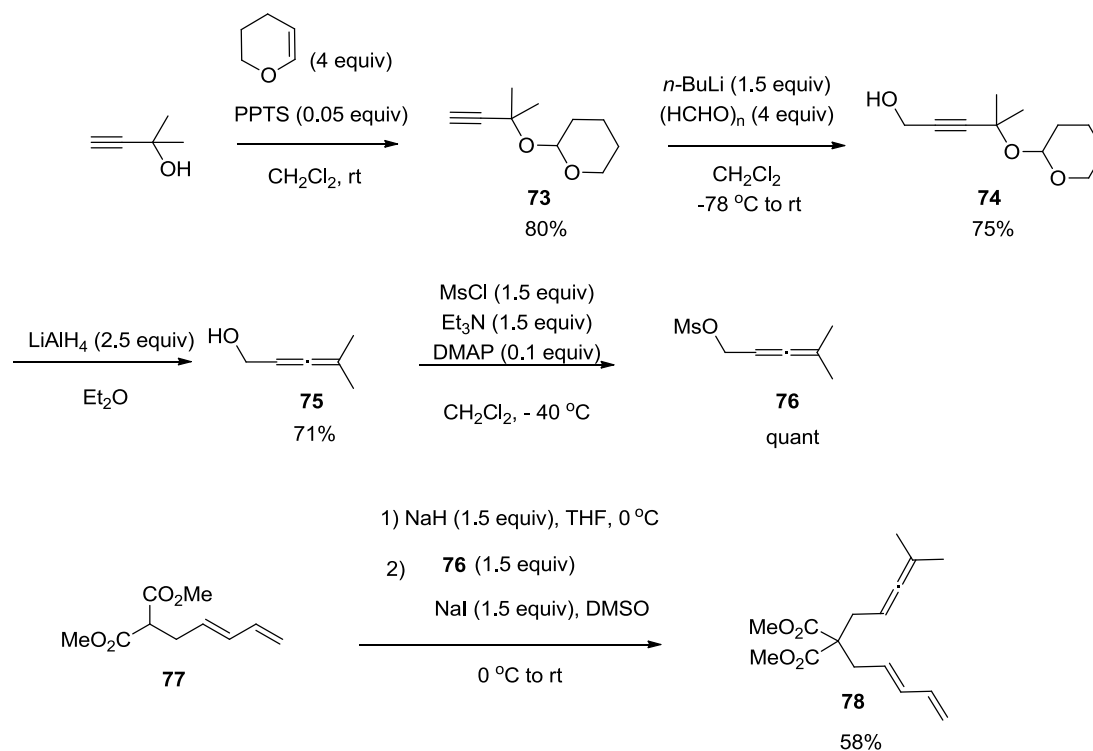
IR (neat): $\tilde{\nu}$ (cm⁻¹) = 3544, 3445, 3057, 3024, 2930, 2854, 1954, 1599, 1495, 1444, 1020, 699.

¹H NMR (300 MHz, CDCl₃) δ 7.37-7.23 (m, 10H, H_{ar}), 4.80-4.73 (m, 1H, H₅), 4.63-4.59 (m, 2H, H₇), 4.22 (d, *J* = 6.9 Hz, 2H, H₂), 2.98 (dt, *J* = 7.7, 2.5 Hz, 2H, H₄), 1.35 (s, 1H, H₁).

¹³C NMR (75 MHz, CDCl₃) δ 209.8 (C, C₆), 145.0 (2C, C_{8,9}), 128.4(4CH), 128.3 (4CH), 126.5 (2CH), 85.7 (CH, C₅), 74.0 (CH₂, C₇), 68.2 (C, C₃), 52.2 (CH₂, C₂), 36.4 (CH₂, C₄).

The procedure and characterization of allenol **69**,^[15] allenyl amine **70**,^[14] allenyl carbamate **71**,^[14] and allenyl-mesyamide **72**^[14] have been described in the literature.

2.7. Preparation of allene diene derivative



According to a modification of a procedure reported by the Toste group^[16], to a solution of 2-methylbut-3-yn-2-ol (5.76 mL, 60.00 mmol, 1 equiv) and 3,4-dihydropyran (21.16 mL, 0.25 mol, 4 equiv) in CH_2Cl_2 (25 mL) was added PPTS (0.75g, 2.98 mmol, 0.05 equiv) and stirred at rt. After stirring for 16 h, the mixture was quenched with H_2O (30 mL) and diluted with Et_2O . The aqueous phase was extracted with Et_2O (3x 20 mL). The combined organic layers were washed with brine (20 mL), dried over anhydrous MgSO_4 , filtered and concentrated under reduced pressure. Purification by distillation ($55\text{ }^\circ\text{C}$, 2 mmHg) afforded **73** (8.07 g, 80% yield) as colourless oil.

IR (neat): $\tilde{\nu}$ (cm^{-1}) = 3309, 2986, 2940, 2871, 1440, 1381, 1361, 1207, 1124, 1076, 1021, 985.

$^1\text{H NMR}$ (400 MHz, CDCl_3) δ 5.07-5.05 (m, 1H), 3.97-3.92 (m, 1H), 3.53-3.48 (m, 1H), 2.43 (s, 1H), 1.85-1.83 (m, 1H), 1.74-1.70 (m, 1H), 1.55 (s, 3H), 1.53-1.52 (m, 3H), 1.51 (s, 3H).

$^{13}\text{C NMR}$ (75 MHz, CDCl_3) δ 96.0 (C), 86.3 (C), 71.9 (C), 70.8 (CH), 63.1 (CH_2), 31.8 (CH_2), 30.5 (CH_3), 29.7 (CH_3), 25.4 (CH_2), 20.3 (CH_2).

To a solution of **73** (9.2 g, 54.8 mmol, 1 equiv) in THF (20 mL) was slowly added *n*-BuLi (33 mL of a 2.5 M in hexanes, 82.2 mmol, 1.5 equiv) at $-78\text{ }^{\circ}\text{C}$ and warmed to $0\text{ }^{\circ}\text{C}$ for 30 min. The organolithium was added *via* cannula into the solution of *p*-formaldehyde (6.6 g, 219.2 mmol, 4 equiv) in THF (20 mL) and slowly warmed to rt. After stirring for 12 h and completion of reaction (TLC monitoring), the reaction mixture was diluted with Et₂O (40 mL) and quenched with a saturated aqueous NH₄Cl solution (40 mL). The aqueous phase was extracted with Et₂O (3x40 mL). The combined organic layers were washed with brine (40 mL), dried over anhydrous MgSO₄, filtered and concentrated under reduced pressure. Purification by column chromatography on silica gel using EtOAc/pentane (2/8) as eluent afforded alcohol **74** (8.1 g, 75% yield) as yellow oil. $R_f = 0.25$ (EtOAc/pentane: 1/4).

¹H NMR (300 MHz, CDCl₃) δ 5.05 (bs, 1H), 4.30 (s, 2H), 3.99-3.92 (m, 1H), 3.52-3.48 (m, 1H), 1.87-1.83 (m, 1H), 1.73-1.70 (m, 3H), 1.53 (s, 6H), 1.49 (s, 3H).

A solution of alcohol **74** (4 g, 19.9 mmol, 1 equiv) in Et₂O (20 mL) was added dropwise into the solution of LiAlH₄ (1.9 g, 49.8 mmol, 2.5 equiv) in Et₂O (40 mL). After stirring for 4 h and completion of reaction, the reaction mixture was slowly treated the aqueous solution of saturated Na₂SO₄ until the bubble disappeared. The white solid was precipitated. The white solid was removed by filtration. The solution was concentrated under reduced pressure. Purification by Kugelrohr distillation ($50\text{ }^{\circ}\text{C}$, 0.1 mmHg) afforded the alcohol allene **75** (1.38 g, 71% yield) as colourless oil.

$R_f = 0.1$ (EtOAc/pentane: 1/15).

IR (neat): $\tilde{\nu}$ (cm⁻¹) = 3300, 2937, 2869, 2854, 2712, 1968, 1408, 1363, 1343, 1239, 1154, 1058, 1005.

¹H NMR (400 MHz, CDCl₃) δ 5.14-5.10 (m, 1H), 4.01 (d, $J = 5.8$ Hz, 2H), 2.25 (bs, 1H), 1.66 (d, $J = 2.9$ Hz, 6H).

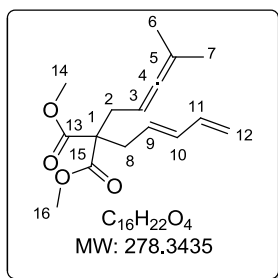
¹³C NMR (100 MHz, CDCl₃) δ 200.8 (C), 97.9 (C), 89.8 (CH), 61.0 (CH₂), 20.5 (CH₃).

To a solution of **75** (1 g, 10.19 mmol, 1 equiv) in CH₂Cl₂ (54 mL) were added DMAP (0.13 g, 1.02 mmol, 0.1 equiv) and Et₃N (2.12 mL, 15.29 mmol, 1.5 equiv). The mixture was stirred at $-40\text{ }^{\circ}\text{C}$ for 10 min. Methanesulfonyl chloride (1.75 g, 15.29 mmol, 1.5 equiv) was added dropwise at the same temperature. After stirring for 1 h, the reaction was quenched with water (20 mL), diluted with CH₂Cl₂ (30 mL). The aqueous phase was extracted with CH₂Cl₂ (3x10 mL). The combined organic layers were washed with brine (40 mL), dried over anhydrous MgSO₄, filtered and concentrated under reduced pressure to afford **76** (1.79 g, quant) as colourless oil. The crude product was used without further purification.

$^1\text{H NMR}$ (400 MHz, CD_2Cl_2) δ 5.20-5.16 (m, 1H), 4.64 (d, $J = 7.2$ Hz, 2H), 3.00 (s, 3H), 1.73 (d, $J = 2.8$ Hz, 6H).

To a solution of NaH (60 % dispersion in mineral oil) (0.4 g, 10.2 mmol, 1.5 equiv) in THF (27 mL) was slowly added a solution of the prepared diene-malonate **77**^[17] (1.3 g, 6.8 mmol, 1 equiv) at 0 °C and stirred for 30 min. The mixture of a solution of a crude mesylate **76** (1.8 g, 10.2 mmol, 1.5 equiv) in distilled DMSO (10.2 mL) and NaI (1.5 g, 10.2 mmol, 1.5 equiv) was sequentially added. The mixture was warmed to rt. After stirring for 16 h, the reaction mixture was quenched with saturated NaHCO_3 and diluted with EtOAc (20 mL). The aqueous phase was extracted with EtOAc (3x10 mL). The combined organic layers were washed with brine (40 mL), dried over anhydrous MgSO_4 , filtered and concentrated under reduced pressure. Purification by column chromatography on silica gel using EtOAc/pentane (1/15) as eluent afforded allene diene **78** (1.1 g, 58% yield) as colourless oil.

Dimethyl 2-(4-methylpenta-2,3-dien-1-yl)-2-(penta-2,4-dien-1-yl)malonate (**78**)



The characterization data were identical to those previously reported.^[16]

$R_f = 0.34$ (EtOAc/pentane: 1/15).

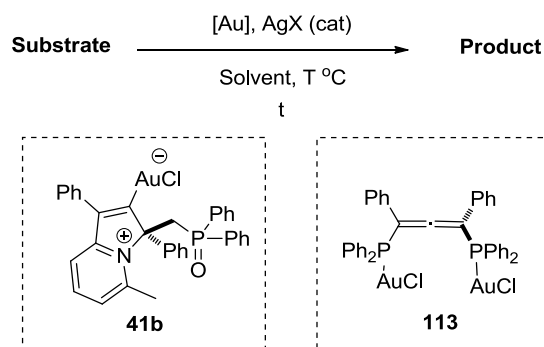
IR (neat): $\tilde{\nu}$ (cm^{-1}) = 2979, 2953, 2909, 2970, 1733, 1651, 1435, 1206, 1180, 1005.

$^1\text{H NMR}$ (300 MHz, CDCl_3) δ 6.27 (dt, $J = 16.9, 9.4$ Hz, 1H, H_{11}), 6.08 (m, $J = 15.0, 10.5$ Hz, 1H, H_{10}), 5.51 (q, 7.5 Hz, 1H, H_9), 5.10 (d, $J = 16.7$ Hz, 1H, H_{12}), 5.00 (d, $J = 10.2$ Hz, 1H, H_{12}), 4.80-4.73 (m, 1H, H_3), 3.70 (s, 6H, $\text{H}_{14, 16}$), 2.71 (d, $J = 7.6$ Hz, 2H, H_2), 2.54 (d, $J = 7.6$ Hz, 2H, H_8), 1.65 (d, $J = 2.7$ Hz, 6H, $\text{H}_{6, 7}$).

$^{13}\text{C NMR}$ (75 MHz, CDCl_3) δ 203.9 (C, C_4), 171.3 (2C, $\text{C}_{13, 15}$), 136.8 (CH, C_{11}), 135.1 (CH, C_{10}), 128.2 (CH, C_9), 116.5 (CH_2 , C_{12}), 95.4 (C, C_5), 82.8 (CH, C_3), 58.2 (C, C_1), 52.6 (CH_3 , $\text{C}_{14, 16}$), 35.7 (CH_2 , C_8), 33.0 (CH_2 , C_2), 20.7 (CH_3 , $\text{C}_{6, 7}$).

2.8. Gold(I)-catalyzed cyclization reactions

Table S1 Optimization of the catalytic conditions



Substrate	[Au] (mol%)	AgX (mol%)	Solvent	T (°C)	t (h)	Yield ^[a] (%)	ee (%)	Product
48	(±)- 113 (3)	AgSbF ₆ (3)	CH ₂ Cl ₂	rt	3	74	-	79
48	(±)- 113 (3)	AgSbF ₆ (6)	CH ₂ Cl ₂	rt	3	76	-	79
45	(±)- 113 (3)	AgSbF ₆ (6)	CH ₂ Cl ₂	rt	1	50	-	80
49	(±)- 113 (3)	AgSbF ₆ (6)	CH ₂ Cl ₂	rt	1	quant	-	81
49	(<i>aS</i>)- 113 (3)	AgSbF ₆ (6)	CH ₂ Cl ₂	-20	15	91	32	81
49	(<i>aR</i>)- 113 (3)	AgBF ₄ (6)	CH ₂ Cl ₂	-20	18	74	5	81
49	(<i>aR</i>)- 113 (3)	AgOTf(6)	toluene	60	4	42	18	81
50	(±)- 113 (3)	AgSbF ₆ (6)	CH ₂ Cl ₂	rt	1	85	-	82
50	(<i>aS</i>)- 113 (3)	AgSbF ₆ (6)	CH ₂ Cl ₂	-20	15	quant	29	82
50	(<i>aR</i>)- 113 (3)	AgBF ₄ (6)	CH ₂ Cl ₂	-20	30	46	8	82
50	(<i>aR</i>)- 113 (3)	AgOTf(6)	toluene	60	4	75	13	82
50	(±)- 41b (5)	AgSbF ₆ (10)	CH ₂ Cl ₂	reflux	16	50	-	82
50	(±)- 41b (3)	AgSbF ₆ (3.5)	CH ₂ Cl ₂	reflux	4	50	-	82
51	(±)- 113 (3)	AgSbF ₆ (6)	CH ₂ Cl ₂	rt	1	60	-	83
51	(<i>aS</i>)- 113 (3)	AgSbF ₆ (6)	CH ₂ Cl ₂	rt	1	58	1	83
52	(±)- 113 (3)	AgSbF ₆ (6)	CH ₂ Cl ₂	rt	2	90	-	84
53	(±)- 113 (3)	AgSbF ₆ (6)	CH ₂ Cl ₂	rt	1	76	-	85
54	(±)- 113 (3)	AgSbF ₆ (6)	CH ₂ Cl ₂	rt	1	74	-	86
54	(<i>aS</i>)- 113 (3)	AgSbF ₆ (6)	CH ₂ Cl ₂	-20	14	74	2	86
55	(±)- 113 (3)	AgSbF ₆ (6)	CH ₂ Cl ₂	rt	2.5	23	-	87
						21	-	88

Experimental part

55	(aS)-113 (3)	AgSbF ₆ (6)	CH ₂ Cl ₂	0 °C	18	29	5	87
						13	6	
56	(±)-113 (3)	AgSbF ₆ (6)	CH ₂ Cl ₂	rt	2.5	59	-	89
57	(aR)-113(3)	AgBF ₄ (6)	toluene	reflux	20	50	0	89
58	(±)-113 (3)	AgSbF ₆ (6)	CH ₂ Cl ₂	rt	2.5	81	-	90
59	(±)-113 (3)	AgSbF ₆ (6)	CH ₂ Cl ₂	rt	1	61	-	91
59	(aS)-113 (3)	AgSbF ₆ (6)	CH ₂ Cl ₂	rt	3	70	4	91
						10	nd ^[b]	
59	(±)-113 (3)	AgSbF ₆ (6)	CH ₂ Cl ₂	0	3	80	-	93
59	(aS)-113 (3)	AgSbF ₆ (6)	CH ₂ Cl ₂	-5	18	61	7	93
63	(±)-113 (3)	AgSbF ₆ (6)	CH ₂ Cl ₂	rt	1	70(2:1)	-	94a,b
63	(±)-41b (5)	AgSbF ₆ (5)	CH ₂ Cl ₂	rt	1	quant (2:1)	-	94a,b
63	(±)-113 (3)	AgSbF ₆ (6)	CH ₂ Cl ₂	rt	1	70(2:1)	-	94a,b
63	(±)-41b (5)	AgSbF ₆ (5)	CH ₂ Cl ₂	rt	1	quant (2:1)	-	94a,b
65	(±)-113 (3)	AgSbF ₆ (6)	CH ₂ Cl ₂	rt	1	quant	-	95
65	(aS)-113 (3)	AgSbF ₆ (6)	CH ₂ Cl ₂	-20	15	quant	0	95
65	(±)-41b (5)	AgSbF ₆ (10)	CH ₂ Cl ₂	reflux	16	76	-	95
65	(±)-41b (3)	AgSbF ₆ (3.5)	CH ₂ Cl ₂	rt	3	75	-	95
65	(R)-41b (3)	AgSbF ₆ (3.5)	CH ₂ Cl ₂	0	4	63	0	95
78	(±)-113(3)	AgSbF ₆ (6)	CH ₂ Cl ₂	rt	2	67 (4:1)	0	96a,b
78	(±)-41b (3)	AgSbF ₆ (3.5)	CH ₂ Cl ₂	rt	3	65 (3:2)	0	96a,b
61	(±)-113 (3)	AgSbF ₆ (6)	CH ₂ Cl ₂	20	3	20	-	97
62	(aR)-113(3)	AgSbF ₆ (6)	CH ₂ Cl ₂	rt	1	40	0	98
62	(R)-41b (3)	AgSbF ₆ (3.5)	CH ₂ Cl ₂	rt	20	25	0	98
68	(±)-113 (3)	AgSbF ₆ (6)	CH ₂ Cl ₂	rt	1.5	26	-	99
68	(aR)-113 (3)	AgOTs (6)	toluene	70	1	70	4	99
68	(±)-41b (3)	AgOTs (4.5)	toluene	70	1	76	-	99
68	(R)-41b (3)	AgOTs (4.5)	toluene	rt	5	58	38	99
69	(±)-41b (3)	AgOTs (4.5)	CH ₂ Cl ₂	rt	1	81	-	100
69	(R)-41b (3)	AgOTs (4.5)	CH ₂ Cl ₂	0	3	quant	^[c]	100
71	(±)-41b (3)	AgOTs (4.5)	toluene	reflux	4	70	-	101

72	(±)- 41b (3)	AgOTs (4.5)	toluene	rt	17	40	-	102
63	(<i>aS</i>)- 113 (3)	AgSbF ₆ (6)	MeOH	rt	24	70	0	103
104, styrene	(<i>aS</i>)- 113 (3)	AgSbF ₆ (6)	MeNO ₂	rt	15	60	11	105 (>20:1 <i>cis: trans</i>)
104, styrene	(±)- 41b (3)	AgSbF ₆ (3.5)	MeNO ₂	reflux	3	32	-	105 (13:1 <i>cis: trans</i>)

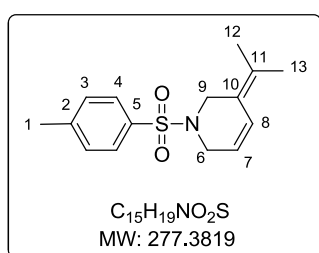
^[a]= Isolated product., ^[b] No data for enantiomeric excess, ^[c] the chiral HPLC analysis of this product is on process.

2.8.1 Cycloisomerization of 1,6-enynes

GP5 : Gold(I)-catalyzed cycloisomerization of enynes

To a solution of [Au] (0.03-0.05 equiv) in dry and degassed solvent was added AgX (X= SbF₆, OTf, BF₄ or OTs) (0.03-0.06 equiv). After 10 min stirring at rt, the formation of AgCl was occurred as a white solid. Then, a solution of 1,6-enyne (1 equiv) in dry and degassed solvent (final concentration 0.05 M) was added. The mixture was stirred and monitored by TLC. When the reaction was complete, the mixture was filtered over a short pad of Celite® and washed with CH₂Cl₂. The solution was concentrated under reduced pressure. Subsequent purification by flash-chromatography on silica gel afforded the desired products.

3-(Propan-2-ylidene)-1-tosyl-1,2,3,6-tetrahydropyridine (79)



The compound was prepared according to the general procedure **GP5** from enyne **48**, followed the conditions as shown in Table **S1** as a white solid.

The characterization data were identical to those previously reported.^[8]

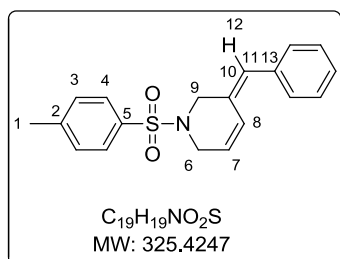
R_f = 0.11 (EtOAc/cyclohexane: 1/10).

IR (neat): $\tilde{\nu}$ (cm⁻¹) = 2956, 2854, 1597, 1494, 1381, 1346, 1164, 1091, 1035, 955, 910, 816, 734, 664.

¹H NMR (400 MHz, CDCl₃) δ 7.64 (d, *J* = 8.2, 2H, H₄), 7.26 (d, *J* = 7.9 Hz, 2H, H₃), 6.32 (dt, *J* = 10.4, 2.1 Hz, 1H, H₈), 5.51 (dt, *J* = 10.4, 3.6 Hz, 1H, H₇), 3.89 (s, 2H, H₆), 3.75 (bs, 2H, H₉), 2.39 (s, 3H, H₁), 1.75 (s, 3H, H₁₂ or ₁₃), 1.66 (s, 3H, H₁₂ or ₁₃).

¹³C NMR (100 MHz, CDCl₃) δ 143.4 (C, C₅), 134.3 (C, C₂), 129.9 (C, C₁₀), 129.4 (2CH, C₄), 127.7 (2CH, C₃), 124.6 (CH, C₈), 122.4 (C, C₁₁), 121.0 (CH, C₇), 45.1 (2CH₂, C_{6,9}), 21.6 (CH₃, C₁), 20.4 (CH₃, C_{12 or 13}), 19.7 (CH₃, C_{12 or 13}).

3-Benzylidene-1-tosyl-1,2,3,6-tetrahydropyridine (80)



The compound was prepared according to the general procedure **GPS** from enyne **45**, followed the conditions as shown in Table **S1** as a white solid.

The characterization data were identical to those previously reported.^[8]

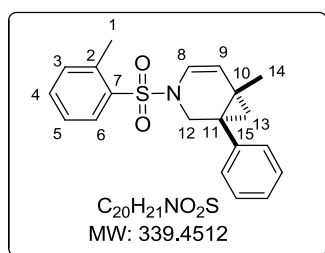
R_f = 0.11 (EtOAc/cyclohexane: 1/10).

IR (neat): $\tilde{\nu}$ (cm⁻¹) = 3061, 2959, 2923, 2852, 1721, 1597, 1493, 1450, 1346, 1162, 1093, 976, 936.

¹H NMR (400 MHz, CDCl₃) δ 7.70 (d, *J* = 8.2 Hz, 2H, H₄), 7.32-7.23 (m, 5H, H_{ar}), 7.09 (d, *J* = 7.3 Hz, 2H, H₃), 6.50 (d, *J* = 10.2, 1H, H₈), 6.32 (s, 1H, H₁₂), 5.77-5.72 (m, 1H, H₇), 3.98 (d, *J* = 1.1 Hz, 2H, H₆), 3.92 (bs, 2H, H₉), 2.39 (s, 3H, H₁).

¹³C NMR (100 MHz, CDCl₃) δ 143.6 (C, C₅), 136.1 (C, C₁₀), 134.5 (C, C₂), 129.7 (2CH, C₄), 129.2 (2CH, 129.1 (C, C₁₃), 128.3 (2CH), 127.9 (2CH, C₃), 127.3 (CH), 127.2 (CH, C₁₁), 126.2 (C, C₈), 124.3 (C, C₇), 50.0 (CH₂, C₆), 46.0 (CH₂, C₉), 21.6 (CH₃, C₁).

6-Methyl-1-phenyl-3-(*o*-tolylsulfonyl)-3-azabicyclo[4.1.0]hept-4-ene (81)



The compound was prepared according to the general procedure **GPS** from enyne **49**, followed the conditions as shown in Table **S1** as a white solid.

The characterization data were identical to those previously reported.^[8]

R_f = 0.4 (EtOAc/pentane: 1/10).

IR (neat): $\tilde{\nu}$ (cm⁻¹) = 3061, 2927, 2871, 2851, 2361, 2257, 1643, 1600, 1496, 1446, 1348, 1329, 1281, 1242, 1177, 1161, 1092, 1069, 979, 906.

¹H NMR (300 MHz, CDCl₃) δ 7.89 (d, *J* = 7.7 Hz, 1H, H₆), 7.44 (d, *J* = 7.1 Hz, 1H, H₃), 7.33-7.21 (m, 7H, H_{4, 5, ar}), 6.47 (d, *J* = 7.9 Hz, 1H, H₈), 5.39 (d, *J* = 8.0 Hz, 1H, H₉), 3.81 (d, *J* = 12.0 Hz, 1H, H₁₂), 3.19 (d, *J* = 11.9 Hz, 1H, H₁₂), 2.61 (s, 3H, H₁), 1.19 (d, *J* = 4.4 Hz, 1H, H₁₃), 1.02 (d, *J* = 4.1 Hz, 1H, H₁₃), 0.88 (s, 3H, H₁₄).

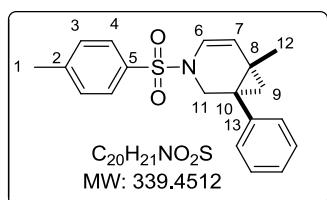
¹³C NMR (100 MHz, CDCl₃) δ 139.0 (C, C_{ar}), 137.7 (C, C₇), 136.9 (C, C₂), 133.1 (CH, C₄), 132.9 (CH, C₃), 130.1 (CH, C₆), 129.9 (2CH), 128.6 (2CH), 127.3 (CH), 126.4 (CH, C₅), 120.9 (CH, C₈), 117.6 (CH, C₉), 48.0 (CH₂, C₁₂), 40.1 (C, C₁₁), 24.6 (CH₂, C₁₃), 21.0 (CH₃, C₁₄), 20.9 (CH₃, C₁), 19.1 (C, C₁₀).

Chiral HPLC analysis: Prepared (+)-**81** by using (*αS*)-**113** (3 mol%), AgSbF₆ (6 mol%) in CH₂Cl₂ at –20°C for 15 h.

Chiralpak AS-H, 95/5 *n*-heptane/*i*-PrOH, 1 mL/min. Retention time for minor enantiomer = 6.46 min; for major enantiomer = 7.89 min (*ee* = 32%); [α_D] = 68.9 (c 0.1, CHCl₃).

{[α_D] (*ent*-**81**) = –206 (c 1.42, CHCl₃, *ee* = 75%)}.^[18]

6-Methyl-1-phenyl-3-tosyl-3-azabicyclo[4.1.0]hept-4-ene (**82**)



The compound was prepared according to the general procedure **GP5** from enyne **50**, followed the conditions as shown in Table **S1** as a white solid.

The characterization data were identical to those previously reported.^[8]

R_f = 0.3 (EtOAc/pentane: 1/10).

IR (neat): $\tilde{\nu}$ (cm⁻¹) = 3059, 3027, 2973, 2926, 2869, 2255, 1642, 1597, 1494, 1445, 1349, 1306, 1237, 1125, 1026, 981, 907, 814.

¹H NMR (400 MHz, CDCl₃) δ 7.66 (d, *J* = 8.3 Hz, 2H, H₄), 7.34–7.22 (m, 7H, H₃, ar), 6.40 (dd, *J* = 8.0, 1.0 Hz, 1H, H₆), 5.38 (d, *J* = 8.0 Hz, 1H, H₇), 3.97 (d, *J* = 11.5 Hz, 1H, H₁₁), 3.02 (d, *J* = 11.5, 1H, H₁₁), 2.45 (s, 3H, H₁), 1.22 (d, *J* = 4.6 Hz, 1H, H₉), 0.99 (dd, *J* = 4.6, 1.3 Hz, 1H, H₉), 0.87 (s, 3H, H₁₂).

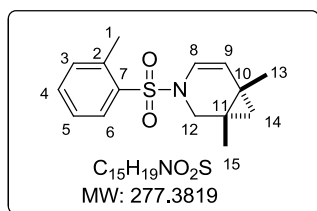
¹³C NMR (100 MHz, CDCl₃) δ 143.8 (C, C₅), 139.1 (C, C₂), 135.1 (C, C₁₃), 129.9 (4CH, C_{3,4}), 128.6 (2CH), 127.3 (CH), 127.2 (2CH), 121.0 (CH, C₆), 118.1 (CH, C₇), 48.2 (CH₂, C₁₁), 39.8 (C, C₁₀), 24.3 (CH₂, C₉), 21.7 (CH₃, C₁₂), 20.9 (CH₃, C₁), 18.9 (C, C₈).

Chiral HPLC analysis: Prepared (+)-**82** by using (*αS*)-**113** (3 mol%), AgSbF₆ (6 mol%) in CH₂Cl₂ at –20°C for 15 h.

Chiralpak AS-H, 95/5 *n*-heptane/*i*-PrOH, 1 mL/min. Retention time for minor enantiomer = 9.91 min; for major enantiomer = 11.45 min (*ee* = 29%); [α_D] = 28.9 (c 0.1, CHCl₃)

{[α_D] (*ent*-**82**) = –72 (c 0.85, CHCl₃, *ee* = 52%)}.^[18]

1,6-Dimethyl-3-(*o*-tolylsulfonyl)-3-azabicyclo[4.1.0]hept-4-ene (**83**)



The compound was prepared according to the general procedure **GP5** from enyne **51**, followed the conditions as shown in Table **S1** as a white solid.

$R_f = 0.27$ (EtOAc/pentane: 1/10).

IR (neat): $\tilde{\nu}$ (cm⁻¹) = 3061, 2989, 2948, 2873, 1642, 1458, 1398, 1274, 1177, 1136, 1112, 1065, 1037, 983, 842, 739.

¹H NMR (300MHz, CDCl₃) δ 7.84 (d, $J = 7.9, 1.5$ Hz, 1H, H₆), 7.38 (d, $J = 7.5$ Hz, 1H, H₃), 7.29-7.21 (m, 2H, H_{4,5}), 6.28 (d, $J = 7.9$, 1H, H₈), 5.14 (d, $J = 8.0$ Hz, 1H, H₉), 3.57 (d, $J = 11.6$ Hz, 1H, H₁₂), 2.81 (d, $J = 11.6$, 1H, H₁₂), 2.53 (s, 3H, H₁), 1.10 (s, 3H, H₁₃), 1.06 (s, 3H, H₁₅), 0.71 (d, $J = 4.4$ Hz, 1H, H₁₄), 0.31 (d, $J = 4.3$, 1H, H₁₄).

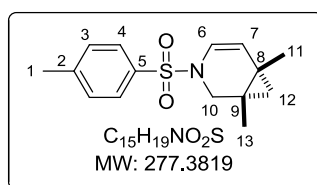
¹³C NMR (75 MHz, CDCl₃) δ 137.7 (C, C₇), 136.9 (C, C₂), 133.0 (CH, C₃), 132.9 (CH, C₄), 129.9 (CH, C₆), 126.3 (CH, C₅), 120.1 (CH, C₈), 117.5 (CH, C₉), 46.5 (CH₂, C₁₂), 29.8 (C, C₁₀), 26.6 (CH₂, C₁₄), 20.9 (CH₃, C₁), 18.9 (CH₃, C₁₃), 17.9 (C, C₁₁), 17.5 (CH₃, C₁₅).

HRMS (ESI) calcd for C₁₅H₁₉NO₂SNa ([M + Na]⁺) 300.1029, found 300.1019

Chiral HPLC analysis: Prepared **83** by using (*α*S)-**113** (3 mol%), AgSbF₆ (6 mol%) in CH₂Cl₂ at rt for 1 h.

Chiralpak AZ-H, 95/5 *n*-heptane/*i*-PrOH, 1 mL/min. Retention time for first enantiomer = 9.07 min; for second enantiomer = 9.61 min (*ee* = 1%).

1,6-Dimethyl-3-tosyl-3-azabicyclo[4.1.0]hept-4-ene (**84**)



The compound was prepared according to the general procedure **GP5** from enyne **52**, followed the conditions as shown in Table **S1** as a white solid.

The characterization data were identical to those previously reported.^[5]

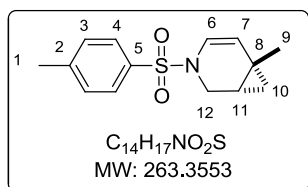
$R_f = 0.20$ (EtOAc/pentane: 1/10).

IR (neat): $\tilde{\nu}$ (cm⁻¹) = 2989, 2949, 2874, 1646, 1598, 1473, 1399, 1274, 1133, 1090, 1018, 990, 667.

¹H NMR (400 MHz, CDCl₃) δ 7.65 (d, $J = 8.4$ Hz, 2H, H₄), 7.30 (d, $J = 8.0$ Hz, 2H, H₃), 6.25 (dd, $J = 8.0, 1.2$ Hz, 1H, H₆), 5.17 (d, $J = 11.2$ Hz, 1H, H₇), 3.77 (d, $J = 11.2$ Hz, 1H, H₁₀), 2.67 (d, $J = 11.2$ Hz, 1H, H₁₀), 2.42 (s, 3H, H₁), 1.11 (s, 3H, H₁₁), 1.03 (s, 3H, H₁₃), 0.72 (d, $J = 4.4$ Hz, 1H, H₁₂), 0.32 (dd, $J = 4.4, 1.2$ Hz, 1H, H₁₂).

^{13}C NMR (75 MHz, CDCl_3) δ 143.7 (C, C₅), 135.1 (C, C₂), 129.8 (2CH, C₄), 127.2 (2CH, C₃), 120.1 (CH, C₆), 118.3 (CH, C₇), 46.8 (CH₂, C₁₀), 29.5 (C, C₈), 26.4 (CH₂, C₁₂), 21.7 (CH₃, C₁), 18.8 (CH₃, C₁₁), 17.7 (C, C₉), 17.6 (CH₃, C₁₃).

6-Methyl-3-tosyl-3-azabicyclo[4.1.0]hept-4-ene (85)



The compound was prepared according to the general procedure **GP5** from enyne **53**, followed the conditions as shown in Table **S1** as a white solid.

The characterization data were identical to those previously reported.^[19]

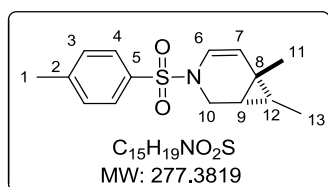
R_f = 0.34 (EtOAc/pentane: 1/10).

IR (neat): $\tilde{\nu}$ (cm⁻¹) = 2920, 2871, 1647, 1597, 1402, 1348, 1262, 1156, 1098, 1025.

^1H NMR (300 MHz, CDCl_3) δ 7.64 (d, J = 8.2 Hz, 2H, H₄), 7.30 (d, J = 8.2 Hz, 2H, H₃), 6.29 (d, J = 8.1 Hz, 1H, H₆), 5.22 (d, J = 8.1 Hz, 1H, H₇), 3.83 (d, J = 11.8 Hz, 1H, H₁₂), 3.03 (dd, J = 11.5, 2.7 Hz, 1H, H₁₂), 2.41 (s, 3H, H₁), 1.25 (bs, 1H, H₁₁), 1.09 (s, 3H, H₉), 0.57 (dd, J = 8.4, 4.4 Hz, 1H, H₁₀), 0.45 (t, J = 5.0 Hz, 1H, H₁₀).

^{13}C NMR (75 MHz, CDCl_3) δ 143.7 (C, C₅), 135.0 (C, C₂), 129.8 (2CH, C₄), 128.0 (2CH, C₃), 120.3 (CH, C₆), 116.6 (CH, C₇), 41.1 (CH₂, C₁₂), 25.8 (CH, C₁₁), 23.3 (CH₃, C₉), 21.6 (CH₃, C₁), 20.9 (CH₂, C₁₀), 12.8 (C, C₈).

6,7-Dimethyl-3-tosyl-3-azabicyclo[4.1.0]hept-4-ene (86)



The compound was prepared according to the general procedure **GP5** from enyne **54** ($E:Z$ = 9:1), followed the conditions as shown in Table **S1** as a white solid ($E:Z$ = 9:1).

The characterization data were identical to those previously reported.^[9]

R_f = 0.39 (EtOAc/ pentane: 1/10).

IR (neat): $\tilde{\nu}$ (cm⁻¹) = 2951, 2924, 1647, 1597, 1360, 1167, 1093, 928.

^1H NMR (300 MHz, CDCl_3) δ 7.73 (dd, J = 9.0, 5.1 Hz, H_{4-Z}), 7.63 (d, J = 8.1 Hz, 2H, H_{4-E}), 7.30 (d, J = 7.8 Hz, 2H, H_{3-E,Z}), 6.57 (d, J = 8.4 Hz, H_{6-Z}), 6.25 (d, J = 8.4 Hz, 1H, H_{6-E}), 5.19 (d, J = 8.1 Hz, 1H, H_{7-E}), 4.85 (d, J = 8.4 Hz, H_{7-Z}), 3.99 (bs, H_{10-Z}), 3.87 (d, J = 11.4 Hz, 1H, H_{10-E}), 3.71 (d, J = 6.9 Hz, H_{10-Z}), 3.47-3.34 (m, H_{10-Z}), 2.92 (dd, J = 11.4, 2.7 Hz, 1H, H_{10-E}), 2.41 (s, 3H, H_{1-E,Z}), 1.10 (s, H_{11-Z}), 1.04 (s,

Experimental part

3H, H_{11-E}), 0.93 (d, *J* = 6.3 Hz, 3H, H_{13-E,Z}), 0.87 (b, 1H, H_{9-E,Z}), 0.72-0.69 (m, H_{12-Z}), 0.61 (p, *J* = 6 Hz, 1H, H_{12-E}).

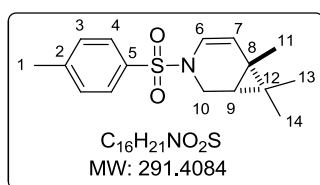
¹³C NMR (75 MHz, CDCl₃) δ 143.7 (C, C₅), 135.0 (C, C₂), 129.8 (2CH, C₄), 127.2 (2CH, C₃), 119.8 (CH, C₆), 118.2 (CH, C₇), 40.5 (CH₂, C₁₀), 32.5 (CH, C₉), 25.2 (CH₃, C₁₁), 21.6 (CH₃, C₁), 17.3 (CH, C₁₂), 16.4 (C, C₈), 13.0 (CH₃, C₁₃).

HRMS (ESI) calcd for C₁₅H₁₉NO₂SNa ([M + Na]⁺) 300.1029, found 300.1016.

Chiral HPLC analysis: Prepared **86** by using (*αS*)-**113** (3 mol%), AgSbF₆ (6 mol%) in CH₂Cl₂ at -20 °C for 14 h.

Lux-Cellulose-2 column, 95/5 *n*-heptane/*i*-PrOH, 1 mL/min. Retention time for first enantiomer = 17.61 min; for second enantiomer = 18.78 min (*ee* = 2%).

6,7,7-Trimethyl-3-tosyl-3-azabicyclo[4.1.0]hept-4-ene (**87**)



The compound was prepared according to the general procedure **GP5** from enyne **55**, followed the conditions as shown in Table **S1** as a white solid.

The characterization data were identical to those previously reported.^[20]

R_f = 0.47 (EtOAc/ pentane: 1/10).

IR (neat): $\tilde{\nu}$ (cm⁻¹) = 2920, 2871, 1402, 1348, 1262, 1156, 1098, 1025.

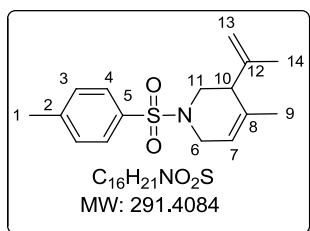
¹H NMR (300 MHz, CDCl₃) δ 7.67 (d, *J* = 8.3 Hz, 2H, H₄), 7.30 (d, *J* = 8.2 Hz, 2H, H₃), 6.54 (d, *J* = 8.4 Hz, 1H, H₆), 4.86 (d, *J* = 8.4 Hz, 1H, H₇), 3.42 -3.35 (m, 2H, H₁₀), 2.42 (s, 3H, H₁), 1.12 (s, 3H, H₁₁), 1.07 (s, 3H, H₁₃ or 14), 0.73 (s, 3H, H₁₃ or 14), 0.07 (s, 1H, H₉).

¹³C NMR (100 MHz, CDCl₃) δ 143.7 (C, C₅), 135.0 (C, C₂), 129.8 (2CH, C₄), 127.3 (2CH, C₃), 121.7 (CH, C₆), 110.7 (C, C₇), 38.7 (CH₂, C₁₀), 28.3 (CH, C₉), 28.1 (C, C₈), 23.0 (CH₃, C₁₁), 21.7 (CH₃, C₁), 19.6 (C, C₁₂), 19.2 (CH₃, C₁₃ or 14), 16.3 (CH₃, C₁₃ or 14).

HRMS (ESI) calcd for C₁₆H₂₁NO₂SNa ([M + Na]⁺) 314.1185, found 314.1179

Chiral HPLC analysis: Prepared **87** by using (*αS*)-**113** (3 mol%), AgSbF₆ (6 mol%) in CH₂Cl₂ at 0 °C for 18 h.

Chiralpak AD-H, 95/5 *n*-heptane/*i*-PrOH, 1 mL/min. Retention time for first enantiomer = 8.05 min; for second enantiomer = 8.77 min (*ee* = 5%)

4-Methyl-3-(prop-1-en-2-yl)-1-tosyl-1,2,3,6-tetrahydropyridine (88)

According to the synthesis of **87** from enyne **55**, followed the conditions as shown in Table **S1**, gave the minor product as colourless oil.

R_f = 0.29 (EtOAc/pentane: 1/10).

IR (neat): $\tilde{\nu}$ (cm⁻¹) = 2967, 2917, 1734, 1434, 1344, 1168, 671.

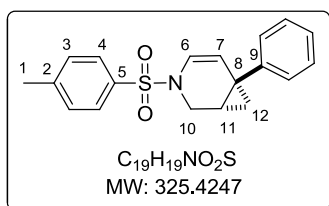
¹H NMR (300 MHz, CDCl₃) δ 7.65 (d, *J* = 8.2 Hz, 2H, H₄), 7.30 (d, *J* = 8.1 Hz, 2H, H₃), 5.45 (bs, 1H, H₇), 4.89 (s, 1H, H₁₃), 4.78 (s, 1H, H₁₃), 3.67 (d, *J* = 15.8 Hz, 1H, H₆), 3.35 (bs, 1H, H₆), 3.30 (dd, *J* = 11.4, 4.2 Hz, 1H, H₁₁), 2.94 (dd, *J* = 11.6, 4.9 Hz, 1H, H₁₁), 2.73 (bs, 1H, H₁₀), 2.42 (s, 3H, H₁), 1.72 (s, 3H, H₉), 1.60 (s, 3H, H₁₄).

¹³C NMR (100 MHz, CDCl₃) δ 144.1 (C, C₁₂), 143.5 (C, C₅), 134.1 (C, C₂), 133.5 (C, C₈), 129.7 (2CH, C₄), 127.9 (2CH, C₃), 118.5 (CH, C₇), 114.3 (CH₂, C₁₃), 47.7 (CH, C₁₀), 47.2 (CH₂, C₁₁), 44.9 (CH₂, C₆), 21.6 (CH₃, C₁), 21.4 (CH₃, C₉), 20.5 (CH₃, C₁₄).

HRMS (ESI) calcd for C₁₆H₂₁NO₂SNa ([M + Na]⁺) 314.1185, found 314.1181.

Chiral HPLC analysis: Prepared **88** by using (*α*S)-**113** (3 mol%), AgSbF₆ (6 mol%) in CH₂Cl₂ at 0 °C for 18 h.

Chiralpak AD-H, 95/5 *n*-heptane/*i*-PrOH, 1 mL/min. Retention time for first enantiomer = 12.85 min; for second enantiomer = 14.20 min (*ee* = 6 %)

6-Phenyl-3-tosyl-3-azabicyclo[4.1.0]hept-4-ene (89)

The compound was prepared according to the general procedure **GP5** from enyne **57**, followed the conditions as shown in Table **S1** as a white solid.

The characterization data were identical to those previously reported.^[20,21]

R_f = 0.15 (EtOAc/pentane: 1/20) (*Note*: the spot of product and starting enyne is the same R_f on TLC silica gel).

IR (neat): $\tilde{\nu}$ (cm⁻¹) = 3060, 3026, 2920, 1641, 1495, 1447, 1345, 1167, 1099, 951.

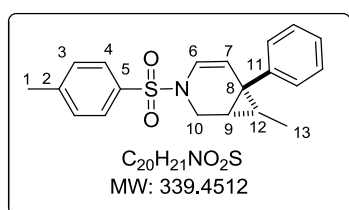
¹H NMR (400 MHz, CDCl₃) δ 7.78 (d, *J* = 8.4 Hz, 2H, H₄), 7.42 (d, *J* = 8.4 Hz, 2H, H₃), 7.36-7.33 (m, 2H, H_{ar}), 7.27-7.24 (m, 3H, H_{ar}), 6.55 (d, *J* = 8.4 Hz, 1H, H₆), 5.59 (d, *J* = 8.4 Hz, 1H, H₇), 4.08 (d, *J* = 11.6 Hz, 1H, H₁₀), 3.24 (dd, *J* = 11.6, 2.4 Hz, 1H, H₁₀), 2.52 (s, 3H, H₁), 1.80 (t, *J* = 7.6 Hz, 1H, H₁₁), 1.45 (dd, *J* = 8.8, 4.8 Hz, 1H, H₁₂), 0.97 (t, *J* = 5.2 Hz, 1H, H₁₂).

¹³C NMR (100 MHz, CDCl₃) δ 143.9 (C, C₅), 143.7 (C, C₉), 135.0 (C, C₂), 129.9 (2CH, C₄), 128.6 (2CH, C₃), 127.2 (2CH, C_{ar}), 127.0 (2CH, C_{ar}), 126.4 (CH, C_{ar}), 121.1 (CH, C₆), 114.9 (CH, C₇), 40.8 (CH₂, C₁₀), 28.7 (CH, C₁₁), 21.8 (C, C₈), 21.7 (CH₃, C₁), 21.0 (CH₂, C₁₂).

Chiral HPLC analysis: Prepared **89** by using (aR)-**113** (3 mol%), AgBF₄ (6 mol%) in toluene at reflux for 20 h.

Chiralpak IA, Heptane/Ethanol 95/5, 1 ml/min. Retention time for first enantiomer = 9.19 min; for second enantiomer = 25.37 min (*ee* = 0%).

7-Methyl-6-phenyl-3-tosyl-3-azabicyclo[4.1.0]hept-4-ene (**90**)



The compound was prepared according to the general procedure **GP5** from enyne **58** (*E/Z* = 9:1), followed the conditions as shown in Table **S1** as a white solid (*E/Z* = 9:1).

The characterization data were identical to those previously reported.^[13]

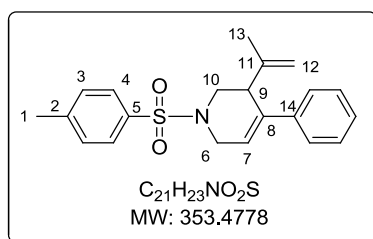
R_f = 0.31 (EtOAc/pentane: 1/10).

IR (neat): $\tilde{\nu}$ (cm⁻¹) = 3026, 2952, 2924, 1599, 1495, 1465, 1445, 1344, 1306, 1244, 1166, 1039, 950, 799, 675.

¹H NMR (400 MHz, CDCl₃) δ 7.69 (d, *J* = 8.2 Hz, 2H, H_{4-E}), 7.33 (d, *J* = 7.9 Hz, 2H, H_{3-E}), 7.29-7.26 (m, 2H, H_{ar-E,Z}), 7.22-7.16 (m, 3H, H_{ar-E,Z}), 6.75 (d, *J* = 8.0 Hz, H_{6-Z}), 6.35 (dd, *J* = 8.4, 0.9 Hz, 1H, H_{6-E}), 5.16 (dd, *J* = 8.4, 0.8 Hz, H_{6-Z}), 5.44 (dd, *J* = 8.2, 1.0 Hz, 1H, H_{7-E}), 5.16 (d, *J* = 8.2, 1.0 Hz, H_{7-Z}), 4.11 (d, *J* = 11.5 Hz, 1H, H_{10-E}), 3.66 (d, *J* = 12.0 Hz, H_{10-Z}), 3.50 (dd, *J* = 12.0, 5.4 Hz, H_{10-Z}), 3.12 (dd, *J* = 11.5, 2.6 Hz, 1H, H_{10-E}), 2.44 (s, 3H, H_{1-E,Z}), 1.69 (bs, 1H, H_{9-E,Z}), 1.07 (p, *J* = 6.0 Hz, 1H, H_{12-E,Z}), 0.95 (d, *J* = 6.2 Hz, H_{13-Z}), 0.67 (d, *J* = 6.3 Hz, 1H, H_{13-E}).

¹³C NMR (100 MHz, CDCl₃) δ 143.8 (C, C₅), 140.6 (C, C₁₁), 134.9 (C, C₂), 129.9 (2CH, C₄), 129.3 (2CH, C₃), 128.5 (2CH, C_{ar}), 127.2 (2CH, C_{ar}), 126.6 (CH, C_{ar}), 119.8 (CH, C₆), 117.6 (CH, C₇), 40.6 (CH₂, C₁₀), 31.1 (CH, C₉), 27.6 (CH, C₁₂), 27.5 (C, C₈), 21.6 (CH₃, C₁), 14.7 (CH₃, C₁₃).

3-Benzylidene-4-(prop-1-en-2-yl)-1-tosylpyrrolidine (**91**)



The compound was prepared according to the general procedure **GP5** from enyne **59**, followed the conditions as shown in Table **S1** as a white solid.

The characterization data were identical to those previously reported^[13]

$R_f = 0.14$ (EtOAc/pentane: 1/10).

m.p. = 97–100 °C.

IR (neat): $\tilde{\nu}$ (cm⁻¹) = 3062, 3029, 2920, 2851, 2256, 1641, 1597, 1575, 1458, 1445, 1400, 1274, 1036, 996, 908, 815, 730.

¹H NMR (300 MHz, CDCl₃) δ 7.70 (d, $J = 10.1$ Hz, 2H, H₄), 7.32 (d, $J = 8.0$ Hz, 2H, H₃), 7.28–7.22 (m, 5H, H_{ar}), 6.03 (t, $J = 3.8$ Hz, 1H, H₇), 4.87 (t, $J = 1.5$ Hz, 1H, H₁₂), 4.78 (bs, 1H, H₁₂), 3.99 (dd, $J = 17.1, 3.3$ Hz, 1H, H₆), 3.64 (dd, $J = 11.4, 3.5$ Hz, 1H, H₁₀), 3.50 (dt, $J = 17.0, 2.8$ Hz, 1H, H₆), 3.38 (bs, 1H, H₉), 2.96 (dd, $J = 11.6, 4.3$ Hz, 1H, H₁₀), 2.42 (s, 3H, H₁), 1.74 (s, 3H, H₁₃).

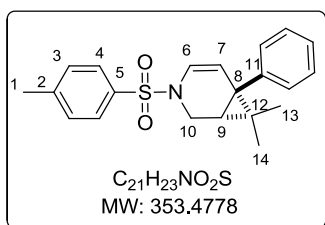
¹³C NMR (75 MHz, CDCl₃) δ 143.7 (C, C₅), 143.6 (C, C₁₁), 139.9 (C, C₈), 137.7 (C, C₂), 133.5 (C, C₁₄), 129.7 (2CH, C₄), 128.4 (2CH, C₃), 127.8 (2CH, C_{15,17}), 127.5 (CH, C₁₆), 125.8 (2CH, C_{14,16}), 121.0 (CH, C₇), 115.2 (CH₂, C₁₂), 47.5 (CH₂, C₁₀), 45.3 (CH₂, C₆), 45.0 (CH, C₉), 21.6 (CH₃, C₁), 21.3 (CH₃, C₁₃).

HRMS (ESI) calcd for C₂₁H₂₃NO₂SH₂ONa ([M + NaH₂O]⁺) 394.1447, found 394.1444.

Chiral HPLC analysis: Prepared **91** by using (*α*S)-**113** (3 mol%), AgSbF₆ (6 mol%) in CH₂Cl₂ at rt for 3 h.

Chiralpak AD-H, 95/5 *n*-heptane/*i*-PrOH, 1 mL/min. Retention time for first enantiomer = 18.80 min; for second enantiomer = 21.17 min (*ee* = 4%).

7,7-Dimethyl-6-phenyl-3-tosyl-3-azabicyclo[4.1.0]hept-4-ene (**92**)



According to the synthesis of **91** from enyne **59**, followed the conditions as shown in Table **S1**, gave the minor product as colourless oil (10 mg), 10% yield.

The characterization data were identical to those previously reported.^[22]

$R_f = 0.28$ (EtOAc/ pentane: 1/10).

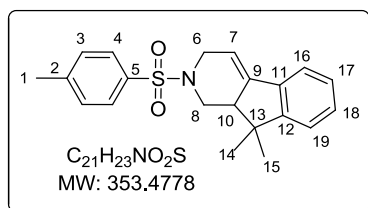
IR (neat): $\tilde{\nu}$ (cm⁻¹) = 3059, 2021, 2867, 1647, 1598, 1446, 1347, 1264, 1167, 1097, 954.

¹H NMR (400 MHz, C₆D₆) δ 7.60 (d, $J = 8.3$ Hz, 2H, H₄), 7.22 (d, $J = 8.0$ Hz, 2H, H₃), 7.20–7.13 (m, 3H, H_{ar}), 7.09–7.07 (m, 1H, H_{ar}), 6.99–6.97 (m, 1H, H_{ar}), 6.50 (d, $J = 8.4$ Hz, 1H, H₆), 4.99 (dd, $J = 8.4, 0.9$ Hz, 1H, H₇), 3.61 (dd, $J = 12.2, 1.6$ Hz, 1H, H₁₀), 3.44 (dd, $J = 12.3, 6.0$ Hz, 1H, H₁₀), 2.34 (s, 3H, H₁), 1.45 (s, H₉), 0.86 (s, 3H, H₁₃ or 14), 0.64 (s, 3H, H₁₃ or 14).

¹³C NMR (100 MHz, C₆D₆) δ 143.9 (C, C₅), 142.5 (C, C₁₁), 135.0 (C, C₂), 129.9 (2CH, C₄), 128.9 (2CH, C₃), 128.5 (2CH, C_{ar}), 127.3 (2CH), 126.4 (CH), 121.6 (CH, C₆), 110.6 (CH, C₇), 38.9 (CH₂, C₁₀), 31.0 (C, C₈), 30.5 (C, C₁₂), 27.3 (CH₃, C₁₃ or 14), 25.0 (CH, C₉), 21.7 (CH₃, C₁), 16.0 (2CH₃, C₁₃ or 14).

HRMS (ESI) calcd for C₂₁H₂₃NO₂SNa ([M + Na]⁺) 376.1342, found 376.1350.

4,4-Dimethyl-2-tosyl-2,3,4-tetrahydro-1H-benzoisoindole (93)



The compound was prepared according to the general procedure **GP5** from enyne **59**, followed the conditions as shown in Table **S1** as a white solid.

R_f = 0.03 (EtOAc/pentane: 1/10).

m.p. = 66–67 °C.

IR (neat): $\tilde{\nu}$ (cm⁻¹) = 3058, 3027, 2969, 2926, 2853, 1650, 1460, 1443, 1345, 1290, 1164, 1091, 977, 932, 760.

¹H NMR (400 MHz, C₆D₆) δ 7.75 (d, J = 8.2 Hz, 2H, H₄), 7.25 (s, 1H, H_{ar}), 7.21-7.19 (m, 2H, H_{ar}), 7.14 (s, 1H, H_{ar}), 6.96 (d, J = 8.0 Hz, 2H, H₃), 5.47 (t, J = 3.3 Hz, 1H, H₇), 4.51 (dd, J = 11.8, 1.1 Hz, 1H, H₉), 4.14 (dd, J = 17.2, 3.8 Hz, 1H, H₆), 3.09 (dt, J = 17.2, 2.6 Hz, 1H, H₆), 2.78 (bs, 1H, H₁₀), 2.27 (dd, J = 11.8, 3.6 Hz, 1H, H₉), 2.05 (s, 3H, H₁), 1.43 (s, 3H, H_{14 or 15}), 1.23 (s, 3H, H_{14 or 15}).

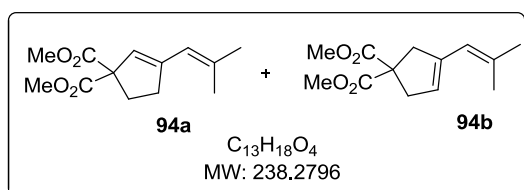
¹³C NMR (100 MHz, C₆D₆) δ 143.4 (C, C₅), 143.3 (C, C₁₁), 139.0 (C, C₂), 133.8 (C, C₁₂), 129.8 (2CH, C₄), 128.7 (2CH, C₃), 128.2 (2CH), 127.5 (CH), 126.8 (2CH), 124.0 (CH, C₇), 73.6 (C, C₁₃), 47.8 (CH, C₁₀), 45.8 (CH₂, C₆), 45.4 (CH₂, C₉), 31.1 (CH₃, C_{14 or 15}), 28.6 (CH₃, C_{14 or 15}), 21.2 (CH₃, C₁).

HRMS (ESI) calcd for C₂₁H₂₃NNaO₂S ([M + Na]⁺) 376.1342, found 376.1346.

Chiral HPLC analysis: Prepared **93** by using (α S)-**113** (3 mol%), AgSbF₆ (6 mol%) in CH₂Cl₂ at -5 °C for 18 h.

Chiralcel AS-H-A, 80/20 *n*-heptane/EtOH+TFA, 1 mL/min. Retention time for major enantiomer = 6.20 min; for minor enantiomer = 9.22 min (*ee* = 7%).

Inseparable mixture of dimethyl-5-(propan-2-ylidene)cyclopent-2-ene-1,1-dicarboxylate (a) and dimethyl 5-(propan-2-ylidene)cyclopent-3-ene-1,1-dicarboxylate (b) with a ratio (2:1) (94)



The compound was prepared according to the general procedure **GP5** from enyne **63**, followed the conditions as shown in Table **S1** as yellow oil of the mixture a and b (2:1).

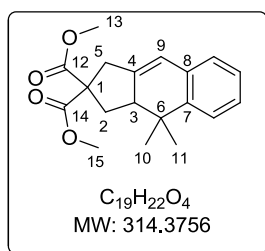
R_f = 0.17 (EtOAc/Pentane: 0.2/10).

IR (neat): $\tilde{\nu}$ (cm⁻¹) = 2954, 2911, 1731, 1453, 1379, 1248, 1155, 1060, 865.

¹H NMR (300 MHz, CDCl₃) δ 5.77 (s, 1H, a), 5.70 (s, 1H, b), 5.56 (s, 1H, a), 5.35 (s, 1H, b), 3.70 (s, 6H, b), 3.69 (s, 6H, a), 3.16 (bs, 2H, b), 3.01 (bs, 2H, a), 2.62 (t, J = 6.6 Hz, 2H, b), 2.46-2.42 (m, 2H, a), 1.80 (s, 3H, a), 1.79 (s, 3H, b), 1.77 (s, 3H, a), 1.75 (s, 3H, b).

¹³C NMR (75 MHz, CDCl₃) δ 172.6 (C, b), 172.0 (C, a), 146.1 (C, a), 138.8 (C, b), 138.0 (C, a), 135.6 (C, b), 124.9 (CH, a), 124.5 (CH, b), 120.7 (2CH, a, b), 66.0 (C, a), 59.4 (C, b), 52.8 (C, b), 52.6 (CH, a), 43.3 (CH₂, b), 40.3 (CH₂, b), 34.8 (CH₂, a), 32.2 (CH₂, a), 27.4 (CH₃, a), 27.3 (CH₃, b), 19.9 (2CH₃, a, b).

Dimethyl 4,4-dimethyl-3a,4-dihydro-1H-cyclopenta[b]naphthalene-2,2(3H)-dicarboxylate (**95**)



The compound was prepared according to the general procedure **GP5** from enyne **65**, followed the conditions as shown in Table **S1** as a white solid.

The characterization data were identical to those previously reported.^[4]

R_f = 0.14 (EtOAc/pentane: 1/10).

IR (neat): $\tilde{\nu}$ (cm⁻¹) = 2954, 2868, 2843, 1731, 1433, 1200, 1129, 1113, 1066, 989, 888, 752.

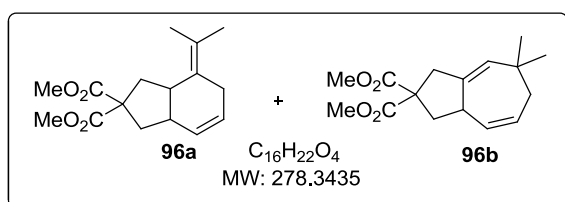
¹H NMR (400 MHz, CDCl₃) δ 7.31-7.29 (m, 1H, H_{ar}), 7.16-7.13 (m, 2H, H_{ar}), 7.03-7.01 (m, 1H, H_{ar}), 6.37 (d, *J* = 2.2 Hz, 1H, H₉), 3.78 (s, 3H, H_{13 or 15}), 3.73 (s, 3H, H_{13 or 15}), 3.32 (dd, *J* = 18.0, 1.5 Hz, 1H, H₅), 3.01 (dt, *J* = 18.0 Hz, 3 Hz, 1H, H₅), 2.75-2.70 (m, 1H, H₂), 2.62 (ddd, *J* = 12.3, 7.5, 1.4 Hz, 1H, H₂), 2.17 (t, *J* = 12.4 Hz, 1H, H₃), 1.44 (s, 3H, H_{10 or 11}), 0.94 (s, 3H, H_{10 or 11}).

¹³C NMR (100 MHz, CDCl₃) δ 172.2 (C, C_{12 or 14}), 172.0 (C, C_{12 or 14}), 144.1 (C, C₇), 143.0 (C, C₄), 134.0 (C, C₈), 127.0 (CH), 126.4 (CH), 126.3 (CH), 123.5 (CH), 119.5 (CH, C₉), 59.0 (C, C₁), 52.9 (CH₃, C_{13 or 15}), 52.9 (CH₃, C_{13 or 15}), 48.5 (CH, C₃), 39.3 (CH₂, C₂), 36.7 (C, C₆), 34.9 (CH₂, C₅), 25.7 (CH₃, C_{10 or 11}), 22.1 (CH₃, C_{10 or 11}).

Chiral HPLC analysis: Prepared **95** by using (*αS*)-**113** (3 mol%), AgSbF₆ (6 mol%) in CH₂Cl₂ at -20 °C for 18 h.

Chiralpak AD-H, 95/5 *n*-heptane/*i*-PrOH, 1 mL/min. Retention time for first enantiomer = 5.56 min; for second enantiomer = 6.80 min (*ee* = 0 %).

Inseparable mixture of dimethyl 7-(propan-2-ylidene)-3,3a,7,7a-tetrahydro-1H-indene-2,2(6H)-dicarboxylate (**a**) and dimethyl 3,3a,6,7-tetrahydroazulene-2,2(1H)-dicarboxylate (**b**) (**96**)



The compound was prepared according to the general procedure **GP5** from enyne **78**, followed the conditions as shown in Table **S1** as colorless oil.

The characterization data were identical to those previously reported.^[16]

R_f = 0.24 (EtOAc/Pentane: 1/10).

The mixture of **96a:96b** = 80:20 for (±)-**113**.

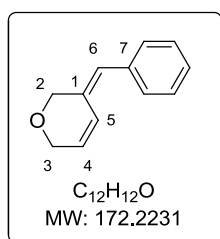
¹H NMR (300 MHz, CDCl₃) δ 5.85-5.82(m, 1H), 5.70-5.69 (m, 1H), 5.16 (bs, 0.5H), 3.71 (m, 10H), 2.99-2.60 (m, 6H), 2.20-2.14 (bm, 3H), 1.77 (s, 3H), 1.71-1.67 (m, 1H), 1.63 (s, 3H), 0.99 (s, 1H), 0.94 (s, 1H).

¹³C NMR (75 MHz, CDCl₃) δ 173.3, 172.3, 136.7, 135.1, 132.6, 129.2, 129.1, 128.1, 124.0, 58.5, 52.8, 48.3, 44.5, 42.1, 41.1, 39.9, 39.2, 39.1, 37.6, 34.4, 31.6, 28.7, 22.1, 21.9.

The mixture of **96a: 96b** = 60:40 for (±)-**41b**.

¹H NMR (400 MHz, CDCl₃) δ 5.88 (dd, *J* = 10.0, 2.8 Hz, 0.3H), 5.83 (d, *J* = 10.8 Hz, 1H), 5.73-5.68 (m, 2H), 5.16 (bs, 1H), 3.73-3.69 (m, 13H), 2.99-2.45 (m, 11H), 2.19-2.16 (m, 2H), 2.07 (dd, *J* = 12.0, 11.2 Hz, 1H), 1.77 (s, 3H), 1.64(s, 3H), 0.99 (s, 2H), 0.94 (s, 2H).

3-Benzylidene-3,6-dihydro-2H-pyran (97)



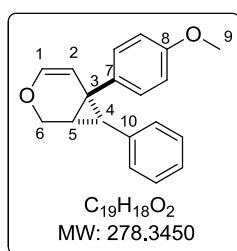
The compound was prepared according to the general procedure **GP5** from enyne **61**, followed the conditions as shown in Table **S1** as colorless oil, 20% yield.

R_f = 0.4 (EtOAc/pentane: 1/20).

¹H NMR (400 MHz, CDCl₃) δ 7.37-7.29 (m, 5H, H_{ar}), 6.76 (dtd, *J* = 12.0, 4.0, 1.1 Hz, 1H, H₅), 6.26 (s, 1H, H₆), 5.97 (dtd, *J* = 12.0, 4.0, 1.7 Hz, 1H, H₄), 4.36 (d, *J* = 1.3 Hz, 2H, H₃), 4.34-4.32 (m, 1H, H₂).

¹³C NMR (100 MHz, CDCl₃) δ 136.6 (C, C₁), 131.7 (C, C₇), 130.2 (CH, C₅), 129.2 (2CH), 128.3 (2CH), 127.0 (CH), 124.1 (CH, C₆), 123.0 (CH, C₄), 70.4 (CH₂, C₃), 66.4 (CH₂, C₂).

6-(4-Methoxyphenyl)-7-phenyl-3-oxabicyclo[4.1.0]hept-4-ene (98)



The compound was prepared according to the general procedure **GP5** from enyne **62**, followed the conditions as shown in Table **S1** as a white solid.

The characterization data were identical to those previously reported.^[23]

R_f = 0.4 (EtOAc/pentane: 1/10).

IR (neat): $\tilde{\nu}$ (cm⁻¹) = 2923, 2855, 1733, 1611, 1509, 1459, 1241, 1172, 1086, 1025, 985, 806.

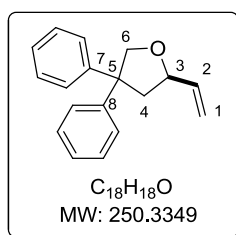
¹H NMR (300 MHz, CDCl₃) δ 7.07-6.97 (m, 5H, H_{ar}), 6.78-6.69 (m, 4H, H_{ar}), 6.24 (d, *J* = 6.0 Hz, 1H, H₁), 5.31 (d, *J* = 5.4 Hz, 1H, H₂), 4.40 (dd, *J* = 10.5, 1.2 Hz, 1H, H₆), 4.07 (dd, *J* = 10.5, 1.8 Hz, 1H, H₆), 3.73 (s, 3H, H₉), 2.73 (d, *J* = 5.9 Hz, 1H, H₄), 2.39 (d, *J* = 5.3 Hz, 1H, H₅).

^{13}C NMR (75 MHz, CDCl_3) δ 158.2 (C, C_8), 140.5 (CH, C_1), 137.9 (C, C_{10}), 132.1 (C, C_7), 130.9 (2CH), 127.8 (4CH), 125.7 (CH), 113.8 (2CH), 112.1 (CH, C_2), 61.6 (CH_2 , C_6), 55.3 (CH, C_5), 37.4 (CH_3 , C_9), 30.4 (C, C_3), 30.3 (CH, C_4).

Chiral HPLC analysis: Prepared **98** by using (*oR*)-**113** (3 mol%), AgSbF_6 (6 mol%) in CH_2Cl_2 at rt for 1 h. and (*R*)-**41b** (3 mol%), AgSbF_6 (3.5 mol%) in CH_2Cl_2 at rt for 20 h.

Lux-Cellulose-4, 95/5 *n*-heptane/*i*-PrOH, 1 mL/min. Retention time for first enantiomer = 5.09 min; for second enantiomer = 5.73 min (*ee* = 0 %).

4,4-Diphenyl-2-vinyltetrahydrofuran (**99**)



The compound was prepared according to the general procedure **GP5** from enyne **68**, followed the conditions as shown in Table **S1** as colorless oil.

The characterization data were identical to those previously reported.^[14]

R_f = 0.43 (EtOAc/pentane: 1/9).

IR (neat): $\tilde{\nu}$ (cm^{-1}) = 3086, 3058, 2983, 2921, 2862, 1947, 1873, 1804, 1599, 1493, 1445, 1260, 1083, 926, 754, 731.

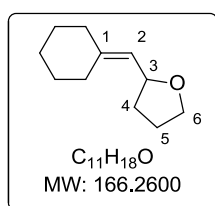
^1H NMR (400 MHz, CDCl_3) δ 7.39-7.32 (m, 6H, H_{ar}), 7.27-7.22 (m, 4H, H_{ar}), 5.99-5.91 (m, 1H, H_2), 5.29 (dt, J = 17.2, 1.2 Hz, 1H, H_1), 5.15 (dt, J = 10.4, 1.2 Hz, 1H, H_1), 4.72 (dd, J = 8.4, 1.2 Hz, 1H, H_3), 4.52-4.46 (m, 1H, H_6), 4.21 (d, J = 8.8 Hz, 1H, H_6), 2.71 (ddd, J = 12.0, 6.0, 1.2 Hz, 1H, H_4), 2.49 (dd, J = 10.0, 9.6 Hz, 1H, H_4).

^{13}C NMR (75 MHz, CDCl_3) δ 146.1 (C, $\text{C}_{7 \text{ or } 8}$), 145.7 (C, $\text{C}_{7 \text{ or } 8}$), 138.9 (CH, C_2), 128.5 (2CH), 128.5 (2CH), 127.3 (2CH), 127.2 (2CH), 126.6 (CH), 126.4 (CH), 116.0 (CH_2 , C_1), 79.8 (CH, C_3), 77.2 (CH_2 , C_6), 56.3 (C, C_5), 45.3 (CH_2 , C_4).

Chiral HPLC analysis: Prepared **99** by using (*R*)-**41b** (3 mol%), AgOTs (4.5 mol%) in toluene at rt for 5 h.

Lux-Cellulose-4, 95/5 *n*-heptane/*i*-PrOH, 1 mL/min. Retention time for first enantiomer = 4.66 min; for second enantiomer = 5.06 min (*ee* = 38 %).

2-(Cyclohexylidenemethyl)tetrahydrofuran (**100**)



The compound was prepared according to the general procedure **GP5** from allenol **69**, followed the conditions as shown in Table **S1** as colorless oil.

The characterization data were identical to those previously reported.^[15]

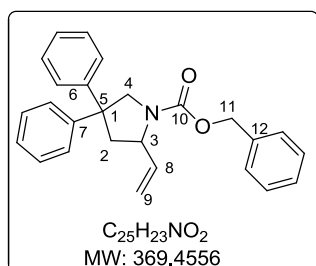
R_f = 0.50 (EtOAc/pentane: 1/10).

IR (neat): $\tilde{\nu}$ (cm^{-1}) = 2924, 2853, 1670, 1446, 1051, 936.

¹H NMR (400 MHz, CDCl₃) δ 5.12 (d, *J* = 8.4 Hz, 1H, H₂), 4.54-4.49 (m, 1H, H₃), 3.90-3.85 (m, 1H, H₆), 3.74-3.68 (m, 1H, H₆), 2.20-1.82 (m, 7H), 1.54-1.48 (m, 7H)

¹³C NMR (100 MHz, CDCl₃) δ 143.7 (C, C₁), 122.7 (CH, C₂), 75.0 (CH, C₃), 67.8 (CH₂, C₆), 37.2 (CH₂, C₄), 32.9 (CH₂, C₄), 29.3 (CH₂, C_{cy}), 28.4 (CH₂, C_{cy}), 27.9 (CH₂, C_{cy}), 26.8 (CH₂, C_{cy}), 26.3 (CH₂, C₅).

Phenyl 4,4-diphenyl-2-vinylpyrrolidine-1-carboxylate (101)



The compound was prepared according to the general procedure **GP5** from allenol **71**, followed the conditions as shown in Table **S1** as colorless oil.

The characterization data were identical to those previously reported.^[14]

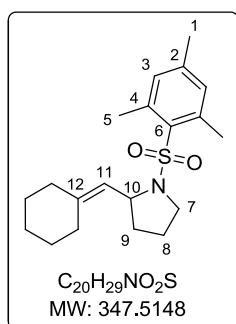
R_f = 0.33 (EtOAc/pentane: 1/10).

IR (neat): $\tilde{\nu}$ (cm⁻¹) = 3060, 1695, 1405, 1355, 1211, 1195, 1096, 918.

¹H NMR (300 MHz, CDCl₃) δ 7.37-7.15 (s, 15H, H_{ar}), 5.81-5.70 (m, 1H, H₈), 5.31-4.99 (m, 4H, H_{9,11}), [4.74 (d, *J* = 11.4 Hz), 4.59 (d, *J* = 11.4)], 1H, H₃, 4.17-4.06 (m, 1H, H₄), 3.70 (dd, *J* = 11.4, 5.4 Hz, 1H, H₄), 2.86-2.79 (m, 1H, H₂), 2.48-2.36 (m, 1H, H₂).

¹³C NMR (100 MHz, CDCl₃) δ 155.6 (C, C₇), 154.8 (2C, C_{6,7}), 145.5 (C, C₁₂), 144.8 (CH, C₈), 139.3 (CH), 138.6 (CH), 137.1, 137.0, 128.8, 128.7, 128.4, 128.3, 128.2, 128.1, 127.8, 127.6, 126.9, 126.7, 126.6, 126.5, 115.8 (CH₂, C₉), 115.2 (CH₂, C₉), 67.0 (2CH₂, C₁₁), [59.6, 59.1 (CH, C₃)], 56.3 (2CH₂, C₄), [53.1, 52.8 (C, C₅)], 45.7 (CH₂, C₂), 44.7 (CH₂, C₂).

2-(Cyclohexylidenemethyl)-1-(mesitylsulfonyl)pyrrolidine (102)



The compound was prepared according to the general procedure **GP5** from allene **72**, followed the conditions as shown in Table **S1** as colorless oil.

IR (neat): $\tilde{\nu}$ (cm⁻¹) = 2923, 1670, 1445, 1380, 1149, 1059.

The characterization data were identical to those previously reported.^[15]

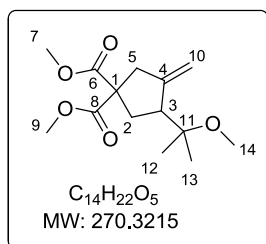
R_f = 0.50 (EtOAc/pentane: 1/20).

¹H NMR (400 MHz, CDCl₃) δ 6.88 (s, 2H, 2H₃), 4.68 (d, *J* = 9.2 Hz, 1H, H₁₁), 4.52-4.46 (m, 1H, H₁₀), 3.60 (dt, *J* = 10.0, 6.8 Hz, 1H, H₇), 3.28 (dt, *J* = 10.0, 6.8 Hz, 1H, H₇), 2.60 (s, 6H, H₅), 2.26 (s, 3H, H₁), 2.12-2.04 (m, 1H, H₉), 2.00-1.98 (m, 2H, H_{cy}), 1.93-1.84 (m, 2H, H₈), 1.77-1.75 (m, 1H, H_{cy}), 1.70-1.67 (m, 1H, H_{cy}), 1.61-1.55 (m, 1H, H₉), 1.44-1.25 (m, 6H, H_{cy}).

¹³C NMR (100 MHz, CDCl₃) δ 142.1 (C, C₁₂), 140.7 (C, C₂ or C₆), 140.3 (C,2C, C₄), 134.2 (C, C₂ or C₆), 131.7 (2CH, 2C₃), 122.1 (CH, C₁₁), 56.5 (CH, C₁₀), 47.6 (CH₂, C₇), 36.9 (CH₂, C_{Cy}), 34.8 (CH₂, C₉), 28.9 (CH₂, C_{Cy}), 28.2 (CH₂, C_{Cy}), 27.5 (CH₂, C_{Cy}), 26.7 (CH₂,C_{Cy}), 24.9 (CH₂, C₈), 23.0 (2CH₃, 2C₅), 21.0 (CH₃, C₁).

2.8.2. Methoxycyclization reaction

3-(2-Methoxypropan-2-yl)-4-methylene-1-tosylpyrrolidine (103)



The compound was prepared according to the general procedure **GP5** from enyne **63**, followed the conditions as shown in Table **S1** as colorless oil.

The characterization data were identical to those previously reported.^[24]

R_f = 0.38 (EtOAc/pentane: 1/10).

IR (neat): $\tilde{\nu}$ (cm⁻¹) = 2953, 1733, 1434, 1364, 1272, 1230, 1202, 1077.

¹H NMR (400 MHz, CDCl₃) δ, 5.05(bs, 1H, H₁₀), 5.00 (bs, 1H, H₁₀), 3.75 (s, 3H, H₇ or ₉), 3.73 (s, 3H, H₇ or ₉), 3.21 (s, 3H, H₁₄), 2.96-2.84 (m, 3H, H_{3,5}), 2.57 (ddd, *J* = 13.5, 8.5, 1.7 Hz, 1H, H₂), 2.03 (dd, *J* = 12.0, 9.4 Hz, 1H, H₂), 1.20 (s, 3H₁₂ or ₁₃), 1.14 (s, 3H, H₁₂ or ₁₃).

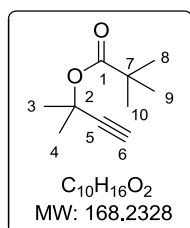
¹³C NMR (75 MHz, CDCl₃) δ 172.2 (C, C₆), 172.1 (C, C₈), 148.3 (C, C₄), 110.7 (CH₂, C₁₀), 76.9 (C, C₁₁), 58.7 (CH, C₃), 52.9 (C, C₁), 52.8(CH₂, C₂), 49.3 (CH₃, C₇ or ₉), 49.2 (CH₃, C₇ or ₉), 43.5 (CH₃, C₁₄), 36.1 (CH₂, C₅), 22.8 (CH₃, C₁₂ or ₁₃), 22.3 (CH₃, C₁₂ or ₁₃).

Chiral HPLC analysis: Prepared **103** by using (*αS*)-**113** (3 mol%), AgSbF₆ (6 mol%) in MeOH at rt for 24 h.

Lux-Cellulose-2, 95/5 *n*-heptane/*i*-PrOH, 1 mL/min. Retention time for minor enantiomer = 5.92 min; for major enantiomer = 12.52 min (*ee* = 18%).

2.8.3. Olefin cyclopropanation reaction

2-Methylbut-3-yn-2-yl pivalate (104)



To a solution of 2-methylbut-3-yn-2-ol (1.1 mL, 11.9 mmol, 1 equiv) in CH₂Cl₂ (15 mL) was added DMAP (0.3 g, 2.45 mmol, 0.2 equiv) and Et₃N (2.5 mL, 1.82 mmol, 1.5 equiv) at rt. The pivaloyl chloride (1.77 mL, 14.37 mmol, 1.2 equiv) was slowly added at 0 °C and the mixture was refluxed for 15 h. The reaction

was quenched with NaHCO₃ sat (20 mL) and diluted with hexanes (20 mL). The mixture was stirred until the bubble of CO₂ gas was disappeared. NH₄OH solution (10 mL) was

added into the mixture to remove the excess pivaloyl chloride. The aqueous phase was extracted with hexanes (3x 20 mL). The combined organic layers were washed with brine (20 mL), dried over anhydrous MgSO₄, filtered and concentrated on rotary evaporation under reduced pressure in cold bath (the product is a volatile). The residue was purified by filtered over a short pad of silica gel and concentrate under reduced pressure to give **104** (49 mg, 25% yield).

The characterization data were identical to those previously reported.^[12]

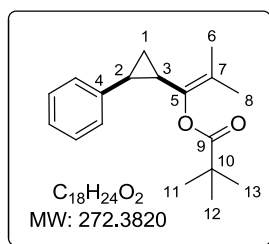
R_f = 0.68 (EtOAc/pentane: 1/10).

IR (neat): $\tilde{\nu}$ (cm⁻¹) = 3269, 2985, 1737, 1481, 1365, 1286, 1117.

¹H NMR (400 MHz, CDCl₃) δ 2.50 (s, 1H, H₆), 1.66 (s, 6H, H_{3,4}), 1.18 (s, 9H, H₈₋₁₀).

¹³C NMR (75 MHz, CDCl₃) δ 176.9 (C, C₁), 85.1 (C, C₅), 72.0 (CH, C₆), 71.3 (C, C₂), 39.2 (C, C₇), 29.0 (2CH₃, C_{3,4}), 27.2 (3CH₃, C₈₋₁₀).

2-Methyl-1-(2-phenylcyclopropyl)prop-1-en-1-yl pivalate (**105**)



To a solution of gold complex (**113** or **41b**) (0.025 equiv) in MeNO₂ was added the solution of AgSbF₆ (2.52 mL of 0.01 M in MeNO₂, 0.02 mmol, 0.05 equiv) at rt. The mixture was stirred for 5 min. Styrene (4 equiv) and the solution of **104** (1 equiv) in MeNO₂ (The final concentration = 0.05 M) was added into the mixture at rt or reflux. After stirring for 15 h, the

mixture was filtered over a short pad of silica and washed with Et₂O, and then concentrated under reduced pressure. Purification by column chromatography on silica gel using EtOAc/pentane (1/20) as eluent afforded **105** as colourless oil. All reaction conditions are shown in Table **S1**. (Note: The reaction could give a pivalyl allene as a volatile side-product).

The characterization data were identical to those previously reported.^[12]

R_f = 0.45 (EtOAc/pentane: 1/20).

IR (neat): $\tilde{\nu}$ (cm⁻¹) = 2979, 2933, 2872, 1738, 1604, 1395, 1363, 1257, 1157, 767, 697.

¹H NMR (300 MHz, CDCl₃) δ 7.24-7.14 (m, 3H, H_{ar}), 7.05-7.02 (m, 2H, H_{ar}), 2.32-2.18 (t, *J* = 7.1 Hz, 2H, H_{2,3}), 1.48 (s, 3H, H_{6 or 8}), 1.41 (s, 3H, H_{6 or 8}), 1.29-1.26 (m, 1H, H₁), 1.22 (s, 9H, H₁₁₋₁₃), 1.00 (dd, *J* = 11.8 Hz, 6.3 Hz, 1H, H₁).

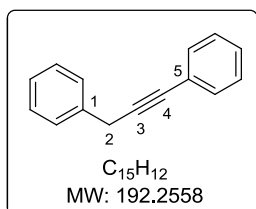
¹³C NMR (75 MHz, CDCl₃) δ 176.8 (C, C₉), 139.6 (C, C₅), 138.2 (C, C₄), 127.6 (2CH), 127.4 (2CH), 125.6 (CH), 123.2 (C, C₇), 39.0 (C, C₁₀), 27.4 (CH₃, C₁₁₋₁₃), 24.1 (CH, C₂), 21.9 (CH, C₃), 18.7 (CH₃, C_{6 or 8}), 17.4 (CH₃, C_{6 or 8}), 11.9 (CH₂, C₁).

Chiral HPLC analysis: Prepared **105** by using styrene (4 equiv), (*αS*)-**113** (3 mol%) and AgSbF₆ (6 mol%) in MeNO₂ at rt for 15 h.

chiralpak AZ-H column, 95/5 *n*-heptane/*i*-PrOH, 1 mL/min. Retention time for minor enantiomer = 3.82 min; for major enantiomer = 4.16 min (*ee* = 11%).

2.9. Preparation of allenyl bisphosphine derivatives

1,3-Diphenyl-1-propyne (106)



To a solution of PdCl₂(PPh₃) (120 mg, 0.17 mmol, 0.02 equiv) in Et₃N (35 mL) was added 3-phenyl-1-propyne (1.0 g, 8.6 mmol, 1.0 equiv) and PhI (1.44 mL, 12.9 mmol, 1.5 equiv) and stirred at rt. CuI (20 mg, 0.09 mmol, 0.01 equiv) was then added portion-wise into the mixture. After stirring for 2 h, the mixture was filtered over a short pad of Celite® to remove the black solid. The solution was added a saturated NH₄Cl solution (20 mL) and diluted with EtOAc (20 mL). The aqueous solution was extracted with EtOAc (2x 20mL). The combined organic layers were washed with brine (10 mL), dried over anhydrous MgSO₄, filtered and concentrated under reduced pressure. The product was purified by flash chromatography (100% pentane) to afford **106** (1.30 g, 79% yield) as yellow oil.

The characterization data were identical to those previously reported.^[25]

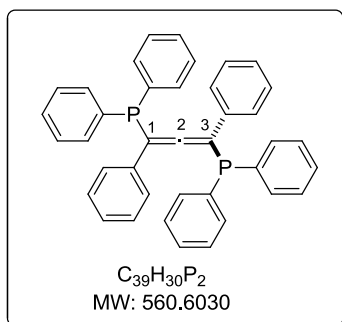
R_f = 0.25 (100% pentane).

IR (neat): $\tilde{\nu}$ (cm⁻¹) = 3085, 3062, 2883, 1949, 1879, 1805, 1571, 1491, 1441, 1388, 795, 712.

¹H NMR (400 MHz, CDCl₃) δ 7.71 (d, *J* = 8.0 Hz, 1H, H_{ar}), 7.47-7.42 (m, 3H, H_{ar}), 7.37-7.26 (m, 5H, H_{ar}), 7.11 (t, *J* = 7.8 Hz, 1H, H_{ar}), 3.85 (s, 2H, H₂).

¹³C NMR (75 MHz, CDCl₃) δ 136.9 (C, C₁), 131.8 (3CH), 128.7 (2CH), 128.4 (2CH), 128.1 (2CH), 127.9 (CH), 126.8 (CH), 123.8 (C, C₅), 87.7 (C, C₃), 82.8 (C, C₄), 25.9 (CH₂, C₂).

1,3-Bis(diphenylphosphino)-1,3-diphenylpropa-1,2-diene (107)



To a solution of **106** (1.50 g, 7.81 mmol, 1 equiv) in THF (80 mL) was added *n*-BuLi (6.50 mL of a 2.5 M in hexanes, 16.17 mmol, 2.1 equiv) at -78 °C. After 1 h, the solution of chlorodiphenyl phosphine (3.0 mL, 16.17 mmol, 2.1 equiv) in THF (10 mL) was added into the mixture at the same temperature. The mixture was slowly warmed to rt for 15 h and concentrated under reduced pressure. The residue was precipitated in the mixture of ethanol and water (1:1) to obtain **107** (2.12 g, 48% yield) as a white solid. (Note: The product is stable in the solid state under argon atmosphere and gets slowly oxidized with small amount of oxygen).

The characterization data were identical to those previously reported.^[26]

$R_f = 0.23$ (Et₂O/pentane: 4/1).

m.p. = 160–163 °C.

IR (neat): $\tilde{\nu}$ (cm⁻¹) = 3057, 2226, 1902, 1595, 1492, 1437, 1187, 1120, 910, 729, 694.

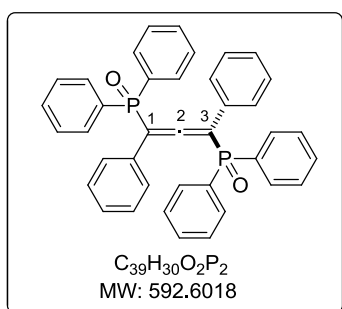
¹H NMR (400 MHz, CDCl₃) δ 7.47 (d, $J = 8.4$ Hz, 5H, H_{ar}), 7.35–7.12 (m, 22H, H_{ar}), 7.01 (t, $J = 7.7$ Hz, 3H, H_{ar}).

¹³C NMR (100 MHz, CDCl₃) δ 209.9 (d, $^2J_{CP} = 3.5$ Hz, C, C₂), 136.0 (C), 135.9 (C), 135.8 (C), 135.6 (C), 135.2 (CH), 135.0 (C), 134.9 (CH), 134.8 (C), 133.8 (2CH), 133.6 (CH), 132.0 (CH), 131.7 (CH), 131.6 (CH), 129.6 (CH), 129.2 (2CH), 128.8 (CH), 128.7 (CH), 128.6 (CH), 128.5 (2CH), 128.4 (2CH), 128.3 (2CH), 128.2 (2CH), 128.1 (2CH), 128.0 (CH), 127.7 (CH), 127.4 (CH), 127.2 (CH), 127.1 (CH), 127.0 (CH), 104.9 (dd, $^1J_{CP} = 21.0, 3.6$ Hz, C, C_{1,3}).

³¹P NMR (162 MHz, CDCl₃) δ – 8.8.

HRMS (ESI) calcd. for C₃₉H₃₁P₂ ([M + H]⁺) 561.18955 found 561.18941.

(1,3-Diphenylpropa-1,2-diene-1,3-diyl)bis(diphenylphosphine oxide) (**108**)



To a solution of **107** (350 mg, 0.62 mmol, 1 equiv) in THF at 0 °C was added H₂O₂ (0.69 mL of 30% w/w in H₂O, 5.75 mmol, 9.2 equiv) and stirred for 1 h. The mixture was warmed to rt and stirred for 20 h. The solution was added H₂O (20 mL) and CH₂Cl₂ (20 mL). The aqueous solution was extracted with CH₂Cl₂ (2x 20 mL). The combined organic layers were washed with brine (10 mL), dried over anhydrous MgSO₄, filtered and concentrated under reduced pressure. The product was recrystallized with EtOAc/pentane (2/8) to obtain **108** (300 mg, 82 %yield) as a white solid.

The characterization data were identical to those previously reported.^[26]

IR (neat): $\tilde{\nu}$ (cm⁻¹) = 3057, 2227, 1909, 1592, 1492, 1437, 1180, 1119, 1099, 927, 724, 691.

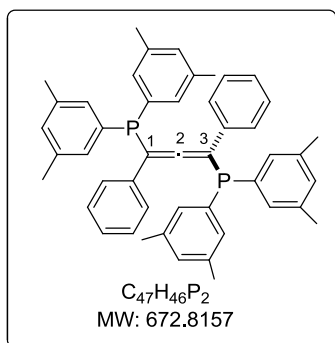
¹H NMR (400 MHz, CDCl₃) δ 7.55–7.21 (m, 30H, H_{ar}).

¹³C NMR (100 MHz, CDCl₃) δ 213.7 (t, $^2J_{CP} = 6.3$ Hz, C, C₂), 132.6 (C), 132.3 (2CH), 132.2 (2CH), 132.1 (2CH), 132.0 (3CH), 131.9 (3CH), 131.8 (2CH), 131.5 (C), 131.0 (3C), 130.8 (C), 128.9 (5CH), 128.8 (2CH), 128.7 (3CH), 128.6 (4CH), 128.5 (2CH), 105.3 (d, $^1J_{CP} = 9.3$ Hz, C, C_{1 or 3}), 104.3 (d, $^1J_{CP} = 9.4$ Hz, C, C_{1 or 3}).

³¹P NMR (162 MHz, CDCl₃) δ 28.3.

Chiral HPLC analysis: Lux Cellulose-4 (250 x 10 mm), hexanes/ethanol (50/50), 5 mL/min. Retention time for first enantiomer = 6.34 min ((-, CD 254nm)-**108**) with *ee* > 98%; for second enantiomer = 7.28 min ((+, CD 254 nm)-**108**) with *ee* > 97%, $[\alpha_D] = 155.55$ (c 0.5, CHCl₃).

1,3-Bis(bis(3,5-dimethylphenyl)phosphino)-1,3-diphenylpropa-1,2-diene (**115**)^[27]



To a solution of **106** (1.0 g, 5.19 mmol, 1 equiv) in THF (67 mL) was added *n*-BuLi (4.30 mL of a 2.5 M in hexanes, 10.7 mmol, 2.07 equiv) at -78 °C. The solution of chlorobis(3,5-dimethylphenyl) phosphine (3.0 g, 10.9 mmol, 2.1 equiv) in THF (7 mL) was added into the mixture at the same temperature. The mixture was slowly warmed to rt for 15 h and concentrated under reduced pressure to obtain **115** (3.5 g, quant) as brown oil. The crude product was

directly engaged in next step. (Note: The product was stable in the solid under argon atmosphere and slowly oxidized in small amount of oxygen).

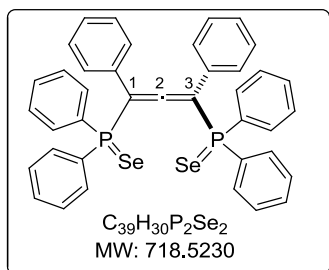
$R_f = 0.23$ (Et₂O/pentane: 4/1).

IR (neat): $\tilde{\nu}$ (cm⁻¹) = 2919, 2852, 1905, 1600, 1466, 1180, 1001.

³¹P NMR (162 MHz, CDCl₃) δ -8.0.

2.10. Metal complexes bearing allenyl bisphosphine ligands

(1,3-Diphenylpropa-1,2-diene-1,3-diyl)-bis(diphenylphosphine selenide) (**109**)



The solution of **107** (100 mg, 0.18 mmol, 1 equiv) and small pieces of Selenium (80 mg, 1.03 mmol, 7.2 equiv) in CDCl₃ (17 mL) was stirred at reflux for overnight (24 h). After monitoring the reaction by ³¹P NMR, the mixture was filtered to remove selenium and concentrated to afford **109** (170 mg, quant) as a yellow solid.

The characterization data were identical to those previously reported.^[26]

m.p. = 207–208 °C.

IR (neat): $\tilde{\nu}$ (cm⁻¹) = 3079, 2221, 1899, 1594, 1492, 1435, 1335, 1184, 1095, 1029, 999, 908, 715.

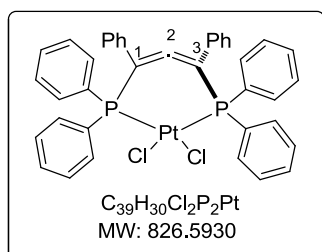
¹H NMR (300 MHz, CDCl₃) δ 7.66–7.19 (m, 30H, H_{ar}).

¹³C NMR (100 MHz, CDCl₃) δ 211.9 (²J_{CP} = 2.0 Hz, C, C₂), 133.2 (2CH), 133.1 (2CH), 132.7 (2CH), 132.6 (2CH), 132.0 (2CH), 131.4 (C), 130.8 (2C), 130.7 (C), 129.7 (C), 128.8 (C), 128.7 (6CH), 128.6 (8CH), 128.5 (6CH), 105.4 (d, ¹J_{CP} = 8.1 Hz, C_{1 or 3}), 105.0 (d, ¹J_{CP} = 8.3 Hz, C, C_{1 or 3}).

^{31}P NMR (162 MHz, CDCl_3) δ 35.5 (d, $^4J_{PP} = 15.7$ Hz), 33.2 (P=Se, $^1J_{PSe} = 751$ Hz), 30.86 (d, $^4J_{PP} = 16.0$ Hz).

(Se = ^{77}Se isotope)

Dichloroplatinum(II)-(1,3-Diphenylpropa-1,2-diene-1,3-diyl)-bis(diphenylphosphine) (**110**)



A solution of **107** (150 mg, 0.27 mmol, 1 equiv) and *cis*-bis(benzonitrile)dichloroplatinum(II) (120 g, 0.27 mmol, 1 equiv) in toluene (6 mL) was stirred at 80 °C for 20 h. The mixture was filtered over a short pad of Celite® and concentrated under reduced pressure. The product was recrystallized by diffusion of toluene into

the solution of crude product in CHCl_3 to give **110** (240 mg, quant) as a brown solid. (Note: the product is not stable in the air and moisture).

IR (neat): $\tilde{\nu}$ (cm^{-1}) = 3080, 3058, 2228, 1903, 1714, 1593, 1482, 1436, 1215, 1099, 758, 716.

^1H NMR (300 MHz, CDCl_3) δ 10.53-10.47 (m, 3H, H_{ar}), 9.72-9.66 (m, 6H, H_{ar}), 9.28-9.13 (m, 11H, H_{ar}), 8.98 (t, $J = 7.5$ Hz, 3H, H_{ar}), 8.79 (t, $J = 7.7$ Hz, 4H, H_{ar}), 8.07 (d, $J = 7.6$ Hz, 3H, H_{ar}).

^{13}C NMR (100 MHz, CD_2Cl_2) δ 198.9 (t, $^2J_{CP} = 5.1$ Hz, C, C_2), 136.6 (2CH), 136.5 (CH), 134.2 (2CH), 134.1 (CH), 133.2 (2CH), 131.8 (2CH), 131.7 (C), 131.1 (C), 130.0 (2CH), 129.9 (2CH), 129.8 (4CH), 129.7 (CH), 129.2 (C), 128.9 (4CH), 128.7 (6CH), 128.5 (C), 128.4 (CH), 128.3 (CH), 128.2 (CH), 128.0 (C), 104.5 (dd, $^1J_{CP} = 32.8, 21.5$ Hz, 2C, $\text{C}_{1,3}$).

^{31}P NMR (162 MHz, CDCl_3) δ 98.7 (P-Pt, $^1J_{P-Pt} = 4371$ Hz).

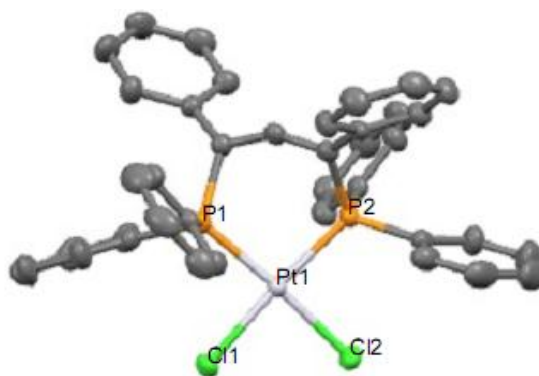
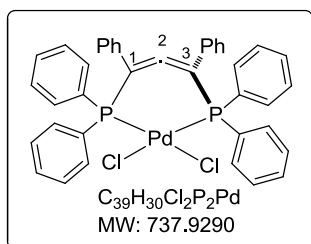


Figure S2. X-ray structure of **110** in the solid state. (The hydrogen atoms are omitted for clarity)

Dichloropalladium(II)-(1,3-Diphenylpropa-1,2-diene-1,3-diyl)-bis(diphenylphosphine) (111)

A solution of **107** (70 mg, 0.12 mmol, 1 equiv) and *cis*-bis(acetonitrile)dichloropalladium(II) (32 mg, 0.12 mmol, 1 equiv) in toluene (1.4 mL) was stirred at 80 °C for 4 h. The mixture was concentrated under reduced pressure. The orange solid was washed with Et₂O and dried to give **111** (74 mg, 84% yield) as a yellow solid.

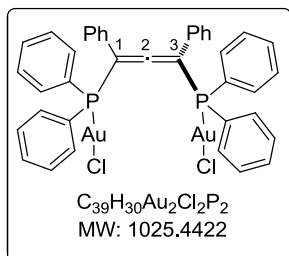
m.p. = 236–237 °C.

IR (neat): $\tilde{\nu}$ (cm⁻¹) = 3055, 1734, 1597, 1493, 1481, 1310, 1098, 729, 690.

¹H NMR (400 MHz, CD₂Cl₂) δ 8.62 (dd, *J* = 12.0, 7.2 Hz, 4H, H_{ar}), 7.80–7.72 (m, 6H, H_{ar}), 7.35–7.33 (m, 2H, H_{ar}), 7.24–7.19 (m, 8H, H_{ar}), 7.05 (t, *J* = 7.6 Hz, 2H, H_{ar}), 6.86 (t, *J* = 7.6 Hz, 4H, H_{ar}), 6.10 (d, *J* = 7.6 Hz, 4H, H_{ar}).

¹³C NMR (100 MHz, CD₂Cl₂) δ 193.3 (t, ²*J*_{CP} = 3.8 Hz, C, C₂), 136.9 (CH), 136.8 (2CH), 136.7 (CH), 134.0 (CH), 133.9 (2CH), 133.5 (C), 133.3 (2CH), 133.3 (C), 133.1 (C), 131.9 (2CH), 130.1 (2CH), 130.0 (CH), 129.9 (2CH), 129.8 (CH), 129.5 (2CH), 129.1 (C), 129.0 (2CH), 128.8 (C), 128.7 (5CH), 128.5 (C), 128.4 (CH), 128.4 (2CH), 128.3 (CH), 105.6 (t, ¹*J*_{CP} = 21.7 Hz, 2C, C_{1,3}).

³¹P NMR (162 MHz, CD₂Cl₂) δ 128.3.

Dichlorogold(I)-(1,3-diphenylpropa-1,2-diene-1,3-diyl)-bis(diphenylphosphine) (113)

A solution of AuCl(Me₂S) (40 mg, 0.14 mmol, 2 equiv) and **107** (40 mg, 0.07 mmol, 1 equiv) in CH₂Cl₂ (2 mL) was stirred at rt for 3 h. The mixture was concentrated under reduced pressure. The residue was purified by a precipitation with pentane and CH₂Cl₂ to obtain **113** (90 mg, quant) as a white solid. The product was recrystallized by diffusion

of cyclohexane into the solution of crude product in CH₂Cl₂ to give colorless crystals quantitatively.

R_f = 0.13 (cyclohexane/EtOAc: 4/1).

m.p. = 259–261 °C

IR (neat): $\tilde{\nu}$ (cm⁻¹) = 3055, 2924, 2237, 1908, 1490, 1436, 1101, 911, 730, 689.

¹H NMR (400 MHz, CDCl₃) δ 7.60–7.31 (m, 30H, H_{ar}).

¹³C NMR (100 MHz, CDCl₃) δ 213.1 (t, ²*J*_{CP} = 3.5 Hz, C, C₂), 135.2 (CH), 135.1 (CH), 135.0 (CH), 134.1 (2CH), 134.0 (CH), 133.5 (2CH), 132.9 (2CH), 132.7 (CH), 132.4 (CH), 131.8 (d, *J* = 9.7 Hz, CH), 131.5 (d, *J* = 9.9 Hz, CH), 130.3 (C), 130.2 (C), 130.1 (CH), 129.8 (2CH), 129.7 (2CH), 129.6 (CH), 129.5 (CH), 129.4 (2CH), 129.3 (CH), 129.2 (CH), 129.1 (CH), 129.0 (CH), 128.9 (CH), 127.8 (CH), 127.7

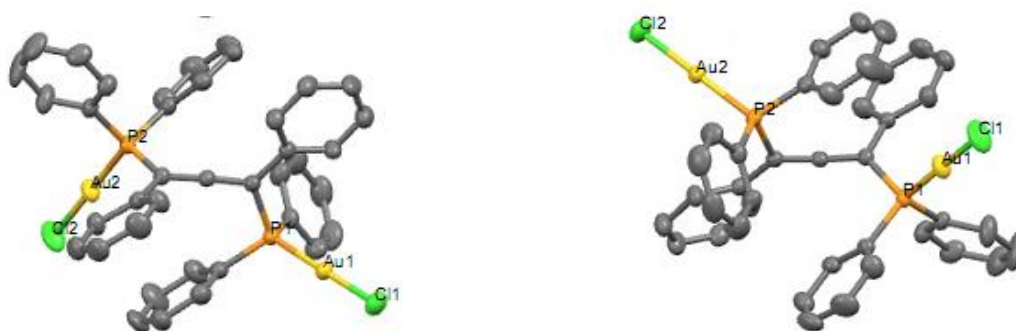
Experimental part

(CH), 127.5 (C), 127.2 (C), 126.8 (C), 126.6 (C), 104.4 (d, $^1J_{CP} = 8.1$ Hz, C, C_{1 or 3}), 103.9 (d, $^1J_{CP} = 8.1$ Hz, C, C_{1 or 3}).

^{31}P NMR (162 MHz, CDCl₃) δ 30.2.

HRMS (ESI) calcd for C₃₉H₃₀Au₂Cl₂P₂ ([M + Na]⁺) 1047.04230, found 1047.04241.

Chiral HPLC separation Chromatographic conditions: Chiralpak IE, hexanes / 2-PrOH / Chloroform (5/2/35) as mobile phase, flow-rate = 5 mL/min UV detection at 254 nm (First column) and circular dichroism detector (Second column). Retention time for first enantiomer = 6.21 min ((-, CD 254nm)-**113**) with *ee* > 98%, [α_D] = + 28.2 (c 0.17, CH₂Cl₂), (*R*)-form; for second enantiomer = 7.28 min ((+, CD 254 nm)-**113**) with *ee* > 97%, [α_D] = - 28.2 (c 0.17, CH₂Cl₂), (*S*)-form).

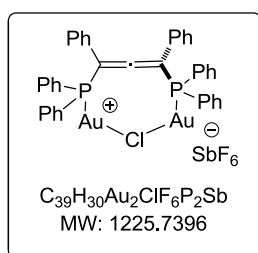


(*aR*)-form, (-, CD 254 nm)-enantiomer

(*aS*)-form, (+, CD 254 nm)-enantiomer

Figure S3. Structure of (*aR*)- and (*aS*)-**113** in the solid-state. (The hydrogen atoms are omitted for clarity)

Chloride bridged-(1,3-diphenylpropa-1,2-diene-1,3-diyl)-bis(gold(I) diphenylphosphine) (114**)**



A solution of **113** (20 mg, 0.02 mmol, 1 equiv) and AgSbF₆ (6.8 mg, 0.02 mmol, 1 equiv) in CD₂Cl₂ (0.4 mL) was stirred for 3 h. The mixture was concentrated under reduced pressure to obtain **114** (20 mg, quant) as a brown solid (*Note*: This product cannot be characterized by NMR analysis).

MS (ESI) calcd for C₃₉H₃₀Au₂ClP₂ 989.1, found 989.2 (Figure S4)

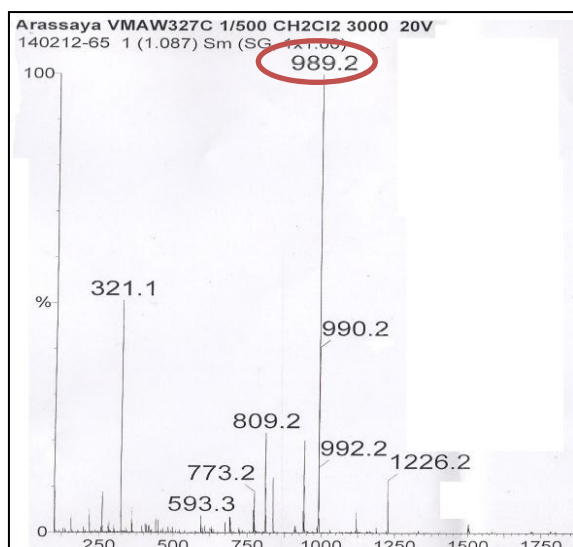
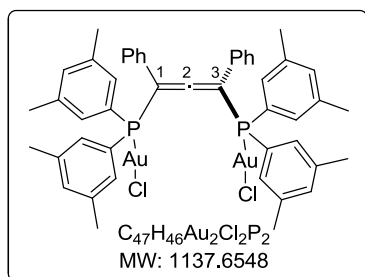


Figure S4. The characterization of Chloride bridged-dinuclear gold (I) complex **114** by Mass Spectrometry **(1,3-Diphenylpropa-1,2-diene-1,3-diyl)-bis(chlorogold(I))bis(3,5dimethylphenylphosphine) (116)**^[27]



The compound was prepared from the crude **115** (200 mg, 0.30 mmol, 1 equiv), according to the similar procedure as complex **113**. A white solid was obtained by a precipitation in the mixture $\text{CH}_2\text{Cl}_2/\text{hexanes}$ (1/7) (0.17 g, 50 % yield).

m.p. = 267–269°C.

IR (neat): $\tilde{\nu}$ (cm^{-1}) = 3029, 2917, 2237, 1911, 1599, 1491, 1416,

1186.

^1H NMR (300 MHz, CDCl_3) δ 7.66–7.63 (m, 4H, H_{ar}), 7.37–7.34 (m, 6H, H_{ar}), 7.24–7.20 (m, 6H, H_{ar}), 7.09 (s, 2H, H_{ar}), 6.93 (d, $J = 15$ Hz, 4H, H_{ar}), 2.25 (s, 12H, CH_3), 2.15 (s, 12H, CH_3).

^{13}C NMR (75 MHz, CDCl_3) δ 212.3 (t, $J_{\text{CP}} = 3.0$ Hz, C, C_2), 139.1 (t, $J = 6.1$ Hz, 2C), 138.7 (t, $J = 6.8$ Hz, 2C), 136.4 (4CH), 134.3 (4CH), 133.1 (t, $J = 7.5$ Hz, 4CH), 131.4 (t, $J = 6.8$ Hz, 4CH), 130.53 (t, $J = 2.6$ Hz, 2C), 129.2 (6CH), 127.8 (4CH), 127.3 (2C), 126.6 (2C), 126.5 (2C), 125.7 (2C), 104.5 (d, $^1J_{\text{CP}} = 6.2$, C, $\text{C}_{1\text{or}3}$), 103.8 (d, $^1J_{\text{CP}} = 6.2$ Hz, $\text{C}_{1\text{or}3}$), 21.4 (d, $J = 10.6$ Hz, 8 CH_3).

^{31}P NMR (162 MHz, CDCl_3) δ 29.3.

Chiral HPLC separation Chromatographic conditions: (S,S)-Whelk-O1, Heptane/Ethanol/Chloroform (50/40/10) as mobile phase, flow-rate = 1 mL/min UV detection at 254nm (First column) and circular dichroism detector (Second column). Retention time for first enantiomer = 6.99 min ((+, CD 254nm)-**116**) with $ee > 98\%$, $[\alpha]_{\text{D}} = +189.6$ (c 0.16, CH_2Cl_2), for second enantiomer = 8.01 min ((-, CD 254 nm)-**113**) with $ee > 97\%$, $[\alpha]_{\text{D}} = -189.6$ (c 0.16, CH_2Cl_2).

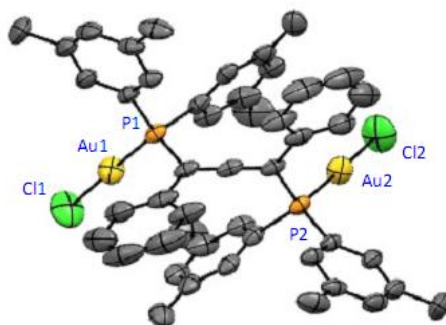
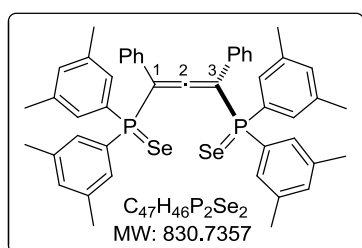


Figure S5. Structure of (±)-116 (The hydrogen atoms are omitted for clarity)

(1,3-diphenylpropa-1,2-diene-1,3-diyl)bis(bis(3,5dimethylphenyl)phosphineselenide) (117) [27]



The solution of **115** (100 mg, 0.15 mmol, 1 equiv) and small pieces of Selenium (80 mg, 1.08 mmol, 7.2 equiv) in CDCl_3 (15 mL) was stirred at reflux for 6 h. After monitoring the reaction by ^{31}P NMR, the mixture was filtered to remove Selenium and concentrated to afford crude product **117** (0.15 g, quant) as a

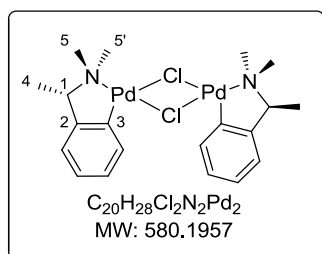
brown solid.

^{31}P NMR (162 MHz, CDCl_3) δ 35.5 (d, $^4J_{\text{PP}} = 15.4$ Hz), 33.7 (P=Se, $^1J_{\text{PSe}} = 744$ Hz), 31.4 (d, $^4J_{\text{PP}} = 15.6$ Hz).

^{31}P NMR (162 MHz, CD_2Cl_2) δ 36.0 (d, $^4J_{\text{PP}} = 16.2$ Hz), 33.7 (P=Se, $^1J_{\text{PSe}} = 750$ Hz), 31.4 (d, $^4J_{\text{PP}} = 16.2$ Hz). (Se = ^{77}Se isotope)

2.11. Resolutions of allenyl bisphosphines

Di- μ -chloro-bis[(*S,S*)-(1-(dimethylamino-ethyl))-2- benzylamine-C,N] dipalladium(II) (118)



A solution of PdCl_2 (120 mg, 0.65 mmol, 1 equiv) and dried LiCl (60 mg, 1.42 mmol, 2.3 equiv) in MeOH (15 mL) was stirred at rt. After 2 h until PdCl_2 was completely dissolved, the color of solution was changed to dark red. (*S*)-*N,N*-dimethyl-1-phenyl ethylamine (0.3 mL, 1.81 mmol, 2.8 equiv) was added and the mixture was stirred for 5

h. The yellow solid product was precipitated, filtered and washed with methanol and Et_2O to afford **118** (300 mg, 81% yield) as yellow solid. The product was recrystallized by diffusion of methanol into the solution of crude product in CH_2Cl_2 to give colorless crystals.

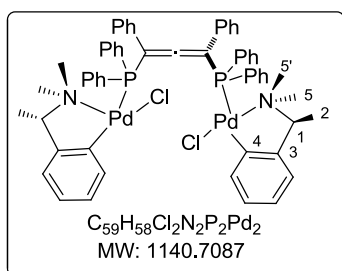
The characterization data were identical to those previously reported. [28,29]

Specific optical rotation: $[\alpha]_D = 53.0$ (c 1, benzene).

$^1\text{H NMR}$ (300 MHz, CDCl_3) δ 7.23-7.15 (m, 2H, H_{ar}), 7.00-6.77 (m, 6H, H_{ar}), 3.88 (t, $J = 6.2$ Hz, 2H, H_1), 2.94 (s, 3H, H_5 or $5'$), 2.91 (s, 3H, H_5 or $5'$), 2.67 (s, 3H, H_5 or $5'$), 2.64 (s, 3H, H_5 or $5'$), 1.59 (d, $J = 6.6$ Hz, 6H, H_4).

HRMS (ESI) calcd for $\text{C}_{20}\text{H}_{28}\text{Cl}_2\text{N}_2\text{NaPd}_2$ ($[\text{M} + \text{Na}]^+$) 600.9592 found 600.9614.

(1,3-diphenylpropa-1,2-diene-1,3-diyl)bis(chloro-(*S,S*)-[(1-(dimethylamino-ethyl))-2-benzylamine-C,N]-palladium(II))-diphenyl phosphine) (119)



A solution of **107** (100 mg, 0.18 mmol, 1 equiv) and **118** (0.11 g, 0.18 mmol, 1 equiv) in toluene (2 mL) was stirred for 2 h. The mixture was concentrated under reduced pressure to afford the yellow oil. The crude was purified by column chromatography on silica gel using EtOAc/cyclohexane (1/1) as eluent to afford the mixture of palladium complexes (210 mg, 0.18 mmol, quant) as

mononuclear palladium complexes (\pm)-**119b** (minor product) and dinuclear palladium complexes (\pm)-**119a** (major product) with 2 diastereomers (1:1.5 minor:major). The product was recrystallized by diffusion of methanol into the solution of crude product in CH_2Cl_2 to give the dinuclear palladium complex (\pm)-**119a** with 2 diastereomer as shown in Figure S6.

$R_f = 0.32, 0.21$ (cyclohexane/EtOAc: 1/1) (*Note*: these diastereomers could not be separated by column chromatography and recrystallization).

IR (neat): $\tilde{\nu}$ (cm^{-1}) = 3055, 2974, 2922, 1908, 1619, 1576, 1527, 1453, 1338, 1218, 1073, 940, 743.

$^1\text{H NMR}$ (400 MHz, CDCl_3) δ 7.82 (d, $J = 7.6$ Hz, 4H, H_{ar}), 7.77-7.68 (m, 8H, H_{ar}), 7.55-7.53 (m, 4H, H_{ar}), 7.36-6.93 (m, 50H, H_{ar}), 6.80-6.72 (m, 8H, H_{ar}), 6.63 (t, $J = 8$ Hz, 2H, H_{ar}), 6.54 (d, $J = 7.6$ Hz, 2H, H_{ar}), 6.31 (t, $J = 7.2$ Hz, 2H, H_{ar}), 6.17 (t, $J = 6.4$ Hz, 2H, H_{ar}), 3.67 (t, $J = 6.0$ Hz, 2H, H_1), 3.55 (t, $J = 5.2$ Hz, 2H, $\text{H}_{1\text{-dias}}$), 2.69-2.57 (m, 24H, $\text{H}_{5,5'}$), 1.64 (d, $J = 6.4$ Hz, 6H, $\text{H}_{2\text{-dias}}$), 1.43 (s, 6H, H_2), 1.42 (s, 3H, $\text{H}_{2\text{-dias}}$).

$^{31}\text{P NMR}$ (162 MHz, CDCl_3) δ 42.6 (major), 42.5 (minor, dias).

HRMS (ESI) calcd for $\text{C}_{59}\text{H}_{58}\text{N}_2\text{P}_2\text{Pd}_2\text{OH}$ ($[\text{M}-2\text{Cl}+\text{OH}]^+$) 1087.22, found 1087.22.

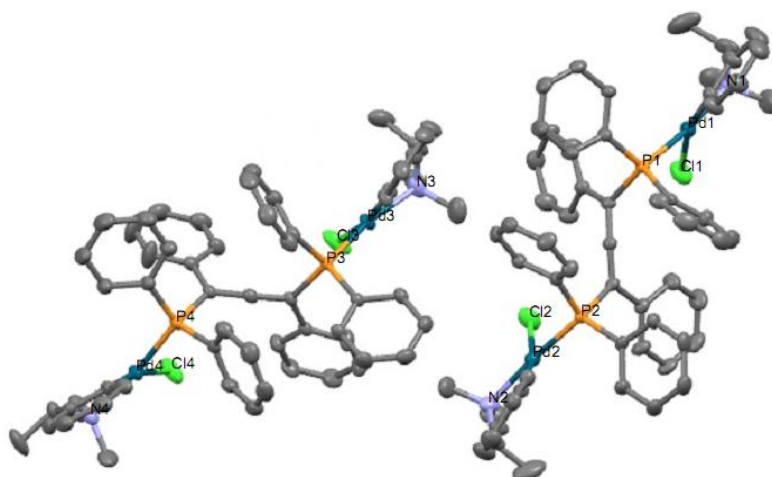
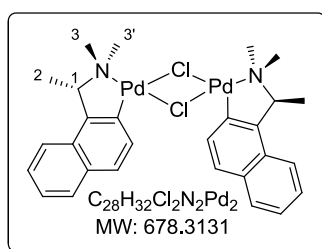


Figure S6. X-ray structure of dinuclear palladium complex (±)-119a in the solid-state. (The hydrogen atoms are omitted for clarity).

Di- μ -chloro-bis[(*S,S*)-(1-(dimethylamino-ethyl))-2-naphthylamine-C,N]-dipalladium(II) (120**)**



A solution of $PdCl_2$ (200 mg, 1.13 mmol, 1 equiv) and dried $LiCl$ (110 mg, 2.48 mmol, 2.2 equiv) in $MeOH$ (20 mL) was stirred at rt. After 4 h, the color solution was changed to dark red. (*S*)-*N,N*-dimethyl-1-(1-naphthyl) ethylamine (0.63 mL, 3.16 mmol, 2.8 equiv) was added and the mixture was stirred for 20 h. The yellow solid was precipitated, filtered and washed with methanol and Et_2O to afford **120** (0.35 g, 46% yield) as yellow solid. The product was recrystallized by diffusion of methanol into the solution of crude product in CH_2Cl_2 to give the pure palladium complex.

The characterization data were identical to those previously reported.^[28]

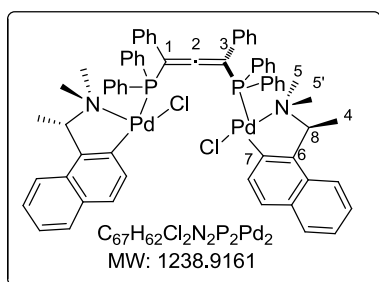
m.p. = 205–208 °C.

1H NMR (400 MHz, $CDCl_3$) δ 7.78 (d, J = 7.5 Hz, 2H, H_{ar}), 7.57 (d, J = 7.2 Hz, 2H, H_{ar}), 7.48-7.33 (m, 6H, H_{ar}), 4.19 (bs, 2H, H_1), 3.49 (s, 2H, H_{ar}), 3.00 (s, 3H, H_3 or $3'$), 2.97 (s, 3H, H_3 or $3'$), 2.80 (s, 3H, H_3 or $3'$), 2.75 (s, 3H, H_3 or $3'$), 1.92 (bs, 6H, H_2).

HRMS (ESI) calcd for $C_{28}H_{32}Cl_2N_2NaPd_2$ ($[M + Na]^+$) 700.9905 found 700.9887.

(1,3-Diphenylpropa-1,2-diene-1,3-diyl)bis(chloro-(*S,S*)-[(1-(dimethylamino-ethyl))-2-naphthylamine-C,N]-palladium(II))-diphenyl phosphine (121**)**

A solution of **107** (100 mg, 0.18 mmol, 1 equiv) and **120** (120 mg, 0.18 mmol, 1.0 equiv) in toluene (8 mL) was stirred at 50 °C for 20 h (monitoring by TLC). The mixture was concentrated under reduced pressure to give a yellow solid. The residue was purified by column chromatography on



silica gel using EtOAc/cyclohexane (1/4) as eluent to afford **121** (172 mg, 77% yield). The product **119** was recrystallized by diffusion of methanol into the solution of crude product in CH_2Cl_2 . The 2 diastereomers: a yellow solid in solid phase as major diastereomer (S,S,S,S)-**121b**, 95.8 mg, yielded 43%, $[\alpha_D] = -134.36$ (c 0.1, CH_2Cl_2) and a yellow solid in liquid phase as

minor diastereomer (S,S,S,S)-**121a**, 60.2 mg, 27% yield, $[\alpha_D] = 43.16$ (c 0.1, CH_2Cl_2).

$R_f = 0.06$ (cyclohexane/EtOAc: 4/1).

m.p. = 195–199 °C.

IR (neat): $\tilde{\nu}$ (cm^{-1}) = 3078, 2970, 2921, 1893, 1573, 1502, 1435, 1383, 1096, 939, 758, 691.

1H NMR (400 MHz, $CDCl_3$) δ 7.80–7.75 (m, 4H, H_{ar}), 7.56–7.07 (m, 21H, H_{ar}), 7.14–7.07 (m, 14H, H_{ar}), 6.64 (dd, $J = 6.6, 6.2$ Hz, 2H, H_{ar}), 6.44 (d, $J = 8.6$ Hz, 2H, H_{ar}), 4.16 (t, $J = 6.2$ Hz, 1H, H_8), 2.84 (d, $J = 2.9$ Hz, 6H, $H_{5\text{ or }5'}$), 2.61 (s, 6H, $H_{5\text{ or }5'}$), 1.69 (d, $J = 6.32$ Hz, 6H, H_4).

^{13}C NMR (75 MHz, $CDCl_3$) δ 210.8 (C, C_2), 150.4 (C, C_6), 148.2 (C, C_7), 136.1 (2CH), 135.9 (2CH), 135.6 (2CH), 135.4 (2CH), 135.0 (CH), 134.9 (CH), 134.6 (C), 134.4 (C), 131.2 (2C), 131.1 (2C), 131.0 (3CH), 130.5 (2C), 130.4 (2C), 129.9 (3CH), 128.6 (3CH), 128.5 (2C), 128.3 (3CH), 128.2 (3CH), 128.1 (6CH), 128.0 (3CH), 127.9 (2CH), 127.8 (2CH), 125.5 (2CH), 124.5 (CH), 123.9 (2CH), 123.3 (2CH), 103.8 (d, $^1J_{CP} = 6.8$ Hz, C, $C_{1\text{ or }3}$), 103.2 (d, $^1J_{CP} = 6.9$ Hz, $C_{1\text{ or }3}$), 73.2 (CH, C_8), 51.3 (CH_3 , $C_{5\text{ or }5'}$), 48.5 (CH_3 , $C_{5\text{ or }5'}$), 23.0 (CH_3 , C_4).

^{31}P NMR (162 MHz, $CDCl_3$) δ 42.1.

HRMS (ESI) calcd for $C_{67}H_{62}Cl_2N_2P_2Pd_2CH_3OH$ ($[M + CH_3OH]^+$) 1237.24262, found 1237.24080.

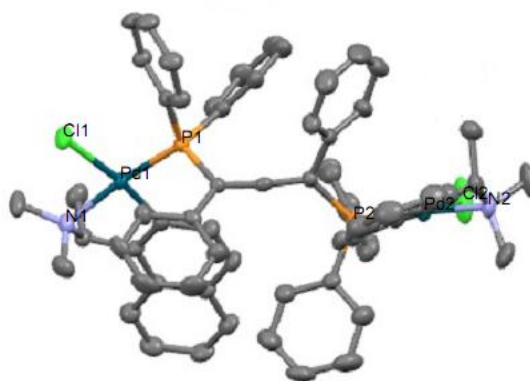
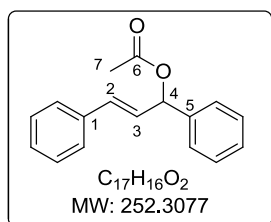


Figure S7. X-ray structure of dinuclear palladium complex (S,S,S,S)-**121b** as a major diastereomer in the solid-state. (The hydrogen atoms are omitted for clarity) (a= axial chirality, c = center chirality)

2.12. Asymmetric catalytic allylation using palladium chiral phosphine complex

(E)-1,3-Diphenylallyl acetate (123)



To a solution of (*E*)-1,3-diphenylprop-2-en-1-ol (500 mg, 2.38 mmol, 1.0 equiv) in CH₂Cl₂ (15 mL) was added DMAP (29 mg, 0.24 mmol, 0.10 equiv), NEt₃ (0.81 mL, 5.9 mmol, 2.5 equiv), and acetic anhydride (0.56 mL, 5.9 mmol, 2.5 equiv). The reaction mixture was stirred at rt for 4 h until completion of reaction (TLC monitoring). The reaction mixture was diluted with EtOAc (30 mL) and quenched with a saturated aqueous NH₄Cl solution (30 mL). The aqueous phase was extracted with EtOAc (2x30 mL). The combined organic layers were washed with brine (20 mL), dried over anhydrous MgSO₄, filtered and concentrated under reduced pressure. Purification by column chromatography on silica gel using EtOAc/pentane (1/5) as eluent afforded **123** (0.50 g, 84% yield) as a colourless oil.

The characterization data were identical to those previously reported.^[30]

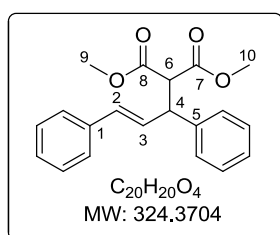
R_f = 0.40 (pentane/EtOAc: 4/1).

IR (neat): $\tilde{\nu}$ (cm⁻¹) = 3028, 2360, 1735, 1494, 1430, 1224, 1016, 963.

¹H NMR (400 MHz, CDCl₃) δ 7.45-7.37(m, 6H), 7.34-7.29 (m, 3H), 7.26-7.24 (m, 1H), 6.66 (d, *J* = 16.0 Hz, 1H), 6.48 (d, *J* = 6.8 Hz, 1H), 6.38 (dd, *J* = 16.0, 6.8 Hz, 1H), 2.14 (s, 3H).

¹³C NMR (100 MHz, CDCl₃) δ 169.7 (C, C₆), 139.3 (C, C₅), 136.2 (C, C₁), 132.6 (CH, C₂), 128.7 (2CH), 128.6 (2CH), 128.2 (CH), 128.1 (CH), 127.6 (CH, C₃), 127.1 (2CH), 126.7 (2CH), 76.2 (CH, C₄), 21.3 (CH₃, C₇).

(E)-dimethyl 2-(1,3-diphenylallyl)malonate (124)



a) Preparation of chiral phosphine ligand 107

In schlenk tube under argon atmosphere, to a solution of palladium phosphine (*S_cR_aS_c*)-**121b** (15 mg, 0.012 mmol, 1.0 equiv) and NaCN (5.0 mg, 0.096 mmol, 8.0 equiv) in degassed CH₂Cl₂ (3 mL) was added degassed water (1 mL) and stirred until NaCN solid disappeared. The reaction was stopped and let it to separate layers. The organic phase was extracted with water (2x 1 mL) and aqueous phase was removed by syringe. Then, the organic solution was dried by MgSO₄ and transferred to another schlenk tube. The solution was concentrated under reduced pressure to give optically pure **107** as a yellow solid.

b) Catalytic allylic alkylation reaction

A solution of NaH (60 % dispersion in mineral oil, 90 mg, 2.1 mmol, 1.8 equiv) in THF was cooled at 0 °C. Dimethyl malonate (0.27 mL, 2.4 mmol, 2 equiv) was added dropwise into the solution. The mixture was warmed at rt. To solution of **107** and [Pd(allyl)Cl]₂ (4.0 mg, 0.012 mmol) in degassed THF (6 mL) was added **123** (0.25 g, 1.19 mmol, 1 equiv) at rt. Then, the solution was added into the mixture of NaH and dimethyl malonate. The color of solution turned to be brown. After 4 h, the solution mixture was hydrolyzed with a saturated aqueous NH₄Cl solution (50 mL). The aqueous phase was extracted with Et₂O (2x20 mL). The combined organic layers were washed with brine (20 mL), dried over anhydrous MgSO₄, filtered and concentrated under reduced pressure. Purification by column chromatography on silica gel using EtOAc/pentane (5/95) as eluent afforded **124** (0.30 g, 78% yield) as a white solid.

The characterization data were identical to those previously reported.^[31]

R_f = 0.35 (pentane/EtOAc: 10/2).

IR (neat): $\tilde{\nu}$ (cm⁻¹) = 3060, 2952, 1733, 1599, 1494, 1434, 1254, 1143, 1025, 965.

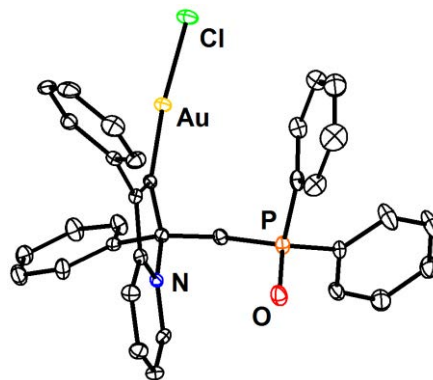
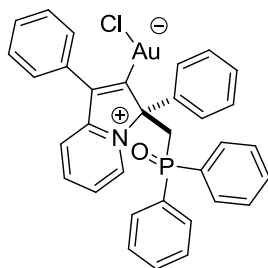
¹H NMR (400 MHz, CDCl₃) δ 7.34-7.28 (m, 8H, H_{ar}), 7.25-7.20 (m, 2H, H_{ar}), 6.48 (d, *J* = 16.0 Hz, 1H, H₃), 6.34 (dd, *J* = 16.0, 8.4 Hz, 1H, H₂), 4.27 (dd, *J* = 10.8, 8.8 Hz, 1H, H₄), 3.96 (d, *J* = 10.8 Hz, 1H, H₆), 3.71 (s, 3H, H_{9 or 10}), 3.52 (s, 3H, H_{9 or 10}).

¹³C NMR (100 MHz, CDCl₃) δ 168.3 (C, C_{7 or 8}), 167.9 (C, C_{7 or 8}), 140.3 (C, C₅), 137.0 (C, C₁), 132.0 (CH, C₂), 129.3 (CH, C₃), 128.9 (2CH), 128.6 (2CH), 128.0 (2CH), 127.7 (CH), 127.3 (CH), 126.5 (2CH), 57.8 (CH, C₆), 52.8 (CH₃, C_{9 or 10}), 52.6 (CH₃, C_{9 or 10}), 49.3 (CH, C₄).

3. X-ray crystal structure determination of compounds

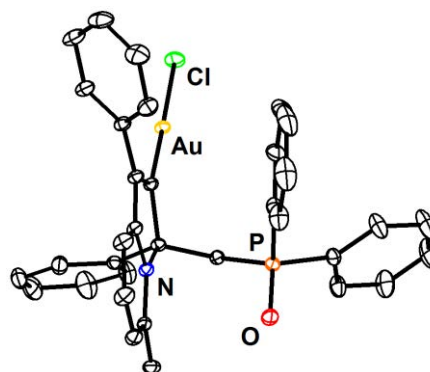
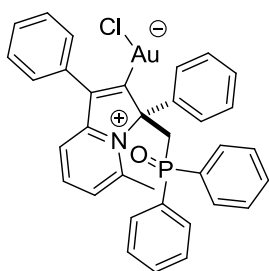
A single crystal was selected, mounted and transferred into a cold nitrogen gas stream. Intensity data was collected with Bruker Kappa-APEX2 systems using Mo-K α fine-focus sealed tube or Cu-K α micro-source. Unit-cell parameters determination, data collection strategy and integration were carried out with the Bruker APEX2 suite of programs. Multi-scan absorption correction was applied.^[33] The structures were solved using SIR92^[34] and refined anisotropically by full-matrix least-squares methods using SHELXL-2013.^[35] Crystallographic data for these structures was deposited at the Cambridge Crystallographic Data Centre. Data can be obtained free of charge *via* www.ccdc.cam.ac.uk.

Experimental part



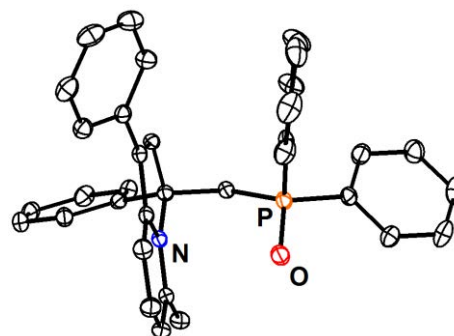
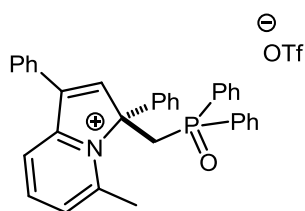
Crystal data and structure refinement for **41a**

Empirical formula	C ₃₃ H ₂₆ Au Cl N O P
Formula weight	715.93
Temperature	200(1) K
Wavelength	0.71073 Å
Crystal system	Orthorhombic
Space group	P 21 21 21
Unit cell dimensions	a = 10.0727(3) Å α = 90° b = 14.4248(4) Å β = 90° c = 37.5204(11) Å γ = 90°
Volume	5451.6(3) Å ³
Z	8
Density (calculated)	1.745 g.cm ⁻³
Absorption coefficient	5.582 mm ⁻¹
F(000)	2800
Crystal size	0.3 x 0.1 x 0.05 mm ³
θ range for data collection	1.085° to 30.531°
Index ranges	-14 ≤ h ≤ 14, -16 ≤ k ≤ 20, -53 ≤ l ≤ 53
Reflections collected	89860
Independent reflections	16668 [R(int) = 0.0446]
Completeness to θ = 25.242°	99.9 %
Absorption correction	Semi-empirical from equivalents
Max. and min. transmission	0.8651 and 0.4563
Refinement method	Full-matrix least-squares on F ²
Data / restraints / parameters	16668 / 0 / 685
Goodness-of-fit on F ²	1.031
Final R indices [I > 2σ(I)]	R1 = 0.0284, wR2 = 0.0468
R indices (all data)	R1 = 0.0356, wR2 = 0.0484
Absolute structure parameter	-0.008(2)
Largest difference peak and hole	0.819 and -1.054 e.Å ⁻³

Crystal data and structure refinement for **41b**

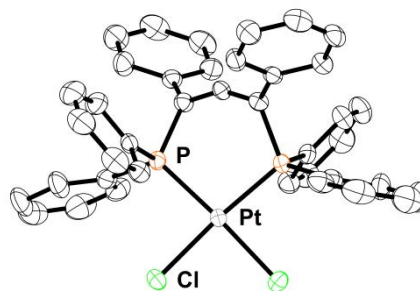
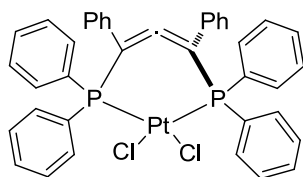
Empirical formula	C ₃₄ H ₂₈ Au Cl N O P	
Formula weight	729.96	
Temperature	200(1) K	
Wavelength	0.71073 Å	
Crystal system	Monoclinic	
Space group	P 2 ₁ /n	
Unit cell dimensions	a = 11.8687(5) Å	α = 90°
	b = 14.4275(6) Å	β = 106.4540(10)°
	c = 17.7634(6) Å	γ = 90°
Volume	2917.2(2) Å ³	
Z	4	
Density (calculated)	1.662 g.cm ⁻³	
Absorption coefficient	5.217 mm ⁻¹	
F(000)	1432	
Crystal size	0.35 x 0.25 x 0.15 mm ³	
θ range for data collection	1.849° to 30.546°	
Index ranges	-16 ≤ h ≤ 16, -20 ≤ k ≤ 20, -25 ≤ l ≤ 24	
Reflections collected	51309	
Independent reflections	8924 [R(int) = 0.0182]	
Completeness to θ = 25.242°	99.9 %	
Absorption correction	Semi-empirical from equivalents	
Max. and min. transmission	0.5396 and 0.3645	
Refinement method	Full-matrix least-squares on F ²	
Data / restraints / parameters	8924 / 0 / 353	
Goodness-of-fit on F ²	1.141	
Final R indices [I > 2σ(I)]	R1 = 0.0175, wR2 = 0.0440	
R indices (all data)	R1 = 0.0212, wR2 = 0.0462	
Largest difference peak and hole	2.082 and -0.828 e.Å ⁻³	

Experimental part

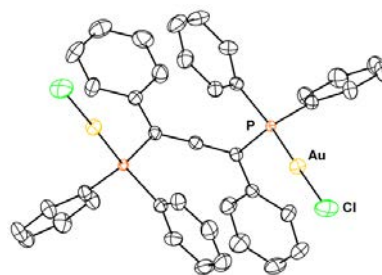
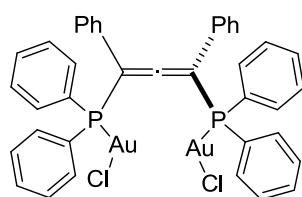


Crystal data and structure refinement for **39**

Empirical formula	C ₃₅ H ₂₉ F ₃ N O ₄ P S
Formula weight	647.62
Temperature	200(1) K
Wavelength	1.54178 Å
Crystal system	Monoclinic
Space group	P 2 ₁ /c
Unit cell dimensions	a = 11.3887(3) Å α = 90° b = 13.3197(4) Å β = 97.896(2)° c = 20.5063(6) Å γ = 90°
Volume	3081.19(15) Å ³
Z	4
Density (calculated)	1.396 g.cm ⁻³
Absorption coefficient	1.934 mm ⁻¹
F(000)	1344
Crystal size	0.3 x 0.05 x 0.05 mm ³
θ range for data collection	3.918° to 66.672°
Index ranges	-13 ≤ h ≤ 13, -15 ≤ k ≤ 10, -24 ≤ l ≤ 24
Reflections collected	22253
Independent reflections	5439 [R(int) = 0.0376]
Completeness to θ = 66.500°	99.8 %
Absorption correction	Semi-empirical from equivalents
Max. and min. transmission	0.992 and 0.726
Refinement method	Full-matrix least-squares on F ²
Data / restraints / parameters	5439 / 9 / 428
Goodness-of-fit on F ²	1.031
Final R indices [I > 2σ(I)]	R1 = 0.0384, wR2 = 0.0945
R indices (all data)	R1 = 0.0520, wR2 = 0.1018
Largest difference peak and hole	0.340 and -0.386 e.Å ⁻³

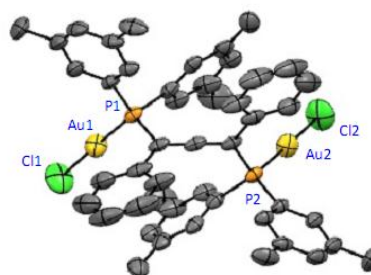
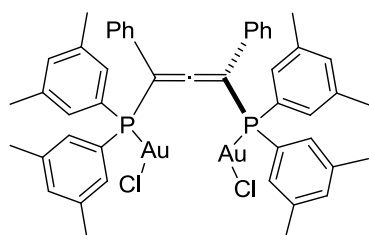
Crystal data and structure refinement for **110**

Empirical formula	C ₄₁ H ₃₂ Cl ₈ P ₂ Pt
Formula weight	1065.29
Temperature	200(1) K
Wavelength	1.54178 Å
Crystal system	Monoclinic
Space group	P 21
Unit cell dimensions	a = 9.9582(3) Å α = 90° b = 21.3845(7) Å β = 103.135(2)° c = 10.1108(3) Å γ = 90°
Volume	2096.77(11) Å ³
Z	2
Density (calculated)	1.687 g.cm ⁻³
Absorption coefficient	11.903 mm ⁻¹
F(000)	1044
Crystal size	0.3 x 0.15 x 0.05 mm ³
θ range for data collection	4.134° to 66.651°
Index ranges	-11 ≤ h ≤ 9, -25 ≤ k ≤ 25, -9 ≤ l ≤ 12
Reflections collected	14108
Independent reflections	6633 [R(int) = 0.0143]
Completeness to θ = 66.500°	99.0 %
Absorption correction	Semi-empirical from equivalents
Max. and min. transmission	0.715 and 0.242
Refinement method	Full-matrix least-squares on F ²
Data / restraints / parameters	6633 / 1 / 469
Goodness-of-fit on F ²	1.031
Final R indices [I > 2σ(I)]	R1 = 0.0183, wR2 = 0.0464
R indices (all data)	R1 = 0.0184, wR2 = 0.0465
Absolute structure parameter	-0.026(5)
Largest difference peak and hole	0.730 and -0.377 e. Å ⁻³

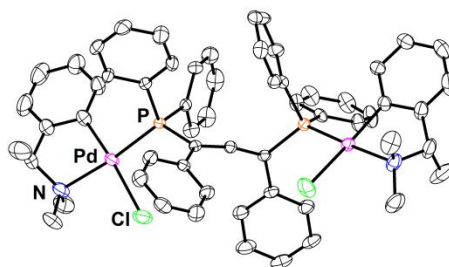
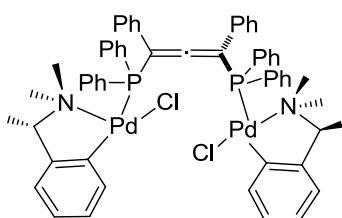


Crystal data and structure refinement for **113**

Empirical formula	C ₄₀ H ₃₂ Au ₂ Cl ₄ P ₂
Formula weight	1110.33
Temperature	200(1) K
Wavelength	0.71073 Å
Crystal system	Monoclinic
Space group	P 2 ₁ /n
Unit cell dimensions	a = 12.6409(3) Å α = 90° b = 16.9730(4) Å β = 104.6610(10)° c = 18.0808(5) Å γ = 90°
Volume	3753.00(16) Å ³
Z	4
Density (calculated)	1.965 g.cm ⁻³
Absorption coefficient	8.208 mm ⁻¹
F(000)	2112
Crystal size	0.5 x 0.2 x 0.15 mm ³
θ range for data collection	2.053° to 30.533°
Index ranges	-18 ≤ h ≤ 18, -24 ≤ k ≤ 24, -25 ≤ l ≤ 25
Reflections collected	55873
Independent reflections	11469 [R(int) = 0.0200]
Completeness to θ = 25.242°	100.0 %
Absorption correction	Semi-empirical from equivalents
Max. and min. transmission	0.4194 and 0.1649
Refinement method	Full-matrix least-squares on F ²
Data / restraints / parameters	11469 / 0 / 433
Goodness-of-fit on F ²	1.077
Final R indices [I > 2σ(I)]	R1 = 0.0191, wR2 = 0.0446
R indices (all data)	R1 = 0.0248, wR2 = 0.0470
Largest difference peak and hole	0.789 and -0.987 e.Å ⁻³

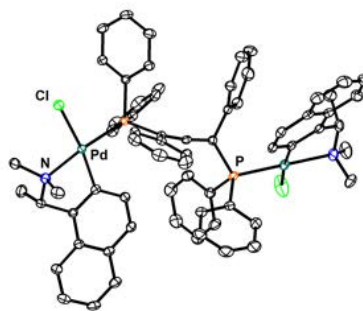
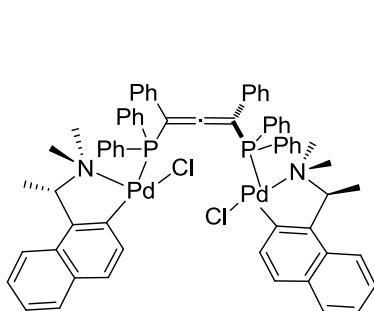
Crystal data and structure refinement for **116**

Empirical formula	C ₅₀ H ₅₃ Au ₂ Cl ₂ P ₂
Formula weight	1180.69
Temperature	200(1) K
Wavelength	0.71073 Å
Crystal system	Monoclinic
Space group	C 2/c
Unit cell dimensions	a = 15.7804(8) Å α = 90° b = 21.3169(10) Å β = 113.037(3)° c = 17.9684(9) Å γ = 90°
Volume	5562.3(5) Å ³
Z	4
Density (calculated)	1.410 g.cm ⁻³
Absorption coefficient	5.450 mm ⁻¹
F(000)	2300
Crystal size	0.3 x 0.25 x 0.2 mm ³
θ range for data collection	1.745° to 30.593°
Index ranges	-22 ≤ h ≤ 22, -30 ≤ k ≤ 30, -25 ≤ l ≤ 25
Reflections collected	51031
Independent reflections	8547 [R(int) = 0.0251]
Completeness to θ = 25.242°	99.9 %
Absorption correction	Semi-empirical from equivalents
Max. and min. transmission	0.172 and 0.122
Refinement method	Full-matrix least-squares on F ²
Data / restraints / parameters	8547 / 36 / 298
Goodness-of-fit on F ²	1.053
Final R indices [I > 2σ(I)]	R1 = 0.0441, wR2 = 0.1455
R indices (all data)	R1 = 0.0648, wR2 = 0.1691
Largest difference peak and hole	2.532 and -1.946 e.Å ⁻³



Crystal data and structure refinement for **119**

Empirical formula	C ₁₁₉ H ₁₂₀ Cl ₄ N ₄ O ₄ Pd ₄	
Formula weight	2313.46	
Temperature	200(1) K	
Wavelength	0.71073 Å	
Crystal system	Triclinic	
Space group	P 1	
Unit cell dimensions	a = 10.1832(3) Å	α = 88.264(2)°
	b = 15.4088(4) Å	β = 82.410(2)°
	c = 17.1707(5) Å	γ = 88.890(2)°
Volume	2669.12(13) Å ³	
Z	1	
Density (calculated)	1.439 g.cm ⁻³	
Absorption coefficient	0.875 mm ⁻¹	
F(000)	1182	
Crystal size	0.2 x 0.2 x 0.06 mm ³	
θ range for data collection	1.197° to 30.590°	
Index ranges	-14 ≤ h ≤ 14, -22 ≤ k ≤ 22, -24 ≤ l ≤ 24	
Reflections collected	115028	
Independent reflections	32066 [R(int) = 0.0251]	
Completeness to θ = 25.242°	99.8 %	
Absorption correction	Semi-empirical from equivalents	
Max. and min. transmission	0.9879 and 0.8643	
Refinement method	Full-matrix least-squares on F ²	
Data / restraints / parameters	32066 / 3 / 1239	
Goodness-of-fit on F ²	1.075	
Final R indices [I > 2θ(I)]	R1 = 0.0395, wR2 = 0.1059	
R indices (all data)	R1 = 0.0459, wR2 = 0.1136	
Absolute structure parameter	-0.025(4)	
Largest difference peak and hole	1.910 and -0.778 e. Å ⁻³	

Crystal data and structure refinement for **120**

Empirical formula	C _{67.50} H ₆₂ Cl ₂ N ₂ O P ₂ Pd ₂	
Formula weight	1262.83	
Temperature	200(1) K	
Wavelength	1.54178 Å	
Crystal system	Monoclinic	
Space group	P 21	
Unit cell dimensions	a = 12.6084(5) Å	$\alpha = 90^\circ$
	b = 12.4687(5) Å	$\beta = 105.173(2)^\circ$
	c = 20.0120(8) Å	$\gamma = 90^\circ$
Volume	3036.4(2) Å ³	
Z	2	
Density (calculated)	1.381 g.cm ⁻³	
Absorption coefficient	6.415 mm ⁻¹	
F(000)	1290	
Crystal size	0.3 x 0.2 x 0.05 mm ³	
θ range for data collection	2.287° to 66.582°	
Index ranges	-15 ≤ h ≤ 15, -10 ≤ k ≤ 14, -23 ≤ l ≤ 23	
Reflections collected	39921	
Independent reflections	9198 [R(int) = 0.0224]	
Completeness to $\theta = 66.500^\circ$	99.7 %	
Absorption correction	Semi-empirical from equivalents	
Max. and min. transmission	0.68 and 0.25	
Refinement method	Full-matrix least-squares on F ²	
Data / restraints / parameters	9198 / 1 / 709	
Goodness-of-fit on F ²	1.128	
Final R indices [I > 2 σ (I)]	R1 = 0.0260, wR2 = 0.0818	
R indices (all data)	R1 = 0.0261, wR2 = 0.0830	
Absolute structure parameter	-0.013(3)	
Largest difference peak and hole	1.155 and -0.454 e. Å ⁻³	

4. Chirality transfer study by chiral HPLC analysis

4.1. Materials and Methods

Chiral HPLC analyses were achieved on an Agilent 1260 infinity unit with pump, autosampler, oven, DAD and Jasco CD-2095 circular dichroism detector, controlled by a SRA Instrument software (Marcy l'Etoile, France).

Lux-Cellulose-4 (250*4.6 mm, 3 μ m) and (250*10 mm, 5 μ m), cellulose tris(4-chloro-3-methylphenylcarbamate), and Lux-Cellulose-2 (250*4.6 mm, 3 μ m), cellulose tris(3-chloro-4-methylphenylcarbamate), chiral stationary phases available from Phenomenex, were used for analytical and preparative separations.

Retention times R_t in minutes, retention factors $k_i = (R_{t_i} - R_{t_0})/R_{t_0}$, enantioselectivity factor $\alpha = k_2/k_1$ and resolution $R_s = 2 (R_{t_2} - R_{t_1}) / (w_1 + w_2)$ are given. R_{t_0} was determined by injection of tri-tertio-butyl benzene and w_i was the width of the peak.

The sign given by the circular dichroism detector is the sign of the enantiomer at 254 nm in the mobile phase used for the separation.

4.2. Chiral HPLC for compound 17, 18, 29 and 30

For compound **17**: Chiralpak AD-H (250*10 mm), heptane / ethanol (80/20), 1 mL/min, 25°C, UV 254 nm and CD 254 nm, $R_t(-, CD 254 nm) = 5.58$ min, $R_t(+, CD 254 nm) = 7.52$ min, $k(-) = 0.89$, $k(+)$ = 1.55, $\alpha = 1.74$ and $R_s = 4.46$.

For compound **18**: Lux-Cellulose-4 (250*4.6 mm, 3 μ m), heptane / ethanol (80/20), 1 mL/min, 25°C, UV 254 nm and CD 254 nm, $R_t(-, CD 254 nm) = 8.01$ min, $R_t(+, CD 254 nm) = 8.77$ min, $k(-) = 1.71$, $k(+)$ = 1.97, $\alpha = 1.15$ and $R_s = 2.23$.

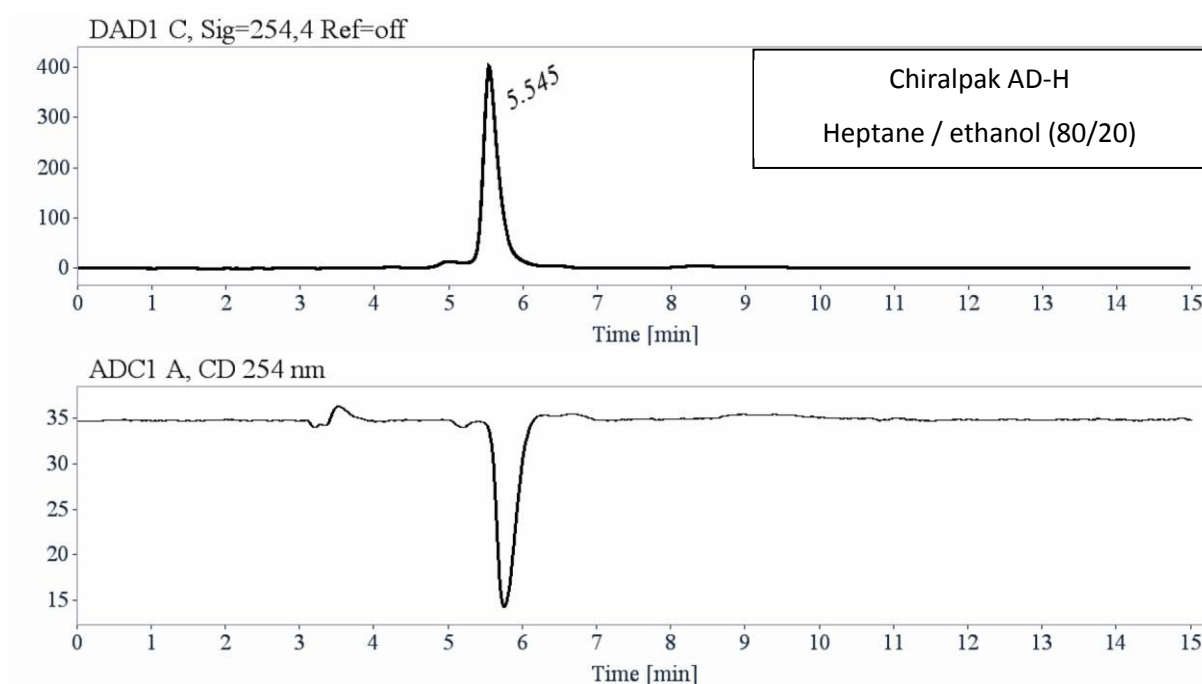
For compound **29**: Lux-Cellulose-4 (250*4.6 mm, 3 μ m), heptane / ethanol (80/20), 1 mL/min, 25°C, UV 254 nm and CD 254 nm, $R_t(-, CD 254 nm) = 6.63$ min, $R_t(+, CD 254 nm) = 7.89$ min, $k(-) = 1.25$, $k(+)$ = 1.67, $\alpha = 1.34$ and $R_s = 3.93$.

For compound **30**: Lux-Cellulose-2 (250*4.6 mm, 3 μ m), heptane / ethanol (70/30), 1 mL/min, 25°C, UV 220 nm and CD 254 nm, $R_t(-, CD 254 nm) = 7.60$ min, $R_t(+, CD 254 nm) = 9.22$ min, $k(-) = 1.58$, $k(+)$ = 2.13, $\alpha = 1.35$ and $R_s = 3.90$.

Semi-preparative separation for compound 17

- Sample preparation: About 160 mg of compound **17** are dissolved in 14 mL of ethanol.
- Chromatographic conditions: Chiralpak AD-H (250 x 10 mm), hexanes/ ethanol (80/20) as mobile phase, flow-rate = 5 mL/min, UV detection at 254 nm.
- Injections: 82 times 170 μ L, every 8 minutes.
- First fraction: 25 mg of the first eluted ((-, CD 254nm)-enantiomer) with *ee* > 99%
- Second fraction: 21 mg of the second eluted ((+, CD 254 nm)-enantiomer) with *ee* > 98%

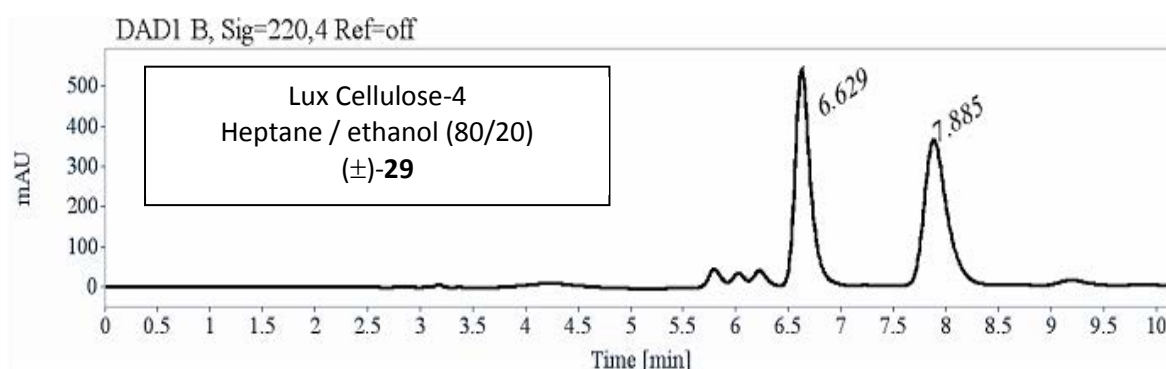
Chromatograms of the collected fractions (**17**):



Signal: DAD1 C, Sig=254,4 Ref=

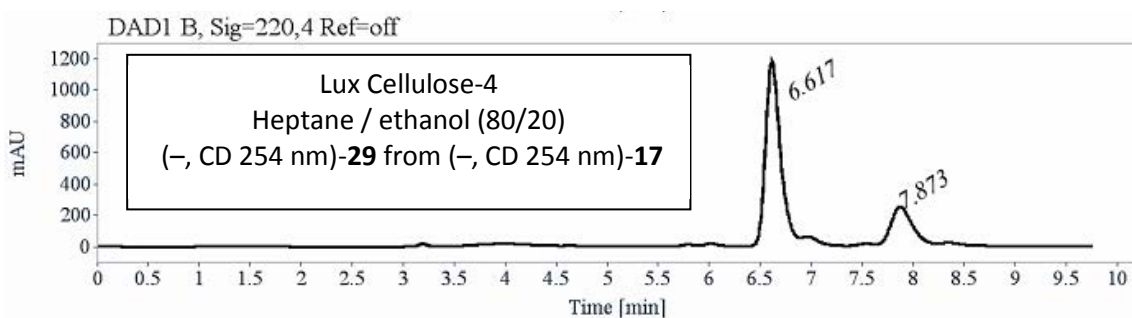
RT [min]	Area	Area%
5.55	5556	100.00
Sum	5556	100.00

- Chromatograms for **29**



Signal: DAD1 B, Sig=220,4 Ref=off

RT [min]	Area	Area%	Capacity Factor	Enantioselectivity	Resolution (USP)
6.63	5405	49.68	1.25		
7.89	5475	50.32	1.67	1.34	3.92
Sum	10879	100.00			



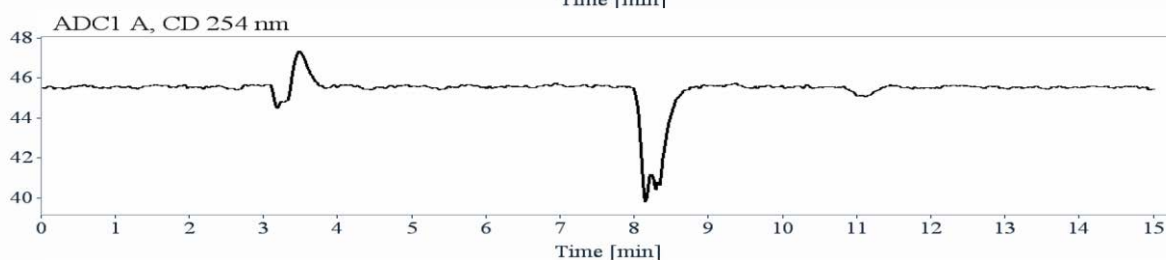
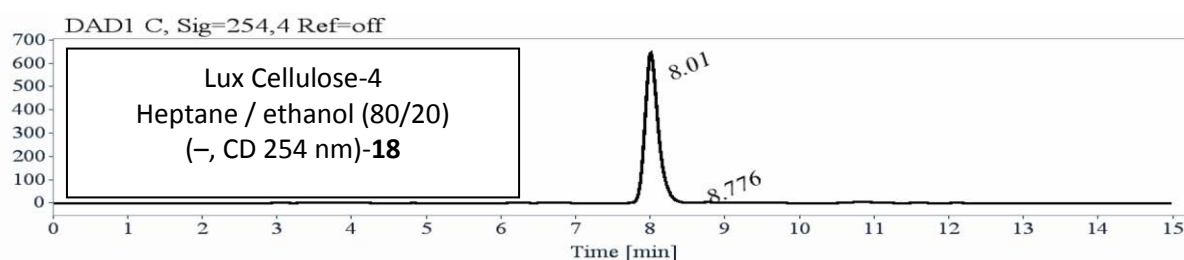
Signal: DAD1 B, Sig=220,4 Ref=off

RT [min]	Area	Area%	Capacity Factor	Enantioselectivity	Resolution (USP)
6.62	12039	77.31	1.24		
7.87	3533	22.69	1.67	1.34	3.93
Sum	15572	100.00			

Semi-preparative separation for enantiomers of **18**:

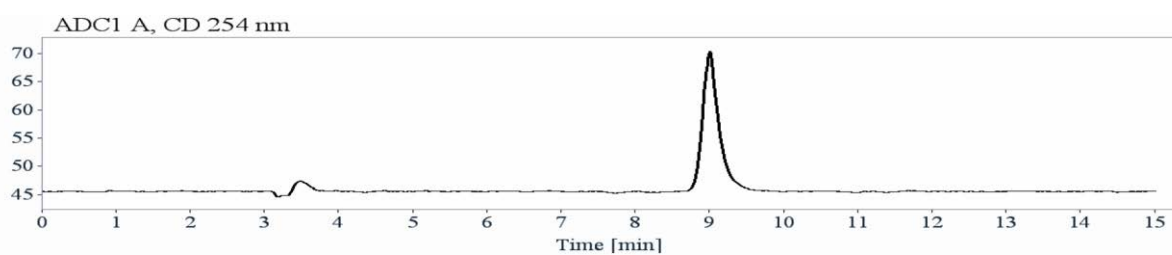
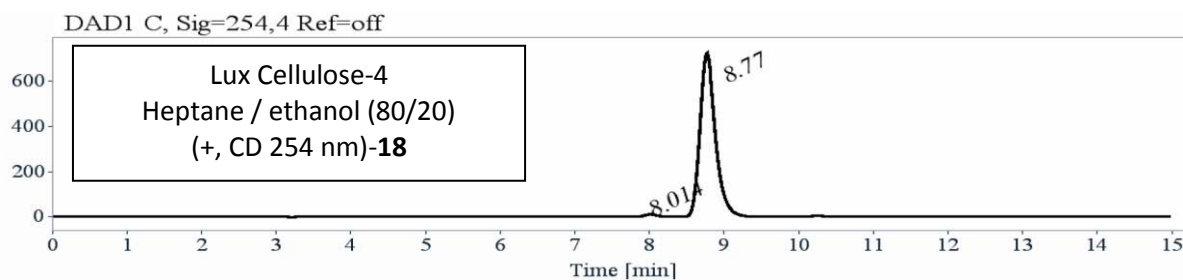
- Sample preparation: About 440 mg of compound **18** are dissolved in 11 mL of ethanol.
- Chromatographic conditions: Lux Cellulose-4 (250 x 10 mm), hexane / ethanol (80/20) as mobile phase, flow-rate = 5 mL/min, UV detection at 280 nm.
- Injections: 275 times 40 µL, every 1.8 minutes.
- First fraction: 181 mg of the first eluted ((-, CD 254nm)-enantiomer) with *ee* > 98.5%
- Second fraction: 203 mg of the second eluted ((+, CD 254 nm)-enantiomer) with *ee* > 97%

- Chromatograms of the collected fractions (**18**):



Signal: DAD1 C, Sig=254,4 Ref=

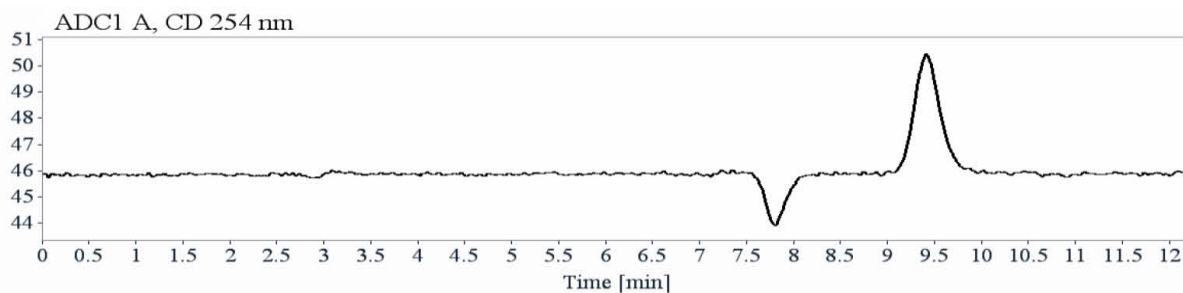
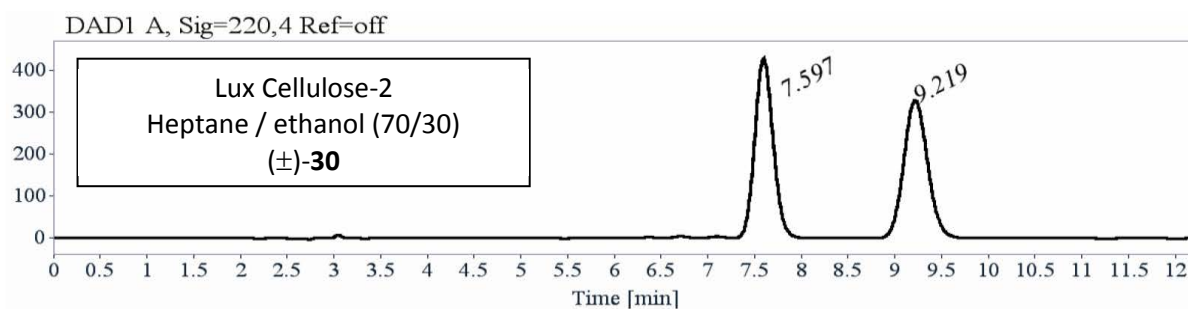
RT [min]	Area	Area%
8.01	8034	99.38
8.78	50	0.62
Sum	8085	100.00



Signal: DAD1 C, Sig=254,4 Ref=

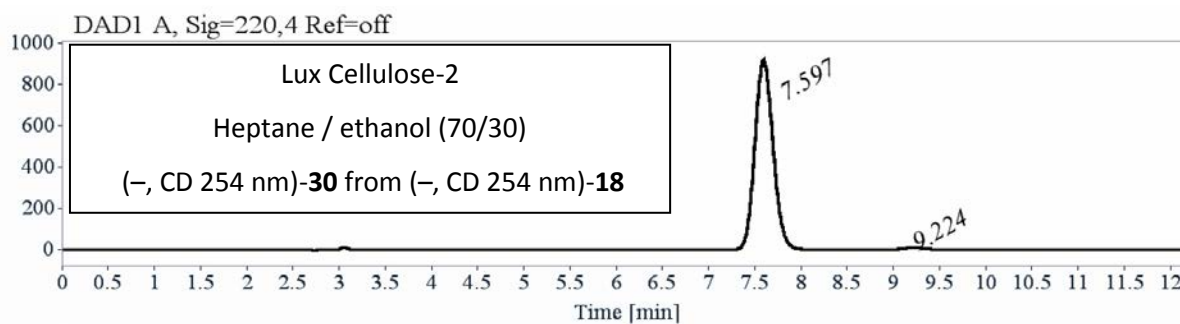
RT [min]	Area	Area%
8.01	133	1.27
8.77	10376	98.73
Sum	10509	100.00

Experimental part



Signal: DAD1 A, Sig=220,4 Ref=off

RT [min]	Area	Area%	Capacity Factor	Enantioselectivity	Resolution (USP)
7.60	5847	49.99	1.58		
9.22	5850	50.01	2.13	1.35	3.90
Sum	11698	100.00			



Signal: DAD1 A, Sig=220,4 Ref=

RT [min]	Area	Area%
7.60	12615	98.65
9.22	173	1.35
Sum	12788	100.00

5. DFT Calculations

XYZ coordinates for calculated complex **41b**

Au	79.0	7.32628059	4.32793951	3.92998505	H	1.0	6.17765808	0.50200272	5.54563808
Cl	17.0	8.44658470	4.65963793	1.90167904	H	1.0	6.39286041	1.73330104	4.29290581
P	15.0	4.06811857	1.26823711	4.83055544	C	6.0	4.14949894	0.25407290	3.31358171
O	8.0	3.31776667	0.57223189	5.94642639	C	6.0	3.40111613	-0.93331349	3.30882502
N	7.0	5.26032734	2.72349262	7.36961174	H	1.0	2.82194877	-1.19771123	4.19862556
C	6.0	6.28060627	3.97176242	5.61689568	C	6.0	3.40654206	-1.75829625	2.17922854
C	6.0	6.27045107	2.58390832	6.25869942	H	1.0	2.82118440	-2.68348503	2.17768168
C	6.0	4.81427956	4.02512884	7.39362288	C	6.0	4.15970564	-1.40231752	1.05516422
C	6.0	5.43581724	4.78503227	6.33481169	H	1.0	4.16438389	-2.04860306	0.17149790
C	6.0	4.88740492	1.78186154	8.28127766	C	6.0	4.91096497	-0.22017910	1.05885041
C	6.0	5.41403723	0.38153851	8.20008564	H	1.0	5.50419712	0.05918600	0.18266310
H	1.0	4.82043648	-0.15916330	7.44116831	C	6.0	4.90799761	0.60860562	2.18395352
H	1.0	5.28690004	-0.12115860	9.17158222	H	1.0	5.50525618	1.52632153	2.16635203
H	1.0	6.47964621	0.35248619	7.92488194	C	6.0	3.27250886	2.84759355	4.38320589
C	6.0	3.98586202	2.16246843	9.27134514	C	6.0	2.05186844	3.12230253	5.02113819
H	1.0	3.66766691	1.41704822	10.00235367	H	1.0	1.67834473	2.42207789	5.77392149
C	6.0	3.49735904	3.47700071	9.32537174	C	6.0	1.33044112	4.27200222	4.68209362
H	1.0	2.79534006	3.76201987	10.11509609	H	1.0	0.37602049	4.48080969	5.17661381
C	6.0	3.91103816	4.41774797	8.39345932	C	6.0	1.82888579	5.15208197	3.71573925
H	1.0	3.57158375	5.45289183	8.42541504	H	1.0	1.26992249	6.05744648	3.45803308
C	6.0	7.67122650	2.34629536	6.85501146	C	6.0	3.05275583	4.88716984	3.09012341
C	6.0	8.00436020	2.84951711	8.12257957	H	1.0	3.46007967	5.58441544	2.35225439
H	1.0	7.25606966	3.37644935	8.72081757	C	6.0	3.77005458	3.73436499	3.41475987
C	6.0	9.29410362	2.69290829	8.63608646	H	1.0	4.72878647	3.55362320	2.92338419
H	1.0	9.53151608	3.08865619	9.62867546	C	6.0	5.16111135	6.21565962	6.07625151
C	6.0	10.27718449	2.04056931	7.88458204	C	6.0	3.84497690	6.71153021	6.04000092
H	1.0	11.28884506	1.92020619	8.28435993	H	1.0	3.00617337	6.02595520	6.18473196
C	6.0	9.95860481	1.55460918	6.61368656	C	6.0	3.59477282	8.05805016	5.76121473
H	1.0	10.72103596	1.05823457	6.00572634	H	1.0	2.56218553	8.42068291	5.72357130
C	6.0	8.66655350	1.70799792	6.10062981	C	6.0	4.65711546	8.93291473	5.51022148
H	1.0	8.45180511	1.34483159	5.09432554	H	1.0	4.46229029	9.98695278	5.28711891
C	6.0	5.85833025	1.50750506	5.22756767	C	6.0	5.97066593	8.44989014	5.53795767
					H	1.0	6.80862331	9.12444210	5.33546638

Experimental part

XYZ Coordinates for carbene moiety of **41b**

C	6.0	-2.74840689	0.16361800	1.04967904	H	1.0	4.72254276	-1.04559195	0.37883800
C	6.0	-1.23403001	-0.47932699	2.80450892	C	6.0	3.24239993	-1.24561298	-3.22212791
C	6.0	-2.21117592	-0.13579100	3.74097800	H	1.0	1.59396505	-0.10320900	-2.47309709
C	6.0	-3.46559906	0.33647901	3.33506489	C	6.0	4.46733093	-1.85513997	-2.93461490
C	6.0	-3.74321294	0.48622599	1.98519301	H	1.0	5.96054888	-2.25958991	-1.41639805
C	6.0	0.07761300	-1.03539395	3.26187992	H	1.0	2.78763795	-1.31276000	-4.21497202
H	1.0	-1.97862005	-0.26020199	4.80000305	H	1.0	5.00358009	-2.40169191	-3.71697092
H	1.0	-4.22493982	0.58110499	4.08398581	C	6.0	2.74152207	2.19515610	0.26164800
H	1.0	-4.71103477	0.84010202	1.62944806	C	6.0	3.23850989	2.84822798	1.40062797
N	7.0	-1.53188503	-0.31246400	1.48214495	C	6.0	2.61613703	2.90115499	-0.94657397
C	6.0	-2.79278398	0.21783599	-0.39379901	C	6.0	3.59720206	4.19831085	1.33320796
C	6.0	-0.65686703	-0.60209501	0.24188501	H	1.0	3.34809899	2.28225803	2.32996702
C	6.0	-1.61386895	-0.25873199	-0.91003501	C	6.0	2.97199392	4.25109100	-1.00802600
C	6.0	0.45199400	0.52260798	0.16439500	H	1.0	2.25435305	2.40182495	-1.85096800
P	15.0	2.29193497	0.42661899	0.44749501	C	6.0	3.46129894	4.90065479	0.13147300
O	8.0	2.71026206	-0.09104000	1.81045401	H	1.0	3.98838592	4.70232105	2.22264695
C	6.0	-0.29730901	-2.10159111	0.22294800	H	1.0	2.87283397	4.79565477	-1.95193505
C	6.0	0.94558901	-2.62027597	0.61131603	H	1.0	3.74329901	5.95701790	0.07926400
C	6.0	-1.29319704	-3.01083302	-0.18566100	C	6.0	-3.97282004	0.70763099	-1.15053403
C	6.0	1.19271600	-3.99809289	0.57287103	C	6.0	-4.51282597	-0.05133900	-2.20492601
H	1.0	1.78876996	-2.68302202	0.88201398	C	6.0	-5.61268282	0.41276601	-2.93046308
C	6.0	-1.05313504	-4.38491297	-0.21009400	C	6.0	-6.19705677	1.64429903	-2.61679006
H	1.0	-2.26905990	-2.63969207	-0.50571197	C	6.0	-5.66791821	2.41267300	-1.57534206
C	6.0	0.19847800	-4.88641787	0.16194201	C	6.0	-4.56630707	1.94870603	-0.85050702
H	1.0	2.17737007	-4.36978817	0.87191099	H	1.0	-4.05789614	-1.01201999	-2.45978498
H	1.0	-1.84500694	-5.06455278	-0.53918999	H	1.0	-6.01303005	-0.19254000	-3.74952412
H	1.0	0.39561501	-5.96240997	0.12879200	H	1.0	-7.05742884	2.00758290	-3.18740010
H	1.0	-0.08159600	1.32779098	0.80168498	H	1.0	-6.10639715	3.38579392	-1.33224499
H	1.0	0.03581100	0.99911100	-0.79895699	H	1.0	-4.14316797	2.57667303	-0.05994600
C	6.0	3.09020209	-0.47072500	-0.92384702	H	1.0	0.95922601	-0.56961101	2.78353500
C	6.0	4.31900215	-1.09254205	-0.63678598	H	1.0	0.16274101	-0.90121198	4.35138178
C	6.0	2.55961299	-0.54949498	-2.22015905	H	1.0	0.13342200	-2.11651707	3.04617810
C	6.0	5.00460386	-1.77687895	-1.64326894					

6. References (Experimental part)

- [1] G. Gao, R.-G. Xie, L. Pu, *Proc. Natl. Acad. Sci.* **2004**, *101*, 5417–5420.
- [2] C. Spino, C. Thibault, S. Gingras, *J. Org. Chem.* **1998**, *63*, 5283–5287.
- [3] D. Alagille, R. M. Baldwin, B. L. Roth, J. T. Wroblewski, E. Grajkowska, G. D. Tamagnan, *Bioorg. Med. Chem.* **2005**, *13*, 197–209.
- [4] C. Nieto-Oberhuber, P. Pérez-Galán, E. Herrero-Gómez, T. Lauterbach, C. Rodríguez, S. López, C. Bour, A. Rosellón, D. J. Cárdenas, A. M. Echavarren, *J. Am. Chem. Soc.* **2008**, *130*, 269–279.
- [5] M. Barbazanges, M. Augé, J. Moussa, H. Amouri, C. Aubert, C. Desmarests, L. Fensterbank, V. Gandon, M. Malacria, C. Ollivier, *Chem. - Eur. J.* **2011**, *17*, 13789–13794.
- [6] W. Wang, J. Yang, F. Wang, M. Shi, *Organometallics* **2011**, *30*, 3859–3869.
- [7] K. T. Sylvester, P. J. Chirik, *J. Am. Chem. Soc.* **2009**, *131*, 8772–8774.
- [8] F. Schröder, C. Tugny, E. Salanouve, H. Clavier, L. Giordano, D. Moraleda, Y. Gimbert, V. Mouriès-Mansuy, J.-P. Goddard, L. Fensterbank, *Organometallics* **2014**, *33*, 4051–4056.
- [9] E. Benedetti, A. Simonneau, A. Hours, H. Amouri, A. Penoni, G. Palmisano, M. Malacria, J.-P. Goddard, L. Fensterbank, *Adv. Synth. Catal.* **2011**, *353*, 1908–1912.
- [10] C. Nevado, L. Charruault, V. Michelet, C. Nieto-Oberhuber, M. P. Muñoz, M. Méndez, M.-N. Rager, J.-P. Genêt, A. M. Echavarren, *Eur. J. Org. Chem.* **2003**, *2003*, 706–713.
- [11] Z.-C. Duan, X.-P. Hu, C. Zhang, D.-Y. Wang, S.-B. Yu, Z. Zheng, *J. Org. Chem.* **2009**, *74*, 9191–9194.
- [12] H. W. Lee, L. N. Lee, A. S. C. Chan, F. Y. Kwong, *Eur. J. Org. Chem.* **2008**, *2008*, 3403–3406.
- [13] S. Lee, S. Kim, S. Kim, Y. Chung, *Synlett* **2006**, *2006*, 2256–2260.
- [14] Z. Zhang, C. Liu, R. E. Kinder, X. Han, H. Qian, R. A. Widenhoefer, *J. Am. Chem. Soc.* **2006**, *128*, 9066–9073.
- [15] G. L. Hamilton, E. J. Kang, M. Mba, F. D. Toste, *Science* **2007**, *317*, 496–499.
- [16] P. Mauleón, R. M. Zeldin, A. Z. González, F. D. Toste, *J. Am. Chem. Soc.* **2009**, *131*, 6348–6349.
- [17] M. Murakami, S. Kadowaki, T. Matsuda, *Org. Lett.* **2005**, *7*, 3953–3956.
- [18] T. Shibata, Y. Kobayashi, S. Maekawa, N. Toshida, K. Takagi, *Tetrahedron* **2005**, *61*, 9018–9024.
- [19] T. Nishimura, Y. Maeda, T. Hayashi, *Org. Lett.* **2011**, *13*, 3674–3677.
- [20] A. Fürstner, F. Stelzer, H. Szillat, *J. Am. Chem. Soc.* **2001**, *123*, 11863–11869.
- [21] K. Yavari, P. Aillard, Y. Zhang, F. Nuter, P. Retailleau, A. Voituriez, A. Marinetti, *Angew. Chem. Int. Ed.* **2014**, *53*, 861–865.

- [22] C. Nieto-Oberhuber, P. Pérez-Galán, E. Herrero-Gómez, T. Lauterbach, C. Rodríguez, S. López, C. Bour, A. Rosellón, D. J. Cárdenas, A. M. Echavarren, *J. Am. Chem. Soc.* **2008**, *130*, 269–279.
- [23] C.-M. Chao, D. Beltrami, P. Y. Toullec, V. Michelet, *Chem. Commun.* **2009**, 6988–6990.
- [24] C.-M. Chao, M. R. Vitale, P. Y. Toullec, J.-P. Genêt, V. Michelet, *Chem. Eur. J.* **2009**, *15*, 1319–1323.
- [25] X. Zhang, S. Sarkar, R. C. Larock, *J. Org. Chem.* **2006**, *71*, 236–243.
- [26] H. Schmidbaur, C. M. Frazão, G. Reber, G. Müller, *Chem. Ber.* **1989**, *122*, 259–263.
- [27] C. Damelincourt, *Rapport de Stage 5C101: Les allénés en catalyse organométallique: réactifs, ligands, catalyseurs*, UPMC, **2015**.
- [28] D. H. Kim, J. K. Im, D. W. Kim, H. Lee, H. Kim, H. S. Kim, M. Cheong, D. K. Mukherjee, *Transit. Met. Chem.* **2010**, *35*, 949–957.
- [29] S. Otsuka, A. Nakamura, T. Kano, K. Tani, *J. Am. Chem. Soc.* **1971**, *93*, 4301–4303.
- [30] F.-Q. Yuan, L.-X. Gao, F.-S. Han, *Chem. Commun.* **2011**, *47*, 5289–5291.
- [31] A. Xing, Z. Pang, H. Li, L. Wang, *Tetrahedron* **2014**, *70*, 8822–8828.
- [32] A. Vanitcha, G. Gontard, N. Vanthuyne, E. Derat, V. Mouriès-Mansuy, L. Fensterbank, *Adv. Synth. Catal.* **2015**, *357*, 2213–2218.
- [33] Blessing, R.H. An empirical correction for absorption anisotropy *Acta Cryst. A* **1995**, *51*, 33-38.
- [34] Altomare, A. ; Cascarano, G. ; Giacovazzo, C. ; Guagliardi, A. Completion and refinement of crystal structures with SIR92 *J. Appl. Cryst.* **1993**, *26*, 343-350.
- [35] Sheldrick, G.M. A short history of SHELX *Acta Cryst. A* **2008**, *64*, 112-122.

Synthesis of Allenes Bearing Phosphine Oxide Groups and Investigation of Their Reactivity toward Gold Complexes

Avassaya Vanitcha,^a Geoffrey Gontard,^a Nicolas Vanthuyne,^b Etienne Derat,^a Virginie Mouriès-Mansuy,^{a,*} and Louis Fensterbank^{a,*}

^a Sorbonne Universités UPMC Univ Paris 06, UMR CNRS 8232, Institut Parisien de Chimie Moléculaire, 4 place Jussieu, C.229, F-75005 Paris, France

Fax: (+33) 1-4427-7360; e-mail: virginie.mansuy@upmc.fr or louis.fensterbank@upmc.fr

^b Aix-Marseille Université, Centrale Marseille, CNRS, iSm2 UMR 7313, 13397, Marseille, France

Received: April 6, 2015; Revised: May 21, 2015; Published online: July 14, 2015

Dedicated to Prof. Steve Buchwald on the occasion of his 60th birthday.

Supporting information for this article is available on the WWW under <http://dx.doi.org/10.1002/adsc.201500345>.

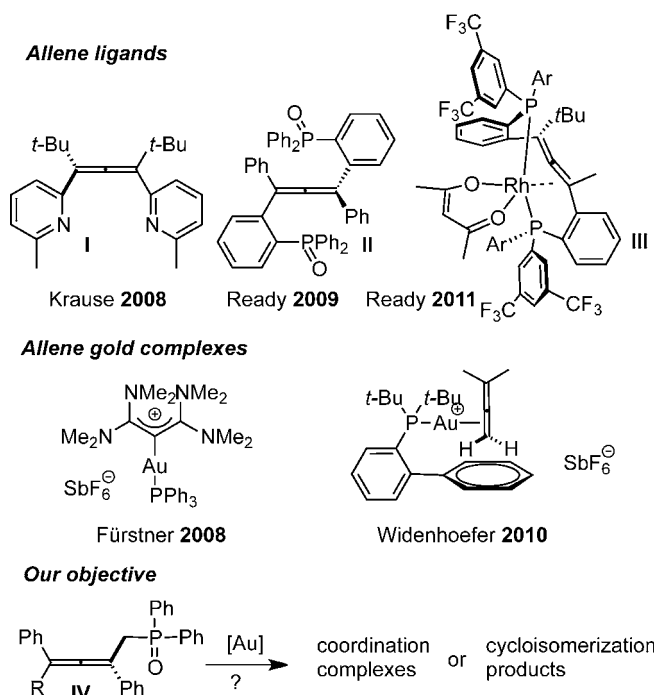
Abstract: A collection of phosphine oxide allenens has been prepared. Their coordination to gold(I) has been studied giving new coordination complexes when a pendant pyridine moiety was present. Alternatively, their gold(I)-catalyzed cycloisomerization has proven to be quite efficient. An almost complete axial-to-central chirality transfer in the cyclization process was observed, opening the potential access to valuable enantiopure phosphorus derivatives.

Keywords: allenens; gold carbenes; gold catalysis; phosphines

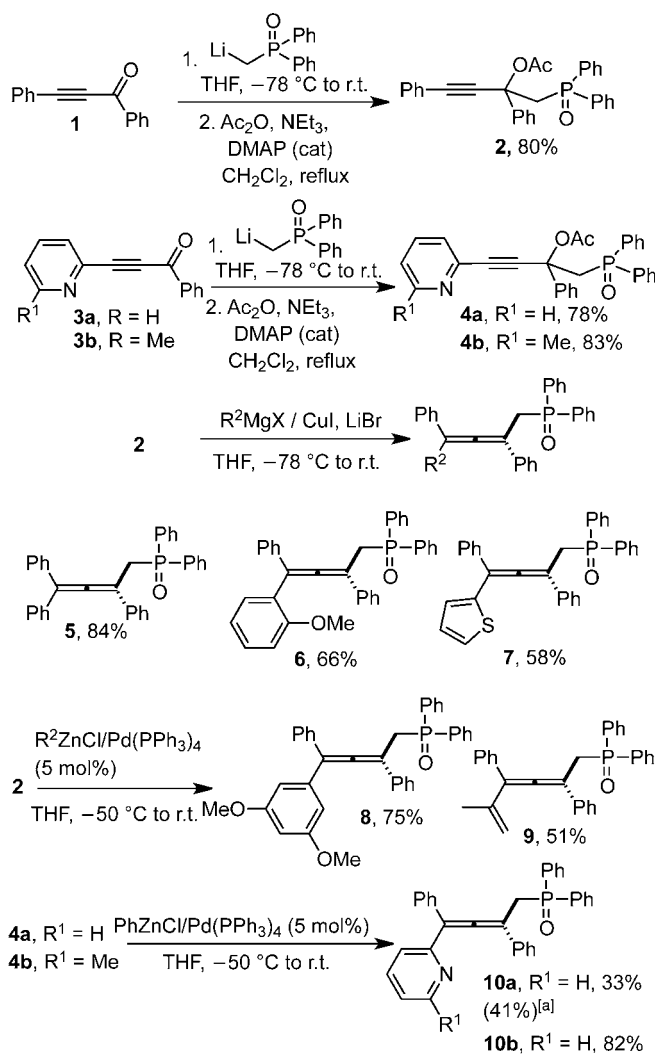
Allenens are fascinating molecular substrates. Their specific electronic configuration coupled to their extended tetrahedral spatial arrangement guarantee special and valuable properties.^[1] When substituted by Lewis base substituents, the allene assembly can serve as a ligand,^[2] possibly conveying axial chirality. Illustration of this principle was initially provided in 2008 by Krause, who reported the preparation of allenic bipyridines **I** and the corresponding silver and copper complexes.^[3] In 2009, Ready developed chiral phosphine oxide allenens **II** as versatile organocatalysts for the asymmetric ring opening of *meso*-epoxides.^[4] The same group then further adapted the parent structure **II** to append phosphine groups bearing CF₃ electron-withdrawing groups in place of the phosphine oxide ones. The resulting ligand could coordinate to Rh(I), featuring coordination to the allene moiety, and provide complex **III**, which proved to be a highly effi-

cient catalyst for the enantioselective arylation of α -keto esters (Scheme 1).^[5]

Because of our long-standing interest in gold catalysis,^[6] we wished to investigate the reactivity of new allene scaffolds bearing phosphine oxide groups as coordinating units. Coordination of gold(I) to allenens has indeed been theoretically studied in order to rationalize some reaction pathways.^[7] In addition, some coordination complexes have also been isolated and characterized by X-ray crystallography. Fürstner isolated a complex between tetradimethylaminoallene



Scheme 1. Allene ligands and complexes.



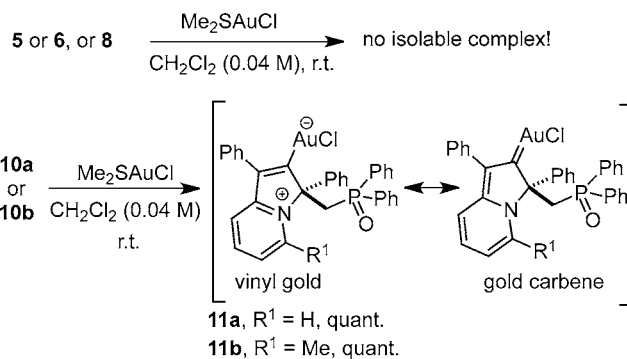
^[a] From the addition of PyZnBr on 2.

Scheme 2. Preparation of allene ligands.

and $\text{Ph}_3\text{PAuSbF}_6$ featuring η^1 central coordination^[8] while Widenhofer has also reported an X-ray crystal structure of the η^2 dimethylallene- Au^+PPh_3 complex.^[9]

Our objective was to use allenylphosphine oxides **IV** as probes for two types of applications. The first aim was the generation of new gold coordination complexes, possibly implying the phosphine oxide moiety.^[10] These could be new precatalytic species or models of proposed intermediates. The second objective was to involve these substrates in cycloisomerization reactions when using appropriate R substituent on **IV** in order to deliver new phosphorus-containing chiral substrates.

Allenylphosphine oxide precursors were easily obtained in a few steps as shown in Scheme 2. Ketone **1** is smoothly alkylated by the lithium anion of methyldiphenylphosphine oxide. The resulting alcohol is then acylated (**2**), setting the stage for a copper-cata-



Scheme 3. Formation of gold chloride complexes **11a** and **11b**.

lyzed $\text{S}_{\text{N}}2'$ process which allows the introduction of various R^2 groups and furnishes allenes **5–7**.^[11a,b,11] Alternatively, we also used the $\text{Pd}(0)$ coupling reaction between a zinc reagent and propargyl acetate **2** to obtain **8** and **9**, as well as pyridyl allenes **10a** and **10b** from acetates **4a** and **4b**.^[3] It should be noted that **10a** could also be prepared in slightly better yield (41%), based on the addition of PyZnBr to **2**.

Our initial attempts to obtain new allene-gold complexes consisted in mixing 1 equiv. of allenes **5–7** with 1 equiv. of Me_2SAuCl . However, we could not isolate any complex from these substrates. So we turned our attention to pyridyl-allenes **10a** and **10b** which incorporate an additional stronger Lewis base site of coordination. In the presence of Me_2SAuCl , a quantitative reaction took place delivering gold complexes **11a** and **11b** for which the structures were secured by single-crystal X-ray diffraction (Scheme 3 and Figure 1).^[12] Careful examination of the literature provided pieces of rationalization for the unforeseen formation of complexes **11a** and **11b**. Gevorgyan showed that similar allenylpyridine units could be activated by gold providing indolizines through nucleophilic addition of the pyridine nitrogen on the electrophilic allene gold complex.^[13] Quite recently, Kumar and Waldmann described a synthesis of cyclic alkyl aminocarbene gold(I) complexes from the addition of Me_2SAuCl to 1,7-enynes.^[14]

Post-functionalization of vinylgold complexes has been documented in the literature.^[13b,15] However,

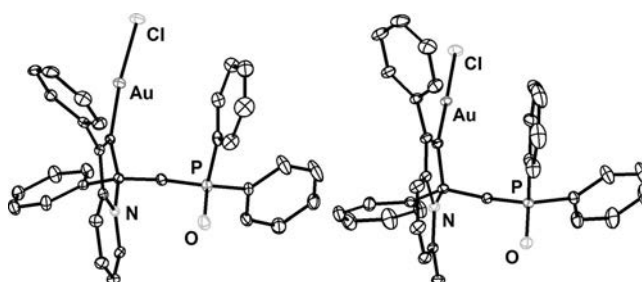


Figure 1. Crystal structures of complexes **11a** and **11b**.

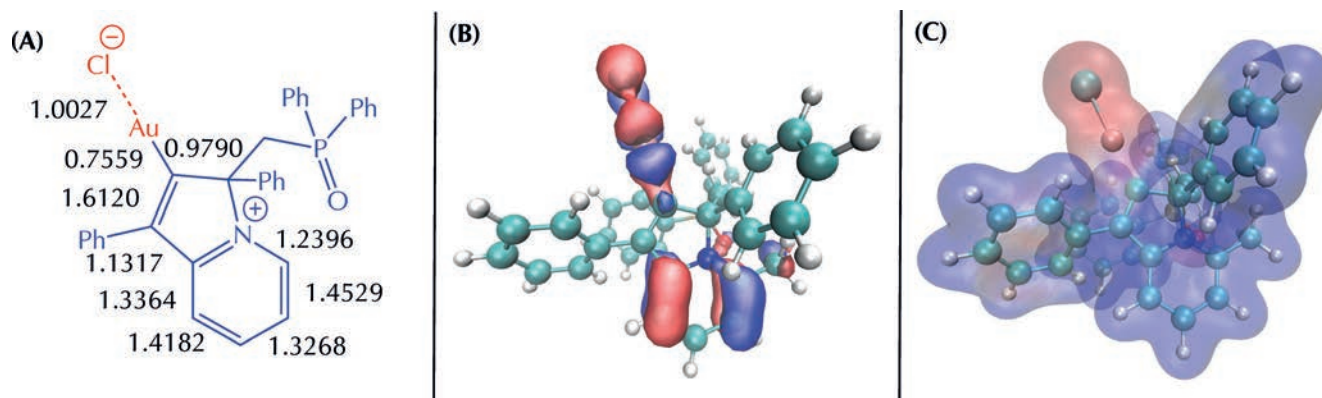


Figure 2. Summary of calculations for complex **11b**: (A) Mayer bond order, (B) molecular orbital showing the delocalization between AuCl and carbene, (C) electrostatic potential (blue: positive; red: negative).

complexes **11a** and **11b** proved quite unreactive to treatment with triflic acid to promote protodeauration,^[15d] addition of electrophilic halide sources (I₂, NIS), and attempts of palladium couplings with aryl halides.^[16] This excited our curiosity and led us to taking a closer look at the crystal structures of **11a** and **11b**. Interestingly, gold carbenes without a stabilizing heteroatom in the α position have been isolated only recently.^[17] The Au–C bond distances of 1.993(4) Å for **11a** and 1.984(2) Å for **11b** are in the low range of previously isolated gold carbenes,^[18] similar to the shortest 1.984(4) Å Au–C bond so far observed by Miqueu, Amgoune and Bourissou for an *o*-carborane diphenylphosphine gold(I) diphenylcarbene complex.^[17d]

To get more insight into the mesomeric structures **11a** and **11b** (vinylgold vs. gold carbene), we performed DFT calculations using the Turbomole program package (V6.4). B3LYP, supplemented by the D3 correction which was used as functional and the def2-SV(P) as basis set. Namely, structure **11b** was optimized starting from X-ray crystallographic data. In order to better understand the electronic structure of this unusual gold-carbene complex, various theoretical analyses were conducted. First, using the Mayer bond order analysis (Figure 2A), it was possible to conclude that the main mesomeric form for complex **11b** is the vinylgold one, as written in Scheme 3. The specific reactivity of this complex can be better understood by looking at one of the orbitals involving interactions between the AuCl fragment and the carbene part (Figure 2B). π -bonding between gold and chloride is also delocalized on the pyridinium moiety of the carbene, thus enhancing what is traditionally described as the back-donation. The fact that the carbene is a good electron acceptor is further confirmed by plotting the electrostatic potential (Figure 2C). While the Au–Cl fragment is found to be electron-rich, the *in-situ* created carbene moiety has a positive electrostatic potential and is thus a good electron-ac-

Table 1. HOMO and LUMO energy (in eV) for various gold ligands.

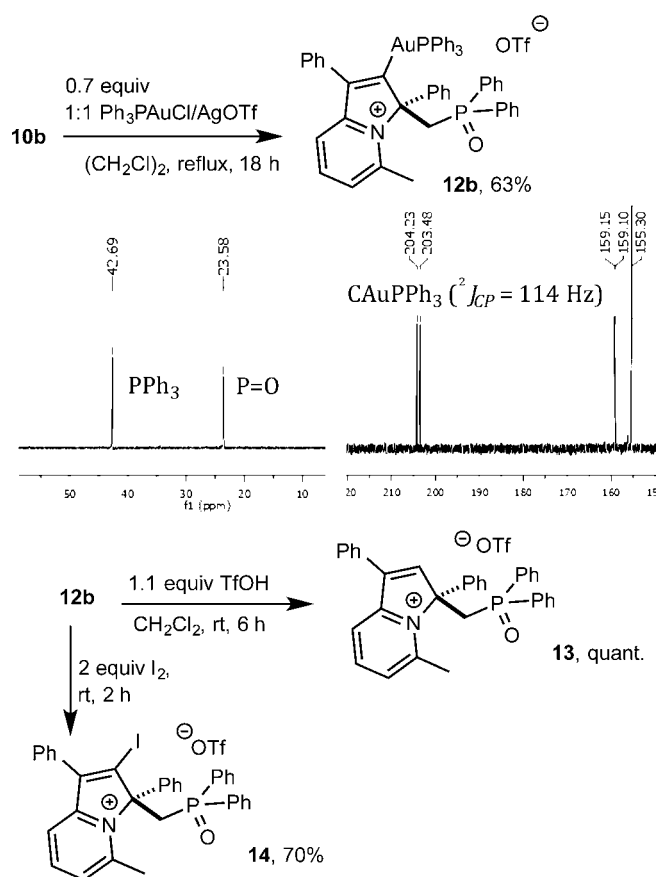
	PPh ₃	DIPP-NHC	SPhos	11b (no AuCl)
LUMO	−0.77	0.82	−0.52	−1.11
HOMO	−5.55	−5.75	−4.85	−4.55

ceptor. To further substantiate these findings, comparisons were made with other classical gold ligands. Namely we compared the HOMO/LUMO energies of a typical phosphine (PPh₃), a standard carbene (DIPP-NHC), a π -accepting phosphine (SPhos, Buchwald ligand^[19]) and our new carbene. The data are summarized in Table 1.

It appears from Table 1 that the carbene derived from **11b** is more electrophilic than the usual carbene (DIPP-NHC) and in the same range as a phosphine, especially the SPhos or Buchwald phosphine.

We then wanted to test the generality of the formation of gold complexes such as **11a** and **11b**. We used a cationic gold precursor and exposed substrate **10b** to 0.7 equiv. of a 1:1 mixture of Ph₃PAuCl and AgOTf (Scheme 4) in refluxing dichloroethane for 18 h. The corresponding complex **12b** was obtained in fair yield (63%) exhibiting characteristic spectral data by ³¹P NMR as shown in Scheme 4 and also a ¹³C NMR resonance at 203 ppm (doublet, ²J_{C,P} = 114 Hz) diagnostic of a vinylgold species.^[20] We also tried to further functionalize this complex. Protodeauration with triflic acid smoothly provided indolizinium salt **13**, whose structure was confirmed by X-ray crystallography,^[12] while iodolysis gave vinyliodine derivative **14**.

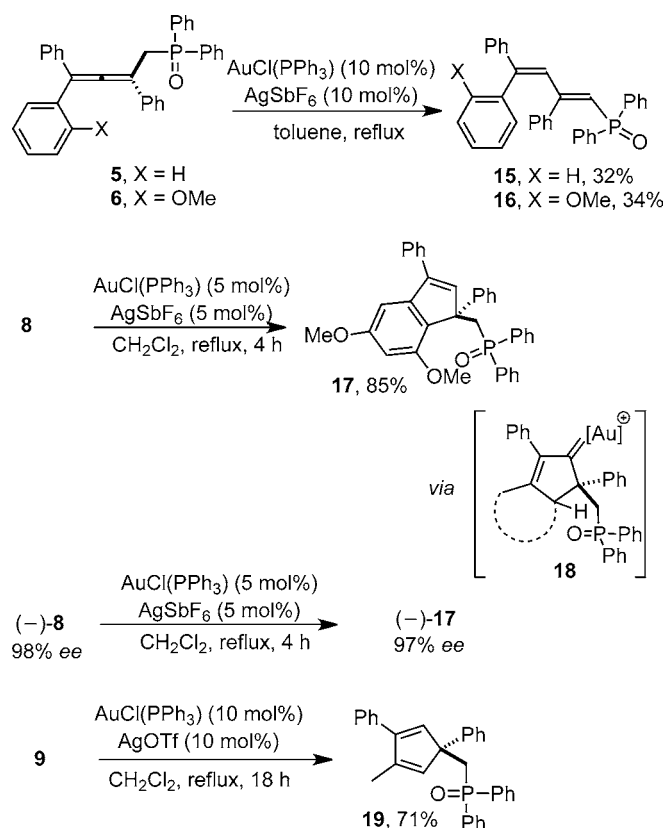
Complexes **11a**, **11b** and **12b** are chemical cul-de-sacs with no possible evolution in these reaction conditions. We hypothesized that the intervention of a nucleophile on the activated allene that liberates a proton would trigger a protodeauration and regenerate the gold catalyst. We therefore examined the reactivity of allenes **5** and **6** in the presence of a catalytic



Scheme 4. Ph₃PAu–vinyl gold complex and reactivity.

quantity of gold catalyst. However, these reactions proved to be rather sluggish giving among a mixture of dienic products **15** and **16** as major components and single diastereomers. We deduced that the involved nucleophilic component was not electron-rich enough. Gratifyingly, allene **8** underwent the expected hydroarylation reaction in satisfactory yield providing indenylphosphine oxide **17**. Our next attempt focused on the Au(I)-catalyzed rearrangement of vinylallene **9**.^[21] In that case, the expected cyclopentadiene product **19** was formed in 71% yield (Scheme 5). All these reactions must transit *via* gold intermediate **18** bearing a stereogenic center. We surmised that if chirality transfer^[22] takes place in the cycloisomerization step, then access to novel enantiopure phosphines whose chirality relies on a quaternary center β to the phosphorus atom should be possible. To probe this point, we ran a preparative chiral HPLC on **8** and obtained both enantiomers with *ees* > 98%. We engaged (–, CD 254 nm)-**8**^[23] in the same conditions as above and gratifyingly isolated (–, CD 254 nm)-**17** with a 97% *ee* evidencing an almost total transfer of chirality. To the best of our knowledge, this is the first example of chirality transfer for a tetrasubstituted allene.

In conclusion, we herein report the reactivity of readily accessible phosphine oxides containing allenes



Scheme 5. Catalytic reactions.

with gold(I) salts. With a pendant pyridine moiety, some new examples of gold carbene complexes with no adjacent heteroatoms have been isolated and fully characterized, both analytically and theoretically. Alternatively, with a nucleophilic component bearing a labile proton, cycloisomerization takes place and delivers highly valuable scaffolds bearing a phosphine oxide moiety. The complete axial-to-central chirality transfer observed in one case augurs well for the preparation of enantiopure phosphines.

Experimental Section

Synthesis of Ph₃PAu–Vinyl Gold Complex **12b**

A mixture of Ph₃PAuCl (140 mg, 0.28 mmol, 1 equiv.) and AgOTf (72 mg, 0.28 mmol, 1 equiv.) in DCE (4 mL) was stirred for 3.5 h at room temperature. The mixture was filtered to remove the AgCl and added to a solution of allene **10b** (200 mg, 0.39 mmol, 1.4 equiv.) in DCE (10 mL) and heated at 50 °C for overnight. After 16 h, the reaction was monitored by ³¹P NMR, the peak at ~45 ppm (Ph₃PAuOTf) had disappeared. The mixture was concentrated under reduced pressure to afford **12b** as a brown solid; yield: 250 mg (63%).

Synthesis of Indolizinium Salt **13**

To a solution of gold complex **12b** (140 mg, 0.13 mmol, 1 equiv.) in CH₂Cl₂ (2 mL) was added dropwise TfOH (12 μL, 0.14 mmol, 1.08 equiv.). After 6 h at room temperature, a black solid precipitated. The reaction was monitored by ³¹P NMR until disappearance of the peaks of starting gold complex **12b**. The black solid was removed by filtration on Celite®. Water was added to the residue (10 mL) and the resultant mixture was diluted with CH₂Cl₂ (5 mL). The aqueous phase was extracted with CH₂Cl₂ (3 × 10 mL) and the combined organic layers were washed with brine (10 mL), dried over anhydrous MgSO₄, filtered and concentrated under reduced pressure. The residue was purified by precipitation in CH₂Cl₂ and Et₂O to afford **13** as a pale brown solid; yield: 84 mg (quant.).

Synthesis of (–)-**17** from Allene (–)-**8**

To a solution of Ph₃PAuCl (4 mg, 0.009 mmol, 0.05 equiv.) in dry and degassed CH₂Cl₂ (1.8 mL) was added AgSbF₆ (3 mg, 0.009 mmol, 0.05 equiv.). After 5 min stirring at room temperature, the formation of AgCl was observed as a white solid. Then, a solution of allene (–)-**8** (98 mg, 98% ee, 0.18 mmol, 1 equiv.) in CH₂Cl₂ (8.5 mL) was added. The reaction mixture was stirred at reflux temperature for 4 h and monitored by TLC. When the reaction was complete, the mixture was filtered through a short pad of Celite® and washed with Et₂O and CH₂Cl₂. The solution was concentrated under reduced pressure. The residue was purified by silica gel chromatography with EtOAc/Pentane (gradient: from 3:7 until 1:1) as eluent to afford cyclic product (–)-**17** as a pale yellow solid; yield: 83 mg (97% ee, 85%).

Acknowledgements

We thank UPMC, CNRS, IUF, the Franco Thai Scholarship Program administered by CAMPUS FRANCE. We are grateful to Marc Petit (IPCM) for fruitful discussions, Omar Khaled (IPCM) for mass spectrometry.

References

- [1] For a monograph, see: a) N. Krause, A. S. K. Hashmi, (Eds.), *Modern Allene Chemistry*, Wiley-VCH, Weinheim, **2004**; b) for a review, see: S. Yu, S. Ma, *Angew. Chem.* **2012**, *124*, 3128–3167; *Angew. Chem. Int. Ed.* **2012**, *51*, 3074–3112; for some recent examples, see: c) M. Hasegawa, Y. Sone, S. Iwata, H. Matsuzawa, Y. Mazaki, *Org. Lett.* **2011**, *13*, 4688–4691.
- [2] For selected examples, see: a) S. Sentets, R. Serres, Y. Ortin, N. Lugan, G. Lavigne, *Organometallics* **2008**, *27*, 2078–2091; b) E. V. Banide, J. P. Grealis, H. Müller-Bunz, Y. Ortin, M. Casey, C. Mendicute-Fierro, M. C. Lagunas, M. J. McGlinchey, *J. Organomet. Chem.* **2008**, *693*, 1759–1770; c) S. Milosevic, E. V. Banide, H. Müller-Bunz, D. G. Gilheany, M. J. McGlinchey, *Organometallics* **2011**, *30*, 3804–3817.
- [3] S. Löhr, J. Averbeck, M. Schürmann, N. Krause, *Eur. J. Inorg. Chem.* **2008**, 552–556.
- [4] X. Pu, X. Qi, J. M. Ready, *J. Am. Chem. Soc.* **2009**, *131*, 10364–10365.
- [5] F. Cai, X. Pu, X. Qi, V. Lynch, A. Radha, J. M. Ready, *J. Am. Chem. Soc.* **2011**, *133*, 18066–18069.
- [6] a) L. Fensterbank, M. Malacria, *Acc. Chem. Res.* **2014**, *47*, 953–965; see also: b) A. Simonneau, F. Jaroschik, D. Lesage, M. Karanik, R. Guillot, M. Malacria, J.-C. Tabet, J.-P. Goddard, L. Fensterbank, V. Gandon, Y. Gimbert, *Chem. Sci.* **2011**, *2*, 2417–2422; c) F. Schröder, C. Tugny, E. Salanouve, H. Clavier, L. Giordano, D. Moraleda, Y. Gimbert, V. Mourières-Mansuy, J.-P. Goddard, L. Fensterbank, *Organometallics* **2014**, *33*, 4051–4056; d) M. Guitet, P. Zhang, F. Marcelo, C. Tugny, J. Jimenez-Barbero, O. Buriez, C. Amatore, V. Mourières-Mansuy, J.-P. Goddard, L. Fensterbank, Y. Zhang, S. Roland, M. Ménand, M. Sollogoub, *Angew. Chem.* **2013**, *125*, 7354–7359; *Angew. Chem. Int. Ed.* **2013**, *52*, 7213–7218; e) F. Nzulu, A. Bontemps, J. Robert, M. Barbazanges, L. Fensterbank, J.-P. Goddard, M. Malacria, C. Ollivier, M. Petit, J. Rieger, F. Stoffelbach, *Macromolecules* **2014**, *47*, 6652–6656.
- [7] a) M. Malacria, L. Fensterbank, V. Gandon, *Top. Curr. Chem.* **2011**, *302*, 157–182; b) E. Soriano, I. Fernandez, *Chem. Soc. Rev.* **2014**, *43*, 3041–3105; c) W. Yang, A. S. K. Hashmi, *Chem. Soc. Rev.* **2014**, *43*, 2941–2955.
- [8] A. Fürstner, M. Alcarazo, R. Goddard, C. W. Lehmann, *Angew. Chem.* **2008**, *120*, 3254–3258; *Angew. Chem. Int. Ed.* **2008**, *47*, 3210–3214.
- [9] T. J. Brown, A. Sugie, M. G. Dickens, R. A. Widenhofer, *Organometallics* **2010**, *29*, 4207–4209.
- [10] For a review on poly-coordinate gold(I) salts, see: a) M. C. Gimeno, A. Laguna, *Chem. Rev.* **1997**, *97*, 511–522; for the extra-coordination by a P=O moiety, see: b) C. Hahn, L. Cruz, A. Villalobos, L. Garza, S. Adeosun, *Dalton Trans.* **2014**, *43*, 16300–16309.
- [11] S. Yu, S. Ma, *Chem. Commun.* **2011**, *47*, 5384–5418.
- [12] Crystallographic data for structures of compounds **11a**, **11b** and **13** were deposited at the Cambridge Crystallographic Data Centre with numbers CCDC 1055995 (**11a**), CCDC 1055996 (**11b**) and CCDC 1055997 (**13**). These data can be obtained free of charge from The Cambridge Crystallographic Data Centre via www.ccdc.cam.ac.uk/data_request/cif.
- [13] a) T. Schwier, A. W. Sromek, D. M. L. Yab, D. Chernyak, V. Gevorgyan, *J. Am. Chem. Soc.* **2007**, *129*, 9868–9878; for related species that are based on oxygen rather than nitrogen, see: b) L.-P. Liu, B. Xu, M. S. Mashuta, G. B. Hammond, *J. Am. Chem. Soc.* **2008**, *130*, 17642–17643; c) R. Döpp, C. Lothschütz, T. Wurms, M. Pernpointer, S. Keller, F. Rominger, A. S. K. Hashmi, *Organometallics* **2011**, *30*, 5894–5903.
- [14] F. Kolundzic, A. Murali, P. Perez-Galan, J. O. Bauer, C. Strohmann, K. Kumar, H. Waldmann, *Angew. Chem.* **2014**, *126*, 8260–8264; *Angew. Chem. Int. Ed.* **2014**, *53*, 8122–8126.
- [15] For reviews, see: a) L.-P. Liu, G. B. Hammond, *Chem. Soc. Rev.* **2012**, *41*, 3129–3139; b) A. S. K. Hashmi, *Angew. Chem.* **2010**, *122*, 5360–5369; *Angew. Chem. Int. Ed.* **2010**, *49*, 5232–5241; see also: c) A. S. K. Hashmi, L. Schwarz, J.-H. Choi, T. M. Frost, *Angew. Chem.* **2000**, *112*, 2382–2385; *Angew. Chem. Int. Ed.* **2000**, *39*, 2285–2288; d) Y. Chen, D. Wang, J. L. Peter-

- sen, N. G. Akhmedov, X. Shi, *Chem. Commun.* **2010**, 46, 6147–6149; e) D. Weber, M. A. Tarselli, M. R. Gagné, *Angew. Chem.* **2009**, 121, 5843–5846; *Angew. Chem. Int. Ed.* **2009**, 48, 5733–5736; f) A. S. K. Hashmi, T. D. Ramamurthi, F. Rominger, *Adv. Synth. Catal.* **2010**, 352, 971–975; g) X. Zeng, R. Kinjo, B. Donnadieu, G. Bertrand, *Angew. Chem.* **2010**, 122, 954–957; *Angew. Chem. Int. Ed.* **2010**, 49, 942–945; h) A. S. K. Hashmi, T. D. Ramamurthi, M. H. Todd, A. S.-K. Tsang, K. Graf, *Aust. J. Chem.* **2010**, 63, 1619–1626; i) A. S. K. Hashmi, T. D. Ramamurthi, F. Rominger, *J. Organomet. Chem.* **2009**, 694, 592–597; j) T. Wang, S. Shi, M. Rudolph, A. S. K. Hashmi, *Adv. Synth. Catal.* **2014**, 356, 2337–2342.
- [16] a) Y. Shi, S. D. Ramgren, S. A. Blum, *Organometallics* **2009**, 28, 1275–1277; b) P. Garcia, M. Malacria, C. Aubert, V. Gandon, L. Fensterbank, *ChemCatChem* **2010**, 2, 493–497; c) M. M. Hansmann, M. Pernpointner, R. Döpp, A. S. K. Hashmi, *Chem. Eur. J.* **2013**, 19, 15290–15303.
- [17] For examples of gold carbenes with two C-substituents see: a) G. Seidel, A. Fürstner, *Angew. Chem.* **2014**, 126, 4907–4910; *Angew. Chem. Int. Ed.* **2014**, 53, 4807–4811; b) M. W. Hussong, F. Rominger, P. Krämer, B. F. Straub, *Angew. Chem.* **2014**, 126, 9526–9529; *Angew. Chem. Int. Ed.* **2014**, 53, 9372–9375; c) R. J. Harris, R. A. Widenhoefer, *Angew. Chem.* **2014**, 126, 9523–9525; *Angew. Chem. Int. Ed.* **2014**, 53, 9369–9371; d) M. Joost, L. Estevez, S. Mallet-Ladeira, K. Miqueu, A. Amgoune, D. Bourissou, *Angew. Chem.* **2014**, 126, 14740–14744; *Angew. Chem. Int. Ed.* **2014**, 53, 14512–14516.
- [18] For very interesting discussions, see: a) D. Benitez, N. D. Shapiro, E. Tkatchouk, Y. Wang, W. A. Goddard III, F. D. Toste, *Nat. Chem.* **2009**, 1, 482–486; b) Y. Wang, M. E. Muratore, A. M. Echavarren, *Chem. Eur. J.* **2015**, 21, 7332–7339; c) L. Nunes dos Santos Compidos, J. E. M. N. Klein, G. Knizia, J. Kästner, A. S. K. Hashmi, *Angew. Chem.* **2015**, 127, DOI: 10.1002/ange.201412401; *Angew. Chem. Int. Ed.* **2015**, 54, DOI: 10.1002/anie.201412401.
- [19] D. S. Surry, S. L. Buchwald, *Angew. Chem.* **2008**, 120, 6438–6461; *Angew. Chem. Int. Ed.* **2008**, 47, 6338–6361.
- [20] For a similar ¹³C NMR spectrum, see: ref.^[13b]
- [21] a) H. Funami, H. Kusama, N. Iwasawa, *Angew. Chem.* **2007**, 119, 927–929; *Angew. Chem. Int. Ed.* **2007**, 46, 909–911; b) J. H. Lee, F. D. Toste, *Angew. Chem.* **2007**, 119, 930–932; *Angew. Chem. Int. Ed.* **2007**, 46, 912–914; c) G. Lemièrre, V. Gandon, K. Cariou, T. Fukuyama, A.-L. Dhimane, L. Fensterbank, M. Malacria, *Org. Lett.* **2007**, 9, 2207–2209; d) V. Gandon, G. Lemièrre, A. Hours, L. Fensterbank, M. Malacria, *Angew. Chem.* **2008**, 120, 7644–7648; *Angew. Chem. Int. Ed.* **2008**, 47, 7534–7538; e) G. Lemièrre, V. Gandon, K. Cariou, A. Hours, T. Fukuyama, A.-L. Dhimane, L. Fensterbank, M. Malacria, *J. Am. Chem. Soc.* **2009**, 131, 2993–3006.
- [22] For a review on chirality transfers in gold catalysis, see: a) N. T. Patil, *Chem. Asian J.* **2012**, 7, 2186–2194; see also with allenes: b) Z. Liu, A. S. Wasmuth, S. G. Nelson, *J. Am. Chem. Soc.* **2006**, 128, 10352–10353; c) N. Morita, N. Krause, *Org. Lett.* **2004**, 6, 4121–4123; d) Z. Zhang, C. Liu, R. E. Kinder, X. Han, H. Qian, R. A. Widenhoefer, *J. Am. Chem. Soc.* **2006**, 128, 9066–9073; e) C.-Y. Yang, G.-Y. Lin, H.-Y. Liao, S. Datta, R. S. Liu, *J. Org. Chem.* **2008**, 73, 4907–4914; for a review on axial-to-central chirality transfer in cyclization processes, see: f) D. Campolo, S. Gastaldi, C. Roussel, M. P. Bertrand, M. Nechab, *Chem. Soc. Rev.* **2013**, 42, 8434–8466.
- [23] The sign has been determined by the circular dichroism detector at 254 nm in the mobile phase used for the chiral HPLC separation (see the Supporting Information).

NEW LIGANDS FOR ASYMMETRIC CATALYSIS FROM ALLENES

Abstract: This thesis has focused on the synthesis of new ligands bearing chirality for asymmetric catalysis. We first aimed to synthesize chiral allenes with phosphine moieties and use them as ligands of transition metals such as gold(I) species. Allenes bearing a phosphine oxide group were prepared from the corresponding propargylic acetate precursors in moderate to high yields. When substituted by a pyridine substituent, these substrates efficiently combined with gold(I) species to afford two types of new vinyl gold complexes. One cationic vinyl complex featuring a triphenylphosphine gold(I) moiety can be further functionalized to give an indolizinium salt and a vinyl iodide derivative. The other one bearing a chlorogold(I) group can be used as a catalyst in gold-catalyzed cyclization. Moreover, other allenes have been investigated in gold(I)-catalyzed rearrangements. To our delight, the allenes featuring a 3,5-methoxyphenyl substituent and a vinylallene can produce respectively indenyl and cyclopentadienyl phosphine oxide products bearing stereogenic centers. In addition, a complete axial-to-center chirality transfer was observed on the indenylphosphine oxide product starting from the optically pure allene. In a next attempt, we have prepared some new digold-allenyl bisphosphine precatalysts. These new complexes can be used in gold-catalyzed intermolecular reactions and cyclization reactions. Several carbo- and heterocyclic products were produced in moderate to excellent yields. These chiral gold complexes could be separated by preparative chiral HPLC. Some promising enantiomeric excesses were observed in cycloisomerization reactions.

Keywords: allenes, gold catalysis, phosphine, gold carbene, cycloisomerization, chirality

NOUVEAUX LIGANDS EN CATALYSE ASYMETRIQUE PAR DES ALLENES

Résumé: Ce travail de thèse décrit la synthèse de nouveaux ligands chiraux pour des applications en catalyse asymétrique. Nous avons ainsi synthétisé différents allènes chiraux possédant des groupements phosphines et nous les avons testés sur des métaux de transition comme l'or(I). Les allènes possédant des oxydes de phosphine ont été préparés à partir de précurseurs de l'acétate propargylique correspondant avec des rendements modérés à élevés. Nous avons pu montrer que les allènes possédant un motif pyridine se coordinent efficacement avec de l'or(I), donnant deux nouveaux types de complexes d'or vinylique. Un complexe cationique vinylique avec un fragment triphénylphosphine d'or(I) permet de préparer des dérivés fonctionnalisés tels qu'un sel d'indolizinium et un iodure de vinyle. L'autre complexe contenant le groupement de chlore d'or a été utilisé comme catalyseur dans des réactions de cyclisation catalysées par de l'or. De plus, les différents allènes synthétisés ont été étudiés dans le cadre de réarrangements catalysés par l'or. Les allènes avec les groupements 3,5-méthoxyphényl et vinylallène peuvent conduire respectivement à des produits indényle et cyclopentadiényle, portant tous deux un centre stéréogène. En outre, un transfert complet de chiralité axiale en chiralité centrée a été observé sur le produit d'indényle - oxyde de phosphine à partir de l'allène optiquement pur. L'étape suivante, nous avons préparé quelques nouveaux précatalyseurs alléniques bisphosphine bimétalliques à base d'or. Ces nouveaux complexes peuvent être utilisés dans des réactions intermoléculaires et des réactions de cyclisation catalysées à l'or. Plusieurs produits carbocycliques et hétérocycliques ont été obtenus avec des rendements modérés à excellents. Ces complexes d'or chiraux peuvent être séparés par HPLC chirale préparative. Certains des excès énantiomériques obtenus dans les réactions des cycloisomérisations sont prometteurs.

Mots clés: allènes, catalyse à l'or, phosphine, carbènes d'or, cycloisomérisations, chiralité